

**MOLECULAR INTERACTIONS IN MIXTURES OF
SOME INDUSTRIALLY IMPORTANT SOLVENTS:
A PHYSICO-CHEMICAL STUDY**

*A Thesis submitted to the
UNIVERSITY OF NORTH BENGAL*

**For the Award of
DOCTOR OF PHILOSOPHY
in
CHEMISTRY**

**By
Mr. RAJENDRA PRADHAN
(M.Sc. in Chemistry)**

**Supervisor
DR. BISWAJIT SINHA**

**DEPARTMENT OF CHEMISTRY
UNIVERSITY OF NORTH BENGAL**

May, 2018

Dedicated
To
My Beloved Parents
Specially To My Mother
Late Kamala Pradhan

DECLARATION

I declare that the thesis entitled “**MOLECULAR INTERACTIONS IN MIXTURES OF SOME INDUSTRIALLY IMPORTANT SOLVENTS: A PHYSICO-CHEMICAL STUDY**” has been prepared by me under the guidance of Dr. Biswajit Sinha, Assistant Professor, Department of Chemistry, University of North Bengal. No part of this thesis has formed the basis for the award of any degree or fellowship previously.

Rajendra Pradhan

RAJENDRA PRADHAN

Department of Chemistry

University of North Bengal

Darjeeling-734013

West Bengal, India

DATE: 28.05.2018

UNIVERSITY OF NORTH BENGAL

Dr. Biswajit Sinha, Ph. D
Associate Professor
Department of Chemistry
E-mail: biswachem@gmail.com
M: 9932738973, 9641967211



Ph: +91-353-2776381
University of North Bengal,
Darjeeling 734 013
INDIA
May 24, 2018

ENLIGHTENMENT TO PERFECTION
Accredited by NAAC with Grade A

CERTIFICATE

I declare that Mr. RAJENDRA PRADHAN has prepared the thesis entitled "MOLECULAR INTERACTIONS IN MIXTURES OF SOME INDUSTRIALLY IMPORTANT SOLVENTS: A PHYSICO-CHEMICAL STUDY" for the award of Ph. D degree of University of North Bengal, under my guidance. He has carried out the work at the Department of Chemistry, University of North Bengal.

Dr. Biswajit Sinha

Department of Chemistry

University of North Bengal

Darjeeling-734013

West Bengal, India

Dr. B. Sinha
Associate Professor
Department of Chemistry
University of North Bengal
Darjeeling - 734013, India

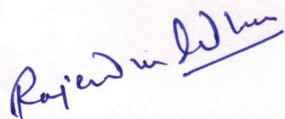
DATE: 28.05.2018

Anti-plagiarism Report of the Ph. D Thesis

Title of the thesis: MOLECULAR INTERACTIONS IN MIXTURES OF SOME INDUSTRIALLY IMPORTANT SOLVENTS: A PHYSICO-CHEMICAL STUDY

Urkund Analysis Result

Analysed Document: Thesis_Rajendra Pradhan.pdf (D38939154)
Submitted: 5/21/2018 7:17:00 AM
Submitted By: nbuplg@gmail.com
Significance: 3 %



Signature of the Candidate



Signature of the Supervisor

Dr. B. Sinha
Associate Professor
Department of Chemistry
University of North Bengal
Darjeeling - 734013, India



Signature of HOD, Dept. of Chemistry

University of North Bengal

Head
Department of Chemistry
University of North Bengal
Darjeeling - 734013, India

ABSTRACT

The present dissertation entitled “*Molecular Interactions in Mixtures of Some Industrially Important Solvents: A Physico-Chemical Study*” has been organized in eleven chapters. Chapter I describes the importance of physico-chemical studies on multi-component liquid mixtures with special reference to solvent effects, preferential solvation and various kinds of molecular interactions, *etc.* This chapter also describes the importance and scope of different physico-chemical parameters generally studied for such studies including objectives, applications of the research work and a brief literature review.

Chapter II contains a thorough theoretical background for the research works embodied in this thesis. Chapter III contains details of the chemicals and measurement techniques for different physico-chemical parameters like density, viscosity, ultrasonic speeds of sound, refractive index, *etc.*

Chapter IV describes the thermophysical properties of the binary mixtures of N, N-dimethylformamide (DMF) with some cyclic ethers, *viz.*, tetrahydrofuran (THF), 1,3-dioxolane (1,3-DO) and 1,4-dioxane (1,4-DO) at several temperatures. Excess molar volumes (V_m^E), viscosity deviations ($\Delta\eta$) and excess isentropic compressibilities (κ_s^E), *etc.*, were derived from the experimental results. These derived properties were discussed in terms of the nature of component liquids and molecular interactions in the mixtures. The molecular interactions in these binary mixtures were attributed to dipole-dipole and dipole induced dipole interactions. Several empirical and semi-empirical models were used to correlate/predict some of the derived properties.

Chapter V describes the thermophysical properties of the binary mixtures of 2-ethyl-1-hexanol (2-EH) with ethylenediamine (EDA), 1,2-dichloroethane (DCE) and monoethanolamine (MEA) at several temperatures. From the experimental data, various properties like excess molar volumes (V_m^E), viscosity deviations ($\Delta\eta$), excess Gibb’s free energy of viscous flow (ΔG^{*E}) and different acoustic properties were derived and discussed in terms of molecular interactions like dipole-dipole interaction, hydrogen bond interaction and interstitial accommodation, *etc.* Excess molar volume (V_m^E) and viscosities (η) of the mixtures were correlated with

Prigogine-Flory-Patterson theory, Peng-Robinson Equation of State and Bloomfield-Dewan model, respectively. The results were substantiated with FTIR spectra of these binary mixtures.

Chapter VI describes the molecular interactions of 1,4-dioxane (1,4-DO) with ethylenediamine (EDA), 1,2-dichloroethane (DCE) and monoethanolamine (MEA) at several temperatures. From the experimental physico-chemical properties, several excess or deviation properties (V_m^E , $\Delta\eta$, κ_S^E and R_m^E , *etc.*) were derived and discussed. The study revealed that the degree of molecular interactions follow the order: (1,4-DO + MEA) > (1,4-DO + EDA) > (1,4-DO + DCE). This order of molecular interactions can be ascribed to intermolecular hydrogen bond formation and interstitial accommodation depending on the nature (shape and size) of the mixing components. The nature and extent of molecular interactions were well corroborated with the FTIR spectra of these mixtures.

Chapter VII describes the thermophysical properties of the binary mixtures of cyclohexane (CH) with three esters, *viz.*, methyl acetate (MA), ethyl acetate (EA) and methyl salicylate (MS) at several temperatures. Experimental densities, viscosities, ultrasonic speeds of sound and refractive indices were utilized to derive various excess or deviation properties (V_m^E , $\Delta\eta$, κ_S^E and R_m^E , *etc.*), which were discussed in terms of the nature of the component liquids and the molecular interactions like breaking of dipolar association or the three dimensional hydrogen bonded network as well as interstitial accommodation, *etc.*, in the mixtures. The order of molecular interactions: (CH + MS) > (CH + EA) > (CH + MA) was well corroborated with FTIR spectra of these binary mixtures. Such an order of molecular interactions manifests a combined effect of several factors like molecular size, shape and nature of the component liquids.

Chapter VIII describes the thermophysical properties of the binary mixtures of cyclohexanone (CHN) with methyl acetate (MA), ethyl acetate (EA) and methyl salicylate (MS). From the experimental densities, viscosities, *etc.*, various thermodynamic, transport and acoustic properties were derived and used to explain the molecular interactions in these binary mixtures in the light of breaking up of dipolar interaction, hydrogen bond interaction and interstitial accommodation, *etc.* The order of molecular interactions: (CHN + MS) > (CHN + EA) > (CHN + MA) was

discussed on the basis of the nature of the liquids and the molecular interactions in the mixtures. The above order of molecular interactions was well substantiated by the FTIR spectra of these binary mixtures.

Chapter IX describes the thermophysical properties of the ternary mixtures consisting of cyclohexane (CH) and cyclohexanone (CHN) with methyl acetate (MA), ethyl acetate (EA) and methyl salicylate (MS). The experimental densities, viscosities, ultrasonic speeds of sound and refractive indices of seven ternary mixtures and three binary mixtures, *viz.*, (MA + EA), (MA + MS) and (EA + MS) were used to derive various excess/deviation properties like V_m^E , $\Delta\eta$, κ_S^E and R_m^E , *etc.* These properties were discussed on the basis of the nature of the mixing components and the molecular interactions in these mixtures. The excess/deviation properties were fitted to Redlich-Kister polynomial (for the binary mixtures) and Cibulka polynomial (for the ternary mixtures). Several empirical/semi-empirical relations like Rastogi, Köhler, Jacob-Fitzner, Colinet, Tsao-Smith, *etc.*, were used to correlate/predict the excess or deviation properties of these ternary mixtures. The so-called ternary contributions determined for the ternary mixtures suggested their non-homogeneity.

Chapter X describes the thermophysical properties of two quaternary mixtures consisting of cyclohexane (CH) and cyclohexanone (CHN) with methyl acetate (MA), ethyl acetate (EA) and methyl salicylate (MS). The experimental densities, viscosities, ultrasonic speeds of sound and refractive indices were utilized to derive V_m^E , $\Delta\eta$, κ_S^E and R_m^E , *etc.*, which helped to reveal the nature of the molecular interactions in these quaternary mixtures. The excess/deviation properties were fitted to Cibulka polynomial for the quaternary mixtures. The study revealed the following order of molecular interactions: (CHN + MA + EA + MA) > (CH + MA + EA + MA) suggesting that the molecular interactions in these quaternary mixtures depend on the nature of the mixing components as well as on the molecular interactions of the associated ternary and binary mixtures at least qualitatively.

Finally in chapter XI concluding remarks on the research works embodied in different chapters (chapters IV to X) of this thesis have been made.

PREFACE

I started my research presented in this thesis entitled “**MOLECULAR INTERACTIONS IN MIXTURES OF SOME INDUSTRIALLY IMPORTANT SOLVENTS: A PHYSICO-CHEMICAL STUDY**” in the year 2014 under the esteemed supervision of Dr. Biswajit Sinha at the Department of Chemistry, University of North Bengal, India with an aim to investigate into the physico-chemical and thermodynamic properties of the multi-component liquid mixtures. These properties of multi-component liquid mixtures can be altered within a reasonable range by varying the concentration till an optimum value of a desired property is obtained. The knowledge of such properties of non-aqueous liquid mixtures has industrial relevance and is frequently required in the theoretical and applied areas of research including many chemical, biochemical and industrial processes. These properties provide valuable information about the structural character of the mixtures in liquid state and such properties have important roles in elucidating the molecular interactions among the components of the mixtures and thus help to develop new theoretical models. A knowledge about the molecular interactions amongst the component liquids of a multi-component liquid mixture can be established from a study of characteristic departure from the ideal behavior of the thermodynamic, transport and acoustic properties like excess molar volumes (V_m^E), viscosity deviations ($\Delta\eta$) and excess isentropic compressibilities (κ_s^E) and excess molar refractions (R_m^E), *etc.*, derived from the experimental densities, viscosities, ultrasonic speeds and refractive indices, *etc.* These excess or deviation properties can well be interpreted in the light of the nature of the individual liquids and the molecular interactions interplaying in their mixtures. Therefore, the research works embodied in this thesis include the physico-chemical studies on various binary, ternary and quaternary liquid mixtures of some industrially important solvents through the determinations of different physico-chemical properties of their mixtures and FTIR spectroscopy.

ACKNOWLEDGEMENT

With deep appreciation and reverence I deem it a great pleasure to express my deep sense of gratitude to my venerable supervisor Dr. Biswajit Sinha for his valuable advise, persistent guidance and stimulating discussions during my doctoral research. He constantly forced me to remain focused on achieving my goal. His observation and comments helped me to establish the overall direction of the research and to move forward expeditiously with investigations in depth. Once again I thank him for providing me the opportunity to work with numerous local and global peers. Special thanks are also due to Prof. S. K. Saha, Prof. M. N. Roy and Prof P. Ghosh of the Department of Chemistry, University of North Bengal for their persistent help and concern whenever required. Above all, needless to say “Thanks” to express my deep indebtedness to my lab mates Dr. Dhiraj Brahman, Dr. Abhijit Sarkar, Mr. Dipu Kumar Mishra, Mrs. Ananya Das, Mr. Uttam Kumar Singha. They always stood beside me with their helping hands and cordial support. I am equally thankful to all the non-teaching staff of the Department of Chemistry, University of North Bengal, for extending their help and cooperation.

I owe many thanks to my friends Dr. D. Lama, Mr. Pravat Dangal for their constant inspiration with keen interest. I am also thankful to the Principal, St. Joseph’s College, Darjeeling and my beloved colleagues at the Department of Chemistry, St. Joseph’s College, Darjeeling for their valuable moral support and inspirations. My special appreciation is reserved to my family- my late parents, my brothers for their love, care and prayers over all these years. I am greatly indebted to my wife and my sweet daughter for their endless love, support and patient endurance that made this venture successful. I would also like to thank all those who directly and indirectly supported me in completing my thesis in due time.

Mr. Rajendra Pradhan
Research Scholar
Department of Chemistry
University of North Bengal
Darjeeling -734013, INDIA

TABLE OF CONTENTS

Topic	Page No.
Abstract	i-iii
Preface	iv
Acknowledgement	v
Table of Contents	vi-xiv
List of Tables	xv-xix
List of Figures	xx-xxvii
List of Appendices	xxviii
<hr/>	
CHAPTER I: General Introduction	1-28
<hr/>	
Introduction	1-3
1.1. Solvent Effects	3-7
1.1.1. Solvation	5-6
1.1.2. Preferential Solvation	6-7
1.2. Importance and scope of the Physico-Chemical Parameters	8-10
1.3. Objectives and Application of the Research Work	10-12
1.4. Importance of Solvents and Solvent Mixtures Studied	12-14
1.5. Literature Review	14-22
References	22-28
<hr/>	
CHAPTER II: Theoretical Background	29-82
<hr/>	
2.1 Importance of Mixed Solvent Systems	29-29
2.2 Intermolecular Forces	30-34
2.2.1 Dipole-Dipole Interaction	30-30
2.2.2. Induced Dipole interaction	31-31
2.2.3. Instantaneous Dipole-Induced Dipole interaction	31-32
2.2.4. Hydrogen Bond	32-34

Contd....

Topic	Page No.
2.3. Theory of Mixed Solvents	34-35
2.4 Excess molar Volume	35-36
2.5. Partial molar Volume	36-40
2.6. Viscosity Deviation	40-41
2.7. Thermodynamics for Viscous Flow	42-44
2.7.1 Excess Gibb's Free Energy of Activation of Viscous Flow	42-43
2.7.2. Viscous Entropy and Enthalpy	43-44
2.8. Ultrasonic Speed of Sound	44-49
2.8.1. Isentropic Compressibility	45-46
2.8.2. Excess Isentropic Compressibility	46-46
2.8.3. Intermolecular Free Length	46-47
2.8.4. Specific Acoustic Impedance	47-47
2.8.5. Free Volume	48-48
2.8.6. Internal Pressure	48-49
2.9. Refractive Index	49-51
2.9.1. Deviation in Refractive index	50-50
2.9.2. Molar Refraction and Excess Molar Refraction	51-51
2.10. Predictive Models	51-59
2.10.1. Excess Molar Volume Models	52-59
2.10.1.1. Cubic Equation of State	52-53
2.10.1.2. Peng-Robinson Equation of State	53-55
2.10.1.3. Flory Theory	55-57
2.10.1.4. Prigogine-Flory-Patterson (PFP) Theory	57-59
2.11. Viscosity Models	59-61
2.11.1. Model Based on Eyring Theory Coupled with a Cubic Equation of State	59-60

Contd...

Topic	Page No.
2.11.2. Bloomfield-Dewan Viscosity Model	60-61
2.12. Viscosity Correlative Models	62-64
2.12.1. Grunberg and Nissan Model	62-62
2.12.2 Tamura and Kurata Model	62-63
2.12.3. Hind Model	63-63
2.12.4. Heric-Brewer Model	63-63
2.12.5. McAllister Models	63-64
2.12.6. Katti-Chaudhri Model	64-64
2.12.7. Lobe Model	64-64
2.12.8. Krishnan-Laddha model	64-64
2.13. Other Correlative Models	65-65
2.14. Predictive Symmetric and Asymmetric Models for Ternary and Quaternary Systems	65-68
2.14.1. Symmetrical Models	66-67
2.14.1.1. Köhler Model	66-66
2.14.1.2. Jacob–Fitzner Model	66-66
2.14.1.3. Colinet Model	66-67
2.14.1.4. Rastogi Model	67-67
2.14.2. Asymmetrical Models	67-68
2.14.2.1. Tsao-Smit model	67-67
2.14.2.2. Toop Model	67-67
2.14.2.3. Scatchard Model	67-68
2.14.2.4. Mathieson-Thynne Model	68-68
2.15. Theoretical Estimation of Ultrasonic Speed	68-70
2.15.1. Nomoto Relation (NOM)	68-68

Contd....

Topic	Page No.
2.15.2 Schaaff's Collision Factor Theory (CFT)	68-69
2.15.3. Impedance Dependence Relation (IDR)	69-69
2.15.4. Vandeaal Vangeal Ideal Mixture Relation (IMR)	69-69
2.15.5. Jacobson's Free Length Theory (FLT)	69-70
2.15.6. Junjie's Equation (JUN)	70-70
2.16. Theoretical Estimation of Refractive Indices of Liquid Mixtures	71-72
2.16.1. Lorentz-Lorenz Relation	71-71
2.16.2. Gladstone-Dale Relation	71-71
2.16.3. Arago-Biot Relation	71-71
2.16.4. Weiner Model Relation	71-71
2.16.5. Eyring-John Relation	72-72
2.16.6. Heller Relation	72-72
2.16.7. Eykman Relation	72-72
2.16.8. Newton Relation	72-72
2.17. Response Surface Model	72-73
2.18. Standard Deviation	73-73
References	73-81
CHAPTER III: Experimental Section	82-96
3.1. Source and Purification of the Chemicals Used	82-84
3.1.1. Solvents	82-83
3.1.2. Mixed Solvents	83-84
3.2. Experimental Methods	84-94
3.2.1. Density measurement	84-86
3.2.2. Measurement of Viscosity	86-87
3.2.3. Measurement of Mass	87-87

Contd...

Topic	Page No.
3.2.4. Refractive Index Measurement	88-89
3.2.5. Measurement of Ultrasonic Speed	89-92
3.2.5. Measurement of FT-IR Spectra	93-94
3.2.6. Methodology	94-95
References	95-96
CHAPTER IV: Thermophysical properties of binary mixtures of N, N-dimethylformamide with three cyclic ethers	97-122
4.1. Introduction	97-98
4.2. Experimental section	98-99
4.2.1. Materials	98-98
4.2.2. Apparatus and Procedure	98-99
4.3. Results and discussion	100-120
4.3.1. Excess molar volumes	100-105
4.3.2. Excess partial molar volumes	105-108
4.3.3. Prigogine-Flory-Patterson theory (PFP)	108-112
4.3.4. Viscosity Deviation	112-114
4.3.5. Thermodynamics of viscous flow	114-115
4.3.6. Excess Isentropic Compressibilities	116-118
4.3.7. Theoretical prediction of ultrasonic speeds	118-120
4.4. Conclusion	120-120
References	120-122
CHAPTER V: Thermophysical properties of the binary mixtures of 2-ethyl-1-hexanol with 1, 2-disubstituted ethanes at $T = (298.15- 318.15)$ K	123-157
5.1. Introduction	123-124
5.2. Experimental section	124-125
5.2.1. Material	124-124
	Contd...

Topic	Page No.
5.2.2. Apparatus and Procedure	124-125
5.3. Results and discussion	125-154
5.3.1. Excess molar volume	128-131
5.3.2. Excess Partial molar volumes	131-133
5.3.3. Predictions of excess molar volumes	133-137
5.3.4. Viscosity deviations	137-139
5.3.5. Thermodynamics of viscous flow	139-141
5.3.6. Viscosity prediction	141-144
5.3.7. Ultrasonic speed of sound and derived functions	144-149
5.3.8. Prediction of ultrasonic speed of sound	149-149
5.3.9. Excess molar refraction	149-152
5.3.10. IR spectroscopic study	152-154
5.4. Conclusion	154-155
Reference	155-157
CHAPTER VI: Hydrogen bond interactions in the mixtures of 1,4-Dioxane with some 1,2 disubstituted ethanes at $T = (298.15 - 318.15)$ K	158-188
6.1. Introduction	158-160
6.2. Experimental section	160-161
6.2.1. Materials	160-160
6.2.2. Apparatus and Procedure	160-161
6.3. Results and discussion	161-186
6.3.1. Excess molar volumes	161-166
6.3.2. Excess partial molar volumes	166-168
6.3.3. Predictions of excess molar volumes	168-171
6.3.4. Viscosity deviations	171-172

Contd...

Topic	Page No.
6.3.5. Thermodynamics of viscous flow	172-174
6.3.6. Viscosity prediction	174-177
6.3.7. Ultrasonic speed of sound and derived functions	177-182
6.3.8. Molar refractions	182-184
6.3.9. IR spectroscopic study	184-186
6.4. Conclusion	184-186
References	186-188
CHAPTER VII: Thermophysical properties of the binary mixtures of cyclohexane with some esters	189-220
7.1. Introduction	189-190
7.2. Experimental section	190-192
7.2.1. Materials	190-190
7.2.2. Apparatus and procedure	190-192
7.3. Results and discussion	192-218
7.3.1. Excess molar volumes	192-197
7.3.2. Excess partial molar volumes	197-198
7.3.3. Predictions of excess molar volumes	198-203
7.3.4. Viscosity deviation	203-204
7.3.5. Thermodynamics of viscous flow	205-207
7.3.6. Viscosity models	207-209
7.3.7. Ultrasonic speed of sound and derived acoustic functions	209-212
7.3.8. Prediction of ultrasonic speed of sound	212-213
7.3.9. Excess molar refractions	213-215
7.3.10. IR spectroscopic study	216-218
7.4. Conclusion	218-218
References	218-220

Contd....

Topic	Page No.
CHAPTER VIII: Thermophysical properties of the binary mixtures of cyclohexanone with some esters	221-250
8.1. Introduction	221-222
8.2. Experimental section	222-222
8.2.1. Materials	222-222
8.2.2. Apparatus and procedures	222-222
8.3. Results and discussion	222-248
8.3.1. Excess molar volumes	223-230
8.3.2. Predictions of excess molar volumes	230-233
8.3.3. Viscosity deviation	234-235
8.3.4. Thermodynamics of viscous flow	235-237
8.3.5. Viscosity correlation	238-239
8.3.6. Ultrasonic speed of sound & derived functions	240-243
8.3.7. Prediction of ultrasonic speed of sound	244-244
8.3.8. Excess molar refractions	244-245
8.3.9. IR spectroscopic study	246-248
8.4. Conclusion	248-248
References	248-250
CHAPTER IX: Thermophysical properties of the ternary mixtures of cyclohexane and cyclohexanone with some esters at $T = (298.15-318.15)$ K	251-295
9.1. Introduction	251-251
9.2. Experimental section	251-252
9.2.1. Material	251-251
9.2.2. Apparatus and procedure	252-252
9.3. Results and discussion	252-293
9.3.1. Excess molar volumes and excess partial molar volumes	252-273
Contd...	

Topic	Page No.
9.3.2. Viscosity Deviations	274-278
9.3.3. Excess Isentropic Compressibility	278-284
9.3.4. Excess Molar Refraction	284-290
9.3.5. Empirical and correlative models	291-293
9.4. Conclusion	293-294
References	294-295
CHAPTER X: Thermophysical properties of the quaternary mixtures of cyclohexane and cyclohexanone with some esters at $T = (298.15-318.15)$ K	296-311
10.1. Introduction	296-296
10.2. Experimental section	296-297
10.2.1. Material	296-297
10.2.2. Measurements	297-297
10.3. Results and discussion	297-310
10.3.1. Excess molar volumes	297-303
10.3.2. Viscosity Deviations	303-304
10.3.3. Excess Isentropic Compressibility	304-306
10.3.4. Excess Molar Refraction	306-307
10.3.5. Empirical and correlative models	307-310
10.4. Conclusion	310-310
References	310-311
CHAPTER XI: Concluding Remarks	312-316
APPENDIX I	317-317
APPENDIX II	318-318
BIBLIOGRAPHY	319-330
INDEX	331-336

LIST OF TABLES

Table	Page No.
3.1. Provenance and purity of the solvents used.	83-83
4.1. Physical properties of various pure liquids at $T = (298.15-318.15)$ K.	99-99
4.2. Densities (ρ), viscosities (η), excess molar volumes (V_m^E) and viscosity deviations ($\Delta\eta$) for the binary mixtures of DMF (1) with three cyclic ethers (2) at $T = (298.15-318.15)$ K.	101-103
4.3. Redlich-Kister coefficients (a_i), standard deviations (σ) for least squares fitting of excess molar volumes (V_m^E), excess partial molar volumes, ($\bar{V}_{m,1}^E$ and $\bar{V}_{m,2}^E$) and excess partial molar volumes ($\bar{V}_{m,1}^{0,E}$ and $\bar{V}_{m,2}^{0,E}$) at infinite dilution of each component in the studied binary mixtures at $T = (298.15-318.15)$ K.	106-106
4.4. Flory's parameters for pure liquids at 298.15 K.	109-109
4.5. Values of interaction parameter ($\chi_{1,2}$) calculated and experimental values of excess molar volumes ($V_{m, PFP}^E$ and $V_{m, exp}^E$), their deviations (ΔV_m^E) and different PFP contributions at 298.15 K.	111-111
4.6. Values of enthalpy (ΔH^*) and entropy (ΔS^*) of activation of viscous flow for the binary mixtures.	115-115
4.7. Ultrasonic speeds (u), isentropic compressibilities (κ_S) and excess isentropic compressibilities (κ_S^E) of binary mixtures of DMF (1) + the cyclic ethers (2) at 298.15 K.	117-117
4.8. Relative predictive capabilities of various theories and empirical relations for ultrasonic speeds of the binary mixtures at 298.15 K.	119-119
5.1. Physical properties of the pure liquids at $T = (298.15$ to $318.15)$ K.	125-125
5.2. Density (ρ), viscosity (η), excess molar volume (V_m^E) and viscosity deviation ($\Delta\eta$) for the binary mixtures studied at $T = (298.15$ to $318.15)$ K.	126-128
5.3. Molar volumes ($V_{m,1}^*$ and $V_{m,2}^*$), partial molar volumes at infinite dilution ($\bar{V}_{m,1}^0$ and $\bar{V}_{m,2}^0$) and excess partial molar volumes at infinite dilution ($\bar{V}_{m,1}^{0,E}$ and $\bar{V}_{m,2}^{0,E}$) for each component in the binary mixtures at 298.15 K.	132-132

Contd....

Table	Page No.
5.4. Isobaric molar heat capacities (c_p), expansion coefficient (α), isothermal compressibility (κ_T) and Flory's parameters for pure liquids at 298.15 K.	134-134
5.5. Interaction parameter ($\chi_{1,2}$), calculated and experimental values of excess molar volumes ($V_{m,exp}^E$ and $V_{m,PFPP}^E$), their deviations (ΔV_m^E) and different PFP contributions at 298.15 K.	135-135
5.6. Free energy (ΔG^*), enthalpy (ΔH^*) and entropy (ΔS^*) of activation of viscous flow for the binary mixtures.	140-140
5.7. Ultrasonic speeds (u), isentropic compressibility (κ_S) and excess isentropic compressibility (κ_S^E) for binary mixtures at 298.15 K.	146-146
5.8. Intermolecular free length (L_f), specific acoustic impedance (z_{im}), excess intermolecular free lengths (L_f^E) and excess acoustic impedances (z_{im}^E) for the studied binaries at 298.15 K.	148-148
5.9. Refractive indices (n_D), molar refractions (R_m) and excess molar refractions (R_m^E) for the binary mixtures at 298.15 K.	151-151
6.1. Densities (ρ) and viscosities (η) of the pure liquids at $T = (298.15 \text{ to } 318.15) \text{ K}$.	160-160
6.2. Density (ρ), viscosity (η), excess molar volume (V_m^E) and viscosity deviation ($\Delta\eta$) for the binary mixtures studied at $T = (298.15 \text{ to } 318.15) \text{ K}$.	162-164
6.3. Molar volumes ($V_{m,1}^*$ and $V_{m,2}^*$), partial molar volumes at infinite dilution ($\bar{V}_{m,1}^0$ and $\bar{V}_{m,2}^0$) and excess partial molar volume at infinite dilution ($\bar{V}_{m,1}^{0,E}$ and $\bar{V}_{m,2}^{0,E}$) for each component in the binary mixtures at 298.15 K.	167-167
6.4. Isobaric molar heat capacities (c_p), expansion coefficient (α), isothermal compressibility (κ_T) and Flory's parameters for pure liquids at 298.15 K.	168-168
6.5. Interaction parameter ($\chi_{1,2}$), calculated and experimental values of excess molar volumes ($V_{m,exp}^E$ and $V_{m,PFPP}^E$), their deviations (ΔV_m^E) and different PFP contributions at 298.15 K.	170-170
6.6. Free energy (ΔG^*), enthalpy (ΔH^*) and entropy (ΔS^*) of activation of viscous flow for the binary mixtures.	173-173

Contd...

Table	Page No.
6.7. Ultrasonic speeds (u), isentropic compressibility (κ_s) and excess isentropic compressibility (κ_s^E) for binary mixtures at 298.15 K.	179-179
6.8. Intermolecular free length (L_f), specific acoustic impedance (z_{im}), excess intermolecular free lengths (L_f^E) and excess acoustic impedances (z_{im}^E) for the studied binaries at 298.15 K.	181-182
6.9. Refractive indices (n_D), molar refractions (R_m) and excess molar refractions (R_m^E) for the binary mixtures at 298.15 K.	183-183
7.1. Densities (ρ) and viscosities (η) of the pure liquids at 298.15, 308.15 and 313.15 K.	191-191
7.2. Density (ρ), viscosity (η), excess molar volume (V_m^E) and viscosity deviation ($\Delta\eta$) for the binary mixtures studied at $T = (298.15 \text{ to } 313.15) \text{ K}$.	193-195
7.3. Molar volumes ($V_{m,1}^*$ and $V_{m,2}^*$), partial molar volumes at infinite dilution ($\bar{V}_{m,1}^0$ and $\bar{V}_{m,2}^0$) and excess partial molar volumes at infinite dilution ($\bar{V}_{m,1}^{0,E}$ and $\bar{V}_{m,2}^{0,E}$) for each component in the binary mixtures at 298.15 K.	199-199
7.4. Isobaric molar heat capacities (C_p), expansion coefficient (α), isothermal compressibility (κ_T) and Flory's parameters for pure liquids at 298.15 K.	201-201
7.5. Interaction parameter ($\chi_{1,2}$), calculated and experimental values of excess molar volumes ($V_{m,exp}^E$ and $V_{m,PFP}^E$), their deviations (ΔV_m^E) and different PFP contributions at 298.15 K.	201-201
7.6. Free energy (ΔG^*), enthalpy (ΔH^*) and entropy (ΔS^*) of activation of viscous flow for the binary mixtures.	206-206
7.7. Different viscosity models coefficients and corresponding standard deviations (σ) for the binary mixtures studied at $T = 298.15 \text{ K}$.	208-208
7.8. Ultrasonic speeds (u), isentropic compressibilities (κ_s), intermolecular free lengths (L_f), free volumes (V_f), excess isentropic compressibilities (κ_s^E), excess intermolecular free lengths (L_f^E) and excess free volumes (V_f^E) for binary mixtures at 298.15 K.	211-211

Contd...

Table	Page No.
7.9. Refractive indices (n_D), molar refractions (R_m) and excess molar refractions (R_m^E) for the binary mixtures at 298.15 K.	215-215
8.1. Densities (ρ) and viscosities (η) of the pure liquids at 298.15, 308.15 and 313.15 K.	223-223
8.2. Density (ρ), viscosity (η), excess molar volume (V_m^E) and viscosity deviation ($\Delta\eta$) for the binary mixtures studied at $T = (298.15 \text{ to } 318.15)$ K.	225-227
8.3. Molar volumes ($V_{m,1}^*$ and $V_{m,2}^*$), partial molar volumes at infinite dilution ($\bar{V}_{m,1}^0$ and $\bar{V}_{m,2}^0$) and excess partial molar volumes at infinite dilution ($\bar{V}_{m,1}^{0,E}$ and $\bar{V}_{m,2}^{0,E}$) for each component in the binary mixtures at 298.15 K	229-229
8.4. Isobaric molar heat capacities (C_p), expansion coefficient (α), isothermal compressibility (κ_T) and Flory's parameters for pure liquids at 298.15 K.	231-231
8.5. Interaction parameters ($\chi_{1,2}$), calculated and experimental values of excess molar volumes ($V_{m,exp}^E$ and $V_{m,PFPP}^E$), their deviations (ΔV_m^E) and different PFP contributions at 298.15 K.	232-232
8.6. Free energy (ΔG^*), enthalpy (ΔH^*) and entropy (ΔS^*) of activation of viscous flow for the binary mixtures.	237-237
8.7. Ultrasonic speeds (u), isentropic compressibilities (κ_S), intermolecular free lengths (L_f), free volumes (V_f), excess isentropic compressibilities (κ_S^E), excess intermolecular free lengths (L_f^E) and excess free volumes (V_f^E) for binary mixtures at 298.15 K.	241-241
8.8. Refractive indices (n_D), molar refractions (R_m) and excess molar refractions (R_m^E) for the binary mixtures at 298.15 K.	245-245
9.1. Densities (ρ), viscosities (η), excess molar volumes (V_m^E) and viscosity deviations ($\Delta\eta$) for the three binary mixtures studied at $T = (298.15 \text{ to } 318.15)$ K.	254-256
9.2. Molar volumes ($V_{m,1}^*$ and $V_{m,2}^*$), partial molar volumes at infinite dilution ($\bar{V}_{m,1}^0$ and $\bar{V}_{m,2}^0$) and excess partial molar volumes at infinite dilution ($\bar{V}_{m,1}^{0,E}$ and $\bar{V}_{m,2}^{0,E}$) for each component in the studied binary mixtures at 298.15 K.	258-258

Contd...

Table	Page No.
9.3. Densities (ρ), viscosities (η), excess molar volumes ($V_{m,123}^E$) and viscosity deviations ($\Delta\eta_{123}$) for the ternary mixtures studied at $T = (298.15 \text{ to } 318.15) \text{ K}$.	260-268
9.4. Coefficients (c_i) of the Cibulka equation for different excess or deviation properties of the ternary mixtures at 298.15 K.	269-269
9.5. Maxima and minima of the ternary contributions to different excess or deviation properties of the ternary mixtures at 298.15 K	272-273
9.6. Ultrasonic speeds (u), isentropic compressibility (κ_S), excess isentropic compressibility (κ_S^E), refractive indices (n_D), molar refractions (R_m) and excess molar refractions (R_m^E) for the binary mixtures at 298.15 K.	280-280
9.7. Ultrasonic speeds (u), isentropic compressibility (κ_S), excess isentropic compressibility (κ_S^E), refractive indices (n_D), molar refractions (R_m) and excess molar refractions (R_m^E) for the ternary mixtures at 298.15 K.	285-287
9.8. Standard deviations between the experimental and calculated excess or deviation properties for the ternary mixtures derived from different semi-empirical equations at 298.15 K.	291-293
10.1. Densities (ρ), viscosities (η), excess molar volumes (V_m^E) and viscosity deviations ($\Delta\eta$) for the quaternary mixtures studied at $T = (298.15 \text{ to } 318.15) \text{ K}$.	298-300
10.2. Coefficients (c_i) of the Cibulka equation for different excess or deviation properties of the quaternary mixtures at 298.15 K.	302-302
10.3 Ultrasonic speeds (u), isentropic compressibility (κ_S) and excess isentropic compressibility (κ_S^E) for the quaternary mixtures at 298.15 K.	305-305
10.4. Refractive indices (n_D), molar refractions (R_m) and excess molar refractions (R_m^E) for the quaternary mixtures at 298.15 K	308-308
10.5. Standard deviations (σ) between the experimental and calculated excess or deviation properties for the quaternary mixtures derived from Köhler and Jacob-Fitzner model at 298.15 K.	310-310

LIST OF FIGURES

Figure	Page No.
1.1. A schematic representation of solvation shell.	5
1.2. Stepwise process involving the endothermic separation of solute and solvent species (Steps 1 and 2) and exothermic solvation of a solute in a solvent (Step 3).	6
1.3. Schematic representation of preferential solvation, A: mixture of solvent 1 and solvent 2 in 1:1 composition; B: ideal solvation of the solute; C: preferential solvation of the solute by solvent 1.	7
1.4. Schematic model for the selective solvation of ions by one component of a binary 1:1 mixture of the solvents A and B: (I), Homoselective solvation; (II), heteroselective solvation.	7
2.1. Dipole-dipole interactions: (a), head to tail orientation; (b), lateral orientation.	30
2.2. Induced dipole interaction.	31
2.3. Induced dipole-induced dipole interaction.	32
2.4. Inter molecular hydrogen bonding between the water molecules and the hydration of chloride ion through hydrogen bonding.	33
2.5. Intramolecular hydrogen bonds in o-nitrophenol, salicylic acid and salicylaldehyde.	34
2.6. Partial molar volumes of water and ethanol in aqueous ethanol at 20 °C.	38
2.7. Spectrum of acoustics.	44
3.1. Anton Paar densitometer (DMA 4500M).	84
3.2. Main screen view of Anton Paar densitometer.	84
3.3. Filling sample with a syringe.	85
3.4. Drying the measuring cell.	85
3.5. A suspended-level Cannon type Ubbelohde viscometer (capillary viscometer).	87
3.6. Digital electronic analytical balance (Mettler Toledo, AG 285).	87
3.7. Schematic diagram of Abbe-refractometer optical system.	88

Contd...

Figure	Page No.
3.8. A: Abbe-refractometer (Cyberlab, MA01527, USA); B: View of the refractometer through the eyepiece.	89
3.9. Ultrasonic interferometer (F-05, Mittal Enterprises, New Delhi, India).	91
3.10. (A) Cross-section of the measuring cell of a multi-frequency ultrasonic interferometer and (B) position of reflector vs. crystal current.	92
3.11. Perkin–Elmer FT-IR spectrophotometer (Spectrum RX-1).	93
3.12. Appearance of a Liquid Cell.	94
3.13. Hierarchy of combination of different solvent mixtures.	94
4.1. Excess molar volume (V_m^E) versus mole fraction of DMF (x_1) for binary mixtures of DMF + cyclic ethers: A, at $T = 298.15$ K; B, at $T = 308.15$ K; C, at $T = 318.15$ K.	104
4.2. Excess partial molar volumes ($\bar{V}_{m,i}^E$) for the i^{th} component against mole fraction of DMF (x_1) for binary mixtures of DMF + cyclic ethers: A, at $T = 298.15$ K; B, at $T = 308.15$ K; C, at $T = 318.15$ K.	107
4.3. Comparison between experimental excess molar volumes and those obtained from Prigogine-Flory-Patterson theory as a function of mole fraction of DMF (x_1) for binary mixtures of DMF + cyclic ethers at $T = 298.15$ K.	111
4.4. Viscosity deviations ($\Delta\eta$) versus mole fraction of DMF (x_1) for binary mixtures of DMF + cyclic ethers: A, at $T = 298.15$ K; B, at $T = 308.15$ K; C, at $T = 318.15$ K.	113
4.5. Excess isentropic compressibility (κ_S^E) versus mole fraction of DMF (x_1) for binary mixtures of DMF + cyclic ethers at $T = 298.15$ K.	118
4.6. MRSD% values for theoretical prediction of ultrasonic speeds by different theories and empirical relations for binary mixtures of DMF + cyclic ethers at $T = 298.15$ K.	120
5.1. Excess molar volume (V_m^E) versus mole fraction of 2-EH (x_1) for the binary mixtures of 2-EH + 1,2-disubstituted ethanes at $T = 298.15$ K.	129
5.2. Excess partial molar volume ($\bar{V}_{m,i}^E$) against mole fraction of 2-EH (x_1) for the binary mixtures of 2-EH + 1,2-disubstituted ethanes at $T = 298.15$ K.	133

Contd...

Figure	Page No.
5.3. A comparison between the excess molar volumes (V_m^E) against mole fraction of 2-EH (x_1) for the binary mixtures of 2-EH + 1,2-disubstituted ethanes at $T = 298.15$ K.	136
5.4. Viscosity deviation ($\Delta\eta$) versus mole fraction of 2-EH (x_1) for the binary mixtures of 2-EH + 1,2-disubstituted ethanes at $T = 298.15$ K.	138
5.5. Excess free energy of activation of viscous flow (ΔG^{*E}) versus mole fraction of 2-EH (x_1) for the binary mixtures of 2-EH + 1,2-disubstituted ethanes at $T = 298.15$ K.	141
5.6. A comparison between the viscosities (η) against mole fraction of 2-EH (x_1) for the binary mixtures of 2-EH + 1,2-disubstituted ethanes at $T = 298.15$ K.	143
5.7. Excess isentropic compressibility (κ_s^E) versus mole fraction of 2-EH (x_1) for the binary mixtures of 2-EH + 1,2-disubstituted ethanes at $T = 298.15$ K.	147
5.8. Excess intermolecular free length (L_t^E) and excess acoustic impedances (z_{im}^E) versus mole fraction of 2-EH (x_1) for the binary mixtures of 2-EH + 1,2-disubstituted ethanes at $T = 298.15$ K.	147
5.9. Percent standard deviations ($\sigma\%$) for theoretical prediction of ultrasonic speeds by different empirical relations at $T = 298.15$ K for the binary mixtures.	150
5.10. FTIR spectra of the various binary mixtures of (2-EH + DCE): A, pure 2-EH ($x_{DCE} = 0.00$); B, ($x_{DCE} = 0.20$); C, ($x_{DCE} = 0.40$); D, ($x_{DCE} = 0.60$); E, ($x_{DCE} = 0.80$); F, Pure DCE ($x_{DCE} = 1.00$).	153
5.11. FTIR spectra of the various binary mixtures of (2-EH + EDA): A, pure 2-EH ($x_{EDA} = 0.00$); B, $x_{EDA} = 0.20$; C, $x_{EDA} = 0.40$; D, $x_{EDA} = 0.60$; E, $x_{EDA} = 0.80$; F, Pure EDA ($x_{EDA} = 1.00$).	153
5.12. FTIR spectra of the various binary mixtures of (2-EH + MEA): A, pure 2-EH ($x_{MEA} = 0.00$); B, $x_{MEA} = 0.20$; C, $x_{MEA} = 0.40$; D, $x_{MEA} = 0.60$; E, $x_{MEA} = 0.80$; F, Pure MEA ($x_{MEA} = 1.00$).	154
6.1. Excess molar volume (V_m^E) versus mole fraction of 1,4-DO (x_1) for the binary mixtures of 1,4-DO + 1,2-disubstituted ethanes at $T = 298.15$ K.	164
6.2. Excess partial molar volume ($\bar{V}_{m,i}^E$) against mole fraction of 1,4-DO (x_1) for the binary mixtures of 1,4-DO + 1,2-disubstituted ethanes at $T = 298.15$ K.	167

Contd...

Figure	Page No.
6.3. A comparison between the excess molar volumes (V_m^E) against mole fraction of 1,4-DO (x_1) for the binary mixtures of 1,4-DO + 1,2-disubstituted ethanes at $T = 298.15$ K.	171
6.4. Viscosity deviation ($\Delta\eta$) versus mole fraction of 1,4-DO (x_1) for the binary mixtures of 1,4-DO + 1,2-disubstituted ethanes at $T = 298.15$ K.	172
6.5. A comparison between the viscosities (η) against mole fraction of 1,4-DO (x_1) for the binary mixtures of 1,4-DO + 1,2-disubstituted ethanes at $T = 298.15$ K.	177
6.6. Excess isentropic compressibility (κ_S^E) versus mole fraction of 1,4-DO (x_1) for the binary mixtures of 1,4-DO + 1,2-disubstituted ethanes at $T = 298.15$ K.	180
6.7. Excess intermolecular free length (L_f^E) and excess acoustic impedances (z_{im}^E) versus mole fraction of 1,4-DO (x_1) for the binary mixtures of 1,4-DO + 1,2-disubstituted ethanes at $T = 298.15$ K.	182
6.8. FTIR spectra of the various binary mixtures of (1,4-DO + DCE): A, pure 1,4-DO ($x_{DCE} = 0.0000$); B, $x_{DCE} = 0.1820$; C, $x_{DCE} = 0.3725$; D, $x_{DCE} = 0.5718$; E, $x_{DCE} = 0.7807$; F, Pure DCE ($x_{DCE} = 1.0000$).	185
6.9. FTIR spectra of the various binary mixtures of (1,4-DO + EDA): A, pure 1,4-DO ($x_{EDA} = 0.0000$); B, $x_{EDA} = 0.2682$; C, $x_{EDA} = 0.4943$; D, $x_{EDA} = 0.6874$; E, $x_{EDA} = 0.8543$; F, Pure EDA ($x_{EDA} = 1.0000$).	185
6.10. FTIR spectra of the various binary mixtures of (1,4-DO + MEA): A, pure 1,4-DO ($x_{MEA} = 0.0000$); B, $x_{MEA} = 0.2651$; C, $x_{MEA} = 0.4902$; D, $x_{MEA} = 0.6839$; E, $x_{MEA} = 0.8523$; F, Pure MEA ($x_{MEA} = 1.0000$).	186
7.1. Excess molar volume (V_m^E) versus mole fraction of CH (x_1) for the binary mixtures of CH + some esters at $T = 298.15$ K.	195
7.2. Excess partial molar volume ($\bar{V}_{m,i}^E$) against mole fraction of CH (x_1) for the binary mixtures of CH + some esters at $T = 298.15$ K: A, for CH; B, for the esters.	199
7.3. A comparison between the excess molar volumes (V_m^E) against mole fraction of CH (x_1) for the binary mixtures of CH + some esters at $T = 298.15$ K.	203

Contd...

Figure	Page No.
7.4. Viscosity deviation ($\Delta\eta$) versus mole fraction of CH (x_1) for the binary mixtures of CH + some esters at $T = 298.15$ K.	204
7.5. Excess free energy of activation of viscous flow (ΔG^{*E}) versus mole fraction of CH (x_1) for the binary mixtures of CH + some esters at $T = 298.15$	207
7.6. Excess isentropic compressibility (κ_s^E) versus mole fraction of CH (x_1) for the binary mixtures of CH + some esters at $T = 298.15$ K.	212
7.7. Percent standard deviations ($\sigma\%$) for theoretical prediction of ultrasonic speeds by different empirical relations at $T = 298.15$ K for the binary mixtures studied.	213
7.8. Percent standard deviations ($\sigma\%$) for theoretical prediction of refractive indices by various models at $T = 298.15$ K for the binary mixtures studied.	214
7.9. FTIR spectra of the various binary mixtures of CH (1) + MA (2): A, pure CH ($x_2 = 0.00$); B, $x_2 = 0.20$; C, $x_2 = 0.40$; D, $x_2 = 0.60$; E, $x_2 = 0.80$; F, pure MA ($x_2 = 1.00$).	216
7.10. FTIR spectra of the various binary mixtures of CH (1) + EA (2): A, pure CH ($x_2 = 0.00$); B, $x_2 = 0.20$; C, $x_2 = 0.40$; D, $x_2 = 0.60$; E, $x_2 = 0.80$; F, pure EA ($x_2 = 1.00$).	217
7.11. FTIR spectra of the various binary mixtures of CH (1) + MS (2): A, pure CH ($x_2 = 0.00$); B, $x_2 = 0.20$; C, $x_2 = 0.40$; D, $x_2 = 0.60$; E, $x_2 = 0.80$; F, pure MS ($x_2 = 1.00$).	217
8.1. Excess molar volume (V_m^E) versus mole fraction of CHN (x_1) for the binary mixtures of CHN + some esters at $T = 298.15$ K.	227
8.2. Excess partial molar volume ($\bar{V}_{m,i}^E$) for the i^{th} component against mole fraction of CHN (x_1) for the binary mixtures of CHN + some esters at $T = 298.15$ K.	229
8.3. A comparison between the excess molar volumes (V_m^E) against mole fraction of CHN (x_1) for the binary mixtures of CHN (1) + some esters (2) at $T = 298.15$ K.	233
8.4. Viscosity deviations ($\Delta\eta$) versus mole fraction of CHN (x_1) for the binary mixtures of CHN + some esters at $T = 298.15$ K.	234

Contd...

Figure	Page No.
8.5. Excess free energy of activation of viscous flow (ΔG^{*E}) vs. mole fraction of CH (x_1) for the binary mixtures of CHN + some esters at $T = 298.15$ K.	236
8.6. A comparison between the viscosities (η) obtained from various models against mole fraction of CHN (x_1) for the binary mixtures of CHN (1) +: A, MA (2); B, EA (2); MS (2) at $T = 298.15$ K.	239
8.7. Excess isentropic compressibility (κ_S^E) versus mole fraction of CHN (x_1) for the binary mixtures of CH + some esters at $T = 298.15$ K.	242
8.8. Percent standard deviations ($\sigma\%$) for theoretical prediction of ultrasonic speeds by different empirical relations at $T = 298.15$ K for the binary mixtures studied.	243
8.9. Percent standard deviations ($\sigma\%$) for theoretical prediction of refractive indices by various models at $T = 298.15$ K for the binary mixtures studied.	244
8.10. FTIR spectra of the various binary mixtures of CHN (1) + MA (2): A, pure CHN ($x_2 = 0.00$); B, $x_2 = 0.20$; C, $x_2 = 0.40$; D, $x_2 = 0.60$; E, $x_2 = 0.80$; F, pure MA ($x_2 = 1.00$).	246
8.11. FTIR spectra of the various binary mixtures of CHN (1) + EA (2): A, pure CHN ($x_2 = 0.00$); B, $x_2 = 0.20$; C, $x_2 = 0.40$; D, $x_2 = 0.60$; E, $x_2 = 0.80$; F, pure EA ($x_2 = 1.00$).	247
8.12. FTIR spectra of the various binary mixtures of CHN (1) + MS (2): A, pure CHN ($x_2 = 0.00$); B, $x_2 = 0.20$; C, $x_2 = 0.40$; D, $x_2 = 0.60$; E, $x_2 = 0.80$; F, pure MS ($x_2 = 1.00$).	247
9.1. Excess molar volume (V_m^E) versus the mole fractions (x_i) of the first component in all the binary mixtures studied at $T = 298.15$ K.	256
9.2. Excess partial molar volume ($\bar{V}_{m,i}^E$) for the i^{th} component against mole fraction (x_1) of the first component in the studied binary mixtures at $T = 298.15$ K.	258
9.3. Three dimensional mesh plots of excess molar volumes ($V_{m,123}^E$) for the ternary mixtures: A, CH (1) + MA (2) + EA (3); B, CH (1) + MA (2) + MS (3) and C, CH (1) + EA (2) + MS (3) and the corresponding pseudo-two dimensional contour plot of constant $V_{m,123}^E$ values for these mixtures.	270
9.4. Three dimensional mesh plots of excess molar volumes ($V_{m,123}^E$) for the ternary mixtures: A, CHN (1) + MA (2) + EA (3); B, CHN (1) + MA (2) + MS (3) and C, CHN (1) + EA (2) + MS (3) and the corresponding pseudo-two dimensional contour plot of constant $V_{m,123}^E$ values for these mixtures.	271

Contd...

Figure	Page No.
9.5. Three dimensional mesh plots of excess molar volumes ($V_{m,123}^E$) for the ternary mixture MA (1) + EA (2) + MS (3) and the corresponding pseudo-two dimensional contour plot of constant $V_{m,123}^E$ values.	272
9.6. Viscosity deviations ($\Delta\eta$) versus the mole fractions (x_1) of the first component in all the binary mixtures studied at $T = 298.15$ K.	275
9.7. Three dimensional mesh plots of viscosity deviations ($\Delta\eta_{123}$) for the ternary mixtures: A, CH (1) + MA (2) + EA (3); B, CH (1) + MA (2) + MS (3) and C, CH (1) + EA (2) + MS (3) and the corresponding pseudo-two dimensional contour plot of constant $\Delta\eta_{123}$ values for these mixtures.	276
9.8. Three dimensional mesh plots of viscosity deviations ($\Delta\eta_{123}$) for the ternary mixtures: A, CHN (1) + MA (2) + EA (3); B, CHN (1) + MA (2) + MS (3) and C, CHN (1) + EA (2) + MS (3) and the corresponding pseudo-two dimensional contour plot of constant $\Delta\eta_{123}$ values for these mixtures.	277
9.9. Three dimensional mesh plots of viscosity deviations ($\Delta\eta_{123}$) for the ternary mixture MA (1) + EA (2) + MS (3) and the corresponding pseudo-two dimensional contour plot of constant $\Delta\eta_{123}$ values.	278
9.10. Excess isentropic compressibility (κ_s^E) versus the mole fractions (x_1) of the first component in all the binary mixtures studied at $T = 298.15$ K.	281
9.11. Three dimensional mesh plots of isentropic compressibility ($\kappa_{S,123}^E$) for the ternary mixtures: A, CH (1) + MA (2) + EA (3); B, CH (1) + MA (2) + MS (3) and C, CH (1) + EA (2) + MS (3) and the corresponding pseudo-two dimensional contour plot of constant $\kappa_{S,123}^E$ values for these mixtures.	282
9.12. Three dimensional mesh plots of isentropic compressibility ($\kappa_{S,123}^E$) for the ternary mixtures: A, CHN (1) + MA (2) + EA (3); B, CHN (1) + MA (2) + MS (3) and C, CHN (1) + EA (2) + MS (3) and the corresponding pseudo-two dimensional contour plot of constant $\kappa_{S,123}^E$ values for these mixtures.	283
9.13. Three dimensional mesh plots of isentropic compressibility ($\kappa_{S,123}^E$) for the ternary mixture MA (1) + EA (2) + MS (3) and the corresponding pseudo-two dimensional contour plot of constant $\kappa_{S,123}^E$ values.	284

Contd...

Figure	Page No.
<p>9.14. Three dimensional mesh plots of excess molar refractions ($R_{m,123}^E$) for the ternary mixtures: A, CH (1) + MA (2) + EA (3); B, CH (1) + MA (2) + MS (3) and C, CH (1) + EA (2) + MS (3) and the corresponding pseudo-two dimensional contour plot of constant $R_{m,123}^E$ values for these mixtures.</p>	288
<p>9.15. Three dimensional mesh plots of excess molar refractions ($R_{m,123}^E$) for the ternary mixtures: A, CHN (1) + MA (2) + EA (3); B, CHN (1) + MA (2) + MS (3) and C, CHN (1) + EA (2) + MS (3) and the corresponding pseudo-two dimensional contour plot of constant $R_{m,123}^E$ values for these mixtures.</p>	289
<p>9.16. Three dimensional mesh plots of excess molar refractions ($R_{m,123}^E$) for the ternary mixture MA (1) + EA (2) + MS (3) and the corresponding pseudo-two dimensional contour plot of constant $R_{m,123}^E$ values.</p>	290
<p>10.1. Three-dimensional mesh plots of excess molar volumes (V_m^E) for the quaternary mixtures: A, CH (1) + MA (2) + EA (3) + MS (4); B, CHN (1) + MA (2) + EA (3) + MS (4) at 298.15 K.</p>	302
<p>10.2. Three-dimensional mesh plots of viscosity deviations ($\Delta\eta$) for the quaternary mixtures: A, CH (1) + MA (2) + EA (3) + MS (4); B, CHN (1) + MA (2) + EA (3) + MS (4) at 298.15 K.</p>	304
<p>10.3. Three-dimensional mesh plots of excess isentropic compressibility (κ_S^E) for the quaternary mixtures: A, CH (1) + MA (2) + EA (3) + MS (4); B, CHN (1) + MA (2) + EA (3) + MS (4).</p>	307
<p>10.4. Three-dimensional mesh plots of excess molar refractions (R_m^E) for the quaternary mixtures: A, CH (1) + MA (2) + EA (3) + MS (4); B, CHN (1) + MA (2) + EA (3) + MS (4).</p>	309

LIST OF APPENDICES

Appendix	Page No.
I: List of Publications	317-317
II: Participation in Seminar, Symposium & Conventions	318-318

CHAPTER I

Introduction

Industrial revolution both energized and freshly unleashed an increased use of scientifically produced knowledge in industrial productions. Like for any other branch of scientific knowledge, increased knowledge of chemistry as a science and technology appear to be increasingly used by chemical industry for the production of consumables and allied products. Ever-growing demand of newer chemicals, their synthesis and their hitherto unknown effects came to be emphatically observed in biophysical processes both in the natural world and in the human body. Until quite recently the adverse effects of such newer chemicals and their concentrations remained unnoticed and the chemical industries in this regard remained in a state of inertia. However, with the emergent public criticisms through media and political debates on such impacts of newly discovered or synthesized chemicals and their concentrates and more particularly the solvents with multiple uses and high volume productions, the chemical industry began to respond to such impacts in line with the standards set for environmental protection and public health and safety by regimes at multiple levels both locally and globally. The utilities of such solvents and chemicals and their syntheses in the broader human welfare require differentiation of such solvents, identification of their fundamental properties and the prior understanding of their risks and utilities. Therefore, the proper selection of suitable solvents becomes necessary and for this the knowledge of solution properties is very essential. Especially the thermodynamic and transport properties are required to make proper selection of these solvents. Naturally it is seen that matter exists in a state of mixtures in an overwhelming manner and hence the possibility of existence of pure substances is a rarity. Liquid-liquid mixtures uniquely exhibit such unusual behavior bereft of pure substances, thereby attracting the attention of scientists and scholars to undertake studies on liquid and liquid mixtures. Thus the physico-chemical behavior and the nature of the molecular interactions in the multi-component liquid mixtures has been a major subject of interest from the point of view of their applications in many branches of science such as pharmaceutical industries, polymer industries, cosmetic industries, molecular biology, *etc.* The non-aqueous systems have been of immense importance

General Introduction

to the technologist and theoretician as many chemical processes occur in these systems.^{1,2}

The classification of different organic solvents are based on the types of organic groups, donor-acceptor properties,^{3,4} hydrogen bonding,⁵ hard and soft acid base properties,⁶ and dielectric constants, *etc.* As a result the different solvent shows a wide divergence in properties that ultimately influence their thermodynamic, transport, acoustic and optical properties, especially when they are mixed to give a homogeneous mixture. The study of such properties in solvent mixtures (binary/ternary/quaternary) would thus provide important information for understanding solvent-solvent interactions. Knowledge of the nature of intermolecular interactions amongst the mixed components can be had from rheological⁷ and thermodynamic study of physico-chemical properties of solvent-solvent systems.^{8,9} That's why various experimental data on thermodynamic, acoustic, transport and optical properties of pure liquid and liquid mixtures are of significant importance to understand the intermolecular forces and in testing the theories which attempt to estimate the mixture properties. The prediction of the properties of a multi-component (binary/ternary/quaternary) liquid mixtures can be made either from pure component properties as developed by Eyring,¹⁰ Flory *et al.*,¹¹⁻¹⁷ or from the properties of their contributing binary systems as advanced by Bertrand *et al.*,^{18,19} The theoretical as well as experimental estimation of the different parameters such as density, viscosity, ultrasonic speed and refractive indices of the pure components and their mixtures have been extensively used both as qualitatively and quantitatively to predict the changes in the volume, viscosity, speed of sound, *etc.*, and the extent of complex formation when different organic solvents are mixed. Such changes in the properties of the mixed solvents arise as a result of several contributions like combinational, energetic, molecular orientation, free volume, steric hindrance, *etc.* If the polar components are involved the additional contribution like hydrogen bonding, dipole-induced dipole, disruption of molecular order due to dipole-dipole interactions come into play. The interstitial accommodation due to different size and large difference in molar volume also leads to such changes. The interpretation of such properties has been made with the introduction of several solution theories of liquid and liquid mixtures of non-electrolytic components. Prigogine and co-workers²⁰⁻²³ employed the cell model of liquid state put forward by Eyring *et al.*^{10,24,25} in correlating the

General Introduction

thermodynamic properties of liquid mixtures with intermolecular energy parameters. They assumed random mixing of the components and showed that the thermodynamic excess functions are affected only to a small extent when the molecules are of same size. Prigogine and Bellemans²⁶ extended this theory to liquid mixtures assuming the cells of two sizes exist in liquid mixtures. This model failed to predict the correct values of the thermodynamic functions for any liquid. As a result of this, a number of theories have been developed based on the theorem of corresponding states.²⁷ Like the cell model theory, Flory and co-workers^{14-17,28,29} developed a theory that relates the thermodynamic excess properties of liquid mixtures to measurable macroscopic properties of the pure components. Patterson and Delmas^{30,31} analysed the theory proposed by Prigogine and Flory and found that Flory theory was superior to those originally proposed by Prigogine and collaborator²⁰⁻²³ using their average potential cell model. In more general form, the Prigogine-Flory-Patterson (PFP) theory has been successfully employed to binary liquid mixtures to estimate the combinational contribution, free volume contribution, interaction contribution and the various thermodynamic properties of the binary mixtures. This theory has also been applied to calculate surface tension,³²⁻³⁵ ultrasonic speeds of sound³²⁻³⁹ and viscosities⁴⁰⁻⁴³ of the liquid mixtures satisfactorily.

1.1. Solvent Effects

Most of the chemical and biological processes occur in solution phase. The role of solvation in chemistry and biology is obvious. The influence of the solvent on chemical phenomena has received the attention of researchers from both experimental and theoretical fields related to chemistry. A solvent can influence the interaction of the local environment with the individual species undergoing the reactions and thus also influences the outcome of a chemical reaction. The solvent, on one level, provides an energy path for the stabilization of energetic products formed during reactions and also provides physical barriers to the motion of the reactive species. On a more subtle level, the solvent perturbs the potential energy curves that govern these reactions.⁴⁴ Since the solvent species around a solute form a structure that determines the outcome of chemical and/or biological events, the solvent species are not just “spectator” species rather they are part of the chemical or biochemical process. Solvation has been proved to be of fundamental importance in diverse areas like biological activities and atmospheric processes.⁴⁵ Solvated ions appear in high

General Introduction

concentrations in living organisms where their presence or absence can fundamentally alter the functions of life. Ions solvated in organic solvents or mixtures of water and organic solvents are also very common⁴⁶ and the exchange of solvent molecules around ions in solutions is fundamental in understanding the reactivity of ions in solution.⁴⁷ Solvated ions also play a key role in electrochemical applications simply because the conductivity of electrolytes depend on the ion-solvent interactions.⁴⁸ Majority of the chemical reactions are usually performed in solutions and solvents can influence reactions in a number of ways. Solvents may be used as a reaction medium to bring reactants together, as a reactant to react with a solute to make it soluble and as a carrier to deliver chemical compounds in solutions to their point of use in the required amounts.

Solvents also control the temperature in exothermic and endothermic reactions. In endothermic reactions, heat could be supplied through a heated inert solvent having a high heat capacity while in exothermic reactions, the surplus heat can be removed by allowing the solvent to boil or absorb heat. If reactions involve solid reactants, solvents could be used to create a homogenous reaction phase (*i.e.*, solution) through which the solid reactants can be brought into contact. It is important to select the most appropriate solvent so as to get most effective results or optimum yield of the products. A good solvent should be able to meet all the necessary standards such as it should be an inert to all the reaction conditions, the boiling point of the solvent should be appropriate, at the end of the reaction there should not be any difficulty in its removal and it should dissolve the reagents and reactants. In essence, the reaction rates are influenced by differential solvation of the starting material and the transition state by the solvent. When the molecules of the reactant start moving towards the transition state, the molecules of the solvent orient themselves and render the transition state stable. Greater the extent of stability of the transition state compared to the starting material, faster the reaction proceeds and vice-versa. However, in practice a differential solvation is realized if the solvent undergoes rapid relaxation or re-orientation to the ground state orientation from the transition state orientation. So reactions involving weakly dipolar solvents that are rapidly relaxing with a tendency for having sharp barriers exhibit equilibrium solvent effects.

General Introduction

1.1.1. Solvation

Solvation is basically the process of association through interactions of the solvent molecules with the solute molecules or ions. A solvated complex is formed when the solute molecules or ions dissolve in a solvent, spread out and become surrounded by the molecules of the solvent. Alternatively solvation refers to surrounding of the solute molecules or ions by solvent molecules. The region around a solute, up to which the solvent molecules are reoriented due to the force created by the solute, is known as solvation shell or cybotactic region. Figure 1.1 shows a typical solvation shell and how the solvent molecules orient themselves to form the solvation shell. Three types of intermolecular attractive forces are relevant to the solvation process: solute-solute, solvent-solvent, and solute-solvent. As illustrated in Figure 1.2, the process of solvation may be viewed as a stepwise process in which energy is consumed to overcome solute-solute and solvent-solvent attractions (endothermic processes) and released when solute-solvent attractions are established (an exothermic process referred to as solvation). The relative magnitudes of the energy changes associated with these stepwise processes determine whether the overall dissolution process will release or absorb energy.

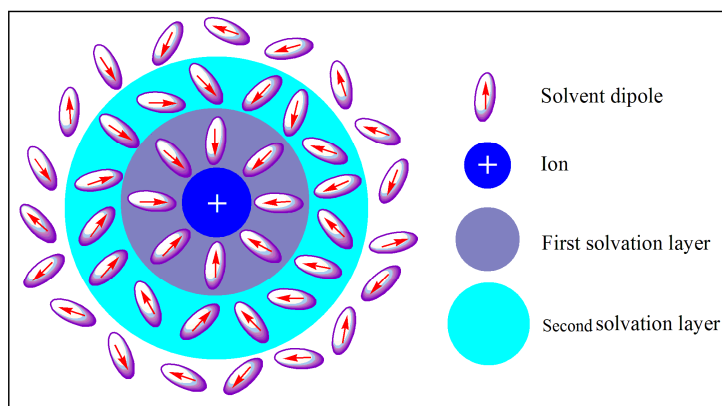


Fig 1.1. A schematic representation of solvation shell

For solvation to occur, energy is required to release individual ions or molecules from the lattice in which they are present. This is necessary to break the attractions that the ions have with each other and is equal to the lattice free energy. The energy released in the process of solvation is called the free energy of solvation. If the liberated solvation energy is lower than the lattice energy, the overall dissolution process is endothermic and if the solvation energy is higher than the lattice energy, the overall

General Introduction

process is exothermic. For the spontaneity of the dissolving process the dissolution process should be endothermic.

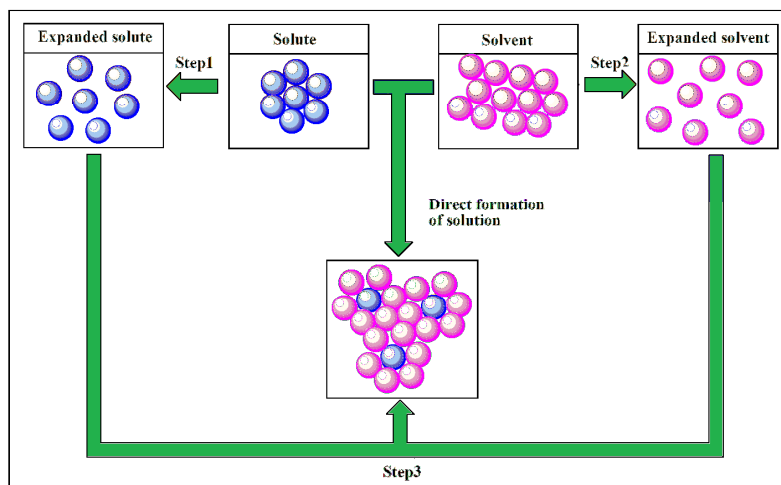


Fig. 1.2. Stepwise process involving the endothermic separation of solute and solvent species (Steps 1 and 2) and exothermic solvation of a solute in a solvent (Step 3).

1.1.2. Preferential Solvation

In the mixtures containing two or more solvents the solvation process is more complicated as compared to pure solvent. It is observed that an increase in the number of component molecules in the mixture increases the number of the solute-solvent interactions. Besides the intermolecular interactions between the solute-solvent molecules in the mixtures, the interactions amongst the unlike solvent molecules play a vital role leading to a large departure from ideal behaviour as expected from the Raoult's law of depression of vapour pressure. In order to understand how the solvent composition affects the solute behavior, we need to know the composition that the solute has in its immediate vicinity different from the bulk composition of the mixed solvent. The solute is surrounded preferably by the component of the mixture, which leads to more negative Gibb's free energy of solvation. The observation that the solvent shell has a composition other than the macroscopic ratio is termed as selective solvation or preferential solvation.⁴⁹ If one of the solvent of the mixture is practically excluded from the solvation shell of the solute then it is regarded as selective solvation. This phenomenon is represented in Figure 1.3.

General Introduction

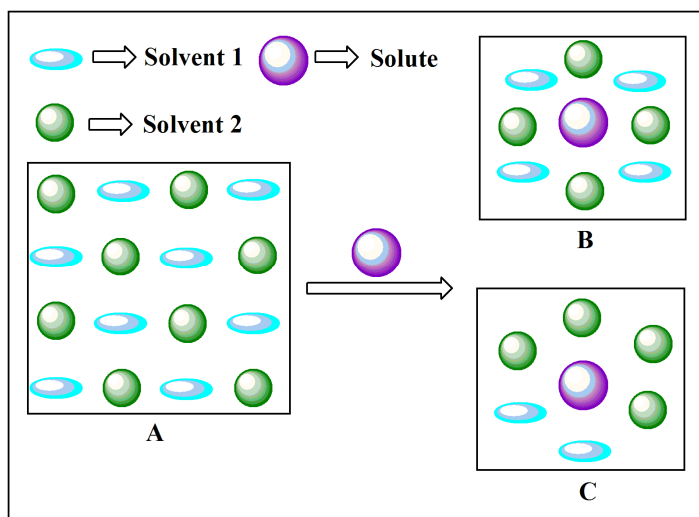


Fig. 1.3. Schematic representation of preferential solvation, A: mixture of solvent 1 and solvent 2 in 1:1 composition; B: ideal solvation of the solute; C: preferential solvation of the solute by solvent 1.

These terms are generally used to describe the molecular microscopic local solute-induced inhomogeneity in a multi-component solvent mixture. They include both (i) non-specific solute/solvent association caused by dielectric enrichment in the solvent shell of solute, ions or dipolar solute molecules and (ii) specific solute/solvent association such as hydrogen-bonding or electron pair donor/electron pair acceptor interactions.

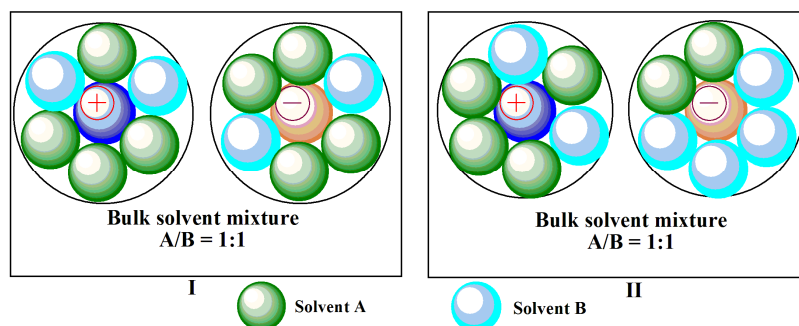


Fig. 1.4. Schematic model for the selective solvation of ions by one component of a binary 1:1 mixture of the solvents A and B: (I), Homoselective solvation; (II), heteroselective solvation.

Homoselective solvation occurs when both the ions of a dissolved molecule or salt are solvated preferentially by the same solvent in a mixture of two solvents and heteroselective solvation occurs when the preferential solvation of the cation by one, and the anion by the other solvent (Figure 1.4).

General Introduction

1.2. Importance and Scope of the Physico-Chemical Parameters

Density and viscosity of liquid mixtures are indispensable physical parameters, required in most engineering calculations where fluid flow of mixture is an important factor and are essential in the design processes involving chemical separations, equipment design, heat transfer, fluid flow and molecular dynamics, *etc.* The knowledge of the dependence of these parameters on composition is of great interest from a theoretical stand point, since it may lead to better understanding of the fundamental behavior; for instance the molecular interactions among the components of the liquid mixture. Such behavior and their change with composition and temperature are generally studied by estimating the different physico-chemical and thermodynamic properties. Among the different thermodynamic parameters the excess or deviation parameters gives better understanding of the molecular interactions. The density and the related volumetric properties such as excess molar volume and apparent molar volume are of great importance in characterizing such behavior and structural aspects of solutions. Though viscosity is not a thermodynamic parameter but still is of great importance in many chemical disciplines and commercial applications. The deviation in viscosity provides a proper understanding of molecular motions and interaction patterns in non-electrolytic solvent mixtures involving both hydrogen bonding and non-hydrogen bonding solvents.^{50,51} The other thermodynamic parameters such as excess free energy of activation of viscous flow, excess enthalpy and excess entropy can also be evaluated using experimental density and viscosity. These excess parameters are also important in estimating the molecular interactions in the liquid mixtures of variable compositions and temperature. The sign and magnitude of these excess parameters imparts estimate of strength of unlike interactions in the binary, ternary, *etc.*, solvent systems.

The experimental viscosity data are valuable for testing the different theories and empirical relations such as Grunberg and Nissan,⁵² Hind *et al.*,⁵³ Heric-Brewer,⁵⁴ Katti and Chaudhri⁵⁵ and McAllister,⁵⁶ *etc.*, for liquid mixtures. Apart from these, viscosity models based on Eyring theory coupled with Peng-Robinson cubic equation of state for non-ideal liquid mixtures⁵⁷ and Bloomfield-Dewan model,⁵⁸ a relation between viscosity and thermodynamic properties of mixing on the basis of absolute reaction rate are used to correlate and estimate the viscosities of non-ideal liquid mixtures under experimental temperature with different compositions.

General Introduction

Amongst the different methods used, ultrasonic method is found to be sensitive and reliable; thus this method has been used by many researchers to explain the molecular interactions in pure liquids as well as in liquid mixtures. Prior to the application of ultrasonic methods to mixtures/solutions, the spectroscopic, dielectric techniques, excess molar volume and viscosity deviations, *etc.*, were only the tool to study the nature and strength of molecular interactions. However, the application of ultrasonic methods has made possible not only the evaluation of physico-chemical properties of the mixtures/solutions but also more reliability on the interpretation of molecular interactions. Therefore, in the present study the experimental speed of sound and density data are used to evaluate acoustic and thermodynamic parameters such as isentropic compressibility, intermolecular free length, specific acoustic impedance, free volume and internal pressure. These parameters are found to be very sensitive to molecular interactions⁵⁹⁻⁶² but the excess properties of these parameters provide better understanding of the nature and strength of molecular interactions and are sensitive to molecular forces as well as the size of the molecules.⁶³ Furthermore, the density and ultrasonic sound speed are valuable tools to develop new theoretical models and learn about the liquid state.⁶⁴ It is observed that a number of workers have extensively applied various empirical and semi-empirical theories to study the ultrasonic speeds in binary and ternary mixtures. Among them the commonly used theories are Nomoto relation (NOM),⁶⁵ Schaaff's collision factor theory (CFT),^{66,67} Impedance dependence relation (IDR),⁶⁸ Vandael Vangeal Ideal mixture relation (IMR),⁶⁹ Jacobson's Free Length Theory (FLT),^{70,71} Junjie's equation (JUN)⁷² and Flory's theory,¹⁴ *etc.* Theoretical evaluation of ultrasonic speed in binary liquid mixtures and its correlation to study the molecular interaction has been successfully performed in recent years⁷³⁻⁸² using the above theoretical relations. The refractive index is one of the important physical properties of liquid and liquid mixtures and is being increasingly used as a tool⁸³⁻⁸⁷ for the investigation of the nature of intermolecular interaction between the liquid mixture constituents. Knowledge of refractive index of multi-component mixtures provides information regarding the interactions in these mixtures.⁸⁸⁻⁹⁰ Pandey *et al.*⁹¹ have made refractive index measurements in liquid mixtures and have suggested that such studies are very much helpful for understanding the molecular interactions in the components of the mixture. Refractive indices can also be used to estimate the different elastic properties of the molecule from which the type of

General Introduction

molecular interactions can be very well understood.⁹² In addition to binary liquid mixtures, a few ternary^{93,94} and quaternary mixtures⁹⁵ have also been studied employing refractive index measurements. Prediction of refractive index of multi-component liquid mixtures theoretically is essential for many physico-chemical calculations that include correlation of refractive index with density.⁹⁶⁻⁹⁸ A number of empirical/semi-empirical mixing rules and models has been suggested by different researchers to correlate the experimental refractive index of the liquid mixtures. Some of the common mixing rules used are Lorentz-Lorentz relation,^{99,100} Gladstone-Dale,¹⁰¹ Arago-Biot,¹⁰² Weiner model,¹⁰³ Eyring-John,¹⁰⁴ Heller,¹⁰⁵ Eykman,¹⁰⁶ and Newton,¹⁰⁷ *etc.*

1.3. Objective and Application of the Research work

The study of physico-chemical properties involving excess or deviation properties as well as the other derived thermodynamic parameters play an important role in understanding the structure and many molecular interactions amongst the molecules of the components in liquid mixture. These properties can provide a precise knowledge about the behavior of the molecules on mixing. It is also seen that the results of one experimental technique often contradicts the results obtained from some other technique; therefore attempts has been made using more than one technique to establish the nature and strength of molecular interactions. With this approach the precise correlation between the microscopic structure and macroscopic properties can be establish. In the present thesis, emphasis has been laid mainly on the measurements of four physical properties, *viz.*, density, viscosity, speed of sound and refractive index of the liquid mixtures (binary, ternary and quaternary) containing: (i) cyclohexane and cyclohexanone with some esters like methyl acetate, ethyl acetate and methyl salicylate, (ii) 1,4-dioxane and 2-ethyl-1-hexanol with ethylenediamine, 1,2-dichloroethane and monoethanolamine at varying temperatures covering the entire composition range. These solvents have drawn much attention of the scientists due to their varied industrial applications.¹⁰⁸⁻¹¹⁸ Therefore the main objectives of the present dissertation are:

- i) to study the molecular interactions through various physico-chemical and derived parameters like excess or deviation properties (such as excess molar volumes and viscosity deviation, *etc.*) in various selected solvent systems.

General Introduction

- ii) to enrich the physico-chemical database of properties of the components and their mixtures (binary, ternary and quaternary liquid mixtures).
- iii) To employ experimental or derived data to critically test some of the empirical and semi-empirical models (involving volume, viscosity, ultrasonic speed and refractive index) and compare their predictive capabilities.

So, a number of parameters such as excess molar volume, partial molar volume, viscosity deviation, isentropic compressibility, excess isentropic compressibility, intermolecular free length, acoustic impedance, free volume, internal pressure and molar refraction, *etc.*, were derived using measured experimental (density, viscosity, ultrasonic speed and refractive index) data for each set of liquid mixtures. The above mentioned parameters, particularly the excess or deviation functions, were found to be very sensitive to the intermolecular interactions between the unlike components of a mixture. Again the model approach has several immediate advantages. The empirical and semi-empirical models often help in understanding these interactions in terms of individual component properties as well as offer a visual picture and hence provide a physical explanation for a variety of phenomenon operating in liquids and liquid mixtures. In this context Peng-Robinson equation of states, Flory and Proggone-Flory-Patterson theories were applied to analyse the excess molar volumes (V_m^E). The viscosity data were correlated with models like Grunberg and Nissan, Hind, Heric-Brewer, Katti and Chaudhri and McAllister, *etc.*, for liquid mixtures. Apart from these, a viscosity model based on Eyring theory coupled with Peng-Robinson cubic equation of state for non-ideal liquid mixtures and Bloomfield-Dewan model were tested. The experimental speeds of sound have been analysed in terms of Nomoto relation, Schaaff's collision factor theory, Impedance dependence relation, Vandael Vangeal Ideal mixture relation, Jacobson's Free Length Theory, Junjie's equation and Flory's theory, *etc.* The experimental refractive indices and molar refractions were correlated in terms of various mixing rules, *viz.*, Lorentz-Lorenz, Gladstone-Dale, Arago-Biot, Eykman, Wiener and Heller relations, *etc.* Relative merits of these mixing rules have been discussed in terms of standard deviation or root mean square percent deviations (RMSD%). The nature of molecular interactions observed in

General Introduction

different solvent systems also corroborated with structural changes and substantiated by the infrared spectroscopic study¹¹⁹ of the respective solvent systems.

1.4. Importance of Solvents and Solvent Mixtures Studied

1,4-dioxane, 2-ethyl-1-hexanol, 1,2-disubstituted ethanes (*viz.*, ethylenediamine, 1,2-dichloroethane, monoethanolamine), cyclohexane, cyclohexanone and some alkyl acetates (*viz.*, methyl acetate, ethyl acetate and methyl salicylate) were chosen as the subject liquids in the works embodied in this dissertation. The study of these solvents and their mixtures is of immense interest because of their wide application as solvents and solubilizing agents in many industries like pharmaceutical, cosmetics, *etc.* 1,4-dioxane is very hygroscopic and miscible in all proportions with water. It is a non-polar, aprotic, non-hydrogen bonded cyclic diether and finds numerous applications in organic syntheses and industrial processes as a solvent for saturated and unsaturated hydrocarbons¹²⁰ as well as in the high-energy battery technology.¹²¹ Ethylenediamine is a strongly basic colorless liquid with ammonia like odour and reacts readily with moisture in humid air to produce a corrosive, toxic and irritating mist. It is an important raw material for the production of polymers, pharmaceuticals, pesticides, herbicides and dye fixing agent. It is widely used as bleach activators, chelating agents, corrosion inhibitors, elastomeric fibers, plastic lubricants, polyamide resins, rubber processing additives, lube oil and fuel additives. 1,2-dichloroethane, commonly known as ethylene dichloride, is a colourless liquid with chloroform like odour. It is a σ -acceptor and is used as a solvent, degreaser, as a precursor for the synthesis of other chemical agents. It is also used in the production of vinyl chloride which is used to make a variety of plastic and vinyl products including polyvinyl chloride (PVC) pipes, furniture and automobile upholstery, wall coverings, house wares, and automobile parts, *etc.*¹²² Its other uses include: as a solvent for resins and fats, photography, photocopying, cosmetics, drugs and as a fumigant for grains and orchards. Monoethanolamine is a colourless, viscous liquid with an odour reminiscent to that of ammonia and is a compound containing both primary amine and a primary alcohol. It is used in cement to enhance strength, reduce drying time and protect against the affects of freezing and thawing; metal working fluids to neutralize acid components in lubricants, prevent corrosion, rusting and biocides; in personal care products to make ethanolamine based

General Introduction

soaps for use in hand lotions, cosmetic creams, cleansing creams, shaving creams, and shampoos; also for dry-cleaning solvents and heavy-duty liquid laundry detergents, in printing inks to control the pH; also used in the purification of petroleum, as a remover of H₂S and CO₂ from refinery and natural gas streams and as an ingredient in paints and pharmaceuticals.¹²³ 2-ethyl-1-hexanol is a colourless branched chiral alcohol. It is poorly soluble in water but soluble in most organic solvents. It is produced in bulk for use in multiple applications, say for instance, as solvents, as flavors and fragrances. It is also used as a precursor for the production of other chemicals like the plasticizers and emollients. It is encountered in natural plant fragrances and the odour has been reported as "heavy earthy and slightly floral" for the R-enantiomer and "light sweet floral fragrance" for the S-enantiomer.¹²⁴ Its main application is as a feedstock in the manufacture of low-volatility esters, the most important of which is di-(2-ethylhexyl) phthalate, an all purpose plasticizer for PVC and vinyl chloride copolymers. Cyclohexane is a cycloparaffinic non-polar, unassociated, inert hydrocarbon with globular structure¹²⁵ with petroleum like odour. It is used in industrial adhesive formulations in particular non-toluene formulation. Nearly all the cyclohexane is consumed in the production of cyclohexanol and cyclohexanone which are then used as a raw material for the industrial production of two important intermediates (*viz.*, adipic acid and caprolactam)¹¹⁸ used in the production of intermediates for nylon, which has a variety of common applications such as clothing, tents, carpets as well as thermoplastics. Other use of cyclohexane includes various solvent applications and recently has been substituted for benzene in many applications. Cyclohexanone is a colourless oily liquid with acetone like odour and consists of six carbon cyclic structure as well as a ketone functional group. Over time, the liquid may assume yellow colour due to oxidation. It is slightly soluble in water and miscible with common organic solvents. It is used in organic synthesis, particularly in the production of adipic acid and caprolactam, polyvinyl chloride and its copolymers, methacrylate ester polymers, cyclohexanone resins, cyclohexanone oxime, caprolactam and nylon.¹¹⁸ Additional uses include paint and varnish removers, spot remover, degreasing of metals, polishes, levelling agents, dyeing and delustering silk, lubricating oil additives, solvent for herbicides, natural and synthetic resins, waxes, fats, insecticides, *etc.* Esters exist as a dipolar associates in their pure state.¹²⁶ Methyl acetate, also known as methyl ethanoate, is a

General Introduction

carboxylate ester. It is a flammable liquid with a characteristically pleasant smell reminiscent of some glues and nail polish removers. Ethyl acetate, also known as ethyl ethanoate, is a colorless liquid with a characteristic sweet smell. Both the aliphatic esters methyl acetate and ethyl acetate are commonly used as solvents in glues, nail polish remover, *etc.* Methyl acetate is also used as a solvent for polyurethane coatings and adhesives, blowing agent for polyurethane and other foams intermediates, as paint strippers, fuel system cleaners and additives, battery electrolytes, polymerization solvents, cleaners for electronics and precision parts, *etc.* Ethyl acetate is used to decaffeinate coffee beans and tea leaves also used in paints as an activator or hardener, as a solvent and diluent. Methyl salicylate, also known as oil of wintergreen, is a phenolic ester having strong intramolecular hydrogen bond between its hydroxyl and carbonyl group.¹²⁷ It is naturally produced by many species of plants, particularly wintergreens. It is also synthetically produced and used as a fragrance, in foods and beverages and in liniments. This compound is mainly used for relieving muscle aches and pains when applied externally to the affected area. The increasing use of the above mentioned solvents and their mixtures in many industrial processes have greatly stimulated the need for extensive information on their various properties.

1.5. Literature Review

Multi-component liquid mixtures were being investigated over the years in terms of various thermodynamics, acoustic, transport and allied properties. So the literature is vast and extensive. Therefore the literature review has been kept confined to some important works that dealt with the liquids and liquid mixtures related to those liquids or liquid mixtures studied in the present dissertation.

Azhagiri *et al.*¹²⁸ measured the densities and ultrasonic speeds of the binary mixtures of benzaldehyde with *n*-hexane and cyclohexane over the entire composition range at 30 °C. Various acoustic parameters indicated association amongst the molecules of the mixtures through dipole–dipole interactions. Further, theoretical values of the ultrasonic speeds for binaries were evaluated using several theories and empirical relations. Sinha *et al.*¹²⁹ measured the densities, viscosities and ultrasonic speeds for the binary mixtures of some alkoxyethanols and amines in cyclohexanone over the entire range of composition at 298.15 K. The large negative excess molar

General Introduction

volumes indicated the presence of strong intermolecular hydrogen bond interactions between the amine and the cyclohexanone molecules. But alkoxyethanols systems are characterized by the presence of weak intermolecular interactions probably due to the formation of intramolecular associates *via* the interaction of the etheric oxygen and hydrogen of –OH group in the same alkoxyethanol molecule. Farhan *et al.*¹³⁰ reported the densities, viscosities and refractive indices for binary mixtures: (i) cyclohexane + n-decane and (ii) cyclohexane + 1-pentanol over the whole mole fraction range at several temperatures. From these results, excess molar volumes, viscosity deviations and excess refractive indices were calculated. Derived excess or deviation properties suggested that the globular cyclohexane disturbs the orientation order in n-alkanes and hydrogen bond interactions in alkanols and thus resulted into less packed structure. The same group¹³¹ also reported the densities, viscosities and refractive indices for the ternary mixtures: i) cyclohexane + 1-pentanol + n-hexane and ii) cyclohexane + 3-hexanol + n-hexane at $T = (298.15-328.15)$ K. For the ternary mixture (i), the excess molar volumes were negative at high mole fraction of n-hexane and become positive at low mole fraction of n-hexane but for the ternary mixture (ii), the excess molar volumes were negative over the whole mole fraction range indicating the orientation order and packed structure in these mixtures. Rathnam *et al.*¹³² reported the densities, viscosities and refractive indices for the binary mixtures of diethylmalonate with ketones (*viz.*, acetophenone, cyclopentanone, cyclohexanone and 3-pentanone) over the entire composition range at $T = (303.15-313.15)$ K. Various excess or deviation properties were interpreted in terms of molecular interactions and were also fitted to the Redlich–Kister polynomial equation. Furthermore, different empirical relations were used to correlate the binary mixture viscosities and refractive indices. Malek *et al.*¹³³ reported the densities, speeds of sound, molar isentropic compressibilities and thermal expansion coefficients for the binary mixtures: (i) cyclohexane + benzene and (ii) cyclohexane + benzaldehyde at $T = (293.15-323.15)$ K over the entire range of composition at atmospheric pressure. Various results indicated enhancement of molecular order in the (cyclohexane + benzene) mixture through closer molecular packing. But results for the (cyclohexane + benzaldehyde) mixture indicated the breaking of dipole-dipole and π - π interactions in benzaldehyde by addition of globular cyclohexane molecules. Gowrisankar *et al.*¹³⁴ reported the densities, viscosities and ultrasonic speeds of methyl isobutylketone,

General Introduction

diethylketone, cyclopentanone, cyclohexanone, 2-methyl cyclohexanone and those of their binary mixtures with N-methyl aniline over the entire composition range at 303.15 K. Various excess or deviation properties like excess molar volumes, excess isentropic compressibility, *etc.*, were discussed in terms of dipole-dipole interactions, interstitial accommodation and hydrogen bond interactions for these binaries. Kannappan *et al.*¹³⁵ studied four ternary mixtures of 1-propanol, 1-butanol, 1-pentanol and 1-hexanol with N, N-dimethylformamide and cyclohexanone at several temperatures to characterize the molecular interactions in these systems. Results such as the excess free volume, excess internal pressure and Gibb's free energy, *etc.*, revealed the mixtures to be characterized by dipole-dipole interactions and rupture of hydrogen bond interactions in the pure components. Also excess free volumes of the mixtures suggested that association between 1-alkanols with N, N-dimethylformamide is more than those with cyclohexanone. Roy *et al.*¹³⁶ reported densities, viscosities and derived parameters for the ternary mixtures of some alkyl esters with cyclohexane and cyclohexanone and related binary mixtures at 298.15 K under atmospheric pressure. Results such as the excess molar volumes and viscosity deviations suggested that specific interactions for the alkyl acetates with cyclohexane and cyclohexanone increase as the chain length of the acetates increase and non-homogeneity prevails in the ternary mixtures. Venis *et al.*¹³⁷ reported the densities, viscosities and ultrasonic speeds for the ternary mixture involving morpholine + cyclohexanone + 1-hexanol at 308.15 K and 318.15 K over the entire range of mole fraction. Parameters like excess molar volume, adiabatic compressibility and free volume, *etc.*, revealed the presence of strong intermolecular interactions between the constituent liquids in the mixtures, chiefly due to strong hydrogen bonding between 1-hexanol and morpholine and electron donor – acceptor complex formation nature of cyclohexanone and geometrical fitting between mixing liquids. The same group¹³⁸ has also reported the densities, viscosities and ultrasonic speeds for the ternary mixture involving anisole + cyclohexanone + 1-hexanol over the entire range of mole fraction at 308.15 and 318.15 K. Various derived excess or deviation properties suggested the presence of non-specific physical interactions and unfavorable interactions between the unlike molecules and it was suggested that bond breaking or breaking of liquid order predominates over other type of molecular interactions between the mixing components. Aravinthraj *et al.*¹³⁹ reported the densities, viscosities and ultrasonic

General Introduction

speeds for three ternary liquid mixtures: (i) p-cresol + cyclohexane + formaldehyde, (ii) p-cresol + cyclohexane + acetaldehyde and (iii) p-cresol + cyclohexane + benzaldehyde at $T = (303-323)$ K. Various derived acoustical parameters such as adiabatic compressibility, free length, free volume and internal pressure, *etc.*, revealed the occurrence of dipole-dipole interactions and molecular association through intermolecular hydrogen bonding in these ternary mixtures and significant interactions occur only after introduction of p-cresol in these mixtures. This is due to the intermolecular hydrogen bonding between carbonyl oxygen of aldehydes with hydroxyl hydrogen in p-cresol and dipole-dipole interactions between the same compounds with carbonyl carbon of aldehydes and hydroxyl oxygen. Mistry *et al.*¹⁴⁰ reported the densities, viscosities and ultrasonic speeds for the ternary mixtures of toluene + cyclohexane + nitrobenzene over the entire range of composition at 308 K and calculated various acoustic parameters like adiabatic compressibility, free length and free volume, *etc.* Based on these results it was suggested that there exists dipole-induced dipole interactions between nitrobenzene and cyclohexane and the donor-acceptor complex between toluene and nitrobenzene molecules. Vanathi *et al.*¹⁴¹ reported densities, viscosities and ultrasonic speeds for the ternary mixture of toluene + chloroform + cyclohexane at $T = (303.15-313.15)$ K. Various acoustic parameters such as adiabatic compressibility, intermolecular free length, free volume and internal pressure, *etc.*, were derived using the experimental data and it was found that strong intermolecular interactions (association) exist between the components in the mixtures, *i.e.*, greater solute-solvent interactions than solute-solute interactions. Dey *et al.*¹¹³ reported the ultrasonic speeds for four binary, one ternary and one quaternary liquid mixture consisting of cyclohexane, benzene, n-hexane and n-decane at 298.15K. Computation of ultrasonic speeds by various approaches, *i.e.*, van Deal, Nomoto, Junjie and Collision factor theory, *etc.*, were carried out for the six mixtures. A comparative study of the merits of the different approaches has been carried out and all the mixing rules used gave reasonably good results for ultrasonic speeds for the binary as well as the multi-component mixtures. They¹⁴² also reported the viscosities of the above referred mixtures at 298.15 K and estimated viscosities of these solutions by various empirical and semi-empirical models such as McAllister 3 and 4 body, Grunberg-Nissan, Wijk, Hind, Katti-Chaudhri and Tamura-Kurata, *etc.* Sharma *et al.*¹⁴³ reported the densities and speeds of sound for ternary mixtures of o-

General Introduction

chlorotoluene + tetrahydropyran + N-methylformamide or N, N-dimethylformamide or cyclohexane and their sub-binary mixtures at $T = (298.15-308.15)$ K and $P = 0.1$ MPa. The excess molar volumes and excess isentropic compressibilities for ternary and binary mixtures were discussed in terms of molecular interactions. The thermodynamic properties were also analyzed in terms of Graph and Prigogine–Flory–Patterson (PFP) theories. S. Kumar *et al.*¹⁴⁴ reported the excess molar volumes for the binary mixtures of 1,4-dioxane with some formamides and anilines over entire composition range at 308.15 K. The excess molar volumes were also rationalized by Graph theoretical arguments, which has further yielded information about the state of association in aniline, formamide and N, N-dimethylformamide. The existence of molecular interactions in these mixtures has also been supported by their infrared spectral studies. The same group¹⁴⁵ has also reported speeds of sound, isentropic and excess isentropic compressibilities of 1,3-dioxolane or 1,4-dioxane + benzene or toluene + formamide or N, N-dimethylformamide ternary and their sub-binary mixtures at 308.15 K and analyzed the excess isentropic compressibilities of the mixtures by Graph and Flory theories. Jangra *et al.*¹⁴⁶ reported the excess molar volumes for the ternary mixtures consisting of 1,4-dioxane + o-toluidine + benzene or toluene or m- or p-xylene as a function of composition at 308.15 K. The resulting excess molar volumes were fitted to Redlich-Kister polynomial to evaluate ternary adjustable parameters and corresponding standard deviations. The observed excess molar volumes were also analyzed in terms of Graph and PFP theories. Bedare *et al.*¹⁴⁷ reported the densities, viscosities and ultrasonic speeds for the binary systems of 1,4-dioxane with ethanol and methanol over the whole range of composition at 308 K. Various acoustic parameters such as adiabatic compressibility, intermolecular free length, free volume and internal pressure were calculated and discussed in terms of molecular interactions between the components of the mixtures. Sinha *et al.*¹⁴⁸ reported the densities and viscosities of binary mixtures consisting of tetrahydrofuran, 1,3-dioxolane and 1,4-dioxane with N, N-dimethylformamide over the entire range of composition at 298.15, 308.15 and 318.15 K. Based on the nature and magnitude of various excess functions and other derived parameters, the molecular interactions in the binary mixtures were primarily attributed to dipole-dipole or dipole-induced dipole interactions. The excess molar volumes as a function of composition at ambient temperature and atmospheric pressure were used to test the applicability of

General Introduction

PFP theory to the experimental binaries. Bhatia *et al.*¹⁴⁹ reported the densities and ultrasonic speeds of binary mixtures of hexan-1-ol with 1,2-dichloroethane, 1,2-dibromoethane, and 1,1,2,2-tetrachloroethene at several temperatures over the entire range of composition. From these data, the excess molar volumes, deviations of ultrasonic speed, excess molar isentropic compressibility, intermolecular free lengths, mean molecular radii and thermal expansion coefficients were calculated. The positive excess molar volumes at all temperatures for these mixtures over the whole composition range in conjunction with the excess molar isentropic compressibilities and intermolecular free lengths for the studied mixtures confirmed that the hydrogen bond interactions of the type $\text{Cl}\cdots\text{H}-\text{O}$, $\text{Br}\cdots\text{H}-\text{O}$, $\pi\cdots\text{H}$ and weak physical intermolecular interactions between hexan-1-ol and the halohydrocarbons dominate over the structure-breaking effect of hexan-1-ol on the addition of halohydrocarbons. Kumar *et al.*¹⁵⁰ reported the densities and ultrasonic speeds for the binary mixtures of p-xylene with 1,2-dichloroethane over the different range of composition at 303.15 K. Various excess properties were discussed in terms of the molecular interactions between the components of the mixture and it was suggested that mixing of p-xylene with 1,2-dichloroethane disrupted the dispersive interactions amongst the 1,2-dichloroethane molecules and the mixture is characterized by the presence of specific interactions amongst the dissimilar molecules. They¹⁵¹ also reported the densities, ultrasonic speeds, excess molar volumes and excess enthalpies for the binary mixture of benzene and 1,2-dichloroethane over the entire composition range at 303.15 K. It is found that intermolecular interactions present in the binary mixtures were stronger than pure solvent-solvent interactions. Observed negative excess molar volumes and positive excess molar enthalpies confirmed the presence of specific chemical attractive forces between the two liquids in the mixture. Kondaiah *et al.*¹⁵² reported the densities, the excess molar volumes and related volumetric properties for the binary mixtures: (i) 1,2-dichloroethane + N, N-dimethylformamide, (ii) 1,2-dichloroethane + dimethylsulphoxide, (iii) dichloromethane + N, N-dimethylformamide and (iv) dichloromethane + dimethylsulphoxide at 308.15 K. The variations of excess properties with composition of the mixtures revealed that hydrogen bond formation between the unlike molecules, dipole-dipole interactions and interstitial accommodation of the unlike molecules were the factors for the

General Introduction

observed molecular interactions. Ranjbar *et al.*¹⁵³ measured the densities and viscosities of binary and ternary liquid mixtures consisting of 1-propanol, benzaldehyde and 1,2-dichloroethane at several temperatures over entire composition range under atmospheric pressure. The interpreted negative viscosity deviations qualitatively by considering the strength of intermolecular hydrogen bonding, molecular size and shapes of the components and suggested that the OH-Cl and OH-O interactions increase the viscosity for the studied mixtures but the effect is not as important as the breaking of associations. Dean *et al.*¹⁵⁴ measured densities and ultrasonic speeds for the binary mixtures of four aliphatic alcohols with monoethanolamine over the entire composition range at several temperatures. Volumetric and acoustic properties of aliphatic alcohols with monoethanolamine were found to depend on the hydrophobicity and hydrogen bonding ability of the alcohols and alcohols with higher hydrophobic character interact more strongly with monoethanolamine. Yasmin *et al.*¹¹¹ reported the densities, viscosities, ultrasonic speeds and refractive indices of binary mixtures of poly(ethylene glycol) 200 with ethanolamine, m-cresol and aniline over the entire composition range at 298.15 K under atmospheric pressure. The different excess parameters derived were explained in terms of specific intermolecular and intramolecular interactions present in the mixtures. The stronger interactions in the binary mixture of poly (ethylene glycol) 200 with ethanolamine than with m-cresol and least with aniline were attributed to the hydrogen bond interactions between $-NH_2$ or $-OH$ groups in ethanolamine, $-OH$ group in m-cresol and $-NH_2$ group in aniline with the hydroxyl groups at the chain terminals of poly (ethylene glycol) 200 molecules. Blanco *et al.*¹⁵⁵ reported the density, viscosity and speed of sound for the ternary mixture consisting of N-methyl-2-pyrrolidone + ethanolamine + water over the entire composition range at several temperatures under a pressure of 10^5 Pa. Various excess or deviation properties were then derived and discussed in terms of molecular interactions. The negative excess molar volumes and excess isentropic compressibilities suggested that the present mixture has a more compact structure as compared to the pure component liquids due to the hydrogen bond interactions. Li *et al.*¹⁵⁶ determined the densities and viscosities for the binary mixtures consisting of 1,2-diaminoethane + 1,2-ethanediol over the whole concentration range at (298.15-308.15) K and molecular interactions in the mixtures were interpreted in terms of excess molar volumes. Tumberphale *et al.*¹¹²

General Introduction

reported densities, viscosities and ultrasonic speeds for the binary mixtures of n-propyl alcohol with ethylenediamine at 303 K. Different excess properties were discussed in terms of intermolecular interactions between the unlike components in the mixture. Vasudha *et al.*¹⁵⁷ reported the densities and viscosities for the binary mixtures of 2-propanol with methyl acetate, ethyl acetate, butyl acetate and iso-amyl acetate over the entire range of composition at 303.15 K. The derived excess properties revealed that the degree of molecular interactions between dissimilar molecules in the mixtures increase as the chain length of the alkyl acetates increases. S. Sharma *et al.*¹⁵⁸ reported the densities, viscosities and speeds of sound for binary mixtures of oleic acid with methyl acetate, ethyl acetate, n-propyl acetate and n-butyl acetate over the entire composition range at several temperatures under atmospheric pressure. Various excess properties suggested that the interactions in these mixtures are due to dipole-dipole type forces originating from the polarizability of ester molecules by the dipoles of oleic acid molecules and it was found that as the chain length in esters increases structure-making effect precedes the structure breaking effect for these binary mixtures. Karuna Kumar *et al.*¹⁵⁹ reported the densities, the ultrasonic speeds and excess molar volume and excess isentropic compressibility, *etc.*, the binary mixtures consisting of N-methyl-2-pyrrolidone, methyl acetate, ethyl acetate, butyl acetate over the entire range of composition at $T = (303.15-318.15)$ K. Various thermo-acoustic results suggested that molecular interactions are due to differences in free volumes between the unlike molecules, dipole-dipole and dipole-induced dipole interactions between unlike molecules. The FTIR spectra of these liquid mixtures also supported the presence of interactions between unlike molecules. The temperature effect on the shapes of the interacting molecules in the binary mixture was also analyzed with the scaled particle theory. Cunha *et al.*¹⁶⁰ reported new experimental data of speeds of sound and densities for seven pure components of pyrolysis bio-oil at atmospheric pressure for several phenols (phenol, o-, m-, and p-cresol), two phenolic ethers (2-methoxyphenol and eugenol) and one phenolic ester (methyl salicylate) at $T = (288.15-343.15)$ K. They correlated measured densities and sound speeds with PFP theory. Kareem *et al.*¹⁶¹ reported the densities, refractive indices, viscosities and derived parameters like the excess molar volumes, excess refractive indices and excess viscosities for quaternary mixtures: i) cyclohexane + n-heptane + n-decane + n-hexane and ii) cyclohexane + 1-pentanol + 3-hexanol + n-

General Introduction

hexane at the temperature range (298.15- 328.15) K. The derived parameters were found to be fluctuating between positive and negative values from ideal ones depending on the nature of molecular interactions in these mixtures. Such behavior was attributed to the interstitial accommodation of the globular cyclohexane molecules between n-alkane molecules and distortion of the hydrogen bond interactions in alkanols by the cyclohexane molecules. Furthermore, the Flory's theory was extended for the theoretical prediction of excess molar volume of these mixtures. The theory predicted the volumetric behavior and magnitudes of excess molar volume satisfactorily.

Anyway, from the above concise literature survey it is obvious that there is a lot of reports on the thermodynamic, acoustic, transport and allied properties for the binary and ternary mixtures consisting of one or more of the liquids studied in the chapters embodied in the present dissertation but reports on the thermodynamics, acoustic and allied properties on the compositions of the various mixtures (binary, ternary and quaternary) studied herein this dissertation are rare to the best of our present knowledge, at least at multi-temperature range.

References

- [1] O. Popvykh, R.P.T. Tomkins, *Nonaqueous Solution Chemistry*, Wiley-Interscience, New York, (1981), Chapter 4.
- [2] A.J. Matheson, *Molecular Acoustics*, Wiley-Interscience, London, 1971.
- [3] V. Gutmann, *Electrochim. Acta*, 21 (1967) 661.
- [4] U. Mayer, V. Gutmann, *Adv. Inorg. Chem. Radiochem*, 17 (1975) 189.
- [5] J.E. Gordon, *The Organic Chemistry of Electrolyte Solutions*, Wiley-Interscience, (1975).
- [6] R.G. Pearson, *Hard and Soft Acids and Bases*, Dowden, Hutchinson and Ross, Stroudsburg, (1973).
- [7] J.V. Herraiz, R. Belda, *J. Solution Chem.*, 33 (2004) 217.
- [8] A.J. Queimade, I.M. Marrucho, J.A.P. Coutinho, E.H. Stenby, *Int. J. Thermophys*, 26 (2005) 47.
- [9] N.N. Wankhede, M.K. Lande, B.R. Arbad, *J. Chem. Eng. Data* 50 (2005) 969.
- [10] H. Eyring *J. Chem. Phys.*, 4 (1936) 283.
- [11] B.E. Eichinger, P.J. Flory, *Trans Faraday Soc.*, 64 (1968) 2061.
- [12] B.E. Eichinger, P.J. Flory, *Trans Faraday Soc.*, 64 (1968) 2006.
- [13] B.E. Eichinger, P.J. Flory, *Trans Faraday Soc.*, 64 (1968) 2035.

General Introduction

- [14] P.J. Flory J. Am. Chem. Soc., 87(1965) 1833.
- [15] P.J. Flory, A. Abe, J. Am. Chem. Soc., 87 (1965) 1838.
- [16] R.A. Orwall, P.J. Flory, J. Am. Chem. Soc., 89 (1967) 6814.
- [17] R.A. Orwall, P.J. Flory, J. Am. Chem. Soc., 86 (1964) 3515.
- [18] G.L. Bertrand, W.E. Acree (Jr), T.E. Burhfield, J. Solution Chem., 12 (1983) 327.
- [19] G.L. Bertrand, W.E. Acree (Jr), J. Solution Chem., 12 (1983) 755.
- [20] I. Prigogine, G. Garikian, Physica, 16 (1950) 239.
- [21] I. Prigogine, V. Mathot, J. Chem. Phys., 20 (1952) 49.
- [22] I. Prigogine, A. Bellemans, J. Chem. Phys., 21 (1953) 561.
- [23] I. Prigogine, *The Molecular Theory of Solutions*, North-Holland Pub. Co., Amsterdam, (1957).
- [24] H. Eyring, F. Comuschi, J. Chem. Phys., 7 (1939) 547.
- [25] H. Eyring, J. Hirschfelder, J. Phys. Chem., 41 (1937) 249.
- [26] I. Prigogine, A. Bellemans, J. Chem. Phys., 21 (1953) 561.
- [27] J.W. Leland, P.S. Chappellear, Ind. Eng. Chem., 60 (1968) 15.
- [28] P.J. Flory, A. Vrij, R.A. Orwall, J. Am Chem. Soc., 86 (1964) 3507.
- [29] P.J. Flory, Discuss Faraday Soc., 49 (1970) 7.
- [30] D. Patterson, G. Delmas, Discuss Faraday Soc., 49 (1970) 98.
- [31] D. Patterson, Pure. Appl. Chem., 47 (1976) 305.
- [32] J.D. Panday, U. Gupta, J. Phys. Chem., 86 (1982) 5234.
- [33] J.D. Panday, N. Pant, J. Am. Chem. Soc., 104 (1982) 3299.
- [34] J.D. Panday, R.P. Panday, Phys. Chem. Letters 14 (1985) 253.
- [35] J.D. Panday, R.K. Upadhyay, U. Gupta, Acoustics Letters, 5 (1982) 120.
- [36] J.D. Panday, Electrochimica Acta, 27 (1982) 1097.
- [37] J.D. Panday, A.D.M. David, Chemica Scr., 19 (1982) 39.
- [38] J.D. Panday, U. Gupta, Electrochimica Acta, 28 (1983) 1047.
- [39] J.D. Panday, V.N.P. Srivastava, V. Vyas, N. Pant, Ind. J. Pure and Appl. Phys., 25 (1987) 467.
- [40] A.K. Doolittle, J. Appl. Phys., 23 (1952) 236.
- [41] M.L. Williams, R.F. Landel, J.D. Ferry, J. Am. Chem. Soc., 77 (1955) 3701.
- [42] R.C.L. Bosworth, Trans Faraday Soc., 43 (1947) 308.
- [43] N. Auerbach, Experientia, 4 (1948) 473.

General Introduction

- [44] W.T. Keeton, J.L. Gould, *Biological Science*, 5th edn., W. W. Norton & Co, New York, 1993.
- [45] A.R. Ravishankara. *Science*, 276 (1997) 1058.
- [46] K. Ibuki, M. Nakahara *J. Phys. Chem.*, 94 (1990) 8370.
- [47] A. Henni, J.H. Jonathan. T. Paitoon, C. Amit, *J. Chem. Eng. Data* 48 (2003) 1062.
- [48] J. Burgess, *Metal Ions in Solutions*, Ellis Horwood, New York, (1978).
- [49] C. Reichardt, *Solvents and Solvent Effects in Organic Chemistry*, 3rd edn., Wiley-VCH, (2003).
- [50] A. Ali, A.K Nain, *J. Pure. Appl. Ultrason.*, 22 (2000) 121.
- [51] J.H. Dymond, *Chem. Soc. Rev.*, 14 (1985) 417.
- [52] L. Grunberg, A.H. Nissan, *Nature (London)*, 164 (1949) 799.
- [53] R.K. Hind, E. McLaughlin, A.R. Ubbelohde, *Trans. Faraday. Soc.*, 56 (1960) 328.
- [54] E.L. Heric, J. G. Brewer, *J. Chem. Eng. Data* 12 (1967) 574.
- [55] P.K. Katti, M. M. Choudhri, *J. Chem. Eng. Data* 9 (1964) 442.
- [56] R.A. McAllister, *AIChE J.*, 6 (1960) 427.
- [57] R. Macias-Salinas, F. Garcia-Sanchez, G. Eliosa-Jimencz. *Fluid Phase Equilib.*, 210 (2003) 319.
- [58] V.A. Bloomfield, R.K. Dewan, *J. Phys. Chem.*, 75 (1971) 3113.
- [59] D.S. Wankaede, N.N. Wankhede, M.K. Lande, B. R. Arbad, *Ind. J. Pure Appl. Phys.*, 44 (2006) 909.
- [60] M. Palaiologou, G.K. Arianas, N.G. Tsierkezo, *J. Sol. Chem.*, 35 (2006) 1551.
- [61] A.B. Pereiro, A. Rodriguez, *J. Chem. Eng. Data* 52 (2007) 600.
- [62] A.F. Ribeiro, E. Langa, A.M. Mainar, J.J. Pardo, J.S. Urieta, *J. Chem. Eng. Data* 52 (2006) 1.
- [63] M. Aravinthraj, C. Venkatesan, D. Meera, *J. Chem. Pharm. Res.*, 3 (2009) 623.
- [64] C.R. Reid, B. E. Poling, *The properties of gases and liquids*, McGraw Hill, New York, (1998), Chap. 1.
- [65] O. Nomoto, *J. Phys. Soc. Jpn.*, 13 (1958) 1528.
- [66] W. Schaaffs, *Acoustica*, 33 (1975) 272.
- [67] W. Schaaffs, *Molekularakustic*, Springer Verlag, Berlin, (1963), Chap., 11-12.
- [68] M. Kalidoss, R. Srinivasamoorthy, *J. Pure. Appl. Ultrason.*, 19 (1997) 9.
- [69] W. van Dael, E. Vangael, in abst. paper: *Proc. 1st International Conference on Calorimetry and thermodynamics*, Warsaw. Poland. (1969), pp. 555.

General Introduction

- [70] B. Jacobson, *J. Chem. Phys.*, 6 (1952) 927.
- [71] B. Jacobson, *Acta Chem. Scand.*, A6 (1952) 1485.
- [72] Z. Junjie, *J. China Univ. Sci. Tech.*, 14 (1984) 298.
- [73] J.D. Pandey, N. Pant, N. Agarwal, Shikha. *Acustica*, 68 (1969) 225.
- [74] A. Ali, K. Tewari, A.K. Nain, V. Chakravorthy, *Phys. Chem. Liq.*, 38 (2000) 459.
- [75] A. Ali, A.K. Nain, S. Hyder, *J. Pure Appl. Ultrason.*, 23 (2001) 73.
- [76] P.S Naidu, K.R. Prasad, *J. Pure Appl. Ultrason.*, 24 (2002) 1824.
- [77] M. Rastogi, A. Awasthi, M. Gupta, J.P. Shukla, *Ind. J. Pure Appl. Phys.*, 40 (2002) 256.
- [78] M. Meyappan, Sethupathy. *J. Pure Appl. Ultrason.*, 25 (2003) 1.
- [79] A. Pal, H. Kumar, *Ind. J. Phys.*, 78 (2004) 1319.
- [80] G.V.R. Rao, A.V. Sarma, J.S.R. Krishna, C. Rambabu, *Ind. J. Pure Appl. Phys.*, 43 (2005) 345.
- [81] J.A. Al-Kandary, A.S. Al-Jimaz, A. Haq, A. Latif, *J. Chem. Eng. Data* 51 (2006) 2074.
- [82] D.K. Sravana, D.K. Rao D. *Ind. J. Pure Appl. Phys.*, 45 (2007) 210.
- [83] T.M. Aminabhavi, K. Banerjee and R.H. Balundgi, *Ind. J. Chem.*, 38 (1999) 768.
- [84] A. Pal and A. Kumar, *J. Chem. Eng. Data* 43 (1998) 143.
- [85] A.H. Al-Dujali, A.A. Yassen, A.M. Awwad, *J. Chem. Eng. Data* 45 (2000) 647.
- [86] A.K. Nain, P. Chandra, J.D. Pandey, S. Gopal, *J. Chem. Eng. Data* 53 (2008) 2654.
- [87] A.K. Nain, *Fluid Phase Equilib.*, 265 (2008) 56.
- [88] B. Giner, S. Martin, H. Artigas, M.C. Lopez, C.J. Lafuente, *J. Phys. Chem. B.*, 110 (2006) 17683.
- [89] B. Garcia, R. Alcalde, S. Aparicio, J.M. Leal, *Phys. Chem. Chem. Phys.*, 4 (2002) 5833.
- [90] M.I. Aralaguppi, T.M. Aminabhavi, S.B. Harogoppad, R.H. Balundgi, *J. Chem. Eng. Data* 37 (1992) 298.
- [91] J.D. Pandey, V. Vyas, G.P. Dubey, N. Tripathi, R. Dey, *J. Mol. Liq.*, 81 (1999) 123.
- [92] M.I. Aralaguppi, C.V. Jadar, T.M. Aminabhavi, *J. Chem. Eng. Data* 44 (1999) 446.
- [93] J.A. Acosta, E. Rodil, A. Soto, *J. Chem. Eng. Data* 46 (2001) 1176.
- [94] C.C. Wang, H.W. Chen, C.H. Tu, *J. Chem. Eng. Data* 50 (2005) 1687.
- [95] S.H. Canzonieri, M.A. Postigo, J.A. Salas, M. Katz, *J. Argen. chem. Soc.*, 1 (2002) 31.
- [96] A.F. Fucaloro, *J. Chem. Educ.*, 79 (2002) 865.
- [97] B. Giner, C. Lafuente, A. Villares, M. Haro, M.C. Lopez, *J. Chem. Thermodyn.*, 3 (2007) 148.

General Introduction

- [98] A. Pineiro, P. Brocos, A. Amigo, M. Pintos, R. Bravo, *Phys. Chem. Liq.*, 38 (2000) 251.
- [99] A. Lorentz, *Weid. Ann.*, 9 (1880) 641.
- [100] L. Lorenz, *Weid. Ann.*, 11 (1880) 70.
- [101] F. Gladstone, D. Dale, *Philos. Trans. R. Soc. London*, 148 (1858) 887.
- [102] D.F.J. Arago, J.B. Biot, *Mem. Acad. Fr.*, 17 (1806) 7.
- [103] O. Weiner, *Berichte (Leipzig)*, 62 (1910), 256.
- [104] H. Eyring, M.S. John, *Significant Liquid Structures*; Wiley, New York, (1969).
- [105] W. Heller, *Phys. Rev.*, 68 (1945) 5.
- [106] J.F. Eykman, A.F. Holleman, *Research Refractometers*, De Erven Loosjes, (1919).
- [107] S.S. Kurtz, A.L. Ward, *J. Franklin Inst.*, 222 (1936) 563.
- [108] M. Gupta and I. Vibhu, J.P. Shukla. *J. Phys. Chem. Liq.*, 41 (2003) 575.
- [109] M.M. Hossain Bhuiyan and Kaxuhiro Tamura, *J. Chem. Thermodyn.*, 36 (2004) 549.
- [110] H. Kumar, D. Kumar. *Int. J. of Thermodyn.*, 16 (2013) 123.
- [111] M. Yasmin, M. Gupta, *J. Solution Chem.*, 40 (2011) 1458.
- [112] U.B. Tumberphale, R.S. Kawale, N.P. Pawar, V.G. Kalamse, *Int. J. Phys. Math. Sci.*, 5 (2015) 25.
- [113] R. Dey, A. Harshavardhan, *J. Ener. Chem. Eng.*, 2 (2014) 1.
- [114] M.A. Tejraj, H.T.S. Phayde, R.S. Khinnavar, G.K. Bindu, *J. Chem. Eng. Data* 39 (1994) 251.
- [115] K. Saravanakumar, R. Basharan, T.R. Kubendra, *E-J. Chem.*, 9 (2012) 1711.
- [116] S. Ismadji, *J. Chem. Eng. Data* 53 (2008) 2207.
- [117] G.A. Shabir, T.K. Bradshaw, *Turk J. Pharm. Sci.*, 8 (2011) 117.
- [118] M.T. Musser "*Cyclohexanol and Cyclohexanone*" in *Ullmann's Encyclopedia of Industrial Chemistry*, Wiley-VCH, Weinheim, (2005).
- [119] R. Hammker, R. Clegg, P. Paderson, P. Ridder, S. Rock, *J. Phys. Chem.*, 72 (1968) 1837.
- [120] P. Brocos, E. Calvo, A. Pineiro, R. Bravo, A. Amigo, *J. Chem. Eng. Data* 44 (1999) 1341.
- [121] C.G. Janz, R.P.T. Tomkins, *Non-Aqueous Electrolytes Handbook*, Academic, New York, 2 (1973).
- [122] J. Nath, G. Singh, *J. Chem. Eng. Data* 33 (1988) 58.

General Introduction

- [123] V.D. Spassjevic, B.D. Bjordjevic, S.P. Serbanovic, I.R. Radovic, M.Lj. Kijevcenin, J. Chem. Eng. Data 59 (2014) 1817.
- [124] K. Rettinger, C. Burschka, P. Scheeben, H. Fuchs, A. Mosandl, Tetrahedron Asymmetry, 2 (1991) 965.
- [125] R. Mehra, A. Gupta, R. Israni, Ind. J. Chem., 40 (2001) 505.
- [126] M. Indhumathi, G. Meenakshi, Mid. East. J. Sci. Res., 20 (2014) 546.
- [127] S. Aparicio, R. Alcalde, Eur. J. Chem., 1 (2010) 162.
- [128] S. Azhagiri, S. Jayakumar, R. Padmanaban, S. Gunasekaran, S. Srinivasan, J. Sol. Chem., 38 (2009) 441.
- [129] B. Sinha, Phys. Chem. Liq., 48 (2010) 183.
- [130] A.M. Farhan, E.T. Kareem, A.N. Abd, Bag. Sci. J., 8 (2011) 348.
- [131] A.M. Farhan, E.T. Kareem, A.N. Abd, J. Kerb. Univ., 8 (2010) 184.
- [132] M.V. Rathnam, S. Mohite, M.S. Kumar, J. Serb. Chem. Soc., 77 (2012) 507.
- [133] N.I. Malek, S.P. Ijardar, S.B. Oswal, Thermochemica Acta, 539 (2012) 71.
- [134] M. Gowrisankar, P. Venkateswarlu, K. Sivakumar, S. Sivarambabu, J. Sol. Chem., 42 (2013) 916.
- [135] A.N. Kannappan, S. Thirumaran, R. Palani, J. Phys. Sci., 20 (2009) 97.
- [136] M.N. Roy, B.K. Sarkar, B. Sinha, J. Chem. Eng. Data 54 (2009) 1076.
- [137] A.R. Venis, R. Rajkumar, Orient. J. Chem., 27 (2011) 105.
- [138] R. Venis, R. Rajkumar, J. Chem. Pharm. Res., 3 (2011) 878.
- [139] M. Aravinthraj, S. Venkatesan, M. Kamaraj, Int. J. Chem. Enviro. Pharm. Res., 2 (2011) 5.
- [140] A.A. Mistry, V.D. Bhandakkar, O.P. Chimankar, J. Chem. Pharm. Res., 4 (2012) 170.
- [141] V. Vanathi, S. Mullainathan, S. Nithiyantham, Rus. J. Phys. Chem. A, 86 (2012) 1204.
- [142] R. Dey, A. Harshavardhan, S. Verma, J. Mol. Liq., 211 (2015) 686.
- [143] V.K. Sharma, R. Dua, D. Sharma, J. Chem. Thermodyn., 78 (2014) 241.
- [144] S. Kumar, A. Maken, S. Agarwal and S. Maken, J. Mol. Liq., 155 (2010) 115.
- [145] S. Kumar, W. Lim, Y. Lee, J.S. Yadav, D. Sharma, V.K. Sharma, Il Moon, J. Mol. Liq., 155 (2010) 8.
- [146] S.K. Jangra, N. Saini, J.S. Yadav, R.K. Siwach, D. Sharma and V.K. Sharma, J. Mol. Liq., 158 (2011) 192.

General Introduction

- [147] G.R. Bedare, V. D. Bhandakkar, B. M. Suryavanshi, Euro. J. Appl. Eng. Sci. Res., 1 (2012) 1.
- [148] B. Sinha, R. Pradhan, S. Saha, D. Brahman, A. Sarkar, J. Serb. Chem. Soc., 78 (2013) 1443.
- [149] S.C. Bhatia, R. Bhatia, G.P. Dubey, Int. J. Thermophys., 31 (2010) 2119.
- [150] H. Kumar, D. Kumar, S. Yadav, J. Pure Appl. Ind. Phys., 2 (2012) 248.
- [151] H. Kumar, D. Kumar, Int. J. Thermodyn., 16 (2013) 123.
- [152] M. Kondaiah, D. K. Rao, Int. J. Res. Pure. Appl. Phys., 3 (2013) 43.
- [153] S. Ranjbar, K. Fakhri, B. Jahan, J. B. Ghasemi, J. Chem. Eng. Data 54 (2009) 3284.
- [154] R. Dean, J. Moulines, A. MacInnis, R.M. Palepu, Phys. Chem. Liq., 47 (2009) 302.
- [155] A. Blanco, A. García-Abuín, D. Gómez-Díaz, J.M. Navaza, J. Chem. Eng. Data 57 (2012) 3136.
- [156] C. Li, J. Zhang, T. Zhang, X. Wei, E. Zhang, N. Yang, N. Zhao, M. Su, H. Zhou, J. Chem. Eng. Data 55 (2010) 4104.
- [157] K. Vasudha, D. Vijaya Kumari, G. Yuvaraja, A. Krishnaiah, J. Chem. Pharm. Res., 3 (2011) 108.
- [158] S. Sharma, J. Bhalodia, J. Ramani, R. Patel, Int. J. Phys. Sci., 7 (2012) 1205.
- [159] D.B. Karuna Kumar, K.R. Reddy, G.S. Rao, P.B. Sandhyasri, Z. Begum, C. Rambabu, J. Mol. Liq., 183 (2013) 31.
- [160] D.L. Cunha, J.A.P. Coutinho, J.L. Daridon, R.A. Reis, M.L.L. Paredes, J. Chem. Eng. Data 58 (2013) 2925.
- [161] E.T. Kareem, Nat. J. Chem., 39 (2010) 515.

CHAPTER II

2.1. Importance of Mixed Solvent Systems

For the past few decades, a considerable progress has been made in theoretical understanding of liquid-liquid mixtures. Besides the theoretical importance, the knowledge of physico-chemical properties of multi-components mixtures is indispensable for many chemical process industries. Importantly, for accurate designing equipment it is necessary to know the interactions between the components of the mixtures. Physico-chemical analysis can be used for getting information about the specific interactions amongst the unlike components and the structure of the liquid mixtures. The mixtures that result upon mixing two or more different liquids give rise to a solution that often do not behave ideally. A solution is said to be an ideal if the escaping tendency of each component is proportional to the mole fraction of that component in the solution. That is the partial vapour pressure of the component is directly proportional to its mole fraction in the solution (Raoult's Law). An ideal solution is characterized by the following points: i) it should obey Raoult's law at all temperatures and compositions of the solute in the solvent, ii) $\Delta H_{mixing} = 0$, *i.e.*, no heat should be absorbed or evolved and iii) $\Delta V_{mixing} = 0$, *i.e.*, no expansion or contraction on mixing. But in real cases it is observed that on mixing two or more solvents the resulting mixture do not behave ideally or in other words it deviates from ideal behaviour (Raoult's Law). Thus, in case of liquid-liquid mixtures such deviation from ideal behaviour can be expressed in terms of many thermodynamic properties referred to as excess functions or properties. These excess properties of binary and ternary liquid mixtures are the difference between the actual property of the system and the property if the system behaves ideally. These properties are useful in the study of molecular arrangements and interactions that interplay between the different components of a mixture. The addition of one liquid into another may modify their structure to some extent depending on the interactions taking place between the similar molecules of the pure components and between the dissimilar molecules of the components in the mixture. Therefore, experimental studies involving densitometry, viscometry, interferometry, refractometry and other suitable methods help in interpreting the nature of various interactions in the liquid mixtures as well as in understanding their structures.

Theoretical Background

2.2. Intermolecular Forces

Intermolecular forces are the forces of attraction or repulsion that act between neighbouring molecules and hold them together. These forces of attraction exist between polar as well as non-polar molecules and are known as cohesive forces or van der Waals forces, because van der Waal recognized these forces to be responsible for the non-ideal behaviour of gases.^{1,2} These forces are very short lived electrostatic attractive forces and exist between all kinds of atoms, molecules and ions. Generally there are two types of intermolecular forces; the first type comprises of non-specific dispersion forces while the second type involves the specific forces like hydrogen bonding, charge transfer, electron pair donor-acceptor force, *etc.* The various types of molecular interactions are briefly described below:

2.2.1. Dipole-Dipole Interaction

A key force of attraction between molecules is the dipole-dipole interaction. This type of interaction comes into play between two polar molecules having permanent dipole moments. A dipole consists of two opposite charges separated by a distance. Therefore, a molecule with a dipole has a 'positive end' and a 'negative end'. When two or more such molecules get together, the 'positive end' of one molecular dipole attracts the 'negative end' of another dipole and they orient themselves in such a way that they maximize the attractive forces (negative end near positive end) or minimize the potential energy and minimize the repulsive forces (like charges). Hence these interactions are directional in character. This type of interaction is inversely proportional to the third power of the distance between the two dipoles and is, therefore, effective over short intermolecular distances.^{3,4} This type of interaction may occur through head to tail or lateral orientations as shown in Figure 2.1. There will always be some repulsive interactions but, in general, the molecule will arrange to favour the attractive forces (lower potential energy).

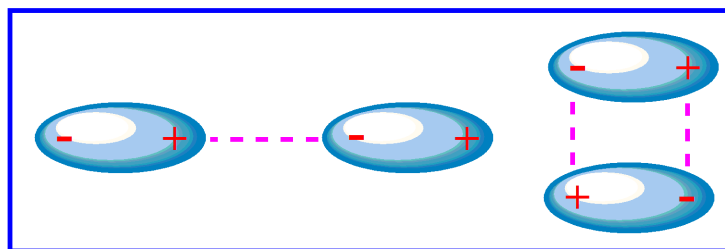


Fig. 2.1. Dipole-dipole interactions: (a) head to tail orientation; (b) lateral orientation.

2.2.2. Induced Dipole Interaction

Some times a polar molecule having a permanent dipole moment distorts a non-polar molecule and induces a dipole moment in it. The forces developed due to interactions between a dipole and an induced dipole are called 'Debye forces'.⁵⁻⁸ This type of forces comes into play when a polar molecule is brought closer to a non-polar molecule. The positive end of the polar molecule attracts the mobile electrons of the non-polar molecule, distorts it and changes it into an individual dipole (Figure 2.2). The 'positive end' of the permanent dipole can now attract the displaced electron cloud of the induced dipole and the two may held together by electrostatic attractions. This type of forces depends upon the distance between dipole and induced dipole. Such forces vary inversely as the sixth power of the distance between the dipole and the induced dipole.⁸ It is effective over an extremely short range and very weak in nature.

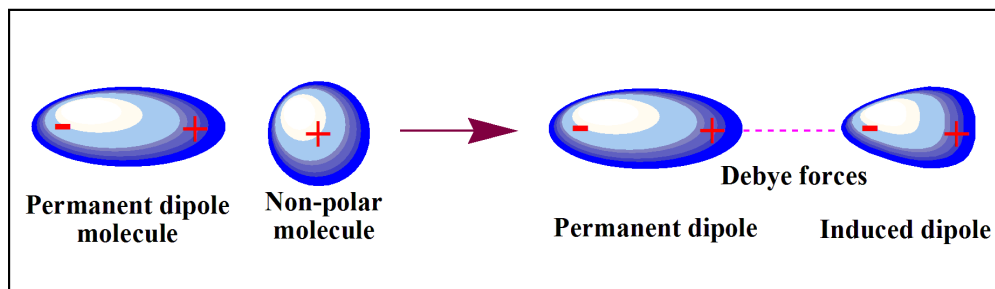


Fig. 2.2. Induced dipole interaction.

2.2.3. Instantaneous Dipole-Induced Dipole Interaction

Non-polar molecules are electrically neutral and as such do not have any dipole moment. In such molecules electrons are continuously moving and visualised as distributed symmetrically. However, the centre of negative charge density due to electrons does not always coincide with the centre of positive charge density of the proton. This disturbs the electrical symmetry of the non-polar molecule momentarily and the molecule becomes momentarily polar with an instantaneous, temporary but random dipole formed (Figure 2.3). The negative side of the instantaneous dipole repels the electron cloud of the adjacent molecules. As a result, this adjacent molecule also acquires a dipole by the induced polarity. Thus the instantaneous dipole and the induced dipole attract each other by an attractive force called instantaneous dipole - induced dipole interaction.⁸ It is true that the instantaneous dipole and induced dipole

Theoretical Background

are changing constantly to a neutral state. Still the attractive force so generated is able to bind the molecules together and is called London force. This force is directly proportional to the molar volume because the London force acts between the surfaces of the concerned molecules when the non-polar molecules come very close to one another.

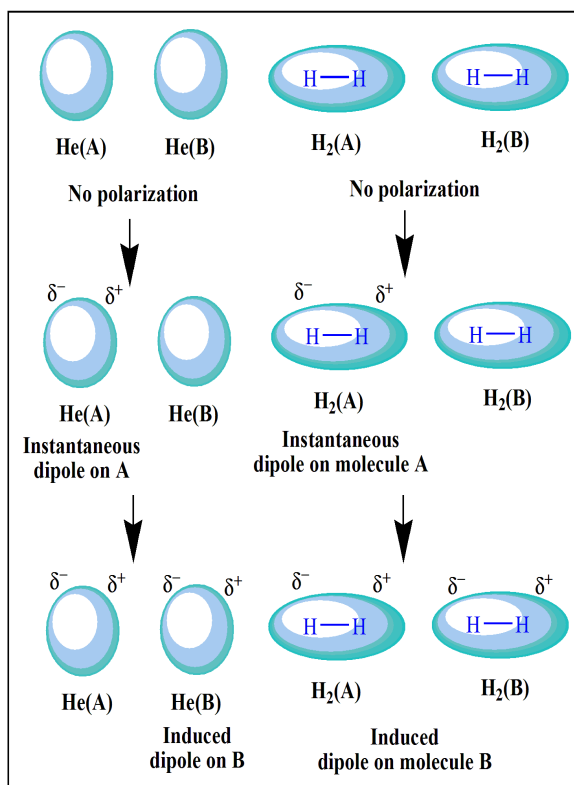


Fig. 2.3. Induced dipole-induced dipole interaction.

2.2.4. Hydrogen Bond

The hydrogen bond is a special case of dipole forces and is considered as a weak chemical force operating both within and between certain types of molecules. Such interaction arises when a hydrogen atom attached to another atom by a covalent bond is attracted to a neighbouring electronegative atom (such as oxygen, nitrogen or fluorine, *etc.*) present either in the same molecule or in a separate molecule. The separation distance determines the strength or energy of the attraction; closer the distance, lower is the energy and hence more stable is the configuration. This is actually not a sharing of electrons, as in a covalent bond, instead this is an attraction between the positive and negative poles of charged atoms. Hydrogen bonding is not

Theoretical Background

nearly as strong as normal covalent bonds but is typically stronger than normal dipole forces between molecules. Although only about 10% as strong as covalent bonds, hydrogen bonds are crucial to biological systems. Hydrogen bonds are responsible for many of the unique properties of water, for the tertiary structure of protein, for the interaction between purine and pyrimidine bases contributing to the stability of the DNA double helix and many more. Normally hydrogen bonds are of two types: intermolecular hydrogen bond and intramolecular hydrogen bond. Intermolecular hydrogen bond is the bonding between the H-atom of one molecule and electronegative atoms of another molecule, *e.g.*, hydrogen bonding among the water molecules (Figure 2.4). It is observed that intermolecular hydrogen bond results into association of molecules leading to an increase in the melting point, boiling point, density, viscosity, surface tension, solubility, *etc.* On the contrary, intramolecular hydrogen bond is formed within the same molecule between the hydrogen atom and the electronegative atoms like F, O and N (Figure 2.5), *etc.* As the intramolecular hydrogen bond results in the cyclization of the molecules, such bonds may prevent their molecular association. Consequently, the effect of this bond on the physical properties is negligible, *e.g.*, o-nitrophenol, salicylic acid, salicylaldehyde, *etc.*

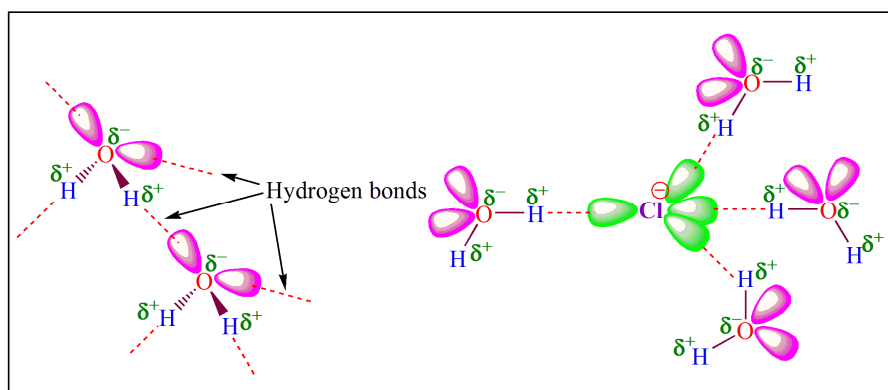


Fig. 2.4. Inter molecular hydrogen bonding between the water molecules and the hydration of chloride ion through hydrogen bonding.

All these different types of intermolecular forces discussed above play an important role in determining the physical properties of molecules and their interactions with one another in pure state as well as in their mixtures. In most cases a combination of forces acts together to contribute to the overall properties of the system, so it is helpful to examine each of them as well as the factors that affect their

Theoretical Background

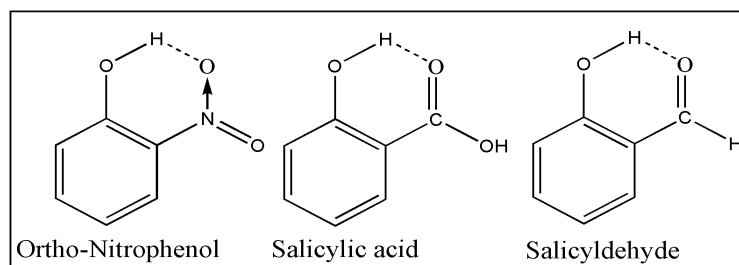


Fig.2.5. Intramolecular hydrogen bonds in o-nitrophenol, salicylic acid and salicylaldehyde.

strength in order to understand their relative importance with respect to molecular interactions in the liquid mixtures.

2.3. Theory of Mixed Solvents

It is observed that much of the chemistry is carried out in solution phase; therefore, the prime necessity and the widely employed requisite in chemical processes are solvents both in industry and in the laboratory. In many industrial applications solvents are substantially employed in pure form called neat or pure solvents. However, for certain applications neat solvents fall short as far as their dissolving strength as well as other properties are concerned. It is then expedient to use solvent mixtures containing two or more solvents rather than the neat solvents. The prime reason to use mixed solvents is to enhance the solubility of substances that have too low solubility in neat solvent, *i.e.*, for their solubilization.⁹ Again the mixed solvents improves the physical properties compared with its neat components with respect to density, viscosity, *etc.*⁹ These properties changes with change in the internal structure on mixing mainly due to the interplay of various types of molecular interactions. The hydrogen bond network, charge transfer complexation, loose association arising from dipole-dipole interaction, dipole-induced dipole interactions, dispersion and diffusion are some familiar and probable interactions generally encountered within liquids and liquid mixtures. The various experimental data on thermodynamic, acoustic, transport and optical properties of pure liquid and liquid mixtures are of significant importance to understand the intermolecular forces and in testing the theories which attempt to estimate the mixture properties. The prediction of the properties of a multi-component (binary/ternary/quaternary) liquid mixtures can be made either from pure component properties as developed by Eyring,¹⁰ Flory *et al.*¹¹⁻¹⁷ or from the properties of their contributing binary systems as advanced by Bertrand *et al.*^{18,19} The theoretical as well as experimental estimation of the different

Theoretical Background

parameters such as density, viscosity, ultrasonic speed and refractive indices of the pure components and their mixtures have been extensively used both as qualitatively and quantitatively to predict the changes in the volume, viscosity, speed of sound, *etc.* and the extent of complex formation when the non-polar organic solvents are mixed. Such changes in the properties of the mixed solvents arise from a result of several contributions like combinational, energetic, molecular orientation, free volume and steric hindrance, *etc.* If the polar components are involved the additional contributions like hydrogen bond, dipole-induced dipole, disruption of molecular order due to dipole-dipole interactions come into play. The interstitial accommodation due to different size and large difference in molar volumes also leads to such changes. Introduction of several theories for the liquids and liquid mixtures has made interpretation of such interactions feasible. Liquid mixtures are usually more easily dealt with properties that measure their deviation from ideal behaviour, *i.e.*, through excess or deviation properties as a function of temperature, pressure and compositions.²⁰

2.4. Excess Molar Volume

Excess molar volume (V_m^E) is one of the most important and commonly used thermodynamic properties. This property is of great interest from both theoretical and engineering point of view. The V_m^E data of binary liquid mixtures have been extensively studied by different researchers and it depends not only on solute-solute, solute-solvent and solvent-solvent interactions but also on the interstitial accommodation of the liquid components into each others cavity (clathrate formation) due to differences in their molar mass, shape, size and free volumes.²¹⁻³¹ Thus it reflects packing effect, molecular arrangement and interactions operating among the constituents of a mixture. The excess molar volumes (V_m^E) for each composition can be calculated from the measured densities using the following relation:³²⁻³⁴

$$V_m^E = V_m - V_m^{\text{id}} \quad (1)$$

where V_m , V_m^{id} are the molar volume and the ideal molar volume of the mixture, respectively and are defined as $V_m = M / \rho$, $M = \sum_{i=1}^n x_i M_i$ and $V_m^{\text{id}} = \sum_{i=1}^n x_i M_i / \rho_i$; n , ρ , M , ρ_i , M_i and x_i stand for the number of components, density of the mixture,

Theoretical Background

molar mass of the mixture, density, molar mass and the mole fraction of the i^{th} pure component in the mixture, respectively.

According to Treszczanowicz *et al.*³⁵ the excess molar volume results from several effects: physical, chemical and geometrical contributions. The physical interactions result in volume expansion and involve mainly the dispersion forces and non-specific interactions in the mixture and thus have positive contribution to V_m^E . The chemical or specific interactions result in volume contraction and involve hydrogen bond formation, charge transfer type forces, dipole-dipole, dipole induced dipole and other complex forming interactions³⁶ between dissimilar species and thus have negative contribution to V_m^E . Structural contributions arising from the variation of molecular packing due to interstitial accommodation of one component into other owing to difference in size, shape, free volume and molar volume of the components also have negative contribution to V_m^E . Therefore, the actual volume change and their magnitude would depend on the relative strength of these effects. The negative excess volume values of the mixture are indicative of molecular interactions and positive values suggests less interactions between the unlike components of the liquid mixture. This can be explained by considering the following facts: i) in an ideal solution there is no interaction between the component molecules, *i.e.*, volumes are just additive and $V_m^E = 0$, ii) but in the case of real solutions due to the existence of interactions (attractive or repulsive) amongst the component molecules either contraction or expansion in the volume takes place on mixing, *i.e.*, volumes are not additive and $V_m^E \neq 0$. Thus the final volume after mixing becomes less than that of the ideal solution due to molecular interactions amongst the dissimilar components, *i.e.*, $V_m^E < 0$. On the contrary disruption of molecular order of the pure components increases the volume of the mixture and the final volume becomes more than that of the ideal solution, *i.e.*, $V_m^E > 0$.

2.5. Partial Molar Volume

The thermodynamic approach, based on the concept of partial properties was proposed in order to determine the effect of each component and their concentration on thermodynamic state properties like volume, enthalpy, entropy, Gibb's free energy, *etc.* They are extensive properties and depend upon the mass (number of moles). In a

Theoretical Background

closed system, these parameters being a state dependent function depends upon any two of the state variables, *viz.*, pressure, temperature and volume of a system of fixed composition. But in an open system of variable composition (*e.g.*, liquid system) containing two or more components, where the interchange of matter occurs with its surroundings undergo a change of composition (number of moles). Therefore, the total value of any extensive property is not only a function of T and P , but also of the actual number of moles of each species present in the system. Thus for a multi-component system a thermodynamic state function Y can be expressed as follows:^{37,38}

$$Y = f(T, P, n_1, n_2, n_3, \dots) \quad (2)$$

The net change in this property (dY) at constant temperature and pressure is given by:

$$dY = \left(\frac{dY}{dn_1} \right)_{T, P, n_2, n_3, \dots} dn_1 + \left(\frac{dY}{dn_2} \right)_{T, P, n_1, n_3, \dots} dn_2 + \dots \quad (3)$$

The term $(dY/dn_i)_{T, P, n_{j \neq i}}$ is called the partial molar property of the i^{th} component and is usually denoted by putting a bar over the symbol of thermodynamic property, *i.e.*, $\bar{Y}_{m,i} = (dY/dn_i)_{T, P, n_2, n_3, \dots}$. Thus it can be defined as the rate at which the property Y changes with the amount of the i^{th} species added to the mixture keeping temperature, pressure and the amount of all other species constant. Partial molar quantities are intensive properties and are related to the changes in extensive properties of the solution (such as V , G , H , S and A) to the concentration changes. Of all the extensive thermodynamic properties, the volume is easiest to visualize. Taking Y as volume rearrangement of Eq. (3) gives:

$$dV = \left(\frac{dV}{dn_1} \right)_{T, P, n_2, n_3, \dots} dn_1 + \left(\frac{dV}{dn_2} \right)_{T, P, n_1, n_3, \dots} dn_2 + \dots \quad (4)$$

$$\text{or } dV = \bar{V}_{m,1} dn_1 + \bar{V}_{m,2} dn_2 + \dots \quad (5)$$

where $\bar{V}_{m,1}$ and $\bar{V}_{m,2}$ are the partial molar volume of component 1 and 2, respectively.

In the molecular level, it is seen that the solute-solvent interaction or solvation also has some influence on partial molar volume. For instance the partial molar volume of lithium ion is negative. In fact such strange negative value of volume is a clear indication of electrostriction,³⁹ *i.e.*, strong electrostatic interaction between the lithium ion and the water molecules. Thus the partial molar volume includes some significant

Theoretical Background

information regarding the solute-solvent interactions in solution. Integration of Eq. (5) gives the Euler relation indicating that partial molar quantities are additive and yields:

$$V = \bar{V}_{m,1}n_1 + \bar{V}_{m,2}n_2 + \dots \quad (6)$$

For an ideal solution, the total volume is just the sum of the molar volume of the components in a mixture and is given by:

$$V = V_{m,1}^*n_1 + V_{m,2}^*n_2 + \dots \quad (7)$$

where $V_{m,1}^*$ and $V_{m,2}^*$ are the molar volumes of components 1 and 2, respectively. In case of ideal solutions, the partial molar volume of each component will be identical to their molar volume in the absence of the other component. However, in the case of non-ideal solutions, the presence of the second component has a measurable influence on the molar volume of the first component and *vice versa*, i.e., $\bar{V}_{m,1} \neq V_{m,1}^*$ and $\bar{V}_{m,2} \neq V_{m,2}^*$. So for non-ideal mixtures total volumes are not just additive but are actually smaller (volumetric contraction) or larger (volumetric dilatation). Thus partial molar volume of a component is not equal to its molar volume in such cases. The partial molar volumes of component vary with composition of the mixture because the molecular environment of each molecule changes (i.e., packing, solvation, etc.) and the molecular interactions are well reflected by these properties. This is illustrated below in Figure 2.6 for water-ethanol system⁴⁰ at 20 °C across all possible composition.

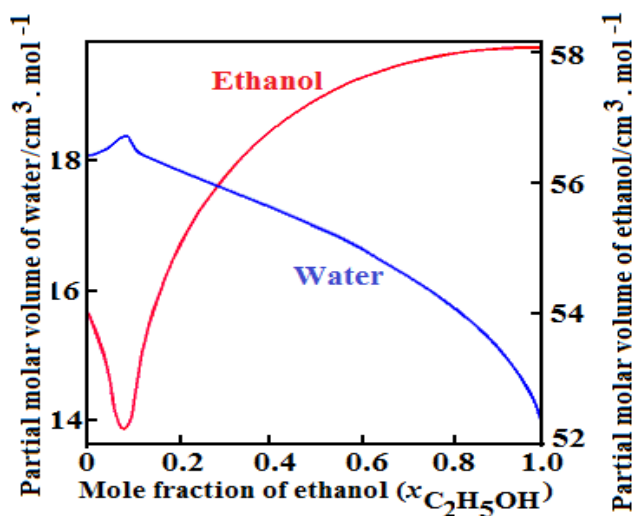


Fig. 2.6. Partial molar volumes of water and ethanol in aqueous ethanol at 20 °C.

Theoretical Background

Thus the partial molar volume is of fundamental importance in understanding the molecular interactions in the liquid mixtures of variable compositions. However, the application of Eq. (6) requires an accurate knowledge of the partial molar volumes of each component at a given concentration. The partial molar volumes $\bar{V}_{m,1}$ and $\bar{V}_{m,2}$ of component 1 and 2, respectively in a binary mixture at the experimental temperature can be had from the excess molar volumes (V_m^E) using the following relations:⁴¹⁻⁴⁹

$$\bar{V}_{m,1} = V_m^E + V_{m,1}^* + x_2 \left(\frac{\partial V_m^E}{\partial x_1} \right)_{T,P} \quad (8)$$

$$\bar{V}_{m,2} = V_m^E + V_{m,2}^* + x_1 \left(\frac{\partial V_m^E}{\partial x_1} \right)_{T,P} \quad (9)$$

To determine the partial molar volumes ($\bar{V}_{m,1}$ and $\bar{V}_{m,2}$) generally an analytical method is used⁵⁰ by fitting the excess molar volumes (V_m^E) to a suitable polynomial in mole fraction and then the necessary derivative $(\partial V_m^E / \partial x_1)_{T,P}$ is found analytically. Regarding this the excess molar volumes (V_m^E) are generally fitted to the Redlich-Kister polynomial:⁵¹

$$Y^E = V_m^E = x_1 x_2 \sum_{i=0}^j a_i (1 - 2x_2)^i \quad (10)$$

where Y^E , x_1 , x_2 are the excess or deviation properties, mole fractions of the component 1 and 2, respectively and a_i represents the multiple-regression coefficients and the corresponding standard deviation (σ) is given by the relation:

$$\sigma = \left[\sum_{i=1}^n (V_{m,\text{expt}}^E - V_{m,\text{calc}}^E)^2 / (n - p) \right]^{1/2} \quad (11)$$

where n is the number of experimental points and p is the number of coefficients (a_i), which can be optimised by the method of least squares regression following Marquardt algorithm.⁵² The $V_{m,\text{Calc}}^E$ values are obtained from Eq. (10) using the best-fit values of the coefficients (a_i) and small values of standard deviation (σ) indicate that Eq. (10) fits the data well for a mixture at the experimental temperature. The derivative, $(\partial V_m^E / \partial x_1)_{T,P}$ used in Eq.(8) and Eq.(9) can be obtained⁵³ by differentiating Eq. (10) with respect to x_1 and when this derivative is substituted in Eq. (8) and (9) the following relations for $\bar{V}_{m,1}$ and $\bar{V}_{m,2}$ are obtained:

Theoretical Background

$$\bar{V}_{m,1} = V_{m,1}^* + x_2^2 \sum_{i=0}^j a_i (1 - 2x_1)^i - 2x_1 x_2^2 \sum_{i=1}^j a_i (1 - 2x_1)^{i-1} \quad (12)$$

$$\bar{V}_{m,2} = V_{m,2}^* + x_1^2 \sum_{i=0}^j a_i (1 - 2x_1)^i + 2x_1^2 x_2 \sum_{i=1}^j a_i (1 - 2x_1)^{i-1} \quad (13)$$

The excess partial molar volumes ($\bar{V}_{m,1}^E$ and $\bar{V}_{m,2}^E$) were evaluated by using the following relations:^{47,48}

$$\bar{V}_{m,1}^E = \bar{V}_{m,1} - V_{m,1}^* \quad (14)$$

$$\bar{V}_{m,2}^E = \bar{V}_{m,2} - V_{m,2}^* \quad (15)$$

The excess partial molar volumes at infinite dilution ($\bar{V}_{m,i}^{0,E}$) can be determined from the relation:

$$\bar{V}_{m,i}^{0,E} = (\partial V_m^E / \partial x_i)_{x_i=0, T, P} \quad (16)$$

The excess partial molar volumes ($\bar{V}_{m,i}^{0,E}$) at infinite dilution are of fundamental importance since they provide insight into the solute–solvent interactions, because at infinite dilution the solute–solute interactions are negligible.⁵⁴

2.6. Viscosity Deviation

Viscosity is not a thermodynamic property but a transport property and refers to a fluid's resistance to flow to shear stress. Knowledge of viscosity of pure liquids and liquid mixtures is of significant importance for practical and theoretical purposes, especially for chemical engineering and industrial purposes such as heat and mass transfer operations and pipeline flow applications, *etc.* For liquid mixtures the viscosity of the system mainly depends on the temperature and the composition of the liquid mixture and thus eventually leads to a better understanding of the structure of liquids as well as molecular interactions in liquid mixtures. The viscosity deviation ($\Delta\eta$) can be expressed by the difference between the measured viscosity (η) and the ideal viscosity (η_{id}) of a mixture and is given by:^{43,46,55-60}

$$\Delta\eta = \eta - \eta_{id} \quad (17)$$

Using the Eyring's approach of viscosity as a rate process⁶¹ η_{id} can be defined as:

$$\eta_{id} = \exp\left(\sum_{i=1}^n x_i \ln \eta_i\right) \quad (18)$$

Theoretical Background

where n is the number of the components in the mixture and η_i is the viscosity of the i^{th} component in the mixture and the additivity law in a logarithm form is considered for ideal mixtures. Ideal viscosity (η_{id}) of a mixture can also be expressed on the basis of additivity of mole fraction average of component viscosities as follows:

$$\eta_{\text{id}} = \sum_{i=1}^n x_i \eta_i \quad (19)$$

According to Kauzman and Eyring,⁶² the viscosity of a liquid mixture depends on the entropy of the mixture, which in turn is related to liquid structure and enthalpy. Thus viscosity is related to the molecular interactions between the unlike components of the mixture. Therefore, the viscosity deviation is a function of molecular interactions, the size and shape of molecules involved. Vogel and Weiss⁶³ established that the positive $\Delta\eta$ values suggest the presence of specific intermolecular interactions amongst the unlike molecules resulting into more compact structure. On the contrary, negative $\Delta\eta$ values⁶⁴ suggest the easier flow of liquid mixture as compared with the pure liquids. This may be due to difference in size and shape of mixing components, dispersion due to breaking of liquid order that involves breaking of hydrogen bond, dipole-dipole specific interactions, *etc.*, on mixing with the second component and the formation of unfavourable non-specific interaction amongst the dissimilar molecules of the mixture. Alternatively the terms ‘viscous synergy’ and ‘viscous antagonism’ are also used to present the viscosity deviation. Generally viscous synergy is the term applied to the interaction between the component molecules of a mixture that causes the total viscosity of the system to be greater than the sum of the viscosities of individual components considered separately.^{65,66} In contraposition to viscous synergy, viscous antagonism is the term used in respect to the interaction between the components of a system that cause the overall viscosity of the mixture to be less than the sum of the viscosities of the individual components in the system.⁶⁷ If the total viscosity of the system is equal to the sum of the viscosities of each component considered separately, the system is said to lack interaction.^{65,66} Eventually this method compares the experimentally obtained viscosity with the calculated viscosity in the absence of interaction. When $\eta_{\text{exp}} > \eta_{\text{cal}}$, it is referred to as ‘viscous synergy’ and when $\eta_{\text{exp}} < \eta_{\text{cal}}$, it is referred to as ‘viscous antagonism’.

Theoretical Background

2.7. Thermodynamics for Viscous Flow

2.7.1. Excess Gibb's Free Energy of Activation of Viscous Flow

The viscosity of a liquid or a liquid mixture imparts resistance to flow and in laminar flow the component molecules flowing must attain a definite amount of energy called the free energy of activation of flow per mole. In general, higher the free energy of activation of flow, more viscous is the liquid. Eyring⁶⁸ proposed a simple theory of liquid in which he suggested that the viscous flow in liquid involves the migration of molecules from a lattice site into nearby hole from which it can move to another site. Thus some work is required to create the hole against the potential barrier. Therefore, the process is analogous to chemical reaction proceeding through a transition state. The absolute reaction rate approach of Eyring^{10,61,69} provides the following expression which correlates the viscosity to the energy required for a molecule to overcome the attractive force field of its neighbour so that it can flow:

$$\eta V_m = Nh \exp\left(\frac{\Delta G^*}{RT}\right) \quad (20)$$

or,

$$\Delta G^* = RT \ln\left(\frac{\eta V_m}{Nh}\right) \quad (21)$$

where ΔG^* is the molar Gibb's free energy of activation for the viscous flow required to move the molecules within the fluid from their energetically most favourable state to the activated state and the other quantities V_m , N , h , R and T are the molar volume of the mixture, Avagadro's number, Plank constant, universal gas constant and the absolute temperature, respectively. In principle Eq. (20) can be used either for a pure liquid or a liquid mixture. For a liquid mixture the molar Gibb's free energy of activation of viscous flow (ΔG^*) can be regarded as the sum of an ideal contribution and a correction or excess term, *i.e.*,

$$\Delta G^* = \Delta G^{*,id} + \Delta G^{*E} \quad (22)$$

where ΔG^{*E} stands for the excess free energy of activation of viscous flow per mole and $\Delta G^{*,id}$ is the ideal mixture contribution under the same condition of temperature, pressure and composition as for the real system per mole and is given by:

Theoretical Background

$$(\eta V_m)^{id} = Nh \exp\left(\frac{\Delta G^{*,id}}{RT}\right) \quad (23)$$

or,

$$\Delta G^{*,id} = RT \ln \frac{(\eta V_m)^{id}}{Nh} \quad (24)$$

A combination of Eqs. (21), (22) and (24) yields to the expression:

$$RT \ln\left(\frac{\eta V_m}{Nh}\right) = RT \ln \frac{(\eta V_m)^{id}}{Nh} + \Delta G^{*E} \quad (25)$$

On rearrangement Eq. (25) yields:

$$\Delta G^{*E} = RT \left[\ln(\eta V_m) - \ln(\eta V_m)^{id} \right] \quad (26)$$

The term $\ln(\eta V_m)^{id}$ for n-component liquid mixture is given by:⁶¹

$$\ln(\eta V_m)^{id} = \sum_{i=1}^n x_i \ln(\eta_i V_{m,i}) \quad (27)$$

and

$$\Delta G^{*E} = RT \left[\ln(\eta V_m) - \sum_{i=1}^n x_i \ln(\eta_i V_{m,i}) \right] \quad (28)$$

According to Mayer,⁷⁰ ΔG^{*E} may be considered as a reliable measure to detect the presence of interaction between the molecule and its magnitude represents the strength of interaction between unlike molecules.^{71,72} The positive value of excess Gibbs free energy of activation of viscous flow suggests the presence of specific and strong interactions in the systems under investigation.⁷³⁻⁷⁶ It also suggests the size effect of the mixing components.⁷⁷ On the contrary negative values of ΔG^{*E} may be attributed to the dominance of dispersion forces.⁷⁸

2.7.2. Viscous Entropy and Enthalpy

Further, the molar entropy (ΔS^*) and molar enthalpy (ΔH^*) of viscous flow are related to Gibbs free energy of activation for viscous flow (ΔG^*) by the following relation:

$$\Delta G^* = \Delta H^* - T\Delta S^* \quad (29)$$

Combination of Eqs. (20) and (29) leads to the following expression:

$$R \ln\left(\frac{\eta V}{Nh}\right) = \left(\frac{\Delta H^*}{T}\right) - \Delta S^* \quad (30)$$

Theoretical Background

Therefore a plot of $R \ln(\eta V / Nh)$ against $1/T$ gives a straight line⁷⁹⁻⁸² with a slope equal to ΔH^* and the intercept equal to ΔS^* . The enthalpy of activation of viscous flow provides valuable information regarding the degree of collaboration between the species taking part in viscous flow.⁸³ It depends upon the intermolecular interactions as well as geometrical effect.⁸³⁻⁸⁵ For a highly structured liquid, a large heat of activation is generally required for collaborative flow. Thus the positive value of ΔH^* suggests the presence of molecular interactions between the unlike component molecules and *vice versa*. On the contrary the negative values of ΔS^* indicates the formation of activated complex leading to molecular order due to interactions between the two components of a mixture.⁸⁶

2.8. Ultrasonic Speed of Sound

Ultrasonics, being a sub-category of acoustics, deals with acoustics beyond the frequency range 20 kHz and for ultrasound the range is from 20 kHz to 10 MHz and has been proved a useful tool for obtaining information about the dynamics of liquid systems. Ultrasound needs a medium to propagate and hence different from electromagnetic waves. It is an oscillating sound pressure wave with a frequency greater than the upper limit of the human hearing range. It can also be defined by its frequency, speed and amplitude or intensity like any other wave. It is approximately sub-divided into three main regions, *viz.*, low frequency ultrasound (20-100 KHz), intermediate frequency ultrasound (100 KHz-1 MHz) and high frequency ultrasound (1-10 MHz). The range from 20 KHz to about 1 MHz is used in sonochemistry, *i.e.*, application of ultrasound for the chemical reactions and processes, whereas frequencies far above 1MHz are used in medical diagnosis.

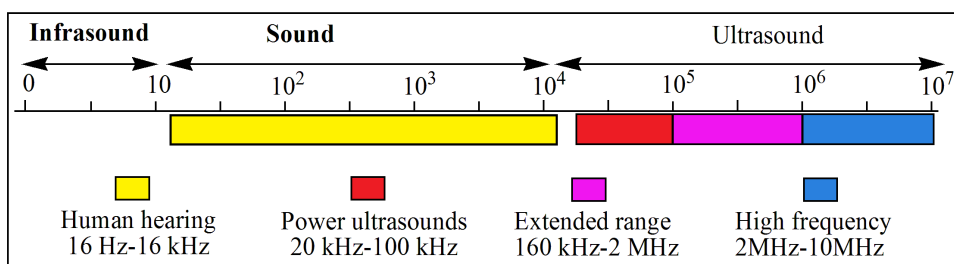


Fig. 2.7. Spectrum of acoustics.

Experimental determination of ultrasonic speeds of sound in various media such as liquids, liquid mixtures, electrolyte solutions, suspensions, polymers, *etc.*, has been

Theoretical Background

found to be an effective means for examining certain physical properties of the media.⁸⁷⁻⁹⁴ The speed of such sound wave varies depending on the medium through which it is traveling and is affected by the medium's density and elastic properties. These experimental data and thermodynamic properties derived from them are found to be the property sensitive to different kinds of association in pure liquid and liquid mixtures.⁹⁵ These properties are of fundamental interest for the researchers to study the physico-chemical behaviour and molecular interactions in liquid mixtures. They are required for the design of industrial plants, pipelines, pumps, *etc.* Different researcher⁹⁶⁻¹¹⁵ have investigated and extensively used acoustic properties of liquid mixtures to obtain the important information about the molecular interactions operating among the component molecules and their physical behaviour. In order to understand the specific molecular interactions in the mixtures various thermodynamic parameters based on the speeds of sound can be derived. Some of these significant acoustic parameters of mixture are discussed below:

2.8.1. Isentropic Compressibility

Ultrasonic investigation is very useful to understand the behaviour of liquid systems. In fluid mechanics, compressibility is a measure of the relative volume change of a fluid as response to a pressure change. The isentropic condition means that when the sound wave passes through a liquid medium the entropy remains constant although the pressure and temperature fluctuate within each microscopic volume. Thus the isentropic compressibility is the fractional decrease of volume per unit increase of pressure when no heat flows in or out and is affected by intra-molecular and inter-molecular association, complex formation and related structural changes. The speed of sound at low frequencies can be measured precisely.^{116,117} The condition of low frequency is important because at high frequencies (>100 MHz), there is a dispersion and absorption of sound wave couples with molecular processes within the liquid.¹¹⁸⁻¹²⁰ So at frequencies where dispersion is not important, the determination of ultrasonic speed of the pure liquid and liquid mixtures enables the accurate determination of isentropic compressibilities (κ_s) through the following Newton-Laplace equation:^{120,121}

$$\kappa_s = (u^2 \rho)^{-1} \quad (31)$$

Theoretical Background

where ρ , u are the experimental density and the ultrasonic speed of sound of the liquid system.

2.8.2. Excess Isentropic Compressibility

According to Rowlinson *et al.*¹²¹ the speed of sound (u) defined by Eq. (31) is a thermodynamic quantity. The excess isentropic compressibilities (κ_S^E) can be had from the relation:

$$\kappa_S^E = \kappa_S - \kappa_S^{\text{id}} \quad (32)$$

where the isentropic compressibility for the ideal mixture (κ_S^{id}) and for a liquid mixture with n components at the absolute temperature T is given by:^{122, 123}

$$\kappa_S^{\text{id}} = \sum_{i=1}^n \phi_i \left[\kappa_{S,i} + \frac{TV_i \alpha_i^2}{c_{P,i}} \right] - T \left(\sum_{i=1}^n x_i V_i \right) \left(\sum_{i=1}^n \phi_i \alpha_i \right)^2 / \left(\sum_{i=1}^n x_i c_{P,i} \right) \quad (33)$$

where x_i , V_i , $\kappa_{S,i}$, α_i and $c_{P,i}$ are the mole fraction, the molar volume, the isentropic compressibility, the isobaric thermal expansion coefficient and the molar heat capacity of the i^{th} pure component in the mixture, respectively. The volume fraction (ϕ_i) of the i^{th} component in the mixture is given by:

$$\phi_i = x_i V_i / \sum_{i=1}^n x_i V_i \quad (34)$$

The excess isentropic compressibility and their sign play a vital role in deciding the molecular compactness in the liquid mixtures. The negative κ_S^E values generally arise as a consequence of two effects, *viz.*, an interaction contribution and a free volume contribution.¹²⁴ As far as the interaction part is concerned, the interactions may be dipole-dipole, dipole-induced dipole, charge transfer, hydrogen bond type which enhance the ordered structure in the mixture yielding negative contribution^{64,125,126-128} to κ_S^E values. The free volume contribution¹²⁴ involves the interstitial accommodation of the molecules of one component into the structure of another. However, positive κ_S^E values are indicative of weak interactions due to dispersion forces coming into play.⁶⁴

2.8.3. Intermolecular Free Length (L_f)

Intermolecular free length (L_f) is the distance between the surfaces of the neighbouring molecules. This property is mainly dependent on the forces between the

Theoretical Background

molecules and has been extensively used to study the molecular interactions in the liquids and liquid mixtures. In the year 1951, Jacobson¹²⁹⁻¹³¹ suggested that the adiabatic compressibility of a liquid can be understood in terms of the intermolecular free length and suggested an empirical relation for the liquid mixture:

$$L_f = K(\kappa_s)^{\frac{1}{2}} \quad (35)$$

where K is a temperature dependent Jacobson's constant. It has been observed that the decrease in intermolecular free length leads to positive deviation in speeds of sound and negative deviation in compressibility. Therefore, the negative L_f values indicate molecular interactions among the component molecules in mixture whereas the positive L_f values indicate the weak interaction due to dispersion forces operating in the mixture. The excess intermolecular free length (L_f^E) can be computed using the expression:

$$L_f^E = L_f - \sum_i^n x_i L_{f,i} \quad (36)$$

where L_f is the intermolecular free length of the mixture; x_i and $L_{f,i}$ are the mole fraction and the intermolecular free length of the i^{th} pure component in the mixture, respectively. According to Fort and Moore,¹²⁵ the positive L_f^E values indicate the dispersion force and negative L_f^E values suggest the molecular interactions due to charge transfer and hydrogen bond interactions in the mixtures.

2.8.4. Specific Acoustic Impedance (z_{im})

Acoustic impedance indicates how much sound pressure is generated by the vibration of molecules of a particular acoustic medium at a given frequency. It is given by the equation:¹³²

$$z_{im} = u\rho \quad (37)$$

and the excess acoustic impedance of a n-component mixture is given by:

$$z_{im}^E = z_{im} - \sum_i^n x_i z_{im,i} \quad (38)$$

Literature survey^{133,134} have shown that negative z_{im}^E values suggest the presence of dispersion force or weak interactions between the unlike component molecules and positive z_{im}^E values suggest the structure making effect or intermolecular interaction between the component molecules in mixture.¹³⁴⁻¹³⁷

Theoretical Background

2.8.5. Free Volume (V_f)

Free volume is one of the important properties that describe the difference in the physiochemical properties of liquids and liquid mixtures. The free space has close connection with the molecular structure and show remarkable features about the interactions when two or more liquids are mixed together. These molecular interactions are influenced by structural arrangements along with shape and size of the molecules involved. A liquid may be treated as if it were composed of individual molecules each moving in a volume V_f in an average potential due to its neighbour or in other words the molecules are not closely packed and there are some free space between the molecules for free movement and is called the free volume.⁶¹ Eyring and Kincaid¹³⁸ defined the free volume as the effective volume in which particular molecule of a liquid can move and obey perfect gas laws. Suryanarayana *et al.*¹³⁹ obtained a relation for free volume (V_f) in terms of speeds of sound (u) and the viscosity of the liquid (η) as follows:

$$V_f = (M_{\text{eff}}u/k_a\eta)^{\frac{3}{2}} \quad (39)$$

and excess free volume (V_f^E) for a n-component mixture is given by:

$$V_f^E = V_f - \sum_i^n x_i V_{f,i} \quad (40)$$

where M_{eff} is the effective molecular weight ($M_{\text{eff}} = \sum M_i x_i$), in which M_i and x_i are the molecular weight and the mole fraction of the i^{th} component in the mixture, respectively. k_a is a temperature independent constant equal to 4.28×10^9 for all liquids. The negative V_f^E values suggests that the component molecules in the mixture are more close together than in the pure liquids and thus suggests that the presence of strong attractive interactions between component molecules such as hydrogen bond, dipole-dipole interactions, *etc.*¹³⁵ However, positive V_f^E values point out to a loose packing^{133,136,140-142} of molecules in the mixtures.

2.8.6. Internal Pressure (π_{in})

The internal pressure is a cohesive force that is actually the resultant of attractive and repulsive forces between the interacting molecules in a mixture.^{143,144} Internal pressure also gives an idea of the solubility characteristics. Dissolved solutes

Theoretical Background

exist under the internal pressure of the medium and their interactions with the solvent arises through hydrogen bonding, charge transfer, van der Waals interaction, *etc.* It varies due to all types of solvent-solute, solute-solute and solvent-solvent interactions. Thus the internal pressure data are highly useful in understanding and establishing the nature of the molecular interactions between the unlike components of a liquid mixture. Suryanarayana *et al.*¹³⁹ derived an expression for the determination of internal pressure on the basis of the statistical thermodynamics using the free volume concept and is expressed as:

$$\pi_{\text{in}} = b_c RT (k_a \eta / u)^{\frac{1}{2}} \left(\rho^{\frac{1}{3}} / M_{\text{eff}}^{\frac{7}{6}} \right) \quad (41)$$

$$\pi_{\text{in}}^{\text{E}} = \pi_{\text{in}} - \sum_i^n x_i \pi_{\text{in},i} \quad (42)$$

where b_c stands for the cubic packing factor and is assumed to be 2 for all liquids and liquid mixtures. According to van der Waals equation,¹⁴⁵ internal pressure (a/V^2) is a measure of the attractive force and is inversely proportional to the square of the total volume. So if there is contraction in the volume due to specific molecular interactions or interstitial accommodation of one molecule into other owing to difference in their size, free volume, *etc.*, the internal pressure will be high. Similarly if there is expansion in volume due to destruction of molecular packing the internal pressure will be low. Thus it is clear that high π_{in} values indicate strong molecular interaction and low π_{in} values indicate loose packing of the component molecules in the mixture.^{133-136,142}

2.9. Refractive Index

The refractive index (n_D) of a liquid is an important additive physical property and its measurement is expected to shed some light on the solvent-solvent interactions and configuration of their mixtures.¹⁴⁶⁻¹⁴⁹ Also its theoretical and empirical correlation to density, surface tension, dielectric permittivity and excess molar volume of multi-component mixtures can provide important information on intermolecular interactions. Therefore this property has been used to study the structure and the molecular interactions among the component molecules of the liquid mixtures. The refractive index (n_D) is the ratio of angle of incident to the angle of refraction. Stated

Theoretical Background

more simply, the refractive index describes the ability to refract light as it passes from one medium to another medium. Thus higher the refractive index (n_D), more is the light refracted.¹⁵⁰ The extent of refraction depends on the relative concentration and the structure of the component molecules. So refractive index (n_D) can give an idea about the geometry and the structure of molecules.

2.9.1. Deviation in Refractive Index (Δn_D)

The deviation in refractive index correlates well with the excess molar volumes and can be obtained using the relation defined as:¹⁵¹

$$\Delta n_D = n_D - n_D^{\text{id}} \quad (43)$$

The ideal refractive index (n_D^{id}) of a mixture can be defined on a volume fraction (ϕ_i) basis but it is usually defined on a mole fraction basis (x_i), *i.e.*, for a binary mixture:

$$n_D^{\text{id}} = \sum_{i=1}^2 \phi_i n_{D,i} \quad (44)$$

or,

$$n_D^{\text{id}} = \sum_{i=1}^2 x_i n_{D,i} \quad (45)$$

According to Iglesias-Otero *et al.*,¹⁵² the ideal refractive index (n_D^{id}) for a binary mixture can also be had from the relation:

$$n_D^{\text{id}} = \left[\frac{(n_{D,1})^2 (n_{D,2})^2 + 2\phi_1 (n_{D,1})^2 + 2\phi_2 (n_{D,2})^2}{2 + \phi_1 (n_{D,2})^2 + \phi_2 (n_{D,1})^2} \right]^{\frac{1}{2}} \quad (46)$$

where $n_{D,i}$ and ϕ_i are the refractive index and volume fraction of the i^{th} pure component in the mixture under experimental temperature and pressure. As stated by Deetlefs *et al.*,¹⁵³ the refractive index of a substance is higher when its molecules are more tightly packed or in general when the compound is denser. This indicates that more is the molecular interactions denser is the liquid, more is the refractive index. This can be followed from the calculated values of the deviation in refractive indices, *i.e.*, positive Δn_D values attribute to strong solvent-solvent interactions and negative Δn_D values indicate weak solvent-solvent¹⁵⁴ interactions.

Theoretical Background

2.9.2. Molar Refraction (R_m) and Excess Molar Refraction (R_m^E)

Excess properties are defined for thermodynamic variables only.¹⁵⁵ Since molar refraction is a volumetric property, the notation R_m^E for excess molar refraction is quite acceptable provided the reference state used for its calculation is a thermodynamically ideal mixture.¹⁵⁶ The molar refraction (R_m) of a mixture can easily be calculated using the experimental refractive indices (n_D) from the Lorentz-Lorentz equation:^{146,150,157, 158}

$$R_m = \left[\frac{n_D^2 - 1}{n_D^2 + 2} \right] V_m \quad (47)$$

and the molar volume of the mixture (V_m) is defined as follows:

$$V_m = \frac{M}{\rho} = \sum_{i=1}^n \frac{x_i M_i}{\rho} \quad (48)$$

where n_D is the refractive index of the mixture. Therefore, excess molar refraction (R_m^E) can be had from the relation:

$$R_m^E = R_m - R_m^{\text{id}} \quad (49)$$

Fermeglia and Torri-ano¹⁵⁹ defined excess molar refraction (R_m^E) on mole fraction basis, while it is defined on the basis of volume fraction¹⁶⁰ by some authors. The ideal molar refraction (R_m^{id}) for n-component mixture can be defined by the following relation:¹⁶¹

$$R_m^{\text{id}} = \sum_{i=1}^n \left[\frac{(n_{D,i}^2 - 1)M_i}{(n_{D,i}^2 + 2)\rho_i} \right] \phi_i \quad (50)$$

where the symbols have their usual meanings as defined above. The positive R_m^E values indicate that the dispersion forces are higher in the mixtures than in the pure liquids, whereas negative R_m^E values indicate the presence of interactions between the unlike components in the mixture.¹⁶² Excess molar refractions give more information than Δn values about the mixture phenomenon, because it takes into account the electronic perturbation of molecular orbital during the mixing process.¹⁶³

2.10. Predictive Models

On the contrary to solids and gases, there exists no simple theory/model for the liquids for explaining their behaviour. This fact can be attributed partly to: i) the

Theoretical Background

mobility of the molecules in liquids like gases and partly to ii) short-range attractive and repulsive forces between the molecules resulting in limited volume. Again closeness of the molecules or molecular packing in liquids decreases with a rise in temperatures till it behaves like a compressed gas at a particular condition of temperature and pressure. However, a comparison of the experimental data of multi-component mixtures with those calculated by means of various predictive or correlative models is very useful from the points of view: (i) it suggests which model is more appropriate to characterize the system, (ii) it may indicate which parameters should be improved and (iii) it may allow the identification of some model as a convenient reference for the interpretation of the deviations in the observed properties. Correlative models generally contain adjustable parameters or coefficients determined by fitting experimental data to these models. Predictive models on the contrary use the dependence of molecular properties on some physical parameter or *vice-versa*. Predictive models can be semi-empirical or empirical. Semi-empirical models are developed on some theoretical basis and requires limited experimental data but empirical models require huge experimental data to develop itself.

2.10.1. Excess Molar Volume Models

There are several empirical models that can simulate the excess molar volumes for the liquid mixtures like Peng-Robinson cubic equation of state,¹⁶⁴ Flory's theory¹⁴⁻¹⁷ and Prigogine-Flory-Patterson^{165,166} model. Empirical methods have also been developed using the corresponding state principle based on van der Waals hypothesis.¹⁶⁷ Some of them are described briefly below:

2.10.1.1. Cubic Equation of State

Cubic equations of state (CEOS) are well focused because of their widespread use and simple form. Basically cubic equations of state are those equations that on expanding are cubic in volume or cubic in compressibility factor. These equations are modified forms of the van der Waals equation of state¹⁶⁸ and were the first equation to predict vapour-liquid coexistence. To improve the accuracy, Redlich and Kwong¹⁶⁹ (1949) modified this equation by introducing temperature dependence for the attractive term. Later, Soave¹⁷⁰ (1972) and Peng and Robinson¹⁶⁴ (1976) proposed further modifications to calculate more accurately the vapour pressure, liquid density and equilibrium ratio. These equations of state are widely used in the design and analysis of industrial processes for the calculation and prediction of the properties of

Theoretical Background

fluid and fluid mixtures.¹⁷¹ This is due to the fact that they offer a balance between accuracy, reliability, simplicity and speed of computation. In addition, they have the advantage of representing multiple phases and multi-component mixtures using the same model. At the beginning these equations of state were used only for the mixtures of non-polar (Soave, 1972; Peng and Robinson, 1976) and for slightly polar compounds [Huron *et al.*¹⁷² (1978); Asselineau *et al.*¹⁷³ (1978); Graboski and Daubert¹⁷⁴ (1978)]. Equation of states involving two constants can be expressed by the general form as suggested by Schmidt and Wenzel:¹⁷⁵

$$P = \frac{RT}{V_m - b} - \frac{a(T)}{V_m^2 + ubV_m + wb^2} \quad (51)$$

With different values of u and w , most of the well known cubic equations of state can be reproduced. For instance Peng-Robinson equation of state is reproduced if we take $u = 2$ and $w = -1$. Although there are many equations of state, Peng-Robinson equation of state (PREOS) was used for the mixtures studied herein this dissertation to predict and correlate the excess molar volumes and viscosity deviations for the selected liquid mixtures.

2.10.1.2. Peng-Robinson Equation of State

This equation was developed during the 1970s anticipating that the parameters a and b should be expressible in terms of the critical properties and acentric factor and should provide reasonable accuracy near the critical point, particularly for the calculation of compressibility factor and liquid density. Peng and Robinson introduced the following modified van der Waals EOS:¹⁶⁴

$$P = \frac{RT}{V_m - b} - \frac{a}{V_m(V_m + b) + b(V_m - b)} \quad (52)$$

For a pure component the attractive parameter a and co-volume parameters b are given by the following relations:

$$a = a(T) = a(T_c) \left[1 + \xi \left(1 - \sqrt{\frac{T}{T_c}} \right) \right]^2 \quad (53)$$

$$b = b(T) = b(T_c) \quad (54)$$

$$a(T_c) = 0.45724 R^2 T_c^2 / P_c \quad (55)$$

$$b(T_c) = 0.07780 RT_c / P_c \quad (56)$$

Theoretical Background

where T_c and P_c are critical temperature and pressure of the pure components. The parameter ξ in terms of acentric factor (ω)¹⁷⁶ is defined by:

$$\xi = 0.37464 + 1.54226\omega - 0.26992\omega^2 \quad (57)$$

In addition, the Peng-Robinson equation can be extended to liquid mixtures also by obtaining the mixture parameters. This is commonly achieved by using mixing or combining rules that relates the properties of the pure components to that of the mixture. Therefore, application of this equation of state to mixtures containing n-components with composition (x_i) requires the evaluation of parameters a and b using some mixing rules.¹⁷⁷ Most commonly used relations are as follows:

$$a(T) = \sum_{i=1}^n \sum_{j=1}^n x_i x_j a_{ij} \quad (58)$$

$$a_{ij} = \sqrt{a_i a_j} (1 - k_{ij}) \quad (59)$$

$$b(T) = \sum_{i=1}^n x_i b_i \quad (60)$$

The parameter k_{ij} is the binary interaction coefficient characterizing the binary formed by components i and j . This coefficient is zero for $i = j$; for $i \neq j$ it is close to zero. This binary interaction coefficient takes into account the difference in the interaction of unlike molecules. This equation of state can be used to calculate the excess molar volume of the mixture. To make the calculation easy the cubic equations of state are often expressed in terms of compressibility factor. Therefore, on rearrangement Peng-Robinson equation of state [Eq. (52)] in terms of the compressibility factor (Z) becomes:

$$Z^3 - (1 - B)Z^2 + (A - 3B^2 - 2B)Z - (AB - B^2 - B^3) = 0 \quad (61)$$

$$\text{where } Z = \frac{PV}{RT}, \quad B = \frac{Pb}{RT} \quad \text{and} \quad A = \frac{aP}{(RT)^2}$$

Thus from a knowledge of the compressibility factors of the pure components and their mixtures, the excess molar volumes can be calculated by calculating the corresponding molar volume of the pure components and their mixtures with the optimized value of k_{ij} . The molar volume of the pure components and their mixtures are therefore calculated in terms of the compressibility factors as:

Theoretical Background

$$V_1 = \frac{Z_1 RT}{P} \quad (62)$$

$$V_2 = \frac{Z_2 RT}{P} \quad (63)$$

$$V_m = \frac{Z_m RT}{P} \quad (64)$$

where Z_1 , Z_2 and Z_m are the compressibility factors of the component 1, the component 2 and the mixture, respectively. Using these calculated compressibility factors, the excess molar volume of the mixtures of variable compositions can be had from the relation:

$$V_m^E = \frac{Z_m RT}{P} - \left(\frac{x_1 Z_1 RT}{P} + \frac{x_2 Z_2 RT}{P} \right) \quad (65)$$

The correlating ability of this model can be judged from the standard deviation [Eq. (11)] between the experimental and the calculated excess molar volumes. The smaller value of standard deviation represents the best fit.

2.10.1.3. Flory Theory

Flory *et al.*,^{14,15} dealing particularly with mixtures suitable for non-polar molecules of different size and shape, formulated a partition function. In this theory, the PVT variables are all expressed in reduced form and the properties of the liquid mixtures are expressed in terms of the characteristic parameter of the pure component and an energy parameter characteristic of molecular interactions in the mixture. Prediction of excess properties can be made by evaluating these parameters. A simple van der Waals type model was found to be suitable.^{14,15} The resulting reduced equation of state from the partition function in terms of Flory's notation is expressed as:

$$\frac{\tilde{P}\tilde{v}}{\tilde{T}} = \frac{\tilde{v}^{1/3}}{\tilde{v}^{1/3} - 1} - \frac{1}{\tilde{v}\tilde{T}} \quad (66)$$

and the reduced pressure (\tilde{P}), volume (\tilde{v}) and temperature (\tilde{T}) are given by:

$$\tilde{P} = \frac{P}{P^*} \quad (67)$$

$$\tilde{v} = \frac{v}{v^*} = \frac{V}{V^*} \quad (68)$$

$$\tilde{T} = \frac{T}{T^*} \quad (69)$$

Theoretical Background

Extending this treatment with an assumption of random mixing of the two species to the binary mixtures, the mean intermolecular energy was shown to be equal to $P^* v^* / \tilde{v}$, where v^* represents the characteristic volume of the mixture and the characteristic pressure P^* of the mixture is given by:

$$P^* = \phi_{s,1} P_1^* + \phi_{s,2} P_2^* - \phi_{s,1} \theta_2 \chi_{12} \quad (70)$$

where θ_2 , $\phi_{s,i}$ and P_i^* represents the molecular site fraction for the component 2, segment or hardcore volume fraction and characteristic pressure of the i^{th} components in the mixture and χ_{12} is the interaction energy parameter characteristic of the system and it is a measure of the dissimilarity of the interaction energy between the unlike pair and the mean of the like pairs. This parameter is a constant at a given temperature and is independent of the composition for the system involving spherical and similar sized non polar molecules.^{178,179} The site fractions, θ_i for the i^{th} component is defined as:

$$\theta_2 = 1 - \theta_1 = - \frac{\phi_{s,2}}{\phi_{s,2} + \phi_{s,1} (v_2^*/v_1^*)^{\frac{1}{3}}} \quad (71)$$

and the segment fraction, $\phi_{s,i}$ of the i^{th} component for nearly spherical molecules is given by:

$$\phi_{s,2} = 1 - \phi_{s,1} = - \frac{x_2 v_2^*}{x_1 v_1^* + x_2 v_2^*} \quad (72)$$

where v_1^* and v_2^* are the characteristic volume of the component 1 and 2, respectively. The characteristic pressure (P_i^*), volume (v_i^*) and temperature (T_i^*) of the pure liquids can be related with their physical properties through Eq. (66) by putting $P = 0$.

$$P_i^* = \frac{\alpha_i}{\kappa_{T,i}} T \tilde{v}_i^2 \quad (73)$$

$$v_i^* = \frac{V_i}{\tilde{v}_i} \quad (74)$$

$$T_i^* = \frac{T_i}{\tilde{T}_i} = \frac{T \tilde{v}_i^{4/3}}{\tilde{v}_i^{1/3} - 1} \quad (75)$$

where $\kappa_{T,i}$ is the isothermal compressibility of the i^{th} component and can be evaluated using the relation:

$$\kappa_{T,i} = \kappa_{s,i} + \frac{T \alpha_i^2 V_i}{c_{p,i}} \quad (76)$$

Theoretical Background

According to Flory's theory, the excess molar volume can be evaluated from the following relation:

$$V_m^E = \tilde{v}^E \sum_i^n (x_i v_i^*) \quad (77)$$

where \tilde{v}^E represents the reduced excess volume per segment and is defined as:

$$\tilde{v}^E = \tilde{v} - \tilde{v}_0 \quad (78)$$

\tilde{v}_0 in the above equation represents the reduced volume per segment. For an ideal liquid mixture:

$$\tilde{v}_0 = \sum_i^k (\phi_{s,i} \tilde{v}_i) \quad (79)$$

Therefore, the actual expression for the excess molar volume for the mixture can be obtained by combining Eq. (77) to Eq. (79) as:

$$V_m^E = \left(\tilde{v} - \sum_i^n (\phi_{s,i} \tilde{v}_i) \right) \sum_i^n (x_i v_i^*) \quad (80)$$

2.10.1.4. Prigogine-Flory-Patterson (PFP) Theory

The Flory theory was proposed to account for the major discrepancies in the lattice theory, which failed to account for the volume changes and changes in local disorder with composition. This one parameter theory was basically installed for explaining the thermodynamic properties of hydrocarbon mixtures and then extended to non-polar molecules of varied shape and size. This theory treats excess thermodynamic properties to be sum of three contributions: i) a combinatorial term, ii) an interactional term and iii) a free volume function. Anyway, in the recent years Prigogine-Flory-Patterson (PFP) theory,^{165,166} a modified version of Flory's statistical theory^{14,15,17,180} has been successfully employed to estimate and analyze excess thermodynamic functions of non-electrolyte liquid mixture¹⁸⁰⁻¹⁸² theoretically. This theory is the first successful theoretical approach of an equation of states model for polymer solutions and is a van der Waals like theory based on the corresponding state. The use of this theory requires the knowledge of isobaric coefficient of thermal expansion (α), isothermal compressibility (κ_T) and Flory's parameters (already defined in the previous section). This theory considers the excess molar volume (V_m^E) of binary mixtures to be the sum of three contributions: (i) the interactional

Theoretical Background

contribution, $V_{m,(int)}^E$, which is proportional to the interaction parameter, $\chi_{1,2}$; (ii) the free volume contribution, $V_{m,(fv)}^E$, which arises from the dependence of the reduced volume upon the reduced temperature as a result of the difference between the degree of thermal expansion of the two components; and (iii) the internal pressure contribution, $V_{m,(P^*)}^E$, which depends both on the differences of the characteristic pressures and on the differences of reduced volumes of the components. The expressions for these three contributions are:

$$V_{m,(int)}^E = \frac{(\tilde{v}^{1/3} - 1)\tilde{v}^{2/3}\psi_1\theta_2}{[(4/3)\tilde{v}^{-1/3} - 1]P_1^*} \chi_{1,2} \quad (81)$$

$$V_{m,(fv)}^E = \frac{(\tilde{v}_1 - \tilde{v}_2)^2[(14/9)\tilde{v}^{-1/3} - 1]\psi_1\psi_2}{[(4/3)\tilde{v}^{-1/3} - 1]\tilde{v}} \quad (82)$$

$$V_{m,(P^*)}^E = \frac{(\tilde{v}_1 - \tilde{v}_2)(P_1^* - P_2^*)\psi_1\psi_2}{(P_1^*\psi_2 + P_2^*\psi_1)} \quad (83)$$

Thus the excess molar volume (V_m^E) is given as:

$$\frac{V_m^E}{x_1V_1^* + x_2V_2^*} = V_{m,(int)}^E - V_{m,(fv)}^E + V_{m,(P^*)}^E \quad (84)$$

$$\text{or} \quad \frac{V_m^E}{x_1V_1^* + x_2V_2^*} = \frac{(\tilde{v}^{1/3} - 1)\tilde{v}^{2/3}\psi_1\theta_2}{[(4/3)\tilde{v}^{-1/3} - 1]P_1^*} \chi_{1,2} - \frac{(\tilde{v}_1 - \tilde{v}_2)^2[(14/9)\tilde{v}^{-1/3} - 1]\psi_1\psi_2}{[(4/3)\tilde{v}^{-1/3} - 1]\tilde{v}} + \frac{(\tilde{v}_1 - \tilde{v}_2)(P_1^* - P_2^*)\psi_1\psi_2}{(P_1^*\psi_2 + P_2^*\psi_1)} \quad (85)$$

where ψ_i is the contact energy fraction for the pure i^{th} component and is calculated using the relation:

$$\psi_1 = 1 - \psi_2 = \frac{\phi_{s,1}P_1^*}{\phi_{s,1}P_1^* + \phi_{s,2}P_2^*} \quad (86)$$

θ_i and $\phi_{s,i}$ for the i^{th} components in mixture has already been defined in the previous section, Eq. (71) and (72). The other symbols have their usual meaning. The first term on the right hand side of Eq. (85) represents the interactional contribution (χ_{12}), second term represents the \tilde{v} contribution and the last term represents the P^* contribution. In order to compute V_m^E from Eq. (85), the interactional energy parameter χ_{12} is required. This can be evaluated by fitting the experimental V_m^E

Theoretical Background

values of each composition for each system to Eq. (85). The calculation is carried out using a computer program that finally provides an optimized value of the interaction parameter $\chi_{1,2}$ with least error. Among the calculated values of the interaction coefficients (χ_{12}), the value with the minimum standard deviation is taken into consideration to calculate the excess molar volume of the mixture. The estimating ability of this model can be judged from the standard deviations [Eq. (11)] between the experimental and the calculated V_m^E values using this model.

2.11. Viscosity Models

Several empirical models can simulate the viscosity of liquids or liquid mixtures and practical implications of such viscosity models were reviewed by Mehrotra *et al.*¹⁸³ The viscosity of the different systems studied were predicted using Peng-Robinson cubic equation of state¹⁶⁴ and Bloomfield–Dewan model.¹⁸⁴ Apart from these models several semiempirical relations have been put forward to correlate the viscosity of binary liquid mixtures in terms of their pure component data.

2.11.1. Model Based on Eyring's Theory Coupled with a Cubic Equation of State:

A viscosity model based, on Eyring's theory coupled with Peng-Robinson cubic equation of state for non-ideal liquid mixtures, is used to correlate and estimate the liquid viscosity of non-ideal liquid mixtures at experimental temperature and different compositions. The estimating ability of this model can be judged from the standard deviations between the experimental and calculated viscosities. Macias-Salinas *et al.*¹⁸⁵ developed a model based on Eyring's theory coupled with a cubic equation of state to suitably correlate and predict the liquid viscosities of the non-ideal binary solutions over a wide range of temperature, pressure and compositions and is given by:

$$\eta = \frac{(\eta V)^{\text{id}}}{V_m} \exp\left(\frac{\Delta G^{*E}}{RT}\right) \quad (87)$$

where $(\eta V)^{\text{id}}$ and ΔG^{*E} are the kinematic viscosity of an ideal solution and excess activation free energy of flow, respectively which can be expressed as:

$$(\eta V)^{\text{id}} = \exp\left[\sum_{i=1}^n x_i \ln(\eta_i V_i)\right] \quad (88)$$

Theoretical Background

In order to incorporate the binary interaction parameter g_{12} ($g_{ii} = 0$ and $g_{ij} = g_{ji}$), ΔG^{*E} for a binary mixture is given as:

$$\frac{\Delta G^{*E}}{RT} = \frac{\Delta G^E}{RT} + \frac{1}{2} \sum_{i=1}^n \sum_{j=1}^n x_i x_j g_{ij} \quad (89)$$

$$\text{and } g_{ii} = 0 \text{ and } g_{ij} = g_{ji}$$

For a binary mixture it takes the form:

$$\frac{\Delta G^{*E}}{RT} = \frac{\Delta G^E}{RT} + x_1 x_2 g_{12} \quad (90)$$

where g_{12} is the binary interaction parameter. Its value can be obtained by non-linear regression analysis and optimized by comparing the experimental viscosity data with those produced from Eq. (87). The value of ΔG^E , the excess Gibbs free energy of the mixture was calculated using the relation:

$$\frac{\Delta G^E}{RT} = \sum_{i=1}^n x_i (\ln \varphi_i - \ln \varphi_i^o) \quad (91)$$

where φ_i^o and φ_i are the fugacity coefficient of the pure component and that of the i^{th} component in the mixture, respectively. As per PREOS, fugacity coefficient of a pure component and that of the i^{th} component in the mixture are given by:

$$\ln \varphi = (Z - 1) - \ln(Z - B) - \frac{A}{2\sqrt{2}B} \ln \left(\frac{Z + (1 + \sqrt{2})B}{Z + (1 - \sqrt{2})B} \right) \quad (92)$$

$$\begin{aligned} \ln \varphi_i &= \frac{b_i}{b} (Z - 1) - \ln(Z - B) \\ &- \frac{A}{2\sqrt{2}B} \left(\frac{2}{a} \sum_{j=1}^n x_j (a_i a_j)^{\frac{1}{2}} (1 - k_{ij}) - \frac{b_i}{b} \right) \ln \left(\frac{Z + (1 + \sqrt{2})B}{Z + (1 - \sqrt{2})B} \right) \end{aligned} \quad (93)$$

Combining Eq. (87) to Eq. (91), the final expression for the mixture viscosity is as follows:

$$\eta = \frac{(\eta V)^{\text{id}}}{V_m} \exp \left[\sum_{i=1}^n x_i (\ln \varphi_i - \ln \varphi_i^o) + \frac{1}{2} \sum_{i=1}^n \sum_{j=1}^n x_i x_j g_{ij} \right] \quad (94)$$

2.11.2. Bloomfield-Dewan Viscosity Model:

It combines two major semi-empirical theories of liquid viscosities in order to assess viscosity deviation of liquid mixtures. The first one is the absolute reaction rate theory¹⁸⁰ that relates the viscosity to the free energy required by a molecule to

Theoretical Background

overcome the attractive force field of its neighbours in order to jump to a new equilibrium position, *i.e.*, to flow. The second one is the free volume theory^{186,187} that relates the viscosity to the probability of occurrence of an empty neighbouring site into which a molecule can jump and the probability depends exponentially on the free volume of the liquid. Thus the probability of viscous flow has been considered as a product of the probabilities of acquiring sufficient activation energy and the occurrence of an empty site. All the thermodynamic quantities involved in Bloomfield-Dewan model can be calculated using the equation of states of Flory^{14,15,17,180} without numerical adjustment, already discussed in section 2.10.1.4. Bloomfield and Dewan¹⁸⁴ proposed the following expression for the viscosity of the mixture as:

$$\Delta \ln \eta = f(\tilde{v}) - \frac{\Delta G^R}{RT} \quad (95)$$

$$\text{where, } \Delta \ln \eta = \ln \eta - \sum_{i=1}^2 (x_i \eta_i) \quad (96)$$

and $f(\tilde{v})$ is the characteristic function of the free volume and is defined as:

$$f(\tilde{v}) = \frac{1}{\tilde{v} - 1} - \sum_{i=1}^2 \frac{x_i}{\tilde{v}_i - 1} \quad (97)$$

ΔG^R is the residual free energy of mixing and can be calculated using the relation¹⁸⁸ as:

$$\Delta G^R = \Delta G^E + RT \sum_{i=1}^2 x_i \ln(x_i / \phi_{s,i}) \quad (98)$$

where $\phi_{s,i}$ is the segment fraction of the i^{th} component in a binary mixture. The excess energy ΔG^E can be obtained from the Flory's statistical theory of liquid mixtures^{15,17} by using the relation:

$$\begin{aligned} \Delta G^E = & \sum_{i=1}^2 x_i P_i^* V_i^* [(1/\tilde{v}_i - 1/\tilde{v}) + 3\tilde{T}_i \ln\{(\tilde{v}_i^{1/3} - 1)/(\tilde{v}^{1/3} - 1)\}] \\ & + (x_1 \theta_2 V_1^* \chi_{12}) / \tilde{v} \end{aligned} \quad (99)$$

Using the χ_{12} values from fitting values of V_m^E and the values of the parameters for the pure liquid components, ΔG^E , $f(\tilde{v})$ and finally $\Delta \ln \eta$ can be calculated and compared with the experimental viscosity to test the estimating ability of the model by calculating the standard deviations.

2.12. Viscosity Correlative Models

These models involve interaction parameters (one or more) generally obtained by employing some optimization technique. These models require some experimental data in order to establish the value of an interaction parameter and have specific values for each mixture at the defined temperature and pressure. Several empirical and semi-empirical relations have been proposed to evaluate and correlate dynamic viscosity (η) as well as kinematic viscosities ($\nu = \eta\rho^{-1}$) and to check the suitability of the equation taking into account the number of empirical adjustable coefficients. Irving^{189,190} surveyed more than fifty equations for describing the viscosity of binary liquid mixtures. Some of them are as follows:

2.12.1. Grunberg and Nissan Model:

Grunberg and Nissan¹⁹¹ suggested the following logarithmic relation between the dynamic viscosity (η) of the binary mixtures and its pure components (η_i):

$$\ln \eta = x_1 \ln \eta_1 + x_2 \ln \eta_2 + x_1 x_2 d_{12} \quad (100)$$

where d_{12} represents Grunberg-Nissan interaction parameter that reflects the non-ideal behaviour and strength of the molecular interactions between the component molecules of the mixture. Its value may be positive or negative depending upon the liquid mixture. Generally a positive d_{12} value suggests the presence of strong interactions and negative value suggests the presence of weak interaction between the components molecules in the mixture. This equation can be extended to ternary and quaternary systems as represented by the following Eqs. (101) and (102):

$$\ln \eta = x_1 \ln \eta_1 + x_2 \ln \eta_2 + x_3 \ln \eta_3 + x_1 x_2 x_3 d_{123} \quad (101)$$

$$\ln \eta = x_1 \ln \eta_1 + x_2 \ln \eta_2 + x_3 \ln \eta_3 + x_4 \ln \eta_4 + x_1 x_2 x_3 x_4 d_{1234} \quad (102)$$

In 1998 Canosa¹⁹² proposed an extension of Grunberg-Nissan equation to the ternary system by introducing a ternary adjustable parameter and is given by:

$$\ln \eta = \sum_i^n x_i \ln \eta_i + \sum_i^n \sum_{j>i}^n x_i x_j d_{ij} + \sum_i^n \sum_{j>i}^n \sum_{n>j}^n x_i x_j x_k d_{ijn} \quad (103)$$

2.12.2. Tamura and Kurata Model:

Tamura-Kurata¹⁹³ have provided the following equation for the dynamic viscosity of binary mixtures:

Theoretical Background

$$\eta = \sum_{i=1}^n x_i \phi_i \eta_i + \sum_{i=1}^n \sum_{j=1}^n (x_i x_j \phi_i \phi_j)^{0.5} T_{ij} \quad (104)$$

$$\text{and } T_{ij} \neq T_{ji}; j \neq i$$

In this equation, the notations are same as in the earlier equations. Additionally ϕ_i and ϕ_j are the volume fractions of the components i and j in the mixture. The interaction coefficient T_{ij} is constant at a chosen temperature and it follows similar kind of temperature dependence as pure liquid viscosity.

2.12.3. Hind Model:

Hind *et al.*¹⁹⁴ suggested the following dynamic viscosity model for the calculation of the viscosity of binary mixtures:

$$\eta = x_1^2 \eta_1 + x_2^2 \eta_2 + 2x_1 x_2 H_{12} \quad (105)$$

where H_{12} is Hind interaction parameter, generally attributed to unlike pair interactions¹⁹⁵ and for ternary mixtures,¹⁹⁴ the model is as follows:

$$\eta = \sum_i x_i^2 \eta_i + \sum_i \sum_{j>i} x_i x_j H_{ij} + \sum_i \sum_{j>i} \sum_{n>j} x_i x_j x_k H_{ijn} \quad (106)$$

2.12.4. Heric-Brewer Model:

Heric–Brewer¹⁹⁶ proposed two parameter model of the following form:

$$\ln \eta = x_1 \ln \eta_1 + x_2 \ln \eta_2 + x_1 \ln M_1 + x_2 \ln M_2 - \ln(x_1 M_1 + x_2 M_2) + x_1 x_2 [\vartheta_{12} + \vartheta_{21}(x_1 - x_2)] \quad (107)$$

where M_1 and M_2 are the molecular weights of component 1 and 2; ϑ_{12} and ϑ_{21} are interaction parameters which can be calculated from the least squares method.

2.12.5. McAllister Models:

McAllister¹⁹⁷ suggested a model based on Eyring's theory of absolute reaction rate to correlate the kinematic viscosities of the liquid mixtures. He considered the interactions to involve activated jumps of molecules between layers of molecules in the velocity gradient and the molecular motion was treated as if the molecules were undergoing a chemical reaction with a potential barrier to overcome. On the basis of the three-body model, McAllister derived the following formula for the kinematic viscosity (ν) of the liquid mixtures:

Theoretical Background

$$\begin{aligned} \ln \nu = & x_1^3 \ln \nu_1 + x_2^3 \ln \nu_2 + 3x_1^2 x_2 \ln \nu_{12} + 3x_2^3 x_1 \ln \nu_{21} - \ln \left[x_1 + x_2 \frac{M_2}{M_1} \right] \\ & + 3x_1^2 x_2 \ln \left[\frac{2}{3} + \frac{M_2}{3M_1} \right] + 3x_2^2 x_1 \ln \left[\frac{1}{3} + \frac{2M_2}{3M_1} \right] + x_2^3 \ln \left[\frac{M_2}{M_1} \right] \end{aligned} \quad (108)$$

If the ratio of the molecular weights (M_1/M_2) = 1, the last four terms vanish. The equation has two interaction coefficients ν_{12} and ν_{21} ; which can be determined from the viscosity-composition data of the mixture. Similarly, the McAllister four-body model is defined by the relation:

$$\begin{aligned} \ln \nu = & x_1^4 \ln \nu_1 + x_2^4 \ln \nu_2 + 4x_1^3 x_2 \ln \nu_{1112} + 6x_1^2 x_2^2 \ln \nu_{1122} + 4x_1 x_2^3 \ln \nu_{2221} \\ & - \ln \left[x_1 + x_2 \frac{M_2}{M_1} \right] + 3x_1^2 x_2 \ln \left[\frac{(3 + M_2 / M_1)}{4} \right] + 6x_1^2 x_2^2 \ln \left[\frac{(1 + M_2 / M_1)}{2} \right] \end{aligned} \quad (109)$$

where ν_{1112} , ν_{1122} , and ν_{2221} are model coefficients and these have to be determined from viscosity-composition data. All these parameters are temperature dependent.

2.12.6. Katti-Chaudhri Model:

Katti-Chaudhri¹⁹⁸ proposed the following relation:

$$\ln(V\eta) = x_1 \ln(\eta_1 V_1) + x_2 \ln(\eta_2 V_2) + x_1 x_2 \left(\frac{W_{vis}}{RT} \right) \quad (110)$$

where W_{vis} is interaction energy for activation of viscous flow.

2.12.7. Lobe Model:

The Lobe Equation¹⁹⁹ involves the volume fraction of the components ϕ_1 and ϕ_2 and is given by:

$$\nu = \phi_1 \nu_1 \exp \left[\phi_2 \tau_{12} \ln \left(\frac{\nu_2}{\nu_1} \right) \right] + \phi_2 \nu_2 \exp \left[\phi_1 \tau_{21} \ln \left(\frac{\nu_2}{\nu_1} \right) \right] \quad (111)$$

where ν_1 , ν_2 , τ_{12} and τ_{21} are the kinematic viscosities of the component 1, component 2 and interaction coefficients, respectively.

2.12.8. Krishnan-Laddha Model:

Krishnan-Ladda²⁰⁰ model is based on Eyring's theory of absolute reaction rate and is given by:

$$\begin{aligned} \ln \nu = & x_1 \ln \nu_1 + x_2 \ln \nu_2 + x_1 \ln M_1 + x_2 \ln M_2 - \ln(x_1 M_1 + x_2 M_2) \\ & - 2.303 x_1 x_2 \{ a + b(x_1 - x_2) + c(x_1 - x_2)^2 \} \end{aligned} \quad (112)$$

where a , b and c are the model coefficients.

2.13. Other Correlative Models

Several empirical models,^{201,202} correlative as well as predictive models suggested by different researchers can be used to estimate the experimental binary ternary and quaternary properties. For this purpose the Redlich-Kister⁵¹ polynomial [Eq. (10)] has been used to correlate the excess or deviation properties of binary mixtures (already discussed in section 2.5) and Cibulka polynomial²⁰³ has been used for the ternary and quaternary excess or deviation properties. For the ternary mixtures, Cibulka polynomial equation is as follows:

$$X_{123}^E = X_{\text{Bin}}^E + x_1 x_2 x_3 (c_1 + c_2 x_1 + c_3 x_2 + \dots) \quad (113)$$

and for the quaternary mixtures, it has the following form:

$$X_{1234}^E = X_{\text{Bin}}^E + x_1 x_2 x_3 x_4 (c_1 + c_2 x_1 + c_3 x_2 + c_4 x_3 + \dots) \quad (114)$$

where X_{123}^E and X_{1234}^E are the excess or deviation properties for the ternary and quaternary systems, respectively. The term X_{Bin}^E is the sum of the corresponding binary excess or deviation properties expressed as:

$$X_{\text{Bin}}^E = X_{12}^E + X_{13}^E + X_{23}^E \quad (\text{for ternary mixtures}) \quad (115)$$

$$X_{\text{Bin}}^E = X_{12}^E + X_{13}^E + X_{14}^E + X_{23}^E + X_{24}^E + X_{34}^E \quad (\text{for quaternary mixtures}) \quad (116)$$

The adjustable ternary and quaternary Cibulka coefficients (c_i) are essential for the calculation of the theoretical excess or deviation properties and can be obtained by least-squares analysis.

2.14. Predictive Symmetric and Asymmetric Models for Ternary and Quaternary Systems

Several predictive empirical models (symmetrical and asymmetrical) have been proposed to predict the ternary excess or deviation properties by utilizing the experimental binary data. Originally some of these models were suggested to predict some specific properties like excess molar enthalpy, Gibbs free energy, *etc.* However, they are applicable to other excess or deviation properties²⁰⁴ and they consider only binary contributions into account. In this dissertation the excess molar volumes and the viscosity deviations were predicted and compared with corresponding experimental values.

Theoretical Background

2.14.1. Symmetrical Models

2.14.1.1. Köhler Model:

Köhler²⁰⁵ expressed the excess or deviation properties for a ternary mixture as:

$$X_{123}^E = (x_1 + x_2)^2 X_{12}^E[x_1^0, x_2^0] + (x_1 + x_3)^2 X_{13}^E[x_1^0, x_3^0] + (x_2 + x_3)^2 X_{23}^E[x_2^0, x_3^0] \quad (117)$$

where X_{ij}^E is the excess or deviation property for the binary mixture at binary composition x_i^0 and x_j^0 , such that $x_i^0 = 1 - x_j^0 = x_i / (x_i + x_j)$, x_i and x_j refers to ternary compositions. When extended for quaternary mixture it takes the form:

$$\begin{aligned} X_{1234}^E = & (x_1 + x_2)^2 X_{12}^E[x_1^0, x_2^0] + (x_1 + x_3)^2 X_{13}^E[x_1^0, x_3^0] \\ & + (x_1 + x_4)^2 X_{14}^E[x_1^0, x_4^0] + (x_2 + x_3)^2 X_{23}^E[x_2^0, x_3^0] \\ & + (x_2 + x_4)^2 X_{24}^E[x_2^0, x_4^0] + (x_3 + x_4)^2 X_{34}^E[x_3^0, x_4^0] \end{aligned} \quad (118)$$

and it considers six binary contributions (X_{ij}^E) with similar definition of composition as given for Eq. (117).

2.14.1.2. Jacob-Fitzner Model:

The Jacob-Fitzner model²⁰⁶ for expressing the excess or deviation properties of a ternary mixture is given by:

$$\begin{aligned} X_{123}^E = & \frac{x_1 x_2 X_{12}^E[x_1^0, x_2^0]}{(x_1 + \frac{x_3}{2})(x_2 + \frac{x_3}{2})} + \frac{x_1 x_3 X_{13}^E[x_1^0, x_3^0]}{(x_1 + \frac{x_2}{2})(x_3 + \frac{x_2}{2})} \\ & + \frac{x_2 x_3 X_{23}^E[x_2^0, x_3^0]}{(x_2 + \frac{x_1}{2})(x_3 + \frac{x_1}{2})} \end{aligned} \quad (119)$$

where $x_i^0 = 1 - x_j^0 = (1 + x_i - x_j) / 2$. When extended for quaternary mixtures, it takes the form:

$$\begin{aligned} X_{1234}^E = & \frac{x_1 x_2 X_{12}^E[x_1^0, x_2^0]}{(x_1 + \frac{x_3}{2})(x_2 + \frac{x_4}{2})} + \frac{x_1 x_3 X_{13}^E[x_1^0, x_3^0]}{(x_1 + \frac{x_2}{2})(x_3 + \frac{x_4}{2})} \\ & + \frac{x_1 x_4 X_{14}^E[x_1^0, x_4^0]}{(x_1 + \frac{x_2}{2})(x_4 + \frac{x_3}{2})} + \frac{x_2 x_3 X_{23}^E[x_2^0, x_3^0]}{(x_2 + \frac{x_1}{2})(x_3 + \frac{x_4}{2})} \\ & + \frac{x_2 x_4 X_{24}^E[x_2^0, x_4^0]}{(x_2 + \frac{x_1}{2})(x_4 + \frac{x_3}{2})} + \frac{x_3 x_4 X_{34}^E[x_3^0, x_4^0]}{(x_3 + \frac{x_1}{2})(x_4 + \frac{x_2}{2})} \end{aligned} \quad (120)$$

and it considers six binary contributions (X_{ij}^E) with similar definition of composition as given for Eq. (119).

2.14.1.3. Colinet Model:

Colinet²⁰⁷ expressed the ternary excess or deviation properties as follows:

Theoretical Background

$$X_{123}^E = 0.5 \left[\begin{array}{l} x_2 X_{12}^E[x_1, 1-x_1]/(1-x_1) + x_1 X_{12}^E[1-x_2, x_2]/(1-x_2) \\ + x_3 X_{13}^E[x_1, 1-x_1]/(1-x_1) + x_1 X_{13}^E[1-x_3, x_3]/(1-x_3) \\ + x_3 X_{23}^E[x_2, 1-x_2]/(1-x_2) + x_2 X_{23}^E[1-x_3, x_3]/(1-x_3) \end{array} \right] \quad (121)$$

This symmetrical model considers six binary contributions (X_{ij}^E) with compositions as defined within third braces.

2.14.1.4. Rastogi model:

Rastogi *et al.*²⁰⁸ suggested the equation:

$$X_{123}^E = 0.5 \left[\begin{array}{l} (x_1 + x_2) X_{12}^E[x_1^0, x_2^0] + (x_1 + x_3) X_{13}^E[x_1^0, x_3^0] \\ + (x_2 + x_3) X_{23}^E[x_2^0, x_3^0] \end{array} \right] \quad (122)$$

where the three binary contributions (X_{ij}^E) have similar definition of composition as given for Eq. (117).

2.14.2. Asymmetrical Models

2.14.2.1. Tsao-Smith model:

Tsao-Smith²⁰⁹ for ternary system is expressed as:

$$X_{123}^E = \frac{x_2}{(1-x_1)} X_{12}^E[x_1^0, x_2^0] + \frac{x_3}{(1-x_1)} X_{13}^E[x_1^0, x_3^0] + (1-x_1) X_{23}^E[x_2^0, x_3^0] \quad (123)$$

where X_{ij}^E is the excess or deviation property for the binary mixture at binary composition x_i^0 and x_j^0 , such that $x_i^0 = x_i$ and $x_j^0 = 1 - x_i$ for the mixtures 1-2 and 1-3 and $x_j^0 = 1 - x_i^0 = x_2 / (x_2 + x_3)$ for the mixture 2-3.

2.14.2.2. Toop Model:

Toop²¹⁰ proposed the equation of the form:

$$X_{123}^E = \frac{x_2}{(1-x_1)} X_{12}^E[x_1^0, x_2^0] + \frac{x_3}{(1-x_1)} X_{13}^E[x_1^0, x_3^0] + (1-x_1)^2 X_{23}^E[x_2^0, x_3^0] \quad (124)$$

where the binary contributions (X_{ij}^E) have similar compositions as defined for Tsao-Smith model.

2.14.2.3. Scatchard Model:

Scatchard²¹¹ proposed the model in the form:

$$X_{123}^E = \frac{x_2}{(1-x_1)} X_{12}^E[x_1^0, x_2^0] + \frac{x_3}{(1-x_1)} X_{13}^E[x_1^0, x_3^0] + X_{23}^E[x_2^0, x_3^0] \quad (125)$$

Theoretical Background

where the binary contributions (X_{ij}^E) have similar compositions as defined for Tsao-Smith model.

2.14.2.4. Mathieson-Thynne Model:

Mathieson and Thynne²¹² proposed an equation of the form:

$$X_{123}^E = \frac{x_1 x_2}{x_1^0 x_2^0} X_{12}^E[x_1^0, x_2^0] + \frac{x_1 x_3}{x_1^0 x_3^0} X_{13}^E[x_1^0, x_3^0] + X_{23}^E[x_2, x_3] \quad (126)$$

where the binary contributions (X_{ij}^E) have compositions as defined as follows: $x_1^0 - x_2^0 = x_1 - x_2 - x_3 / 2$ and $x_1^0 - x_3^0 = x_1 - x_3 - x_2 / 2$.

Predictive capability of these models can be ascertained from the standard deviations (σ) between the experimental and the calculated excess or deviation properties of the mixtures at the experimental temperature.

2.15. Theoretical Estimation of Ultrasonic Speed

The experimental ultrasonic speeds of sound for the liquid mixtures can be theoretically estimated with the various empirical and semi-empirical models as suggested by different researchers. Some of these models are discussed briefly as follows:

2.15.1. Nomoto Relation (NOM):

Assuming the additivity of molar sound velocity Nomoto (NOM)²¹³ proposed the following relation:

$$u_{\text{NOM}} = \left[\frac{\sum_{i=1}^n (x_i R_i)}{\sum_{i=1}^n (x_i V_{m,i})} \right]^3 \quad (127)$$

where R_i and $V_{m,i}$ stand for the molar speed of sound and the molar volume of the i^{th} component in the mixture, respectively. R_i is given by:²¹⁴

$$R_i = V_{m,i} u_i^{\frac{1}{3}} \quad (128)$$

2.15.2 Schaaff's Collision Factor Theory (CFT):

Schaaff's collision factor theory^{215,216} yields the following relation:

$$u_{\text{CFT}} = u_{\infty} \frac{\sum_{i=1}^n (x_i S_i) \sum_{i=1}^n (x_i B_i)}{V_m} \quad (129)$$

Theoretical Background

where $u_\infty = 1600 \text{ m}\cdot\text{s}^{-1}$, S_i and B_i represent collision factor and actual volume of a molecule per mole for i^{th} pure component in the mixtures, respectively. B_i , the actual volume of the molecule per mole of component i , can be evaluated as

$$B = \frac{4}{3}\pi r^3 N_0 \quad (130)$$

where N_0 is the Avogadro's number and r is the molecular radius of the pure component. Molecular radius can be computed using the Schaaff's relation.²¹⁶

$$r = \left[\frac{3b}{16\pi N} \right]^{1/3} \quad (131)$$

where b is the van der Waals constant.

2.15.3. Impedance Dependence Relation (IDR):

The product of sound speed (u) and the density (ρ) of the mixture is termed as acoustic impedance (z_{im}) of the mixture. Hence, from the knowledge of the density and the acoustic impedance of pure components the speed of the sound in the mixture can be predicted. The relation²¹⁷ is given by:

$$u_{\text{IDR}} = \frac{\sum_{i=1}^n (x_i z_{\text{im},i})}{\sum_{i=1}^n (x_i \rho_i)} \quad (132)$$

where $z_{\text{im},i}$ stands for specific acoustic impedance for the i^{th} pure component in the mixtures.

2.15.4. Vandael Vangeal Ideal Mixture Relation (IMR):

Vandael Vangeal Ideal mixture relation²¹⁸ is given by:

$$u_{\text{IMR}} = \left[\frac{\sum_{i=1}^n (x_i M_i) \sum_{i=1}^n (x_i / M_i u_i^2)}{\sum_{i=1}^n (x_i M_i)} \right]^{1/2} \quad (133)$$

where u_i is ultrasonic speed of sound for the i^{th} pure component in the mixtures.

2.15.5. Jacobson's Free Length Theory (FLT):

Free length concept in liquid mixtures was introduced by Jacobson^{219,220} and is given by:

$$u_{\text{FLT}} = K_j / (L_f \rho^{1/2}) \quad (134)$$

where K_j is the temperature dependent Jacobson constant defined as $(93.875 + 0.375T) \times 10^{-8}$ at temperature T in Kelvin., the intermolecular free length

Theoretical Background

(L_f) in the binary mixtures is given by $L_f = 2V_a/Y_s$. Here V_a represents the available volume per mole and Y_s is the surface area per mole and may be expressed as:

$$V_a = (V_T - V_0) \quad (135)$$

$$Y_s = (36\pi NV_0^2)^{\frac{1}{3}} \quad (136)$$

Here V_0 and V_T are the molar volumes at absolute zero and at temperature T , respectively. The V_0 can be obtained from the following relation using critical temperature (T_c):

$$V_0 = V_T \left[1 - \frac{T}{T_c} \right]^{0.3} \quad (137)$$

The critical temperature (T_c) for a mixture can be taken as an additive of the mole fraction average of the T_c values of its pure components, *i.e.*,

$$T_c = \sum_i^n x_i T_{c,i} \quad (138)$$

The thermodynamic intermolecular free lengths (L_f) in the binary liquid mixtures have been calculated using the relation:

$$L_f = 2 \left[V_T - \sum_i^n x_i V_{0,i} \right] / \sum_i^n x_i V_i \quad (139)$$

The intermolecular free lengths (L_f) can also be computed using the Schaaff's relation for available volume (V_a) as given below:

$$V_a = V_T \left[1 - \frac{u}{u_\infty} \right] \quad (140)$$

where the symbols used have their usual meanings.

2.15.6. Junjie's Equation (JUN):

Junjie²²¹ proposed the following equation:

$$u_{\text{JUN}} = \frac{\sum_{i=1}^n (x_i V_i)}{\sum_{i=1}^n (x_i M_i)^{\frac{1}{2}} \left[\sum_{i=1}^n (x_i V_i / \rho_i u_i^2)^{\frac{1}{2}} \right]} \quad (141)$$

where the symbols used have their usual meanings.

2.16. Theoretical Estimation of Refractive Indices of Liquid Mixtures

There are several mixing rules to correlate the experimental refractive indices of the liquid mixtures. A comparative study can be made between the experimental and theoretically calculated refractive indices at the experimental temperatures using the different empirical/semi-empirical mixing rules and models suggested by different researchers from time to time. These mixing rules for the prediction of refractive index can be theoretically applied to the liquid mixtures. Some commonly used mixing rules used in the present dissertation are as follows:

2.16.1. Lorentz-Lorentz Relation:

The Lorentz-Lorentz relation^{222,223} for refractive index is based on the change in the molecular polarizability with volume fraction. This mixing rule is the most frequently used in the analysis of refractive index data and is expressed as:

$$\left[\frac{n_D^2 - 1}{n_D^2 + 2} \right] = \sum_i^n \frac{n_{D,i}^2 - 1}{n_{D,i}^2 + 2} \phi_i \quad (142)$$

where $n_{D,i}$ is the refractive index of the i^{th} pure component and the other symbols used have their usual meanings.

2.16.2. Gladstone-Dale Relation:

Gladstone-Dale²²⁴ proposed the following relation:

$$(n_D - 1) = \sum_i^n (n_{D,i} - 1) \phi_i \quad (143)$$

2.16.3. Arago-Biot Relation:

Arago-Biot²²⁵ suggested the following expression:

$$n_D = \sum_i^n n_{D,i} \phi_i \quad (144)$$

2.16.4. Weiner Model Relation:

Weiner model²²⁶ is given by the following expression:

$$\frac{n_D^2 - n_{D,1}^2}{n_D^2 + 2n_{D,1}^2} = \phi_2 \left[\frac{n_{D,2}^2 - n_{D,1}^2}{n_{D,2}^2 + 2n_{D,1}^2} \right] \quad (145)$$

These mixing rules are also used in the analysis of refractive indices for the ternary and quaternary systems along with binary systems in the present dissertation.

2.16.5. Eyring-John Relation:

Eyring-John²²⁷ proposed the following expression:

$$n_D = n_{D,1}\phi_1^2 + 2(n_{D,1}n_{D,2})^{\frac{1}{2}}\phi_1\phi_2 + n_{D,2}\phi_2^2 \quad (146)$$

2.16.6. Heller Relation:

Heller²²⁸ suggested the following expression:

$$\frac{n_D - n_{D,1}}{n_{D,1}} = \frac{3}{2} \left[\frac{(n_{D,2} - n_{D,1})^2 - 1}{(n_{D,2} - n_{D,1})^2 + 2} \right] \quad (147)$$

2.16.7. Eykman Relation:

The expression suggested by Eykman²²⁹ has the following form:

$$\frac{n_D^2 - 1}{n_D^2 + 0.4} = \left(\frac{n_{D,1}^2 - 1}{n_{D,1}^2 + 0.4} \right) \phi_1 + \left(\frac{n_{D,2}^2 - 1}{n_{D,2}^2 + 0.4} \right) \phi_2 \quad (148)$$

2.16.8. Newton Relation:

Newton²³⁰ suggested the following expression:

$$n_{D,1}^2 - 1 = (n_{D,1}^2 - 1)\phi_1 + (n_{D,2}^2 - 1)\phi_2 \quad (149)$$

2.17. Response Surface Model

Recently a response surface model²³¹ has been successfully utilized to determine the partial molar volume and partial molar refraction of highly interacting solutes from very dilute multi-component data alone.²³² Neither densities nor refractive indices of any of the pure component are required and also no binary information is required for such analysis. A response surface model for the total volume, $V_m(T, P, x)$, consisting of three sets of terms, viz., linear, bilinear and higher interaction terms is shown by Eq. (150) and for the partial molar volume at infinite dilution, $\bar{V}_{m,i}^0(T, P)$, is shown by Eq. (151).

$$V_m(T, P, x) = \sum_{i=1}^n \alpha_{r,i} x_i + \sum_{i=1}^{n-1} \sum_{j>i}^n \alpha_{r,ij} x_i x_j + \sum_{i=1}^{n-1} \sum_{j>i}^i \gamma_{ij} x_i x_j (x_i - x_j) \quad (150)$$

$$\bar{V}_{m,i}^0(T, P) = \alpha_{r,i} + \alpha_{r,i4} - \gamma_{r,i4} \quad (151)$$

where $\alpha_{r,i}$, $\alpha_{r,i4}$ and $\gamma_{r,i4}$ are regression coefficients and the other symbol have their usual meanings. Similarly a response surface model for the molar refraction (R_m) and

Theoretical Background

the partial molar refraction at infinite dilution ($\overline{R_{m,i}^\infty}$) are given by Eq. (152) and Eq. (153), respectively as shown below:

$$R_m(T, P, x) = \sum_{i=1}^n \beta_i x_i + \sum_{i=1}^{n-1} \sum_{j>i}^n \beta_{ij} x_i x_j \quad (152)$$

$$\overline{R_{m,i}^\infty}(T, P) = \beta_i + \beta_{i4} \quad (153)$$

where β_{ij} are the regression coefficients. This methodology works well for thermodynamic system identification at very dilute concentration range.

2.18. Standard Deviation

The numerical comparison of the correlating and predictive capability of the different models used in the present dissertation can be made by calculating the standard deviations [Eq. (11)], standard percentage deviations ($\sigma\%$)^{233,234} and percent root mean square deviation using the following expressions:

$$\sigma\% = \left[\frac{1}{n-p} \sum \left(\frac{y_{\text{exp}} - y_{\text{cal}}}{y_{\text{exp}}} \right)^2 \right]^{0.5} \quad (154)$$

where y_{exp} , y_{cal} are the experimental and calculated values of the mixture property, n and p are the number of experimental points and the number of adjustable parameters, respectively. The percent root mean square deviation (RMSD%) can be evaluated using the expression:

$$\text{RMSD}\% = 100 \times \left[\frac{1}{n} \sum \left(\frac{y_{\text{exp}} - y_{\text{cal}}}{y_{\text{exp}}} \right)^2 \right]^{0.5} \quad (155)$$

The minimum values of these parameters represent the best fit.

References

- [1] M.M. Cox, *Molecular Biology*, Palgrave Macmillan, 18 November, (2011), pp. 73.
- [2] *Intermolecular force*, Rory Adams Free High School Science Text Project Heather Williams, Version 1.2, July 7 (2001).
- [3] P. Muller, *Pure Appl. Chem.*, 66 (1994) 1077.
- [4] P.W. Atkins, *Physical Chemistry*, 6th edn., Oxford University Press, Oxford, Chap. 22, (1998).
- [5] R.J. Hunter, *Fundation of colloidal science*, 2nd edn., Oxford University Press, Oxford, (2004), pp. 533.

Theoretical Background

- [6] P.W. Atkins, *Physical Chemistry*, 6th edn., Oxford University Press, Oxford, (1993), pp. 763.
- [7] J. Israelachvili, *Intermolecular and surface Force*, Academic Press, London, (1992).
- [8] P. Atkins, J. de Paula, *Elements of Physical Chemistry*, Fifth Edition, W. H. Freeman and Company, New York, (2009), pp. 351.
- [9] Y. Marcus, *Solvent Mixtures: Properties and Selective Solvation*, Marcel Dekker, Inc., New York, Basel, (2002).
- [10] H. Eyring, *J. Chem. Phys.*, 4 (1936) 283.
- [11] B.E. Eichinger, P.J. Flory, *Trans Faraday Soc.*, 64 (1968) 2061.
- [12] B.E. Eichinger, P.J. Flory, *Trans Faraday Soc.*, 64 (1968) 2006.
- [13] B.E. Eichinger, P.J. Flory, *Trans Faraday Soc.*, 64 (1968) 2035.
- [14] P.J. Flory, *J. Am. Chem. Soc.*, 87 (1965) 1833.
- [15] P.J. Flory, A. Abe, *J. Am. Chem. Soc.*, 87 (1965) 1838.
- [16] R.A. Orwall, P.J. Flory, *J. Am. Chem. Soc.*, 89 (1967) 6814.
- [17] R.A. Orwall, P.J. Flory, *J. Am. Chem. Soc.*, 86 (1964) 3515.
- [18] G.L. Bertrand, W.E. Acree (Jr), T.E. Burhfield, *J. Solution Chem.*, 12 (1983) 327.
- [19] G.L. Bertrand, W.E. Acree (Jr), *J. Solution Chem.*, 12 (1983) 755.
- [20] J.P. O'Connell, J.M. Haile, *Thermodynamics: Fundamentals for Applications*, Cambridge University Press, New York, (2005).
- [21] I.A. McLure, J.E. Benette, A.E. Watson, *J. Phys. Chem.*, 69 (1965) 2759.
- [22] W.A. Duncan, J.P. Sheridan, F.L. Swinton, *Trans. Faraday Soc.*, 62 (1966) 1090.
- [23] W.E. Streeti, L.A.K. Stavely, *J. Chem. Phys.*, 47 (1967) 2449.
- [24] R.W. Kershaw, G.N. Makcolm, *Trans. Faraday Soc.*, 64 (1968) 323.
- [25] R.K. Nigam, P.P. Singh, *Trans. Faraday Soc.*, 65 (1969) 950.
- [26] K.R. Harris, P.J. Dunlop, *J. Chem. Thermodyn.*, 2 (1970) 813.
- [27] R. Battino, *Chem. Reviews*, 71 (1971) 5.
- [28] M.I. Aralguppi, C.V. Jadar, T. M. Aminabhavi, J.D. Ortego, S.C. Mehrotra, *J. Chem. Eng. Data* 42 (1977) 301.
- [29] P.P. Singh, R.K. Nigam, K.C. Singh, V.K. Sharma, *Thermochim. Acta*, 46 (1981) 175.
- [30] S. Yamagishi, Y. Takahshi, K. Shiba, *J. Phys. E: Sci. Instrum.*, 17 (1984) 359.
- [31] M.L. Haber, R.A. Perkins, *Fluid Phase Equilib.*, 227 (2005) 44.
- [32] M.I. Davis, *Chem. Soc. Rev.*, 22 (1993) 127.
- [33] G. Douheret, M.I. Davis, *Chem. Soc. Rev.*, 22 (1993) 43.
- [34] M.J. Blandamer, *Chem. Soc. Rev.*, 27 (1998) 73.

Theoretical Background

- [35] A.J. Treszczanowicz, O. Kiyohora, G.C. Benson, *J. Chem. Thermodyn.*, 13 (1981) 253.
- [36] V.A. Tavhane, B.A. Pataki, *Ind. J. Pure Appl. Phys.*, 22 (1984) 447.
- [37] R.P. Rastogi, R.R. Misra, *An introduction to chemical thermodynamics*, Vikash Publishing House, New Delhi, (1978).
- [38] D.N. Bajpai, *Advanced Physical Chemistry*, S. Chand and Company Ltd., 2nd edn., New Delhi, (1998).
- [39] F.J. Millero, *Chem. Rev.*, 71 (1971) 147.
- [40] W.J. Moore, *Physical Chemistry*, 2nd edn., Prentice-Hall, New Jersey, (1972).
- [41] H. Iloukhani, H.A. Zarei, *Phys. Chem. Liq.*, 46 (2008) 154.
- [42] N.V. Sastry, N.M. Vaghela, P.M. Mac, *J. Mol. Liq.*, 180 (2013) 12.
- [43] B.K. Sarkar, A. Choudhury, B. Sinha, *J. Solution Chem.*, 41 (2012) 53.
- [44] A. Pal, G. Dass, *Ind. J. Chem.*, 38 (1999) 237.
- [45] A.J. Treszczanowicz, T. Treszczanowicz, T.S. Pawlowski, T. Kasprzycka-Guttman, *J. Solution Chem.*, 33 (2004) 1049.
- [46] B. Sinha, *Phys. Chem. Liq.*, 48 (2010) 183.
- [47] G.M. Smith, H.C.V. Ness, *Introduction to Chemical Engineering Thermodynamics*. McGraw-Hill, New York, (1987).
- [48] H.A. Zarei, *J. Mol. Liq.*, 130 (2007) 74.
- [49] M. Kondaiaha, D. K. Rao, *Int. J. Res. Pure Appl. Phys.*, 3 (2013) 43.
- [50] S.I. Sandlar, *Chemical Biochemical and engineering Thermodynamics*, 4th edn., Wiley India, (2007), pp. 371.
- [51] O. Redlich, A.T. Kister, *Indus. Eng. Chem.*, 40 (1948) 345.
- [52] D.W. Marquardt, *J. Soc. Indus. Appl. Math.*, 11 (1963) 431.
- [53] A.K. Nain, *J. Solution Chem.*, 35 (2006) 1417.
- [54] I.R. Radovic, M. Lj. Kijevcanin, A.Ž. Tasic, B.D. Djordjevic, S.P. Šerbanovic, *J. Serb. Chem. Soc.*, 75 (2010) 283.
- [55] M.A. Saleh, S. Akhtar, M. S. Ahmed, *Phys. Chem. Liq.*, 44 (2006) 551.
- [56] J.A. Al-Kandary, A.S. Al-Jimaz, A.M. Abdul-Latif, *Phys. Chem. Liq.*, 47 (2009) 210.
- [57] A. Ali, M. Tariq, F. Nabi, *Ind. J. Pure Appl. Phys.*, 46 (2008) 545.
- [58] S.L. Oswal, H.S. Desai, *Fluid Phase Equilib.*, 186 (2001) 81.
- [59] E.D. Dikio1, S.M. Nelana, D.A. Isabirye, E.E. Ebenso, *Int. J. Electrochem. Sci.*, 7 (2012) 11101.
- [60] A.B. Sawant, M. Hasan, V. J. Naukudkar, *Chem. Sci. Trans.*, 2 (2013) 263.
- [61] S. Glasstone, K.J. Laidler, H. Eyring, *The theory of Rate Process*, McGraw-Hill Book Company, Inc., New York, (1941).

Theoretical Background

- [62] W. Kauzman, H. Eyring, *J. Am. Chem. Soc.*, 62 (1940) 3113.
- [63] H. Vogel, A. Weiss, *Phys. Chem. Chem. Phys.*, 86 (1982) 193.
- [64] R.J. Fort, W.R. Moore, *Trans. Faraday. Soc.*, 62 (1966) 1112.
- [65] J. Pellicer, *Sinergia Viscosa*, Valencia, Spain, October, (1997).
- [66] G. Copetti, R. Lapasin, E. R. Morris, *Proceedings of the 4th European Rheology Conference*, Seville, Spain, (1994), pp. 215.
- [67] R. Chanda, A. Banerjee, M.N. Roy, *J. Serb. Chem. Soc.*, 75 (2010) 1721.
- [68] H. Eyring, J. Hirschfelder., *J. Phys. Chem.*, 41 (1937) 249.
- [69] H. Eyring, M.S. John, *Significant Liquid Structures*, John Willey and Sons, New York, (1969).
- [70] M. Mayer, R. Mayer, *J. Chem. Phys.*, 63 (1971) 143.
- [71] P.N. Tshibangu, S.N. Ndwandwe, E.D. Dikio, *Int. J. Electrochem. Sci.*, 6 (2011) 2201.
- [72] M. Shafiq, S. Asif, M. Farooqui, *Asian J. Biochem. Pharm. Res.*, 1 (2011) 419.
- [73] T. M. Reed, T. E. Taylor, *J. Phys. Chem.*, 63 (1959) 58.
- [74] R. Meyer, M. Meyer, J. Metzger, A. Peneloux, *J. Chim. Phys.*, 62 (1971) 405.
- [75] K. Sreekanth, D.S. Kumar, M. Kondaiah, D.K. Rao, *J. Phys. B.*, 406 (2011) 854.
- [76] A.G. Peshwe, B.R. Arbad, S.P. Pachaling, *Int. J. Chem. Sci.*, 7 (2009) 1505.
- [77] S.L. Oswal, A.V. Rao, *Ind. J. Chem. Sec. A*, 24 (1985) 545.
- [78] B.J.I. Shwara, N.S. Varaprasad, *Ind. J. Pure Appl. Phys.*, 41 (2003) 275.
- [79] O. Ciocirlan, O. Iulian, *J. Serb. Chem. Soc.*, 74 (2009) 317.
- [80] A. Ali, M. Tariq, F. Nabi, *Ind. J. Pure App. Phys.*, 46 (2008) 545.
- [81] F. Corradini, L. Marcheselli, A. Marchetti, M. Tagliazucchi, L. Tassi, G. Tosi, *Bull. Chem. Soc. Jpn.*, 65 (1992) 503.
- [82] B. Sinha, R. Pradhan, S. Saha, D. Brahman, *J. Serb. Chem. Soc.*, 78 (2013) 1443.
- [83] K. Rajathi, S.J.A. Ali, A. Rajendra, *J. Chem. Pharma. Res.*, 3 (2011) 348.
- [84] V. Kannapan, R.J. Santhi, *Ind. J. Pure and Appl. Phys.*, 43 (2005) 750.
- [85] S. Bhatiya, J. Sagnwan, R. Bhatiya, *J. Mol. Liq.*, 161 (2011) 96.
- [86] S.S. Nandre, U.G. Deshpande, S.R. Patil, *J. Chem. Pharm. Res.*, 7 (2015) 328.
- [87] R. Truell, C. Elbaum, B.B. Chick, *Ultrasonic Methods in Solid State Physics*, Academic Press, New York, (1969).
- [88] J. Krautkramer, H. Krautkramer, *Ultrasonic Testing of Materials*, Springer Verlag, New York, (1969).
- [89] R.T. Beyer, S.V. Letcher, *Physical Ultrasonics*, Academic Press, New York, (1969).
- [90] K.F. Hertzfeld, T.A. Litovitz, *Absorption and Dispersion of Ultrasonic Waves*, Academic Press, New York, (1959).

Theoretical Background

- [91] V.F. Nozdrev, *The Use of Ultrasonics in Molecular Physics*, Pergamon, London, (1965).
- [92] P. Vigoureux, *Ultrasonics. Chapman and Hall Ltd.*, London, (1952).
- [93] A.B. Bhatia, *Ultrasonic Absorption*, Clarendon Press, Oxford, (1967).
- [94] A.J. Matheson, *Molecular Acoustics*, Wiley Interscience, London, (1971).
- [95] R. Azevedo, J. Szydowski, *J. Chem. Thermodyn.*, 36 (2004) 211.
- [96] O.K. Patrick, P.J.D. Arcy, G.C. Benson, *Canad. J. Chem.*, 57 (1978) 1006.
- [97] J. Nath, S.N. Dubey, *J. Phys. Chem.*, 84 (1980) 2166.
- [98] E. Rajgopal, S.V. Subrahmanyam, *Bull. Chem. Soc. Jpn.*, 54 (1981) 282.
- [99] A.M. Awaad, R.A. Pethrick, *J. Chem. Soc. Faraday Trans.*, 78 (1982) 3203.
- [100] J. Nath, A.P. Dixit, *J. Chem. Eng. Data* 29 (1984) 320.
- [101] K. Tamura, S. Murakami, S. Doi, S. Takagi, *J. Chem. Thermodyn.*, 18 (1986) 489.
- [102] G.C. Benson, C.J. Halpin, *Canad. J. Chem.*, 65 (1987) 322.
- [103] K.C. Kalra, K.C. Singh, D.C. Spah, *J. Chem. Thermodyn.*, 21 (1989) 1243.
- [104] J. Nath, M. Tewari, *J. Chem. Soc. Faraday Trans.*, 88 (1992) 2197.
- [105] D.S. Gill, T. Kaur, H. Kaur, I.M. Joshi, *J. Chem. Soc. Faraday Trans.*, 89 (1993) 1737.
- [106] V. Chakravorty, B.K. Rout, *Ind. J. Chem.*, 33 (1994) 303.
- [107] C. Lafuente, J. Pardo, J. Santafe, F.M. Royo, *J. Chem. Thermodyn.*, 27 (1995) 541.
- [108] V. Rajendran, *Ind. J. Pure Appl. Phys.*, 34 (1996) 152.
- [109] A. Pal, Y.P. Singh, *J. Chem. Thermodyn.*, 28 (1996) 143.
- [110] A. Pal, Y.P. Singh, *Ind. J. Pure Appl. Phys.*, 35 (1997) 310.
- [111] R. Palepu, B. Hawrylak, K. Gracia, *Canad. J. Chem.*, 76 (1998) 464.
- [112] J.A. Pal, S. Sharma, G. Dass, *J. Chem. Thermodyn.*, 31 (1999) 273.
- [113] H. Houkhani, J.B. Parsa, S. Azizian, *J. Chem. Eng. Data* 44 (1999) 152.
- [114] T.S. Banipal, A.P. Toor, V.K. Rattan, *Ind. J. Chem.*, 39 (2000) 809.
- [115] R. Abraham, M. Abdulkhadar, C.V. Asokan, *J. Chem. Thermodyn.*, 32 (2000) 1.
- [116] A.T.J. Hayward, *Brit. J. Appl. Phys.*, 18 (1967) 965.
- [117] A.T.J. Hayward, *J. Phys. D: Appl. Phys.*, 4 (1971) 938.
- [118] J.O. Hirschfelder, C.F. Curtis, R.B. Bird, *Molecular Theory of Gases and Liquids*, Wiley, New York, corrected printing, (1964), Chap. 5, 11.
- [119] A.T.J. Hayward, *Nature*, 221 (1996) 1047.
- [120] M.J. Blandamer, *Introduction to Chemical Ultrasonics*, Academic Press, London, (1973).
- [121] J.S. Rowlinson, F.L. Swinton, *Liquid and Liquid Mixtures*, Butterworths, London, 3rd edn., (1982), pp. 16,17.

Theoretical Background

- [122] G.C. Benson, O.K. Kiyohara, J. Chem. Thermodyn., 11 (1979) 1061.
- [123] W.E. Acree, J. Chem. Eng. Data 28 (1983) 215.
- [124] T.H. Van, D. Patterson, J. Solution Chem., 11 (1982) 793.
- [125] R.J. Fort, W.R. Moore, Trans. Faraday Soc., 61 (1965) 2102.
- [126] M. Karvo, J. Chem. Thermodyn., 15 (1986) 809.
- [127] D.S. Gill, K.N. Arora, J. Tiwari, J. Chem. Soc. Faraday Trans., 1, 84 (1988) 1729.
- [128] W. Haijum, Z. Guokang, C. Mingzhi, J. Chem Thermodyn., 25 (1993) 949.
- [129] B. Jacobson, J. Chem. Phys., 20 (1952) 927.
- [130] B. Jacobson, Acta Chem. Scand., 5 (1951) 1214.
- [131] B. Jacobson, Acta Chem. Scand., 6 (1952) 1485.
- [132] R.K. Dewan, C.M. Gupta, S.K. Mehta, Acustics, 66 (1988) 245.
- [133] K. Saravanakumar, T.G. Lavanya, T.R. Kubendran, Chem. Sci. Trans., 1 (2012) 269.
- [134] J. AsgharI, F.L.A. Khan, K. Subramani, Rasay. J. Chem., 3 (2010), 697.
- [135] R.A. Patil, P.B. Dabrase, B.M. Suryavanshi, J. Chem. Pharm. Res., 5 (2013) 745.
- [136] V.D. Bhandakkar, S. Rode, S. Jajodia, Arch. Appl. Sci. Res., 5 (2013) 12.
- [137] N. Mohanty, R. Paikaray, Res. J. Chem. Sci., 3 (2013) 71.
- [138] H. Erying, J.F. Kincaid, J. Chem. Phy., 6 (1938) 520.
- [139] C.V. Surayanarayana, T. Kuppusamy, J. Acou. Soc. Ind., 4 (1976) 75.
- [140] G.R. Bedare1, V. D. Bhandakkar, B.M. Suryavanshi, Euro. J. Appl. Eng. Sci. Res., 1 (2012) 1.
- [141] J.D. Panday, V. Sanguri, M.K. Yadav, A. Singh, Ind. J chem., 47 (2008) 1020.
- [142] G.V.R. Rao, A.V. Sharma, D. Ramachandran, C. Rambabu, Ind. J. pure Appl. Phys., 43 (2005) 602.
- [143] T.W. Richards, Chem. Rev., 2 (1925) 315.
- [144] J.D. Van der Waals, *Essay on the continuity of the gaseous and liquid States*, London, (1873).
- [145] S. Glasstone, *Thermodynamic for chemist*, D. Van Nostrand Co., Inc., New York, 62 (1947).
- [146] G.J. Moody, J.D.R.Thomas, *Dipole Moments in Inorganic Chemistry*; Edward Arnold: London, (1971).
- [147] J. Nath, J. Chem. Thermodyn., 34 (2002) 1857.
- [148] S.K. Mehta, A.K. Sharma, K.K. Bhasin, Fluid Phase Equilib., 201 (2002) 203.
- [149] T.B. Hoover, J. Phys. Chem., 73 (2002) 57.

Theoretical Background

- [150] M. Born, E. Wolf, *Principles of Optics: Electromagnetic Theory of Propagation, Interference and Diffraction of Light*, 7th edn., Cambridge University Press, London, (1999).
- [151] E. Vercher, F.J. Llopis, M.V. González-Alfaro, A. Martínez-Andreu, *J. Chem. Eng. Data* 55 (2010) 1377.
- [152] M.A. Iglesias-Otero, J. Troncoso, E. Carballo, L. Romani, *J. Chem. Thermodyn.*, 40 (2008) 949.
- [153] M. Deetlefs, K. Seddon, M. Shara, *Phys. Chem. Chem. Phys.*, 8 (2006) 642.
- [154] Farid I. El-Dossoki, *J. Chin. Chem. Soc.*, 54 (2007) 1129.
- [155] R.W. Missen, *Ind. Eng. Chem. Fundam.*, 8 (1969) 81.
- [156] P. Brocos, A. Pineiro, R. Bravo, A. Amigo, *Phys. Chem. Chem. Phys.*, 5 (2003) 550.
- [157] S. Glasstone, *Textbook of Physical Chemistry*, 2nd ed.; D. Van Nostrand Co., London, (1949).
- [158] R.D. Singh, M. Gupta, *Int. J. Inno. Res. Adv. Stud.*, 3 (2016) 407,
- [159] M. Fermeglia, G. Torriano, *J. Chem. Eng. Data* 44 (1999) 965.
- [160] M.I. Aralaguppi, T. M. Aminabhavi, R. H. Balundgi, S. S. Joshi, *J. Phys. Chem.*, 95 (1991) 299.
- [161] S. Singh, S. Parveen, D. Shukla, M. Gupta and J.P. Shukla, *Acta Physi. Polo. A*, 111 (2007) 847.
- [162] A. Pineiro, P. Brocos, A. Amigo, M. Pintos, R. Bravo, *J. Chem. Thermodyn.*, 31 (1999) 931.
- [163] T.M. Aminabhavi, H.T.S. Phayde, R.S. Khinnavar, B. Gopalakrishna, K.C. Hansen, *J. Chem. Eng. Data* 39 (1994) 251.
- [164] D.Y. Peng, D.B. Robinson, *Ind. Eng. Chem. Fundam.*, 15 (1976) 59.
- [165] D. Patterson, G. Delmas, *J. Polym. Sci.*, 30 (1970) 1.
- [166] D. Patterson, *Pure. Appl. Chem.*, 47 (1976) 305.
- [167] R.D. McCarty, *Fluid Phase Equilib.*, 256 (2007) 42.
- [168] J.D. van der Waals, *On the Continuity of the Gaseous and Liquid States*. Ph.D. Dissertation, University Leiden, Leiden, Netherland, (1873).
- [169] O. Redlich, J.N.S. Kwong, *Chem. Rev.*, 44 (1949) 233.
- [170] G. Soave, *Chem. Eng. Sci.*, 27 (1972) 1197.
- [171] H. Renon, *Fluid Phase Equilib.*, 13 (1983) 15.
- [172] M.J. Huron, D.N. Dufour, J. Vidal, *Fluid Phase Equilib.*, 1 (1978) 247.
- [173] L. Asselineau, G. Bogdanic, J. Vidal, *Chem. Eng. Sci.*, 33 (1978) 1269.
- [174] M.S. Graboski, T.E. Daubert, *Ind. Eng. Chem. Process. Des. Dev.*, 17 (1978) 443.

Theoretical Background

- [175] G. Schmidt, H. Wenzel, Chem. Eng. Sci., 35 (1980) 1503.
- [176] S.I Sandler, Chemical, *Biochemical, and Engineering Thermodynamics*, 4th edn., John Wiley India (P) Ltd., (2007), New Delhi, pp. 242, 258.
- [177] S.I Sandler, Chemical, *Biochemical, and Engineering Thermodynamics*, 4th edn, John Wiley India (P) Ltd., (2007), New Delhi, pp. 423.
- [178] J. Singh, H.D. Pflug, G.C. Benson, J. Phys. Chem., 72 (1968) 1939.
- [179] G.C. Benson, J. Singh, J. Phys. Chem., 72 (1968) 1345.
- [180] P.J. Flory, R.A. Orwell, A. Vrij, J. Am. Chem. Soc., 86 (1964) 3507.
- [181] I. Prigogine, *Molecular Theories of Solutions*, North-Holland publishing Co., Amsterdam, (1957).
- [182] D. Patterson, G. Delmas, Discuss Faraday Soc., 49 (1970) 98.
- [183] A.K. Mehrotra, W.D. Monnery, W. Svrcek, Fluid Phase Equilib., 117 (1996) 344.
- [184] V.A. Bloomfield, R.K. Dewan, J. Phys. Chem., 75 (1971) 3113.
- [185] R. Macias-Salinas, F. Garcia-Sanchez, G. Eliosa-Jimencz. Fluid Phase Equilib., 210 (2003) 319.
- [186] M.L. Williams, R.F. Landel, J.D. Ferry, J. Am. Chem. Soc., 77 (1955) 3701.
- [187] M. H. Cohen, D. Turnbull, J. Chem. Phys., 31 (1959) 1164.
- [188] B. Celda, R. Gavara, J. E. Figueruelo, J. Chem. Eng. Data 32 (1987) 31.
- [189] J.B. Irving, *Viscosity of Binary Liquid Mixtures, A Survey of Mixture Equations*, NEL Report No. 630, National Eng. Lab., East Kilbride, Glasgow, (1977).
- [190] J.B. Irving, *The Effectiveness of Mixture Equations*, NEL Report No31, National Eng. Lab., East Kilbride, Glasgow, (1977).
- [191] L. Grunberg, A.H. Nissan, Nature (London), 164 (1949) 799.
- [192] J. Canosa, A. Rodriguez, J. Tojo, J. Chem. Eng. Data 43 (1998) 961.
- [193] M. Tamura, M. Kurata, Bull. Chem. Soc. Jpn., 25 (1952) 32.
- [194] R.K. Hind, E. McLaughlin, A.R. Ubbelohde, Trans. Faraday. Soc., 56 (1960) 328.
- [195] S.L. Oswal, H.S. Desai, Fluid Phase Equilib., 186 (2001) 81.
- [196] E.L. Heric, J.G. Brewer, J. Chem. Eng. Data 12 (1967) 574.
- [197] R.A. McAllister, AIChE J., 6 (1960) 427.
- [198] P.K. Katti, M.M. Choudhri, J. Chem. Eng. Data 9 (1964) 442.
- [199] V.M. Lobe, M.Sc. *Thesis University of Rochester*, New York, (1973).
- [200] M.R.V. Krishnan, G.S. Laddha, Ind. Eng. Chem. Fundam., 7 (1968) 324.
- [201] X. Esteve, K.R. Patil, J. Fernandez, A. Coronas, J. Chem. Thermodyn., 27 (1995) 281.
- [202] S.M. Bardavid, G.C. Pedrosa, M. Katz, J. Solution Chem., 25 (1996) 1125.
- [203] I. Cibulka, Collect. Czech. Chem. Commun., 47 (1982)1414.

Theoretical Background

- [204] B. Jasinski, S. Malanowski, Chem. Eng. Sci., 25 (1970) 913.
- [205] F. Köhler, Monatsh. Chem., 91 (1960) 738.
- [206] K.T. Jacob, K. Fitzner, Thermochim. Acta, 18 (1977) 197.
- [207] C. Colinet: Ph. D thesis, University of Grenoble, France, (1967).
- [208] R.P. Rastogi, J. Nath, S.S. Das, J. Eng. Chem. Data 22 (1977) 249.
- [209] C.C. Tsao, J.M. Smith, Chem. Eng. Prog. Symp. Series, 49 (1953) 107.
- [210] G.W. Toop, Trans. TMS-AIME, 233 (1965) 850.
- [211] G. Scatchard, L.B. Ticknor, J.R. Goates, J. Am. Chem. Soc., 74 (1952) 3721.
- [212] A.R. Mathieson, J.C.J. Thynne, J. Chem. Soc., (1956) 3713.
- [213] O. Nomoto, J. Phys. Soc. Jpn., 13 (1958) 1528.
- [214] S. Balakrisjnan, R. Palani, J. Pure App. Indust. Phys., 5 (2015) 25.
- [215] W. Schaaffs, Acoustica, 33 (1975) 272.
- [216] W. Schaaffs, *Molekularakustic*, Springer Verlag, Berlin, (1963) Chap. 11,12.
- [217] M. Kalidoss, R. Srinivasamoorthy, J. Pure. Appl. Ultrason., 19 (1997) 9.
- [218] W. Van Dael, E. Vangael, in abst. paper: *Proc. 1st International Conference on Calorimetry and thermodynamics*, Warsaw Poland, (1969), pp. 555.
- [219] B. Jacobson, J. Chem. Phys., 6 (1952) 927.
- [220] B. Jacobson, Acta Chem. Scand., 6 (1952) 1485.
- [221] Z. Junjie, J. China Univ. Sci. Tech., 14 (1984) 298.
- [222] A. Lorentz, Weid. Ann., 9 (1880) 641,
- [223] L. Lorenz, Weid. Ann., 11 (1880) 70.
- [224] F. Gladstone, D. Dale, Philos. Trans. R. Soc. London, 148 (1858) 887.
- [225] D.F.J. Arago, J.B. Biot, Mem. Acad. Fr., 17 (1806) 7.
- [226] O. Weiner, Berichte (Leipzig), 62 (1910) 256.
- [227] H. Eyring, M.S. John, *Significant Liquid Structures*, Wiley, New York, (1969).
- [228] W. Heller, Phys. Rev., 68 (1945) 5.
- [229] J.F. Eykman, A.F. Holleman, *Research Refractometers*, De Erven Loosjes, (1919).
- [230] S.S. Kurtz, A.L. Ward, J. Franklin Inst., 222 (1936) 563.
- [231] M. Tjahjono, M. Garland, J. Solution Chem., 36 (2007) 221.
- [232] M. Tjahjono, L. Guo, M. Garland, Chem. Eng.Sci., 60 (2005) 3239.
- [233] S.S. Patil, S.R. Mirgane, B.R. Arbad, Adv. Appl. Sci. Res., 3 (2012) 2378.
- [234] M.V. Rathnam, S. Mohite, M.S. Kumar, J. Serb. Chem. Soc., 76 (2011) 1.

CHAPTER III

3.1. Source and Purification of the Chemicals Used

3.1.1. Solvents

1,4-dioxane ($C_4H_8O_2$, M.W. 88.11), 1,3-dioxolane ($C_3H_6O_2$, M.W. 74.08), ethylenediamine ($C_2H_8N_2$, M.W. 60.09), 1,2-dichloroethane ($C_2H_4Cl_2$, M. W. 98.97), monoethanolamine (C_2H_7NO , M.W. 61.08), 2-ethyl-1-hexanol ($C_8H_{18}O$, M.W. 130.23), cyclohexane (C_6H_{12} , M.W. 84.16), cyclohexanone ($C_6H_{10}O$, M.W. 98.15), methyl acetate ($C_3H_6O_2$, M.W. 74.08), ethyl acetate ($C_4H_8O_2$, M.W. 88.11), methyl salicylate ($C_8H_8O_2$, M.W. 152.15), tetrahydrofuran (C_4H_8O , M.W. 72.11) and dimethylformamide (C_3H_7NO , M.W. 73.10) were used as solvents for preparing different binary/ternary/quaternary solvent mixtures in the research works embodied in this thesis.

Dimethylformamide was purified by distilling the azeotropes obtained by mixing it with a 10% of benzene by volume at a temperature of 80 °C under atmospheric pressure.¹ The product thus obtained was dried over silica gel followed by distillation under reduced pressure. The collected middle fractions were stored in a desiccator over P_2O_5 before use.¹ Tetrahydrofuran was purified by distilling it over $LiAlH_4$ after keeping it for several days over KOH .² 1,3-dioxolane was purified by refluxing it for two hours with PbO_2 . It was cooled and filtered, the filtrate was then fractionally distilled after mixing with xylene and PbO_2 .³ Similarly 1,4-dioxane was purified by refluxing it with concentrated HCl and water for about 12 hours by passing nitrogen slowly. The product obtained was cooled, treated with KOH solution slowly with constant shaking until a second layer was separated. 1,4-dioxane was decanted and again treated with fresh KOH pellets to remove the aqueous phase if any. It was then transferred to a new clean flask and refluxed with sodium for 6-12 hours and then distilled from it.⁴ All other solvents were of spectroscopic grade and were used as received from the vendors. The purity of these solvents was ascertained by comparing their densities and viscosities to literature values⁵⁻³⁹ as presented in the respective chapters wherein they were used. Provenance and purity of these solvents are given in Table 3.1.

Chapter III

Table 3.1. Provenance and purity of the solvents used.

Chemical	Source	Mass Fraction purity	CAS No.
1,4-dioxane	Sigma Aldrich, Germany	>0.998 ^a	123-91-1
	Merck, India	>0.99	
1,3-dioxolane	S.D. Fine Chemicals, India	>0.99	646-06-0
Ethylenediamine	Sigma Aldrich, Germany	>0.998 ^a	107-15-3
1,2-dichloroethane	Sigma Aldrich, Germany	>0.998 ^a	107-06-2
Monoethanolamine	Sigma Aldrich, Germany	>0.998 ^a	141-20-9
2-ethyl-1-hexanol	Sigma Aldrich, Germany	>0.998 ^a	104-76-7
Cyclohexane	Sigma Aldrich, Germany	>0.998 ^a	110-82-7
Cyclohexanone	Sigma Aldrich, Germany	>0.998 ^a	108-94-1
Methyl acetate	Sigma Aldrich, Germany	>0.998 ^a	79-20-9
Ethyl acetate	Sigma Aldrich, Germany	>0.998 ^a	141-78-6
Methyl salicylate	Sigma Aldrich, Germany	>0.998 ^a	119-36-8
N, N-dimethylformamide	S.D. Fine Chemicals, India	>0.99	68-12-2
Tetrahydrofuran	Merck, India	>0.99	109-99-9

^aMoisture content as prescribed by the respective vendors were 0.05%

3.1.2. Mixed Solvents

In this research work the binary/ternary/quaternary mixtures required for the experiments were prepared by mass in specially designed air-tight bottles with stopper inside a dry box at 298.15 K. The binary mixtures containing 10, 20, 30, 40, 50, 60, 70, 80, 90 mass% of component 1 were prepared at 298.15 K so as to cover the whole composition range. The binary mixtures selected for the investigations are as follows: (i) 1,4-dioxane with ethylenediamine, 1,2-dichloroethane and monoethanolamine, (ii) 2-ethyl-1-hexanol with ethylenediamine, 1,2-dichloroethane and monoethanolamine, (iii) cyclohexane with methyl acetate, ethyl acetate and methyl salicylate, (iv) cyclohexanone with methyl acetate, ethyl acetate and methyl salicylate. The ternary mixtures containing varying mass% of the components were also prepared at 298.15 K in order to cover the whole range of mass fractions for each component as much as possible. The ternary mixtures studied are as follows: (i) cyclohexane + methyl acetate + ethyl acetate, (ii) cyclohexane + methyl acetate + methyl salicylate, (iii) cyclohexane + ethyl acetate + methyl salicylate, (iv) methyl acetate + ethyl acetate +

Chapter III

methyl salicylate, (v) cyclohexanone + methyl acetate + ethyl acetate, (vi) cyclohexanone + methyl acetate + methyl salicylate and (vii) cyclohexanone + ethyl acetate + methyl salicylate. Similarly the quaternary mixtures were prepared with varying mass% of the components containing: (i) cyclohexane + methyl acetate + ethyl acetate + methyl salicylate and (ii) cyclohexanone + methyl acetate + ethyl acetate + methyl salicylate at 298.15 K.

3.2. Experimental Methods

3.2.1. Density Measurement

The densities of the experimental liquids or liquid mixtures were measured at the experimental temperatures using a digital density meter (Anton Paar, DMA 4500M) as shown in Figures 3.1-3.4.



Fig. 3.1. Anton Paar densitometer (DMA 4500M).

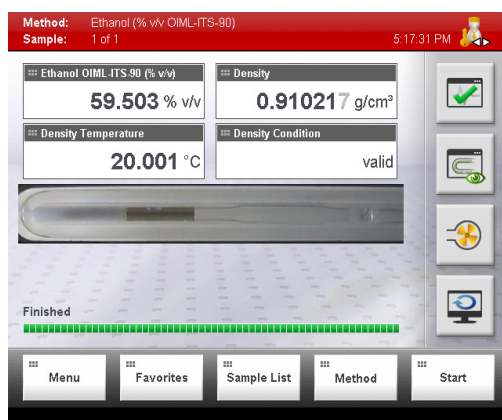


Fig. 3.2. Main screen view of Anton Paar densitometer.

Chapter III



Fig. 3.3. Filling of sample with a syringe.



Fig. 3.4. Drying the measuring cell.

In the digital density meter, the mechanic oscillation of the U-tube is electromagnetically transformed into an alternating voltage of the same frequency. The period of oscillation (τ_0) can be measured with high resolution and it follows a simple relation to the density (ρ) of the sample in the oscillator:⁴⁰

$$\rho = A\tau_0^2 - B \quad (1)$$

where A and B are the respective instrument constants of each oscillator. Their values are determined by calibrating with two liquids of precisely known densities ρ_1 and ρ_2 . For the special adjustment the densities of these two liquids must differ by at least $\pm 0.01 \text{ g} \cdot \text{cm}^{-3}$ and τ_0 values of the adjustment media must differ by at least 0.0001. Modern instruments calculate and store the constants A and B after the two calibration measurements, mostly performed with air and water. They employ suitable measures to compensate various parasitic influences on the measuring result, *e.g.*, the influence of the sample's viscosity and the non-linearity caused by the measuring instrument's finite mass. The density meter was calibrated at the experimental

Chapter III

temperatures with doubly distilled, degassed water and dry air at atmospheric pressure. The temperature was kept constant with an accuracy of $\pm 1 \times 10^{-2}$ K by using an automatic built-in Peltier technique. The stated repeatability and accuracy of the densities were $\pm 1 \times 10^{-5}$ g · cm⁻³ and $\pm 5 \times 10^{-5}$ g · cm⁻³, respectively. However, when the accuracy of the measured densities was tested with the density of an aqueous NaCl solution of known molality using the data given by Pitzer,⁴¹ the estimated uncertainty of the density measurements for most of the solutions was found to be better than $\pm 2 \times 10^{-5}$ g · cm⁻³.

3.2.2. Measurement of Viscosity

The kinematic viscosities were measured by means of a suspended Cannon type Ubbelohde viscometer (capillary viscometer). The time of efflux of a constant volume of the experimental liquid mixtures through the capillary was measured with the aid of a digital stopwatch capable of measuring time accurate to ± 0.01 s. The viscometer was always kept immersed in a vertical position in the thermostatic bath with an accuracy of ± 0.01 K of the desired temperature. After attainment of thermal equilibrium, the flow times of pure liquids or liquid mixtures were measured thrice and the average of the readings were taken into account. During the measurements adequate precautions were taken to minimize evaporation losses. The efflux time for water at 298.15 K was measured to be 428.9 s. The kinematic viscosity (ν) and the absolute viscosity (η) are obtained using the following equations:

$$\nu = kt - \frac{L}{t} \quad (2)$$

$$\eta = \nu\rho \quad (3)$$

where k and L are the viscometer constants and t and ρ are the efflux time of flow in seconds and the density of the experimental liquid, respectively. The values of the constants k and L , determined by using water and methanol as the calibrating liquids, were found to be 1.9602×10^{-3} and 4.2019, respectively. The kinetic energy corrections were done from these values and they were found to be negligible. The uncertainty in viscosity measurements, based on our work on several pure liquids, was within $\pm 4 \times 10^{-4}$ mPa · s. Figure 3.5 depicts the capillary viscometers used for measuring viscosities of the solutions studied.

Chapter III

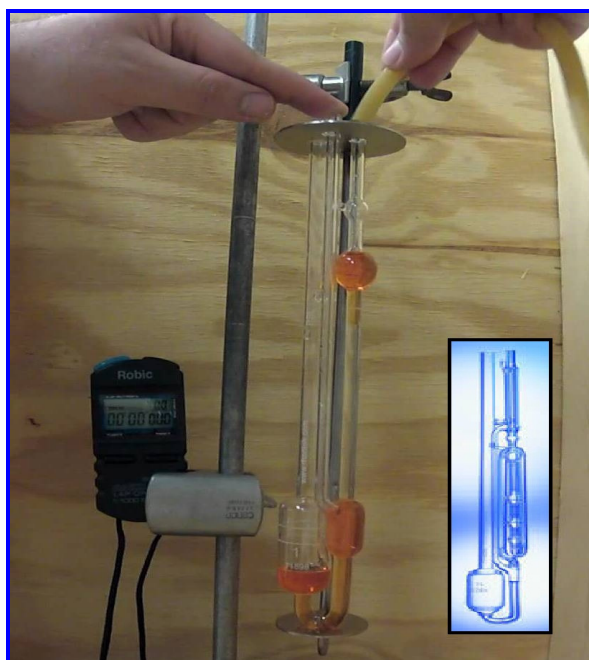


Fig. 3.5. A suspended-level Cannon type Ubbelohde viscometer (capillary viscometer).

3.2.3. Measurement of Mass

Mass measurements were made on digital electronic analytical balance (Mettler Toledo, AG 285, Switzerland) as shown in Figure 3.6.



Fig. 3.6. Digital electronic analytical balance (Mettler Toledo, AG 285).

It can measure mass with a very high precision and accuracy. The weighing pan is inside a transparent enclosure with doors so that dust particles do not collect and any air currents in the room do not affect the operation of the balance. The mass measurements were accurate to ± 0.01 mg.

Chapter III

3.2.4. Refractive Index Measurement

Refractive indices of the experimental liquid mixtures (binary/ternary/quaternary) were measured with an Abbe-refractometer (Cyberlab, MA01527, USA) using yellow sodium D-line light ($\lambda=589.3$ nm, which is the average of the two emission lines at 589.0 nm and 589.6 nm) at 298.15 K. The Abbe-refractometer is one of the most convenient and widely used refractometer and owes its popularity to its wide range ($n_D = 1.3$ to 1.7) and to the minimal sample needed. Figure 3.7 shows a schematic diagram of its optical system. The sample liquid is directly injected into the prism assembly of the instrument using an airtight hypodermic syringe and is sandwiched as a thin layer (~ 0.1 mm) between two prisms. The upper prism is firmly mounted on a bearing that allows its rotation by means of the side arm shown in dotted lines. The lower prism is hinged to the upper to allow separation for cleaning and for introduction of the sample. When light reflects into the prism (the lower surface being rough) effectively becomes the source for an infinite number of rays that passes through the sample at all angels.

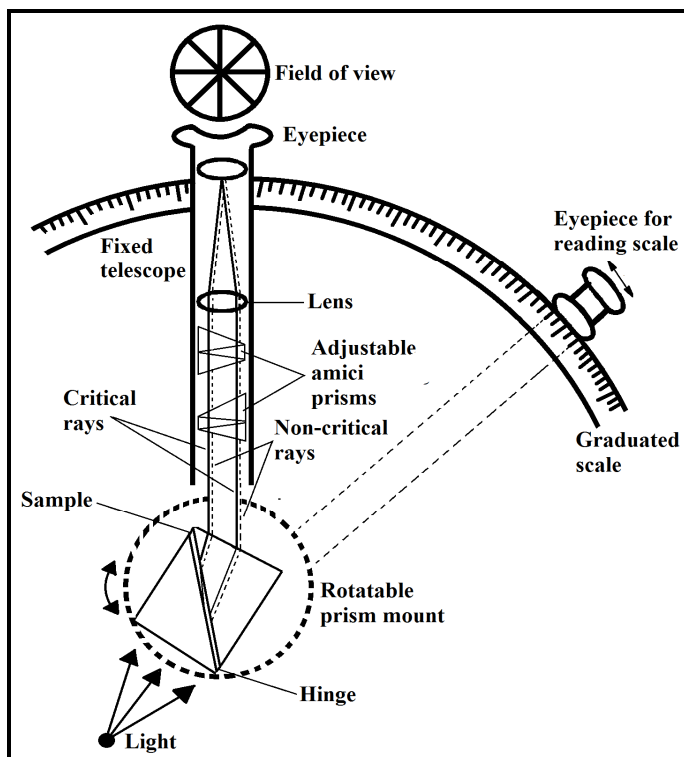


Fig 3.7. Schematic diagram of Abbe-refractometer optical system.

Chapter III

The light rays get refracted at the interface of the sample and the smooth-ground face of the upper prism. After this it passes through the fixed telescope. Two triangular prisms in contact (Amici prisms) serve to collect the divergent rays of different colors into a single white beam that corresponds in path to that of the sodium D ray. The eyepiece of the telescope is provided with crosshairs as shown in Figure 3.8. During the measurement of the refractive index the prism angle is changed until the light-dark interface just coincides with the crosshairs. The position of the prism is then established from the fixed scale. The Abbe-refractometer is depicted in Figure 3.8. Water was circulated through the refractometer from a thermostatic bath maintained at 298.15 ± 0.01 K. It was calibrated by measuring the refractive indices of doubly distilled, degassed water at 298.15 K.^{42,43} The uncertainty in refractive indices was within ± 0.0002 . An average of three measurements was taken for each mixture.

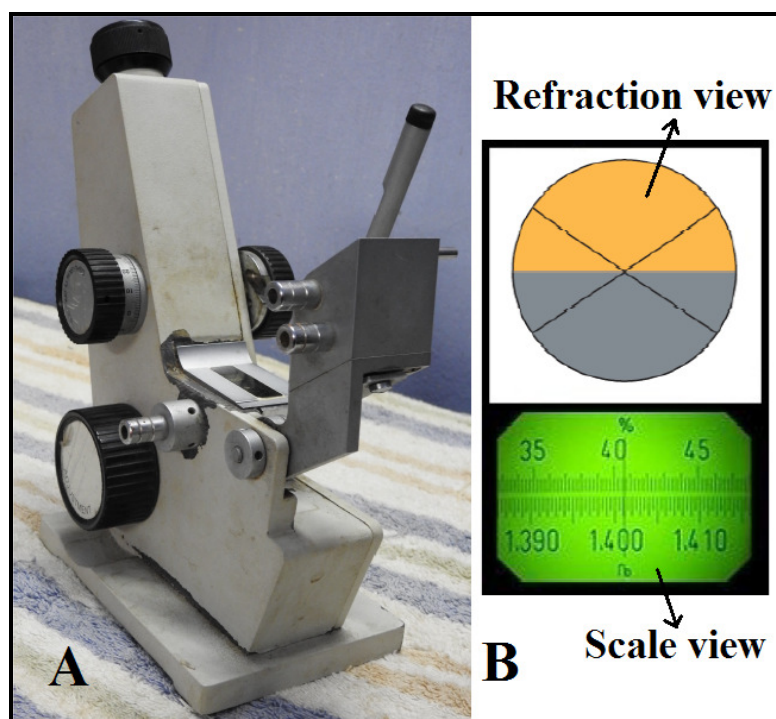


Fig. 3.8. A: Abbe-refractometer (Cyberlab, MA01527, USA); B: View of the refractometer through the eyepiece.

3.2.5. Measurement of Ultrasonic Speed

There are mainly three experimental techniques to measure the velocity of ultrasonic sounds in pure liquids and liquid mixtures. They are: (i) Continuous wave

Chapter III

technique, (ii) Pulse technique and (iii) Interferometer method. From a comparison of the relative merits of the various methods, interferometer method is found to be the most accurate method available for speed measurements. Hunter and Dardy⁴⁴, Dobbs and Fine gold⁴⁵, Fort and Moore⁴⁶ measured the speed of sound for liquids and liquid mixtures by using interferometric technique with $\pm 0.15\%$ uncertainty. In the present research work ultrasonic speeds of the experimental liquid mixtures were measured with an accuracy of 0.3% using a multi-frequency ultrasonic interferometer (F-05, Mittal Enterprises, New Delhi, India) operating at 2 MHz. It was calibrated with doubly distilled degassed water and purified methanol or benzene maintained at 298.15 K by circulating thermostatic water around a jacketed cell (2 MHz) containing the experimental liquids with a circulating pump. The uncertainty in ultrasonic speeds⁴⁷ was around $\pm 0.2 \text{ m s}^{-1}$.

The measurement of the ultrasonic speed (u) by ultrasonic interferometer is based on the accurate determination of the wavelength (λ) in the medium. In this process ultrasonic waves of known frequency (f) are generated by a quartz crystal fixed at the bottom of the cell. These waves are then reflected by a movable metallic plate, which is kept parallel to the quartz crystal. If the distance between these two plates is exactly a whole multiple of the sound wavelength, standing waves are formed in the medium. Under these circumstances, acoustic resonance occurs and this acoustic resonance gives rise to an electrical reaction on the generator driving the quartz crystal and the anode current of the generator becomes a maximum. But If the distance is increased or decreased by exactly one half of the wavelength ($\lambda/2$) or an integer multiple of it, the anode current again becomes maximum. If d is the separation between successive adjacent maxima of anode current and the total number of oscillation (usually $n = 20$) counted. Then the total distance moved by the micrometer in n oscillations is given by:

$$d = n \times \frac{\lambda}{2} \quad (4)$$

Now the speed (u) of the wave and frequency (f) of the cell is related to its wavelength (λ) by the relation,

$$u = \lambda \times f \quad (5)$$

Chapter III

$$\text{or } u = \lambda \times f = \frac{2d}{n} \times f \quad (6)$$

Thus with a known frequency of the cell the ultrasonic speed (u) can be obtained. The ultrasonic interferometer consists of the following three parts: (i) The high frequency generator (Single and Multi-frequency), specially designed to excite the quartz crystal fixed at the bottom of the measuring cell at its resonant frequency to generate ultrasonic wave in the experimental liquid filled in the measuring cell, (ii) The measuring cell (1, 2, 3 and 4 MHz) is specially designed double walled cell for maintaining the temperature of the liquid sample constant during the experiment. A fine micrometer has been provided at the top, which can lower or raise the reflector plate in the liquid in the cell through a known distance and (iii) shielded cable.

The total assembly is shown Figure 3.9 in which the measuring cell is connected to the output terminal of the high frequency generator through a shielded cable. The cell is filled with the experimental liquid before switching on the generator. The ultrasonic waves move normal from the quartz crystal till they are reflected back from the movable plate and the standing waves are formed in the liquid in between the reflector plate and the quartz crystal. The micrometer is slowly moved till the anode current on the meter on the high frequency generator shows a maximum deflection. A number of maxima of anode current are observed and the total number of oscillation (n) is counted. The total distance (d) thus moved by the micrometer gives the value of the wavelength (λ) using the Eq. (4).



Fig 3.9. ultrasonic interferometer (F-05, Mittal Enterprises, New Delhi, India).

Chapter III

Further, the speed (u) determined thus is used for the calculation of the isentropic compressibility (K_s) using the following formula:

$$K_s = 1/(u^2 \rho) \quad (7)$$

where ρ is the density of the experimental liquid. In Figure 3.10(A) cross-section of the measuring cell of a multi-frequency ultrasonic interferometer and (B) position of reflector *versus* crystal current are depicted. However, the extra peaks [Figure 3.10(B)] in between minima and maxima occur due to a number of reasons but these do not effect the $\lambda/2$ values.

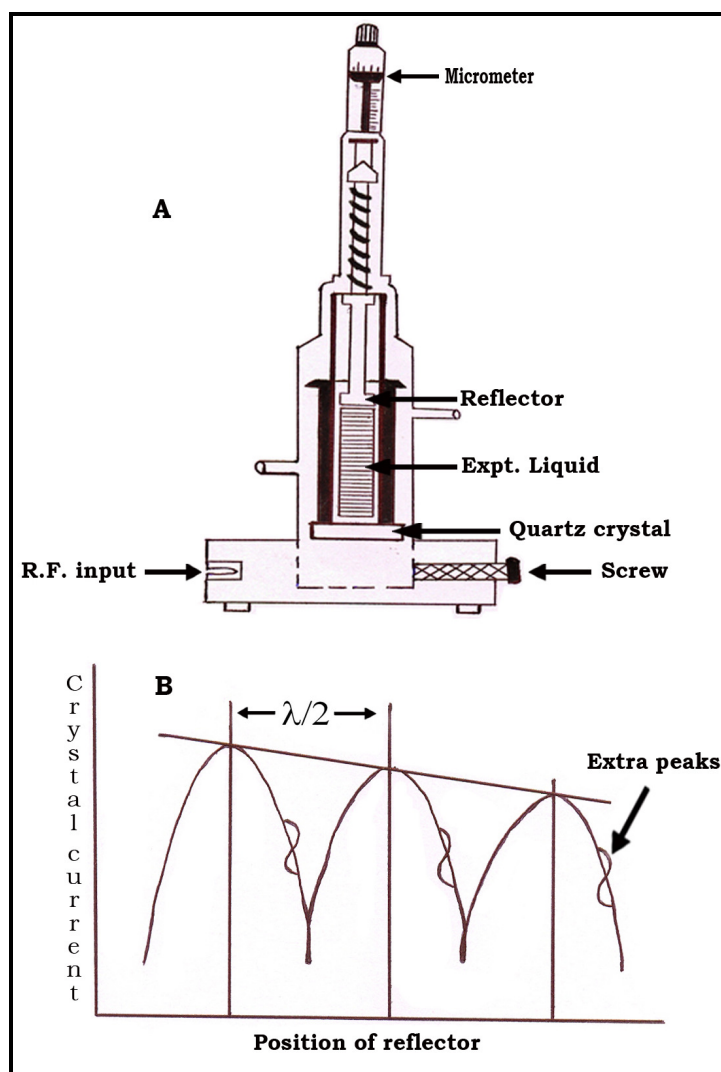


Figure 3.10. (A) Cross-section of the measuring cell of a multi-frequency ultrasonic interferometer and (B) position of reflector vs. crystal current.

Chapter III

3.2.5. Measurement of FTIR Spectra

Fourier transform infrared spectroscopy (FTIR)⁴⁸ is a technique which is used to obtain an infrared spectrum of absorption or emission of a solid, liquid or gas. An FTIR spectrometer simultaneously collects high spectral resolution data over a wide spectral range. The term Fourier transform infrared spectroscopy originates from the fact that a Fourier transform (a mathematical process) is required to convert the raw data into the actual spectrum. In the present study FT-IR spectra of the experimental liquid mixtures (binary/ternary/quaternary) were recorded at 298.15 K using Elmer FT-IR spectrophotometer (Spectrum RX-1) in the range 400-4000 cm^{-1} and is depicted in Figure 3.11. In our study the experimental liquid mixtures were sandwiched between two potassium bromide aperture plates⁴⁹ (Sigma-Aldrich, Germany) taking an adequate precaution such that no gas bubbles are trapped. The thickness of the liquid membrane between the KBr aperture plate is adjusted using spacer of fixed path length and by appropriately tightening the screws (without breaking the aperture plates). These plates are transparent to the infrared light and do not introduce any lines onto the spectra. This type of cell is often called a "liquid cell." Figure 3.12 shows the appearance of a liquid cell.



Fig. 3.11. Perkin-Elmer FTIR spectrophotometer (Spectrum RX-1).

Chapter III



Fig. 3.12. Appearance of a Liquid Cell.

3.2.6. Methodology

To reveal the nature and extent of molecular interactions in liquid mixtures various properties like density, viscosity, ultrasonic speed and refractive index were measured and various excess properties were determined by using standard relations as available in literatures, infra red (IR) spectroscopic technique was used to study molecular interactions and structural changes in the liquid mixtures. To study molecular interactions in a quaternary system, information on various properties of the binary and ternary mixtures of the components comprising the quaternary system is required. So a bottom to top method of study as shown in Figure 3.13 was adopted.

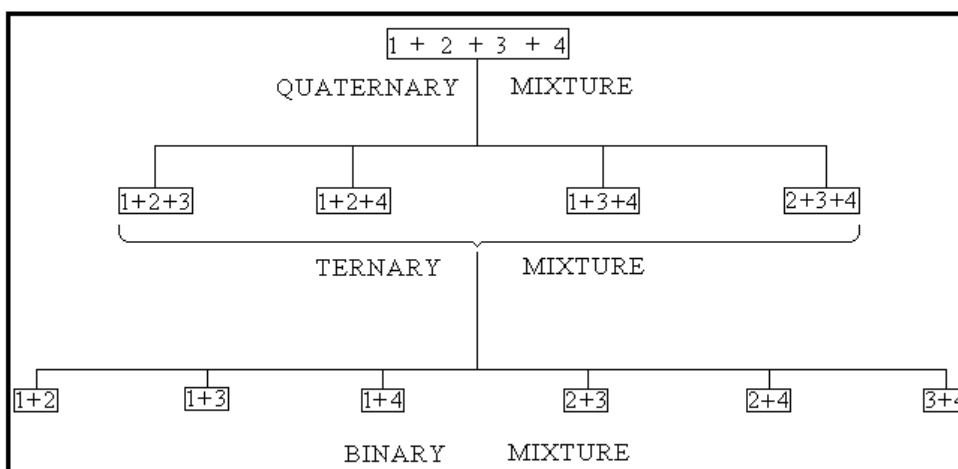


Fig. 3.13. Hierarchy of combination of different solvent mixtures.

Once experimental data for such systems are measured various excess or deviation and thermodynamic properties were derived and discussed in terms of various specific and nonspecific forces, various empirical and semi empirical models for excess molar volume, speed of sound, refractive index, *etc.*, were evaluated for their applicability.

Chapter III

The equation of states like PREOS along with PFP model were used for binary mixtures. However, response surface model⁵⁰ may be utilized to determine the partial molar volume and partial molar refraction for the ternary or quaternary liquid mixtures.

References

- [1] Y. Zhao, J. Wang, X. Xuan, J. Lu, J. Chem. Eng. Data 45 (2000) 440.
- [2] M.N. Roy, R. Dey, A. Jha, J. Chem. Eng. Data 46 (2001) 1327.
- [3] J.A. Riddick, W.B. Bunger, T.K. Sakano, *Organic Solvents. Techniques of Chemistry*, Vol. 2, 4th edn., Wiley Interscience, New York, (1986).
- [4] D.D. Perin, W.L.F. Armarego, *Purification of Laboratory Chemicals*, 3rd edn., Oxford, New York, (1988), pp. 164.
- [5] A. Villares, S. Martin, M. Haro, B. Giner, J. Chem. Thermodyn., 36 (2004) 1027.
- [6] M. Das, M.N. Roy, J. Chem. Eng. Data 51 (2006) 2225.
- [7] S. Akhtar, A.N.Q. Faruk, M.A. Saleh, Phys. Chem. Liq., 39 (2001) 383.
- [8] L. Sarkar, M.N. Roy, J. Chem. Eng. Data 54 (2009) 3307.
- [9] K.P. Rao, K.S. Reddy, J. Chem. Eng. Data 33 (1988) 130.
- [10] C. Li, J. Zhang, T. Zhang, X. Wei, E. Zhang, J. Chem. Eng. Data 55 (2010) 4104.
- [11] J.K. Gladden, J. Chem. Eng. Data 17 (1972) 468.
- [12] M.A. Saleh, M.S. Ahmed, M.S. Islam, Phys. Chem. Liq., 40 (2002) 477.
- [13] S. Ranjbar, K. Fakhri, B. Jahan, J. Ghasemi, J. Chem. Eng. Data 54 (2009) 3284.
- [14] R.K. Biswas, R.A. Banu, M.N. Islam, Hydrometallurgy, 69 (2003) 157.
- [15] S.E. Burke, B. Hawryla, R. Palepu, Thermochim. Acta, 345 (2002) 101
- [16] U.R. Kapadi, D.G. Hundiwale, N.B. Patil, Fluid Phase Equilib., 201 (2002) 335.
- [17] A.M. Awwada, R.A. Pethric, J. Chem. Soc. Faraday Trans. I., 78 (1982) 3203.
- [18] E. Zorebski, M. Dzida, E. Wysocka, J. Chem. Eng. Data 56 (2011) 2680.
- [19] E. Zorebski, M.G. Rybczynska, B. Maciej, J. Chem. Eng. Data 55 (2010) 1025.
- [20] S.C. Bhatia, J. Sangwan, R. Rani, V. Kiran, Int. J. Thermophys., 34 (2013) 2076.
- [21] M.N. Roy, B.K. Sarkar, B. Sinha, J. Chem. Eng. Data 54 (2009) 1076.
- [22] E. Aicart, G. Tardajos, M. Dlaz Peia, J. Chem. Eng. Data 26 (1981) 22.
- [23] K.N. Marsh, *TRC Data Bases for Chemistry and Engineering, TRC Thermodynamic Tables*, Texas A & M University System, College Station, TX, (1994).
- [24] T.M. Aminabhavi, V.B. Patil, M.I. Aralaguppi, J. Chem. Eng. Data 41 (1996) 521.
- [25] V.K. Dakua, B. Sinha, M.N. Roy, Ind. J. Chem., 45 (2006) 1381.
- [26] M.I. Aralaguppi, C.V. Jadar, T.M. Aminabhavi, J. Chem. Eng. Data 44 (1999) 441.

Chapter III

- [27] A. Pal and H. Kumar, *J. Mol. Liq.*, 89 (2000) 189.
- [28] R.M. Pires, H.F. Costa, A.G.M. Ferreira, I.M.A. Fonseca, *J. Chem. Eng. Data* 52 (2007) 1240.
- [29] D.L. Cunha, J.A.P. Coutinho, J.L. Daridon, R.A. Reis, M.L.L. Paredes, *J. Chem. Eng. Data* 58 (2013) 2925.
- [30] T.M. Aminabhavi, H.T.S. Phayde, *J. Chem. Eng. Data* 41(1996) 813
- [31] R. Venis, R. Rajkumar, *J. Chem. Pharm. Res.*, 2 (2011) 878.
- [32] J.A. Riddick, W.B. Bunger, T.K. Sakano, *Organic Solvents, Physical Properties and Methods of Purification, Techniques of Chemistry*, vol. 2, 4th edn., Wiley-Interscience, New York, (1986).
- [33] Y. Zhao, J. Wang, X. Xuan, J. Lu, *J. Chem. Eng. Data* 45 (2000) 440.
- [34] M.N. Roy, R. Dey, A. Jha, *J. Chem. Eng. Data* 46 (2001) 1327.
- [35] I. Johnson, M. Kalidoss, R. Srinivasamoorthy, *J. Chem. Eng. Data* 47 (2002) 1388.
- [36] P.S. Nikam, S.J. Kharat, *J. Chem. Eng. Data* 50 (2005) 455.
- [37] P. Pacak, *J. Solution Chem.*, 16 (1987) 71.
- [38] M. Das, M.N. Roy, *J. Chem. Eng. Data* 51 (2006) 2225.
- [39] L. Sarkar, M.N. Roy, *J. Chem. Eng. Data* 54 (2009) 3307.
- [40] Oscillating U-tube. Electronic document, [http://en.m.wikipedia.org/wiki/Oscillating U-tube](http://en.m.wikipedia.org/wiki/Oscillating_U-tube), accessed on Oct 12, 2013.
- [41] K.S. Pitzer, J.C. Peiper, R.H. Busey, *J. Phys. Chem. Ref. Data*, 13 (1984) 1.
- [42] D. Brahman, R. Pradhan, B. Sinha, *J. Chem. Thermodyn.*, 75 (2014) 96.
- [43] D. Brahman, B. Sinha, *J. Chem. Thermodyn.*, 75 (2014) 136.
- [44] Y.L. Hunter, H.D. Dardy, *J. Acoust. Soc. Amer.*, 36 (1964) 1914.
- [45] E.R. Dobbs, L. Finegold, *Ibid*, 32 (1960) 1215.
- [46] R.J. Fort, W.R. Moore, *Trans Faraday Soc.*, 61 (1965) 2102.
- [47] R. Pradhan, A. Kamath, D. Brahman, B. Sinha, *Fluid Phase Equilib.*, 404 (2015) 131.
- [48] P. Griffiths, J.A. de Hasseth, *Fourier Transform Infrared Spectrometry*, 2nd edn., Wiley-Blackwell, 18 May, 2007.
- [49] L.M. Harwood, C.J. Moody, *Experimental organic chemistry: Principles and Practice*, (Illustrated edn.), Wiley-Blackwell, (1989), pp. 292.
- [50] M. Tjahjono, M. Garland, *J. Solution Chem.*, 36 (2007) 221.

CHAPTER IV

Thermophysical properties of binary mixtures of N, N-dimethylformamide with three cyclic ethers*

4.1. Introduction

The volumetric, viscometric and acoustic properties of liquid-liquid mixtures and their dependence on composition are crucial for many important chemical, industrial and biological processes. The study of excess or deviation properties like excess molar volume and viscosity deviation, *etc.*, of binary mixtures stand as useful tools for understanding the nature and strength of molecular interactions between the component molecules,^{1,2} this is because of the close connection between the liquid state³ and macroscopic properties like density, viscosity, *etc.*, such studies therefore help in understanding the behavior of the liquid-liquid mixtures and developing theoretical models for their description including simulation processes. Anyway, DMF is a polar non-associative aprotic solvent with a dipole moment, $\mu = 3.86$ Debye⁴ and dielectric constant,^{4,5} $\epsilon = 36.71$ at 298.15 K. In the liquid state it remains self-associated through dipole-dipole interactions.⁶ THF, 1,3-DO and 1,4-DO are non-polar aprotic cyclic ethers and differ in the number and position of oxygen and carbon atoms; therefore these liquids differ in quadrupolar and dipolar order.⁷ Again, the above mentioned solvents are versatile solvents used in the separation of saturated and unsaturated hydrocarbons, in pharmaceutical synthesis and serves as solvents for many polymers. So, increasing use of these liquids in many industries make the acoustic, transport and thermodynamic properties of these liquids and their mixtures worthy of further studies. Therefore the present chapter attempts to unravel the nature of molecular interactions in the binary mixtures of DMF with THF, 1,3-DO and 1,4-DO by measuring mixture densities, viscosities and ultrasonic speeds of sound over the entire composition range at different temperature and ambient pressure. The calculated excess molar volumes (V_m^E), viscosity deviations ($\Delta\eta$) and excess isentropic compressibilities (κ_S^E) were interpreted in terms of molecular interactions and structural effects. Partial molar volumes ($\bar{V}_{m,1}^0$ and $\bar{V}_{m,2}^0$) and excess partial molar

**Published in: J. Serb. Chem. Soc.* 78 (2013) 1443-1460.

Chapter IV

volumes ($\bar{V}_{m,1}^{0,E}$ and $\bar{V}_{m,2}^{0,E}$) of each component at infinite dilution were further utilized to derive the excess molar volumes (V_m^E) and interpreted in terms of molecular interactions and the nature of liquid mixtures. Also, a quantitative estimation of different contributions to the excess molar volumes (V_m^E) of the experimental binary systems at ambient temperature and pressure were derived using the PFP theory. Moreover, ultrasonic speeds of sound in all the binary mixtures were calculated using some theories and empirical relations like collision factor theory, nomoto relation, impedance dependence relation and ideal mixture relation and Flory's theory.

4.2. Experimental section

4.2.1. Materials

DMF (S. D. Fine Chemicals, India, AR, purity > 99%) was purified by the method described by Y. Zhao *et al.*⁸ 1, 4-DO and THF (Merck, India, purity > 99%) were purified as described earlier.⁹ 1,3-DO (S. D. Fine Chemicals, India, AR, purity > 99 %) was refluxed with PbO₂ and fractionally distilled after the addition of xylene.⁵ After purification all the purified chemicals were found to be better than 99.5% pure as their purity were ascertained by GLC and also by comparing experimental densities, viscosities at the experimental temperatures with their literature values⁸⁻²⁰ (Table 4.1).

4.2.2. Apparatus and procedure

The binary mixtures were prepared by mass in a dry box and each solution thus prepared was distributed into three recipients (in air-tight bottles) to perform all the measurements in triplicate with the aim of the determining possible dispersion of the results obtained. The mass measurements accurate to ± 0.01 mg were made on a digital electronic analytical balance (Mettler, AG 285, Switzerland). The reproducibility in mole fraction was within ± 0.0002 . The densities were measured with a vibrating-tube density meter (Anton Paar, DMA 4500M), maintained at ± 0.01 K of the desired temperatures and calibrated at the experimental temperatures with doubly distilled water and dry air. The uncertainty in density was estimated to be ± 0.0001 g·cm⁻³ and that of the temperature was ± 0.01 K.

Chapter IV

Table 4.1. Physical properties of various pure liquids at $T = (298.15-318.15)$ K.

Pure liquid	T/K	$\rho \cdot 10^{-3}$ ($\text{kg} \cdot \text{m}^{-3}$)		η ($\text{mPa} \cdot \text{s}$)		u ($\text{m} \cdot \text{s}^{-1}$)	
		Expt.	Lit.	Expt.	Lit.	Expt.	Lit.
DMF	298.15	0.9442	0.9442 ⁸ 0.9445 ⁹	0.803	0.802 ¹⁰ 0.803 ¹¹	1464.8	1465.0 ¹⁰ 1462.0 ¹⁰
	308.15	0.9350	0.9344 ¹⁰ 0.9347 ¹¹	0.709	0.706 ¹²	-	-
	318.15	0.9258	0.9251 ¹⁰ 0.9252 ¹¹	0.617	0.633 ¹²	-	-
THF	298.15	0.8807	0.8807 ¹²	0.463	0.4630 ¹³	1277.8	1292.2 ¹³ 1277.8 ¹⁴
	308.15	0.8712	0.8712 ¹²	0.428	0.4277 ¹³	-	-
	318.15	0.8614	0.8614 ¹²	0.390	0.3902 ¹³	-	-
1,3-DO	298.15	1.0571	1.0577 ¹² 1.0572 ¹³	0.588	0.5878 ¹³ 0.588 ¹⁵	1338.2	1338.2 ¹⁵ 1340.2 ¹⁶
	308.15	1.0459	1.0463 ¹² 1.0462 ¹⁵	0.513	0.5128 ¹³	-	-
	318.15	1.0334	1.03364 ¹⁵	0.458	0.4580 ¹³	-	-
1,4-DO	298.15	1.0265	1.0278 ¹⁶ 1.0282 ¹⁷	1.196	1.196 ¹⁸ 1.178 ¹⁹ 1.1779 ¹³	1343.4	1344.4 ¹³ 1344.8 ¹⁶
	308.15	1.0166	1.0168 ¹²	1.013	0.9985 ¹³ 0.999 ¹⁹	-	-
	318.15	1.0052	1.00526 ¹⁵	0.887	0.901 ²⁰	-	-

The viscosities were measured by means of a suspended Ubbelohde type viscometer thoroughly cleaned, dried and calibrated at the experimental temperatures with triply distilled water and purified methanol.^{4,21,22} The uncertainty in viscosity measurements was within ± 0.003 mPa·s for the mixtures studied. Ultrasonic speeds of sound (u) were measured with an accuracy of 0.3 % by using a single crystal variable-path ultrasonic interferometer (Mittal Enterprise, New Delhi, F-05) working at 2 MHz. It was calibrated with doubly distilled water, purified methanol and benzene at 298.15 ± 0.01 K. The uncertainty of ultrasonic speeds measurements was around ± 0.2 m·s⁻¹ for the systems studied. In all determinations, an average of triplicate measurements was taken into account and adequate precautions were taken to minimize evaporation losses during the actual measurements. The details of the methods and measurement techniques had been described in chapter III.

Chapter IV

4.3. Results and discussion

The experimental densities (ρ), viscosities (η), excess molar volumes (V_m^E) and viscosity deviations ($\Delta\eta$) for the binary mixtures studied at different temperatures are listed in Table 4.2.

4.3.1. Excess molar volumes

The excess molar volumes (V_m^E) were calculated using the following relation:

$$V_m^E = \sum_{i=1}^2 x_i M_i (1/\rho - 1/\rho_i) \quad (1)$$

where ρ is the density of the mixture and x_i , M_i and ρ_i are the mole fraction, molar mass and density of the i^{th} component in the mixture, respectively. The estimated uncertainty for excess molar volumes (V_m^E) was $\pm 0.005 \text{ cm}^3 \cdot \text{mol}^{-1}$. Excess molar volumes (V_m^E) of the binary mixtures as a function of mole fraction (x_1) of DMF at the experimental temperatures are depicted in Figure 4.1. The excess molar volumes (V_m^E) for all the binary systems, except for (DMF + 1,4-DO) system at 298.15 and 308.15 K, are negative over the entire range of composition at all the experimental temperatures. The excess molar volumes (V_m^E) for the three systems were observed to follow the order: (DMF + 1,4-DO) > (DMF + 1,3-DO) > (DMF + THF). According to Treszczanowicz *et al.*²³ V_m^E is a function of several opposing effects categorized into three types: physical, chemical and structural. While physical effects offer a positive contribution to V_m^E , the chemical effects or specific intermolecular interactions (such as hydrogen bond interaction, dipole-dipole/dipole-induced dipole interaction, formation of charge transfer complexes, *etc.*) cause net volume decrease and thus contribute negative values to V_m^E . The structural effects such as interstitial accommodation (due to differences in size and shape of the components) and changes in the free volume also contribute negative values to V_m^E . The actual volume change would, therefore, depend on the relative strength of these effects. The molar volumes of DMF are 77.42, 78.18, and 78.96 $\text{cm}^3 \cdot \text{mol}^{-1}$ and those of THF, 1,3-DO and 1,4-DO

Chapter IV

Table 4.2. Densities (ρ), viscosities (η), excess molar volumes (V_m^E) and viscosity deviations ($\Delta\eta$) for the binary mixtures of DMF (1) with three cyclic ethers (2) at $T = (298.15-318.15)$ K.

x_1^a	$\rho \cdot 10^{-3}$ ($\text{kg} \cdot \text{m}^{-3}$)	η ($\text{mPa} \cdot \text{s}$)	$V_m^E \cdot 10^6$ ($\text{m}^3 \cdot \text{mol}^{-1}$)	$\Delta\eta$ ($\text{mPa} \cdot \text{s}$)
DMF (1) + THF (2)				
<i>T</i> = 298.15 K				
0	0.8807	0.463	0	0
0.0988	0.8873	0.470	-0.058	-0.019
0.1978	0.8938	0.482	-0.099	-0.034
0.2971	0.9003	0.496	-0.131	-0.049
0.3967	0.9067	0.518	-0.146	-0.058
0.4966	0.9131	0.547	-0.153	-0.062
0.5967	0.9193	0.586	-0.135	-0.057
0.6971	0.9254	0.630	-0.101	-0.050
0.7978	0.9315	0.679	-0.061	-0.039
0.8988	0.9377	0.737	-0.021	-0.022
1	0.9442	0.803	0	0
<i>T</i> = 308.15 K				
0	0.8712	0.428	0	0
0.0988	0.8779	0.434	-0.067	-0.016
0.1978	0.8845	0.444	-0.115	-0.029
0.2971	0.8910	0.458	-0.145	-0.039
0.3967	0.8975	0.476	-0.167	-0.047
0.4966	0.9039	0.502	-0.172	-0.048
0.5967	0.9102	0.533	-0.159	-0.045
0.6971	0.9164	0.570	-0.130	-0.038
0.7978	0.9227	0.614	-0.103	-0.026
0.8988	0.9289	0.659	-0.059	-0.015
1	0.9350	0.709	0	0
<i>T</i> = 318.15 K				
0	0.8614	0.390	0	0
0.0988	0.8680	0.410	-0.054	0.002
0.1978	0.8749	0.431	-0.127	0.004
0.2971	0.8817	0.454	-0.181	0.007
0.3967	0.8885	0.478	-0.225	0.010
0.4966	0.8951	0.502	-0.242	0.012
0.5967	0.9013	0.523	-0.214	0.010
0.6971	0.9073	0.545	-0.160	0.008
0.7978	0.9134	0.568	-0.108	0.006
0.8988	0.9195	0.592	-0.049	0.003
1	0.9258	0.617	0	0
DMF (1) + 1, 3-DO (2)				
<i>T</i> = 298.15 K				
0	1.0571	0.588	0	0
0.1012	1.0454	0.567	-0.053	-0.040

Chapter IV

0.2021	1.0338	0.568	-0.096	-0.058
0.3028	1.0222	0.578	-0.121	-0.068
0.4032	1.0106	0.594	-0.127	-0.073
0.5033	0.9991	0.614	-0.120	-0.074
0.6032	0.9876	0.642	-0.095	-0.068
0.7028	0.9764	0.676	-0.073	-0.056
0.8021	0.9654	0.715	-0.046	-0.040
0.9012	0.9546	0.759	-0.017	-0.020
1	0.9442	0.803	0	0.
<hr/>				
<i>T</i> = 308.15 K				
0	1.0459	0.513	0	0
0.1012	1.0345	0.506	-0.059	-0.024
0.2021	1.0232	0.510	-0.108	-0.038
0.3028	1.0119	0.520	-0.140	-0.046
0.4032	1.0006	0.535	-0.153	-0.049
0.5033	0.9895	0.552	-0.162	-0.052
0.6032	0.9783	0.578	-0.145	-0.046
0.7028	0.9673	0.606	-0.124	-0.038
0.8021	0.9564	0.637	-0.091	-0.028
0.9012	0.9456	0.671	-0.047	-0.016
1	0.9350	0.709	0	0
<hr/>				
<i>T</i> = 318.15 K				
0	1.0334	0.458	0	0
0.1012	1.0221	0.467	-0.040	-0.005
0.2021	1.0115	0.477	-0.114	-0.009
0.3028	1.0008	0.488	-0.164	-0.013
0.4032	0.9901	0.500	-0.196	-0.016
0.5033	0.9793	0.515	-0.204	-0.017
0.6032	0.9683	0.534	-0.178	-0.014
0.7028	0.9573	0.555	-0.132	-0.010
0.8021	0.9466	0.576	-0.091	-0.006
0.9012	0.9359	0.597	-0.030	-0.002
1	0.9258	0.617	0	0
<hr/>				
DMF (1) + 1, 4- DO (2)				
<hr/>				
<i>T</i> = 298.15 K				
0	1.0265	1.196	0	0
0.1181	1.0173	1.109	0.028	-0.032
0.2316	1.0082	1.043	0.059	-0.048
0.3406	0.9992	0.984	0.095	-0.060
0.4455	0.9904	0.934	0.126	-0.067
0.5465	0.9820	0.891	0.135	-0.071
0.6439	0.9739	0.859	0.131	-0.066
0.7377	0.9661	0.835	0.113	-0.056
0.8282	0.9586	0.820	0.081	-0.040
0.9156	0.9513	0.811	0.044	-0.019
1	0.9442	0.803	0	0
<hr/>				
<i>T</i> = 308.15 K				
0	1.0166	1.013	0	0
0.1181	1.0077	0.952	0.009	-0.019

Chapter IV

0.2316	0.9988	0.899	0.030	-0.034
0.3406	0.9902	0.849	0.039	-0.048
0.4455	0.9817	0.807	0.052	-0.057
0.5465	0.9735	0.772	0.050	-0.061
0.6439	0.9654	0.746	0.052	-0.059
0.7377	0.9576	0.726	0.039	-0.053
0.8282	0.9499	0.714	0.030	-0.040
0.9156	0.9424	0.708	0.014	-0.023
1	0.9350	0.709	0	0
<hr/>				
<i>T</i> = 318.15 K				
0	1.0052	0.887	0	0
0.1181	0.9968	0.843	-0.013	-0.007
0.2316	0.9886	0.797	-0.031	-0.018
0.3406	0.9804	0.753	-0.036	-0.031
0.4455	0.9724	0.713	-0.046	-0.042
0.5465	0.9644	0.680	-0.045	-0.047
0.6439	0.9564	0.653	-0.034	-0.049
0.7377	0.9486	0.636	-0.028	-0.043
0.8282	0.9408	0.624	-0.012	-0.033
0.9156	0.9332	0.618	-0.002	-0.018
1	0.9258	0.617	0	0

^a Mole fraction of DMF

are 81.87, 82.77, and 83.71 cm³·mol⁻¹; 70.07, 70.83, and 71.68 cm³·mol⁻¹; and (85.83, 86.67, and 87.65) cm³·mol⁻¹ at 298.15, 308.15 and 318.15 K, respectively. Evidently molar volumes of the components in the mixtures differ appreciably and based on the differences in molar volumes of the components, the expected order of mutual or geometrical fitting of the component liquids should be: (DMF + 1,4-DO) > (DMF + 1,3-DO) > (DMF + THF); but a reversed trend in V_m^E values was observed. Figure 4.1 shows that V_m^E values increase in the order: (DMF + THF) < (DMF + 1,3-DO) < (DMF + 1,4-DO) and the dielectric constants of the cyclic ethers follow a reverse order: THF ($\epsilon = 7.58^{24}$) > 1,3- DO ($\epsilon = 7.13^{25}$) > 1,4- DO ($\epsilon = 2.21^{24}$). This suggests that a cyclic ether with a larger dielectric constant than another has greater specific interactions with DMF and the negative V_m^E for all the binary mixture studied can primarily be ascribed to dipole-dipole or dipole-induced dipole interactions between the component liquids in the mixtures. Also V_m^E values decrease as the experimental temperature increases suggesting an increase in intermolecular interactions between

Chapter IV

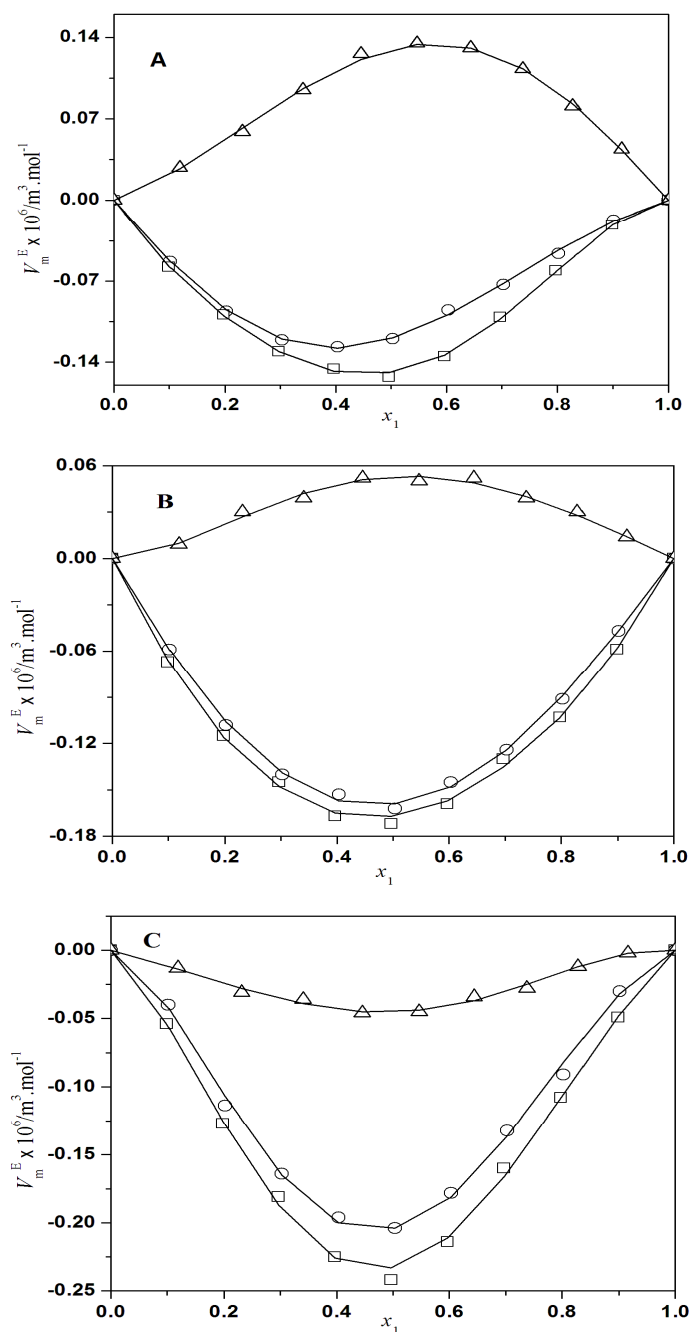


Fig. 4.1. Excess molar volume (V_m^E) versus mole fraction of DMF (x_1) for binary mixtures of DMF + cyclic ethers: A, at $T = 298.15$ K; B, at $T = 308.15$ K; C, at $T = 318.15$ K. Graphical points represent excess molar volumes (V_m^E): \square , THF; \circ , 1,3-DO; Δ , 1,4-DO. Smooth curves represent V_m^E values obtained from Redlich-Kister polynomial.

Chapter IV

the component molecules at higher temperature probably due to greater thermal agitation and enhanced mutual fitting of the components at higher temperatures.

4.3.2. Excess partial molar volumes

The partial molar volumes ($\bar{V}_{m,i}$) of the i^{th} component in the binary mixtures were calculated by using the relation:

$$\bar{V}_{m,i} = V_{m,i}^E + V_{m,i}^* + (1 - x_i)(dV_{m,i}^E/dx_i)_{T,P} \quad (2)$$

where $V_{m,i}^*$ is the molar volume of the i^{th} component in the binary mixture. The derivatives, $(dV_{m,i}^E/dx_i)_{T,P}$ used in Eq. (2) were obtained by following a procedure²⁶ of fitting the excess molar volumes (V_m^E) of the binary mixtures to Redlich–Kister polynomial²⁷ with minimum standard deviations (σ) falling in the range 0.002-0.006. Redlich–Kister polynomial²⁷ is expressed as follows:

$$V_{m,i}^E = x_1 x_2 \sum_{i=1}^2 a_i (1 - 2x_2)^i \quad (3)$$

where x_1 and x_2 are the mole fractions of the liquid 1 and 2, and a_i represents the multiple-regression coefficients. The standard deviations (σ) were calculated using the relation:

$$\sigma = \left[\sum_{i=1}^n (V_{m,\text{calc}}^E - V_{m,\text{expt}}^E)^2 / (n - p) \right]^{1/2} \quad (4)$$

where n is the number of experimental data points and p is the number of a_i coefficients (listed in Table 4.3). From the partial molar volumes ($\bar{V}_{m,i}$) the excess partial molar volumes ($\bar{V}_{m,i}^E$) can be derived using the relation:

$$\bar{V}_{m,i}^E = \bar{V}_{m,i} - V_{m,i}^* \quad (5)$$

and the excess partial molar volume at infinite dilution ($\bar{V}_{m,i}^{0,E}$) can be had from the relation:

$$\bar{V}_{m,i}^{0,E} = (dV_{m,i}^E/dx_i)_{x_i=0,T,P} \quad (6)$$

The excess partial molar volumes ($\bar{V}_{m,1}^{0,E}$ and $\bar{V}_{m,2}^{0,E}$) at infinite dilution for the three binaries at the experimental temperatures are given in Table 4.3.

Chapter IV

Table 4.3. Redlich-Kister coefficients (a_i), standard deviations (σ) for least squares fitting of excess molar volumes (V_m^E), excess partial molar volumes, ($\bar{V}_{m,1}^E$ and $\bar{V}_{m,2}^E$) and excess partial molar volumes ($\bar{V}_{m,1}^{0,E}$ and $\bar{V}_{m,2}^{0,E}$) at infinite dilution of each component in the studied binary mixtures at $T = (298.15-318.15)$ K.

Redlich-Kister coefficients (a_i)	DMF (1) +		
	THF (2)	1,3-DO (2)	1,4-DO (2)
	$T = 298.15$ K		
a_0	-0.596	-0.480	0.520
a_1	0.145	0.290	0.238
a_2	0.251	0.133	-0.180
a_3	0.184	-0.077	-0.058
σ	0.002	0.002	0.003
$\bar{V}_{m,1}^E$	76.75	76.86	77.58
$\bar{V}_{m,2}^E$	81.86	69.94	86.35
$\bar{V}_{m,1}^{0,E}$	-0.674	-0.560	0.160
$\bar{V}_{m,2}^{0,E}$	-0.016	-0.134	0.520
$T = 308.15$ K			
a_0	-0.669	-0.637	0.212
a_1	0.097	0.086	0.041
a_2	-0.040	0.068	-0.119
a_3	-0.053	-0.016	0.040
σ	0.004	0.003	0.003
$\bar{V}_{m,1}^E$	77.43	77.54	78.19
$\bar{V}_{m,2}^E$	82.11	70.33	86.84
$\bar{V}_{m,1}^{0,E}$	-0.753	-0.639	0.012
$\bar{V}_{m,2}^{0,E}$	-0.665	-0.499	0.174
$T = 318.15$ K			
a_0	-0.933	-0.819	-0.182
a_1	0.177	0.190	0.023
a_2	0.568	0.635	0.155
a_3	-0.203	-0.205	0.048
σ	0.006	0.006	0.003
$\bar{V}_{m,1}^E$	78.62	78.79	78.86
$\bar{V}_{m,2}^E$	83.32	71.49	87.70
$\bar{V}_{m,1}^{0,E}$	-0.339	-0.169	-0.098
$\bar{V}_{m,2}^{0,E}$	-0.391	-0.199	0.044

Various molar volumes are given in $\text{cm}^3 \cdot \text{mol}^{-1}$.

Chapter IV

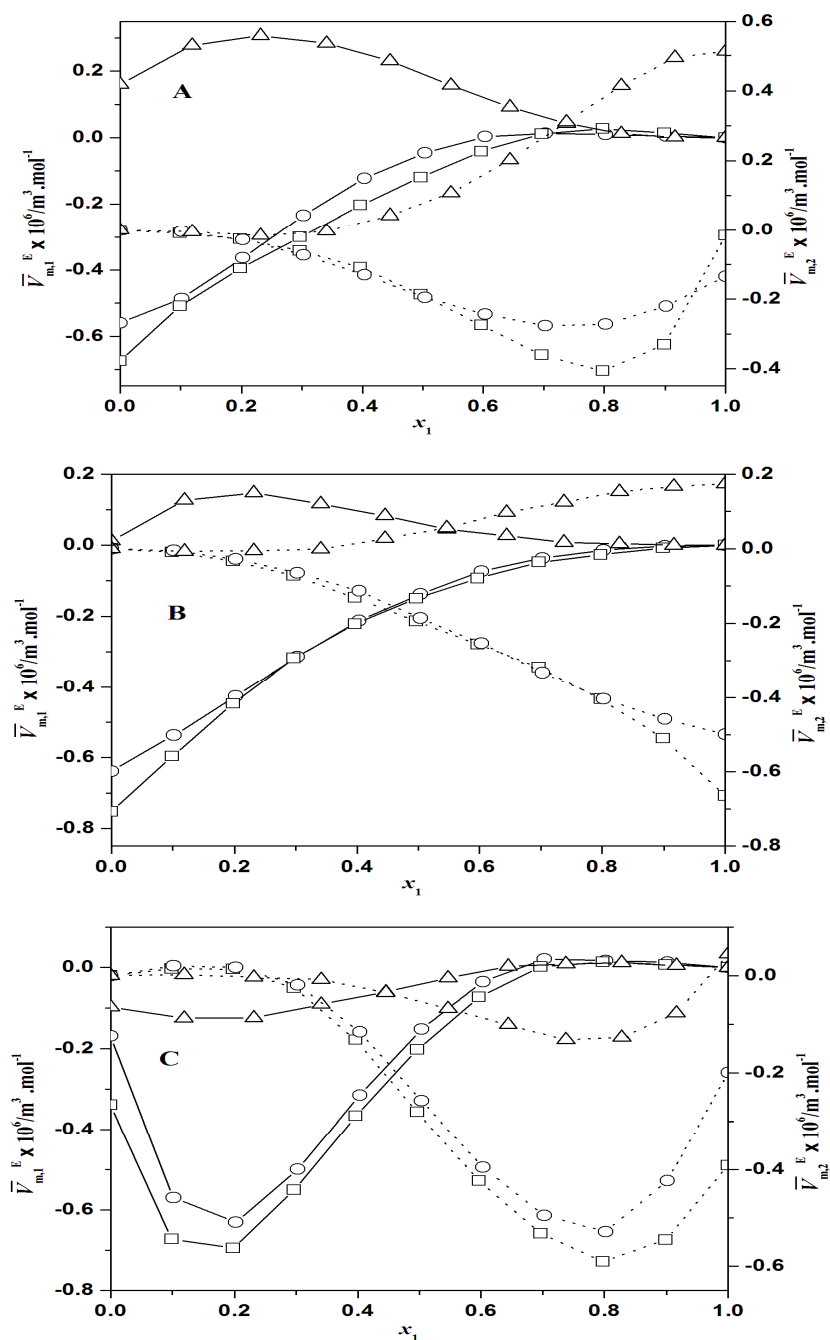


Fig. 4.2. Excess partial molar volumes ($\bar{V}_{m,i}^E$) for the i^{th} component against mole fraction of DMF (x_1) for binary mixtures of DMF + cyclic ethers: A, at $T = 298.15$ K; B, at $T = 308.15$ K; C, at $T = 318.15$ K. Graphical points represent $\bar{V}_{m,i}^E$ values for mixtures of DMF +: THF, \square ; 1,3-DO, \circ ; 1,4-DO, Δ . Solid curves represent $\bar{V}_{m,i}^E$ values for DMF and dotted curves represent $\bar{V}_{m,i}^E$ values for cyclic ethers.

Chapter IV

The excess partial molar volumes ($\bar{V}_{m,1}^E$ and $\bar{V}_{m,2}^E$) of each component in the studied binaries are depicted in Figure 4.2 as a function of x_1 . $\bar{V}_{m,1}^E$ and $\bar{V}_{m,2}^E$ values were found to be negative for all the binary systems except the binary mixture containing 1,4-DO over the entire composition range at the experimental temperatures. Also, the excess partial molar volumes at infinite dilution ($\bar{V}_{m,1}^{0,E}$ and $\bar{V}_{m,2}^{0,E}$) were found to be negative for both components in all the binary systems except for the binary mixture (DMF + 1,4-DO) [However, $\bar{V}_{m,2}^{0,E}$ and $\bar{V}_{m,2}^{0,E}$ values were negative at 318.15 K for this system]. These results suggest that while (DMF + 1,4-DO) system is characterized by volume expansion at 298.15 and 308.15 K, other systems (DMF + 1,3-DO) and (DMF + THF) are characterized by volume contraction.

4.3.3. Prigogine-Flory-Patterson theory (PFP)

In recent years Flory's statistical theory²⁸⁻³¹ and its modified version, *i.e.*, Prigogine-Flory-Patterson theory,^{32,33} have been successfully used to estimate and analyze theoretically the excess thermodynamic functions of the binary liquid mixtures; PFP theory is applicable to mixtures of both non-polar and polar molecules. The reduced equation of state in Flory's notation³⁰ is given by,

$$\frac{\tilde{P}\tilde{V}}{\tilde{T}} = \frac{\tilde{v}^{1/3}}{\tilde{v}^{1/3} - 1} - \frac{1}{\tilde{v}\tilde{T}} \quad (7)$$

$$\tilde{v} = \frac{V}{V^*} \quad (8)$$

$$\tilde{T} = \frac{T}{T^*} \quad (9)$$

$$\tilde{P} = \frac{P}{P^*} \quad (10)$$

where are \tilde{v} , \tilde{T} and \tilde{P} are reduced volume, reduced temperature and reduced pressure; V^* , T^* and P^* are characteristic volume, characteristic temperature and characteristic pressure of each pure liquid components, respectively. In Flory's treatment, the reduced equation of state in the limit of zero pressure (or without appreciable error at 1 atmospheric pressure³¹) takes the following form,

Chapter IV

$$\tilde{T} = \frac{\tilde{v}^{1/3} - 1}{\tilde{v}^{4/3}} \quad (11)$$

$$\tilde{v} = \left[\frac{1 + (4/3)\alpha T}{1 + \alpha T} \right]^3 \quad (12)$$

$$T^* = \frac{T}{\tilde{T}} = \frac{T\tilde{v}^{4/3}}{\tilde{v}^{1/3} - 1} \quad (13)$$

$$P^* = \gamma T \tilde{v}^2 \quad (14)$$

where the thermal expansion coefficient (α) and thermal pressure coefficient (γ) are given by the following relations,

$$\alpha = V^{-1}(dV/dT)_p = -\rho^{-1}(d\rho/dT)_p \quad (15)$$

$$\gamma = (dP/dV)_V = \alpha \kappa_T^{-1} \quad (16)$$

where κ_T is isothermal compressibility and it can be had from the relation,

$$\kappa_T = \kappa_S + \frac{T\alpha^2 V}{c_p} \quad (17)$$

The Flory's parameters for each liquid component are given in Table 4.4.

Table 4.4. Flory's parameters for pure liquids at 298.15 K.

Liquids	\tilde{v}	\tilde{T}	$V^* \cdot 10^6$ ($\text{m}^3 \cdot \text{mol}^{-1}$)	P^* (Pa)	T^* (K)	$\alpha \cdot 10^4$ (K^{-1})	$\kappa_T \cdot 10^{10}$ (Pa^{-1})
DMF	1.2424	0.05618	62.31	701.85	5307.04	9.744	6.389
THF	1.2670	0.05987	64.62	562.13	4980.01	10.957	9.329
1,3-DO	1.2720	0.06067	55.09	726.60	4921.11	11.209	7.442
1,4-DO	1.2553	0.05815	68.37	674.51	5127.02	10.375	7.227

Isobaric molar heat capacity (c_p) for different component liquids were taken from the literature.^{34,35} From Prigogine-Flory-Patterson theory,^{36,37} a quantitative estimation of different contributions to V_m^E can be obtained and the approximate expression for V_m^E is given by:

Chapter IV

$$\begin{aligned}
 \frac{V_m^E}{x_1 V_1^* + x_2 V_2^*} &= \frac{(\tilde{v}^{1/3} - 1)\tilde{v}^{2/3}\psi_1\theta_2}{[(4/3)\tilde{v}^{-1/3} - 1]P_1^*} \chi_{1,2} - \frac{(\tilde{v}_1 - \tilde{v}_2)^2 [(14/9)\tilde{v}^{-1/3} - 1]\psi_1\psi_2}{[(4/3)\tilde{v}^{-1/3} - 1]\tilde{v}} \\
 &\quad (\chi_{1,2} \text{ contribution}) \qquad \qquad \qquad (\tilde{v} \text{ contribution}) \\
 &+ \frac{(\tilde{v}_1 - \tilde{v}_2)(P_1^* - P_2^*)\psi_1\psi_2}{(P_1^*\psi_2 + P_2^*\psi_1)} \\
 &\quad (P^* \text{ contribution})
 \end{aligned} \tag{18}$$

where P_i^* , V_i^* and ψ_i are characteristic pressure, volume and the molecular contact energy fraction of the i^{th} pure component, respectively; the θ_2 is the molecular site fraction of the second component in a binary liquid mixture. The molecular contact energy fractions (ψ_i), the molecular site fractions (θ_i) and molecular segment fractions ($\phi_{s,i}$) are defined by the relations,

$$\psi_1 = 1 - \psi_2 = \frac{\phi_1 P_1^*}{\phi_1 P_1^* + \phi_2 P_2^*} \tag{19}$$

$$\theta_1 = 1 - \theta_2 = \frac{\phi_{s,1}}{\phi_{s,1} + (V_1^*/V_2^*)^{1/3}} \tag{20}$$

$$\phi_{s,1} = 1 - \phi_{s,2} = \frac{x_1 V_1^*}{x_1 V_1^* + x_2 V_2^*} \tag{21}$$

Actually in deriving the interaction parameter ($\chi_{1,2}$), V_m^E values of each composition (of each systems) were fitted to Eq. (18) through the use of Eqs. (11)-(17) using a computer program that finally provided an optimized value of the interaction parameter ($\chi_{1,2}$) with least error. Table 4.5 contains the optimized $\chi_{1,2}$ values, calculated and experimental V_m^E values, their deviation and values of different contributions to V_m^E values for equimolar ($x_1 \approx 0.5$) composition at 298.15 K. It is clear from Table 4.5 that the calculated excess molar volumes ($V_{m,\text{PFP}}^E$) reasonably agree with the experimental excess molar volumes ($V_{m,\text{exp}}^E$) for all the systems studied.

A comparison between $V_{m,\text{exp}}^E$ and $V_{m,\text{PFP}}^E$ values as a function of mole fraction (x_1) of DMF at 298.15 K has been depicted in Figure 4.3. According to PFP theory, the interaction contribution is proportional to the interaction parameter $\chi_{1,2}$, the free volume contribution arises from the dependence of reduced volume on reduced

Chapter IV

Table 4.5. Values of interaction parameter ($\chi_{1,2}$) calculated and experimental values of excess molar volumes ($V_{m,\text{PFP}}^E$ and $V_{m,\text{exp}}^E$), their deviations (ΔV_m^E) and different PFP contributions at 298.15 K.

DMF (1) +	$\chi_{1,2}$ ($\text{J} \cdot \text{m}^{-3}$)	$V_{m,\text{exp}}^E \cdot 10^6$ ($\text{m}^3 \cdot \text{mol}^{-1}$)	$V_{m,\text{PFP}}^E \cdot 10^6$ ($\text{m}^3 \cdot \text{mol}^{-1}$)	$\Delta V_m^E \cdot 10^6$ ($\text{m}^3 \cdot \text{mol}^{-1}$)	PFP contributions $\times 10^3$		
					int ^a	fv ^b	ip ^c
THF (2)	-4.588	-0.1531	-0.1427	-0.0104	-0.826	-0.224	-1.362
1,3-DO (2)	-15.085	-0.1204	-0.1204	0	-1.979	-0.326	0.255
1,4-DO (2)	18.008	0.1353	0.1243	0.0110	2.270	-0.063	-0.128

^ainteraction contribution, ^bfree volume contribution and ^cinternal pressure contribution

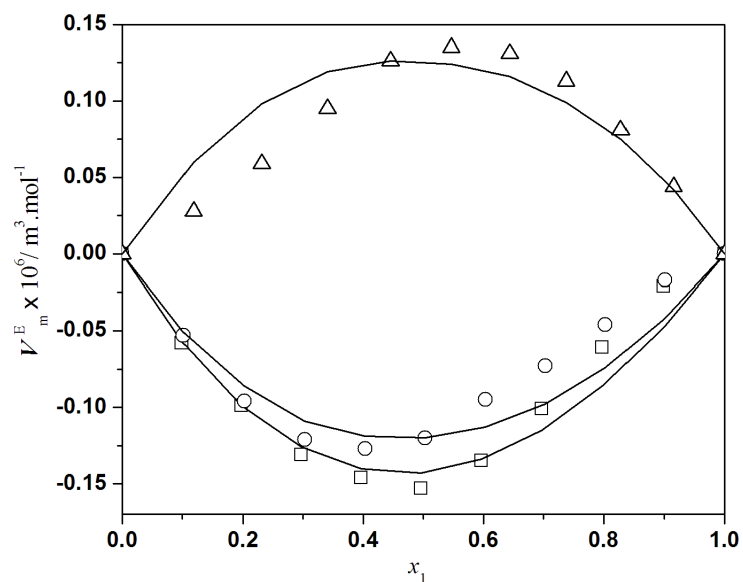


Fig. 4.3. Comparison between experimental excess molar volumes and those obtained from Prigogine-Flory-Patterson theory as a function of mole fraction of DMF (x_1) for binary mixtures of DMF + cyclic ethers at $T = 298.15$ K. Graphical points represent experimental excess molar volumes ($V_{m,\text{exp}}^E$): \square , THF; \circ , 1,3-DO; Δ , 1,4-DO and smooth curves represent $V_{m,\text{PFP}}^E$ values obtained from Prigogine-Flory-Patterson theory.

temperature due to the differences between the degree of expansion of two mixing components (always negative as dV^2/dT^2 is positive) and the internal pressure

Chapter IV

contribution depends on the product of the differences between reduced volumes and characteristic pressures of the mixing components. Table 4.5 shows that the interaction contributions are negative for the systems (DMF + THF) and (DMF + 1,3-DO) but positive for the system (DMF + 1,4-DO); internal pressure contributions, except for 1,3-DO system, are negative for all the studied systems. From Table 4.5 it is evident that while interaction contribution ($\chi_{1,2}$) plays a dominant role in deciding the sign and magnitude of $V_{m,PPF}^E$ values for the systems (DMF + 1,3-DO) and (DMF + 1,4-DO), internal pressure contribution (P^*) plays major role in deciding the nature of $V_{m,PPF}^E$ values for the system (DMF + THF).

4.3.4. Viscosity deviations

The viscosity deviation ($\Delta\eta$) is the difference between the measured viscosity (η) and the ideal viscosity (η_{id}) of a solution as expressed by Eq. (22):³⁸

$$\Delta\eta = \eta - \eta_{id} \quad (22)$$

and η_{id} can be defined by Eq. (23):³⁹

$$\eta_{id} = \exp\left(\sum_{i=1}^2 x_i \ln \eta_i\right) \quad (23)$$

where η_i is the viscosity of the i^{th} component in the mixture and the additivity law in a logarithm form has been considered for ideal mixtures. The estimated uncertainty for viscosity deviation ($\Delta\eta$) was within ± 0.004 mPa.s for the present systems. Plots of viscosity deviations ($\Delta\eta$) versus mole fraction (x_1) of DMF for the different binary mixtures at the experimental temperatures are depicted in Figure 4.4. $\Delta\eta$ values of the binary mixtures were fitted to Redlich–Kister polynomial (shown as curves in Figure 4.4) with standard deviations (σ) lying in the range 0.001-0.002. Figure 4.4 shows that $\Delta\eta$ values, except for the system with THF at 318.15 K, are negative for all the mixtures over the entire composition range at all the experimental temperatures. The negative $\Delta\eta$ values indicate the presence of dispersion forces in these mixtures; while positive $\Delta\eta$ values may be attributed to the presence of specific

Chapter IV

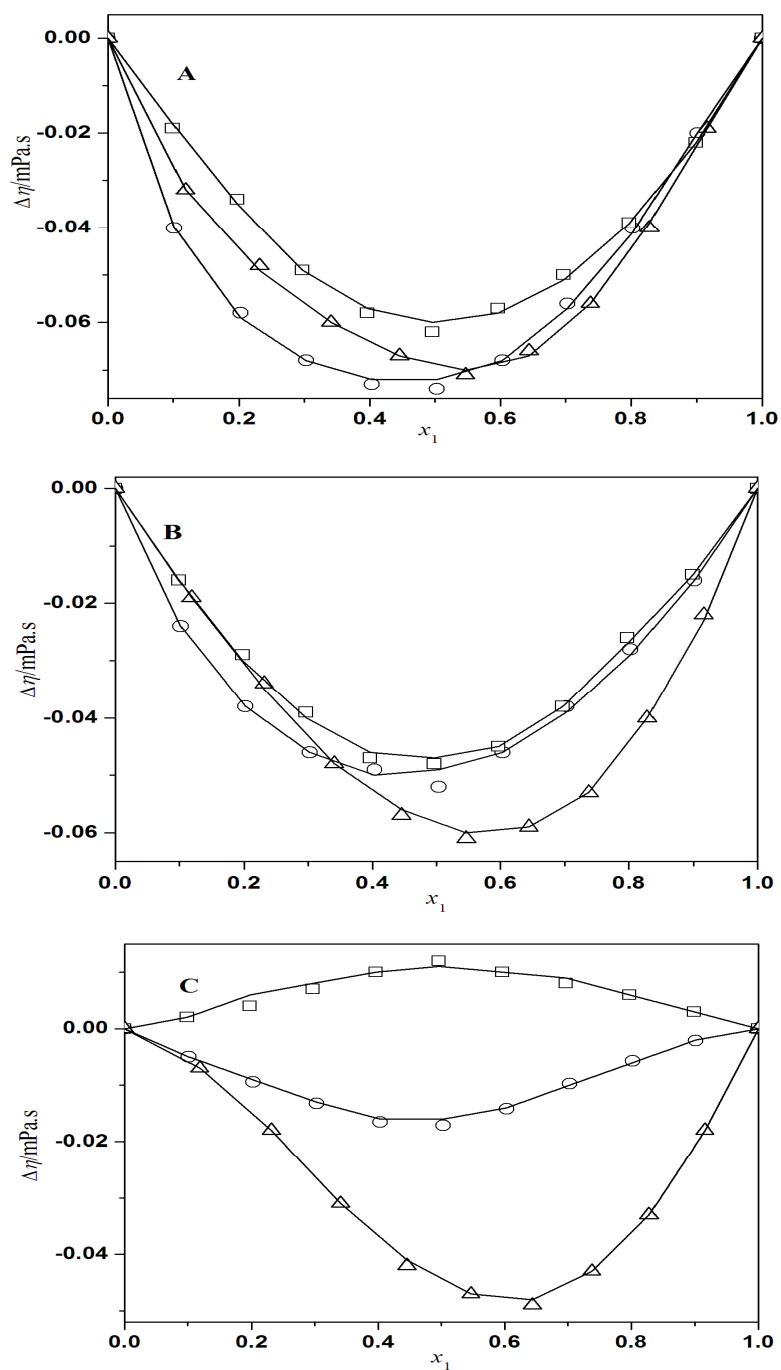


Fig. 4.4. Viscosity deviations ($\Delta\eta$) versus mole fraction of DMF (x_1) for binary mixtures of DMF + cyclic ethers: A, at $T = 298.15$ K; B, at $T = 308.15$ K; C, at $T = 318.15$ K. Graphical points represent experiment $\Delta\eta$ values: \square , THF; \circ , 1,3-DO; Δ , 1,4-DO and smooth curves represent $\Delta\eta$ values obtained from Redlich-Kister polynomial.

Chapter IV

interactions. As expected, the $\Delta\eta$ values become less negative, *i.e.*, increase as the temperature increases but decrease as the dielectric constant of the ethers decrease from THF to 1,4-DO (Figure 4.4). This suggests that the strength of molecular interactions in the mixture follows the order: (DMF + THF) > (DMF + 1,3-DO) > (DMF + 1,4-DO) and increase with the increase in temperature. Thus the functions V_m^E and $\Delta\eta$ compliment each other in describing the behavior of the binary mixtures studied.

4.3.5. Thermodynamics of viscous flow

Eyring's viscosity relation³⁹ yields the following equation for the free energy of viscous flow (ΔG^*),

$$\eta = (hN/V)\exp(\Delta G^*/RT) \quad (24)$$

where h is Planck's constant, N is Avogadro's number and other symbols have their usual meanings. Rearranging Eq. (24) and putting $\Delta G^* = \Delta H^* - T\Delta S^*$ we get the relation,

$$R\ln(\eta V/hN) = (\Delta H^*/T) - \Delta S^* \quad (25)$$

Thus, linear regressions of $R\ln(\eta V/hN)$ against $(1/T)$ can give the values of enthalpy (ΔH^*) and entropy (ΔS^*) of activation of viscous flow from the slope and negative intercept, respectively. The ΔH^* , ΔS^* and the linear regression coefficients (R^2) as given in Table 4.6 show that while ΔH^* values are positive, ΔS^* values are negative for all the studied binary mixtures throughout the entire composition range. According to Corradini *et al.*⁴⁰ the enthalpy of activation of viscous flow may be regarded as a measure of the degree of cooperation between the species taking part in viscous flow. In a highly structured liquid there will be considerable degree of order; hence for cooperative movement of the entities a large heat of activation is required for the flow process. Thus the ΔH^* values indicate that the ease of formation of activated species necessary for viscous flow follows the order: (DMF + THF) > (DMF + 1,3-DO) > (DMF + 1,4 DO). This order is also supported by negative values of ΔS^* for the mixtures.

Chapter IV

Table 4.6. Values of enthalpy (ΔH^*) and entropy (ΔS^*) of activation of viscous flow for the binary mixtures.

x_1^a	ΔH^* (kJ·mol ⁻¹)	ΔS^* (J·K ⁻¹ ·mol ⁻¹)	R^2
DMF (1) + THF (2)			
0	5.884	-18.150	0.9948
0.0988	4.527	-22.725	0.9902
0.1978	3.588	-25.992	0.9089
0.2971	2.695	-29.152	0.7474
0.3967	2.406	-30.410	0.5981
0.4966	2.636	-30.051	0.6587
0.5967	3.736	-26.902	0.8361
0.6971	4.958	-23.390	0.9473
0.7978	6.273	-19.605	0.9956
0.8988	7.865	-14.926	0.9999
1	9.604	-9.790	0.9972
DMF (1) + 1,3-DO (2)			
0	8.965	-8.460	0.9981
0.1012	6.775	-15.570	0.9902
0.2021	6.041	-18.118	0.9809
0.3028	5.856	-18.963	0.9783
0.4032	5.999	-18.804	0.9849
0.5033	6.158	-18.629	0.9856
0.6032	6.494	-17.973	0.9944
0.7028	7.005	-16.778	0.9971
0.8021	7.753	-16.830	0.9992
0.9012	8.687	-12.288	1.0000
1	9.604	-9.790	0.9972
DMF (1) + 1,4-DO (2)			
0	10.970	-9.314	0.9971
0.1181	10.022	-11.775	0.9970
0.2316	9.842	-11.781	0.9977
0.3406	9.810	-11.317	0.9978
0.4455	9.929	-10.405	0.9988
0.5465	9.947	-9.876	0.9996
0.6439	10.097	-8.997	1.0000
0.7377	10.014	-8.957	1.0000
0.8282	10.030	-8.673	0.9999
0.9156	9.956	-8.754	0.9997
1	9.604	-9.790	0.9972

^a Mole fraction of DMF

Chapter IV

4.3.6. Excess isentropic compressibilities

Using the ultrasonic speed (u) and density data, the isentropic compressibilities (κ_S) and excess isentropic compressibility (κ_S^E)⁴¹ of the binary mixtures were determined using the following equations:

$$\kappa_S = 1/u^2 \rho \quad (26)$$

$$\kappa_S^E = \kappa_S - \kappa_S^{\text{id}} \quad (27)$$

$$\kappa_S^{\text{id}} = \sum_{i=1}^2 \phi_i \left[\kappa_{S,i} + \frac{TV_i \alpha_i^2}{c_{P,i}} \right] - \left\{ \frac{T \sum_{i=1}^2 (x_i V_i) \sum_{i=1}^2 (\phi_i \alpha_i)^2}{\sum_{i=1}^2 (x_i c_{P,i})} \right\} \quad (28)$$

where ϕ_i , $\kappa_{S,i}$, V_i , α_i and $c_{P,i}$ are volume fraction, isentropic compressibility, molar volume, thermal expansion coefficient and isobaric enthalpy of the i^{th} pure component in the binary mixtures, respectively at 298.15 K. Experimental speeds of sound, isentropic compressibilities (κ_S) and excess isentropic compressibilities (κ_S^E) at 298.15 K are given in Table 4.7. The estimated uncertainty of isentropic compressibility (κ_S^E) was within $\pm 1.0 \times 10^{10} \text{ Pa}^{-1}$ for the mixtures studied. For all the investigated binary mixtures, excess isentropic compressibilities (κ_S^E) were negative, except for the mixture (DMF + 1, 4-DO) at 1,4-DO rich region (Table 4.7). κ_S^E values of the binary mixtures were also fitted to Redlich–Kister polynomial (shown as curves in Figure 4.5) with standard deviations (σ) lying in the range 0.003-0.007. Figure 4.5 depicts the composition dependence of excess isentropic compressibilities (κ_S^E) for the investigated binary mixtures at 298.15 K. It shows that the values of excess isentropic compressibility (κ_S^E) decrease in the order: (DMF + 1,4-DO) > (DMF + 1,3-DO) > (DMF + THF) supporting the observations obtained from V_m^E and $\Delta\eta$ values.

Chapter IV

Table 4.7. Ultrasonic speeds (u), isentropic compressibilities (κ_s) and excess isentropic compressibilities (κ_s^E) of binary mixtures of DMF (1) + the cyclic ethers (2) at 298.15 K.

x_1^a	u ($\text{m} \cdot \text{s}^{-1}$)	$\kappa_s \times 10^{10}$ (Pa^{-1})	$\kappa_s^E \times 10^{10}$ (Pa^{-1})
DMF (1) + THF (2)			
0	1277.8	6.954	0
0.0988	1313.2	6.535	-0.254
0.1978	1343.8	5.196	-0.420
0.2971	1369.6	5.921	-0.513
0.3967	1395.5	5.663	-0.581
0.4966	1418.8	5.441	-0.605
0.5967	1438.1	5.260	-0.580
0.6971	1452.1	5.125	-0.500
0.7978	1462.9	5.016	-0.387
0.8988	1463.5	4.979	-0.194
1	1464.8	4.936	0
DMF (1) + 1, 3-DO (2)			
0	1338.2	5.283	0
0.1012	1352.6	5.229	-0.028
0.2021	1369.8	5.155	-0.072
0.3028	1387.8	5.079	-0.117
0.4032	1406.2	5.004	-0.159
0.5033	1424.9	4.930	-0.199
0.6032	1440.4	4.880	-0.212
0.7028	1452.3	4.856	-0.199
0.8021	1460.2	4.858	-0.158
0.9012	1462.8	4.896	-0.082
1	1464.8	4.936	0
DMF (1) + 1, 4- DO (2)			
0	1343.4	5.398	0
0.1181	1368.4	5.250	-0.103
0.2316	1386.5	5.160	-0.148
0.3406	1397.5	5.124	-0.137
0.4455	1404.8	5.116	-0.099
0.5465	1408.6	5.132	-0.036
0.6439	1414.5	5.122	0.010
0.7377	1422.7	5.076	0.038
0.8282	1432.7	5.029	0.053
0.9156	1446.9	4.983	0.039
1	1464.8	4.936	0

^a Mole fraction of DMF

Chapter IV

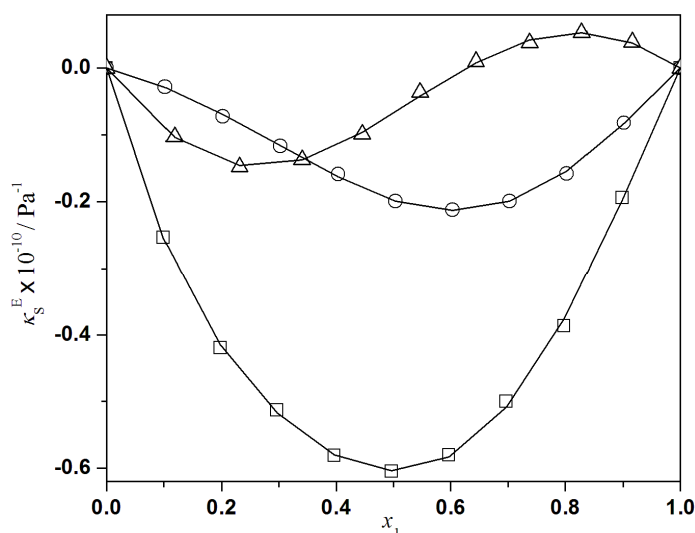


Fig. 4.5. Excess isentropic compressibility (κ_S^E) versus mole fraction of DMF (x_1) for binary mixtures of DMF + cyclic ethers at $T = 298.15$ K. Graphical points represent experimental experimental κ_S^E values: \square , THF; \circ , 1,3-DO; \triangle , 1,4-DO and smooth curves represent κ_S^E values obtained from Redlich-Kister polynomial.

4.3.7. Theoretical prediction of ultrasonic speeds

Ultrasonic speeds of sound for all the three binary mixtures were theoretically predicted using the following theories and empirical relations:

Flory's theory²⁸ yields,

$$u_{\text{FLO}} = \left(\frac{10^4 \sigma_s}{6.3\rho} \right) \quad (29)$$

where σ_s is the surface tension of liquid or liquid mixture calculated following Pandey's approach⁴² through a extension of a work of Patterson and Rastogi.⁴³

Collision factor theory (CFT)⁴⁴ yields:

$$u_{\text{CFT}} = u_{\infty} \frac{\sum_{i=1}^2 (x_i S_i) \sum_{i=1}^2 (x_i B_i)}{V_{\text{mix}}} \quad (30)$$

where $u_{\infty} = 1600 \text{ m}\cdot\text{s}^{-1}$, S_i and B_i represent collision factor and actual volume of a molecule per mole for the i^{th} pure component in the mixtures, respectively.

Chapter IV

Nomoto relation (NOM)⁴⁵ yields,

$$u_{\text{NOM}} = \left(\frac{\sum_{i=1}^2 (x_i R_i)}{\sum_{i=1}^2 (x_i V_i)} \right)^3 \quad (31)$$

where R_i stands for molar speed of sound for the i^{th} pure component in the mixtures.

Impedance dependence relation (IDR)⁴⁶ yields,

$$u_{\text{IDR}} = \frac{\sum_{i=1}^2 (x_i z_{\text{im},i})}{\sum_{i=1}^2 (x_i \rho_i)} \quad (32)$$

where $z_{\text{im},i}$ stands for specific acoustic impedance for the i^{th} pure component in the mixtures.

Ideal mixture relation (IMR)⁴⁷ yields,

$$u_{\text{IMR}} = \left[\sum_{i=1}^2 (x_i M_i) \sum_{i=1}^2 (x_i / M_i u_i^2) \right]^{-\frac{1}{2}} \quad (33)$$

where u_i is ultrasonic speed of sound for the i^{th} pure component in the mixtures. It is observed that values obtained from all of these theories and empirical relations have some deviations from experimental speeds of sound and based on the MRSD% values (listed in Table 4.8 and shown graphically in Figure 4.6), the relative predictive capability for the different relations follows the orders: FLORY > IDR > CFT > NOM >> IMR (for DMF + THF system); CFT ~ NOM > IDR > IMR >> FLORY (for DMF + 1,3-DO system) and CFT > IDR > NOM ~ IMR >> FLORY (DMF + 1,3-DO system).

Table 4.8. Relative predictive capabilities of various theories and empirical relations for ultrasonic speeds of the binary mixtures at 298.15 K

DMF (1) +	MRSD% ^a				
	FLORY	CFT	NOM	IMR	IDR
THF (2)	1.96	2.50	2.86	3.15	2.43
1,3-DO (2)	1.48	1.10	1.10	1.40	1.39
1,4-DO (2)	1.74	0.70	0.76	0.76	0.72

^aMRSD% = $100 \times [1/N \sum \{(u_{\text{exp}} - u_{\text{cal}}) / u_{\text{exp}}\}^2]^{1/2}$, N is number of data points.

Chapter IV

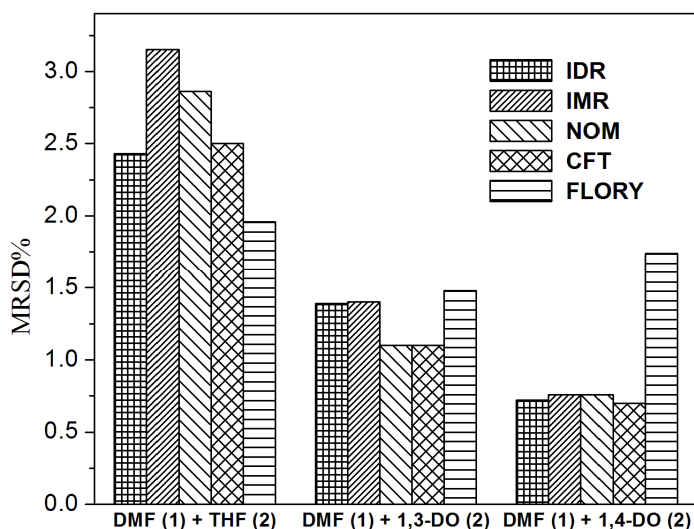


Fig. 4.6. MRSD% values for theoretical prediction of ultrasonic speeds by different theories and empirical relations for binary mixtures of DMF + cyclic ethers at $T = 298.15$ K.

4.4. Conclusion

Based on the nature and magnitude of various excess or deviation functions (V_m^E , $\Delta\eta$ and κ_S^E) and other derived parameters ($\bar{V}_{m,1}^E$, $\bar{V}_{m,2}^E$, $\bar{V}_{m,1}^{0,E}$, $\bar{V}_{m,2}^{0,E}$, etc), evidently molecular interactions in the binary systems studied can primarily be attributed to dipole-dipole or dipole-induced dipole interactions; PFP theory has provided a satisfactory quantitative estimation of different contributions to the excess molar volumes (V_m^E) for the systems at ambient temperature and pressure.

References

- [1] B. Garcia, R. Alcalde, J.M. Leal, J.S. Mantos, *J. Chem. Soc., Faraday Trans.*, 93 (1997) 1115.
- [2] Y. Mahan, C.N. Liew, A.E. Mather, *J. Solution Chem.*, 31 (2002) 743.
- [3] C.R Reid, B.E. Poling, *The properties of Gases and Liquids*, McGraw Hill, New York, (1998), Ch.1
- [4] J.A. Dean, *Lange's Handbook of Chemistry*, 11th ed., McGraw Hill, New York, (1973).
- [5] J.A. Riddick, W.B. Bunger, T.K. Sakano, *Organic solvents. Techniques of Chemistry*, Vol. 2, 4th ed., Wiley Interscience, New York, (1986).
- [6] R. Gopal, S. Agarwal, D.K. Agarwal, *J. Chem. Thermodyn.*, 8 (1976) 1205.

Chapter IV

- [7] P. Brocos, E. Calvo, A. Pineiro, R. Bravo, A. Amigo, J. Chem. Eng. Data 44 (1999) 1341.
- [8] Y. Zhao, J. Wang, X. Xuan, J. Lu, J. Chem. Eng. Data 45 (2000) 440.
- [9] M.N. Roy, R. Dey, A. Jha, J. Chem. Eng. Data 46 (2001) 1327.
- [10] I. Johnson, M. Kalidoss, R. Srinivasamoorthy, J. Chem. Eng. Data 47 (2002) 1388.
- [11] P.S. Nikam, S.J. Kharat, J. Chem. Eng. Data 50 (2005) 455.
- [12] S. Akhtar, A.N.Q. Faruk, M.A. Saleh, Phys. Chem. Liq., 39 (2001) 383.
- [13] M. Das, M.N. Roy, J. Chem. Eng. Data 51 (2006) 2225.
- [14] A. Valen, I. Gascon, C. Lafuente, J.S. Urieta, F.M. Royo, M. Postigo, Int. J. Thermophys., 23 (2002) 1587.
- [15] L. Sarkar, M.N. Roy, J. Chem. Eng. Data 54 (2009) 3307.
- [16] A. Villares, S. Martin, M. Haro, B. Giner, H. Artigas, J. Chem. Thermodyn., 36 (2004) 1027.
- [17] A. Inglese, J.E. Groller, E. Wilhelm, J. Chem. Eng. Data 28 (1983) 124.
- [18] S.M. Contreras, J. Chem. Eng. Data 46 (2001) 1149
- [19] T.M. Aminabhavi, V.B. Patil, J. Chem. Eng. Data 43, (1998) 497.
- [20] K.P. Rao, K.S. Reddy, J. Chem. Eng. Data 33 (1988) 130.
- [21] K.N. Marsh, *Recommended Reference Materials for the Realisation of Physicochemical Properties*, Blackwell Scientific Publications, Oxford, U. K., (1987).
- [22] A. Chatterjee, B. Das, J. Chem. Eng. Data 51 (2006) 1352.
- [23] A.J. Treszczanowicz, O. Kiyohora, G.C. Benson, J. Chem. Thermodyn., 13 (1981) 253.
- [24] J.F. Coetzee, T.-H. Chang, Pure. Appl. Chem., 57 (1985) 633.
- [25] A. Sinha, M.N. Roy, J. Mol. Liq., 140 (2008) 39.
- [26] B. Sinha, Phys. Chem. Liq., 48 (2010) 183.
- [27] O. Redlich, A.T. Kister, Indus. Eng. Chem., 40 (1948) 345.
- [28] P.J. Flory, R.A. Orwell, A. Vrijji, J. Am. Chem. Soc., 86, (1964) 3507.
- [29] P.J. Flory, R.A. Orwell, A. Vrijji, J. Am. Chem. Soc., 86 (1964) 3515.
- [30] P.J. Flory, J. Am. Chem. Soc., 87 (1965) 1833.
- [31] A. Abe, P.J. Flory, J. Am. Chem. Soc. 87 (1965) 1838
- [32] D. Patterson, G. Delmas, J. Polym. Sci., 30 (1970) 1.
- [33] D. Patterson, Pure. Appl. Chem., 47 (1976) 305.
- [34] C.de. Visser, G. Perron, J.E. Desnoyers, J. Chem. Eng. Data 22 (1977) 74.

Chapter IV

- [35] P. Brocos, E. Calvo, R. Bravo, M. Pintos, A. Amigo, J. Chem. Eng. Data 44 (1999) 67.
- [36] I. Prigogine, R. Defay, *Chemical Thermodynamics*, 5th ed., Longman, London, (1994), pp. 8.
- [37] P. Tancrede, P. Bothorel, P.St. Romain, D. Patterson. J. Chem. Soc. Faraday Trans., II 73 (1977) 15.
- [38] M.A. Saleh, S. Akhtar, M.S. Ahmed, Phys. Chem. Liq., 44 (2006) 551.
- [39] S. Glasstone, K.J. Laidler, H. Eyring, *The Theory of Rate Process*, McGraw-Hill Book Company, New York, 1941.
- [40] F. Corradini, L. Marcheselli, A. Marchetti, M. Tagliazucchi, L. Tassi, G. Tosi, Bull. Chem. Soc. Jpn., 65 (1992) 503.
- [41] D. Kiyohora. G.C. Benson, J. Chem. Thermodyn., 11 (1979) 861.
- [42] J.D. Pandey, J. Chem. Soc., Faraday Trans I, 75 (1979) 2160.
- [43] D. Patterson, A.K. Rastogi, J. Phys. Chem., 74 (1970) 1067.
- [44] B. Jacobson, J. Chem. Phys., 20 (1952) 927.
- [45] O. Nomoto, J. Phys. Soc. Jpn., 13 (1958) 1528.
- [46] M. Kalidoss, R. Srinivasamoorthy, J. Pure. Appl. Ultrason., 19 (1997) 9.
- [47] W. Van Dael, E. Vangael, in abst. paper: *Proc. 1st International Conference on Calorimetry and Thermodynamics*, Warsaw, Poland, (1969), pp. 555.

CHAPTER V

Thermophysical properties of the binary mixtures of 2-ethyl-1-hexanol with 1, 2-disubstituted ethanes at $T = (298.15- 318.15)$ K

5.1. Introduction

The molecular interactions, operating between different liquids in liquid-liquid systems, control their physico-chemical properties and are of major significance in relation to their industrial applications.^{1,2} The information based on density and viscosity of pure liquid and their mixtures are important for both practical and theoretical purposes. The excess properties of the binary mixtures reflect the extent of deviation in their properties from ideality and can be successfully employed in understanding the nature and the strength of the molecular interactions in such mixtures. Again ultrasonic study of the liquid systems containing the pure liquids and their mixtures has gained much importance in assessing the nature of molecular interactions and investigating the physicochemical behavior of such systems. The variation of ultrasonic speed along with the derived acoustic properties, specially their excess or deviation properties, are more useful in understanding the interactions between the molecules as they are related with structural effects and packing phenomena.³⁻⁶ The refractive index measurements⁷ are also used to estimate the different parameters like the molar refraction and the excess molar refraction which can be helpful for understanding the type of molecular interactions. Therefore the systematic investigation of the different parameters and their excess or deviation functions are of great importance for a better understanding of the liquid systems and appropriate selection of these systems for their practical applications in various industrial and biological usages. In this chapter densities and viscosities for the binary systems consisting of 2-ethyl-1-hexanol (2-EH) as component 1 and ethylenediamine (EDA), 1,2-dichloroethane (DCE) and monoethanolamine (MEA) as component 2 were measured at 298.15, 308.15 and 318.15 K. Also ultrasonic speeds of sound and refractive indices for such systems were measured at 298.15 K under atmospheric pressure. Different excess or deviation properties derived from these experimental data were discussed in terms of molecular interactions. To the best of our knowledge no volumetric, viscometric, acoustic and refractive index study is available in the

Chapter V

literature for the binary mixtures of 2-ethyl-1-hexanol with ethylenediamine, 1,2-dichloroethane and monoethanolamine at the experimental conditions studied.

5.2. Experimental section

5.2.1. Materials

All the chemicals chosen for this investigation were of spectroscopic grade (Sigma-Aldrich, purity >99%) and were used without any further purification as received from the vendor. The purity of each solvent was ascertained by comparing their experimental densities and viscosities at the experimental temperatures as listed in Table 5.1 with the available literature data.⁸⁻¹⁹

5.2.2. Apparatus and procedure

Different binary mixtures of the selected solvents were prepared at 298.15 K by mass and were kept in special airtight stoppered glass bottles to avoid evaporation. The mass measurements were done on a digital electronic analytical balance (Mettler, AG 285, Switzerland) with an uncertainty of $\pm 1 \cdot 10^{-4}$ g and the uncertainty in mole fraction was evaluated to be ± 0.0002 . The densities of the pure liquids and their binary mixtures were measured with a vibrating-tube density meter (Anton Paar, DMA 4500M). The densitometer was calibrated at the experimental temperatures using doubly distilled and degassed water and dry air under atmospheric pressure. The desired experimental temperatures were automatically kept constant with an accuracy of $\pm 1 \cdot 10^{-2}$ K by using a built-in Peltier technique. The viscosity of the pure liquids and their binary mixtures were measured using a suspended Canon-type Ubbelohde viscometer. Before use the viscometer was thoroughly cleaned, dried and calibrated at the experimental temperatures with triply distilled, degassed water and purified methanol. The efflux times of flow of liquid samples were recorded with a digital stopwatch with an uncertainty of ± 0.01 s. Ultrasonic speeds of sound (u) were measured at $T = (298.15 \pm 0.01)$ K with an accuracy of 0.3 % by using a variable path, single crystal ultrasonic interferometer (Mittal Enterprise, New Delhi, F-05) working at 2 MHz. Refractive indices were measured with an Abbe's refractometer at $T = (298.15 \pm 0.01)$ K. In all determinations, an average of triplicate measurements was taken into account and adequate precautions were taken to minimize evaporation losses during the actual measurements. The details of the methods, uncertainties and measurement techniques have already been described in Chapter III.

Chapter V

Table 5.1. Physical properties of the pure liquids at $T = (298.15 \text{ to } 318.15) \text{ K}$

Pure Liquid	$T \text{ (K)}$	$\rho \cdot 10^{-3}$ ($\text{kg} \cdot \text{m}^{-3}$)		η ($\text{mPa} \cdot \text{s}$)	
		Expt.	Lit.	Expt.	Lit.
2-EH	298.15	0.82907	0.82906 ⁸ 0.82896 ⁹	8.4186	8.418 ¹⁰
	308.15	0.82159	0.82158 ⁹	6.0823	6.090 ¹⁰
	318.15	0.81413	0.81411 ⁹	3.7257	-
EDA	298.15	0.89479	0.8945 ¹¹ 0.8948 ¹¹	1.2758	1.276 ¹¹
	308.15	0.88563	0.8856 ¹²	1.1072	1.107 ¹¹
	318.15	0.86762	0.867667 ¹³	0.9445	0.9445 ¹⁴
DCE	298.15	1.24637	1.2474 ¹⁵	0.7804	0.759 ¹⁵ 0.7805 ¹⁶
	308.15	1.23121	1.2312 ¹⁵	0.6744	0.674 ¹⁵
	318.15	1.21455	1.21455 ¹⁴	0.5719	0.5719 ¹⁴
MEA	298.15	1.01179	1.0118 ¹⁷	18.9538	18.95 ¹⁹
	308.15	1.00468	1.00467 ¹⁷ 1.00431 ¹⁸	11.9630	11.966 ¹⁸
	318.15	0.99815	0.99817 ¹⁷ 0.99635 ¹⁸	7.9132	7.914 ¹⁸

5.3. Results and discussion

The measurement of the different physical properties of pure liquids and their binary mixtures are being used as an important tool for describing the molecular interactions operating among the unlike components of the mixture. Such studies highlight the deviation of these properties from their ideal behavior and help to investigate the molecular interactions between the unlike components in the mixture. These deviations depend upon the nature of the liquids, mixture composition and the experimental temperatures. Thus the investigation on the excess or deviation parameters helps to estimate and understand the extent of the molecular interactions operating in the mixture. The experimentally determined densities (ρ) and viscosities (η) along with the excess molar volumes (V_m^E) and viscosity deviations ($\Delta\eta$) of the binary mixtures studied at the experimental temperatures are listed in Table 5.2.

Chapter V

Table 5.2. Density (ρ), viscosity (η), excess molar volume (V_m^E) and viscosity deviation ($\Delta\eta$) for the binary mixtures studied at $T = (298.15 \text{ to } 318.15) \text{ K}$

x_1	$\rho \cdot 10^{-3}$ ($\text{kg} \cdot \text{m}^{-3}$)	η ($\text{mPa} \cdot \text{s}$)	$V_m^E \cdot 10^6$ ($\text{m}^3 \cdot \text{mol}^{-1}$)	$\Delta\eta$ ($\text{mPa} \cdot \text{s}$)
2-EH (1) + EDA (2)				
$T = 298.15 \text{ K}$				
0	0.89479	1.2758	0	0
0.0488	0.88820	1.4630	-0.036	0.0641
0.1034	0.88175	1.7049	-0.080	0.1542
0.1651	0.87552	2.0516	-0.142	0.3095
0.2352	0.86941	2.4932	-0.215	0.5047
0.3157	0.86323	3.0203	-0.282	0.7057
0.4090	0.85701	3.6868	-0.345	0.9266
0.5185	0.85056	4.3758	-0.376	0.9821
0.6486	0.84376	5.1930	-0.347	0.8551
0.8059	0.83651	6.2905	-0.218	0.4536
1	0.82907	8.4186	0	0
$T = 308.15 \text{ K}$				
0	0.88563	1.1072	0	0
0.0488	0.87910	1.2537	-0.027	0.0505
0.1034	0.87260	1.4332	-0.050	0.1127
0.1651	0.86664	1.7323	-0.119	0.2655
0.2352	0.86031	2.0719	-0.151	0.4190
0.3157	0.85419	2.5380	-0.201	0.6422
0.4090	0.84828	3.0787	-0.274	0.8563
0.5185	0.84206	3.5855	-0.307	0.9074
0.6486	0.83560	4.0757	-0.296	0.7331
0.8059	0.82864	4.7035	-0.181	0.3337
1	0.82159	6.0823	0	0
$T = 318.15 \text{ K}$				
0	0.86762	0.9445	0	0
0.0488	0.86213	1.0491	-0.015	0.0392
0.1034	0.85673	1.1960	-0.033	0.1075
0.1651	0.85166	1.4374	-0.080	0.2527
0.2352	0.84650	1.6815	-0.117	0.3772
0.3157	0.84146	2.0221	-0.167	0.5654
0.4090	0.83639	2.4019	-0.213	0.7463
0.5185	0.83127	2.7433	-0.252	0.8192
0.6486	0.82586	2.9488	-0.243	0.6486
0.8059	0.82008	3.1463	-0.156	0.2918
1	0.81413	3.7257	0	0
2-EH (1) + DCE (2)				
$T = 298.15 \text{ K}$				
0	1.24637	0.7804	0	0
0.0779	1.18639	0.7528	0.016	-0.1865
0.1597	1.13193	0.9344	0.034	-0.2066

Chapter V

0.2457	1.08261	1.2791	0.022	-0.1208
0.3363	1.03773	1.7632	-0.026	0.0266
0.4318	0.99622	2.4669	-0.051	0.2875
0.5327	0.95797	3.2867	-0.088	0.5162
0.6394	0.92248	4.2152	-0.117	0.6444
0.7525	0.88931	5.1569	-0.116	0.4839
0.8724	0.85819	6.3998	-0.067	0.1848
1	0.82907	8.4186	0	0
<hr/>				
<i>T</i> = 308.15 K				
0	1.23121	0.6744	0	0
0.0779	1.17215	0.5472	0.042	-0.2532
0.1597	1.11892	0.6466	0.052	-0.3116
0.2457	1.07068	0.8895	0.030	-0.2682
0.3363	1.02658	1.3328	-0.010	-0.0802
0.4318	0.98582	1.8869	-0.033	0.1437
0.5327	0.94825	2.6389	-0.069	0.4626
0.6394	0.91336	3.4333	-0.096	0.6813
0.7525	0.88076	4.1632	-0.097	0.6341
0.8724	0.85017	4.9219	-0.051	0.3279
1	0.82159	6.0823	0	0
<hr/>				
<i>T</i> = 318.15 K				
0	1.21455	0.5719	0	0
0.0779	1.15698	0.3641	0.046	-0.2977
0.1597	1.10499	0.4412	0.065	-0.3302
0.2457	1.05783	0.5692	0.052	-0.3371
0.3363	1.01485	0.8605	0.002	-0.2136
0.4318	0.97495	1.3005	-0.015	0.0159
0.5327	0.93818	1.8483	-0.050	0.2963
0.6394	0.90394	2.4608	-0.065	0.5653
0.7525	0.87197	2.9102	-0.061	0.5672
0.8724	0.84206	3.2181	-0.029	0.2848
1	0.81413	3.7257	0	0
<hr/>				
2-EH (1) + MEA (2)				
<hr/>				
<i>T</i> = 298.15 K				
0	1.01179	18.9538	0	0
0.0495	0.99182	18.3499	-0.121	0.1424
0.1049	0.97172	17.7102	-0.193	0.3046
0.1674	0.95291	17.0280	-0.312	0.4819
0.2382	0.93455	16.3047	-0.422	0.6825
0.3193	0.9165	15.5619	-0.512	0.9348
0.4020	0.90119	14.7035	-0.623	1.0259
0.5225	0.88222	13.6371	-0.711	1.2338
0.6523	0.86478	12.2476	-0.663	1.0844
0.8085	0.8469	10.4609	-0.423	0.6268
1	0.82907	8.4186	0	0
<hr/>				
<i>T</i> = 308.15 K				
0	1.00468	11.9630	0	0
0.0495	0.98394	11.6681	-0.077	0.0990

Chapter V

0.1049	0.96386	11.4254	-0.152	0.2826
0.1674	0.94459	11.1083	-0.235	0.4261
0.2382	0.92644	10.8491	-0.362	0.6664
0.3193	0.90856	10.5217	-0.467	0.8826
0.4020	0.89325	10.0940	-0.577	0.9793
0.5225	0.87407	9.4923	-0.635	1.0910
0.6523	0.85674	8.6493	-0.592	0.9542
0.8085	0.83907	7.4358	-0.372	0.5123
1	0.82159	6.0823	0	0
<hr/>				
<i>T</i> = 318.15 K				
0	0.99815	7.9132	0	0
0.0495	0.97677	7.6953	-0.045	0.0717
0.1049	0.95624	7.5229	-0.096	0.2115
0.1674	0.93699	7.3377	-0.185	0.3620
0.2382	0.91853	7.1545	-0.290	0.5411
0.3193	0.90064	6.9980	-0.396	0.7765
0.4020	0.88508	6.7868	-0.480	0.9411
0.5225	0.86596	6.4309	-0.542	1.0924
0.6523	0.84875	5.9254	-0.511	1.0842
0.8085	0.83135	5.0766	-0.328	0.7728
1	0.81413	3.7257	0	0

5.3.1. Excess molar volumes

Excess molar volume (V_m^E), a thermodynamic property, is sensitive towards the change in structure during the mixing process and can be had from the relation:

$$V_m^E = \sum_{i=1}^2 x_i M_i (1/\rho - 1/\rho_i) \quad (1)$$

where ρ is the density of the mixture and x_i , M_i and ρ_i are the mole fraction, molar mass and density of the i^{th} component in the mixture, respectively. The estimated uncertainty in the excess molar volumes (V_m^E) was found to be $\pm 0.005 \text{ cm}^3 \cdot \text{mol}^{-1}$. The variation of excess molar volumes (V_m^E) with the mole fraction (x_1) of 2-EH at 298.15 K is depicted in Figure 5.1. It shows that the excess molar volume (V_m^E) varies in a sigmoidal fashion with the mole fraction (x_1) of 2-EH for the binary mixture (2-EH + DCE) with positive V_m^E values at $x_1 \leq 0.2457$ and negative V_m^E values at $x_1 \geq 0.3363$. Similar composition dependence of V_m^E values was observed at other experimental temperatures for this mixture. However, negative V_m^E values were observed for the binary mixtures (2-EH + EDA) and (2-EH + MEA) over the entire composition range

Chapter V

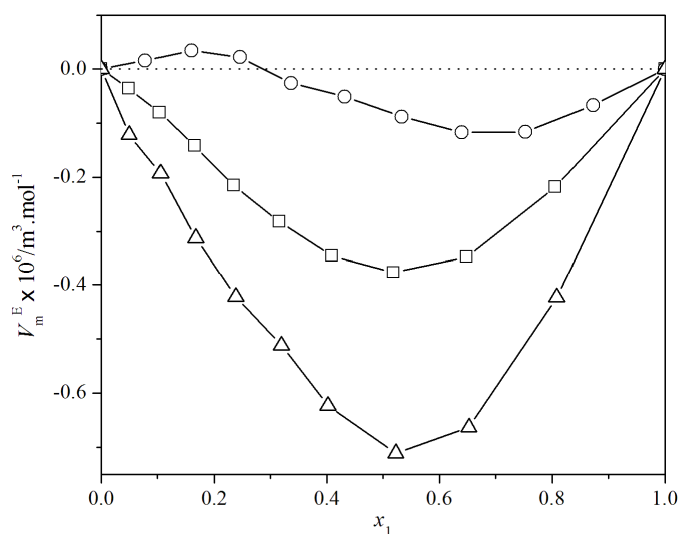


Fig. 5.1. Excess molar volume (V_m^E) versus mole fraction of 2-EH (x_1) for the binary mixtures of 2-EH + 1,2-disubstituted ethanes at $T = 298.15$ K. Symbols: \square , EDA; \circ , DCE; \triangle , MEA.

at all the experimental temperatures. The V_m^E values can be interpreted from their sign and magnitudes reflecting the nature and the extent of the molecular interactions operating between the components of the liquid mixtures. The sign and the magnitude of V_m^E values mainly arise from the involvement of different types of interactions: physical and chemical or specific interactions. The physical interactions involve mainly the dispersion forces and cause volume expansion and thus yield positive V_m^E values. On the contrary the chemical or specific interactions that lead to volume contraction involve mainly the charge transfer type forces, hydrogen bond formation and other complex forming interactions between unlike components of the mixture and thus contribute negative values to V_m^E . Furthermore, the structural contribution that involves the geometrical fitting or interstitial accommodation of one component into other owing to their difference in molar volumes also yields negative V_m^E values. A comparison of the dipole moments (μ) and relative permittivities (ϵ_r)²⁰ of the pure components $\{(\mu_{2\text{-EH}}=1.74 \text{ D}, \mu_{\text{EDA}}=1.99 \text{ D}, \mu_{\text{DCE}}=1.8 \text{ D}, \mu_{\text{MEA}}=2.3 \text{ D})$ and $(\epsilon_{r,2\text{-EH}}=7.54, \epsilon_{r,\text{EDA}}=13.82, \epsilon_{r,\text{DCE}}=10.42, \epsilon_{r,\text{MEA}}=31.94)\}$ suggests that the expected order of molecular interactions between the like components of the studied systems should be: MEA-MEA > EDA-EDA > DCE-DCE > 2-EH-2-EH. The sigmoidal variations of the V_m^E values for the mixture (2-EH + DCE) may be attributed to the breaking of the

Chapter V

dipolar association (through dipole-dipole interactions amongst the DCE molecules) in DCE leading to initial volume expansion ($V_m^E > 0$) on mixing with 2-EH and this effect reaches its maximum at around $x_1 = 0.2457$ and thereafter the V_m^E values drop in magnitude and become negative after $x_1 \geq 0.3363$. The negative V_m^E values for this mixture may be attributed to hydrogen bond interaction between the $-OH$ group of 2-EH molecule and the $-Cl$ group of DCE molecules. The other effect yielding negative V_m^E values for this system is most probably the geometrical fitting or interstitial accommodation of one component into the other due to the large differences in their sizes and molar volumes. As DCE being a smaller molecule with a molar volume of $V_{m,DCE} = 79.41 \text{ cm}^3 \cdot \text{mol}^{-1}$ compared to 2-EH with a molar volume of $V_{m,2-EH} = 157.08 \text{ cm}^3 \cdot \text{mol}^{-1}$ at 298.15 K, it can fit itself into the space/voids formed between the polymeric entities of 2-EH molecules²¹ leading to more compact structure for the mixture (2-EH + DCE), although mixing of DCE with 2-EH also breaks intermolecular hydrogen bonds as well as dipolar associations in 2-EH.

On the contrary the negative V_m^E values for the mixtures (2-EH + EDA) and (2-EH + MEA) over the whole composition range at all the experimental temperatures suggest the presence of strong molecular interactions between the unlike components of the mixtures; most probably due to the following facts: i) the presence of highly polar $-NH_2$ and $-OH$ groups in MEA and two $-NH_2$ groups in EDA leads to hydrogen bond interactions with the $-OH$ group of 2-EH molecules on mutual mixing and ii) the geometrical fitting of EDA and MEA molecules in the intermolecular space or voids between the 2-EH molecules. This is due to difference in the size and molar volume of the participating components in the mixtures. Both EDA with a molar volume of $V_{m,EDA} = 67.15 \text{ cm}^3 \cdot \text{mol}^{-1}$ and MEA with a molar volume of $V_{m,MEA} = 60.37 \text{ cm}^3 \cdot \text{mol}^{-1}$ are smaller molecules than 2-EH ($V_{m,2-EH} = 157.08 \text{ cm}^3 \cdot \text{mol}^{-1}$) and this fact permits the easy fitting of these two molecules (EDA and MEA) in the intermolecular space/voids between the 2-EH molecules and thus more compact structures result for the mixtures (2-EH + EDA) and (2-EH + MEA). Figure 5.1 reveals that V_m^E values have the following order of magnitude for the studied mixtures: (2-EH + DCE) > (2-EH + EDA) > (2-EH + MEA) irrespective of the sign of V_m^E values. This order suggests the following order of molecular

Chapter V

interactions: (2-EH + MEA) > (2-EH + EDA) > (2-EH + DCE). Similar behavior of the V_m^E values against the mole fraction (x_1) of 2-EH was observed for these mixtures at other experimental temperatures. However, for each mixture the V_m^E values increase as the experimental temperature increases. So it is evident that the degree of molecular interactions between the dissimilar species becomes weaker at higher temperatures; most probably due to enhanced thermal agitation and kinetic energy of the component molecules at higher temperatures.

5.3.2. Excess partial molar volumes

The partial molar quantities like partial molar volume, partial molar volume at infinite dilution, *etc.*, are also helpful in understanding the molecular interactions between the component molecules upon mixing. Therefore, these parameters for the i^{th} component of the mixtures were determined at 298.15 K. The partial molar volumes ($\bar{V}_{m,i}$) of the i^{th} component were obtained from the relation:^{22,23}

$$\bar{V}_{m,i} = V_{m,i}^E + V_{m,i}^* + (1 - x_i)(dV_{m,i}^E/dx_i)_{T,P} \quad (2)$$

where $V_{m,i}^*$ and $V_{m,i}^E$ are the molar volume and the excess partial molar volume of the i^{th} component in the binary mixtures, respectively. The derivatives $(\partial V_{m,i}^E/\partial x_i)_{T,P}$ involved in these calculations were obtained using the excess molar volumes (V_m^E) and the Redlich-Kister coefficients (a_i)²⁴ of appropriate degree (as determined by Marquardt algorithm²⁵). The details of these calculations are described in chapter II. The calculated Redlich-Kister coefficients (a_i) and the standard deviations (σ) are as follows $a_0 = -1.4980$, $a_1 = -0.2488$, $a_2 = 0.6669$ for the mixture (2-EH + EDA); $a_0 = -0.3239$, $a_1 = -0.7469$, $a_2 = 0.2529$, $a_3 = 0.2829$ for the mixture (2-EH + DCE) and $a_0 = -2.7839$, $a_1 = -0.9154$, $a_2 = 0.8206$, $a_3 = 1.3550$ for the mixture (2-EH + MEA) with standard deviations (σ) 0.0018, 0.0061, 0.0095, respectively for the mixtures (2-EH + EDA), (2-EH + DCE) and (2-EH + MEA). For a better understanding of the overall state of molecular interactions, the excess partial molar volumes ($\bar{V}_{m,i}^E$) and excess partial molar volumes ($\bar{V}_{m,i}^{0,E}$) at infinite dilution were calculated by using the standard relations described in chapter II. These parameters are more sensitive to the change in the aggregation arising due to mixing of the components. The $\bar{V}_{m,i}^E$ values of a binary

Chapter V

Table 5.3. Molar volumes ($V_{m,1}^*$ and $V_{m,2}^*$), partial molar volumes at infinite dilution ($\bar{V}_{m,1}^0$ and $\bar{V}_{m,2}^0$) and excess partial molar volumes at infinite dilution ($\bar{V}_{m,1}^{0,E}$ and $\bar{V}_{m,2}^{0,E}$) for each component in the binary mixtures at 298.15 K

Volume parameters	2-EH (1) +		
	EDA (2)	DCE (2)	MEA (2)
$V_{m,1}^*$	157.08	157.08	157.08
$\bar{V}_{m,1}^0$	156.49	157.47	154.68
$V_{m,2}^*$	67.15	79.41	60.37
$\bar{V}_{m,2}^0$	66.07	78.87	58.84
$\bar{V}_{m,1}^{0,E}$	-0.58	0.39	-2.40
$\bar{V}_{m,2}^{0,E}$	-1.08	-0.53	-1.52

Volume parameters are given in $\text{cm}^3 \cdot \text{mol}^{-1}$.

mixture provide valuable information regarding the individual component's response to the molecular interactions. These parameters for the studied mixtures at 298.15 K are listed in Table 5.3. The excess partial molar volumes ($\bar{V}_{m,i}^E$) for each component in the studied binaries are represented in Figure 5.2 as a function of the mole fraction (x_1) of 2-EH. Figure 5.2 shows that $\bar{V}_{m,1}^E$ values initially decrease for the mixture containing DCE (up to $x_1 = 0.4318$) and EDA (up to $x_1 = 0.2352$) and thereafter gradually increase for both the mixtures. But for the mixture with MEA $\bar{V}_{m,1}^E$ values gradually increase with increasing mole fraction (x_1) of 2-EH. However, for all the studied mixtures $\bar{V}_{m,2}^E$ values behave in opposite fashion as compared to $\bar{V}_{m,1}^E$ values as expected. Partial molar volumes ($\bar{V}_{m,1}^0$) at infinite dilution for 2-EH in the mixture (2-EH + DCE) was found to be greater than its molar volume ($V_{m,1}^*$), *i.e.*, 2-EH expands in volume but that of DCE ($\bar{V}_{m,2}^0$) was found to lower than its molar volume ($V_{m,2}^*$), *i.e.*, DCE contracts in volume. Partial molar volumes ($\bar{V}_{m,1}^0$ and $\bar{V}_{m,2}^0$) at infinite dilution for both the components in the mixtures (2-EH + EDA) and (2-EH + MEA) were also found to be lower than their respective molar volumes ($V_{m,1}^*$ and $V_{m,2}^*$). Again more negative $\bar{V}_{m,i}^E$ values for the mixture (2-EH + MEA) compared to the mixtures (2-EH + EDA) and (2-EH + DCE) are significantly more apparent and this

Chapter V

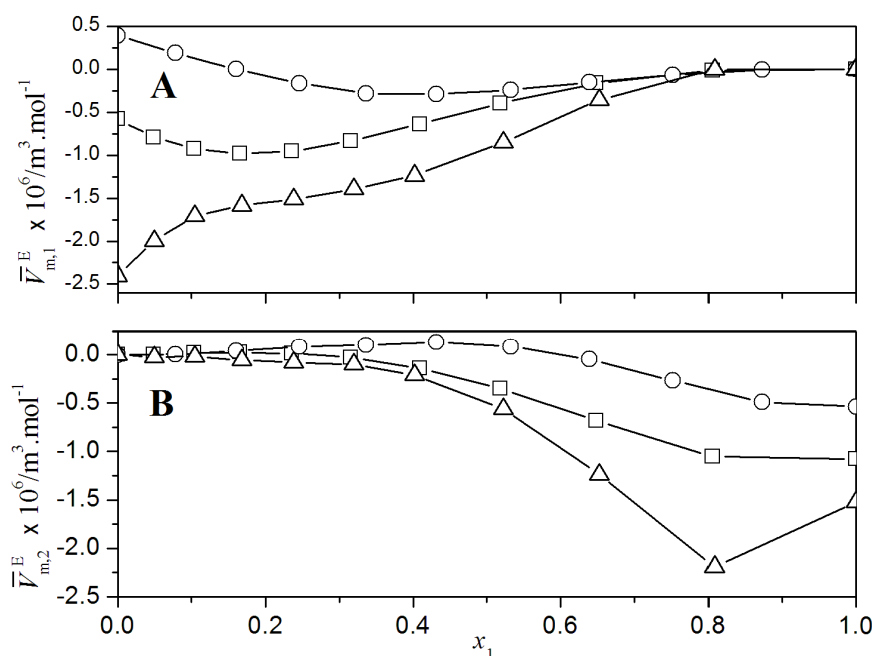


Fig. 5.2. Excess partial molar volume ($\bar{V}_{m,i}^E$) against mole fraction of 2-EH (x_1) for the binary mixtures of 2-EH + 1,2-disubstituted ethanes at $T = 298.15$ K: A, for 2-EH; B, for 1,2-disubstituted ethanes. Symbols: \square , EDA; \circ , DCE; Δ , MEA.

fact supports comparatively more compact structure for the mixture (2-EH + MEA) than other two mixtures. These results suggest the interstitial accommodation of these disubstituted ethanes in the voids of 2-EH ensemble and thus corroborates with the following order of packing efficiency or structure compactness in the mixtures:

$$(2\text{-EH} + \text{MEA}) > (2\text{-EH} + \text{EDA}) > (2\text{-EH} + \text{DCE}).$$

5.3.3. Predictions of excess molar volumes

Of late several theoretical models have been used to correlate the experimental and theoretical excess molar volumes (V_m^E). Herein this chapter Prigogine-Flory-Patterson (PFP) theory^{26,27} and the Peng Robinson equation of state²⁸⁻³¹ at 298.15 K were used for the studied binary mixtures.

i) *Prigogine-Flory-Patterson theory (PFP):*

The Prigogine-Flory-Patterson (PFP) theory^{26,27} is a modified version of Flory's statistical theory and has been successfully tested to correlate and analyze the excess thermodynamic functions like excess molar volume (V_m^E) of the liquid mixtures theoretically. According to this theory the excess molar volume (V_m^E)

Chapter V

originates from a combination of interactional, a free volume and internal pressure combinations and V_m^E is given by:

$$\begin{aligned} \frac{V_m^E}{x_1V_1^* + x_2V_2^*} = & \frac{(\tilde{v}^{1/3} - 1)\tilde{v}^{2/3}\psi_1\theta_2}{[(4/3)\tilde{v}^{-1/3} - 1]P_1^*} \chi_{1,2} \\ & (\chi_{1,2} \text{ contribution}) \\ & - \frac{(\tilde{v}_1 - \tilde{v}_2)^2[(14/9)\tilde{v}^{-1/3} - 1]\psi_1\psi_2}{[(4/3)\tilde{v}^{-1/3} - 1]\tilde{v}} \\ & (\tilde{v} \text{ contribution}) \\ & + \frac{(\tilde{v}_1 - \tilde{v}_2)(P_1^* - P_2^*)\psi_1\psi_2}{(P_1^*\psi_2 + P_2^*\psi_1)} \quad (3) \\ & (P^* \text{ contribution}) \end{aligned}$$

The first term on the right hand side of the Eq. (3) relates to the interactional contribution, the second term relates to free volume contribution and the last term is the internal pressure contribution. The different parameters (θ , ψ and P^*) involved in Eq. (3) are the molecular surface fraction, molecular contact energy fraction and characteristic pressure respectively. The other terms and notations involved in this theory for the pure components and their mixtures were obtained using Flory's theory²⁸⁻³¹ and are given in Table 5.4.

Table 5.4. Isobaric molar heat capacities (c_p), expansion coefficient (α), isothermal compressibility (κ_T) and Flory's parameters for pure liquids at 298.15 K

Liquids	c_p^a	\tilde{v}	\tilde{T}	$V^* \cdot 10^6$ ($\text{m}^3 \cdot \text{mol}^{-1}$)	P^* (Pa)	T^* (K)	$\alpha \cdot 10^4$ (K^{-1})	$\kappa_T \cdot 10^{10}$ (Pa^{-1})
2-EH	317.50 ⁹	1.2271	0.0537	128.01	496.96	5548.96	9.010	8.139
EDA	172.60 ²⁰	1.3451	0.0699	49.93	1226.52	4262.04	15.182	6.677
DCE	128.40 ²⁰	1.3018	0.0646	60.99	746.81	4611.90	12.765	8.636
MEA	195.50 ²⁰	1.1768	0.0449	51.30	737.98	6641.29	6.740	3.771

^a Unit : $\text{J} \cdot \text{K}^{-1} \cdot \text{mol}^{-1}$.

For the prediction of V_m^E values the interaction parameter ($\chi_{1,2}$) is required and so it was obtained by fitting the experimental equimolar ($x_1 \approx 0.5$) V_m^E values to Eq. (3) by using computer program as detailed in chapter II. The theoretically calculated and experimentally obtained excess molar volumes, their deviation and the optimized $\chi_{1,2}$ value near equimolar ($x_1 \approx 0.5$) composition for the studied binaries at 298.15 K are given in Table 5.5. It suggests that the calculated excess molar volumes ($V_{m,\text{FFP}}^E$)

Chapter V

Table 5.5. Interaction parameter ($\chi_{1,2}$), calculated and experimental values of excess molar volumes ($V_{m,\text{exp}}^E$ and $V_{m,\text{PFP}}^E$), their deviations (ΔV_m^E) and different PFP contributions at 298.15 K

2-EH (1) +	$\chi_{1,2}$ ($\text{J} \cdot \text{m}^{-3}$)	$V_{m,\text{exp}}^E \cdot 10^6$ ($\text{m}^3 \cdot \text{mol}^{-1}$)	$V_{m,\text{PFP}}^E \cdot 10^6$ ($\text{m}^3 \cdot \text{mol}^{-1}$)	$\Delta V_m^E \cdot 10^6$ ($\text{m}^3 \cdot \text{mol}^{-1}$)	PFP contributions $\times 10^3$		
					int ^a	fv ^b	ip ^c
DA (2)	-149.559	-0.3763	-0.3182	-0.0581	-0.0233	0.0052	0.0243
DCE (2)	-32.092	-0.0880	-0.0497	-0.0383	-0.0057	0.0020	0.0068
MEA (2)	-11.657	-0.7110	-0.6211	-0.0899	-0.0027	0.0009	-0.0042

^a interaction contribution, ^b free volume contribution and ^c internal pressure contribution

do not agree well with the experimental excess molar volumes (V_m^E) for all the mixtures studied.

ii) Peng-Robinson Equation of State (PREOS):

In recent years the cubic equation of states has gained more importance because of their simplicity, computational efficiency, reliability and their easy application in the liquid mixtures through mixing or combination rules. These equations of state are commonly used to describe the phase equilibria of hydrocarbon system and finds wide applications in the prediction of properties of the solution. In the present chapter the classical cubic Peng-Robinson equation of state (PREOS) has been used to predict the excess molar volume ($V_{m,\text{PREOS}}^E$) of the mixtures at 298.15 K. The general form of the two parameter PREOS is given by:³²

$$P = \frac{RT}{V-b} - \frac{a}{V(V+b)+b(V-b)} \quad (4)$$

where a and b are the attraction parameter and van der Waals co-volume parameters, respectively. a and b can be obtained by using the standard relations as described in chapter II. For the pure components:

$$a = a(T) = a(T_c) \left[1 + \xi \left(1 - \sqrt{\frac{T}{T_c}} \right) \right]^2 \quad (5)$$

$$b = b(T) = b(T_c) \quad (6)$$

$$a(T_c) = 0.45724 \frac{R^2 T_c^2}{P_c} \quad (7)$$

$$b(T_c) = 0.07780 \frac{RT_c}{P_c} \quad (8)$$

Chapter V

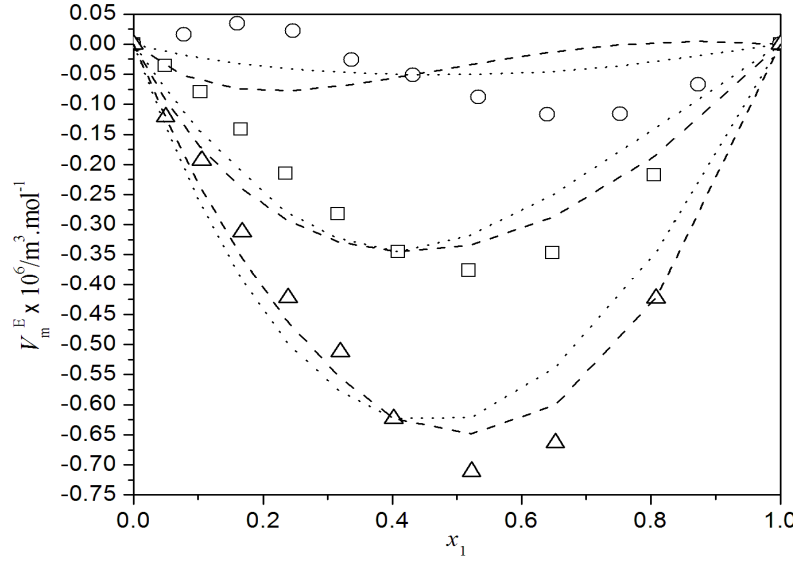


Fig. 5.3. A comparison between the excess molar volumes (V_m^E) against mole fraction of 2-EH (x_1) for the binary mixtures of 2-EH + 1,2-disubstituted ethanes at $T = 298.15$ K. Symbols represent experimental excess molar volumes (V_m^E): \square , EDA; \circ , DCE; Δ , MEA. Dashed lines and dotted lines represent excess molar volumes (V_m^E) obtained from PREOS and PFP theory, respectively.

where T_c and P_c are critical temperature and pressure of the pure components. The parameter ξ can be defined in terms of acentric factor (ω)³³ as:

$$\xi = 0.37464 + 1.54226\omega - 0.26992\omega^2 \quad (9)$$

The parameters (T_c , P_c and ω) for the pure components were taken from the literature.^{20,33} For the binary mixtures the attraction parameter a and co-volume parameter b were calculated using the following standard relation:³³

$$a(T) = \sum_{i=1}^2 \sum_{j=1}^2 x_i x_j \sqrt{a_i a_j} (1 - k_{ij}) \quad (10)$$

$$b(T) = \sum_{i=1}^2 x_i b_i \quad (11)$$

where k_{ij} is the interaction coefficient of the components i and j for a binary mixture.

Rearrangement of Eq. (4) in terms of compressibility factor yields:

$$Z^3 - (1 - B)Z^2 + (A - 3B^2 - 2B)Z - (AB - B^2 - B^3) = 0 \quad (12)$$

Chapter V

In Eq. (12) the terms, $Z = PV/RT$, $A = aP/(RT)^2$ and $B = Pb/RT$. Thus from the knowledge of the compressibility factor (Z) for pure components and their mixtures, the corresponding volumes and the excess molar volumes of the systems were calculated. The interaction coefficient (k_{ij}) for the mixtures (2-EH + EDA), (2-EH + DCE) and (2-EH + MEA) were found to be -0.1668, -0.0624 and -0.1235 with standard deviations (σ) 0.0661, 0.0866 and 0.0441, respectively. The experimental excess molar volumes (V_m^E) and the calculated excess molar volumes ($V_{m, PFP}^E$ and $V_{m, PREOS}^E$) as a function of mole fraction (x_1) of 2-EH in the present system at 298.15 K are depicted in Figure 5.3. It reveals that the calculated excess molar volumes ($V_{m, PFP}^E$ and $V_{m, PREOS}^E$) although agree to some extent with the experimental excess molar volumes (V_m^E) for the mixtures (2-EH + EDA) and (2-EH + MEA) but for the mixture (2-EH + DCE), both the models (PREOS and PFP) fail to predict its excess molar volumes.

5.3.4. Viscosity deviations

The study of transport properties of the liquid mixture is very useful in process design, development of the liquid state theories and predictive methods, *etc.* Viscosity deviation ($\Delta\eta$) depends on the strength of intermolecular hydrogen bonding, molecular size and shape of the components. Hence it is very important and useful tool for understanding the nature of intermolecular interactions between the unlike components. Therefore, the viscosity deviations ($\Delta\eta$) of all the studied binaries were evaluated at $T = (298.15-318.15)$ K from the relation:³⁴

$$\Delta\eta = \eta - \eta_{id} \quad (13)$$

where η_{id} is the ideal viscosity of the solution as given by:³⁵

$$\eta_{id} = \exp\left(\sum_{i=1}^2 x_i \ln \eta_{id}\right) \quad (14)$$

Figure 5.4 ($\Delta\eta$ versus x_1 at 298.15 K) shows that the $\Delta\eta$ values are positive for the mixtures (2-EH + EDA) and (2-EH+MEA) over the entire composition range. However, for the mixture (2-EH + DCE), $\Delta\eta$ values vary in a sigmoidal fashion with negative $\Delta\eta$ values at the lower mole fraction of 2-EH (up to $x_1 \leq 0.2457$) and positive $\Delta\eta$ values at 2-EH rich regions ($x_1 \geq 0.2457$). Similar composition dependence of $\Delta\eta$ values was observed at other experimental temperatures for these mixtures.

Chapter V

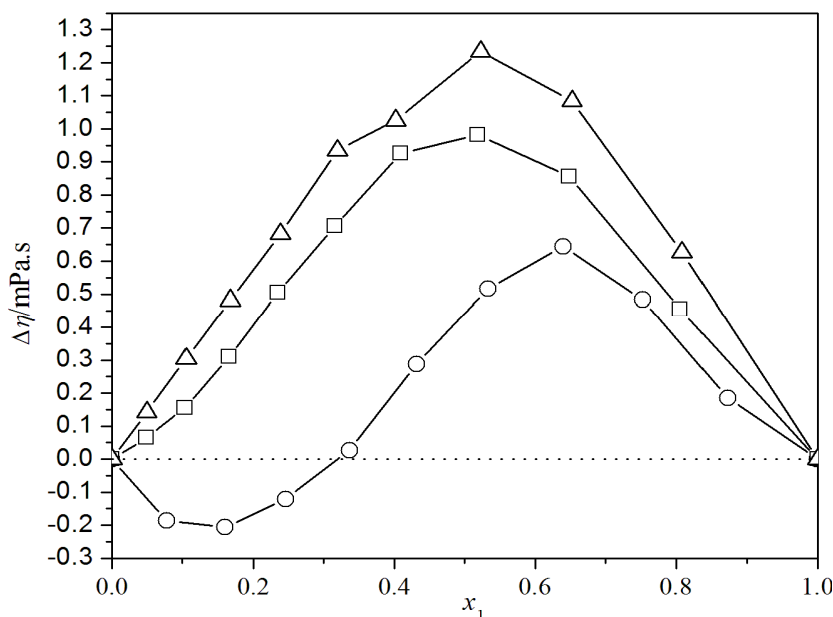


Fig. 5.4. Viscosity deviation ($\Delta\eta$) versus mole fraction of 2-EH (x_1) for the binary mixtures of 2-EH + 1,2-disubstituted ethanes at $T = 298.15$ K. Symbols represent experimental points: □, EDA; ○, DCE; △, MEA.

For many liquid-liquid systems the $\Delta\eta$ versus x_1 plot often shows a reversed trend compared to the V_m^E versus x_1 plots; *i.e.*, if V_m^E is positive $\Delta\eta$ will be negative and *vice-versa*.³⁶ Such a coincidence was observed for all the studied binaries. According to Vogel and Weiss,³⁷ viscosity deviations are positive for mixtures with strong molecular interactions and negative for the mixtures without specific interaction or with weak interactions. The negative $\Delta\eta$ values for the mixture (2-EH + DCE) at dilute 2-EH regions is most probably due to loss of dipolar association of DCE on mixing with 2-EH. But at 2-EH rich regions $\Delta\eta$ values gradually increase and become positive suggesting predominance of specific interactions like dipole-dipole interactions, hydrogen bond interaction and interstitial accommodation or geometrical fitting as described earlier. The positive $\Delta\eta$ values for the mixtures (2-EH + EDA) and (2-EH + MEA) over the entire composition range entails that these two binary mixtures are characterized by strong molecular interactions (amongst the dissimilar species) arising out of specific dipole-dipole interactions, hydrogen bonds and interstitial accommodation. Thus the $\Delta\eta$ values also suggest the same order of molecular interactions for the mixtures as discussed earlier. Anyway, for each mixture

Chapter V

$\Delta\eta$ values decrease at higher temperatures reflecting the fact that the molecular interactions amongst the dissimilar species become weaker at higher temperatures.

5.3.5. Thermodynamics of viscous flow

According to Eyring's viscosity relation,³⁵ the free energy of viscous flow (ΔG^*) is given by the relation:

$$\eta = (hN/V) \exp(\Delta G^* / RT) \quad (15)$$

where h is Planck's constant, N is Avogadro's number and other symbols have their usual meanings. Rearranging Eq. (15) and putting $\Delta G^* = \Delta H^* - T\Delta S^*$ yields the following relation:

$$R \ln(\eta V / hN) = \Delta H^* / T - \Delta S^* \quad (16)$$

Thus, linear regressions of $R \ln(\eta V / hN)$ against $(1/T)$ give the enthalpy (ΔH^*) and entropy (ΔS^*) of activation of viscous flow from the corresponding slope and negative intercept, respectively. ΔG^* , ΔH^* , ΔS^* and the regression coefficients (R^2) are given in Table 5.6. It shows that while ΔH^* and ΔS^* values are positive for the mixtures (2-EH + DCE) and (2-EH + MEA), the ΔS^* values are mostly negative for the binary mixtures (2-EH + EDA) except at $x_1 \geq 0.6486$. Such a trend in ΔH^* and ΔS^* values indicate that formation of transition state for viscous flow is accompanied by disruption of the dipolar association as well as specific interactions between the components of the mixtures. According to Corradini *et al.*,³⁸ the enthalpy of activation of viscous flow is regarded as a measure of the degree of cooperation between the species involved in viscous flow. In a highly structured liquid there will be considerable degree of order; hence for cooperative movement of the species a large heat of activation is required for the viscous flow. Thus the ΔH^* values indicate that the molecular compactness follows the order: (2-EH + MEA) > (2-EH + + EDA) > (2-EH + + DCE). This order is also supported by the ΔS^* values for the mixtures studied. The ΔG^{*E} values are plotted against the mole fraction of 2-EH (x_1) in Figure 5.5 at 298.15 K. Reid and Taylor³⁹ suggested that the positive ΔG^{*E} stands for molecular interactions or compactness due to geometrical fittings of one component into the other on mixing and negative ΔG^{*E} indicate the dominance of dispersion forces in the mixtures. From Figure 5.5 it is evident that the ΔG^{*E} values for the mixtures stand in support of the order of the molecular interactions discussed above.

Chapter V

Table 5.6. Free energy (ΔG^*), enthalpy (ΔH^*) and entropy (ΔS^*) of activation of viscous flow for the binary mixtures.

x_1	ΔG^*			ΔH^* (kJ·mol ⁻¹)	ΔS^* (J·K ⁻¹ ·mol ⁻¹)	R^2
	(kJ·mol ⁻¹)					
	298.15 K	308.15 K	318.15 K			
2-EH (1) + EDA (2)						
0	13.309	13.419	13.488	10.634	-8.995	0.9988
0.0488	13.804	13.898	13.929	11.928	-6.325	0.9978
0.1034	14.347	14.410	14.448	12.840	-5.066	0.9999
0.1651	14.978	15.073	15.114	12.931	-6.893	0.9987
0.2352	15.643	15.720	15.721	14.466	-3.988	0.9978
0.3157	16.312	16.440	16.413	14.788	-5.195	0.9913
0.4090	17.014	17.149	17.086	15.903	-3.829	0.9879
0.5185	17.663	17.771	17.674	17.473	-0.745	0.9892
0.6486	18.332	18.351	18.121	21.428	10.256	0.9895
0.8059	19.075	18.994	18.574	26.480	24.662	0.9872
1	20.093	19.957	19.332	31.346	37.488	0.9812
2-EH (1) + DCE (2)						
0	12.506	12.583	12.591	11.226	-4.330	0.9971
0.0779	12.599	12.236	11.590	27.605	50.182	0.9918
0.1597	13.313	12.846	12.285	28.624	51.305	0.9991
0.2457	14.265	13.842	13.142	30.968	55.877	0.9938
0.3363	15.231	15.053	14.414	27.332	40.345	0.9781
0.4318	16.231	16.116	15.684	24.341	27.034	0.9868
0.5327	17.108	17.146	16.788	21.809	15.560	0.9748
0.6394	17.889	17.989	17.719	20.361	8.096	0.9747
0.7525	18.552	18.651	18.335	21.714	10.389	0.9721
0.8724	19.250	19.247	18.774	26.282	23.337	0.9753
1	20.093	19.957	19.332	32.346	37.488	0.9812
2-EH (1) + MEA (2)						
0	19.734	19.235	18.783	33.915	47.589	0.9998
0.0495	19.838	19.364	18.911	33.667	46.394	0.9999
0.1049	19.944	19.511	19.060	33.125	44.199	0.9999
0.1674	20.047	19.648	19.210	32.524	41.828	0.9999
0.2382	20.150	19.804	19.368	31.784	38.974	0.9994
0.3193	20.255	19.954	19.546	30.808	35.337	0.9991
0.4020	20.321	20.062	19.687	29.755	31.579	0.9988
0.5225	20.410	20.190	19.840	28.885	28.358	0.9984
0.6523	20.412	20.229	19.910	27.870	24.945	0.9981
0.8085	20.313	20.143	19.812	27.752	24.866	0.9973
1	20.093	19.957	19.332	31.346	37.488	0.9812

Chapter V

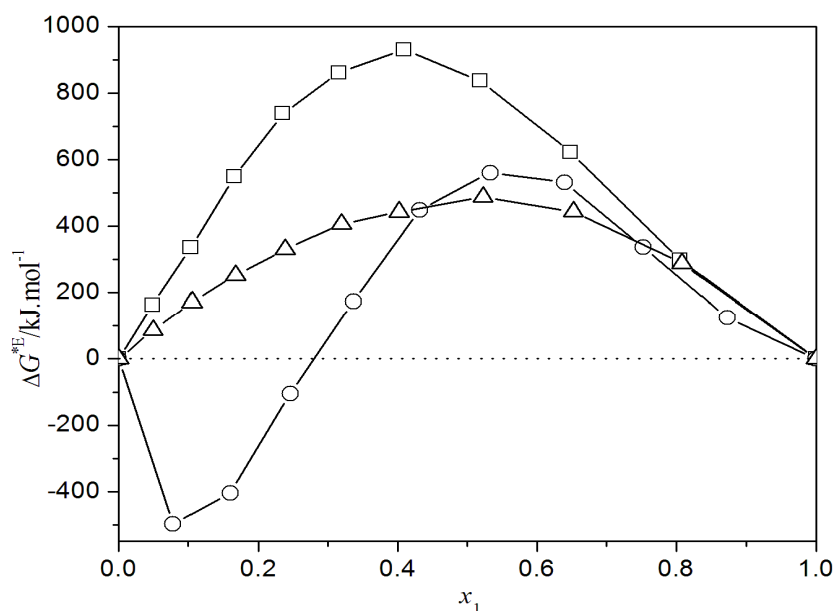


Fig. 5.5. Excess free energy of activation of viscous flow (ΔG^{*E}) versus mole fraction of 2-EH (x_1) for the binary mixtures of 2-EH + 1,2-disubstituted ethanes at $T = 298.15$ K. Symbols represent experimental points: \square , EDA; \circ , DCE; Δ , MEA.

5.3.6. Viscosity prediction

Several theoretical models, empirical and semi empirical based relations have been proposed to represent the dependence of viscosity on mole fraction in binary liquid mixtures. The simulation of the viscosity of liquid mixtures can be obtained by the use of these empirical models. Mehrotra *et al*⁴⁰ have reviewed the practical implication of these models. Such empirical models have also been developed based on van der waals' theory and the corresponding state principle by using the reduced thermodynamic properties of the substances.⁴¹ In the present chapter the viscosities of the binary liquid mixtures were theoretically evaluated and correlated with the experimental viscosities using the cubic equation of state based on Peng-Robinson model³² and the Bloomfield-Dewan model⁴² at 298.15 K.

i) *Viscosity model using Peng-Robinson Equation of State:*

According to this model, the viscosity of a mixture is given by:

$$\eta = \frac{(\eta V)^{\text{id}}}{V_m} \exp \left[\sum_{i=1}^2 x_i (\ln \phi_i - \ln \phi_i^0) + \frac{1}{2} \sum_{i=1}^2 \sum_{j=1}^2 x_i x_j g_{ij} \right] \quad (17)$$

Chapter V

This expression is a combination of Eyring's viscosity expression with the Peng-Robinson equation of state. In Eq. (17) V_m , $(\eta V)^{id}$, φ_i^0 , φ_i and g_{12} are the molar volume, kinematic viscosity of an ideal mixture, fugacity coefficient of the i^{th} component in pure state, fugacity coefficient of the i^{th} component in a binary mixture and the binary interaction parameter, respectively. $(\eta V)^{id}$ can be had from the expression:

$$(\eta V)^{id} = \exp \left[\sum_{i=1}^2 x_i \ln(\eta_i V_i) \right] \quad (18)$$

According to PREOS, fugacity coefficient for a pure component and for the i^{th} component in their binary mixture are given by:

$$\ln \varphi^0 = (Z-1) - \ln(Z-B) - \frac{A}{2\sqrt{2}B} \ln \left(\frac{Z+(1+\sqrt{2})B}{Z+(1-\sqrt{2})B} \right) \quad (19)$$

$$\begin{aligned} \ln \varphi_i &= \frac{b_i}{b} (Z-1) - \ln(Z-B) \\ &\quad - \frac{A}{2\sqrt{2}B} \left(\frac{2}{a} \sum_{j=1}^2 x_j (a_i a_j)^{\frac{1}{2}} (1-k_{ij}) - \frac{b_i}{b} \right) \ln \left(\frac{Z+(1+\sqrt{2})B}{Z+(1-\sqrt{2})B} \right) \end{aligned} \quad (20)$$

The inter relationship between the binary interaction parameter g_{12} ($g_{ii} = 0$ and $g_{ij} = g_{ji}$) and the excess activation free energy of viscous flow, ΔG^{*E} is given by:

$$\frac{\Delta G^{*E}}{RT} = \frac{G^{*E}}{RT} + \frac{1}{2} \sum_{i=1}^2 \sum_{j=1}^2 x_i x_j g_{ij} = \frac{G^{*E}}{RT} + x_1 x_2 g_{12} \quad (21)$$

and ΔG^{*E} were obtained from the relation:³⁴

$$\Delta G^{*E} = \Delta G^* - \sum_{i=1}^2 (x_i \Delta G_i^*) \quad (22)$$

The binary interaction parameters (g_{12}) were obtained from a C-program utilizing a non-linear regression analysis to yield minimum standard deviations (σ) between the experimental and the calculated viscosities for the studied mixtures. The binary interaction parameters (g_{12}) were found to be 0.423 ($\sigma = 0.029$), 0.338 ($\sigma = 0.145$) and 0.027 ($\sigma = 0.014$) for the mixtures (2-EH + EDA), (2-EH + DCE) and (2-EH + MEA), respectively.

Chapter V

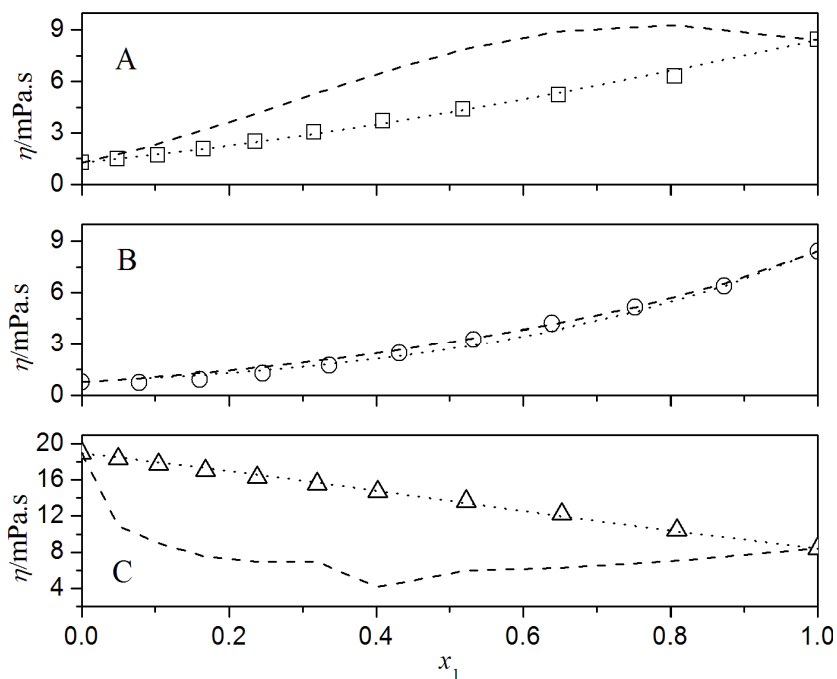


Fig. 5.6. A comparison between the viscosities (η) against mole fraction of 2-EH (x_1) for the binary mixtures of 2-EH + 1,2-disubstituted ethanes at $T = 298.15$ K. Symbols represent experimental viscosities: \square , EDA; \circ , DCE; Δ , MEA. Dashed lines and dotted lines represent viscosities (η) obtained from Bloom Field-Dewar theory and PREOS, respectively.

ii) Bloomfield-Dewar viscosity model:

Bloomfield and Dewar proposed a viscosity model based on the free-volume theory⁴² and the absolute reaction rate theory.³⁵ All the involved thermodynamic parameters used in this model were evaluated using Flory's statistical thermodynamic theory for liquid mixtures.²⁸⁻³¹ The statistical theory from which this equation of state evolved treats the properties of a mixture in terms of reduced properties of the pure components. The proposed expression for the viscosity is given by:

$$\Delta \ln \eta = f(\tilde{v}) - \frac{\Delta G^R}{RT} \quad (23)$$

where $f(\tilde{v})$ and ΔG^R are the characteristic function of the free volume and the residual free energy of mixing, respectively and $\Delta \ln \eta$ is given by the expression:

$$\Delta \ln \eta = \ln \eta - \sum_{i=1}^2 (x_i \eta_i) \quad (24)$$

$f(\tilde{v})$ and ΔG^R were evaluated using the following standard relations:⁴²

Chapter V

$$f(\tilde{v}) = \frac{1}{\tilde{v} - 1} - \sum_{i=1}^2 \frac{x_i}{\tilde{v}_i - 1} \quad (25)$$

$$\Delta G^R = \Delta G^E + RT \sum_{i=1}^2 x_i \ln(x_i / \phi_i) \quad (26)$$

where ϕ_i is the segment fraction of the i^{th} component in a binary mixture.²⁸⁻³¹ The excess energy ΔG^E in the above expression can be obtained from the Flory's statistical theory using the relation:

$$\begin{aligned} \Delta G^E = & \sum_{i=1}^2 x_i P_i^* V_i^* [(1/\tilde{v}_i - 1/\tilde{v}) + 3\tilde{T}_i \ln\{(\tilde{v}_i^{1/3} - 1)/(\tilde{v}^{1/3} - 1)\}] \\ & + (x_1 \theta_2 V_1^* \chi_{12}) / \tilde{v} \end{aligned} \quad (27)$$

The estimating ability of this model was tested by calculating the standard deviations (σ) between the experimental and the calculated viscosities and the standard deviations (σ) were found to be 2.56, 0.25 and 8.66 for the mixtures with EDA, DCE and MEA, respectively. A comparison of the experimental viscosities with the viscosities calculated from these two viscosity prediction models has been illustrated in Figure 5.6. It reveals that the model based on PREOS better predicted the viscosities for all the studied mixtures than the Bloomfield-Dewan model.

5.3.7. Ultrasonic speed of sound and derived functions:

The ultrasonic studies can provide valuable information regarding the strength of molecular interactions in pure liquids and their mixtures. Therefore the measurement of ultrasonic speeds has become one of the important tools to estimate the nature and the strength of the molecular interactions in the binary liquid mixtures. Concentration dependence of the isentropic compressibility (κ_S) and other acoustic properties can impart valuable information about molecular interactions and structural aspects in the binary mixtures. Hence using the experimentally measured densities (ρ) and speed of sound (u) of the binary mixtures at 298.15 K the isentropic compressibility (κ_S), intermolecular free length (L_f), acoustic impedance (z_{im}) and their excess or deviation functions were determined. The variation of these excess or deviation functions with the mole fraction (x_1) of 2-EH provides better understanding of the molecular interactions between the components of the binary mixtures. The excess isentropic compressibility (κ_S^E) can be determined from the relation:

$$\kappa_S^E = \kappa_S - \kappa_S^{\text{id}} \quad (28)$$

Chapter V

The isentropic compressibility, κ_s in the above expression was calculated using the Laplace relation:⁴³

$$\kappa_s = 1/\rho u^2 \quad (29)$$

The experimental speeds of sound for the pure liquids were in good agreement with the literature values^{8,17,44,45} at 298.15 K. According to Benson and Kiyohara⁴⁶ and Acree,⁴⁷ the isentropic compressibility (κ_s^{id}) for an ideal mixture is given by:

$$\kappa_s^{\text{id}} = \sum_{i=1}^2 \tau_i \left[\kappa_{s,i} + \frac{TV_{m,i}^* \alpha_i^2}{c_{p,i}} \right] - \left\{ \frac{T \sum_{i=1}^2 (x_i V_{m,i}^*) \sum_{i=1}^2 (\tau_i \alpha_i)^2}{\sum_{i=1}^2 (x_i c_{p,i})} \right\} \quad (30)$$

where, τ_i is the volume fraction of the i^{th} component in the mixture, $\kappa_{s,i}$, $V_{m,i}^*$, α_i and $c_{p,i}$ are the isentropic compressibility, the molar volume, the expansion coefficient and the molar isobaric heat capacity of the pure components, respectively. The experimental densities were used to calculate the expansion coefficients ($\alpha = -\rho^{-1} (d\rho/dT)_p$) and the $c_{p,i}$ values (required for the calculation) were taken from the literature.^{9,20} The speed of sound (u), isentropic compressibility (κ_s) and excess isentropic compressibility parameters (κ_s^{E}), at 298.15 K are given in Table 5.7. Figure 5.7 illustrates the excess isentropic compressibilities (κ_s^{E}) of the studied mixtures against the mole fraction (x_1) of 2-EH at 298.15 K. While κ_s^{E} values for the mixtures (2-EH + EDA) and (2-EH + MEA) were found to be negative over the entire composition range, those for the mixture (2-EH + DCE) followed a sigmoid trend with positive κ_s^{E} values at DCE rich regions but with negative κ_s^{E} values at 2-EH rich regions. The descending order of negative κ_s^{E} values for the studied mixtures indicates enhanced rigidity or more efficient packing of the dissimilar species in the mixtures.³⁶ The intermolecular free length (L_f), specific acoustic impedance (z_{im}) and their excess functions were determined using the standard relations (detailed in Chapter II). Intermolecular free length (L_f), acoustic impedance (z_{im}) and their excess functions at 298.15 K are given in Table 5.8. The L_f^{E} and z_{im}^{E} values are depicted in Figure 5.8 against the mole fraction (x_1) of 2-EH at 298.15 K.

Chapter V

Table 5.7. Ultrasonic speeds (u), isentropic compressibility (κ_s) and excess isentropic compressibility (κ_s^E) for binary mixtures at 298.15 K

x_1	u ($\text{m} \cdot \text{s}^{-1}$)	$\kappa_s \times 10^{10}$ (Pa^{-1})	$\kappa_s^E \times 10^{10}$ (Pa^{-1})
2-EH (1) + EDA (2)			
0	1670.8	4.003	0
0.0488	1666.2	4.055	-0.275
0.1034	1653.4	4.149	-0.501
0.1651	1636.1	4.267	-0.695
0.2352	1619.5	4.385	-0.881
0.3157	1598.8	4.532	-1.032
0.4090	1569.8	4.735	-1.119
0.5185	1530.4	5.020	-1.117
0.6486	1475.1	5.447	-0.965
0.8059	1395.7	6.137	-0.544
1	1318.2	6.941	0
2-EH (1) + DCE (2)			
0	1193.6	5.632	0
0.0779	1179.8	6.056	0.152
0.1597	1195.4	6.182	0.061
0.2457	1228.0	6.125	-0.174
0.3363	1272.5	5.951	-0.494
0.4318	1310.0	5.849	-0.717
0.5327	1334.8	5.859	-0.809
0.6394	1346.0	5.983	-0.770
0.7525	1342.3	6.241	-0.585
0.8724	1325.9	6.628	-0.260
1	1318.2	6.941	0
2-EH (1) + MEA (2)			
0	1716.8	3.353	0
0.0495	1735.0	3.349	-0.470
0.1049	1740.1	3.399	-0.860
0.1674	1735.2	3.485	-1.188
0.2382	1720.0	3.617	-1.447
0.3193	1697.1	3.788	-1.643
0.4020	1660.3	4.025	-1.714
0.5225	1611.7	4.364	-1.736
0.6523	1538.1	4.888	-1.513
0.8085	1435.6	5.729	-0.952
1	1318.2	6.941	0

Chapter V

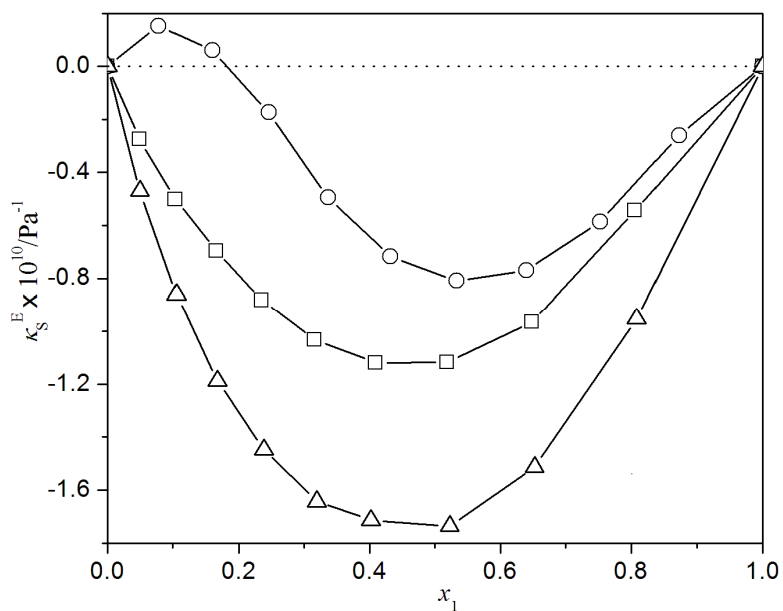


Fig. 5.7. Excess isentropic compressibility (κ_S^E) versus mole fraction of 2-EH (x_1) for the binary mixtures of 2-EH + 1,2-disubstituted ethanes at $T = 298.15$ K. Symbols: \square , EDA; \circ , DCE; \triangle , MEA.

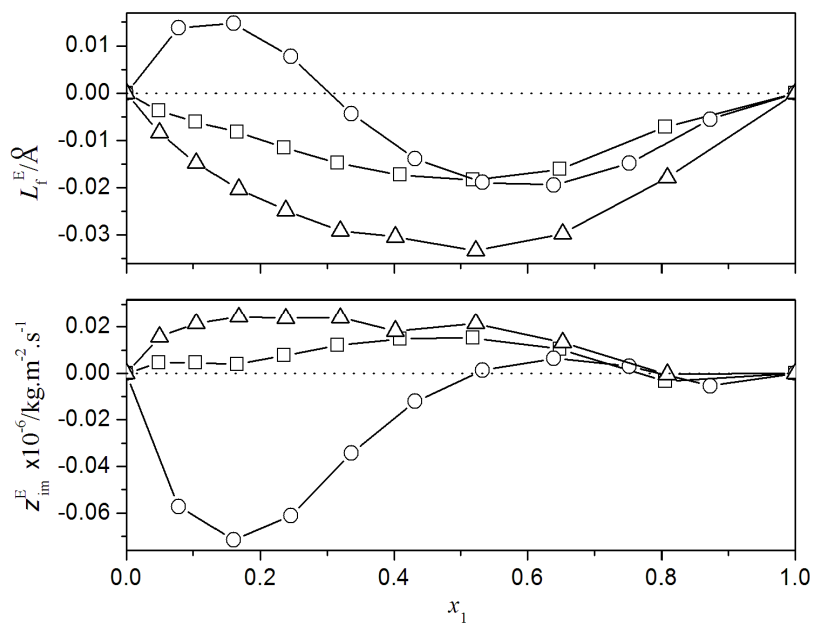


Fig. 5.8. Excess intermolecular free length (L_f^E) and excess acoustic impedances (z_{im}^E) versus mole fraction of 2-EH (x_1) for the binary mixtures of 2-EH + 1,2-disubstituted ethanes at $T = 298.15$ K. Symbols: \square , EDA; \circ , DCE; \triangle , MEA.

Chapter V

Table 5.8. Intermolecular free length (L_f), specific acoustic impedance (z_{im}), excess intermolecular free lengths (L_f^E) and excess acoustic impedances (z_{im}^E) for the studied binaries at 298.15 K

x_1	L_f (Å)	$z_{im} \cdot 10^{-6}$ ($\text{kg} \cdot \text{m}^{-2} \cdot \text{S}^{-1}$)	L_f^E (Å)	$z_{im}^E \cdot 10^{-6}$ ($\text{kg} \cdot \text{m}^{-2} \cdot \text{S}^{-1}$)
2-EH (1) + EDA (2)				
0	0.4115	1.4950	0	0
0.0488	0.4142	1.4799	-0.0037	0.0045
0.1034	0.4189	1.4579	-0.0061	0.0045
0.1651	0.4249	1.4324	-0.0082	0.0038
0.2352	0.4307	1.4080	-0.0115	0.0076
0.3157	0.4379	1.3801	-0.0148	0.0121
0.4090	0.4476	1.3453	-0.0173	0.0148
0.5185	0.4608	1.3017	-0.0183	0.0152
0.6486	0.4800	1.2446	-0.0161	0.0104
0.8059	0.5095	1.1675	-0.0071	-0.0034
1	0.5419	1.0929	0	0
2-EH (1) + DCE (2)				
0	0.4881	1.4877	0	0
0.0779	0.5061	1.3997	0.0138	-0.0572
0.1597	0.5114	1.3531	0.0147	-0.0715
0.2457	0.5090	1.3294	0.0077	-0.0612
0.3363	0.5018	1.3205	-0.0044	-0.0344
0.4318	0.4974	1.3050	-0.0139	-0.0121
0.5327	0.4979	1.2787	-0.0189	0.0013
0.6394	0.5031	1.2417	-0.0194	0.0064
0.7525	0.5138	1.1937	-0.0148	0.0031
0.8724	0.5295	1.1379	-0.0055	-0.0054
1	0.5419	1.0929	0	0
2-EH (1) + MEA (2)				
0	0.3766	1.7370	0	0
0.0495	0.3764	1.7208	-0.0084	0.0157
0.1049	0.3792	1.6909	-0.0148	0.0215
0.1674	0.3840	1.6535	-0.0203	0.0243
0.2382	0.3912	1.6074	-0.0248	0.0238
0.3193	0.4003	1.5554	-0.0291	0.0240
0.4020	0.4127	1.4962	-0.0304	0.0182
0.5225	0.4297	1.4219	-0.0333	0.0214
0.6523	0.4547	1.3301	-0.0297	0.0133
0.8085	0.4923	1.2158	-0.0179	-0.0004
1	0.5419	1.0929	0	0

Chapter V

It is evident that the plots of z_{im}^E versus mole fraction (x_1) of 2-EH are opposite in nature to those of the L_f^E plots. Table 5.8 shows that while the specific acoustic impedances (z_{im}) decrease, the intermolecular free lengths (L_f) increase as the mole fraction (x_1) of 2-EH in the mixtures increase. The magnitude of the intermolecular free lengths (L_f) has the order: (2-EH + DCE) > (2-EH + EDA) > (2-EH + MEA); this indicates that the molecular interactions between dissimilar molecules is also decreasing in the same order. The results, therefore, suggest the order of molecular interactions: (2-EH + MEA) > (2-EH + EDA) > (2-EH + DCE), which has already been discussed earlier.

5.3.8. Prediction of ultrasonic speed of sound

The speeds of sound were predicted theoretically using the Collision factor theory (CFT), Nomoto relation (NOM), Impedance dependence relation (IDR), Ideal mixture relation (IMR) and Jungie (JUN). The details of these empirical models and method of calculation are described in chapter II. Theoretically calculated speeds of sound were correlated with the experimentally obtained ultrasonic speeds and the predictive capabilities of these models were judged on the basis of the percent standard deviations ($\sigma\%$). The comparison of the $\sigma\%$ values has been depicted for each studied binaries in Figure 5.9. Figure 5.9 clearly reveals that the predictive capabilities of the different models used follow the order: CFT > IDR > IMR > NOM > JUN (for 2-EH + EDA mixture); NOM > CFT > JUN > IDR > IMR (for 2-EH + DCE mixture) and IDR > CFT > IMR > NOM > JUN (for 2-EH + MEA mixture), respectively.

5.3.9. Excess molar refractions

Refractive indices can often be correlated with densities, surface tension and dielectric permittivity. That is why refractive index data along with other parameters derived from it provide valuable information regarding the molecular interactions in the liquid mixtures. For example, molar refraction is a volumetric property and thus excess molar refractions (R_m^E) can equally shed light on the molecular interactions in a multi-component liquid mixture like excess molar volumes. Hence the experimental refractive indices and densities at 298.15 K were utilized to evaluate the molar refraction and the excess molar refraction with the help of the following standard relations:⁴⁸

Chapter V

$$R_m = \left[\frac{n_D^2 - 1}{n_D^2 + 2} \right] V_m \quad (31)$$

$$R_m^E = R_m - [x_1 R_{m,1} + x_2 R_{m,2}] \quad (32)$$

The experimental refractive indices, molar refractions and excess molar refractions for the three binaries under investigation at 298.15 K are presented in Table 5.9. The experimental refractive indices (n_D) were in good agreement with literature values^{8,12,49,50} at 298.15 K. Table 5.9 manifests that R_m^E values are negative for the mixtures (2-EH + EDA) and (2-EH + MEA) over the entire composition range but such values vary slightly in a sigmoidal fashion for the mixture (2-EH + DCE). While the negative excess molar refractions suggest the solvent-solvent interactions, positive excess molar refractions suggest the presence of the dispersion forces between the unlike components in the mixtures.^{51,52} Thus these results are also in good agreement with those obtained earlier from other excess or deviations properties.

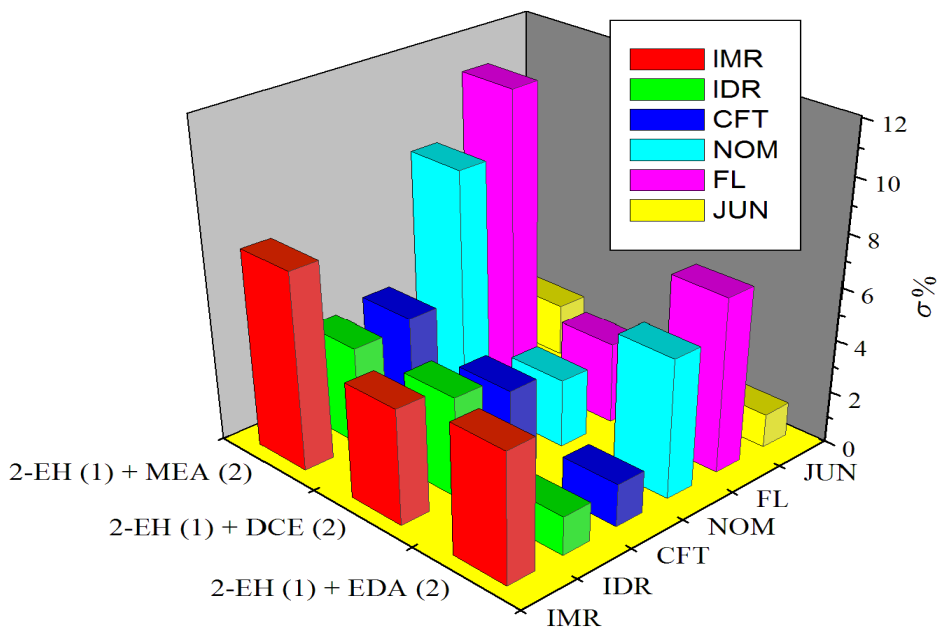


Fig. 5.9. Percent standard deviations ($\sigma\%$) for theoretical prediction of ultrasonic speeds by different empirical relations at $T = 298.15$ K for the binary mixtures studied.

The experimental refractive indices of the studied binaries were also predicted using several empirical or semi-empirical models like Lorentz-Lorenz (LL), Arago-Biot (AB), Gladstone-Dale (GD), Eykma (EYK), Newton (NEW), Heller (HEL), Eyring-

Chapter V

Table 5.9. Refractive indices (n_D), molar refractions (R_m) and excess molar refractions (R_m^E) for the binary mixtures at 298.15 K

x_1	n_D	$R_m \cdot 10^6$ ($\text{m}^3 \cdot \text{mol}^{-1}$)	$R_m^E \cdot 10^6$ ($\text{m}^3 \cdot \text{mol}^{-1}$)
2-EH (1) + EDA (2)			
0	1.4541	18.189	0
0.0488	1.4515	19.272	-0.006
0.1034	1.4488	20.478	-0.020
0.1651	1.4462	21.838	-0.037
0.2352	1.4438	23.391	-0.049
0.3157	1.4416	25.186	-0.051
0.4090	1.4392	27.259	-0.061
0.5185	1.4369	29.704	-0.059
0.6486	1.4345	32.620	-0.048
0.8059	1.4321	36.167	-0.013
1	1.4292	40.512	0
2-EH (1) + DCE (2)			
0	1.4419	21.006	0
0.0779	1.4428	22.531	0.006
0.1597	1.4406	24.124	0.004
0.2457	1.4386	25.793	-0.005
0.3363	1.4369	27.546	-0.019
0.4318	1.4353	29.400	-0.029
0.5327	1.4338	31.356	-0.041
0.6394	1.4326	33.441	-0.038
0.7525	1.4314	35.653	-0.030
0.8724	1.4304	38.008	-0.015
1	1.4292	40.512	0
2-EH (1) + MEA (2)			
0	1.4521	16.289	0
0.0495	1.4498	17.471	-0.017
0.1049	1.447	18.791	-0.041
0.1674	1.4447	20.281	-0.063
0.2382	1.4425	21.978	-0.081
0.3193	1.4402	23.923	-0.100
0.4020	1.4386	25.920	-0.106
0.5225	1.4366	28.845	-0.100
0.6523	1.4345	32.009	-0.080
0.8085	1.432	35.829	-0.044
1	1.4292	40.512	0

Chapter V

John (EJ) and Weiner (WEI) as detailed in chapter II. The predictive capabilities of these models were ascertained by estimating the percent standard deviations ($\sigma\%$). The percent standard deviations were 0.03, 0.01 and 0.06 for the mixtures (2-EH + EDA), (2-EH + DCE) and (2-EH + MEA), respectively for most of the models used and this fact suggests predicted refractive indices were in good agreement with the corresponding experimental values at 298.15 K.

5.3.10. IR spectroscopic study

The results obtained so far are also well reflected in FT-IR spectra of the binary mixtures (Figures 5.10-5.12). The spectra were recorded in a demountable KBr cell for liquid samples with spacer of path length of 0.5 mm at ambient temperature with a Perkin-Elmer Spectrum FT-IR spectrometer (RX-1). 2-EH, being a branched eight carbon alcohol, is a flexible molecule and have a number of thermally accessible geometric conformers. All these conformers contribute to its infrared spectrum with smooth bands.⁵³ The FTIR spectrum of 2-EH exhibits the following characteristic bands: i) fundamental C-H stretching vibrations in the range 2900-2880 cm^{-1} , different C-C stretching vibrations at 1038 cm^{-1} , different H-C-H bending vibrations at around 1463 and 1379 cm^{-1} and a broad O-H band around 3340 cm^{-1} .⁵⁵ DCE has characteristic peaks around 1232 cm^{-1} for *trans* conformer and two peaks around 1313 and 1285 cm^{-1} for *gauche* conformer.⁵⁴ The broad O-H band of 2-EH gradually became less broad and its intensity also decreased as the mole fraction of DCE increased for the mixture (2-EH +DCE). On the contrary the fundamental C-H stretching vibrations of 2-EH in the range 2900-2880 cm^{-1} gradually became more distinct and sharp. Also the bands at 1232, 1285 and 1313 cm^{-1} of DCE shifted slightly in peak position and intensity as the mole fraction (x_1) of 2-EH increased for this mixture. All these changes in the spectrum of the mixture (2-EH + DCE) suggest weak interactions between the components. However, for the mixture (2-EH + EDA) the N-H and N-CH₂ stretching bands (at around 3296 and 2855 cm^{-1} , respectively) of EDA become less intense and broad as the mole fraction (x_1) of 2-EH in the mixture increased. Again the -NH bending vibration⁵⁵ of EDA that appeared at 1598 cm^{-1} slowly shifted to higher frequency (from 1598 to 1600 cm^{-1}) with increasing mole fraction of 2-EH. This indicates formation of inter-molecular hydrogen bonds

Chapter V

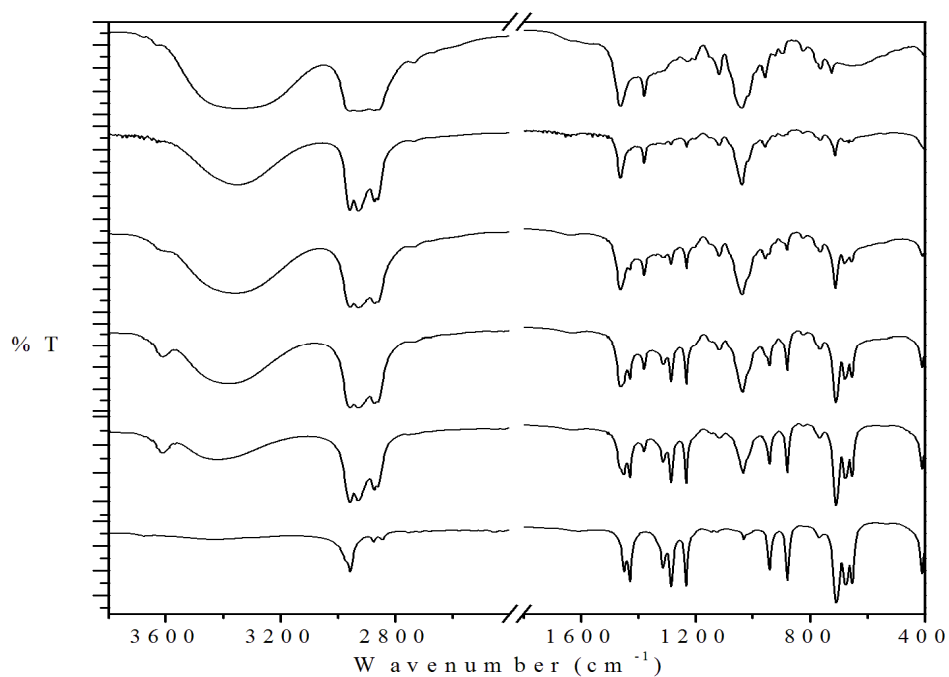


Fig. 5.10. FTIR spectra of the various binary mixtures of (2-EH + DCE): A, pure 2-EH ($x_{\text{DCE}} = 0.00$); B, ($x_{\text{DCE}} = 0.20$); C, ($x_{\text{DCE}} = 0.40$); D, ($x_{\text{DCE}} = 0.60$); E, ($x_{\text{DCE}} = 0.80$); F, Pure DCE ($x_{\text{DCE}} = 1.00$).

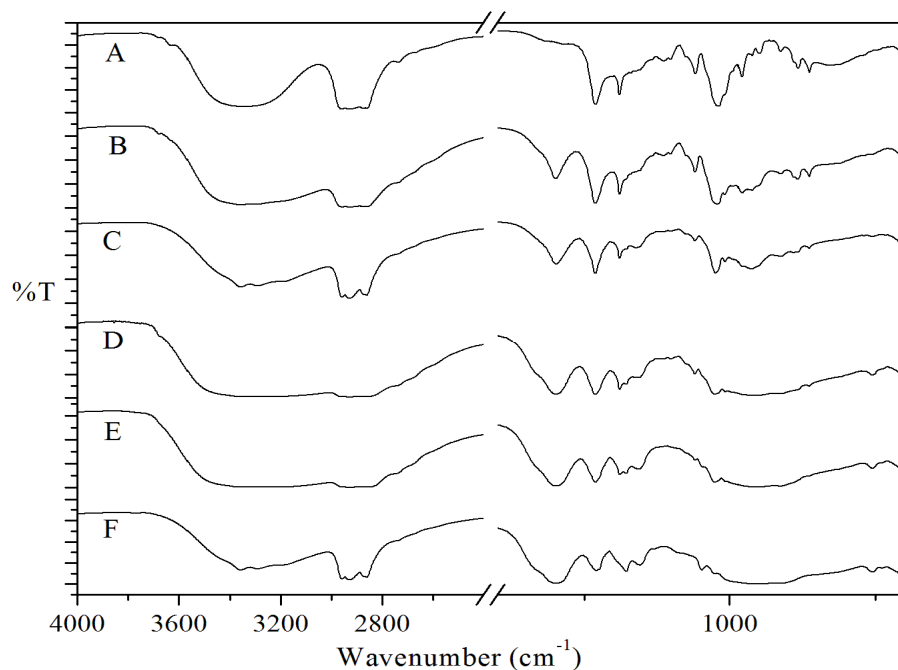


Fig. 5.11. FTIR spectra of the various binary mixtures of (2-EH + EDA): A, pure 2-EH ($x_{\text{EDA}} = 0.00$); B, $x_{\text{EDA}} = 0.20$; C, $x_{\text{EDA}} = 0.40$; D, $x_{\text{EDA}} = 0.60$; E, $x_{\text{EDA}} = 0.80$; F, Pure EDA ($x_{\text{EDA}} = 1.00$).

Chapter V

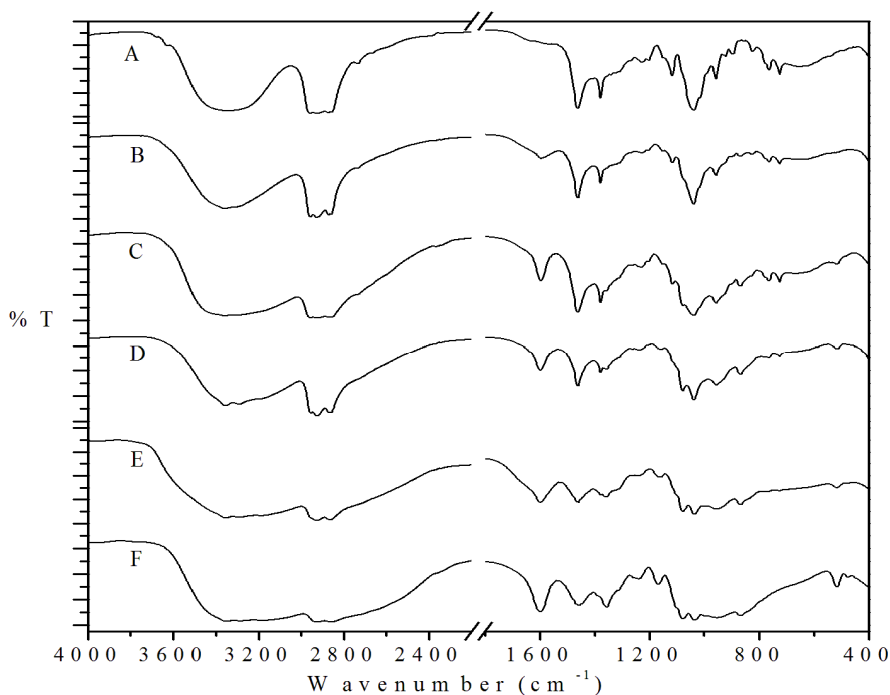


Fig. 5.12. FTIR spectra of the various binary mixtures of (2-EH + MEA): A, pure 2-EH ($x_{\text{MEA}} = 0.00$); B, $x_{\text{MEA}} = 0.20$; C, $x_{\text{MEA}} = 0.40$; D, $x_{\text{MEA}} = 0.60$; E, $x_{\text{MEA}} = 0.80$; F, Pure MEA ($x_{\text{MEA}} = 1.00$).

between dissimilar molecules in the mixture (2-EH + EDA). Similarly for the mixture (2-EH + MEA) the bands due to $-\text{OH}$ and NH_2 groups (in the range $3335\text{--}2850\text{ cm}^{-1}$) became much broader and their intensity decreased significantly as the mole fraction (x_1) of 2-EH decreased in the mixture. Also the fundamental C-H stretching vibrations of 2-EH gradually became less intense and broad, almost overlaps with the broad bands of $-\text{OH}$ and $-\text{NH}_2$ groups. These spectral changes definitely suggest that the mixtures are characterized by intra-molecular and inter-molecular hydrogen bonds.

5.4. Conclusion

The densities, viscosities, ultrasonic speeds of sound and refractive indices for the binary mixtures of 2-EH with EDA, DCE and MEA at 298.15, 308.15 and 318.15 K over the entire composition range were determined. From the experimental data, the excess volumes (V_m^E), viscosity deviations ($\Delta\eta$), excess molar refractions (R_m^E) and different excess acoustic parameters like excess isentropic compressibility (κ_S^E), excess intermolecular free length (L_f^E) and excess acoustic impedance (z_{im}^E) were

Chapter V

obtained. The reported excess or deviation properties show both positive and negative deviations from ideal ones and their variations with mole fraction (x_1) of 2-EH were discussed in terms of molecular interactions like dipole-dipole interactions, hydrogen bond formation and interstitial accommodation, *etc.* This study revealed that the molecular interaction is highest in the mixture (2-EH + MEA) and least in the mixture (2-EH + DCE) and thus the order of molecular interactions follows the order: (2-EH + MEA) > (2-EH + EDA) > (2-EH + DCE). These excess molar volumes were correlated by using PFP, PREOS models and viscosities were correlated using PREOS and Bloomfield-Dewan models. FTIR spectra of the mixtures showed characteristic band shifts in position and intensity reflecting the nature of molecular interaction in the studied mixtures.

References

- [1] A. Ali, H. Soghra, *Ind. J. phys.*, 76 (2002) 23.
- [2] A. Ali, A.K. Nain, N. Kumar, M. Ibrahim, *J. Pure Appl. Ultrason.*, 24 (2002) 27.
- [3] R. Mehra, R. Israni, *Ind. J. Pure Appl. Phys.*, 38 (2000) 81.
- [4] S.I. Oswal, N.B. Patel, *J. Chem. Eng. Data* 40 (1995) 845.
- [5] B. Gracia, R. Alcalde, J. M. Leal, *J. Chem. Soc., Faraday Trans.*, 93 (1997) 1115.
- [6] G.A. Krestov, *Thermodynamics of Solvation*, Ellis Horwood, England, (1991) pp.151.
- [7] M.I. Aralaguppi, C.V. Jadar, T.M. Aminabhavi, *J. Chem. Eng. Data* 44 (1999) 446.
- [8] A.M. Awwada, R.A. Pethric, *J. Chem. Soc. Faraday Trans. I*, 78 (1982) 3203.
- [9] E. Zorebski, M. Dzida, E. Wysocka, *J. Chem. Eng. Data* 56 (2011) 2680.
- [10] S.C. Bhatia, J. Sangwan, R. Rani, V. Kiran, *Int. J. Thermophys.*, 34 (2013) 2076.
- [11] C. Li, J. Zhang, T. Zhang, X. Wei, E. Zhang, N. Yang, N. Zhao, M. Su, H. Zhou, *J. Chem. Eng. Data* 55 (2010) 4104.
- [12] J.K. Gladden, *J. Chem. Eng. Data* 17 (1972) 468.
- [13] M.A. Saleh, M.S. Ahmed, M.S. Islam, *Phys. Chem. Liq.*, 40 (2002) 477.
- [14] R. Pradhan, A. Kamath, D. Brahman, B. Sinha, *Fluid Phase Equilib.*, 404 (2015) 131.
- [15] S. Ranjbar, K. Fakhri, B. Jahan, J. Ghasemi, *J. Chem. Eng. Data* 54 (2009) 3284.
- [16] R.K. Biswas, R.A. Banu, M.N. Islam, *Hydrometallurgy*, 69 (2003) 157.
- [17] S.E. Burke, B. Hawryla, R. Palepu, *Thermochim. Acta.*, 345 (2002) 101.
- [18] U.R. Kapadi, D.G. Hundiwale, N.B. Patil, M.K. Lande, *Fluid Phase Equilib.*, 201 (2002) 335.

Chapter V

- [19] Y. Mahan, C.N. Liew, A.E. Mather, *J. Solution Chem.*, 31 (2002) 743.
- [20] W.M. Haynes, D.R. Lide, T.J. Bruno, *CRC Handbook of Chemistry & Physics*, 93rd edn., Taylor & Francis, Boca Roton, London, 2012-2013.
- [21] S.C. Bhatia, R. Bhatia, G.P. Dubey, *J. Mol. Liq.*, 144 (2009) 163.
- [22] G.M. Smith, H.C. Van Ness, *Introduction to Chemical Engineering Thermodynamics*, McGraw Hill, New York, 1987.
- [23] H.A. Zarei, *J. Mol. Liq.*, 130 (2007) 74.
- [24] O. Redlich, A.T. Kister, *Indus. Eng. Chem.*, 40 (1948) 345.
- [25] D.W. Marquardt, *J. Soc. Ind. Appl. Math.*, 11, (1963) 431.
- [26] D. Patterson, G. Delmas, *J. Polym. Sci.*, 30 (1970) 1.
- [27] D. Patterson, *Pure. Appl. Chem.*, 47 (1976) 305.
- [28] P.J. Flory, R.A. Orwell, A. Vrij, *J. Am. Chem. Soc.*, 86 (1964) 3507.
- [29] P.J. Flory, R.A. Orwell, A. Vrij, *J. Am. Chem. Soc.*, 86 (1964) 3515.
- [30] P.J. Flory, *J. Am. Chem. Soc.*, 87 (1965) 1833.
- [31] A. Abe, P.J. Flory, *J. Am. Chem. Soc.*, 87 (1965) 1838.
- [32] D.Y. Peng, D.B. Robinson, *Ind. Eng. Chem. Fundum.*, 15 (1976) 59.
- [33] S.I Sandler, *Chemical, Biochemical, and Engineering Thermodynamics*, 4th edn, John Wiley & Sons (Asia), New Delhi, 2006, pp. 242, 258.
- [34] M.A. Saleh, S. Akhtar, M.S. Ahmed, *Phys. Chem. Liq.*, 44 (2006) 551.
- [35] S. Glasstone, K.J. Laidler, H. Eyring, *The theory of Rate Process*. McGraw-Hill Book Company, Inc., New York, 1941.
- [36] R.J. Fort, W.R. Moore, *Trans. Faraday Soc.*, 62 (1966) 1112.
- [37] H. Vogel, A. Weiss, *Phys. Chem. Chem. Phys.*, 86 (1982) 193.
- [38] F. Corradini, L. Marcheselli, A. Marchetti, M. Tagliazucchi, L. Tassi, G. Tosi, *Bull. Chem. Soc. Jpn.*, 65 (1992) 503.
- [39] T.M. Reid, T.E. Taylor, *J. Phys. Chem.*, 63 (1959) 58.
- [40] A.K. Mehrotra, W.D. Monnery, W. Svrcek, *Fluid Phase Equilib.*, 117 (1996) 344.
- [41] R.D. McCarty, *Fluid Phase Equilib.*, 256 (2007) 42.
- [42] V.A. Bloomfield, R.K. Dewan, *J. Phys. Chem.*, 75 (1971) 3113.
- [43] J.S. Rowlinson, F.L. Swinton, *Liquid and Liquid Mixtures*, Butterworths, London, 3rd edn., 1982, pp. 16,17.
- [44] G.P. Dubey, K. Kumar, *J. Chem. Eng. Data* 56 (2011) 2995.
- [45] S.C. Bhatia, R. Bhatia ·G.P. Dubey, *Int. J. Thermophys.*, 31(2010) 2119.

Chapter V

- [46] G.C. Benson, O.K. Kiyohara, *J. Chem. Thermodyn.*, 11 (1979) 1061.
- [47] W.E. Acree, *J. Chem. Eng. Data* 28 (1983) 215.
- [48] A. Ali, A.K. Nain, D. Chand, R. Ahmad, *J. Chin. Chem. Soc.*, 53 (2006) 531.
- [49] K.M. Kadish, J.E. Anderson, *Pure. Appl. Chem.*, 59 (1987) 703.
- [50] M. Yasmin, M. Gupta, *J. Solution Chem.*, 40 (2011) 1458.
- [51] A. Pineiro, P. Brocos, A. Amigo, M. Pintos, R, *J. Chem. Thermodyn.*, 31 (1999) 931.
- [52] D.S. Wankhede, *Int. J. Chem. Res.*, 2 (2011) 23.
- [53] T.N. Clasp, S.W. Reeve, H. Koizumi, *J. Theo. Comp. Chem.*, 16 (2017) 1750023.
- [54] R.K. Sreeruttun, R. Ramasami, *Phys. Chem. Liq.*, 44 (2006) 315.
- [55] Q. Li, F. Sha, G. Zhao, M. Yang, L. Zhao, Q. Zhang, J. Zhang, . *Chem. Eng. Data* 61 (2016) 1718.

CHAPTER VI

Hydrogen bond interactions in the mixtures of 1,4-dioxane with some 1, 2-disubstituted ethanes at $T = (298.15-318.15) \text{ K}^*$

6.1. Introduction

Molecular interactions control the physico-chemical properties of different liquids in liquid-liquid systems. Knowledge of such molecular interactions in liquid-liquid systems is very important for their industrial applications¹⁻³ and in the elucidation of the structural properties of the molecules⁴ in the liquid state. Mixed solvents were being used for studying complex reactions and developing theoretical understanding of chemical separations, fluid flow and heat transfers, *etc.* The basis for any process design in chemical industries is a reliable set of chemical and physical properties of the pure components and their mixtures. Therefore the determination of macroscopic properties like density, viscosity and speed of sound, *etc.* help greatly for exploring the liquid state,⁵ this is due to the close connection between the liquid structure and such macroscopic properties. However, experimental values of these properties are not available many-a-time and the measurements are often expensive or difficult; hence estimation methods often become very helpful. These properties functionally depend upon temperature, pressure and the composition of the liquid-liquid systems. For example, density and ultrasonic speed of sound depend on the binding forces between the liquids and are very much sensitive to the liquid structure and composition.⁶ Hence studies on the physico-chemical properties of liquid-liquid systems stand as an efficient guide for the selection of such systems regarding their practical utilization in industrial and consumer applications. 1,2-disubstituted ethanes are excellent prototypes for conformational studies, because the relative stability of the *gauche* and *trans* conformation of 1,2-disubstituted ethanes depend upon the substituents and upon the dielectric constant of the medium.⁷ Ramasmari *et al.*⁸ studied the conformational behavior of 1, 2-dichloroethanes in several solvents by ¹H-NMR, IR, refractive index and theoretical studies. It has been found that *gauche* conformers are preferentially more stabilized in media with higher dielectric constants. Nath *et al.*⁹ studied the binary mixtures of 1,2-dichloroethane with benzene, toluene, p-xylene, quinoline and cyclohexane. Anyway, to the best of our knowledge

**Published in: Fluid Phase Equilibria* 404 (2015) 131–140.

Chapter VI

reports on the physico-chemical properties of the binary mixtures studied in this chapter are rare in the literature. Therefore, herein this chapter an attempt has been undertaken to unravel the nature of molecular interactions in the binary mixtures of 1,4-dioxane (1,4-DO) with ethylenediamine (EDA), 1,2-dichloroethane (DCE) and monoethanolamine (MEA) at 298.15, 308.15 and 318.15 K under ambient pressure.

Among the selected liquids 1,4-DO is a non-polar, aprotic, non-hydrogen bonded cyclic diether and finds numerous applications in industrial processes as a solvent for saturated and unsaturated hydrocarbons.¹⁰ The other three solvents also find industrial importance and consumer applications, *e.g.*, EDA is an important raw material for the production of polymers, pharmaceuticals, pesticides, herbicides and dye fixing agent, *etc*; DCE is a σ -acceptor and is used as a solvent, degreaser, *etc*;⁹ MEA is used in the purification of petroleum, as a solvent in dry cleaning, as a CO₂ adsorbent and as an ingredient in paints and pharmaceuticals.¹¹ Thus the pure liquid components for the present study were chosen based on their varied applications.

The experimental data (ρ , η , u and n_D) were used to determine the excess molar volumes (V_m^E), viscosity deviations ($\Delta\eta$), acoustic parameters like isentropic compressibility (κ_s), intermolecular free length (L_f), specific acoustic impedance (z_{im}), free volume (V_f), excess isentropic compressibility (κ_s^E), excess intermolecular free length (L_f^E), excess specific acoustic impedance (z_{im}^E), excess free volume (V_f^E) and excess molar refractions (R_m^E) for the binary mixtures. Partial molar volumes ($\bar{V}_{m,1}^0$ and $\bar{V}_{m,2}^0$) and excess partial molar volumes ($\bar{V}_{m,1}^{0,E}$ and $\bar{V}_{m,2}^{0,E}$) at infinite dilution of each component were also determined using the excess molar volumes (V_m^E) of the binary mixtures. All these functions were discussed in terms of molecular interactions, structural effects and the nature of liquid mixtures. The excess molar volumes (V_m^E) of the binary mixtures at ambient temperature and pressure were also treated in terms of PFP theory.^{12,13} A comparison between the experimental and calculated V_m^E and η values (based on PFP^{12,13} or Bloomfield-Dewan viscosity model¹⁴ and PREOS¹⁵) was also made to estimate the predictive capability of these theories for the selected binary mixtures. Moreover, ultrasonic speeds of sound and refractive indices for all the binary mixtures were theoretically predicted on the basis

Chapter VI

of several empirical and semi-empirical relations. In addition, IR spectra of the mixtures were correlated to the molecular interactions between the components in the mixtures.

6.2. Experimental section

6.2.1. Materials

All the chemicals used (Reagent/Reagent Plus grade, Sigma-Aldrich, Germany, purity > 99%) were used without any further purification. Provenance and purity of the chemicals used in this chapter have already been given in chapter III. However, purity of the solvents was ascertained by GLC and also a comparison of the experimental densities and viscosities at the experimental temperatures was made in Table 6.1 with the literature data,¹⁶⁻²⁸ whenever available.

Table 6.1. Densities (ρ) and viscosities (η) of the pure liquids at $T = (298.15 \text{ to } 318.15) \text{ K}$

Pure Liquid	$T \text{ (K)}$	$\rho \cdot 10^{-3}$ ($\text{kg} \cdot \text{m}^{-3}$)		η ($\text{mPa} \cdot \text{s}$)	
		Expt.	Lit.	Expt.	Lit.
1,4-DO	298.15	1.02779	1.0265 ¹⁶ 1.0278 ¹⁷	1.1777	1.196 ¹⁶ 1.1779 ¹⁸
	308.15	1.01678	1.0166 ¹⁶ 1.0168 ¹⁹	1.0094	1.013 ¹⁶ 0.9985 ¹⁸
	318.15	1.00524	1.0052 ¹⁶ 1.00526 ²⁰	0.8896	0.887 ¹⁶ 0.901 ²¹
EDA	298.15	0.89479	0.8945 ²² 0.8948 ²³	1.2758	1.276 ²²
	308.15	0.88563	0.8856 ²²	1.1072	1.107 ²²
	318.15	0.86762	0.867667 ²⁴	0.9445	
DCE	298.15	1.24637	1.2474 ²⁵	0.7804	0.759 ²⁵ 0.7805 ²⁶
	308.15	1.23121	1.2312 ²⁵	0.6744	0.674 ²⁵
	318.15	1.21455		0.5719	
MEA	298.15	1.01179	1.0118 ²⁷	18.9538	18.95 ⁵
	308.15	1.00468	1.00467 ²⁷ 1.0043 ²⁸	11.9630	11.966 ²⁸
	318.15	0.99815	0.99817 ²⁷ 0.99635 ²⁸	7.9132	7.914 ²⁸

6.2.2. Apparatus and procedure

The binary mixtures were prepared by mass in air-tight bottles with stopper inside a dry box at 298.15 K as detailed in chapter III. The mass measurements were made on a digital electronic analytical balance (Mettler, AG 285, Switzerland) with an

Chapter VI

uncertainty of $\pm 1 \cdot 10^{-4}$ g. All solutions were prepared afresh before use. The densities were measured with a vibrating-tube density meter (Anton Paar, DMA 4500M). The temperature of the density meter was automatically kept constant with an accuracy of $\pm 1 \cdot 10^{-2}$ K using a built-in Peltier technique. The viscosities were measured with the aid of a suspended Canon-type Ubbelohde viscometer at the experimental temperatures ± 0.01 K. Ultrasonic speeds of sound (u) were measured with an accuracy of 0.3 % by using a single crystal variable-path ultrasonic interferometer (Mittal Enterprise, New Delhi, F-05) working at 2 MHz. Refractive indices were measured with an Abbe's refractometer. In all determinations, an average of triplicate measurements was taken into account and adequate precautions were taken to minimize evaporation losses during the actual measurements. The details of the instruments, their calibrations and uncertainties of the measured properties are given in chapter III.

6.3. Results and discussion

The experimental densities (ρ), viscosities (η), excess molar volumes (V_m^E) and viscosity deviations ($\Delta\eta$) of the binary mixtures at the experimental temperatures are given in Table 6.2. For an understanding of the nature of the molecular interactions between the components of the liquid mixtures, excess/deviations properties are of immense help. Non-ideal liquid mixtures often show deviations from a rectilinear dependence of their properties such as molar volume, viscosity, *etc.*, upon the component mole fractions or compositions. Such deviations basically arise from the strong or weak interactions between the liquid components in a mixture based upon their nature and compositions.

6.3.1. Excess molar volumes

The excess molar volumes (V_m^E) of the mixture can be had from the equation:

$$V_m^E = \sum_{i=1}^2 x_i M_i (1/\rho - 1/\rho_i) \quad (1)$$

where ρ is the density of the mixture and x_i , M_i and ρ_i are the mole fraction, molar mass and density of the i^{th} component in the mixture, respectively. The estimated uncertainty for excess molar volumes (V_m^E) was evaluated to be $\pm 0.005 \text{ cm}^3 \cdot \text{mol}^{-1}$.

Chapter VI

Table 6.2. Density (ρ), viscosity (η), excess molar volume (V_m^E) and viscosity deviation ($\Delta\eta$) for the binary mixtures studied at $T = (298.15 \text{ to } 318.15) \text{ K}$

x_1	$\rho \cdot 10^{-3}$ ($\text{kg} \cdot \text{m}^{-3}$)	η ($\text{mPa} \cdot \text{s}$)	$V_m^E \cdot 10^6$ ($\text{m}^3 \cdot \text{mol}^{-1}$)	$\Delta\eta$ ($\text{mPa} \cdot \text{s}$)
1,4-DO (1) + EDA (2)				
$T = 298.15 \text{ K}$				
0	0.89479	1.2758	0	0
0.0800	0.90717	1.2628	0.068	-0.005
0.1636	0.91948	1.2504	0.144	-0.009
0.2511	0.93176	1.2391	0.223	-0.011
0.3428	0.94428	1.2276	0.286	-0.014
0.3850	0.94992	1.2227	0.308	-0.014
0.5399	0.97035	1.2064	0.334	-0.015
0.6461	0.9841	1.1973	0.302	-0.014
0.7578	0.99837	1.1892	0.227	-0.011
0.8756	1.01303	1.1824	0.119	-0.007
1	1.02779	1.1777	0	0
$T = 308.15 \text{ K}$				
0	0.88563	1.1072	0	0
0.0800	0.89775	1.0922	0.076	-0.007
0.1636	0.90985	1.0784	0.155	-0.012
0.2511	0.92106	1.0655	0.307	-0.016
0.3428	0.93433	1.0527	0.297	-0.020
0.3850	0.93989	1.0480	0.320	-0.020
0.5399	0.95996	1.0329	0.352	-0.020
0.6461	0.97348	1.0259	0.323	-0.017
0.7578	0.98759	1.0193	0.245	-0.013
0.8756	1.00204	1.0156	0.136	-0.005
1	1.01678	1.0094	0	0
$T = 318.15 \text{ K}$				
0	0.86762	0.9445	0	0
0.0800	0.88010	0.9318	0.093	-0.008
0.1636	0.89274	0.9205	0.177	-0.015
0.2511	0.90551	0.9111	0.254	-0.019
0.3428	0.91846	0.9021	0.319	-0.023
0.3850	0.92435	0.8983	0.338	-0.025
0.5399	0.94542	0.8929	0.372	-0.022
0.6461	0.95955	0.8913	0.348	-0.017
0.7578	0.97427	0.8918	0.276	-0.011
0.8756	0.98943	0.8902	0.166	-0.006
1	1.00524	0.8896	0	0
1,4-DO (1) + DCE (2)				
$T = 298.15 \text{ K}$				
0	1.24637	0.7804	0	0
0.0934	1.22134	0.8045	0.207	-0.006
0.1881	1.19717	0.8332	0.368	-0.010
0.2843	1.17399	0.8640	0.469	-0.013
0.3819	1.15177	0.8974	0.507	-0.016
0.4258	1.14209	0.9132	0.511	-0.017
0.5816	1.10956	0.9729	0.422	-0.018

Chapter VI

0.6838	1.08925	1.0159	0.314	-0.018
0.7875	1.06916	1.0636	0.184	-0.015
0.8929	1.04886	1.1171	0.063	-0.010
1	1.02779	1.1777	0	0
<hr/>				
<i>T</i> = 308.15 K				
0	1.23121	0.6744	0	0
0.0934	1.20617	0.6918	0.243	-0.008
0.1881	1.18234	0.7127	0.415	-0.015
0.2843	1.15950	0.7370	0.526	-0.019
0.3819	1.13763	0.7628	0.572	-0.024
0.4258	1.12816	0.7747	0.574	-0.026
0.5816	1.09617	0.8211	0.493	-0.032
0.6838	1.07638	0.8551	0.375	-0.033
0.7875	1.05658	0.8949	0.252	-0.032
0.8929	1.03688	0.9435	0.113	-0.023
1	1.01678	1.0094	0	0
<hr/>				
<i>T</i> = 318.15 K				
0	1.21455	0.5719	0	0
0.0934	1.18914	0.5856	0.313	-0.010
0.1881	1.16497	0.6042	0.555	-0.017
0.2843	1.14196	0.6266	0.724	-0.022
0.3819	1.12000	0.6499	0.822	-0.027
0.4258	1.11067	0.6611	0.834	-0.029
0.5816	1.07943	0.7050	0.764	-0.034
0.6838	1.06046	0.7374	0.623	-0.036
0.7875	1.04221	0.7750	0.414	-0.035
0.8929	1.02408	0.8234	0.183	-0.025
1	1.00524	0.8896	0	0
<hr/>				
1,4-DO (1) + MEA (2)				
<hr/>				
<i>T</i> = 298.15 K				
0	1.01179	18.9538	0	0
0.0597	1.01553	16.0540	-0.147	-0.001
0.1251	1.01805	13.3865	-0.222	-0.002
0.1969	1.02039	10.9652	-0.286	-0.003
0.2760	1.02247	8.7983	-0.333	-0.004
0.3639	1.02423	6.8921	-0.358	-0.005
0.4618	1.02564	5.2493	-0.356	-0.005
0.5716	1.02641	3.8676	-0.302	-0.004
0.6958	1.02709	2.7386	-0.233	-0.003
0.8373	1.02758	1.8488	-0.136	-0.002
1	1.02779	1.1777	0	0
<hr/>				
<i>T</i> = 308.15 K				
0	1.00468	11.9630	0	0
0.0597	1.00750	10.3163	-0.112	-0.004
0.1251	1.01007	8.7723	-0.212	-0.008
0.1969	1.01165	7.3404	-0.250	-0.012
0.2760	1.01321	6.0311	-0.286	-0.014
0.3639	1.01447	4.8507	-0.301	-0.015
0.4618	1.01523	3.8043	-0.279	-0.015
0.5716	1.01549	2.8980	-0.214	-0.013
0.6958	1.01574	2.1319	-0.140	-0.009
0.8373	1.01622	1.5061	-0.072	-0.003

Chapter VI

1	1.01678	1.0094	0	0
$T = 318.15 \text{ K}$				
0	0.99815	7.9132	0	0
0.0597	1.00035	6.9395	-0.101	-0.005
0.1251	1.00177	6.0097	-0.155	-0.010
0.1969	1.00306	5.1318	-0.203	-0.015
0.2760	1.00408	4.3215	-0.234	-0.007
0.3639	1.00475	3.5555	-0.240	-0.017
0.4618	1.00492	2.8675	-0.209	-0.016
0.5716	1.00506	2.2547	-0.171	-0.014
0.6958	1.00496	1.7194	-0.109	-0.010
0.8373	1.00510	1.2664	-0.059	-0.003
1	1.00524	0.8896	0	0

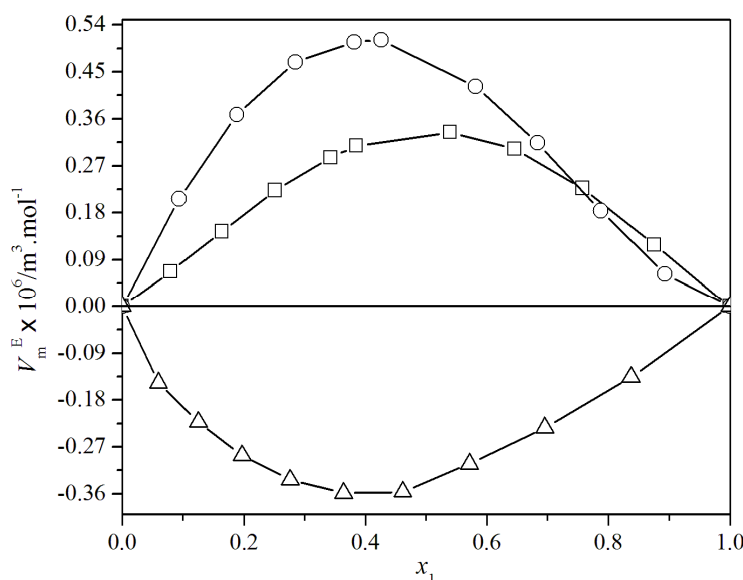


Fig. 6.1. Excess molar volume (V_m^E) versus mole fraction of 1,4-DO (x_1) for the binary mixtures of 1,4-DO + 1,2-disubstituted ethanes at $T = 298.15 \text{ K}$. Symbols: \square , EDA; \circ , DCE; Δ , MEA.

Figure 6.1 (V_m^E versus x_1 at 298.15 K) illustrates that the V_m^E values are positive for the mixtures (1,4-DO + EDA) and (1,4-DO + DCE) mixture but are negative for (1,4-DO + MEA) mixture over the entire range of compositions at all the experimental temperatures. The excess molar volume generally depends upon two factors: (i) variation of intermolecular forces between two components in contact; the physical effects involve dispersion forces and non-specific interactions in the mixture and thus contribute positive values to V_m^E . The chemical or specific interactions result in

Chapter VI

volume decrease or contraction and involve hydrogen bond formation or rupture, charge transfer type forces and other complex forming interactions between dissimilar species and thus contribute negative values to V_m^E ; (ii) variation in molecular packing subject to interstitial accommodation of one component into other may arise due to difference in free volume and molar volume of the components. If the interactions between dissimilar species are weaker than those between similar species excess molar volume (V_m^E) will be positive. As already stated earlier that 1,2-disubstituted ethanes generally prefer *gauche* conformation and possess intra-molecular hydrogen bonding except DCE.²⁹ For DCE, the *gauche* conformer is polar and stabilized by electrostatic interaction between their dipole moments.²⁹ A comparison of the relative permittivity³⁰ of the liquid components $\{\epsilon_{r,1,4-DO} (2.21) < \epsilon_{r,DCE} (10.42) < \epsilon_{r,EDA} (13.82) < \epsilon_{r,MEA} (31.94)\}$ suggests that the following approximate order of molecular interaction between similar components: (MEA-MEA) > (EDA-EDA) > (DCE-DCE) > (1,4-DO-1,4-DO). The positive V_m^E values for the mixtures (1,4-DO + EDA) and (1,4-DO + DCE) indicate breaking of liquid order on mixing and dispersion interactions between dissimilar components. Dispersion interactions may arise from the breaking of cohesive forces or intra-molecular hydrogen bonds between the similar molecules on addition of 1,4-DO to the ethanes. So mixing of 1,4-DO probably results in the breaking of the weak dipole-dipole cohesive forces amongst the DCE molecules²⁹ and intra-molecular hydrogen bonds in EDA molecules.²⁹ 1,4-DO can also form hydrogen bond through its two ethereal O-atoms with NH_2 groups of EDA molecule and thus it can hamper intra-molecular hydrogen bonds in EDA molecules. That is why V_m^E values of the mixture (1,4-DO + EDA) are lower than those of the mixture (1,4-DO + DCE). In the case of the mixture (1,4-DO + MEA), the negative V_m^E values suggest the presence of specific interactions like intermolecular hydrogen bonds between the dissimilar components (through the involvement of the ethereal O-atoms of 1,4-DO and the highly polar $-OH$ and $-NH_2$ group present in MEA molecule) and geometrical fitting of the molecules ($V_{m,1,4-DO} - V_{m,MEA} = 25.36 \text{ cm}^3 \cdot \text{mol}^{-1}$ at 298.15 K) on mixing. Thus the magnitude of V_m^E values have the order: (1,4-DO + DCE) > (1,4-DO + EDA) > (1,4-DO + MEA);

Chapter VI

thus it is apparent that the molecular interaction is least for the mixture (1,4-DO + DCE) and highest for the mixture (1,4-DO + MEA). Furthermore, Table 6.2 suggests that in each case V_m^E values increase as the temperature increases over the whole composition range from 298.15 to 318.15 K. Such a trend in temperature dependence of V_m^E values indicates that temperature enhancement causes a decrease in the interaction between the component molecules; therefore thermal agitation that probably breaks or disturbs the developing dispersion forces and non-specific interactions as well as specific interactions between the liquid components in the studied mixtures.

6.3.2. Excess partial molar volumes

The partial molar volumes ($\bar{V}_{m,i}$) of the i^{th} component in the binaries over the entire composition range at 298.15 K were obtained from the relation:³¹

$$\bar{V}_{m,i} = V_{m,i}^E + V_{m,i}^* + (1 - x_i)(dV_{m,i}^E/dx_i)_{T,P} \quad (2)$$

where $V_{m,i}^*$ is the molar volume of the i^{th} component in the binaries. The derivatives, $(\partial V_{m,i}^E/\partial x_i)_{T,P}$ used in Eq. (2) were obtained by following a procedure described in chapter II by using the Redlich–Kister coefficients (a_i)³² for the excess molar volumes (V_m^E): $a_0 = 1.3439$, $a_1 = 0.0760$, $a_2 = -0.5266$, $a_3 = -0.0272$ for the mixture (1,4-DO + EDA); $a_0 = 1.9370$, $a_1 = -1.0974$, $a_2 = -0.6155$, $a_3 = 0.0604$ for the mixture (1,4-DO + DCE) and $a_0 = -1.3210$, $a_1 = 0.4367$, $a_2 = -0.4153$, $a_3 = 0.8004$ for the mixture (DO + MEA) with standard deviations (σ)³³ 0.0008, 0.0051, 0.0147 for the three mixtures, respectively. Partial molar volumes ($\bar{V}_{m,1}^0$ and $\bar{V}_{m,2}^0$) at infinite dilution, excess partial molar volumes ($\bar{V}_{m,i}^E$) and excess partial molar volumes ($\bar{V}_{m,i}^{0,E}$) at infinite dilution were determined using the standard relations described in chapter II. Partial molar volumes ($\bar{V}_{m,1}^0$ and $\bar{V}_{m,2}^0$) and excess partial molar volumes ($\bar{V}_{m,i}^{0,E}$) at infinite dilution for each component in the binary mixtures are listed in Table 6.3. Excess partial molar volumes ($\bar{V}_{m,1}^E$ and $\bar{V}_{m,2}^E$) of each component in the studied mixtures were depicted in Figure 6.2 as a function of x_1 . Partial molar volume ($\bar{V}_{m,1}^0$ and $\bar{V}_{m,2}^0$) at infinite dilution of each liquid was found to be greater than the molar

Chapter VI

Table 6.3. Molar volumes ($V_{m,1}^*$ and $V_{m,2}^*$), partial molar volumes at infinite dilution ($\bar{V}_{m,1}^0$ and $\bar{V}_{m,2}^0$) and excess partial molar volume at infinite dilution ($\bar{V}_{m,1}^{0,E}$ and $\bar{V}_{m,2}^{0,E}$) for each component in the binary mixtures at 298.15 K.

Volume parameters	1,4-DO (1) +		
	EDA (2)	DCE (2)	MEA (2)
$V_{m,1}^*$	85.73	85.73	85.73
$\bar{V}_{m,1}^0$	86.50	88.09	82.75
$V_{m,2}^*$	67.15	79.41	60.37
$\bar{V}_{m,2}^0$	68.02	79.69	59.87
$\bar{V}_{m,1}^{0,E}$	0.769	2.358	-2.973
$\bar{V}_{m,2}^{0,E}$	0.866	0.285	-0.499

Volume parameters are given in $\text{cm}^3 \cdot \text{mol}^{-1}$.

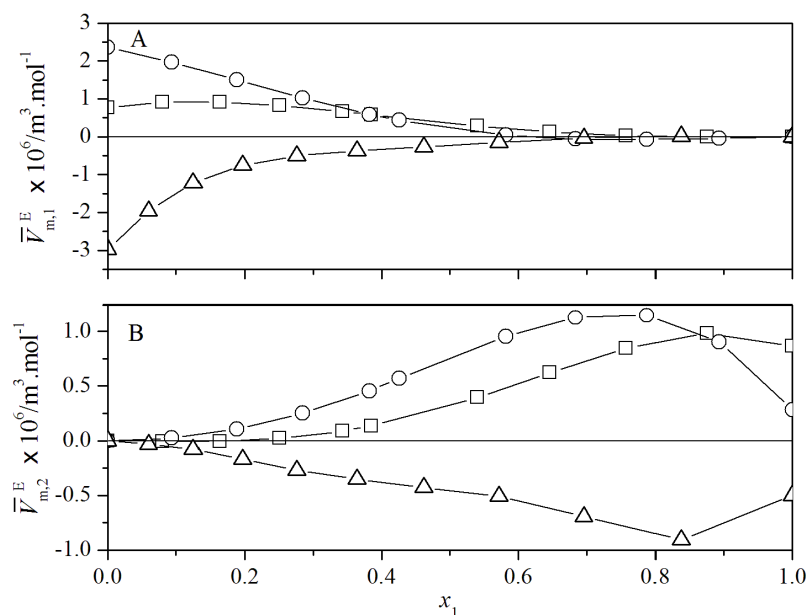


Fig. 6.2. Excess partial molar volume ($\bar{V}_{m,i}^E$) against mole fraction of 1,4-DO (x_1) for the binary mixtures of 1,4-DO + 1,2-disubstituted ethanes at $T = 298.15$ K: A, for DO; B, for 1,2-disubstituted ethanes. Symbols: \square , EDA; \circ , DCE; Δ , MEA.

volume of the respective pure liquid for the studied mixtures except the (1,4-DO + MEA) mixture. Also, the excess partial molar volumes ($\bar{V}_{m,1}^{0,E}$ and $\bar{V}_{m,2}^{0,E}$) at infinite dilution were positive for both components in the mixtures (1,4-DO + EDA) and

Chapter VI

(1,4-DO + DCE) except the mixture (1,4-DO + MEA). This suggests that while the systems with EDA and DCE are characterized by volume expansion on mixing with 1,4-DO, the mixture with MEA is characterized by volume contraction on mixing with 1,4-DO, *i.e.*, the mixture (1,4-DO + MEA) is characterized by a better packing efficiency and intermolecular hydrogen bonds between the dissimilar molecules were not broken at dilute regions.

6.3.3. Predictions of excess molar volumes

i) *Prigogine-Flory-Patterson theory* (PFP):

In recent years, Flory's statistical theory³⁴⁻³⁷ and its modified version known as the Prigogine-Flory-Patterson (PFP) theory^{12,13} has been employed to estimate and analyze excess thermodynamic functions theoretically. The Flory's parameters such as reduced volume (\tilde{v}), reduced temperature (\tilde{T}), characteristic volume (V^*), characteristic pressure (P^*) and characteristic temperature (T^*) for each liquid component are given in Table 6.4. The PFP theory considers excess molar volumes (V_m^E) of the binary mixtures to be the sum of three contributions: (i) the interaction contribution (V_{int}^E), which is proportional to the interaction parameter, $\chi_{1,2}$; (ii) the free volume contribution (V_{fv}^E), which arises from the dependence of the reduced volume upon the reduced temperature as a result of the difference between the degree of expansion of the two components and (iii) the internal pressure contribution (V_p^E),

Table 6.4. Isobaric molar heat capacities (c_p), expansion coefficient (α), isothermal compressibility (κ_T) and Flory's parameters for pure liquids at 298.15 K

Liquids	c_p^a	\tilde{v}	\tilde{T}	$V^* \cdot 10^6$ ($m^3 \cdot mol^{-1}$)	P^* (Pa)	T^* (K)	α (kK^{-1})	κ_T (TPa^{-1})
1, 4-DO	152.10	1.2672	0.0599	67.65	708.53	4976.93	1.0970	741.3
EDA	172.60	1.3451	0.0699	49.93	1226.52	4262.04	1.5182	667.7
DCE	128.40	1.3018	0.0646	60.99	746.81	4611.89	1.2765	863.6
MEA	195.50	1.1768	0.0448	51.30	737.98	6641.29	0.6740	377.1

^a Unit: $J \cdot K^{-1} \cdot mol^{-1}$ and values are adapted from Ref [30].

which depends both on the differences of the characteristic pressures and on the differences of reduced volumes of the components. The following equation was used to estimate V_m^E values:

Chapter VI

$$\begin{aligned}
 \frac{V_m^E}{x_1V_1^* + x_2V_2^*} &= \frac{(\tilde{v}^{1/3} - 1)\tilde{v}^{2/3}\psi_1\theta_2}{[(4/3)\tilde{v}^{-1/3} - 1]P_1^*} \chi_{1,2} && (\chi_{1,2} \text{ contribution}) \\
 &- \frac{(\tilde{v}_1 - \tilde{v}_2)^2[(14/9)\tilde{v}^{-1/3} - 1]\psi_1\psi_2}{[(4/3)\tilde{v}^{-1/3} - 1]\tilde{v}} && (\tilde{v} \text{ contribution}) \\
 &+ \frac{(\tilde{v}_1 - \tilde{v}_2)(P_1^* - P_2^*)\psi_1\psi_2}{(P_1^*\psi_2 + P_2^*\psi_1)} && (P^* \text{ contribution})
 \end{aligned} \tag{3}$$

where ψ_1 and ψ_2 stand for the molecular contact energy fractions of liquid 1 and liquid 2 in a mixture; θ_2 is the molecular site fraction of liquid 2 in a mixture and other symbols have their usual significance^{12,13} (details are given in chapter II). The interaction contributions to V_m^E were obtained from Eq. (3) by using a computer program as mentioned in chapter II. The optimized $\chi_{1,2}$ values, calculated and experimental V_m^E values, their deviation and different contributions to V_m^E values for near equimolar ($x_1 \approx 0.5$) composition at 298.15 K are given in Table 6.5. It reveals that the calculated excess molar volumes ($V_{m,PPF}^E$) reasonably agree well with the experimental excess molar volumes (V_m^E) for all the mixtures studied.

ii) *Peng-Robinson Equation of State* (PREOS):

Cubic equations of state are extensively used in process simulations for the prediction of thermodynamic properties and phase equilibria of hydrocarbon systems due to their simplicity, robustness and computational efficiency. Herein this chapter the classical cubic Peng-Robinson equation of state (PREOS) has been used for predicting the excess molar volumes ($V_{m,PREOS}^E$) of the mixtures at 298.15 K. PREOS is given by:¹⁵

$$P = \frac{RT}{V-b} - \frac{a}{V(V+b) + b(V-b)} \tag{4}$$

For a pure component the energy a and co-volume b parameters can be obtained from the relations:

$$a = a(T) = a(T_c) \left[1 + \xi \left(1 - \sqrt{\frac{T}{T_c}} \right) \right]^2 \tag{5}$$

Chapter VI

Table 6.5. Interaction parameter ($\chi_{1,2}$), calculated and experimental values of excess molar volumes ($V_{m,\text{exp}}^E$ and $V_{m,\text{PFP}}^E$), their deviations (ΔV_m^E) and different PFP contributions at 298.15 K

1,4-DO (1) +	$\chi_{1,2}$ ($\text{J} \cdot \text{m}^{-3}$)	$V_{m,\text{exp}}^E \cdot 10^6$ ($\text{m}^3 \cdot \text{mol}^{-1}$)	$V_{m,\text{PFP}}^E \cdot 10^6$ ($\text{m}^3 \cdot \text{mol}^{-1}$)	$\Delta V_m^E \cdot 10^6$ ($\text{m}^3 \cdot \text{mol}^{-1}$)	PFP contribution $\times 10^3$		
					int ^a	fv ^b	ip ^c
EDA (2)	-20.606	0.334	0.323	0.011	-0.0026	0.0022	0.0105
DCE (2)	42.811	0.511	0.511	0.000	0.0079	0.0004	0.0004
MEA (2)	-14.039	-0.344	-0.344	0.000	-0.0018	0.0030	-0.0009

^a interaction contribution, ^b free volume contribution and ^c internal pressure contribution

$$b = b(T) = b(T_c) \quad (6)$$

$$a(T_c) = 0.45724 \frac{R^2 T_c^2}{P_c} \quad (7)$$

$$b(T_c) = 0.07780 \frac{RT_c}{P_c} \quad (8)$$

where T_c and P_c are critical temperature and pressure of a pure component. The parameter ξ in terms of acentric factor (ω)³⁸ is defined by:

$$\xi = 0.37464 + 1.54226\omega - 0.26992\omega^2 \quad (9)$$

T_c , P_c and ω values of the pure liquids used were taken from the literature.^{22,39} For a binary mixture the energy a and co-volume b parameter can be given by:³⁸

$$a(T) = \sum_{i=1}^2 \sum_{j=1}^2 x_i x_j \sqrt{a_i a_j} (1 - k_{ij}) \quad (10)$$

$$b(T) = \sum_{i=1}^2 x_i b_i \quad (11)$$

where k_{ij} is the interaction coefficient for a binary mixture of components i and j . Rearranging Eq. (4) in terms of the compressibility factor (Z), provides the following relations:

$$Z^3 - (1 - B)Z^2 + (A - 3B^2 - 2B)Z - (AB - B^2 - B^3) = 0 \quad (12)$$

where $Z = PV/RT$, $B = Pb/RT$ and $A = aP/(RT)^2$. Thus from a knowledge of the compressibility factors for the components and their mixtures, the corresponding excess molar volumes ($V_{m,\text{PREOS}}^E$) of the mixtures were calculated. The values of the interaction coefficients (k_{ij}) were found to be 0.0582, 0.0679 and 0.0206 with

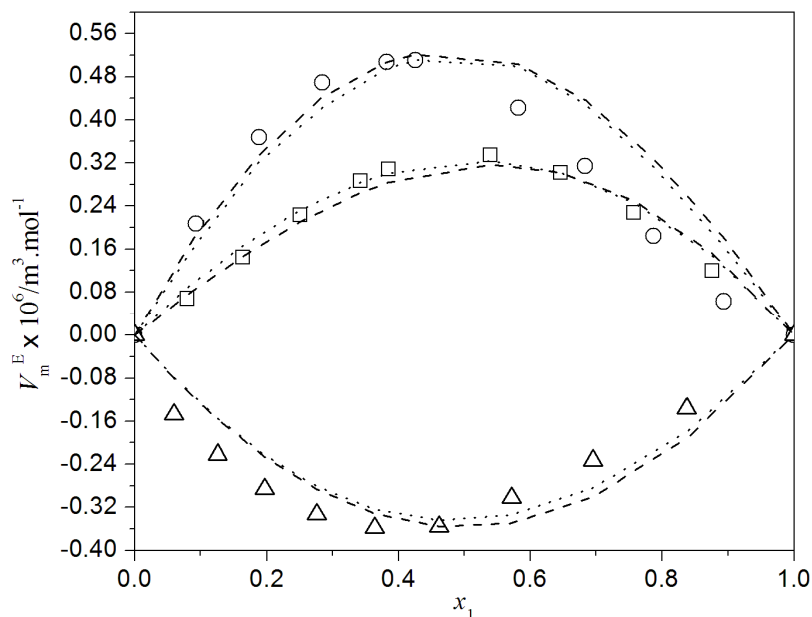


Fig. 6.3. A comparison between the excess molar volumes (V_m^E) against mole fraction of 1,4-DO (x_1) for the binary mixtures of 1,4-DO + 1,2-disubstituted ethanes at $T = 298.15$ K. Symbols represent experimental excess molar volumes (V_m^E): \square , EDA; \circ , DCE; Δ , MEA. Dashed lines and dotted lines represent excess molar volumes (V_m^E) obtained from PREOS and PFP theory, respectively.

standard deviations (σ) 0.019, 0.086 and 0.056, respectively for the mixtures (1,4-DO + EDA), (1,4-DO+ DCE) and (1,4-DO + MEA). A comparison between the experimental excess molar volumes (V_m^E) and the calculated excess molar volumes ($V_{m,PFP}^E$ and $V_{m,PREOS}^E$) from PFP theory and PREOS for the studied mixtures at 298.15 K has been depicted in Figure 6.3.

6.3.4. Viscosity deviations

The viscosity deviation ($\Delta\eta$) can be obtained from the difference between the measured viscosity (η) and the ideal viscosity (η_{id}) of a mixture as follows:^{16, 33}

$$\Delta\eta = \eta - \eta_{id} \quad (13)$$

and the ideal viscosity (η_{id}) is given by:⁴⁰

$$\eta_{id} = \exp\left(\sum_{i=1}^2 x_i \ln \eta_{id}\right) \quad (14)$$

Chapter VI

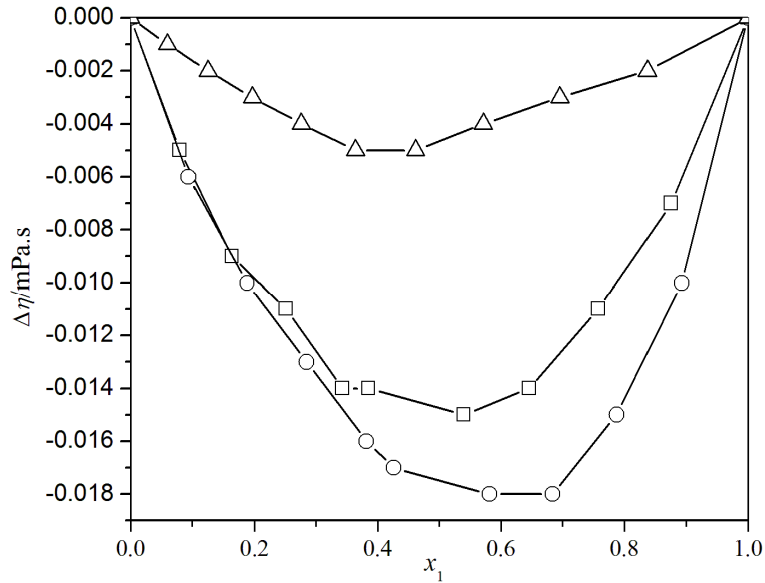


Fig. 6.4. Viscosity deviation ($\Delta\eta$) versus mole fraction of 1,4-DO (x_1) for the binary mixtures of 1,4-DO + 1,2-disubstituted ethanes at $T = 298.15$ K. Symbols: □, EDA; ○, DCE; Δ, MEA.

The estimated uncertainty for viscosity deviation ($\Delta\eta$) was evaluated to be ± 0.0002 mPa · s for the mixtures studied. Figure 6.4 ($\Delta\eta$ versus x_1 at 298.15 K) shows that the $\Delta\eta$ values are negative over the whole composition range for the mixtures at the experimental temperatures. It was observed if V_m^E values are positive, $\Delta\eta$ values become negative for many binary mixtures and *vice-versa*. Such a coincidence was found for the mixtures (1,4-DO + EDA) and (1,4-DO + DCE) but for the mixture (1,4-DO + MEA) both V_m^E and $\Delta\eta$ values are negative. However, for each mixture $\Delta\eta$ values decrease as the experiment temperature increases indicating that the interaction between the dissimilar molecules becomes weaker at higher temperatures (Table 6.2).

6.3.5. Thermodynamics of viscous flow

According to Eyring's viscosity relation,⁴⁰ the free energy of viscous flow (ΔG^*) is given by the relation:

$$\eta = (hN/V)\exp(\Delta G^*/RT) \quad (15)$$

where h is Planck's constant, N is Avogadro's number and other symbols have their usual meanings.

Chapter VI

Table 6.6. Free energy (ΔG^*), enthalpy (ΔH^*) and entropy (ΔS^*) of activation of viscous flow for the binary mixtures.

x_1	ΔG^* (kJ·mol ⁻¹)			ΔH^* (kJ·mol ⁻¹)	ΔS^* (J·K ⁻¹ ·mol ⁻¹)	R^2
	298.15 K	308.15 K	318.15 K			
1,4-DO (1) + EDA (2)						
0	13.309	13.419	13.488	10.634	-8.995	0.9988
0.0800	13.340	13.443	13.511	10.786	-8.586	0.9992
0.1636	13.374	13.471	13.539	10.910	-8.280	0.9994
0.2511	13.411	13.504	13.573	10.994	-8.119	0.9996
0.3428	13.448	13.532	13.608	11.054	-8.033	0.9999
0.3850	13.465	13.549	13.625	11.080	-8.003	0.9999
0.5399	13.526	13.610	13.706	10.842	-8.997	0.9998
0.6461	13.569	13.656	13.765	10.646	-9.793	0.9996
0.7578	13.614	13.703	13.830	10.391	-10.789	0.9989
0.8756	13.662	13.758	13.890	10.269	-11.361	0.9991
1	13.716	13.809	13.953	10.196	-11.779	0.9979
1,4-DO (1) + DCE (2)						
0	12.506	12.583	12.591	11.226	-4.330	0.9971
0.0934	12.606	12.675	12.683	11.459	-3.878	0.9978
0.1881	12.717	12.775	12.792	11.590	-3.800	0.9990
0.2843	12.828	12.883	12.912	11.573	-4.223	0.9996
0.3819	12.942	12.991	13.031	11.619	-4.442	0.9999
0.4258	12.994	13.040	13.085	11.638	-4.547	0.9999
0.5816	13.177	13.216	13.282	11.619	-5.211	0.9995
0.6838	13.301	13.336	13.416	11.585	-5.729	0.9987
0.7875	13.430	13.468	13.561	11.485	-6.496	0.9982
0.8929	13.567	13.619	13.734	11.096	-8.255	0.9974
1	13.716	13.809	13.953	10.196	-11.779	0.9979
1,4-DO (1) + MEA (2)						
0	19.734	19.235	18.783	33.915	47.589	0.9998
0.0597	19.378	18.912	18.499	32.487	43.997	0.9997
0.1251	18.990	18.561	18.188	30.954	40.156	0.9997
0.1969	18.563	18.175	17.846	29.274	35.954	0.9996
0.2760	18.091	15.750	17.472	27.329	31.017	0.9995
0.3639	17.566	17.277	17.045	25.351	26.142	0.9996
0.4618	16.979	16.749	16.572	23.047	20.379	0.9996
0.5716	16.318	16.153	16.041	20.458	13.913	0.9995
0.6958	15.567	15.476	15.437	17.504	6.525	0.9993
0.8373	14.708	14.704	14.752	14.056	-2.160	0.9989
1	13.716	13.809	13.953	10.196	-11.779	0.9979

Rearranging Eq. (15) and putting $\Delta G^* = \Delta H^* - T\Delta S^*$ yields the following relation:

$$R \ln(\eta V / hN) = \Delta H^* / T - \Delta S^* \quad (16)$$

Thus, linear regressions of $R \ln(\eta V / hN)$ against $(1/T)$ give the enthalpy (ΔH^*) and entropy (ΔS^*) of activation of viscous flow from the corresponding slope and

Chapter VI

negative intercept, respectively. ΔG^* , ΔH^* , ΔS^* and the regression coefficients (R^2) are given in Table 6.6. It shows that while ΔH^* values are positive, ΔS^* values are negative for all the binary mixtures except the mixture (1,4-DO + MEA). According to Corradini *et al.*,⁴¹ the enthalpy of activation of viscous flow is regarded as a measure of the degree of cooperation between the species taking part in viscous flow. In a highly structured liquid there will be considerable degree of order; hence for cooperative movement of the species a large heat of activation is required for the flow process. Thus the ΔH^* values indicate that the ease of formation of activated species necessary for viscous flow follows the order: (1,4-DO + DCE) \approx (1,4-DO + EDA) > (1,4-DO + MEA). This order is also supported by negative ΔS^* values for the mixtures (1,4-DO + DCE) and (1,4-DO + EDA) and positive values of ΔS^* for the mixture (1,4-DO + MEA).

6.3.6. Viscosity prediction

Several empirical models can simulate the viscosity of liquids or liquid mixtures and practical implications of such viscosity models were reviewed by Mehrotra *et al.*⁴² Empirical methods have also been developed using the corresponding state principle based on van der Waals' hypothesis⁴³ that the properties of substances in terms of reduced thermodynamic properties show similar behavior. For the mixtures studied viscosities were predicted using Peng-Robinson cubic equation of state¹⁵ and Bloomfield–Dewan model.¹⁹

i) Peng-Robinson Equation of State:

The excess activation free energy of viscous flow (ΔG^{*E}) for the binary mixtures can be obtained from the relation:

$$\Delta G^{*E} = \Delta G^* - \sum_{i=1}^2 (x_i \Delta G_i^*) \quad (17)$$

A simple rearrangement of Eq. (17) gives the viscosity for a mixture:⁴⁴

$$\eta = \frac{(\eta V)^{\text{id}}}{V_m} \exp\left(\frac{\Delta G^{*E}}{RT}\right) \quad (18)$$

where V_m and $(\eta V)^{\text{id}}$ are the molar volume and kinematic viscosity of an ideal mixture, respectively. $(\eta V)^{\text{id}}$ is defined as follows:

$$(\eta V)^{\text{id}} = \exp\left[\sum_{i=1}^2 x_i \ln(\eta_i V_i)\right] \quad (19)$$

Chapter VI

In order to incorporate the binary interaction parameter g_{12} ($g_{ii} = 0$ and $g_{ij} = g_{ji}$), ΔG^{*E} for a binary mixture is given as:

$$\frac{\Delta G^{*E}}{RT} = \frac{G^{*E}}{RT} + \frac{1}{2} \sum_{i=1}^2 \sum_{j=1}^2 x_i x_j g_{ij} = \frac{G^{*E}}{RT} + x_1 x_2 g_{12} \quad (20)$$

The interaction parameter g_{12} can be evaluated from a comparison of the experimental viscosities to those obtained from Eq. (18). The value of G^{*E} can also be obtained from the relation:

$$\frac{G^{*E}}{RT} = \sum_{i=1}^2 x_i (\ln \varphi_i - \ln \varphi_i^0) \quad (21)$$

where φ_i^0 and φ_i stand for the fugacity coefficients of the i^{th} component in pure state and in the mixture, respectively. As per PREOS, fugacity coefficient for a pure component is given by:

$$\ln \varphi = (Z-1) - \ln(Z-B) - \frac{A}{2\sqrt{2}B} \ln \left(\frac{Z+(1+\sqrt{2})B}{Z+(1-\sqrt{2})B} \right) \quad (22)$$

and fugacity coefficient for the i^{th} component in a binary mixture is given by:

$$\begin{aligned} \ln \varphi_i = & \frac{b_i}{b} (Z-1) - \ln(Z-B) \\ & - \frac{A}{2\sqrt{2}B} \left(\frac{2}{a} \sum_{j=1}^2 x_j (a_j a_j)^{\frac{1}{2}} (1-k_{ij}) - \frac{b_i}{b} \right) \ln \left(\frac{Z+(1+\sqrt{2})B}{Z+(1-\sqrt{2})B} \right) \end{aligned} \quad (23)$$

Combination of Eqs. (18-23) yields,

$$\eta = \frac{(\eta V)^{\text{id}}}{V_m} \exp \left[\sum_{i=1}^2 x_i (\ln \varphi_i - \ln \varphi_i^0) + \frac{1}{2} \sum_{i=1}^2 \sum_{j=1}^2 x_i x_j g_{ij} \right] \quad (24)$$

In order to obtain the binary interaction parameter (g_{12}), a non-linear regression analysis was performed iteratively by using a C-program to have minimum standard deviation (σ) for a binary mixture. The binary interaction parameters (g_{12}) were found to be -0.294 ($\sigma = 0.001$), -0.053 ($\sigma = 0.002$) and -0.116 ($\sigma = 0.001$) for the mixtures (1,4-DO + EDA), (1,4-DO + DCE) and (1,4-DO + MEA), respectively.

ii) Bloomfield-Dewan viscosity model:

It combines two major semi-empirical theories of liquid viscosities in order to estimate viscosity of the liquid mixtures. The first one is the absolute reaction rate theory⁴⁰ that relates the viscosity to the free energy required by a molecule to

Chapter VI

overcome the attractive force field of its neighbors in order to jump to a new equilibrium position, *i.e.*, to flow. The second one is the free volume theory⁴⁵ that relates the viscosity to the probability of occurrence of an empty neighboring site into which a molecule can jump and the probability depends exponentially on the free volume of the liquid. Thus the probability of viscous flow has been considered as a product of the probabilities of acquiring sufficient activation energy and the occurrence of an empty site. All the thermodynamic quantities involved in Bloomfield-Dewan model can be had from Flory's statistical thermodynamic theory for liquid mixtures.³⁴⁻³⁷ Bloomfield and Dewan¹⁴ developed the following expression:

$$\Delta \ln \eta = f(\tilde{v}) - \frac{\Delta G^R}{RT} \quad (25)$$

$$\text{where, } \Delta \ln \eta = \ln \eta - \sum_{i=1}^2 (x_i \eta_i) \quad (26)$$

$$\text{and } f(\tilde{v}) = \frac{1}{\tilde{v} - 1} - \sum_{i=1}^2 \frac{x_i}{\tilde{v}_i - 1} \quad (27)$$

ΔG^R is the residual free energy of mixing and can be had from the relation:

$$\Delta G^R = \Delta G^E + RT \sum_{i=1}^2 x_i \ln(x_i / \phi_i) \quad (28)$$

where ϕ_i is the segment fraction of the i^{th} component in a binary mixture and is defined in the literature.³⁴⁻³⁷ The excess free energy ΔG^E can be obtained from the Flory's statistical theory of liquid mixtures by using the relation:

$$\begin{aligned} \Delta G^E = & \sum_{i=1}^2 x_i P_i^* V_i^* [(1/\tilde{v}_i - 1/\tilde{v}) + 3\tilde{T}_i \ln\{(\tilde{v}_i^{1/3} - 1)/(\tilde{v}^{1/3} - 1)\}] \\ & + (x_1 \theta_2 V_1^* \chi_{12}) / \tilde{v} \end{aligned} \quad (29)$$

The standard deviations (σ) between the experimental viscosities and those calculated from Bloomfield and Dewan model were 0.03, 0.39 and 4.99 for the mixtures with EDA, DCE and MEA, respectively. A comparison between the experimental viscosities and the calculated viscosities from these two viscosity prediction models are depicted in Fig 6.5. It is evident that PREOS predicted the viscosities for the mixtures very well

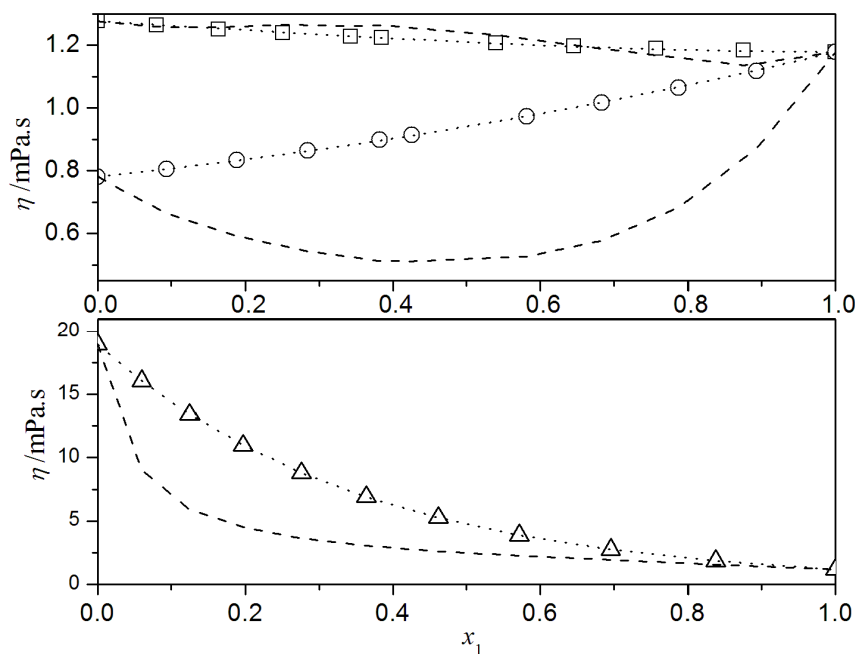


Fig. 6.5. A comparison between the viscosities (η) against mole fraction of 1,4-DO (x_1) for the binary mixtures of 1,4-DO + 1,2-disubstituted ethanes at $T = 298.15$ K. Symbols represent experimental viscosities: \square , EDA; \circ , DCE; Δ , MEA. Dashed lines and dotted lines represent viscosities (η) obtained from Bloom Field-Dewan theory and PREOS, respectively.

6.3.7. Ultrasonic speed of sound and derived functions

The speeds of sound (u) and the densities (ρ) of the binary mixtures at 298.15 K were used to determine their isentropic compressibilities (κ_S), excess isentropic compressibilities (κ_S^E) and the other acoustic parameters. The experimental speeds of sound of each pure liquid were in good agreement with the literature values^{16,27,46,47} at 298.15 K. The excess isentropic compressibilities (κ_S^E) were calculated by using the relation:

$$\kappa_S^E = \kappa_S - \kappa_S^{\text{id}} \quad (30)$$

where $\kappa_S = 1/\rho u^2$ and κ_S^{id} , the isentropic compressibility for an ideal mixture, is given by the relation:⁴⁸

$$\kappa_S^{\text{id}} = \sum_{i=1}^2 \tau_i \left[\kappa_{S,i} + \frac{TV_{m,i}^* \alpha_i^2}{c_{P,i}} \right] - \left\{ \frac{T \sum_{i=1}^2 (x_i V_{m,i}^*) (\sum_{i=1}^2 \tau_i \alpha_i)^2}{\sum_{i=1}^2 (x_i c_{P,i})} \right\} \quad (31)$$

Chapter VI

where τ_i is the volume fraction of the component 'i' in the mixture, $\kappa_{s,i}$, $V_{m,i}^*$, α_i and $c_{p,i}$ are the isentropic compressibility, the molar volume, the expansion coefficient and the molar isobaric heat capacity of the pure components, respectively. The expansion coefficients (α_i) were determined from experimental densities and the values of $c_{p,i}$ were taken from the literature.³⁰ The other acoustic parameters like intermolecular free length (L_f), specific acoustic impedance (z_{im}) and their excess/deviation functions were calculated by using the standard relations as described in chapter II. The parameters u , κ_s and κ_s^E at 298.15 K are listed in Table 6.7. Figure 6.6 illustrates the variation of excess isentropic compressibilities (κ_s^E) of the mixtures against mole fraction of 1,4-DO (x_1) at 298.15 K. It is evident that while the excess isentropic compressibilities (κ_s^E) for the mixtures (1,4-DO + EDA) and (1,4-DO + DCE) are positive, those for the mixture (1,4-DO + MEA) are negative over the entire composition range at 298.15 K. The positive κ_s^E values for the mixtures (1,4-DO + EDA) and (1,4-DO + DCE) are indicative of dispersion interaction between mixing component like breaking up of the weak dipole-dipole cohesive forces present among the DCE molecules and intermolecular hydrogen bonding present in EDA molecules upon mixing. For the mixture (1,4-DO + MEA), the negative κ_s^E values suggest the presence of specific interaction like intermolecular hydrogen bond between the components as well as mutual geometrical fitting of the dissimilar molecules on mixing. The magnitude of κ_s^E values follows the order: (1,4-DO + DCE) > (1,4-DO + EDA) > (1,4-DO + MEA), indicating that the molecular interaction is least for the mixture (1,4-DO + DCE) and highest for the mixture (1,4-DO + MEA). Thus these results stand in parallel to those obtained earlier from excess molar volumes and viscosity deviations. Intermolecular free length (L_f) and specific acoustic impedance (z_{im}) for the studied binaries at 298.15 K are listed in Table 6.8. According to King-Kincaid,⁴⁹ a regular rise in intermolecular free length causes a fall in speeds of sound for the mixtures and *vice-versa*. This is also in accordance with the expected increase in the isentropic compressibility and decrease in specific acoustic impedance.

Chapter VI

Table 6.7. Ultrasonic speeds (u), isentropic compressibility (κ_S) and excess isentropic compressibility (κ_S^E) for binary mixtures at 298.15 K

x_1	u (m · s ⁻¹)	$\kappa_S \cdot 10^{10}$ (Pa ⁻¹)	$\kappa_S^E \cdot 10^{10}$ (Pa ⁻¹)
1,4-DO (1) + EDA (2)			
0	1670.8	4.003	0
0.0800	1625.9	4.170	0.027
0.1636	1585.3	4.327	0.046
0.2511	1546.2	4.489	0.069
0.3428	1506.8	4.664	0.105
0.3850	1488.8	4.749	0.128
0.5399	1428.4	5.051	0.214
0.6461	1395.1	5.221	0.245
0.7578	1369.6	5.340	0.226
0.8756	1353.7	5.387	0.134
1	1343.4	5.391	0
1,4-DO (1) + DCE (2)			
0	1193.6	5.632	0
0.0934	1198.9	5.696	0.075
0.1881	1204.7	5.756	0.148
0.2843	1211.7	5.802	0.210
0.3819	1218.7	5.846	0.275
0.4258	1222.7	5.857	0.295
0.5816	1240.4	5.858	0.335
0.6838	1256.1	5.819	0.325
0.7875	1277.4	5.732	0.270
0.8929	1306.8	5.583	0.155
1	1343.4	5.391	0
1,4-DO (1) + MEA (2)			
0	1716.8	3.353	0
0.0597	1696.8	3.420	-0.172
0.1251	1677.7	3.490	-0.343
0.1969	1654.2	3.581	-0.491
0.2760	1626.7	3.696	-0.614
0.3639	1593.6	3.845	-0.698
0.4618	1557.5	4.019	-0.746
0.5716	1517.9	4.229	-0.744
0.6958	1471.8	4.495	-0.662
0.8373	1417.1	4.846	-0.456
1	1343.4	5.391	0

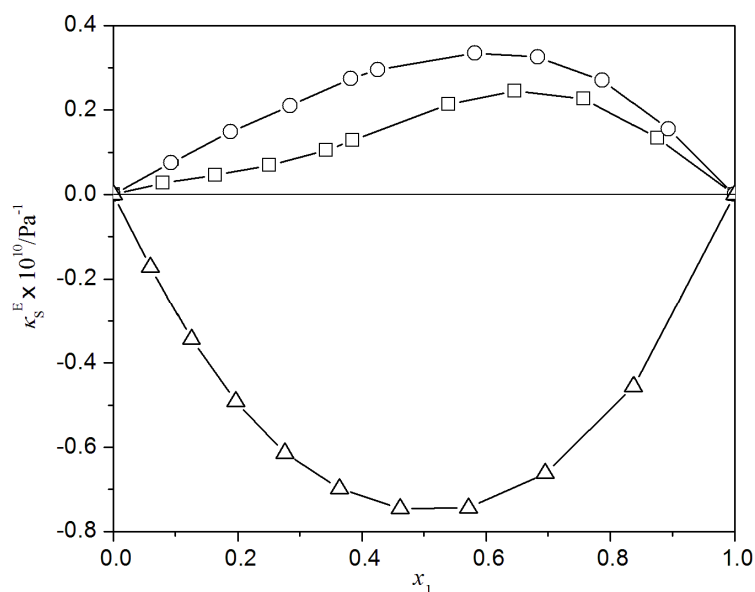


Fig. 6.6. Excess isentropic compressibility (κ_s^E) versus mole fraction of 1,4-DO (x_1) for the binary mixtures of 1,4-DO + 1,2-disubstituted ethanes at $T = 298.15$ K. Symbols: \square , EDA; \circ , DCE; \triangle , MEA.

Table 6.8 shows that while the specific acoustic impedances (z_{im}) decrease, the intermolecular free lengths (L_f) increase as the mole fraction (x_1) of 1,4-DO in the mixtures increase. The magnitude of the intermolecular free lengths (L_f) has the order: (1,4-DO + DCE) > (1,4-DO + EDA) > (1,4-DO + MEA); this indicates that the molecular interactions between dissimilar molecules is also decreasing in the same order. The excess intermolecular free lengths (L_f^E) and excess acoustic impedances (z_{im}^E) are plotted in Figure 6.7 against the mole fraction of 1,4-DO in the mixtures. The negative excess intermolecular free lengths (L_f^E) and positive excess acoustic impedances (z_{im}^E) for the mixture (1,4-DO + MEA) reflect the stronger interactions between the two components in contrast to the mixtures (1,4-DO + EDA) and (1,4-DO + DCE) for which z_{im}^E values are negative and L_f^E values are positive. The negative L_f^E and positive z_{im}^E values for the mixture (1,4-DO + MEA) are due to stronger hetero-association between MEA and 1,4-DO molecules and such hetero-association may be attributed to both hydrogen bonding and interstitial accommodation of MEA molecules within the voids of 1,4-DO structure.

Chapter VI

Table 6.8. Intermolecular free length (L_r), specific acoustic impedance (z_{im}), excess intermolecular free lengths (L_r^E) and excess acoustic impedances (z_{im}^E) for the studied binaries at 298.15 K

x_1	L_r (Å)	$z_{im} \cdot 10^{-6}$ ($\text{kg} \cdot \text{m}^{-2} \cdot \text{s}^{-1}$)	L_r^E (Å)	$z_{im}^E \cdot 10^{-6}$ ($\text{kg} \cdot \text{m}^{-2} \cdot \text{s}^{-1}$)
1,4-DO (1) + EDA (2)				
0	0.4115	1.4950	0	0
0.0800	0.4200	1.4750	0.0032	-0.0109
0.1636	0.4279	1.4577	0.0055	-0.0187
0.2511	0.4358	1.4407	0.0077	-0.0256
0.3428	0.4442	1.4228	0.0100	-0.0330
0.3850	0.4482	1.4142	0.0113	-0.0368
0.5399	0.4623	1.3860	0.0151	-0.0473
0.6461	0.4700	1.3729	0.0158	-0.0483
0.7578	0.4753	1.3674	0.0137	-0.0410
0.8756	0.4774	1.3713	0.0080	-0.0236
1	0.4776	1.3807	0	0
1,4-DO (1) + DCE (2)				
0	0.4881	1.4877	0	0
0.0934	0.4909	1.4643	0.0038	-0.0134
0.1881	0.4934	1.4422	0.0073	-0.0253
0.2843	0.4954	1.4225	0.0103	-0.0347
0.3819	0.4973	1.4037	0.0132	-0.0432
0.4258	0.4978	1.3964	0.0141	-0.0457
0.5816	0.4978	1.3763	0.0158	-0.0492
0.6838	0.4961	1.3682	0.0152	-0.0463
0.7875	0.4924	1.3657	0.0126	-0.0377
0.8929	0.4860	1.3707	0.0073	-0.0215
1	0.4776	1.3807	0	0
1,4-DO (1) + MEA (2)				
0	0.3766	1.7370	0	0
0.0597	0.3804	1.7232	-0.0023	0.0074
0.1251	0.3842	1.7080	-0.0050	0.0155
0.1969	0.3892	1.6879	-0.0073	0.0210

Chapter VI

0.2760	0.3954	1.6633	-0.0091	0.0246
0.3639	0.4033	1.6322	-0.0101	0.0248
0.4618	0.4124	1.5974	-0.0109	0.0249
0.5716	0.4230	1.5580	-0.0114	0.0246
0.6958	0.4361	1.5117	-0.0108	0.0225
0.8373	0.4528	1.4562	-0.0084	0.0175
1	0.4776	1.3807	0	0

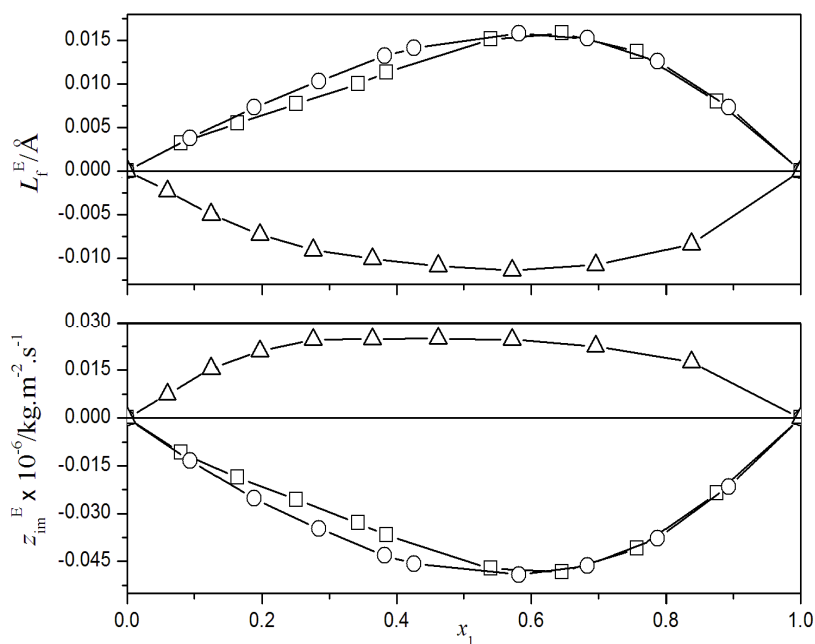


Fig. 6.7. Excess intermolecular free length (L_f^E) and excess acoustic impedances (z_{im}^E) versus mole fraction of 1,4-DO (x_1) for the binary mixtures of 1,4-DO + 1,2-disubstituted ethanes at $T = 298.15$ K. Symbols: \square , EDA; \circ , DCE; Δ , MEA.

6.3.8. Molar refractions

The molar refractions (R_m) for the binary mixtures were calculated from the relation:

$$R_m = \frac{n_D^2 - 1}{n_D^2 + 2} \frac{\sum_{i=1}^2 x_i M_i}{\rho} \quad (33)$$

where ρ is the density of the mixture and x_i , M_i are the mole fraction and molar mass of the i^{th} component in the mixture, respectively.

Chapter VI

Table 6.9. Refractive indices (n_D), molar refractions (R_m) and excess molar refractions (R_m^E) for the binary mixtures at 298.15 K

x_1	n_D	$R_m \times 10^6$ ($\text{m}^3 \cdot \text{mol}^{-1}$)	$R_m^E \times 10^6$ ($\text{m}^3 \cdot \text{mol}^{-1}$)
1,4-DO (1) + EDA (2)			
0	1.4541	18.189	0
0.0800	1.4510	18.501	0.030
0.1636	1.4479	18.826	0.062
0.2511	1.4448	19.166	0.095
0.3428	1.4415	19.510	0.116
0.3850	1.4400	19.665	0.122
0.5399	1.4346	20.211	0.124
0.6461	1.4311	20.572	0.112
0.7578	1.4275	20.935	0.083
0.8756	1.4239	21.312	0.045
1	1.4202	21.703	0
1,4-DO (1) + DCE (2)			
0	1.4419	21.006	0
0.0934	1.4417	21.209	0.137
0.1881	1.4384	21.271	0.133
0.2843	1.4355	21.333	0.129
0.3819	1.4328	21.388	0.116
0.4258	1.4316	21.409	0.106
0.5816	1.4281	21.488	0.076
0.6838	1.4260	21.534	0.051
0.7875	1.4239	21.575	0.020
0.8929	1.4222	21.638	0.009
1	1.4202	21.703	0
1,4-DO (1) + MEA (2)			
0	1.4521	16.289	0
0.0597	1.4501	16.594	-0.018
0.1251	1.4480	16.951	-0.015
0.1969	1.4454	17.333	-0.022
0.2760	1.4425	17.754	-0.029
0.3639	1.4394	18.226	-0.033
0.4618	1.4360	18.753	-0.036
0.5716	1.4324	19.355	-0.029
0.6958	1.4285	20.031	-0.025
0.8373	1.4245	20.809	-0.031
1	1.4202	21.704	0

The excess molar refractions (R_m^E) were obtained from relation,

$$R_m^E = R_m - \sum_{i=1}^2 x_i R_{m,i} \quad (34)$$

where $R_{m,i}$ is the molar refraction of the i^{th} component in the mixture. Excess molar refractions (R_m^E) along with the experimental the refractive indices (n_D) for the three

Chapter VI

binaries are listed in Table 6.9. The experimental refractive indices (n_D) were in good agreement with literature values^{23,50-52} at 298.15 K. The variation of excess refractive indices (R_m^E) with the mole fraction of 1,4-DO (x_1) at 298.15 K also reveals the same order of molecular interactions for the studied mixtures as discussed earlier.

6.3.9. IR spectroscopic study

The results obtained so far are also well reflected in FT-IR spectra of the binary mixtures (Figures 6.8-6.10). The spectra were recorded in a demountable KBr cell for liquid samples with spacer of path length of 0.5 mm at ambient temperature with a Perkin-Elmer Spectrum FT-IR spectrometer (RX-1). Pure 1,4-DO shows characteristic bands at the range 1600-800 cm^{-1} due to vibrations of the ring (around 1122 cm^{-1}), the wagging vibrations (800-1050 cm^{-1}) and fan-like vibrations (1250-1300 cm^{-1}) for CH_2 groups and scissor vibrations (1453 cm^{-1}).⁵³ DCE has characteristic peaks around 1232 cm^{-1} for *trans* conformer and two peaks around 1313 and 1285 cm^{-1} for *gauche* conformer.⁸ These bands shift slightly in peak position and intensity for the mixtures (1,4-DO + DCE) as the mole fraction (x_1) of 1,4-DO increases in the mixtures and thus stand for weak interactions between the components. Of note for the mixture (1,4-DO + EDA) is that the N-H and N- CH_2 stretching bands (around 3296 and 2855 cm^{-1} , respectively) of EDA become less intense and broad as the mole fraction of 1,4-DO (x_1) in the mixture increases. This indicates formation of inter-molecular hydrogen bonds between dissimilar molecules in the mixture (1,4-DO + EDA). Similarly for the mixture (1,4-DO + MEA) the bands due to -OH and NH_2 groups (falling within the range 3335-2850 cm^{-1}) become broader and their intensity decreases significantly as the mole fraction (x_1) of 1,4-DO decreases in the mixture suggesting that the mixtures are characterized by intra-molecular and inter-molecular hydrogen bonds.

6.4. Conclusion

The physico-chemical study revealed that degree of molecular interactions in the binary mixtures follows the order: (1,4-DO + MEA) > (1,4-DO + EDA) > (1,4-DO + DCE). This order of molecular interactions originates from the disruption of weak dipole-dipole interaction/cohesion forces or intra-molecular hydrogen bonds amongst the similar molecules on mixing with 1,4-DO, because mixing of 1,4-DO results in

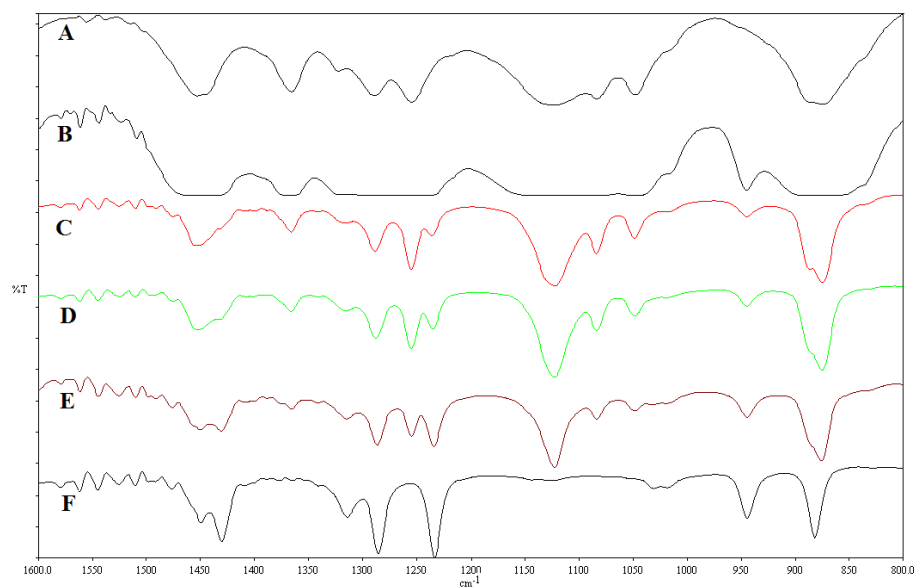


Fig. 6.8. FTIR spectra of the various binary mixtures of (1,4-DO + DCE): A, pure 1,4-DO ($x_{\text{DCE}} = 0.0000$); B, $x_{\text{DCE}} = 0.1820$; C, $x_{\text{DCE}} = 0.3725$; D, $x_{\text{DCE}} = 0.5718$; E, $x_{\text{DCE}} = 0.7807$; F, Pure DCE ($x_{\text{DCE}} = 1.0000$).

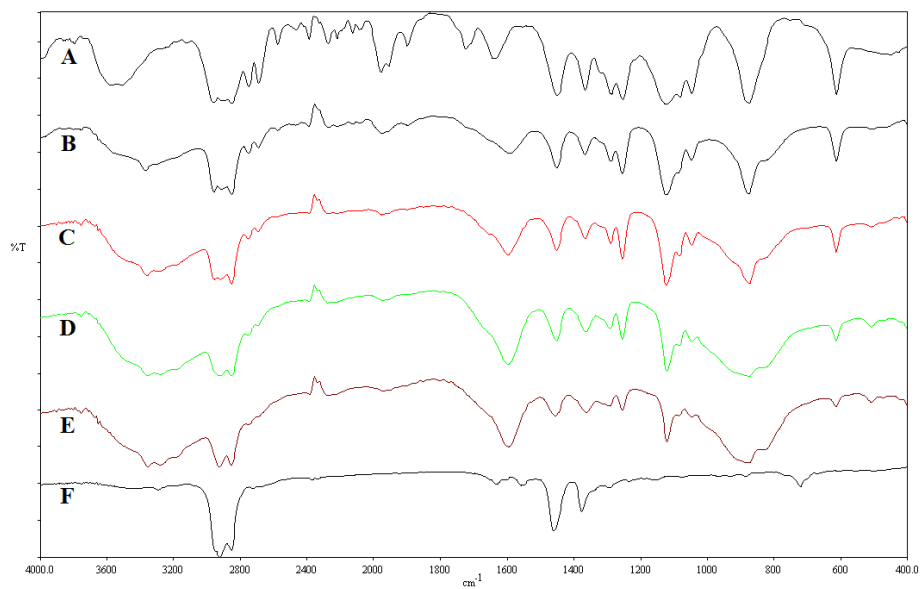


Fig. 6.9. FTIR spectra of the various binary mixtures of (1,4-DO + EDA): A, pure 1,4-DO ($x_{\text{EDA}} = 0.0000$); B, $x_{\text{EDA}} = 0.2682$; C, $x_{\text{EDA}} = 0.4943$; D, $x_{\text{EDA}} = 0.6874$; E, $x_{\text{EDA}} = 0.8543$; F, Pure EDA ($x_{\text{EDA}} = 1.0000$).

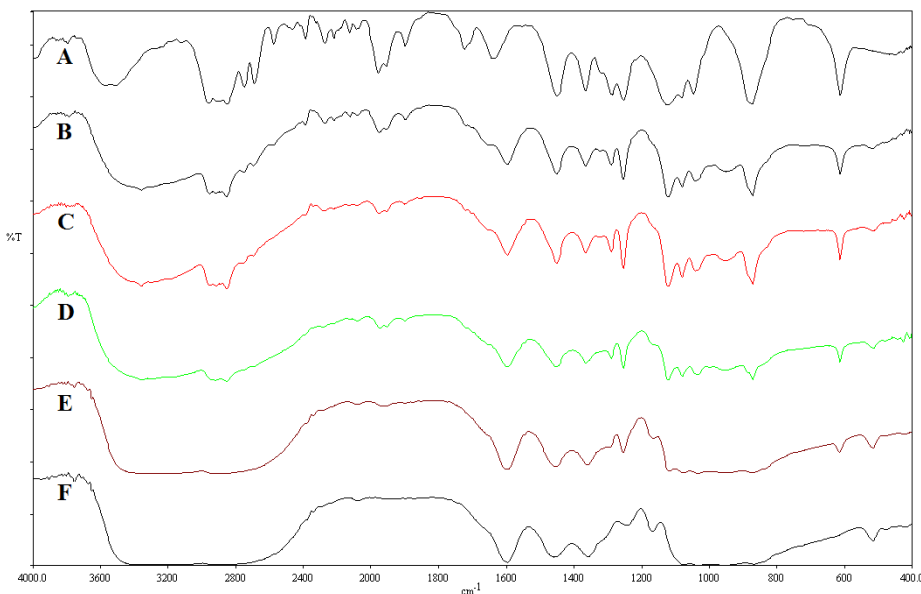


Fig. 6.10. FTIR spectra of the various binary mixtures of (1,4-DO + MEA): A, pure 1,4-DO ($x_{\text{MEA}} = 0.0000$); B, $x_{\text{MEA}} = 0.2651$; C, $x_{\text{MEA}} = 0.4902$; D, $x_{\text{MEA}} = 0.6839$; E, $x_{\text{MEA}} = 0.8523$; F, Pure MEA ($x_{\text{MEA}} = 1.0000$).

the formation of hetero-associates due to inter-molecular hydrogen bond formation and mutual interstitial fitting. Interestingly, a comparison of the partial molar volume ($\bar{V}_{m,1}^0$ and $\bar{V}_{m,2}^0$) at infinite dilution to the molar volume of the respective pure liquid for the studied mixtures revealed that except the mixture (1,4-DO + MEA) other two mixtures are characterized by volume increase. Anyway, FTIR spectra of the mixtures showed characterized band shifts in position and intensity as per the above order of molecular interactions.

References

- [1] C.R. Reid, B.E. Poling, *The properties of Gases and Liquids*, McGraw Hill, New York, 1998, Ch. 1.
- [2] J. George, N.V. Sastry, *J. Chem. Eng. Data* 49 (2004) 1116.
- [3] A.R. Mahajan, S.R. Mirgane, *Chem. Eng. Comm.*, 200 (2013) 1666.
- [4] L. Venkatramana, R.L. Gardas, K.S. Kumar, *Fluid. Phase. Equilib.*, 367 (2014) 7.
- [5] Y. Mahan, C.N. Liew, A.E. Mather, *J. Solution Chem.*, 31 (2002) 743.
- [6] G. Nath, *Chem. Sci. Trans.*, 1 (2012) 516.
- [7] K.B. Wiberg, T.A. Keith, M.J. Frisch, M. Murcko, *J. Phys. Chem.*, 99 (1995) 9072.
- [8] R.K. Sreeruttun, R. Ramasami, *Phys. Chem. Liq.*, 44 (2006) 315.

Chapter VI

- [9] J. Nath, G. Singh, *J. Chem. Eng. Data* 33 (1988) 58.
- [10] P. Brocos, E. Calvo, A. Pineiro, R. Bravo, *J. Chem. Eng. Data* 44 (1999) 1341.
- [11] V.D. Spassjevic, B.D. Bjordjevic, S.P. Serbanovic, I.R. Radovic, M.Lj. Kijevcanin, *J. Chem. Eng. Data* 59 (2014) 1817.
- [12] D. Patterson, G. Delmas, *J. Polym. Sci.*, 30 (1970) 1.
- [13] D. Patterson, *Pure. Appl. Chem.*, 47 (1976) 305.
- [14] V.A. Bloomfield, R.K. Dewan, *J. Phys. Chem.*, 75 (1971) 3113.
- [15] D.Y. Peng, D.B. Robinson, *Ind. Eng. Chem. Fundum.*, 15 (1976) 59.
- [16] B. Sinha, R. Pradhan, S. Saha, D. Brahman, *J. Serb. Chem. Soc.*, 78 (2013) 1443.
- [17] A. Villares, S. Martin, M. Haro, B. Giner, *J. Chem. Thermodyn.*, 36 (2004) 1027.
- [18] M. Das, M.N. Roy, *J. Chem. Eng. Data* 51 (2006) 2225.
- [19] S. Akhtar, A.N.Q. Faruk, M.A. Saleh, *Phys. Chem. Liq.*, 39 (2001) 383.
- [20] L. Sarkar, M.N. Roy, *J. Chem. Eng. Data* 54 (2009) 3307.
- [21] K.P. Rao, K.S. Reddy, *J. Chem. Eng. Data* 33 (1988) 130.
- [22] C. Li, J. Zhang, T. Zhang, X. Wei, E. Zhang, N. Yang, N. Zhao, M. Su, H. Zhou, *J. Chem. Eng. Data* 55 (2010) 4104.
- [23] J.K. Gladden, *J. Chem. Eng. Data* 17 (1972) 468.
- [24] M.A. Saleh, M.S. Ahmed, M.S. Islam, *Phys. Chem. Liq.*, 40 (2002) 477.
- [25] S. Ranjbar, K. Fakhri, B. Jahan, J. Ghasemi, *J. Chem. Eng. Data* 54 (2009) 3284.
- [26] R.K. Biswas, R.A. Banu, M.N. Islam, *Hydrometallurgy*, 69 (2003) 157.
- [27] S.E. Burke, B. Hawryla, R. Palepu, *Thermochim. Acta* 345 (2002) 101.
- [28] U.R. Kapadi, D.G. Hundiwale, N.B. Patil, M.K. Lande, *Fluid Phase Equilib.*, 201 (2002) 335.
- [29] K.M. Marstokk, H. Mollendal, *J. Mol. Struc.*, 49 (1978) 221.
- [30] W.M. Haynes, D.R. Lide, T.J. Bruno, *CRC Handbook of Chemistry & Physics*, 93rd edn., Taylor & Francis, Boca Roton, London, 2012-2013.
- [31] G.M. Smith, H.C. Van Ness, *Introduction to Chemical Engineering Thermodynamics*, McGraw Hill, New York, 1987.
- [32] O. Redlich, A.T. Kister, *Indus. Eng. Chem.*, 40 (1948) 345.
- [33] B.K. Sarkar, A. Choudhury, B. Sinha, *J. Solution Chem.*, 41 (2012) 53.
- [34] P.J. Flory, R.A. Orwell, A. Vrijji, *J. Am. Chem. Soc.*, 86 (1964) 3507.
- [35] P.J. Flory, R.A. Orwell, A. Vrijji, *J. Am. Chem. Soc.*, 86 (1964) 3515.
- [36] P.J. Flory, *J. Am. Chem. Soc.*, 87 (1965) 1833.
- [37] A. Abe, P.J. Flory, *J. Am. Chem. Soc.*, 87 (1965) 1838.

Chapter VI

- [38] S.I. Sandler, Chemical, *Biochemical, and Engineering Thermodynamics*, 4th edn, John Wiley & Sons (Asia), New Delhi, 2006, pp. 242, 258.
- [39] J.J. McKetta, W.A. Cunningham, *Encyclopedia of Chemical Processing and Design*, Vol-36, Marcel Dekker, New York, 1991, pp. 99.
- [40] S. Glasstone, K.J. Laidler, H. Eyring, *The theory of Rate Process*. McGraw-Hill Book Company, New York, 1941.
- [41] F. Corradini, L. Marcheselli, A. Marchetti, M. Tagliazucchi, L. Tassi, G. Tosi, *Bull. Chem. Soc. Jpn.*, 65 (1992) 503.
- [42] A.K. Mehrotra, W.D. Monnery, W. Svrcek, *Fluid. Phase. Equilib.*, 117 (1996) 344.
- [43] R.D. McCarty, *Fluid. Phase. Equilib.*, 256 (2007) 42.
- [44] M.A. Hernandez-Galvan, F. Garcia-Sanchez, R. Macias-Salinas, *Fluid. Phase. Equilib.* 262 (2007) 51.
- [45] M.H. Cohen, D. Turnbull, *J. Chem. Phys.*, 31 (1959) 1164.
- [46] G.P. Dubey, K. Kumar, *J. Chem. Eng. Data* 56 (2011) 2995.
- [47] S.C. Bhatia, R. Bhatia, G.P. Dubey, *Int. J. Thermophys.*, 31 (2010) 2119.
- [48] W.E. Acree, *J. Chem. Eng. Data* 28 (1983) 215.
- [49] H. Eyring, J.F. Kincaid, *J. Chem. Phys.*, 6 (1938) 620.
- [50] T.J. Aminabhavi, V.B. Patil, *J. Chem. Eng. Data* 43 (1998) 497.
- [51] K.M. Kadish, J.E. Anderson, *Pure. Appl. Chem.*, 59 (1987) 703.
- [52] M. Yasmin, M. Gupta, *J Solution Chem.*, 40 (2011) 1458.
- [53] A.P. Kilimov, M.A. Svechnikova, V.I. Shevchenko, V.V. Smirnov, S.B. Zotov, F.V. Kvasnyuk-Mudryi, *Khimiya Geterotsiklicheskikh Soedinenii*, 5 (1969) 208.

CHAPTER VII

Thermophysical properties of the binary mixtures of cyclohexane with some esters*

7.1. Introduction

Instead of a single pure solvent, solvent mixtures containing two or more solvents often provide a wide range of mixtures with varied compositions, which are optimizable for specific chemical engineering purposes like chemical separation, heat transfer, mass transfer and fluid flow, *etc.* This necessitates a prior knowledge of the physico-chemical properties of such liquid mixtures at hand and so systematic studies on thermodynamic and transport properties of binary liquid mixtures such as density, viscosity and speed of sound, *etc.*, were being used as tools for understanding intermolecular interactions and the structural properties of the liquid-liquid mixtures.¹ This is because local structure and macroscopic properties of liquids/liquid mixtures are determined by the interactions operative within the molecules involved.² Excess molar volumes (V_m^E), viscosities deviations ($\Delta\eta$), excess isentropic compressibility (κ_s^E), *etc.*, are frequently being used to understand the intermolecular forces in liquid-liquid mixtures and thus help in the elucidation of their behavior with a purpose of developing theoretical models for their description and simulation processes.^{3,4}

Cyclohexane (CH) is a non-polar, unassociated, inert hydrocarbon with globular structure.⁵ It is used as a raw material for the industrial production of two important intermediates (*viz.*, adipic acid and caprolactam) used in the production of nylon. Esters exist as a dipolar associates in their pure state.⁶ Both the aliphatic esters methyl acetate (MA) and ethyl acetate (EA) are commonly used solvents in glues, nail polish remover, *etc.* Ethyl acetate (EA) is used to decaffeinate coffee beans and tea leaves. Methyl salicylate (MS) is a phenolic ester having strong intramolecular hydrogen bond between its hydroxyl and carbonyl group⁷ and is used for relieving muscle aches and pains when applied externally to the affected area. Previously Rathnam *et al.*⁸ studied the binary mixture of CH with EA in terms of viscosity parameters at 313.15 K and Roy *et al.*⁹ studied the binary and ternary mixtures of CH with MA and EA at 298.15 K. However, there is lack of comprehensive data on the binary mixtures studied in this chapter and studies on the molecular interactions

*Published in: *J. Serb. Chem. Soc.* 82 (2017) 189-202.

Chapter VII

between these liquids in terms of various excess or deviation properties are insufficient in the literature. Furthermore, a quantitative estimation of different contributions (*i.e.*, interaction contribution, free volume contribution and internal pressure contribution) based on PFP theory^{10, 11} to the excess molar volumes (V_m^E) of the selected binary mixtures is rare in the literature. Hence herein the present chapter the binary mixtures of cyclohexane (CH) with methyl acetate (MA), ethyl acetate (EA) and methyl salicylate (MS) were studied at 298.15, 308.15 and 318.15 K under ambient pressure with a view to unravel the nature of molecular interactions in these mixtures in terms of various excess or deviation properties derived from the experimental (ρ , η , u and n_D) data. Also a comparison between the experimental and calculated V_m^E and η values (based on PFP^{10,11} or Bloomfield-Dewan viscosity model¹² and PREOS¹³) were made for the studied binary systems. Moreover, solution viscosities, ultrasonic speeds of sound and refractive indices for all the binary mixtures were theoretically predicted using several empirical and semi-empirical relations/models.

7.2. Experimental section

7.2.1. Materials

All the chemicals used in this work were purchased from Sigma-Aldrich, Germany (Reagent Plus, purity > 99%) and were used as received from the vendor. Purity of the solvents was ascertained by GLC and also by comparing their densities and viscosities at the experimental temperatures with the available literature data,¹⁴⁻²⁵ as shown in Table 7.1.

7.2.2. Apparatus and procedure

The binary mixtures were prepared by mass in specially designed air-tight bottles with stopper inside a dry box at 298.15 K. Actually for each binary system a set of nine binary mixtures were prepared afresh before use with mole fractions varying from 0.1 to 0.9. The uncertainty in mole fraction was evaluated to be ± 0.0002 . The densities (ρ) were measured with a vibrating-tube density meter (Anton Paar, DMA 4500M) calibrated at the experimental temperatures with doubly distilled, degassed water and dry air under atmospheric pressure.

Chapter VII

Table 7.1. Densities (ρ) and viscosities (η) of the pure liquids at $T = (298.15-318.15)$ K

Pure Liquid	T (K)	$\rho \cdot 10^{-3}$ ($\text{kg} \cdot \text{m}^{-3}$)		η ($\text{mPa} \cdot \text{s}$)	
		Expt.	Lit.	Expt.	Lit.
CH	298.15	0.77384	0.7737 ¹⁴	0.8927	0.8859 ¹⁴
			0.77392 ¹⁵		0.892 ¹⁶
			0.7739 ¹⁶		
			0.7740 ¹⁷		
MA	308.15	0.76433	0.76443 ¹⁵	0.7748	0.774 ¹⁷
	318.15	0.75473	0.75471 ¹⁵	0.6620	
	298.15	0.92681	0.9268 ¹⁸	0.3809	0.384 ¹⁸
EA	308.15	0.91524	0.9261 ¹⁹	0.3491	0.3798 ¹⁹
	318.15	0.90225	0.9152 ^{20,21}	0.3132	0.349 ²⁰
	298.15	0.89455	0.9022 ²¹	0.4262	0.313 ²¹
MS	308.15	0.88267	0.8948 ²⁰	0.3874	0.430 ²⁰
			0.8945 ²¹		0.429 ²¹
			0.89444 ²²		0.427 ²²
			0.8827 ²⁰		0.387 ²⁰
MS	318.15	0.86994	0.8821 ²¹	0.3564	0.384 ²¹
	298.15	1.17931	0.8826 ²³	1.5358	0.353 ²¹
			0.8692 ²¹		0.356 ²²
308.15	1.16931	0.86997 ²²	1.4024		
MS	318.15	1.15942	0.8696 ²³	1.3027	
			1.179336 ²⁴		
			1.1782 ²⁵		1.535 ²⁵
			1.169367 ²⁴		
			1.159405 ²⁴		

The stated repeatability and accuracy of the densities were $\pm 1 \times 10^{-5} \text{ g} \cdot \text{cm}^{-3}$ and $\pm 5 \times 10^{-5} \text{ g} \cdot \text{cm}^{-3}$, respectively. Viscosities (η) were measured by means of a suspended Canon-type Ubbelohde viscometer, placed vertically in a glass sided thermostat at a desired experimental temperature for the attainment of thermal equilibrium. The flow times of the liquids or liquid mixtures were measured with a digital stopwatch correct ± 0.01 s. Ultrasonic speeds of sound (u) were measured a single crystal variable-path ultrasonic interferometer (Mittal Enterprise, New Delhi, F-05) working at 2 MHz. It was calibrated with triply distilled, degassed water and methanol maintained at $T = (298.15 \pm 0.01)$ K by circulating thermostated water around the jacketed cell (2 MHz) filled with the experimental liquids. The uncertainty of the ultrasonic speeds was around $\pm 0.2 \text{ m s}^{-1}$. Refractive indices were measured with an Abbe's refractometer, calibrated with triply distilled, degassed water and purified methanol maintained at $T = (298.15 \pm 0.01)$ K. The estimated uncertainty in the

Chapter VII

refractive indices was ± 0.0002 units. In all determinations, an average of triplicate measurements was taken into consideration and adequate precautions were taken to minimize evaporation losses during the measurements. The details of the calibration and measurement techniques have been described in chapter III.

7.3. Results and discussion

The experimental densities (ρ), viscosities (η), excess molar volumes (V_m^E) and viscosity deviations ($\Delta\eta$) of the binary mixtures at the experimental temperatures are listed in Table 7.2.

7.3.1. Excess molar volumes

Excess molar volume is a thermodynamic function sensitive to change of structure (*i.e.*, order) or randomness during the mixing process. Excess molar volumes (V_m^E) can be had from the equation:

$$V_m^E = \sum_{i=1}^2 x_i M_i (1/\rho - 1/\rho_i) \quad (1)$$

where ρ is the density of the mixture and x_i , M_i and ρ_i are the mole fraction, molar mass and density of i^{th} component in the mixture, respectively. The estimated uncertainty for excess molar volumes (V_m^E) was evaluated to be $\pm 0.005 \text{ cm}^3 \cdot \text{mol}^{-1}$. Figure 7.1 (V_m^E versus x_1 at 298.15 K) illustrate that the excess molar volumes (V_m^E) for the (CH + MS) mixture show a slight sigmoid variation with positive V_m^E values at lower mole fractions of CH ($x_1 \leq 0.2294$) but with negative V_m^E values at CH rich regions ($x_1 \geq 0.2294$); however, V_m^E values for the mixtures (CH + MA) and (CH + EA) are positive over the entire composition range at all the experimental temperatures. The excess molar volumes (V_m^E) may be discussed in terms of several effects: physical, chemical and geometrical contributions. The physical interactions result in volume expansion and involve mainly the dispersion forces and non-specific interactions in the mixtures and thus contribute to positive V_m^E values. The chemical or specific interactions result in volume contraction and involve hydrogen bond formation, charge transfer type forces and other complex forming interactions between dissimilar species in the mixtures and thus contribute to negative V_m^E values.

Chapter VII

Table 7.2. Density (ρ), viscosity (η), excess molar volume (V_m^E) and viscosity deviation ($\Delta\eta$) for the binary mixtures studied at $T = (298.15 \text{ to } 318.15) \text{ K}$

x_1	$\rho \cdot 10^{-3}$ ($\text{kg} \cdot \text{m}^{-3}$)	η ($\text{mPa} \cdot \text{s}$)	$V_m^E \cdot 10^6$ ($\text{m}^3 \cdot \text{mol}^{-1}$)	$\Delta\eta$ ($\text{mPa} \cdot \text{s}$)
CH (1) + MA (2)				
$T = 298.15 \text{ K}$				
0	0.92681	0.3810	0	0
0.0754	0.90732	0.3938	0.380	-0.012
0.1551	0.88781	0.4094	0.800	-0.025
0.2393	0.86932	0.4285	1.160	-0.039
0.3286	0.85192	0.4517	1.440	-0.052
0.3700	0.84477	0.4641	1.510	-0.058
0.5241	0.82097	0.5242	1.630	-0.071
0.6314	0.80660	0.5808	1.600	-0.071
0.7460	0.79358	0.6568	1.389	-0.062
0.8686	0.78244	0.7579	0.900	-0.040
1	0.77384	0.8927	0	0
$T = 308.15 \text{ K}$				
0	0.91524	0.3491	0	0
0.0754	0.89370	0.3520	0.601	-0.019
0.1551	0.87433	0.3605	1.051	-0.034
0.2393	0.85607	0.3714	1.430	-0.051
0.3286	0.83895	0.3876	1.722	-0.066
0.3700	0.83151	0.3965	1.841	-0.072
0.5241	0.80796	0.4395	1.997	-0.091
0.6314	0.79386	0.4817	1.974	-0.096
0.7460	0.78118	0.5432	1.756	-0.090
0.8686	0.77086	0.6352	1.182	-0.062
1	0.76433	0.7748	0	0
$T = 318.15 \text{ K}$				
0	0.90225	0.3132	0	0
0.0754	0.87878	0.3057	0.840	-0.026
0.1551	0.85971	0.3094	1.320	-0.042
0.2393	0.84136	0.3155	1.771	-0.059
0.3286	0.82490	0.3228	2.050	-0.078
0.3700	0.81769	0.3297	2.171	-0.083
0.5241	0.79500	0.3556	2.310	-0.108
0.6314	0.78152	0.3889	2.260	-0.113
0.7460	0.76950	0.4386	2.000	-0.109
0.8686	0.75971	0.5201	1.390	-0.080
1	0.75473	0.6620	0	0
CH (1) + EA (2)				
$T = 298.15 \text{ K}$				
0	0.89455	0.4262	0	0
0.0914	0.88047	0.4475	0.227	-0.008
0.1845	0.86626	0.4640	0.480	-0.024
0.2795	0.85214	0.4872	0.737	-0.037
0.3764	0.83873	0.5162	0.919	-0.047
0.4200	0.83290	0.5284	0.987	-0.053
0.5759	0.81413	0.5909	1.025	-0.061

Chapter VII

0.6787	0.80289	0.6462	0.941	-0.058
0.7836	0.79243	0.7107	0.746	-0.050
0.8907	0.78304	0.7925	0.395	-0.031
1	0.77384	0.8927	0	0
<hr/>				
<i>T</i> = 308.15 K				
0	0.88267	0.3874	0	0
0.0914	0.86805	0.3981	0.325	-0.015
0.1845	0.85376	0.4108	0.627	-0.029
0.2795	0.83972	0.4277	0.914	-0.042
0.3764	0.82515	0.4456	1.283	-0.057
0.4200	0.82079	0.4560	1.182	-0.062
0.5759	0.80223	0.5029	1.248	-0.075
0.6787	0.79137	0.5436	1.145	-0.076
0.7836	0.78153	0.6009	0.896	-0.066
0.8907	0.77239	0.6752	0.534	-0.043
1	0.76433	0.7748	0	0
<hr/>				
<i>T</i> = 318.15 K				
0	0.86994	0.3564	0	0
0.0914	0.85474	0.3592	0.443	-0.018
0.1845	0.84042	0.3635	0.802	-0.036
0.2795	0.82682	0.3725	1.086	-0.051
0.3764	0.81389	0.3834	1.297	-0.066
0.4200	0.80830	0.3882	1.374	-0.074
0.5759	0.79017	0.4202	1.455	-0.089
0.6787	0.77936	0.4487	1.389	-0.094
0.7836	0.76955	0.4913	1.175	-0.088
0.8907	0.76152	0.5586	0.690	-0.060
1	0.75473	0.6620	0	0
<hr/>				
CH (1) + MS (2)				
<hr/>				
<i>T</i> = 298.15 K				
0	1.17931	1.5358	0	0
0.1168	1.13610	1.4367	0.281	-0.005
0.2294	1.09741	1.3549	0.060	-0.001
0.3379	1.06052	1.2856	-0.370	0.007
0.4425	1.02285	1.2236	-0.719	0.016
0.4878	1.00603	1.1969	-0.873	0.018
0.6411	0.94605	1.1096	-1.281	0.025
0.7353	0.90552	1.0554	-1.309	0.025
0.8265	0.86273	1.0015	-1.052	0.021
0.9146	0.81950	0.9473	-0.707	0.012
1	0.77384	0.8927	0	0
<hr/>				
<i>T</i> = 308.15 K				
0	1.16931	1.4024	0	0
0.1168	1.12552	1.3008	0.342	-0.008
0.2294	1.08606	1.2194	0.200	-0.004
0.3379	1.04900	1.1489	-0.221	0.001
0.4425	1.01121	1.0892	-0.559	0.011
0.4878	0.99471	1.0639	-0.752	0.014
0.6411	0.93462	0.9777	-1.141	0.019
0.7353	0.89413	0.9256	-1.159	0.019
0.8265	0.85231	0.8744	-1.002	0.016
0.9146	0.80851	0.8249	-0.547	0.010
1	0.76433	0.7748	0	0

Chapter VII

$T = 318.15 \text{ K}$				
0	1.15942	1.3027	0	0
0.1168	1.11418	1.1942	0.502	-0.009
0.2294	1.07371	1.1084	0.469	-0.007
0.3379	1.03673	1.0344	0.028	-0.002
0.4425	0.99954	0.9721	-0.388	0.007
0.4878	0.98303	0.9471	-0.583	0.011
0.6411	0.92305	0.8612	-0.982	0.017
0.7353	0.88228	0.8087	-0.948	0.017
0.8265	0.84081	0.7571	-0.812	0.013
0.9146	0.79715	0.7086	-0.337	0.007
1	0.75473	0.6620	0	0

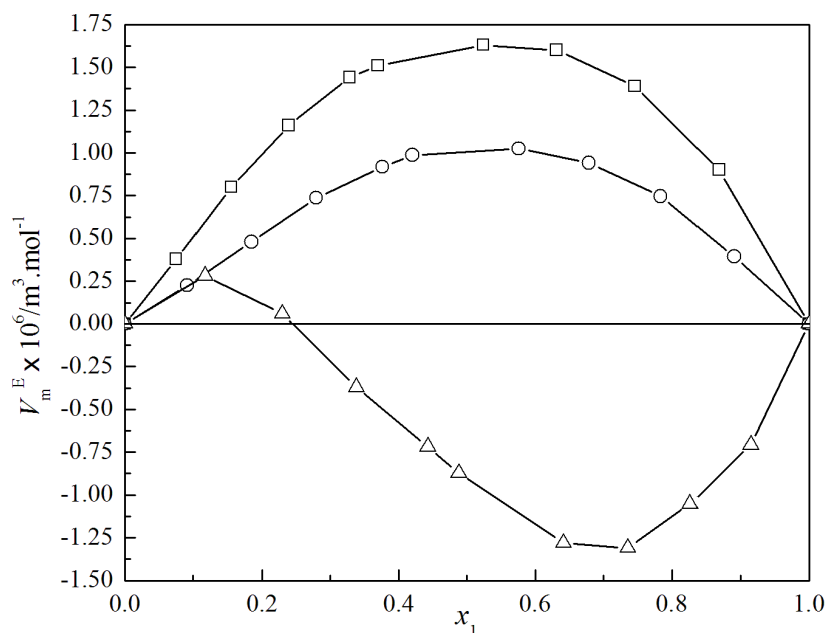


Fig. 7.1. Excess molar volume (V_m^E) versus mole fraction of CH (x_1) for the binary mixtures of CH + some esters at $T = 298.15 \text{ K}$. Symbols: \square , MA; \circ , EA; Δ , MS.

Structural/geometrical contributions arising from the variation of molecular packing due to interstitial accommodation of one component into other owing to difference in free volume and molar volume of the components also contributes to negative V_m^E values. Esters can exist as dipolar associates and an approximate estimate about the nature and the strength of molecular interactions between similar ester molecules can be had from the knowledge of their dipole moments (μ_D). Dipole moment of different components²⁶ used has the order: $\mu_{D, CH}(0.00) < \mu_{D, MA}(1.72) < \mu_{D, EA}(1.78) < \mu_{D, MS}(2.47)$ in Debye. Hence a comparison of the μ_D values reveals

Chapter VII

that the intermolecular interactions should be least in the mixture (CH + MA) and highest for the mixture (CH + MS). Thus the expected order of molecular interactions (based on dipole-induced dipole interactions) between the unlike components of the binary mixtures is: (CH + MS) > (CH + EA) > (CH + MA). If the interactions between dissimilar molecules are less than those between similar molecules the excess molar volume (V_m^E) will be positive. Therefore, the observed positive V_m^E values for the mixtures (CH + MA) and (CH + EA) over the entire composition range indicated breaking up of liquid order on mixing and dispersion interactions between dissimilar components in these mixtures led to volume expansion. Dispersion interaction may arise from breaking of dipole-dipole cohesive forces present between similar molecules (ester-ester) on addition of CH to the esters studied. Similarly if the interactions between dissimilar molecules are more than those between similar molecules (ester-ester) the excess molar volume (V_m^E) will be negative. This was observed for the mixture (CH + MS). The comparison of V_m^E versus x_1 at 298.15 K reveals that the intermolecular interactions amongst the unlike components is highest for the mixture (CH + MS) and lowest for the mixture (CH + MA). Thus the order of molecular interactions based on excess molar volumes (V_m^E) is: (CH + MA) < (CH + EA) < (CH + MS). This order of molecular interactions for the binary mixtures is probably due to combined effects of factors like the molecular size, shape and nature of the components, *etc.* CH is a ring structured globular molecule and can exist either in chair form or twisted boat form or in skew-boat form.²⁷ Spectroscopic study by Garcia *et al.*²⁸ showed that the stable conformer of CH is the chair form with D_{3d} symmetry and CH rotates freely between these two conformations at high temperature (even greater than room temperature)²⁹ and occupies a small space with its flexible ring structure.³⁰ MS molecules are almost planer in shape due to favorable intra-molecular hydrogen bonding rather than inter-molecular hydrogen bonding, because inter-molecular hydrogen bonding requires the –OH group to be out of the plane and interaction between neighboring MS molecules originate predominantly from dipolar interactions; the intra-molecular hydrogen bonding in liquid MS persists even at higher temperatures.⁷ The order of molar volumes: MS > EA > MA indicates that the inter-molecular spacing or vacancies in EA is larger than that in MA. Alkyl esters exist as dipolar associates and are hydrogen bond acceptors. The addition of CH

Chapter VII

(component 1) breaks the inter-molecular association (dipole-dipole interaction in the case of MA and EA) in the structure of the pure component (2) making enough space available for mutual fitting. Therefore, the molecular packing in the mixture (CH + EA) is more compact than that of the mixture (CH + MA); that is why the excess molar volumes (V_m^E) of the mixture (CH + MA) are greater than those of the mixture (CH + EA). In case of the mixture (CH + MS) the initial positive V_m^E values can be attributed to the breaking up of the three dimensional hydrogen bonded (inter-molecular and intra-molecular) network or dipolar interactions in liquid MS due to the addition of CH and beyond the mole fraction (x_1) of CH ≥ 0.2294 as the amount of CH increases further in this mixture, the CH molecules are interstitially accommodated or geometrically fitted in the free space between the voids of planar MS molecules ($V_{m,MS} - V_{m,CH} = 20.21 \text{ cm}^3 \cdot \text{mol}^{-1}$ at 298.15 K). This effect increases the intermolecular compactness, thereby imparting negative contributions to solution volume and compressibility of the mixture (CH + MS). Thus, the order of molecular interactions, based on the V_m^E values, is: (CH + MS) > (CH + EA) > (CH + MA). Nevertheless, it was observed that the V_m^E values increased with increasing experimental temperature for all the mixtures over the entire composition range. Such a trend in temperature dependence of V_m^E values suggests that temperature enhancement disrupts the developing specific and non-specific interactions between the component molecules in the mixtures due to thermal agitations at elevated temperatures.

7.3.2. Excess partial molar volumes

Partial molar volumes ($\bar{V}_{m,i}$) of the i^{th} component in the binaries at 298.15 K were obtained from the relation:^{31, 32}

$$\bar{V}_{m,i} = V_{m,i}^E + V_{m,i}^* + (1 - x_i)(dV_{m,i}^E/dx_i)_{T,P} \quad (2)$$

where $V_{m,i}^*$ is the molar volume of the i^{th} component in the binaries. The derivatives, $(\partial V_{m,i}^E/\partial x_i)_{T,P}$ used in Eq. (2) were obtained using a procedure as mentioned in chapter II, the V_m^E values were fitted to the Redlich–Kister polynomial³³ by the method of least squares regression using the Marquardt algorithm³⁴ to derive the

Chapter VII

following Redlich–Kister coefficients (a_i): $a_0 = 6.5322$, $a_1 = 0.6065$, $a_2 = 2.0832$, $a_3 = 1.2945$, $a_4 = -2.5250$ for the mixture (CH + MA); $a_0 = 4.1742$, $a_1 = 0.8079$, $a_2 = -1.0677$ for the mixture (CH + EA) and $a_0 = -3.7627$, $a_1 = -6.3862$, $a_2 = 1.4985$, $a_3 = -1.3304$ for the mixture (CH + MS) with standard deviations (σ) 0.006, 0.011 and 0.029 for the three binaries, respectively. Partial molar volumes ($\bar{V}_{m,1}^0$ and $\bar{V}_{m,2}^0$) at infinite dilution, excess partial molar volumes ($\bar{V}_{m,i}^E$) and excess partial molar volumes ($\bar{V}_{m,i}^{0,E}$) at infinite dilution were obtained from the standard relations as described earlier.^{31,32} Partial molar volumes ($\bar{V}_{m,1}^{0,E}$ and $\bar{V}_{m,2}^{0,E}$) and excess partial molar volumes ($\bar{V}_{m,i}^E$) at infinite dilution for each component in the binary mixtures are listed in Table 7.3. The excess partial molar volumes ($\bar{V}_{m,1}^E$ and $\bar{V}_{m,2}^E$) of each component in the binary mixtures are depicted in Figure 7.2 against the mole fraction of CH (x_1). Figure 7.2 shows that the $\bar{V}_{m,1}^E$ values gradually decreased (*i.e.*, a decreasing trend as the alkyl chain length increased⁹) but the $\bar{V}_{m,2}^E$ values increased with increasing mole fraction of CH (x_1) for the studied mixtures. The partial molar volume ($\bar{V}_{m,1}^0$ and $\bar{V}_{m,2}^0$) at infinite dilution of each liquid was found to be greater than the molar volume of the respective pure liquid for the studied mixtures, except the mixture (CH + MS). Again the excess partial molar volumes ($\bar{V}_{m,1}^{0,E}$ and $\bar{V}_{m,2}^{0,E}$) at infinite dilution were positive for both components in the mixtures (CH + MA) and (CH + EA) but for the mixture (CH + MS), $\bar{V}_{m,2}^{0,E}$ was found to be negative. This suggests that while the mixtures (CH + MA) and (CH + EA) are characterized by volume expansion, the mixture (CH + MS) is characterized by volume contraction on mutual mixing with CH, *i.e.*, the mixture (CH + MS) is characterized by a better packing efficiency,³⁵ most probably due to combined effects of dipole-induced dipole interactions and interstitial accommodation.

7.3.3. Predictions of excess molar volumes

i) Prigogine-Flory-Patterson theory (PFP):

Prigogine-Flory-Patterson (PFP) theory^{10, 11} is a modified version of Flory's statistical theory.³⁶⁻³⁹ It has been successfully applied to predict, estimate and analyze the excess thermodynamic functions of liquid mixtures with non-polar as well as polar

Chapter VII

Table 7.3. Molar volumes ($V_{m,1}^*$ and $V_{m,2}^*$), partial molar volumes at infinite dilution ($\bar{V}_{m,1}^0$ and $\bar{V}_{m,2}^0$) and excess partial molar volumes at infinite dilution ($\bar{V}_{m,1}^{0,E}$ and $\bar{V}_{m,2}^{0,E}$) for each component in the binary mixtures at 298.15 K

Volume parameters	CH (1) +		
	MA (2)	EA (2)	MS (2)
$V_{m,1}^*$	108.81	108.81	108.81
$\bar{V}_{m,1}^0$	113.71	111.01	114.65
$V_{m,2}^*$	79.93	98.50	129.02
$\bar{V}_{m,2}^0$	89.30	102.32	118.62
$\bar{V}_{m,1}^{0,E}$	4.91	2.20	5.84
$\bar{V}_{m,2}^{0,E}$	9.36	3.82	-10.39

Volume parameters are given in $\text{cm}^3 \cdot \text{mol}^{-1}$.

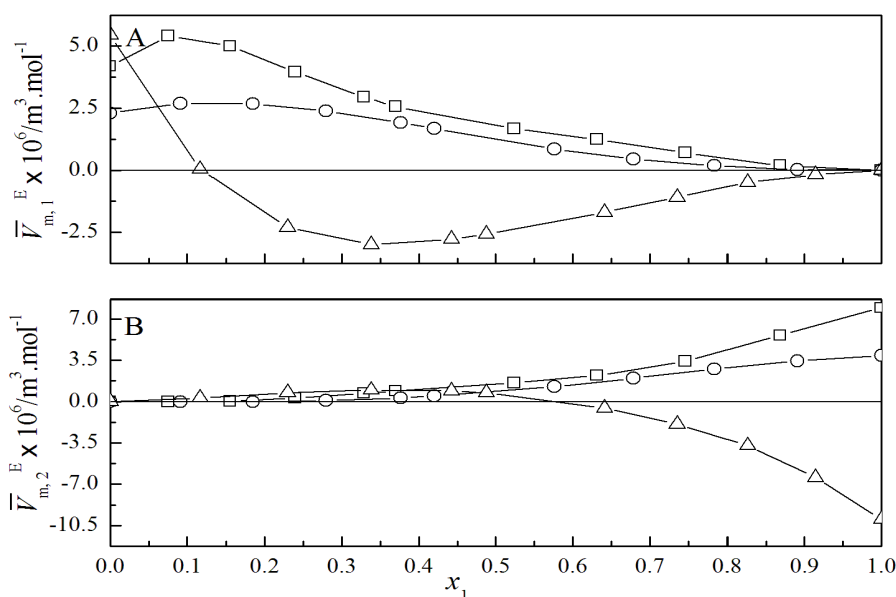


Fig. 7.2. Excess partial molar volume ($\bar{V}_{m,i}^E$) against mole fraction of CH (x_1) for the binary mixtures of CH + some esters at $T = 298.15 \text{ K}$: A, for CH; B, for the esters. Symbols: \square , MA; \circ , EA; Δ , MS.

liquids. This theory considers the excess molar volumes (V_m^E) of binary mixtures to be a sum of three contributions: (i) the interaction contribution (V_{int}^E) that is proportional to the interaction parameter, $\chi_{1,2}$; (ii) the free volume contribution (V_{fv}^E) that arises from the dependence of the reduced volume upon the reduced temperature; and (iii)

Chapter VII

the internal pressure contribution (V_p^E) that depends both on the differences of the characteristic pressures and on the differences of reduced volumes of the components.

The relations for V_m^E in terms the three contributions is as follows:

$$\begin{aligned} \frac{V_m^E}{x_1V_1^* + x_2V_2^*} = & \frac{(\tilde{v}^{1/3} - 1)\tilde{v}^{2/3}\psi_1\theta_2}{[(4/3)\tilde{v}^{-1/3} - 1]P_1^*} \chi_{1,2} \\ & (\chi_{1,2} \text{ contribution}) \\ & - \frac{(\tilde{v}_1 - \tilde{v}_2)^2[(14/9)\tilde{v}^{-1/3} - 1]\psi_1\psi_2}{[(4/3)\tilde{v}^{-1/3} - 1]\tilde{v}} \\ & (\tilde{v} \text{ contribution}) \\ & + \frac{(\tilde{v}_1 - \tilde{v}_2)(P_1^* - P_2^*)\psi_1\psi_2}{(P_1^*\psi_2 + P_2^*\psi_1)} \quad (3) \\ & (P^* \text{ contribution}) \end{aligned}$$

where ψ_1 and ψ_2 stand for the molecular contact energy fractions of liquid 1 and liquid 2 in a mixture; θ_2 is the molecular site fraction of liquid 2 in a mixture and other symbols have their usual significance.^{10,11} The various characteristic and reduced parameters of the pure liquid components (needed for the V_m^E estimation) were calculated using Flory's formalism.³⁶⁻³⁹ and are listed in Table 7.4. The interaction contributions to V_m^E were obtained from Eq. (3) by using a computer program as detailed elsewhere.³² The optimized $\chi_{1,2}$ values, calculated and experimental V_m^E values, their deviation (ΔV_m^E) and different contributions to V_m^E values near equimolar ($x_1 \approx 0.5$) composition at 298.15 K are given in Table 7.5. Table 7.5 revealed that the excess molar volumes ($V_{m,\text{PFP}}^E$) calculated from PFP theory reasonably agree with the experimental excess molar volumes (V_m^E) for all the binary mixtures studied.

ii) *Peng-Robinson Equation of State* (PREOS):

Cubic equations of state are powerful tools for predicting the thermodynamic properties and phase equilibria of hydrocarbon systems. These equations are widely applied in industrial process design for their relatively simple mathematical structure and computational efficiency in the calculation of the volume and other thermodynamic parameters like fugacity coefficient, *etc.*

Chapter VII

Table 7.4. Isobaric molar heat capacities (c_p), expansion coefficient (α), isothermal compressibility (κ_T) and Flory's parameters for pure liquids at 298.15 K

Liquids	c_p^a	\tilde{v}	\tilde{T}	$V^* \cdot 10^6$ ($\text{m}^3 \cdot \text{mol}^{-1}$)	P^* (Pa)	T^* (K)	α (kK^{-1})	κ_T (TPa^{-1})
CH	155.01	1.2939	0.0636	84.09	539.84	4686.95	1.2348	1141.8
MA	141.93	1.3107	0.0658	60.98	609.89	4530.98	1.3250	1112.8
EA	170.66	1.3199	0.0670	74.62	605.88	4452.90	1.3756	1179.3
MS	249.06	1.2147	0.0517	106.22	692.34	5769.79	0.8433	535.8

^a Unit: $\text{J} \cdot \text{mol}^{-1} \cdot \text{K}^{-1}$ and values adapted from Ref [26] were multiplied with molecular weight for unit conversion.

Table 7.5. Interaction parameter ($\chi_{1,2}$), calculated and experimental values of excess molar volumes ($V_{m,\text{exp}}^E$ and $V_{m,\text{PFP}}^E$), their deviations (ΔV_m^E) and different PFP contributions at 298.15 K

CH +	(1)	$\chi_{1,2}$ ($\text{J} \cdot \text{m}^{-3}$)	$V_{m,\text{exp}}^E \cdot 10^6$ ($\text{m}^3 \cdot \text{mol}^{-1}$)	$V_{m,\text{PFP}}^E \cdot 10^6$ ($\text{m}^3 \cdot \text{mol}^{-1}$)	$\Delta V_m^E \cdot 10^6$ ($\text{m}^3 \cdot \text{mol}^{-1}$)	PFP contribution $\times 10^3$		
						int ^a	fv ^b	ip ^c
MA	(2)	76.254	1.630	1.630	0.000	0.0219	0.0001	0.0005
EA	(2)	46.868	1.025	0.991	0.034	0.0123	0.0002	0.0007
MS	(2)	-13.482	-0.870	-0.870	0.000	-0.0022	0.0022	-0.0047

^a interaction contribution, ^b free volume contribution and ^c internal pressure contribution

These equations can correctly predict the solution properties and can also be conveniently extended to mixtures using varied mixing or combination rules. Herein this chapter the classical cubic Peng-Robinson equation of state (PREOS) has been used for predicting the excess molar volumes ($V_{m,\text{PREOS}}^E$) of the mixture studied at 298.15 K. The two parameter PREOS is given by:¹³

$$P = \frac{RT}{V-b} - \frac{a}{V(V+b)+b(V-b)} \quad (4)$$

For a pure component the energy a and co-volume b parameters can be obtained from the relations:

$$a = a(T) = a(T_c) \left[1 + \xi \left(1 - \sqrt{\frac{T}{T_c}} \right) \right]^2 \quad (5)$$

$$b = b(T) = b(T_c) \quad (6)$$

Chapter VII

$$a(T_c) = 0.45724 \frac{R^2 T_c^2}{P_c} \quad (7)$$

$$b(T_c) = 0.07780 \frac{RT_c}{P_c} \quad (8)$$

where T_c and P_c are critical temperature and pressure of a pure component. The parameter ξ in terms of acentric factor (ω) is defined by:

$$\xi = 0.37464 + 1.54226\omega - 0.26992\omega^2 \quad (9)$$

Acentric factor (ω) for each pure liquid was calculated from the relation:⁴⁰

$$\omega = \frac{3T_{br}}{7(1-T_{br})} \log P_c - 1 \quad (10)$$

where $T_{br} = T_b/T_c$ and T_b is the boiling point of a pure liquid. T_b , T_c and P_c values were taken from the literature.²⁶ For a binary mixture the energy a and co-volume b parameters are given by:⁴⁰

$$a(T) = \sum_{i=1}^2 \sum_{j=1}^2 x_i x_j \sqrt{a_i a_j} (1 - k_{ij}) \quad (11)$$

$$b(T) = \sum_{i=1}^2 x_i b_i \quad (12)$$

where k_{ij} is an empirically determined binary interaction coefficient characterizing the binaries formed by component i and component j and $k_{ij} = 0$ for $i = j$. The different parameters related to Eq. (4) can be conveniently expressed in terms of compressibility factor ($Z = PV/RT$) as follows:

$$Z^3 - (1 - B)Z^2 + (A - 3B^2 - 2B)Z - (AB - B^2 - B^3) = 0 \quad (13)$$

where $B = Pb/RT$ and $A = aP/(RT)^2$. Thus from a knowledge of the compressibility factors (Z) of the pure components and their mixtures, the corresponding excess molar volumes ($V_{m,PREOS}^E$) of the studied binary mixtures were calculated. The values of the interaction coefficient (k_{ij}) were found to be 0.1358, 0.0882 and 0.0524 with standard deviations (σ) 0.137, 0.067 and 0.484, respectively for the mixtures (CH + MA), (CH + EA) and (CH + MS).

Chapter VII

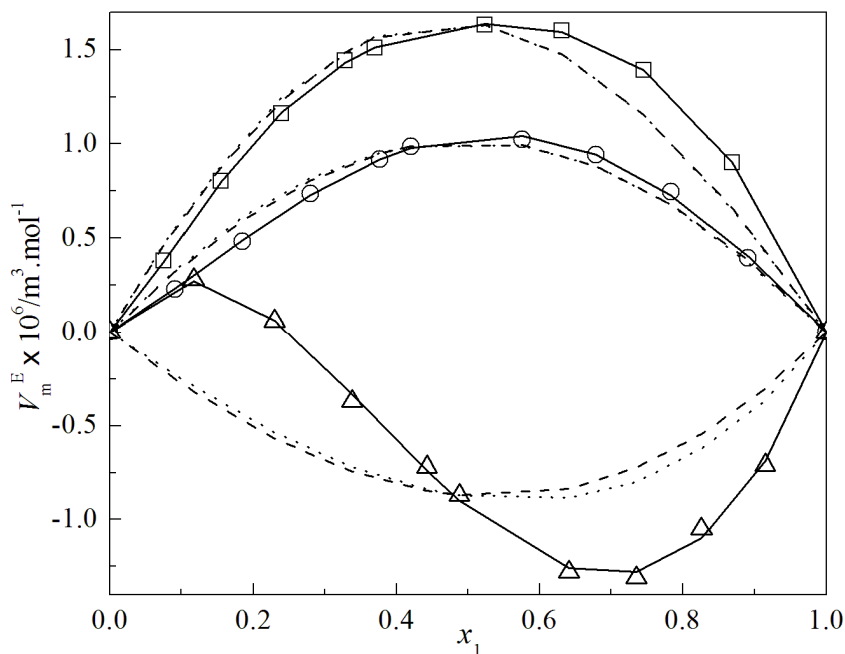


Fig. 7.3. A comparison between the excess molar volumes (V_m^E) against mole fraction of CH (x_1) for the binary mixtures of CH with some esters at $T = 298.15$ K. Symbols represent experimental excess molar volumes (V_m^E): \square , MA; \circ , EA; Δ , MS. Solid lines, dashed lines and dotted lines represent excess molar volumes (V_m^E) obtained from Redlich-Kister polynomial, PREOS and PFP theory, respectively.

A comparison between the experimental excess molar volumes (V_m^E) and the calculated excess molar volumes ($V_{m,PFP}^E$ and $V_{m,PREOS}^E$) as a function of mole fraction of CH (x_1) for the studied mixtures at 298.15 K is depicted in Figure 7.3.

7.3.4. Viscosity deviation

The viscosity deviation ($\Delta\eta$) can be obtained from the difference between the measured viscosity (η) and the ideal viscosity (η_{id}) of a solution as follows:^{41,42}

$$\Delta\eta = \eta - \eta_{id} \quad (14)$$

and the ideal viscosity (η_{id}) is given by:⁴³

$$\eta_{id} = \exp\left(\sum_{i=1}^2 x_i \ln \eta_{id}\right) \quad (15)$$

The estimated uncertainty for viscosity deviation ($\Delta\eta$) was evaluated to be ± 0.004 mPa \cdot s for the mixtures studied.

Chapter VII

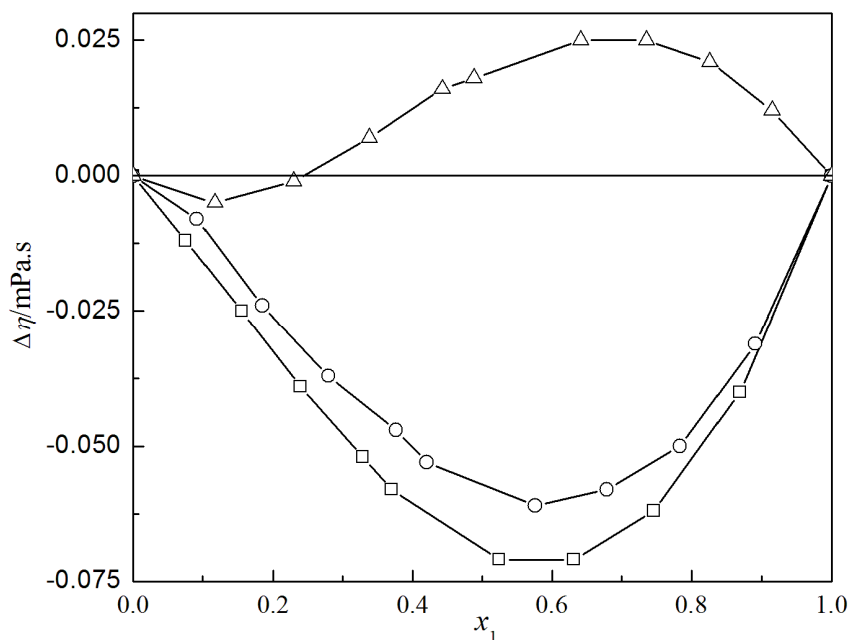


Fig. 7.4. Viscosity deviation ($\Delta\eta$) versus mole fraction of CH (x_1) for the binary mixtures of CH + some esters at $T = 298.15$ K. Symbols: \square , MA; \circ , EA; Δ , MS.

Figure 7.4 ($\Delta\eta$ versus x_1 at 298.15 K) shows that the $\Delta\eta$ values are negative for the mixtures (CH + MA) and (CH + EA), but for the mixture (CH + MS) $\Delta\eta$ values are positive (initially negative at MS rich regions with $x_1 \leq 0.2294$) over the whole composition range. Similar trends in the $\Delta\eta$ values were observed at the other experimental temperatures. Negative $\Delta\eta$ values suggest the easier flow of liquid mixture as compared with the pure liquids. This may be due to difference in size and shape of the mixing components, dispersion due to breaking of liquid order on mixing with a second component and the presence of unfavorable non-specific interactions amongst the unlike molecules. However, positive $\Delta\eta$ values suggest the presence of specific intermolecular interaction amongst the unlike molecules, resulting into more compact structure. Thus, the $\Delta\eta$ values for the studied mixtures suggest that the same order of molecular interactions: (CH + MS) > (CH + EA) > (CH + MA), as discussed earlier based on the V_m^E values. Moreover, the decrease in $\Delta\eta$ values as the experimental temperature increases for each mixture suggests that the interactions between the unlike molecule become weaker at higher temperatures (Table 7.2).

Chapter VII

7.3.5. Thermodynamics of viscous flow

Based on the theory of absolute reaction rate the free energy of activation of viscous flow (ΔG^*) and its excess function (ΔG^{*E}) for the liquid mixtures were obtained by using the Eyring's viscosity relation:⁴³

$$\eta = (hN/V)\exp(\Delta G^*/RT) \quad (16)$$

$$\Delta G^{*E} = \Delta G^* - \sum_{i=1}^2 \Delta G_i^{*E} \quad (17)$$

where N , h and ΔG^* are Avogadro's number, Planck's constant and free energy of activation of viscous flow required to move the fluid particles from ground state to activated state and other symbols have their usual meanings. Rearranging Eq. (16) and putting $\Delta G^* = \Delta H^* - T\Delta S^*$ we get the relation:

$$R\ln(\eta V/hN) = \Delta H^*/T - \Delta S^* \quad (18)$$

Linear regression of $R\ln(\eta V/hN)$ against $(1/T)$ gives the enthalpy (ΔH^*) and entropy (ΔS^*) of activation for viscous flow from the corresponding slope and negative intercept, respectively. ΔG^* , ΔH^* , ΔS^* and the regression coefficients (R^2) are given in Table 7.6. It shows that while ΔH^* values are positive, ΔS^* values are mostly negative for the binary mixtures (CH + EA) and (CH + MS), but are mostly positive for the mixture (CH + MA). Such a trend in ΔH^* and ΔS^* values indicate that formation of transition state for viscous flow is accompanied by disruption of the developing forces or specific interactions between the components of the liquid mixtures. The ΔG^{*E} values are plotted against the mole fraction of CH (x_1) in Figure 7.5 at 298.15 K. Interestingly ΔG^{*E} and $\Delta\eta$ values follow similar variations against the mole fraction of CH (x_1). Reid and Taylor⁴⁴ suggested that the positive ΔG^{*E} stands for molecular interactions or compactness due to geometrical fittings of one component into the other on mixing and negative ΔG^{*E} indicate the dominance of dispersion forces leading to easier flow of a liquid mixture as compared with the pure liquids. From Figure 7.5 it is evident that the ΔG^{*E} values are negative for the mixtures (CH + MA) and (CH + EA) but positive for the mixture (CH + MS) over the whole composition range (similar trends in ΔG^{*E} versus x_1 were found at other experimental temperatures). This fact suggests the breaking of liquid order on mixing and presence of unfavorable non-specific interactions between the unlike molecules.

Chapter VII

Table 7.6. Free energy (ΔG^*), enthalpy (ΔH^*) and entropy (ΔS^*) of activation of viscous flow for the binary mixtures

x_1	ΔG^*			ΔH^* (kJ·mol ⁻¹)	ΔS^* (J·K ⁻¹ ·mol ⁻¹)	R^2
	(kJ·mol ⁻¹)					
	298.15 K	308.15 K	318.15 K			
CH (1) + MA (2)						
0	10.745	10.914	11.019	6.657	-13.744	0.9928
0.0754	10.905	11.022	11.051	8.711	-7.406	0.9920
0.1551	11.082	11.167	11.170	9.761	-4.472	0.9944
0.2393	11.275	11.326	11.308	10.771	-1.727	0.9967
0.3286	11.485	11.517	11.452	11.961	1.547	0.9947
0.3700	11.586	11.612	11.545	12.182	1.951	0.9955
0.5241	12.008	12.000	11.872	14.015	6.667	0.9942
0.6314	12.340	12.315	12.190	14.553	7.372	0.9963
0.7460	12.720	12.701	12.587	14.692	6.562	0.9968
0.8686	13.148	13.174	13.112	13.670	1.705	0.9966
1	13.620	13.746	13.809	10.793	-9.515	0.9974
CH (1) + EA (2)						
0	11.541	11.717	11.915	5.956	-18.719	0.9990
0.0914	11.691	11.820	11.972	7.501	-14.039	0.9992
0.1845	11.811	11.932	12.037	8.429	-11.351	0.9997
0.2795	11.962	12.067	12.134	9.389	-8.648	0.9987
0.3764	12.134	12.206	12.240	10.536	-5.378	0.9990
0.4200	12.204	12.273	12.286	10.967	-4.179	0.9979
0.5759	12.520	12.564	12.537	12.253	-0.933	0.9973
0.6787	12.765	12.787	12.735	13.198	1.414	0.9975
0.7836	13.021	13.063	12.995	13.384	1.161	0.9947
0.8907	13.308	13.379	13.350	12.676	-2.174	0.9950
1	13.620	13.746	13.809	10.793	-9.515	0.9974
CH (1) + MS (2)						
0	15.387	15.693	16.029	5.825	-32.054	0.9977
0.1168	15.182	15.460	15.763	6.526	-29.021	0.9990
0.2294	14.987	15.247	15.519	7.060	-26.583	0.9997
0.3379	14.804	15.041	15.282	7.679	-23.896	0.9999
0.4425	14.631	14.853	15.065	8.162	-21.702	0.9999
0.4878	14.554	14.770	14.973	8.316	-20.928	0.9998
0.6411	14.292	14.478	14.645	9.019	-17.694	0.9996
0.7353	14.126	14.296	14.438	9.469	-15.634	0.9993
0.8265	13.961	14.112	14.225	10.010	-13.271	0.9988
0.9146	13.790	13.933	14.021	10.349	-11.573	0.9978
1	13.620	13.746	13.809	10.793	-9.515	0.9974

Chapter VII

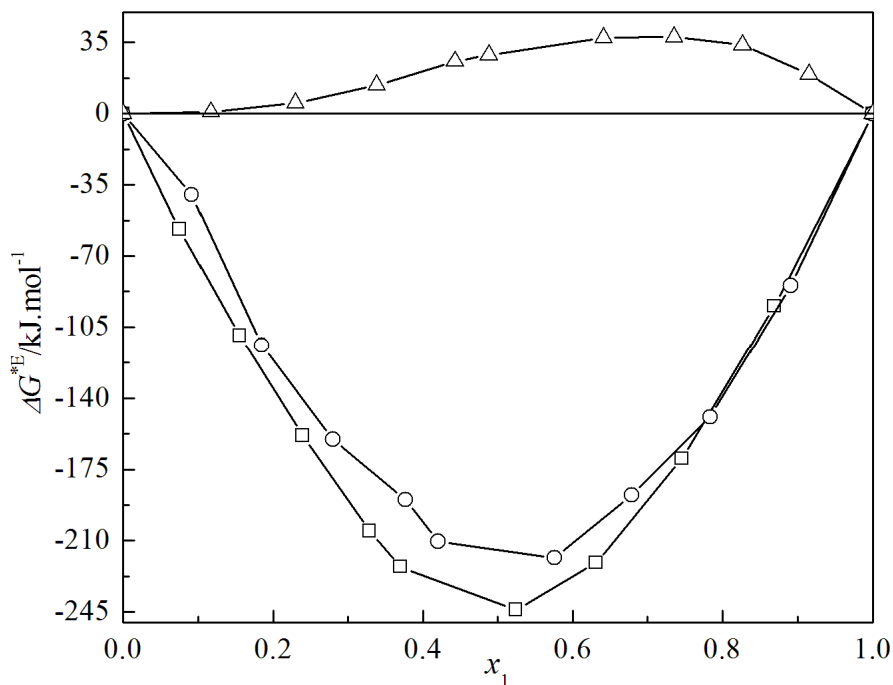


Fig. 7.5. Excess free energy of activation of viscous flow (ΔG^{*E}) versus mole fraction of CH (x_1) for the binary mixtures of CH with some esters at $T = 298.15$ K. Symbols: \square , MA; \circ , EA; Δ , MS.

7.3.6. Viscosity models

Mehrotra *et al.*⁴⁵ reviewed the practical implications of several empirical or semi-empirical viscosity models for liquid mixture viscosities. These models can simulate the viscosity of liquids or liquid mixtures. However, such models that apply the corresponding state principle based on van der Waals' hypothesis⁴⁶ are limited. Therefore, the experimental viscosities of the studied binaries were correlated with Peng-Robinson cubic equation of state (PREOS),^{12,41} Bloomfield–Dewan model (BF)^{13,41} and several popular correlation models like Grunberg–Nissan (GN), Tamura–Kurata (TK), Hind (HN), Katti–Chaudhri (KC), two parameters three body McAllister (McA3), three parameters four body McAllister (McA4), three parameters Heric–Brewer (HB), Krisnan–Laddha (KL) and Lobe (LB) at 298.15 K.^{45,47,48} Various model coefficients were estimated either by linear or non-linear least-squares regression analyses (whichever is required model-wise). Different model coefficients and corresponding standard deviations are listed in Table 7.7.

Chapter VII

Table 7.7. Different viscosity model coefficients and corresponding standard deviations (σ) for the binary mixtures studied at $T = 298.15$.

Model	Coefficients	σ	Model	Coefficients	σ
CH (1) + MA (2)					
GN	$d_{12} = -0.492$	0.003	McA3	$z_{12} = 0.736$	0.034
				$z_{21} = 0.490$	
TK	$T_{12} = 0.366$	0.017	McA4	$z_{1112} = 0.826, z_{1122} = 0.591$	0.025
				$z_{1222} = 0.481$	
HN	$H_{12} = 0.369$	0.011	KL	$a = 0.168$	0.003
				$b = -0.001$	
				$c = -0.041$	
KC	$w_{12} / RT = -0.373$	0.004	LB	$\alpha_{12} = -0.460$	0.156
				$\alpha_{21} = -0.287$	
HB	$a_0 = -0.388, a_1 = 0.001$ $a_2 = 0.095$	0.007			
CH (1) + EA (2)					
GN	$d_{12} = -0.381$	0.006	McA3	$z_{12} = 0.765$	0.031
				$z_{21} = 0.566$	
TK	$T_{12} = 0.451$	0.012	McA4	$z_{1112} = 0.849, z_{1122} = 0.650$	0.072
				$z_{1222} = 0.560$	
HN	$H_{12} = 0.461$	0.011	KL	$a = 0.155$	0.010
				$b = 0.028$	
				$c = -0.051$	
KC	$w_{12} / RT = -0.338$	0.005	LB	$\alpha_{12} = -0.437$	0.140
				$\alpha_{21} = -0.238$	
HB	$a_0 = -0.358, a_1 = -0.066$ $a_2 = 0.118$	0.023			
CH (1) + MS (2)					
GN	$d_{12} = 0.065$	0.010	McA3	$z_{12} = 1.195$	0.045
				$z_{21} = 1.213$	
TK	$T_{12} = 1.141$	0.012	McA4	$z_{1112} = 1.176, z_{1122} = 1.220$	0.109
				$z_{1222} = 1.159$	
HN	$H_{12} = 1.163$	0.011	KL	$a = -0.021$	0.001
				$b = -0.028$	
				$c = -0.001$	
KC	$w_{12} / RT = 0.048$	0.005	LB	$\alpha_{12} = -0.883$	0.108
				$\alpha_{21} = 6.864$	
HB	$a_0 = 0.048, a_1 = 0.064$ $a_2 = 0.003$	0.003			

Chapter VII

The binary interaction parameter (g_{12}) based on Peng-Robinson cubic equation of state was found to be -0.409 ($\sigma = 0.004$), -0.338 ($\sigma = 0.005$) and -0.829 ($\sigma = 0.002$) for the mixtures (CH + MA), (CH + EA) and (CH + MS), respectively. The standard deviations (σ) between the experimental viscosities and those calculated from Bloomfield and Dewan model were 0.28, 0.22 and 0.44 for the mixtures of CH with MA, EA and MS, respectively. Grunberg-Nissan coefficient (d_{12}) is proportional to interchange energy and approximates the strength of molecular interactions between the component liquids in a mixture. d_{12} values were found to be -0.492 ($\sigma = 0.003$), -0.381 ($\sigma = 0.006$) and 0.065 ($\sigma = 0.010$) for the mixtures (CH + MA), (CH + EA) and (CH + MS), respectively. Thus d_{12} values are at par the degree of molecular interactions⁴⁹ for the studied mixtures. Interestingly, Katti-Chaudhri (KC) interactions coefficients (w_{12}/RT) were also found to -0.373 ($\sigma = 0.004$), -0.338 ($\sigma = 0.005$) and 0.048 ($\sigma = 0.005$) in parallel to the order of molecular interactions in the studied mixtures.

7.3.7. Ultrasonic speed of sound and derived acoustic functions

The speeds of sound (u) and the densities (ρ) of the binary mixtures at 298.15 K were further used to determine isentropic compressibility (κ_s), excess isentropic compressibility (κ_s^E) and the other acoustic functions like intermolecular free length (L_f), specific acoustic impedance (z_{im}), free volume (V_f), internal pressure (π_{in}) along with their excess or deviation properties. The experimental speeds of sound for each pure liquid were in good agreement with the literature values^{23,25,50,51} at 298.15 K. The excess isentropic compressibility (κ_s^E) were calculated by using the relation:

$$\kappa_s^E = \kappa_s - \kappa_s^{id} \quad (19)$$

where $\kappa_s = 1/\rho u^2$ and κ_s^{id} is the isentropic compressibility for an ideal mixture.

Benson-Kiyohara⁵² and Acree⁵³ has expressed κ_s^{id} by the relation:

$$\kappa_s^{id} = \sum_{i=1}^2 \tau_i \left[\kappa_{S,i} + \frac{TV_{m,i}^* \alpha_i^2}{c_{P,i}} \right] - \left\{ \frac{T \sum_{i=1}^2 (x_i V_{m,i}^*) \sum_{i=1}^2 (\tau_i \alpha_i)^2}{\sum_{i=1}^2 (x_i c_{P,i})} \right\} \quad (20)$$

Chapter VII

where τ_i is the volume fraction of the component 'i' in the mixture, $\kappa_{s,i}$, $V_{m,i}^*$, α_i and $c_{p,i}$ are the isentropic compressibility, the molar volume, the expansion coefficient and the molar isobaric heat capacity of the pure components, respectively. The expansion coefficients (α_i) were obtained from experimental density values and $c_{p,i}$ values were taken from the literature.²⁸ The intermolecular free length (L_f), excess intermolecular free length (L_f^E), free volume (V_f) and excess free volume (V_f^E) were calculated by using the standard relations⁴² as detailed in chapter II. Various acoustic parameters and their excess functions at 298.15 K are listed in Table 7.8. Figure 7.6 illustrates the variation of excess isentropic compressibility (κ_s^E) of the mixtures against the mole fraction of CH (x_1) at 298.15 K. It shows that the κ_s^E values for the mixtures (CH + MA) and (CH + EA) are positive but mostly negative for the mixture (CH + MS) over the entire composition range. The positive κ_s^E values for the mixture (CH + MA) and (CH + EA) reveal that the component molecules in the mixtures become more compressible or less compact as compared to their pure state. This may be ascribed to the disruption of dipolar associated structure or molecular order in pure liquids (alkyl acetates) due to the breaking up of the dipole-dipole cohesive forces present amongst the individual MA and EA molecules (in pure state) when mixed with CH. For the mixture (CH + MS), the initial positive κ_s^E values at $x_1=0.1168$ probably arises from the sudden perturbation of the three dimensional hydrogen bonded (intermolecular and intramolecular) network in liquid MS on the addition of CH; however, the negative κ_s^E values over moderate to CH-rich regions are most probably associated with favorable mutual (geometrical) fitting of the CH and MS molecules through interstitial accommodation as well as dipole-induced dipole interactions caused by the dipoles of MS. According to Eyring and Kincaid,⁵⁴ isentropic compressibility (κ_s) and intermolecular free length (L_f) inversely vary with the speeds of sound (u). It was observed that the speeds of sound (u) were observed to increase with increasing mole fraction of CH (x_1) for the mixtures (CH + MA) and (CH + EA) but decreased for the mixture (CH + MS); such an increase in the speeds of sound (u) led to a decrease in isentropic compressibility (κ_s) and intermolecular free lengths (L_f).

Chapter VII

Table 7.8. Ultrasonic speeds (u), isentropic compressibilities (κ_s), intermolecular free lengths (L_f), free volumes (V_f), excess isentropic compressibilities (κ_s^E), excess intermolecular free lengths (L_f^E) and excess free volumes (V_f^E) for binary mixtures at 298.15 K; x_1 -mole fraction of CH.

x_1	u (m · s ⁻¹)	$\kappa_s \cdot 10^{10}$ (Pa ⁻¹)	L_f (Å)	$V_f \cdot 10^6$ (m ³ · mol ⁻¹)	$\kappa_s^E \cdot 10^{10}$ (Pa ⁻¹)	L_f^E (Å)	$V_f^E \cdot 10^6$ (m ³ · mol ⁻¹)
CH (1) + MA (2)							
0	1148.5	8.180	0.5883	0.378	0	0	0
0.0754	1146.9	8.379	0.5954	0.363	0.189	0.0070	0.003
0.1551	1152.2	8.484	0.5991	0.351	0.285	0.0106	0.009
0.2393	1160.6	8.540	0.6011	0.337	0.332	0.0124	0.015
0.3286	1171.8	8.549	0.6014	0.321	0.334	0.0126	0.020
0.3700	1177.0	8.545	0.6012	0.313	0.327	0.0124	0.021
0.5241	1197.8	8.490	0.5993	0.276	0.265	0.0102	0.020
0.6314	1212.7	8.430	0.5972	0.246	0.202	0.0079	0.015
0.7460	1226.9	8.371	0.5951	0.213	0.142	0.0056	0.008
0.8686	1240.2	8.309	0.5929	0.178	0.080	0.0032	0.003
1	1253.3	8.227	0.5899	0.145	0	0	0
CH (1) + EA (2)							
0	1144.3	8.537	0.6010	0.411	0	0	0
0.0914	1154.5	8.521	0.6004	0.385	0.013	0.0004	-0.002
0.1845	1165.2	8.503	0.5997	0.367	0.024	0.0008	0.005
0.2795	1176.3	8.481	0.5990	0.344	0.032	0.0011	0.007
0.3764	1187.5	8.455	0.5981	0.318	0.036	0.0012	0.007
0.4200	1192.2	8.447	0.5978	0.308	0.042	0.0015	0.008
0.5759	1209.2	8.401	0.5961	0.263	0.044	0.0015	0.005
0.6787	1220.1	8.367	0.5949	0.231	0.041	0.0014	0.001
0.7836	1231.0	8.328	0.5935	0.202	0.034	0.0012	-0.001
0.8907	1241.5	8.286	0.5920	0.172	0.025	0.0009	-0.002
1	1253.3	8.227	0.5899	0.145	0	0	0
CH (1) + MS (2)							
0	1410.9	4.260	0.4245	0.187	0	0	0
0.1168	1356.0	4.787	0.4500	0.179	0.056	0.0062	-0.002
0.2294	1325.7	5.185	0.4683	0.174	-0.004	0.0059	-0.003
0.3379	1305.2	5.535	0.4839	0.170	-0.098	0.0035	-0.003
0.4425	1292.5	5.852	0.4976	0.165	-0.209	-0.0001	-0.003
0.4878	1286.7	6.004	0.5040	0.163	-0.243	-0.0012	-0.003
0.6411	1268.4	6.570	0.5272	0.156	-0.297	-0.0034	-0.004
0.7353	1258.7	6.970	0.5430	0.152	-0.271	-0.0031	-0.004
0.8265	1252.8	7.385	0.5590	0.149	-0.209	-0.0023	-0.004
0.9146	1249.3	7.818	0.5751	0.146	-0.105	-0.0007	-0.003
1	1253.3	8.227	0.5899	0.145	0	0	0

Chapter VII

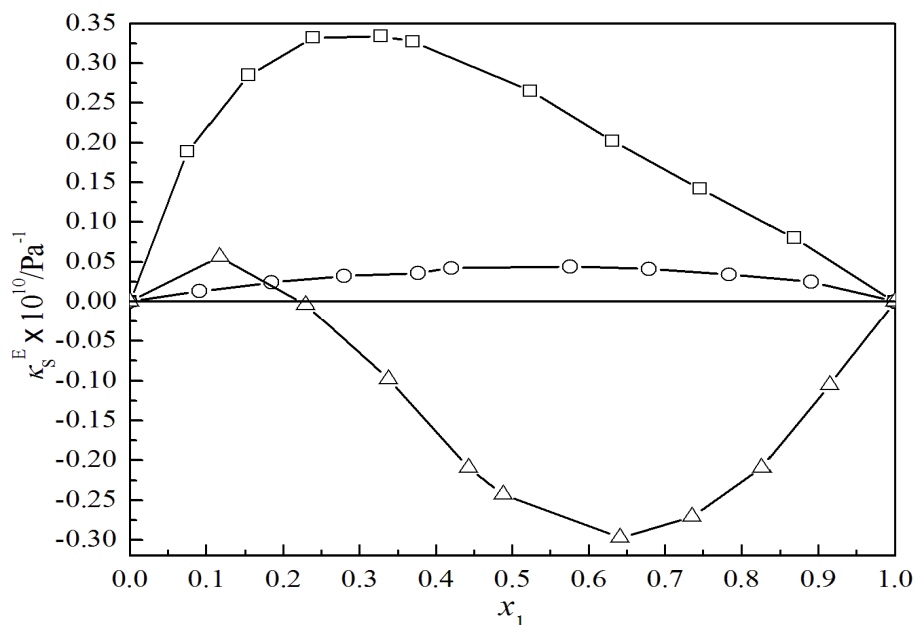


Fig. 7.6. Excess isentropic compressibility (κ_s^E) versus mole fraction of CH (x_1) for the binary mixtures of CH + some esters at $T = 298.15$ K. Symbols: \square , MA; \circ , EA; \triangle , MS.

However, for the mixture (CH + MS), as the speeds of sound (u) decreased with increasing mole fraction of CH (x_1), isentropic compressibility (κ_s) and intermolecular free lengths (L_f) increased monotonously. Positive excess intermolecular free lengths (L_f^E) for the mixture (CH + MA) and (CH + EA) suggest their less compact structure as compared to the mixture (CH + MS) with more compact structure and negative L_f^E values. Interestingly, it was observed that free volumes (V_f) and excess free volumes (V_f^E) for the studied mixtures followed the order: (CH + MA) > (CH + EA) > (CH + MS), i.e., the reversed order of molecular interactions in parallel to the degree of their structural compactness. Thus the study of the various acoustic and their excess functions also stand in support of the following order of molecular interactions: (CH + MS) > (CH + EA) > (CH + MA), as found earlier on the basis of excess molar volumes and viscosity deviations.

7.3.8. Prediction of ultrasonic speed of sound

Ultrasonic speeds of sound for the binary mixtures were estimated with several theoretical models like Flory theory (FL), Collision factor theory (CFT), Nomoto's relation (NOM), Impedance dependence relation (IDR), Ideal mixture relation (IMR), Junjie's relation (JUN). Details of these theoretical models and

Chapter VII

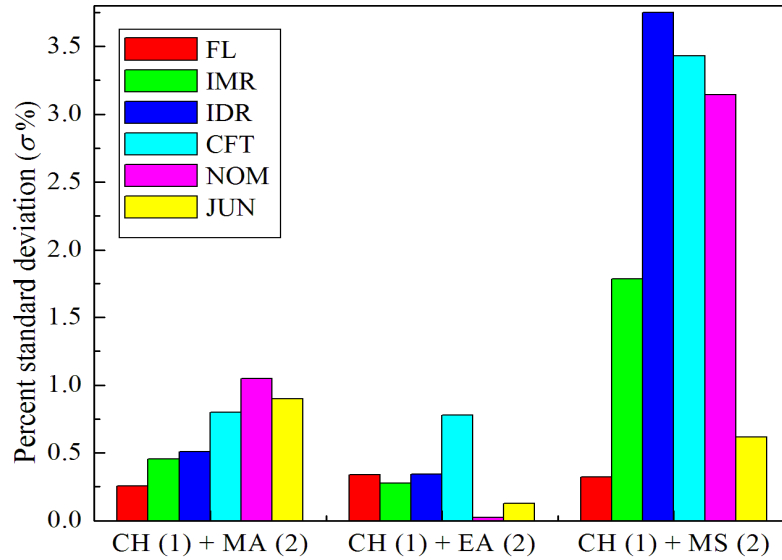


Fig. 7.7. Percent standard deviations ($\sigma\%$) for theoretical prediction of ultrasonic speeds by different empirical relations at $T = 298.15$ K for the binary mixtures studied. Models: FL, Flory theory; IMR, Ideal mixing relation; IDR, Impedance dependence relation; CFT, Collision factor theory; NOM, Nomoto's relation; JUN, Junjie's relation.

calculations are mentioned in chapter II. The goodness of prediction for these models was judged by percent standard deviations ($\sigma\%$) (as illustrated in Figure 7.7) against the experimental speeds of sound (u) for the mixtures studied. Figure 7.7 depicts that the predictive capability of these models follows the orders: $FL > IMR > IDR > CFT > JN > NOM$ (for the mixtures CH + MA); $NOM > JN > IMR > FL > IDR > CFT$ (for the mixture CH + EA) and $FL > JN > IMR > NOM > CFT > IDR$ (for the mixture CH + MS), respectively.

7.3.9. Excess molar refractions

The excess molar refractions (R_m^E) for the mixtures were obtained from relation:⁴⁸

$$R_m^E = R_m - \sum_{i=1}^2 x_i R_{m,i} \quad (21)$$

where $R_{m,i} = \{(n_{D,i}-1)/(n_{D,i}+2)\}M_i/\rho_i$, $n_{D,i}$ and ρ_i stand for the molar refraction, refractive index and density of the i^{th} component in the mixture, respectively. The molar refraction (R_m) for a mixture can be had from the relation:⁴⁸

Chapter VII

$$R_m = \frac{(n_D^2 - 1) \sum_{i=1}^2 x_i M_i}{(n_D^2 + 2) \rho} \quad (22)$$

where ρ and n_D are the mixture density and refractive index; M_i stands for the molar mass of i^{th} component in a mixture, respectively. Excess molar refractions (R_m^E) and the experimental refractive indices (n_D) for the three binaries are listed in Table 7.9. The experimental refractive indices (n_D) of the pure liquids were in good agreement with literature values^{20,24,54} at 298.15 K. The dependence of the excess refractive indices (R_m^E) on the mole fraction of CH (x_1) at 298.15 K also stands in parallel to the same order of molecular interactions for the studied binaries as discussed above. Furthermore the refractive indices of the mixtures were predicted by several models: Lorentz-Lorenz (LL), Gladstone-Dale (GD), Arago-Biot (AB), Newton (NEW), Eykman (EYK), Eyring-John (EJ), Heller (HEL) and Weiner (WEI) as detailed in chapter II and their goodness of prediction was judged by percent standard deviations ($\sigma\%$) (as illustrated in Figure 7.8) against the experimental refractive indices for all the binary mixtures studied.

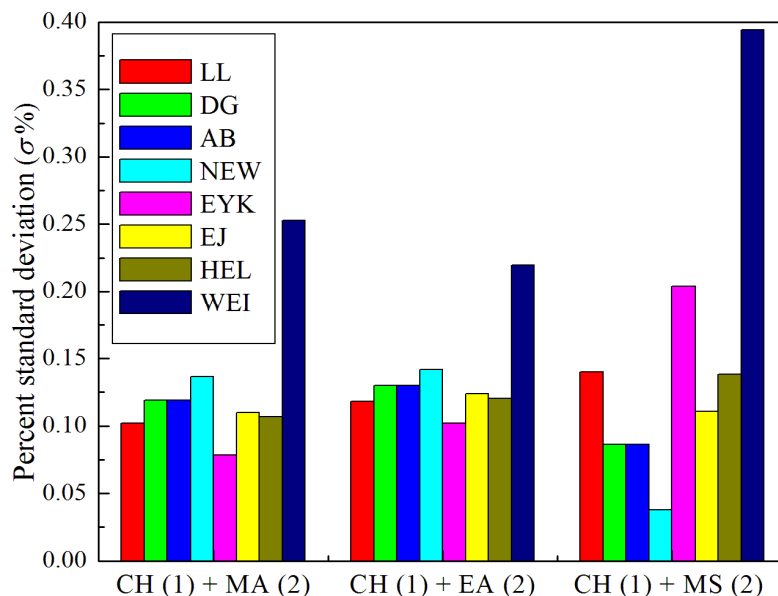


Fig. 7.8. Percent standard deviations ($\sigma\%$) for theoretical prediction of refractive indices by various models at $T = 298.15$ K for the binary mixtures studied. Models: LL, Lorentz-Lorenz; DG, Gladstone-Dale; AB, Arago-Biot; NEW, Newton; EYK, Eykman; EJ, Eyring-John; HEL, Heller; WEI, Weiner.

Chapter VII

Table 7.9. Refractive indices (n_D), molar refractions (R_m) and excess molar refractions (R_m^E) for the binary mixtures at 298.15 K

x_1	n_D	$R_m \cdot 10^6$ ($\text{m}^3 \cdot \text{mol}^{-1}$)	$R_m^E \cdot 10^6$ ($\text{m}^3 \cdot \text{mol}^{-1}$)
CH (1) + MA (2)			
0	1.3604	17.658	0
0.0754	1.3659	18.472	0.055
0.1551	1.3717	19.352	0.132
0.2393	1.3776	20.270	0.201
0.3286	1.3836	21.224	0.256
0.3700	1.3862	21.649	0.264
0.5241	1.3958	23.223	0.286
0.6314	1.4022	24.303	0.285
0.7460	1.4089	25.425	0.253
0.8686	1.4158	26.567	0.160
1	1.4234	27.730	0
CH (1) + EA (2)			
0	1.3712	22.343	0
0.0914	1.3753	22.831	-0.004
0.1845	1.3799	23.362	0.025
0.2795	1.3849	23.925	0.076
0.3764	1.3898	24.475	0.104
0.4200	1.3920	24.721	0.115
0.5759	1.4000	25.566	0.120
0.6787	1.4054	26.110	0.110
0.7836	1.4109	26.642	0.077
0.8907	1.4172	27.190	0.048
1	1.4234	27.730	0
CH (1) + MS (2)			
0	1.5352	40.179	0
0.1168	1.5247	38.882	0.157
0.2294	1.5136	37.439	0.116
0.3379	1.5028	35.999	0.026
0.4425	1.4920	34.627	-0.043
0.4878	1.4872	34.032	-0.074
0.6411	1.4700	32.024	-0.174
0.7353	1.4585	30.820	-0.205
0.8265	1.4470	29.728	-0.162
0.9146	1.4354	28.680	-0.113
1	1.4234	27.730	0

Chapter VII

7.3.10. IR spectroscopic study

The results obtained so far are also well reflected in FT-IR spectra of the binary mixtures (Figures 7.9-7.11). The spectra were recorded in a demountable KBr cell for liquid samples with spacer of path length of 0.5 mm at ambient temperature with a Perkin-Elmer Spectrum FT-IR spectrometer (RX-1). Redondo *et al.*⁵⁵ reported that the stable conformer of CH is the chair configuration with D_{3d} symmetry and its spectra is characterized by the fundamental C-H stretching vibration at 3000-2800 cm^{-1} along with some bands appearing in the range 2700-2600 cm^{-1} with frequency lower than the corresponding C-H stretching vibrations and at higher frequency than other possible C-C stretching, C-H bending vibrations, *etc.*, due to some combinations of the fundamental bands. The IR spectra of the MA and EA are similar in nature with characteristic C=O stretching vibration at 1760 and 1739 cm^{-1} , respectively along with some C-H stretching vibration at 3000-2800 cm^{-1} . As the mole fraction of CH in mixture (CH + MA) and (CH + EA) increases, the C-H fundamental vibrations gradually become sharp with slight changes in peak position.

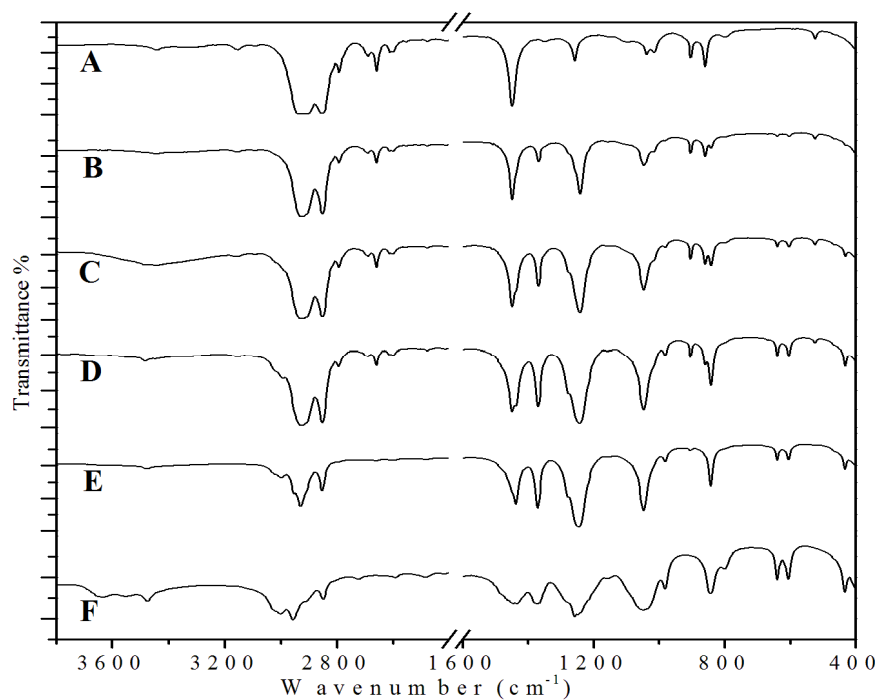


Fig.7.9. FTIR spectra of the various binary mixtures of CH (1) + MA (2): A, pure CH ($x_2 = 0.00$); B, $x_2 = 0.20$; C, $x_2 = 0.40$; D, $x_2 = 0.60$; E, $x_2 = 0.80$; F, pure MA ($x_2 = 1.00$).

Chapter VII

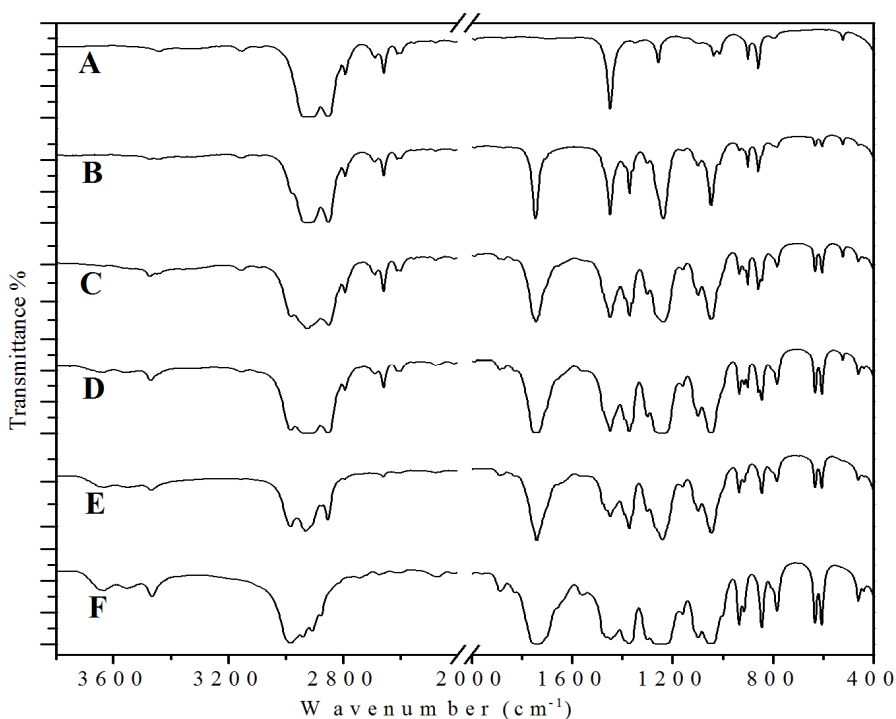


Fig. 7.10. FTIR spectra of the various binary mixtures of CH (1) + EA (2): A, pure CH ($x_2 = 0.00$); B, $x_2 = 0.20$; C, $x_2 = 0.40$; D, $x_2 = 0.60$; E, $x_2 = 0.80$; F, pure EA ($x_2 = 1.00$).

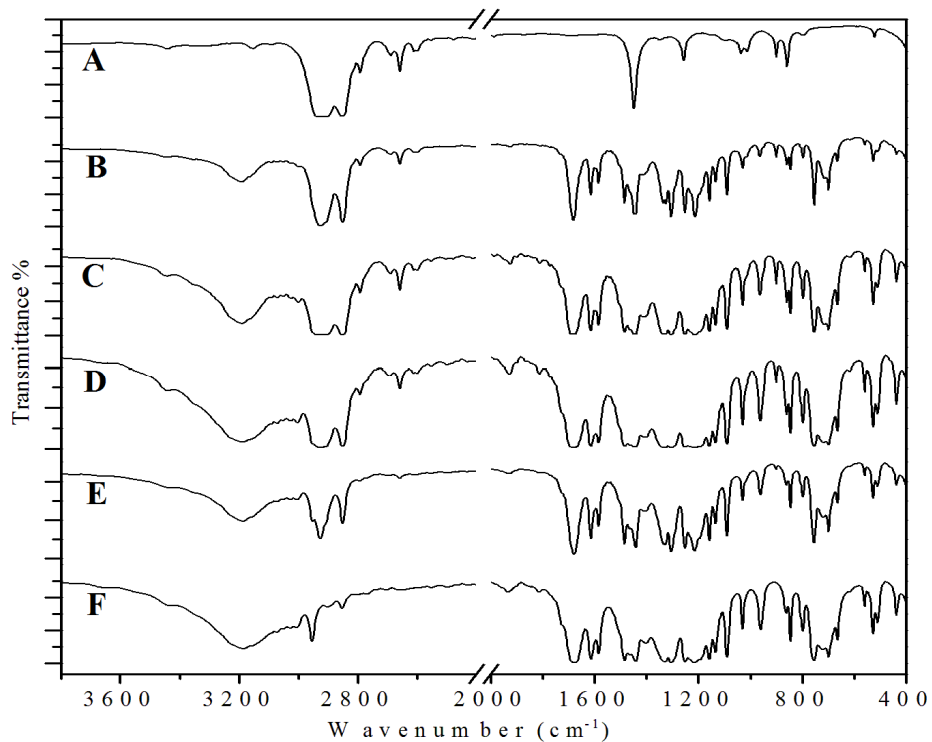


Fig. 7.11. FTIR spectra of the various binary mixtures of CH (1) + MS (2): A, pure CH ($x_2 = 0.00$); B, $x_2 = 0.20$; C, $x_2 = 0.40$; D, $x_2 = 0.60$; E, $x_2 = 0.80$; F, pure MS ($x_2 = 1.00$).

Chapter VII

Again, the characteristic C=O and C-O stretching vibrations become much sharper with corresponding changes in peak position and intensity. All these changes in FTIR spectra of the alkyl esters indicate breaking of dipolar association of the acetate molecules with the advent of CH in the mixtures. The IR spectra of MS is characterized by C=O and C-O stretching vibrations at around 1676 and 1215 cm^{-1} along with a broad band appearing at around 3180 cm^{-1} .⁵⁶ This band becomes less broad as the mole fraction of CH increases in the mixture (CH + MS); these bands shifts to higher frequency (3180 to 3190 cm^{-1}) and also becomes less intense. These results indicate that the dipolar association of MS molecules due to inter and intra molecular H-bonds decreases. Similar shifts were found for the C=O bond of MS. All these results indicate that the molecular interactions mainly involved in all the mixtures studied are the loss of dipolar association of the polar molecules on mixing with the non-polar CH molecules, dipole-induced dipole interactions and interstitial accommodations.

7.4. Conclusion

In summary, the various derived excess properties like excess molar volume (V_m^E), viscosity deviation ($\Delta\eta$), excess isentropic compressibility (κ_s^E), *etc.*, reveals the following order of molecular interactions: (CH + MS) > (CH + EA) > (CH + MA) for the mixtures studied. Such an order of molecular interactions originates from a combined effect of factors like the molecular size, shape and nature of the components; herein the order is attributed to the breaking up of dipolar interactions or the three dimensional hydrogen bonded network as well as interstitial accommodation on mutual mixing of the components. However, these specific and non-specific interactions between the dissimilar molecules in the mixtures decrease at higher temperatures. A comparison of the excess partial molar volumes ($\bar{V}_{m,1}^{0,E}$ and $\bar{V}_{m,2}^{0,E}$) at infinite dilution to the molar volumes of the pure components in the mixtures suggests that while the mixtures with MA and EA are characterized by volume expansion, the mixture with MS is characterized by volume contraction on mixing with CH. FTIR spectra of the mixtures also correlate well with the observed molecular interactions for the mixtures studied.

Chapter VII

References

- [1] C.R. Reid, B.E. Poling, *The properties of Gases and Liquids*, McGraw Hill, New York, 1998, Ch.1.
- [2] J.G. Harris, F.H. Stillinger, *J. Chem. Phys.*, 95 (1991) 5953.
- [3] F. Nabi, M.A. Malik, C.G. Jesudason, S.A. Al-Thabaiti, *Korean. J. Chem. Eng. Data* 31 (2014) 1505.
- [4] M. Shafique, S. Hussain, S. Asif, V. Pradhan, *Res. J. Chem. Sci.*, 3 (2013) 98.
- [5] R. Mehra, A. Gupta, R. Israni, *Ind. J. Chem.*, 40A (2001) 505.
- [6] M. Indhumathi, G. Meenakshi, *Mid. East. J. Sci. Res.*, 20 (2014) 546.
- [7] S. Aparicio, R. Alcalde, *Eur. J. Chem.*, 1 (2010) 162.
- [8] M.V. Rathnam, *Proc. Ind. Natn. Sci. Acad.*, 53A (1987) 588.
- [9] M.N. Roy, B.K. Sarkar, B. Sinha, *J. Chem. Eng. Data* 54 (2009) 1076.
- [10] D. Patterson, G. Delmas, *J. Polym. Sci.*, 30 (1970) 1.
- [11] D. Patterson, *Pure. Appl. Chem.*, 47 (1976) 305.
- [12] V.A. Bloomfield, R.K. Dewan, *J. Phys. Chem.*, 75 (1971) 3113.
- [13] D.Y. Peng, D.B. Robinson, *Ind. Eng. Chem. Fundum.*, 15 (1976) 59.
- [14] I. Gascon, A.M. Mainar, F.M. Royo, J.S. Urieta, *J. Chem. Eng. Data* 45 (2000) 751.
- [15] E. Aicart, G. Tardajos, M. Dlaz Peia, *J. Chem. Eng. Data* 26 (1981) 22.
- [16] K.N. Marsh, *TRC Data Bases for Chemistry and Engineering-TRC Thermodynamic Tables*, Texas A & M University System, College Station, TX, 1994.
- [17] T.M. Aminabhavi, V.B. Patil, M.I. Aralaguppi, *J. Chem. Eng. Data* 41 (1996) 521.
- [18] N.V. Sastry, M.C. Patel, *J. Chem. Eng. Data* 48 (2003) 1019.
- [19] V.K. Dakua, B. Sinha, M.N. Roy, *Ind. J. Chem.*, 45A (2006) 1381.
- [20] M.I. Aralaguppi, C.V. Jadar, T.M. Aminabhavi, *J. Chem. Eng. Data* 44 (1999) 441.
- [21] A. Pal, H. Kumar, *J. Mol. Liq.*, 89 (2000) 189.
- [22] R.M. Pires, H.F. Costa, A.G.M. Ferreira, I.M.A. Fonseca, *J. Chem. Eng. Data* 52 (2007) 1240.
- [23] D.L. Cunha, J.A.P. Coutinho, J.L. Daridon, *J. Chem. Eng. Data* 58 (2013) 925.
- [24] T.M. Aminabhavi, H.T.S. Phayde, *J. Chem. Eng. Data* 41(1996) 813.
- [25] S. Nallani, S. Boodida, S.J. Tangeda, *J. Chem. Eng. Data* 52 (2007) 405.
- [26] W.M. Haynes, D.R. Lide, T.J. Bruno, *CRC Handbook of Chemistry & Physics*, 93rd edn., Taylor & Fransis, Boca Roton, London, 2012-2013.
- [27] D.W.A. Sharp, *Miall's Dictionary of Chemistry*, Essex, 5th edn., UK, Longman, (1981), pp. 121.
- [28] M.V. Garcia, M.I. Redondo, *J. Chem. Edu.*, 62 (1985) 887.

Chapter VII

- [29] F.R. Jensen, D.S. Noyce, C. H. Sederholm, J. Am. Chem. Soc., 84 (1962) 386.
- [30] R. Thiagarajan, L. Palaniappan. Ind. J. Pure. Appl. Phys., 46 (2008) 852.
- [31] G.M. Smith, H.C. Van Ness, *Introduction to Chemical Engineering Thermodynamics*, McGraw Hill, New York, 1987.
- [32] B. Sinha, Phys. Chem. Liq., 48 (2010) 183.
- [33] O. Redlich, A.T. Kister, Indus. Eng. Chem. 40 (1948) 345.
- [34] D. W. Marquardt, J. Soc. Ind. Appl. Math., 11, (1963) 431.
- [35] I.R. Radovic, M.L. Kijevcanin, A.Z. Tasic, B.D. Djordjevic, J. Serb. Chem. Soc., 74 (2009) 1303.
- [36] P.J. Flory, R.A. Orwell, A. Vrijji, J. Am. Chem. Soc., 86 (1964) 3507.
- [37] P.J. Flory, R.A. Orwell, A. Vrijji, J. Am. Chem. Soc., 86 (1964) 3515.
- [38] P.J. Flory, J. Am. Chem. Soc., 87 (1965) 1833.
- [39] A. Abe, P.J. Flory, J. Am. Chem. Soc., 87 (1965) 1838.
- [40] S.I Sandler, *Chemical, Biochemical, and Engineering Thermodynamics*, 4th edn., John Wiley & Sons (Asia), New Delhi, 2006, pp. 242.
- [41] R. Pradhan, A. Kamath, D. Brahman, B. Sinha, Fluid Phase Equilib., 404 (2015) 131.
- [42] B.K. Sarkar, A. Choudhury, B. Sinha, J. Solution Chem., 41 (2012) 53.
- [43] S. Glasstone, K.J. Laidler, H. Eyring, *The theory of Rate Process*. McGraw-Hill Book Company, New York, 1941.
- [44] T.M. Reid, T.E. Taylor, J. Phys. Chem., 63 (1959) 58.
- [45] A.K. Mehrotra, W.D. Monnery, W. Svrcek, Fluid Phase Equilib., 117 (1996) 344.
- [46] R.D. McCarty, Fluid Phase Equilib., 256 (2007) 42.
- [47] M.R.V. Krishnan, G.S. Laddha, Ind. Chem. Eng., Trans., 57 (1963).
- [48] A. Ali, A. K. Nain, D. Chand, R. Ahmad, J. Chinese. Chem. Soc., 53 (2006) 531.
- [49] R.J. Fort, W.R. Moore, Trans. Faraday Soc., 62 (1966) 1112.
- [50] V. Vyas, T. Nautiyal, Pramana-J. Phys., 59 (2002) 663.
- [51] J.M. Resa, J.M. Goenaga, A.I. Sanchez-Ruiz, J. Chem. Eng. Data 51 (2006) 1294.
- [52] G.C. Benson, O.K. Kiyohara, J. Chem. Thermodyn., 11 (1979) 1061.
- [53] W.E. Acree, J. Chem. Eng. Data 28 (1983) 215.
- [54] H. Eyring, J. F. Kincaid, J. Chem. Phys., 6 (1938) 620.
- [55] M.V. Garcia, M.I. Redondo, J. Chem. Edu., 62 (1985) 887.
- [56] H. Yamada, Bull. Chem. Soc. Jpn, 32 (1959) 1051.

CHAPTER VIII

Thermophysical properties of the binary mixtures of cyclohexanone with some esters

8.1. Introduction

The study of molecular interactions in binary and multi-component liquid mixtures is of significant importance and interest to both chemists and chemical engineers in view of their diversified applications. A knowledge of excess functions like excess molar volume, excess isentropic compressibility, *etc.*, may help to interpret, correlate and even predict thermodynamic properties of liquid mixtures as well as simulate their liquid state in order to design new industrial process equipments with better precision at reduced costs and hence such knowledge is an avenue for the study of molecular interactions in terms of structural effects and packing phenomenon.¹⁻⁴ Thus systematic investigation on the different physico-chemical properties (volumetric, viscometric and acoustic, *etc.*) and their excess/deviation functions are of great importance in chemical industry. Therefore herein this chapter an attempt has been undertaken to study the nature of molecular interactions in the binary mixtures of cyclohexanone (CHN) with some esters, *viz.*, methyl acetate (MA), ethyl acetate (EA) and methyl salicylate (MS) at 298.15, 308.15 and 318.15 K under ambient pressure. In chapter VII the thermophysical properties of the binary mixtures of cyclohexane with these esters were studied. The selected liquids were chosen due to their varied applications. Cyclohexanone is used as an intermediate in nylon manufacture and as a solvent for natural resins, lacquers, dyes and insecticides, *etc.* Esters are also industrially important liquids because of their wide usage in flavoring, perfumery, artificial essences and cosmetics, *etc.*, as mentioned in chapter VII.

Herein this chapter experimental data (ρ , η , u and n_D) were used to determine different excess or deviation functions and are discussed in terms of molecular interactions, structural effects and the nature of liquid mixtures. Again a quantitative estimation of different contributions (*i.e.*, interaction contribution, free volume contribution, *etc.*) to the excess molar volumes (V_m^E) of the binary mixtures at ambient temperature and pressure were determined from PFP theory.^{5,6} A comparison was also made between the experimental and calculated V_m^E and η values (based on PFP⁵ or Bloomfield-Dewan viscosity model⁷ and PREOS⁸) to assess the predictive capability

Chapter VIII

of these theories. Furthermore, ultrasonic speeds of sound and refractive indices for all the binary mixtures were theoretically predicted based on several empirical and semi-empirical relations.

8.2. Experimental section

8.2.1. *Materials*

All the chemicals used in this chapter were of spectroscopic grade (Sigma-Aldrich, Germany, Reagent Plus, purity > 99%) and were used as received from the vendor. A comparison between the experimental and literature density and viscosity data of the selected esters at the experimental temperatures and pressure has been shown in the previous chapter and such a comparison between the experimental and literature density and viscosity data⁹⁻¹² of cyclohexanone has been given in Table 8.1 for ascertaining its purity.

8.2.2. *Apparatus and procedures*

All the binary mixtures were prepared afresh by mass before use inside a dry box by mass at 298.15 K and kept in air-tight bottles with stopper. Each prepared solution was distributed into three recipients to perform all the measurements in triplicate. The mass measurements were recorded on a digital electronic analytical balance (Mettler, AG 285, Switzerland) with an uncertainty of ± 0.01 mg. The uncertainty in mole fraction was evaluated to be ± 0.0002 . Densities (ρ) were measured with a vibrating-tube densitometer (Anton Paar, DMA 4500M). Viscosities (η) were measured by means of a suspended Canon-type Ubbelohde viscometer, thoroughly cleaned, dried and placed vertically in a glass sided thermostat maintained to ± 0.01 K of the desired temperature. Ultrasonic speeds of sound (u) were measured with a multi-frequency ultrasonic interferometer (F-05, Mittal Enterprises, New Delhi, India) working at 2 MHz. Refractive indices of pure liquid and their binary mixtures were measured with an Abbe's refractometer. The details of the instruments, their calibrations and uncertainties of the measured properties are given in chapter III.

8.3. Results and discussion

Excess or deviation functions are sensitive to the nature and degree of the intermolecular forces operating amongst the unlike and like components in the liquid mixtures. Therefore, the systematic investigation of the excess or deviation functions

Chapter VIII

Table 8.1. Densities (ρ) and viscosities (η) of the pure liquids at $T = (298.15-318.15)$ K

Pure Liquid	T (K)	$\rho \cdot 10^{-3}$		η	
		(kg · m ⁻³)		(mPa · s)	
		Expt.	Lit.	Expt.	Lit.
CHN	298.15	0.94165	0.9416 ⁹ 0.9418 ¹⁰	2.021	0.020 ⁹ 2.0205 ¹⁰
	308.15	0.93128	0.9312 ¹¹	1.656	1.6562 ¹¹
	318.15	0.92346	0.9234 ¹¹	1.381	1.3809 ¹¹
	318.15	1.15942	1.159405 ¹²	1.303	

for the liquid mixtures (differing in size, shape and polarity, *etc.*) is the initial step for a fundamental understanding of the physico-chemical behavior and the nature of the molecular interactions amongst the unlike molecules in the mixtures. The sign and magnitude of these excess or deviation functions depend upon the relative magnitude of contractive and expansive factors that arise on mutual mixing of the components and often give a measure of non-ideality in the liquid mixtures involved. The experimental values of densities (ρ), viscosities (η), excess molar volumes (V_m^E) and viscosity deviation ($\Delta\eta$) of the binary mixtures under investigation as a function of mole fraction (x_1) of CHN at the experimental temperatures are listed in Table 8.2.

8.3.1. Excess molar volumes

Excess molar volume (V_m^E) reflects the overall state of the packing effects, molecular arrangements and interactions prevailing amongst the components of the binary mixtures and arises as a result of several effects or contributions, *viz.*, physical, chemical and geometrical contribution. The physical contributions (like breaking of liquid order on mutual mixing) mainly involve the dispersion forces, non-specific and unfavorable interactions amongst the unlike components in the mixtures. The chemical or specific interactions involve hydrogen bond formation, dipole-dipole or dipole-induced dipole interactions, charge transfer type forces and other complex forming interactions amongst dissimilar species. Structural contributions arise from the differences in molecular packing due to interstitial accommodation of one component into other's structure provided the components differ in size, shape and volume. While physical contributions cause volume expansion (*i.e.*, positive V_m^E), chemical and geometrical contributions cause volume contraction (*i.e.*, negative V_m^E).

Chapter VIII

Using the measured densities of the mixtures, excess molar volumes (V_m^E) were obtained from the relation:

$$V_m^E = \sum_{i=1}^2 x_i M_i (1/\rho - 1/\rho_i) \quad (1)$$

where ρ is the density of the mixture and x_i , M_i and ρ_i are the mole fraction, molar mass and density of the i^{th} component in a mixture, respectively. The uncertainty in the excess molar volumes (V_m^E) was evaluated to be $\pm 0.006 \text{ cm}^3 \cdot \text{mol}^{-1}$. Figure 8.1 (V_m^E versus x_1 at 298.15 K) illustrate that excess molar volumes (V_m^E) vary in a sigmoid fashion with mole fraction (x_1) of CHN for the binary mixtures with the alkyl esters (MA and EA) at 298.15 K. Similar composition dependence of V_m^E values was observed at other experimental temperatures. The V_m^E values are positive at the lower mole fraction (x_1) of CHN and become negative at the mole fractions $x_1 \geq 0.6378$ and $x_1 \geq 0.4730$ for the mixtures (CHN + MA) and (CHN + EA), respectively but for the mixture (CHN + MS) the V_m^E values are negative over the entire composition range at all the experimental temperatures. Almost similar results were reported earlier for the mixtures with alkyl esters at 298.15 K by Roy *et al.*⁹ CHN is a polar associated liquid through dipole-dipole interactions and esters also exist as dipolar associates. So an approximate estimate of the nature and strength of molecular interactions between similar or dissimilar molecules can be guessed from their dipole moments (μ_D). The ascending order of the dipole moment (μ_D) of the selected liquids is: $\mu_{D, \text{MA}} (1.72) < \mu_{D, \text{EA}} (1.78) < \mu_{D, \text{MS}} (2.47) < \mu_{D, \text{CHN}} (2.87)$ in Debye.¹³ A comparison of the dipole moments (μ_D) reveals that the intermolecular interactions should be lowest in the mixture (CHN + MA) and highest in the mixture (CHN + MS) and the expected order of molecular interactions amongst the unlike components in the mixtures should be (CHN + MS) > (CHN + EA) > (CHN + MA) based on the degree of dipole-dipole interactions. The observed positive variation of V_m^E values for the mixtures (CHN + MA) and (CHN + EA) with mole fraction (x_1) of CHN is due to the breaking of dipole-dipole cohesive forces present amongst the similar molecules on mutual mixing of the dissimilar molecules.

Chapter VIII

Table 8.2. Density (ρ), viscosity (η), excess molar volume (V_m^E) and viscosity deviation ($\Delta\eta$) for the binary mixtures studied at $T = (298.15 \text{ to } 318.15) \text{ K}$.

x_1	$\rho \cdot 10^{-3}$ ($\text{kg} \cdot \text{m}^{-3}$)	η ($\text{mPa} \cdot \text{s}$)	$V_m^E \cdot 10^6$ ($\text{m}^3 \cdot \text{mol}^{-1}$)	$\Delta\eta$ ($\text{mPa} \cdot \text{s}$)
CHN (1) + MA (2)				
<i>T</i> = 298.15 K				
0	0.92681	0.3810	0	0
0.0774	0.92744	0.3952	0.0735	-0.038
0.1587	0.92858	0.4262	0.1047	-0.070
0.2444	0.92995	0.4834	0.1166	-0.089
0.3347	0.93149	0.5647	0.1134	-0.101
0.4301	0.93314	0.6797	0.0999	-0.101
0.5310	0.93522	0.8284	0.0434	-0.095
0.6378	0.93729	1.0332	-0.0144	-0.071
0.7512	0.93917	1.2861	-0.0550	-0.048
0.8717	0.94072	1.6093	-0.0618	-0.022
1	0.94165	2.0209	0	0
<i>T</i> = 308.15 K				
0	0.91524	0.3491	0	0
0.0774	0.91598	0.3429	0.0759	-0.051
0.1587	0.91713	0.3449	0.1178	-0.102
0.2444	0.91856	0.3668	0.1357	-0.144
0.3347	0.92014	0.4167	0.1404	-0.171
0.4301	0.92193	0.5197	0.1250	-0.162
0.5310	0.92409	0.6539	0.0719	-0.144
0.6378	0.92631	0.8255	0.0103	-0.117
0.7512	0.92828	1.0483	-0.0271	-0.076
0.8717	0.92992	1.3266	-0.0296	-0.030
1	0.93128	1.6564	0	0
<i>T</i> = 318.15 K				
0	0.90225	0.3132	0	0
0.0774	0.90320	0.2682	0.1048	-0.083
0.1587	0.90488	0.2551	0.1457	-0.141
0.2444	0.90674	0.2679	0.1718	-0.182
0.3347	0.90890	0.3083	0.1703	-0.206
0.4301	0.91119	0.3907	0.1565	-0.202
0.5310	0.91380	0.5101	0.1099	-0.178
0.6378	0.91643	0.6546	0.0599	-0.152
0.7512	0.91908	0.8514	0.0064	-0.103
0.8717	0.92146	1.0971	-0.0186	-0.044
1	0.92346	1.3807	0	0
CHN (1) + EA (2)				
<i>T</i> = 298.15 K				
0	0.89455	0.4262	0	0
0.0907	0.89863	0.4607	0.0459	-0.030
0.1833	0.90306	0.5139	0.0584	-0.053
0.2778	0.90769	0.5924	0.0536	-0.064
0.3744	0.91256	0.6973	0.0279	-0.066
0.4730	0.91754	0.8297	-0.0051	-0.060

Chapter VIII

0.5738	0.92293	0.9920	-0.0778	-0.049
0.6769	0.92798	1.1849	-0.1076	-0.037
0.7822	0.93298	1.4117	-0.1260	-0.028
0.8899	0.93759	1.6884	-0.0962	-0.014
1	0.94165	2.0209	0	0
<hr/>				
<i>T</i> = 308.15 K				
0	0.88267	0.3875	0	0
0.0907	0.88663	0.3971	0.0760	-0.045
0.1833	0.89104	0.4367	0.1066	-0.069
0.2778	0.89581	0.4971	0.1018	-0.083
0.3744	0.90088	0.5829	0.0692	-0.085
0.4730	0.90602	0.6939	0.0341	-0.076
0.5738	0.91137	0.8286	-0.0186	-0.063
0.6769	0.91662	0.9866	-0.0541	-0.049
0.7822	0.92170	1.1760	-0.0638	-0.031
0.8899	0.92664	1.3920	-0.0519	-0.020
1	0.93128	1.6564	0	0
<hr/>				
<i>T</i> = 318.15 K				
0	0.86994	0.3564	0	0
0.0907	0.87415	0.3451	0.1002	-0.058
0.1833	0.87892	0.3678	0.1421	-0.089
0.2778	0.88413	0.4180	0.1395	-0.101
0.3744	0.88972	0.4938	0.1004	-0.098
0.4730	0.89521	0.5874	0.0798	-0.089
0.5738	0.90111	0.6972	0.0195	-0.078
0.6769	0.90703	0.8321	-0.0356	-0.059
0.7822	0.91261	0.9932	-0.0430	-0.035
0.8899	0.91812	1.1654	-0.0351	-0.024
1	0.92346	1.3807	0	0
<hr/>				
CHN (1) + MS (2)				
<hr/>				
<i>T</i> = 298.15 K				
0	1.17931	1.5358	0	0
0.1469	1.15497	1.6132	-0.5092	0.014
0.2793	1.13044	1.6852	-0.8422	0.027
0.3992	1.10597	1.7545	-1.0413	0.041
0.5082	1.08166	1.8141	-1.1289	0.048
0.6079	1.05751	1.8639	-1.1147	0.049
0.6993	1.03357	1.906	-1.0112	0.045
0.7834	1.00995	1.9394	-0.8366	0.035
0.8611	0.98676	1.9695	-0.6069	0.024
0.9331	0.96381	1.9962	-0.3069	0.012
1	0.94165	2.0209	0	0
<hr/>				
<i>T</i> = 308.15 K				
0	1.16931	1.4024	0	0
0.1469	1.14342	1.4484	-0.3597	0.011
0.2793	1.11840	1.4912	0.6562	0.022
0.3992	1.09389	1.5296	-0.8635	0.031
0.5082	1.06923	1.5609	-0.9211	0.035
0.6079	1.04518	1.5854	-0.9218	0.034
0.6993	1.02094	1.6047	-0.7855	0.029
0.7834	0.99744	1.6199	-0.6207	0.022
0.8611	0.97477	1.6330	-0.4426	0.014
0.9331	0.95299	1.6454	-0.2650	0.007

Chapter VIII

1	0.93128	1.6564	0	0
$T = 318.15 \text{ K}$				
0	1.15942	1.3027	0	0
0.1469	1.13269	1.3210	-0.2428	0.007
0.2793	1.10771	1.3403	-0.5227	0.016
0.3992	1.08335	1.3565	-0.7252	0.023
0.5082	1.05892	1.3682	-0.7849	0.026
0.6079	1.03477	1.3753	-0.7510	0.026
0.6993	1.01120	1.3789	-0.6641	0.022
0.7834	0.98801	1.3806	-0.5092	0.017
0.8611	0.96552	1.3802	-0.3269	0.011
0.9331	0.94431	1.3796	-0.1905	0.004
1	0.92346	1.3807	0	0

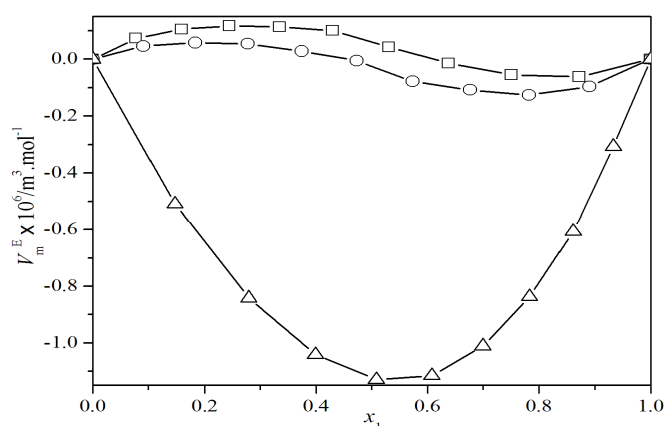


Fig. 8.1. Excess molar volume (V_m^E) versus mole fraction of CHN (x_1) for the binary mixtures of CHN with some esters at $T = 298.15 \text{ K}$. The graphical points represent excess molar volumes (V_m^E) for the mixtures with: \square , MA; \circ , EA; Δ , MS.

At dilute to moderate CHN region V_m^E values augment with increasing mole fraction (x_1) of CHN for the mixtures (CHN + MA) and (CHN + EA) indicating that free volumes amongst the unlike molecules are increasing due to loose packing of the component molecules in the mixtures. This effect is maximum at $x_1 \approx 0.2444$ and $x_1 \approx 0.1833$ for the mixtures (CHN + MA) and (CHN + EA), respectively. However at CHN rich region V_m^E values decrease and become negative for the mixtures (CHN + MA) and (CHN + EA). Hence there is increase in the compactness of the liquid structure due to close packing. This close packing or compactness in the liquid structure may be attributed to: (i) the interstitial accommodation or the geometrical fitting of the ester molecules in the free space or vacancies between the CHN

Chapter VIII

molecules or *vice-versa*, (ii) the dipole-dipole interactions amongst the CHN and the ester molecules and iii) intermolecular hydrogen bond interactions. Furthermore it is seen that although both the mixtures (CHN + MA) and (CHN + EA) follow the similar trend in V_m^E values, the interactions amongst the unlike components in the mixture (CHN + EA) is more compared to those in the mixture (CHN + MA). This may be due to more polar nature of EA compared to that of MA and greater dipole-dipole interactions in the mixture (CHN + EA). On the contrary the V_m^E values for the mixture (CHN + MS) are negative over the entire composition range at all the experimental temperatures. MS is self-associated through dipolar interactions as well as intramolecular hydrogen bonding and the mixing of CHN with MS perturbs the self-associated structure of MS and induce specific hydrogen bond interactions between the -OH group of MS and >C=O group of CHN molecules in the mixture (CHN + MS), strong dipole-dipole interactions as well as interstitial accommodation of CHN molecules in the free space between MS molecules ($V_{m,MS} - V_{m,CHN} = 24.79 \text{ cm}^3 \cdot \text{mol}^{-1}$ at 298.15 K). These effects ultimately increase the intermolecular compactness in this mixture ultimately leading to volume contraction. Therefore, the molecular interactions in the studied binaries follow the order: (CHN + MS) > (CHN + EA) > (CHN + MA). Furthermore, V_m^E values for all the studied mixtures increase with a rise in the experimental temperature from 298.15 to 318.15 K over the entire composition range. Such a temperature dependence of V_m^E values suggests that temperature enhancement reduces or disturbs developing specific and non-specific interactions amongst the component molecules due to thermal agitation.

The partial molar volumes ($\bar{V}_{m,i}$) of the i^{th} component in the mixtures were obtained at 298.15 K from the relation:¹⁴

$$\bar{V}_{m,i} = V_{m,i}^E + V_{m,i}^* + (1 - x_i)(dV_{m,i}^E/dx_i)_{T,P} \quad (2)$$

where $V_{m,i}^*$ is the molar volume of the i^{th} component in the binaries. The derivatives $(\partial V_{m,i}^E/\partial x_i)_{T,P}$ were obtained by following a procedure (as detailed in chapter II) using the Redlich-Kister coefficients (a_i)¹⁵ calculated for the excess molar volumes (V_m^E) for each binary mixture. The coefficients are: $a_0 = 0.2216$, $a_1 = -0.8773$, $a_2 = -0.1140$, $a_3 = -0.1861$ for the mixture (CH + MA); $a_0 = -0.1250$, $a_1 = -0.9933$, $a_2 = -$

Chapter VIII

0.1817, $a_3 = 0.0495$ for the mixture (CH + EA) and $a_0 = -4.5071$, $a_1 = -0.9010$, $a_2 = -0.0375$, $a_3 = 0.5274$ for the mixture (CH + MS) with standard deviations (σ) 0.045, 0.034, 0.054 for the corresponding mixtures, respectively. Partial molar volumes ($\bar{V}_{m,1}^0$ and $\bar{V}_{m,2}^0$) at infinite dilution, excess partial molar volumes ($\bar{V}_{m,i}^E$) and excess partial molar volumes ($\bar{V}_{m,i}^{0,E}$) at infinite dilution were determined at 298.15 K by using the standard relations described in chapter II.

Table 8.3. Molar volumes ($V_{m,1}^*$ and $V_{m,2}^*$), partial molar volumes at infinite dilution ($\bar{V}_{m,1}^0$ and $\bar{V}_{m,2}^0$) and excess partial molar volumes at infinite dilution ($\bar{V}_{m,1}^{0,E}$ and $\bar{V}_{m,2}^{0,E}$) for each component in the binary mixtures at 298.15 K; molar volumes are given in $\text{cm}^3 \cdot \text{mol}^{-1}$.

Parameters	CHN (1) +		
	MA (2)	EA (2)	MS (2)
$V_{m,1}^*$	104.23	104.23	104.23
$\bar{V}_{m,1}^0$	105.40	104.87	100.06
$V_{m,2}^*$	79.93	98.49	129.02
$\bar{V}_{m,2}^0$	78.97	97.24	124.10
$\bar{V}_{m,1}^{0,E}$	1.17	0.64	-4.17
$\bar{V}_{m,2}^{0,E}$	-0.96	-1.25	-4.92

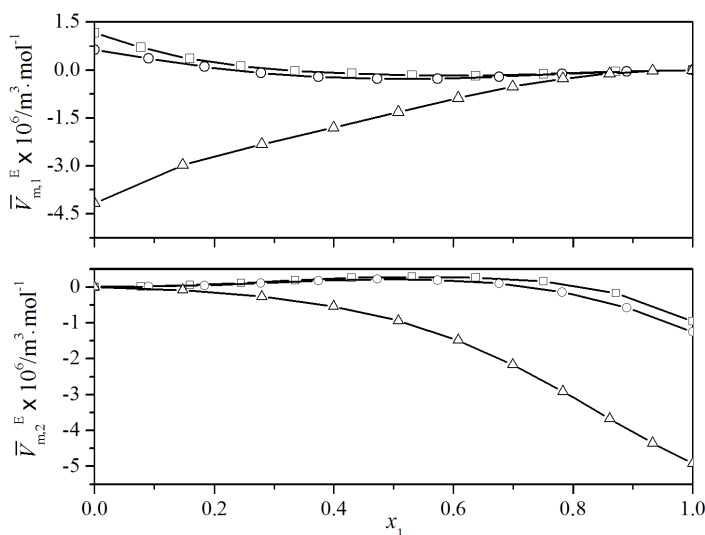


Fig. 8.2. Excess partial molar volume ($\bar{V}_{m,i}^E$) for the i^{th} component against mole fraction of CHN (x_1) for the binary mixtures of CHN with some esters at $T = 298.15$ K. The graphical points represent the $\bar{V}_{m,i}^E$ values for the mixtures with: \square , MA; \circ , EA; Δ , MS.

Chapter VIII

Molar volumes ($V_{m,1}^*$ and $V_{m,2}^*$), partial molar volumes ($\bar{V}_{m,1}^0$ and $\bar{V}_{m,2}^0$) and excess partial molar volumes ($\bar{V}_{m,i}^{0,E}$) at infinite dilution for each component in the mixtures at 298.15 K are listed in Table 8.3. Excess partial molar volumes ($\bar{V}_{m,1}^E$ and $\bar{V}_{m,2}^E$) of each component in the binary mixtures are depicted in Figure 8.2 against the mole fraction (x_1) of CHN. Figure 8.2 shows that $\bar{V}_{m,1}^E$ values gradually decrease (*i.e.*, decreasing trend as the alkyl chain length increases⁹) but $\bar{V}_{m,2}^E$ values increase with increasing mole fraction (x_1) of CHN for the mixtures studied. Partial molar volumes ($\bar{V}_{m,1}^0$) at infinite dilution for CHN in the mixtures (CHN + MA) and (CHN + EA) were found to be greater than its molar volume but those ($\bar{V}_{m,2}^E$) of the esters (MA and EA) were found to be lower than their respective molar volumes. These results corroborate with the interstitial accommodation of these ester molecules in the voids of CHN molecules and these ester molecules suffer volume contraction. Partial molar volumes ($\bar{V}_{m,1}^0$ and $\bar{V}_{m,2}^0$) at infinite dilution for both the components in the mixture (CHN + MS) were found to be lower than their respective molar volumes. These results, therefore, suggest the following order of packing efficiency or structure compactness in the mixtures: (CHN + MA) < (CHN + EA) < (CHN + MS).

8.3.2. Predictions of excess molar volumes

i) Prigogine-Flory-Patterson theory (PFP):

The Prigogine-Flory-Patterson (PFP) theory^{5,6} can be used successfully to correlate, predict and estimate the excess molar volumes (V_m^E) of the binary mixtures theoretically. The interaction parameters ($\chi_{1,2}$) needed for the prediction of V_m^E values were obtained as described in chapter II and was adjusted by fitting the experimental V_m^E values over the entire composition at 298.15 K. According to this theory the excess molar volume (V_m^E) originates from a combination of interactional, a free volume and internal pressure contributions and V_m^E is given by:

Chapter VIII

$$\begin{aligned}
 \frac{V_m^E}{x_1V_1^* + x_2V_2^*} &= \frac{(\tilde{v}^{1/3} - 1)\tilde{v}^{2/3}\psi_1\theta_2}{[(4/3)\tilde{v}^{-1/3} - 1]P_1^*} \chi_{1,2} && \text{(interaction contribution)} \\
 &- \frac{(\tilde{v}_1 - \tilde{v}_2)^2[(14/9)\tilde{v}^{-1/3} - 1]\psi_1\psi_2}{[(4/3)\tilde{v}^{-1/3} - 1]\tilde{v}} && \text{(free volume contribution)} \\
 &+ \frac{(\tilde{v}_1 - \tilde{v}_2)(P_1^* - P_2^*)\psi_1\psi_2}{(P_1^*\psi_2 + P_2^*\psi_1)} && \text{(internal pressure contribution)} \quad (3)
 \end{aligned}$$

where ψ_1 and ψ_2 stand for the molecular contact energy fractions of liquid 1 and liquid 2 in a mixture; θ_2 is the molecular site fraction of liquid 2 in a mixture and other symbols have their usual significance.^{5,6} Various characteristic and reduced parameters of the pure liquid components such as reduced volume (\tilde{v}), reduced temperature (\tilde{T}), characteristic volume (V^*), characteristic pressure (P^*) and characteristic temperature (T^*) for each liquid component (needed for the V_m^E estimation) were calculated using Flory's formalism¹⁶⁻¹⁹ and are listed in Table 8.4.

Table 8.4. Isobaric molar heat capacities (c_p), expansion coefficient (α), isothermal compressibility (κ_T) and Flory's parameters for pure liquids at 298.15 K.

Liquids	c_p^a	\tilde{v}	\tilde{T}	$V^* \cdot 10^6$ ($\text{m}^3 \cdot \text{mol}^{-1}$)	P^* (Pa)	T^* (K)	α (kK^{-1})	κ_T (TPa^{-1})
CH	182.16	1.2407	0.0559	84.01	637.72	5333.17	0.9659	695.1
MA	141.93	1.3107	0.0658	60.98	609.89	4530.98	1.3250	1112.8
EA	170.66	1.3199	0.0670	74.62	605.88	4452.90	1.3756	1179.3
MS	249.06	1.2147	0.0517	106.22	692.34	5769.79	0.8433	535.8

^aValues adapted from Ref. [13] were multiplied with molecular weight for unit conversion.

The interaction contributions to V_m^E were obtained from Eq. (3) by using a computer program as detailed in chapter II. The optimized $\chi_{1,2}$ values, calculated and experimental V_m^E values, their deviation and different contributions to V_m^E values at equimolar ($x_1 \approx 0.5$) composition at 298.15 K are given in Table 8.5. It reveals that the calculated excess molar volumes ($V_{m,\text{PF}}^E$) reasonably agree with the experimental excess molar volumes (V_m^E) for all the mixtures studied.

Chapter VIII

Table 8.5. Interaction parameters ($\chi_{1,2}$), calculated and experimental values of excess molar volumes ($V_{m,\text{exp}}^E$ and $V_{m,\text{PFP}}^E$), their deviations (ΔV_m^E) and different contributions at 298.15 K.

CHN(1) +	$\chi_{1,2}$ (J·mol ⁻¹)	$V_{m,\text{exp}}^E \cdot 10^6$ (m ³ ·mol ⁻¹)	$V_{m,\text{PFP}}^E \cdot 10^6$ (m ³ ·mol ⁻¹)	$\Delta V_m^E \cdot 10^6$ (m ³ ·mol ⁻¹)	PFP contributions ×10 ³		
					int ^a	fv ^b	ip ^c
MA (2)	17.291	0.043	0.043	0.000	0.0031	0.0017	-0.0007
EA (2)	17.046	-0.005	-0.005	0.000	0.0033	0.0023	-0.0010
MS (2)	-78.873	-1.1289	-1.1289	0.000	-0.0111	0.0002	-0.0005

^a interaction contribution; ^b free volume contribution; ^c internal pressure contribution

ii) *Peng-Robinson Equation of State* (PR-EOS):

Cubic equation of states are more commonly used in process simulations to correlate the solution properties and phase equilibria of hydrocarbon systems because they offer the best balance between accuracy, reliability, simplicity, computational efficiency and can also be extended to the liquid mixtures with different mixing or combination rules. Herein this chapter the classical cubic Peng-Robinson equation of state (PREOS) was used for correlating the excess molar volumes ($V_{m,\text{PR-EOS}}^E$) of the mixtures at 298.15 K. The two parametric PR-EOS is given by the relation:⁸

$$P = \frac{RT}{V-b} - \frac{a}{V(V+b)+b(V-b)} \quad (4)$$

For a pure component the attraction parameter (a) and co-volume parameters (b) were obtained by using the standard relations as detailed in chapter II. However, acentric factor (ω) for each pure liquid was calculated from the relation:²⁰

$$\omega = \frac{3T_{br}}{7(1-T_{br})} \log P_c - 1 \quad (5)$$

where $T_{br} = T_b / T_c$ and T_b is the boiling point of a pure liquid. T_b , T_c and P_c values were taken from the literature.¹³ For a binary mixture, the attraction parameter (a) and co-volume (b) parameters are given by the relations:²⁰

$$a(T) = \sum_{i=1}^2 \sum_{j=1}^2 x_i x_j \sqrt{a_i a_j} (1 - k_{ij}) \quad (6)$$

$$b(T) = \sum_{i=1}^2 x_i b_i \quad (7)$$

Chapter VIII

where k_{ij} is the interaction coefficient for a binary mixture of components i and j and $k_{ij} = 0$ for $i = j$. On rearrangement in terms of the compressibility factor ($Z = PV/RT$), Eq. (4) becomes:

$$Z^3 - (1 - B)Z^2 + (A - 3B^2 - 2B)Z - (AB - B^2 - B^3) = 0 \quad (8)$$

where $B = Pb/RT$ and $A = aP/(RT)^2$. Thus from a knowledge of the compressibility factors of both the pure components and their mixtures the corresponding excess molar volumes ($V_{m,PR-EOS}^E$) of the binary mixtures were determined. The values of the interaction coefficient (k_{ij}) were found to be 0.0449, 0.0426 and -0.1672 with standard deviations (σ) 0.041, 0.055 and 0.069, respectively for the mixtures (CHN + MA), (CHN + EA) and (CHN + MS). A comparison between the experimental excess molar volumes (V_m^E) and the calculated excess molar volumes ($V_{m,PFP}^E$ and $V_{m,PR-EOS}^E$) as a function of mole fraction (x_1) of CHN for the studied mixtures at 298.15 K is depicted in Figure 8.3 and it is evident that the calculated excess molar volumes reasonably agree with the experimental excess molar volumes for all the studied mixtures.

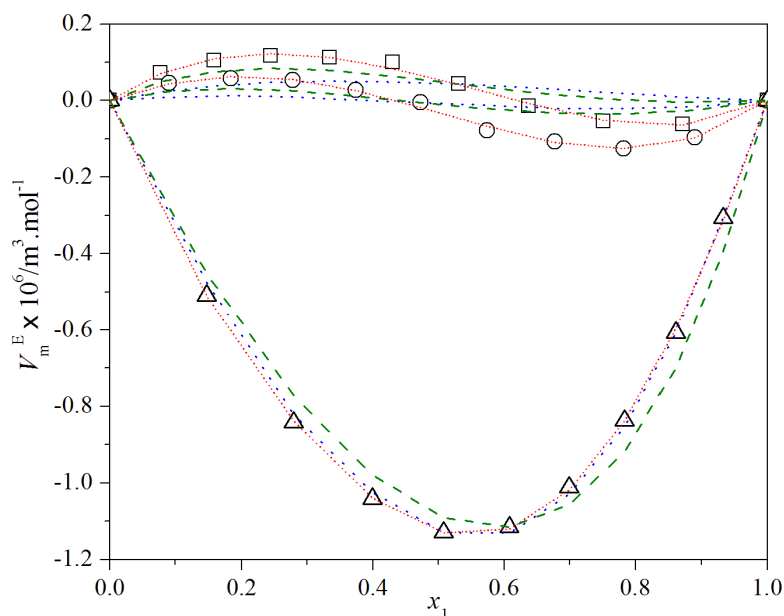


Fig. 8.3. A comparison between the excess molar volumes (V_m^E) versus mole fraction of CHN (x_1) for the binary mixtures of CHN (1) with some esters (2) at $T = 298.15$ K. The symbols represent experimental V_m^E values for the mixtures with: \square , MA; \circ , EA; Δ , MS. Olive dashed lines, PR-EOS; blue dotted lines, PFP; red short dotted lines, Redlich-Kister polynomial.

Chapter VIII

8.3.3. Viscosity deviation

The viscosity deviations ($\Delta\eta$) can be calculated by finding the difference between the measured viscosity (η) and the ideal viscosity (η_{id}) of a mixture as follows:

$$\Delta\eta = \eta - \eta_{id} \quad (9)$$

and the ideal viscosity (η_{id}) is given by:²¹

$$\eta_{id} = \exp\left(\sum_{i=1}^2 x_i \ln \eta_{id}\right) \quad (10)$$

The uncertainty in viscosity deviation ($\Delta\eta$) was evaluated to be ± 0.004 mPa s. Figure 8.4 ($\Delta\eta$ versus x_1 at 298.15 K) shows that the $\Delta\eta$ values are negative for the mixtures (CHN + MA) and (CHN + EA) but positive for the mixture (CHN + MS) over the entire composition range. Similar composition dependence of $\Delta\eta$ values was observed at other experimental temperatures. The negative $\Delta\eta$ values suggest the easier flow of a liquid mixture in comparison to individual pure liquids. This is possibly due to the breaking of liquid order on mutual mixing and unfavorable nonspecific interactions amongst the unlike molecules. The positive $\Delta\eta$ values suggest the presence of strong intermolecular interactions amongst the unlike molecules leading to more compact structure.

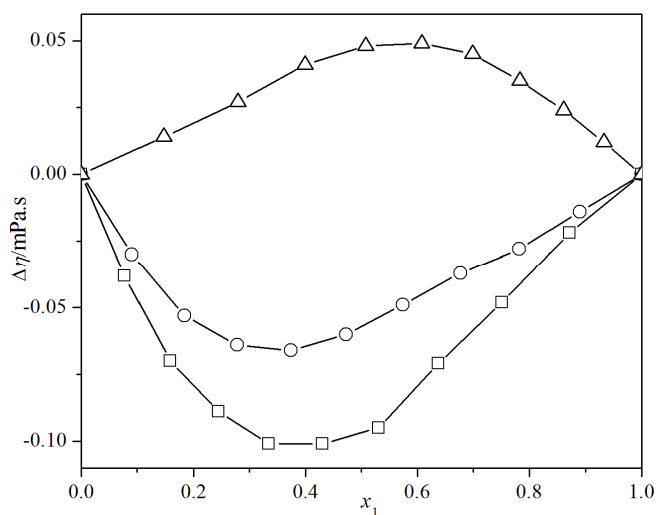


Fig. 8.4. Viscosity deviations ($\Delta\eta$) versus mole fraction of CHN (x_1) for the binary mixtures of CHN with some esters at $T = 298.15$ K. The symbols represent the $\Delta\eta$ values for the mixtures with: \square , MA; \circ , EA; Δ , MS.

Chapter VIII

Negative $\Delta\eta$ values for the mixtures (CHN + MA) and (CHN + EA) at dilute CHN range may be due to the molecular unpacking and unfavorable nonspecific interaction amongst the unlike components in the mixture. This effect is maximum at $x_1 \approx 0.3347$ and $x_1 \approx 0.3744$ for the mixtures (CHN + MA) and (CHN + EA), respectively at all the experimental temperatures. Beyond these compositions, however, the $\Delta\eta$ values increase due to increased dipole-dipole interactions and interstitial accommodation at CHN rich regions. On the contrary positive $\Delta\eta$ values for the mixture (CHN + MS) over the entire composition range suggest that the mixing of CHN with MS is characterized by strong intermolecular interactions amongst the component molecules due to dipole-dipole interactions, specific hydrogen bond interactions as well as interstitial accommodation. Thus the $\Delta\eta$ values also suggest the following order of molecular interactions in the mixtures: (CHN + MS) > (CHN + EA) > (CHN + MA). However, for each mixture the $\Delta\eta$ values decrease with a rise in the experimental temperatures and thus the molecular interactions amongst the dissimilar components become weaker at higher temperatures (Table 8.2.).

8.3.4. Thermodynamics of viscous flow

It is useful to study the activation parameters of viscous flow for a better understanding of different possible physico-chemical interactions prevailing in the mixtures and such parameters can be evaluated using viscosities of the mixtures in terms of Eyring's theory of absolute reaction rate²¹ as expressed by the relation:

$$\eta = \left(\frac{hN}{V} \right) \exp\left(\frac{\Delta G^*}{RT} \right) \quad (11)$$

Substituting $\Delta G^* = \Delta H^* - T\Delta S^*$ in Eq. (11), we get:

$$R \ln\left(\frac{\eta V}{hN} \right) = \frac{\Delta H^*}{T} - \Delta S^* \quad (12)$$

where N is Avogadro's number, h is Planck's constant, ΔG^* , ΔH^* and ΔS^* are the activation free energy, enthalpy and entropy for viscous flow and other symbols have their usual meanings. Therefore linear regressions of $R \ln(\eta V/hN)$ against $(1/T)$ yield the enthalpy (ΔH^*) and entropy (ΔS^*) of activation of viscous flow from the corresponding slope and intercept, respectively.

Chapter VIII

Again the excess free energy of activation of viscous flow of the mixtures (ΔG^{*E}) can be had from the relation:

$$\Delta G^{*E} = \Delta G^* - \sum_{i=1}^2 (x_i \Delta G_i^{*E}) \quad (13)$$

ΔG^* , ΔH^* , ΔS^* and the regression coefficients (R^2) are given in Table 8.6. Table 8.6 manifests that ΔH^* values are positive for all the mixtures but ΔS^* values are mostly negative for the mixtures (CHN + EA) and (CHN + MS) except the mixture (CHN + MA). Interestingly ΔS^* values decrease or become more negative in the order: (CHN + MA) > (CHN + EA) > (CHN + MS) in parallel to the extent of molecular compactness as discussed above. Excess free energies of activation of viscous flow (ΔG^{*E}) were plotted in Figure 8.5 against the mole fraction (x_1) of CHN for all the mixtures at 298.15 K. According to Reid and Taylor²² positive ΔG^{*E} may be ascribed to molecular interactions or structural compactness due to geometrical fittings of one component into the other's structure in the mixture and negative ΔG^{*E} values may be ascribed to the dominance of dispersion forces allowing easier fluid flow.

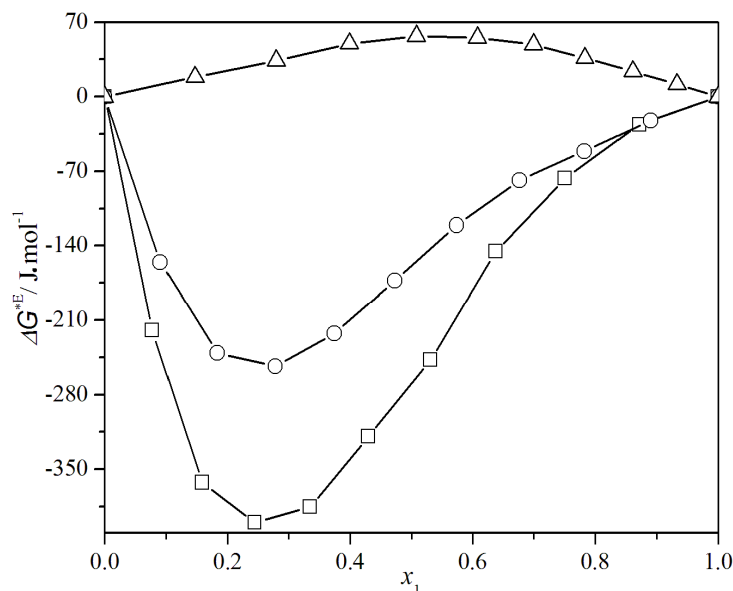


Fig. 8.5. Excess free energy of activation of viscous flow (ΔG^{*E}) versus mole fraction of CH (x_1) for the binary mixtures of CHN with some esters at $T = 298.15$ K. The symbols represent the ΔG^{*E} values for the mixtures with: \square , MA; \circ , EA; Δ , MS.

Chapter VIII

Table 8.6. Free energy (ΔG^*), enthalpy (ΔH^*) and entropy (ΔS^*) of activation of viscous flow for the binary mixtures; x_1 -mole fraction of CHN.

x_1	ΔG^* (kJ·mol ⁻¹)			ΔH^* (kJ·mol ⁻¹)	ΔS^* (J·K ⁻¹ ·mol ⁻¹)	R^2
	298.15 K	308.15 K	318.15 K			
	CHN (1) + MA (2)					
0	10.744	10.914	11.019	6.647	-13.777	0.9927
0.0774	10.896	10.929	10.671	14.193	10.907	0.9677
0.1587	11.143	11.006	10.601	19.174	26.797	0.9848
0.2444	11.516	11.227	10.794	22.253	35.938	0.9967
0.3347	11.964	11.618	11.231	22.890	36.624	0.9997
0.4301	12.487	12.250	11.923	20.881	28.104	0.9986
0.5310	13.043	12.905	12.696	18.195	17.243	0.9988
0.6378	13.657	13.570	13.425	17.099	11.515	0.9991
0.7512	14.269	14.254	14.193	15.405	3.784	0.9993
0.8717	14.898	14.932	14.938	14.287	-2.063	0.9997
1	15.539	15.579	15.625	14.254	-4.308	0.9999
CHN (1) + EA (2)						
0	11.541	11.718	11.915	5.956	-18.721	0.9991
0.0907	11.748	11.796	11.845	10.303	-4.844	0.9999
0.1833	12.032	12.053	12.026	12.113	0.246	0.9988
0.2778	12.398	12.398	12.377	12.709	1.033	0.9998
0.3744	12.815	12.819	12.829	12.609	-0.688	0.9999
0.4730	13.259	13.279	13.300	12.647	-2.052	0.9999
0.5738	13.714	13.746	13.765	12.960	-2.536	0.9999
0.6768	14.169	14.206	14.244	13.037	-3.794	0.9999
0.7822	14.617	14.670	14.726	12.995	-5.439	0.9999
0.8899	15.076	15.117	15.162	13.791	-4.307	0.9999
1	15.539	15.579	15.625	14.254	-4.308	0.9999
CHN (1) + MS (2)						
0	15.387	15.693	16.029	5.825	-32.055	0.9977
0.1469	15.428	15.695	15.986	7.116	-27.869	0.9991
0.2793	15.464	15.696	15.949	8.232	-24.245	0.9995
0.3992	15.498	15.694	15.912	9.333	-20.665	0.9996
0.5082	15.521	15.687	15.873	10.289	-17.538	0.9997
0.6079	15.535	15.672	15.831	11.134	-14.750	0.9997
0.6993	15.543	15.655	15.787	11.905	-12.189	0.9998
0.7834	15.543	15.635	15.744	12.538	-10.068	0.9998
0.8611	15.542	15.614	15.701	13.164	-7.966	0.9999
0.9331	15.541	15.596	15.660	13.764	-5.955	0.9999
1	15.539	15.579	15.625	14.254	-4.308	0.9999

Therefore the observed negative ΔG^{*E} values (Figure 8.5) suggest the easier viscous flow for the mixtures (CHN + MA) and (CHN + EA) as compared to the mixture (CHN + MS). Similar composition dependence of ΔG^{*E} values was observed at other experimental temperatures.

Chapter VIII

8.3.5. Viscosity correlation

Several empirical and semi-empirical relations are used to represent the composition dependence of viscosity in binary liquid mixtures as well as to simulate the viscosity of liquids or liquid mixtures.²³ Such empirical methods have also been developed using the corresponding state principle based on van der Waals' hypothesis.²⁴ Herein this chapter the experimental viscosities at 298.15 K were correlated with models like Bloomfield-Dewan,⁷ cubic equation of state based Peng-Robinson,⁸ Grunberg-Nissan,²⁵ and Katti-Choudhury.²⁶

i) *Peng-Robinson Equation of State (PR-EOS)*:

In this viscosity model Eyring's viscosity expression for liquid mixtures is coupled with Peng-Robinson equation of state. The final form of the viscosity expression is given by:²⁷

$$\eta = \frac{(\eta V)^{\text{id}}}{V_m} \exp \left[\sum_{i=1}^2 x_i (\ln \varphi_i - \ln \varphi_i^0) + \frac{1}{2} \sum_{i=1}^2 \sum_{j=1}^2 x_i x_j g_{ij} \right] \quad (14)$$

where V_m , $(\eta V)^{\text{id}}$, φ_i^0 , φ_i and g_{12} ($g_{ii} = 0$ and $g_{ij} = g_{ji}$) are the molar volume, kinematic viscosity of an ideal mixture, fugacity coefficients of the i^{th} component in pure state, fugacity coefficients of the i^{th} component in a mixture and binary interaction parameter, respectively. The details of the model have been described in chapter II. In order to obtain the binary interaction parameter (g_{12}), a non-linear regression analysis was performed to have minimum standard deviation (σ) for a binary mixture. The binary interaction parameters (g_{12}) were found to be -0.571 ($\sigma = 0.055$), -0.505 ($\sigma = 0.033$) and -0.131 ($\sigma = 0.002$) for the mixtures (CHN + MA), (CHN + EA) and (CHN + MS), respectively.

ii) *Bloomfield-Dewan viscosity model*:

Bloomfield and Dewan developed this model by combining the absolute reaction rate theory²¹ and the free volume theory,²⁸ which treats the properties of a mixture in terms of reduced properties of the pure components. The expression proposed for the viscosity deviation ($\Delta \ln \eta$) of a mixture is given by:

$$\Delta \ln \eta = f(\tilde{v}) - \frac{\Delta G^R}{RT} \quad (15)$$

$$\Delta \ln \eta = \ln \eta - \sum_{i=1}^2 (x_i \eta_i) \quad (16)$$

Chapter VIII

where $f(\tilde{v})$ and ΔG^R are the characteristic function of the free volume and the residual free energy of mixing, respectively. These quantities were obtained by using the standard literature relations.²⁸ Based on Flory's statistical thermodynamic theory for liquid mixtures,¹⁶⁻¹⁹ the excess energy ΔG^E can be obtained from the relation:

$$\Delta G^E = \sum_{i=1}^2 x_i P_i^* V_i^* [(1/\tilde{v}_i - 1/\tilde{v}) + 3\tilde{T}_i \ln\{(\tilde{v}_i^{1/3} - 1)/(\tilde{v}^{1/3} - 1)\}] + (x_1 \theta_2 V_1^* \chi_{12})/\tilde{v} \quad (17)$$

The standard deviations (σ) between the experimental viscosities and those calculated from Bloomfield and Dewan model were 0.115, 0.207 and 0.189 for the mixtures of (CHN + MA), (CHN + EA) and (CHN + MS), respectively. Experimental viscosities were also correlated with Grunberg-Nissan (GN) and Katti-Chaudhri (KC) viscosity models at 298.15 K using required regressions. While Grunberg-Nissan parameters (d_{12}) were determined to be -0.546 ($\sigma = 0.058$), -0.307 ($\sigma = 0.350$) and 0.102 ($\sigma = 0.003$); Katti-Chaudhri parameter (W_{vis}/RT) were found to be -105.52 ($\sigma = 0.057$), -63.65 ($\sigma = 0.034$) and 17.76 ($\sigma = 0.002$), respectively for the mixtures (CHN + MA), (CHN + EA) and (CHN + MS). The variations of experimental and theoretical viscosities with the mole fraction (x_1) of CHN at 298.15 K are depicted in Figure 8.6.

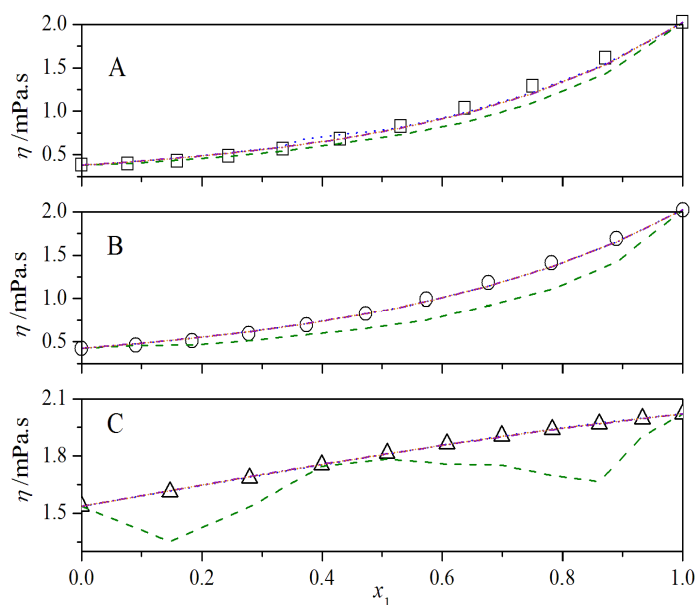


Fig. 8.6. A comparison between the viscosities (η) versus mole fraction of CHN (x_1) for the binary mixtures at $T = 298.15$ K: A, CHN (1) + MA (2); B, CHN (1) + EA (2); C, CHN (1) + MS (1). The symbols represent experimental η values for the mixtures with: \square , MA; \circ , EA; Δ , MS. Olive dashed lines, BF; blue dotted lines, PREOS; violet dash dotted lines, GN; orange short dotted lines, KC.

Chapter VIII

8.3.6. Ultrasonic speed of sound and derived functions

The ultrasonic speed of a liquid is fundamentally related to binding forces amongst component molecules and has been successfully employed to provide qualitative information regarding the physical nature and strength of molecular interactions in pure liquid as well as in liquid mixtures. The experimental speeds of sound (u) and the densities (ρ) of the binary mixtures at 298.15 K were used to determine the isentropic compressibilities (κ_s) and other acoustic parameters along with the corresponding excess or deviation functions. The excess isentropic compressibilities (κ_s^E) were obtained from the relation:

$$\kappa_s^E = \kappa_s - \kappa_s^{\text{id}} \quad (18)$$

where κ_s is the isentropic compressibility and was calculated using the Laplace relation, $\kappa_s = 1/\rho u^2$ and κ_s^{id} is the isentropic compressibility for an ideal mixture. According to Benson and Kiyohara²⁹ and Acree,³⁰ κ_s^{id} is given by the relation:

$$\kappa_s^{\text{id}} = \sum_{i=1}^2 \tau_i \left[\kappa_{s,i} + \frac{TV_{m,i}^* \alpha_i^2}{c_{p,i}} \right] - \left\{ \frac{T \sum_{i=1}^2 (x_i V_{m,i}^*) \sum_{i=1}^2 (\tau_i \alpha_i)^2}{\sum_{i=1}^2 (x_i c_{p,i})} \right\} \quad (19)$$

where τ_i is the volume fraction of the i^{th} component in the mixture, $\kappa_{s,i}$, $V_{m,i}^*$, α_i and $c_{p,i}$ are the isentropic compressibility, molar volume, isobaric expansion coefficient and molar isobaric heat capacity of the pure components, respectively. Isobaric expansion coefficients (α_i) were obtained from experimental densities and $c_{p,i}$ values were adapted from the literature.¹³ The other acoustic parameters like intermolecular free lengths (L_f) and free volumes (V_f) and their excess values were calculated as described in chapter II. The parameters u , κ_s and κ_s^E at 298.15 K are listed in Table 8.7. The experimental speeds of sound of each pure liquid were in good agreement with the literature values³¹⁻³⁴ at 298.15 K. Figure 8.7 represents the variation of excess isentropic compressibilities (κ_s^E) of the mixtures against the mole fraction (x_1) of CHN at 298.15 K. While excess isentropic compressibilities (κ_s^E) for the mixture (CHN + MA) were mostly positive, those for the mixtures (CHN + EA) and (CHN + MS) were mostly negative. Positive κ_s^E values for the mixture (CHN + MA) suggest perturbation of the associated structures or molecular order in the pure liquids leading

Chapter VIII

Table 8.7. Ultrasonic speeds (u), isentropic compressibilities (κ_s), intermolecular free lengths (L_f), free volumes (V_f), excess isentropic compressibilities (κ_s^E), excess intermolecular free lengths (L_f^E) and excess free volumes (V_f^E) for the binary mixtures at 298.15 K; x_1 -mole fraction of CHN.

x_1	u /m · s ⁻¹	κ_s /TPa ⁻¹	$L_f/\text{Å}$	$V_f \cdot 10^8$ /m ³ · mol ⁻¹	κ_s^E /TPa ⁻¹	$L_f^E/\text{Å}$	$V_f^E \cdot 10^8$ /m ³ · mol ⁻¹
CHN (1) + MA (2)							
0	1148.5	818.0	0.5883	37.70	0	0	0
0.0774	1148.8	817.0	0.5879	37.04	25.1	0.0083	1.76
0.1587	1155.3	806.8	0.5842	34.65	41.4	0.0138	1.92
0.2444	1170.9	784.3	0.5760	30.44	45.9	0.0152	0.39
0.3347	1193.0	754.3	0.5649	25.81	43.3	0.0142	-1.40
0.4301	1223.3	716.1	0.5504	21.15	33.1	0.0104	-3.77
0.5310	1256.8	676.9	0.5351	17.08	22.4	0.0064	-3.99
0.6378	1295.9	635.3	0.5184	13.42	9.6	0.0017	-4.31
0.7512	1334.5	597.9	0.5029	10.56	1.6	-0.0011	-3.61
0.8717	1371.3	565.3	0.4890	8.23	-1.0	-0.0015	-2.17
1	1407.7	535.9	0.4761	6.38	0	0	0
CHN (1) + EA (2)							
0	1144.3	853.7	0.6010	41.09	0	0	0
0.0907	1160.7	826.0	0.5911	37.93	0.3	0.0015	-0.01
0.1833	1177.9	798.1	0.5811	33.43	0.7	0.0030	-1.30
0.2778	1197.4	768.4	0.5701	28.13	0.4	0.0039	-3.32
0.3744	1220.1	736.1	0.5580	23.02	-1.5	0.0038	-5.08
0.4730	1247.3	700.5	0.5444	18.63	-5.9	0.0025	-6.05
0.5738	1277.8	663.6	0.5298	15.02	-10.7	0.0005	-6.16
0.6768	1311.3	626.7	0.5149	12.16	-14.5	-0.0016	-5.44
0.7822	1346.5	591.2	0.5001	9.89	-15.9	-0.0032	-4.05
0.8899	1379.6	560.4	0.4869	7.97	-11.6	-0.0030	-2.23
1	1407.7	535.9	0.4761	6.38	0	0	0
CHN (1) + MS (2)							
0	1410.9	426.0	0.4245	18.66	0	0	0
0.1469	1421.1	428.7	0.4259	16.17	-11.4	-0.0062	-0.69
0.2793	1427.5	434.1	0.4285	14.13	-19.4	-0.0104	-1.10
0.3992	1430.8	441.7	0.4323	12.41	-24.3	-0.0129	-1.35
0.5082	1430.4	451.8	0.4372	11.01	-26.0	-0.0135	-1.41
0.6079	1424.3	466.1	0.4441	9.83	-22.8	-0.0118	-1.37
0.6993	1419.5	480.2	0.4507	8.88	-19.2	-0.0099	-1.20
0.7834	1413.9	495.3	0.4577	8.09	-14.0	-0.0072	-0.95
0.8611	1412	508.3	0.4637	7.44	-10.4	-0.0053	-0.64
0.9331	1409.7	522.1	0.4700	6.88	-5.4	-0.0027	-0.32
1	1407.7	535.9	0.4761	6.38	0	0	0

Chapter VIII

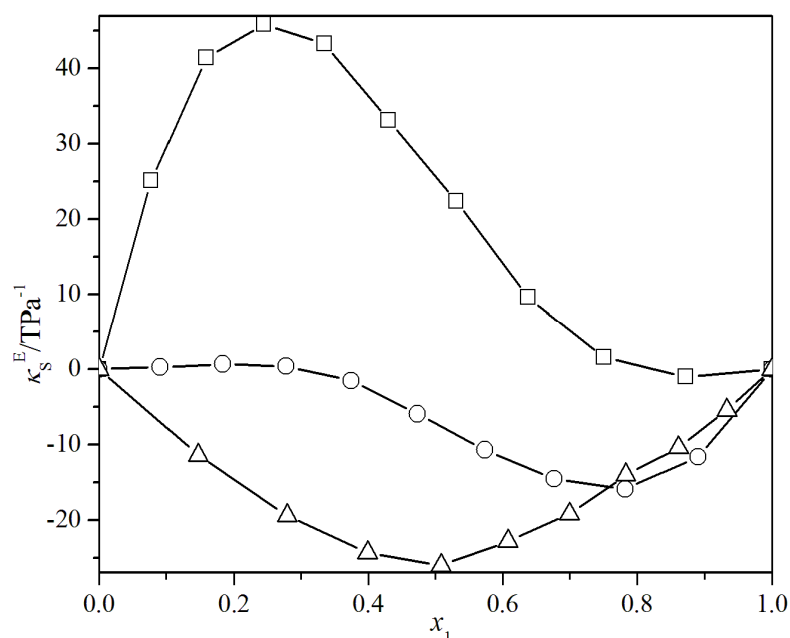


Fig. 8.7. Excess isentropic compressibility (κ_s^E) versus mole fraction of CHN (x_1) for the binary mixtures of CH + some esters at $T = 298.15$ K. The graphical points represent the κ_s^E values for the mixtures with: \square , MA; \circ , EA; \triangle , MS.

to breaking up of the weak dipole-dipole cohesive forces operating amongst the similar molecules on mutual mixing. Negative κ_s^E values for the mixtures (CHN + EA) and (CHN + MS) are associated with structure making or more compact packing of the dissimilar molecules due to combined effects of specific hydrogen bond interactions, dipole-dipole interactions and interstitial accommodation. It is interesting that the speeds of sound (u) increase as the molecular compactness increase for the mixtures. Furthermore, the intermolecular free length, *i.e.*, the distance between the surfaces of neighboring molecules, is generally found to show an opposite behavior to those of ultrasonic speeds, *i.e.*, the decrease in intermolecular free length increases the ultrasonic speeds and acoustic impedances. The decrease in intermolecular free length and increase in ultrasonic speeds and acoustic impedances signify the molecular interactions amongst the component molecules in the mixtures. Variations of these acoustic parameters and the corresponding excess functions with mole fractions (x_1) of CHN at 298.15 K are in Table 8.7. The perusal of Table 8.7 shows that the excess free lengths (L_f^E) are positive in the ester rich region and negative in CHN rich region

Chapter VIII

for the mixtures (CHN + MA) and (CHN + EA) but are negative for the mixture (CHN + MS) throughout the entire composition range at 298.15 K. Interestingly, it was observed that free volumes (V_f) and excess free volumes (V_f^E) for the mixtures studied followed the order: (CHN + MA) > (CHN + EA) > (CHN + MS), *i.e.*, the reversed order of molecular interactions in parallel to the degree of their structural compactness. Thus the study of the various acoustic and their excess functions also stand in support of the order of molecular interactions discussed on the basis of excess molar volumes and viscosity deviations.

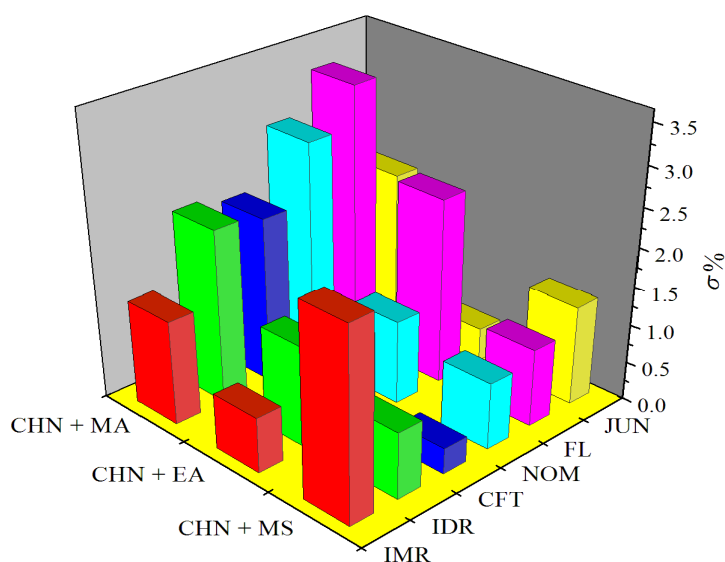


Fig. 8.8. Percent standard deviations ($\sigma\%$) for theoretical prediction of ultrasonic speeds by different empirical relations at $T = 298.15$ K for the binary mixtures studied.

8.3.7. Prediction of ultrasonic speed of sound

The experimentally determined ultrasonic speeds (u) of sound for the studied mixtures were compared with the ultrasonic speeds obtained from Flory theory (FL), Collision factor theory (CFT), Nomoto relation (NOM), Impedance dependence relation (IDR), Ideal mixture relation (IMR) and Junjie's relation (JUN). These empirical models are well described in chapter II. A comparison of the percent standard deviations ($\sigma\%$) reveals that predictive capabilities of these models follow the order: FL > IMR > JUN > CFT > IDR > NOM (for CHN + MA mixture); JUN > IMR > NOM > CFT > IDR > FL (for CHN + EA mixture) and CFT > NOM \approx IDR > JUN > IMR > FL (for CHN + MS mixture), respectively (Figure 8.8.).

Chapter VIII

8.3.8. Excess molar refractions

The study of refractive indices (n_D), molar refractions (R_m) and the excess molar refractions (R_m^E) plays an important role in explaining the molecular interactions in the binary mixtures. The excess molar refractions (R_m^E) for the mixtures were obtained from relation:³⁵

$$R_m^E = R_m - \sum_{i=1}^2 (x_i R_{m,i}) \quad (20)$$

where $R_{m,i} = \{(n_{D,i}-1)/(n_{D,i}+2)\}M_i/\rho_i$, $n_{D,i}$ and ρ_i stand for the molar refraction, refractive index and density of the i th component in the mixture, respectively. The molar refractions (R_m) for a mixture can be had from the relation:³⁵

$$R_m = \frac{n_D^2 - 1}{n_D^2 + 2} \frac{\sum_{i=1}^2 x_i M_i}{\rho} \quad (21)$$

where ρ and n_D are the mixture density and refractive index; M_i stands for the molar mass of i th component in a mixture, respectively. Molar refractions (R_m), excess molar refractions (R_m^E) and the experimental refractive indices (n_D) for the three binaries are listed in Table 8.8. The experimental refractive indices (n_D) of the pure liquids were in good agreement with literature values^{12,31,36} at 298.15 K and the trends in excess molar refractions (R_m^E) for the binary mixtures with respect to composition were found to be in line with the molecular interactions discussed above.

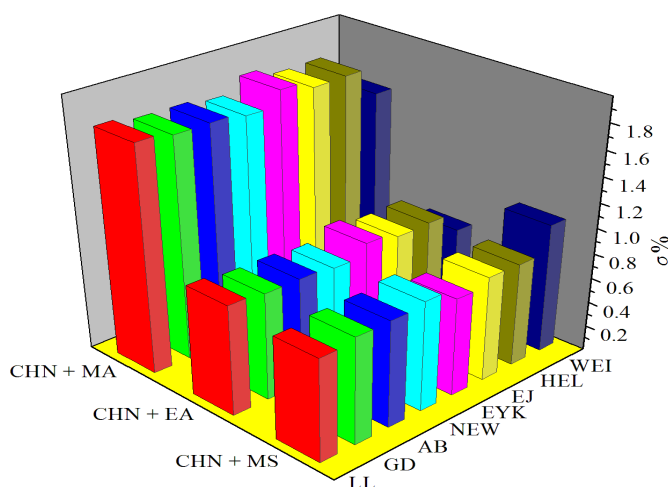


Fig. 8.9. Percent standard deviations ($\sigma\%$) for theoretical prediction of refractive indices by various models at $T = 298.15$ K for the binary mixtures studied.

Chapter VIII

Table 8.8. Refractive indices (n_D), molar refractions (R_m) and excess molar refractions (R_m^E) for the binary mixtures at 298.15 K; x_1 -mole fraction of CHN.

x_1	n_D	$R_m \cdot 10^6$ ($\text{m}^3 \cdot \text{mol}^{-1}$)	$R_m^E \cdot 10^6$ ($\text{m}^3 \cdot \text{mol}^{-1}$)
CHN (1) + MA (2)			
0	1.3604	17.658	0
0.0774	1.3808	19.003	0.550
0.1587	1.4001	20.342	1.054
0.2444	1.4181	21.674	1.506
0.3347	1.4328	22.908	1.813
0.4301	1.4428	23.978	1.904
0.5310	1.4489	24.907	1.797
0.6378	1.4506	25.671	1.465
0.7512	1.4486	26.300	0.930
0.8717	1.4476	27.031	0.424
1	1.4484	27.9249	0
CHN (1) + EA (2)			
0	1.3712	22.343	0
0.0907	1.3861	23.274	0.425
0.1833	1.3978	24.029	0.663
0.2778	1.4079	24.699	0.806
0.3744	1.4170	25.316	0.884
0.4730	1.4256	25.910	0.926
0.5738	1.4331	26.439	0.893
0.6768	1.4398	26.943	0.822
0.7822	1.4446	27.354	0.645
0.8899	1.4468	27.644	0.334
1	1.4484	27.925	0
CHN (1) + MS (2)			
0	1.5352	40.179	0
0.1469	1.5199	37.954	-0.425
0.2793	1.5062	36.036	-0.720
0.3992	1.4914	34.222	-1.065
0.5082	1.4785	32.664	-1.287
0.6079	1.4682	31.378	-1.352
0.6993	1.4595	30.284	-1.326
0.7834	1.4542	29.465	-1.114
0.8611	1.4506	28.806	-0.820
0.9331	1.4503	28.390	-0.354
1	1.4484	27.925	0

Refractive indices were also predicted by models like Lorentz-Lorenz (LL), Gladstone-Dale (GD), Arago-Biot (AB), Newton (NEW), Eykman (EYK), Eyring-John (EJ), Heller (HEL), and Weiner (WEI) as detailed in chapter II and references therein.^{37,38} The correlating abilities of these models were ascertained by percent standard deviations ($\sigma\%$) and a comparison has been illustrated in Figure 8.9.

Chapter VIII

8.3.9. IR spectroscopic study

The results obtained so far are also well reflected in FT-IR spectra of the binary mixtures (Figures 8.10-8.12). The spectra were recorded in a demountable KBr cell for liquid samples with spacer of path length of 0.5 mm at ambient temperature with a Perkin-Elmer Spectrum FT-IR spectrometer (RX-1). MA and EA show characteristic C=O stretching vibrations at 1760 and 1739 cm^{-1} , respectively along with some C-H stretching vibrations in the range 3000-2800 cm^{-1} . In the structure of CHN, chair type monomers were reported to form C-H \cdots O- bonded dimmers through the involvement of -C=O group³⁹ and the corresponding band appearing at around 1713 cm^{-1} is thus broad and strong enough. Gradual intensity loss and shifting to higher frequencies of this band with the advent of the esters (MA and EA) suggests breaking of intermolecular C-H \cdots O interactions within CHN molecules and formation of intermolecular C-H \cdots O interactions between CHN and the ester molecules.

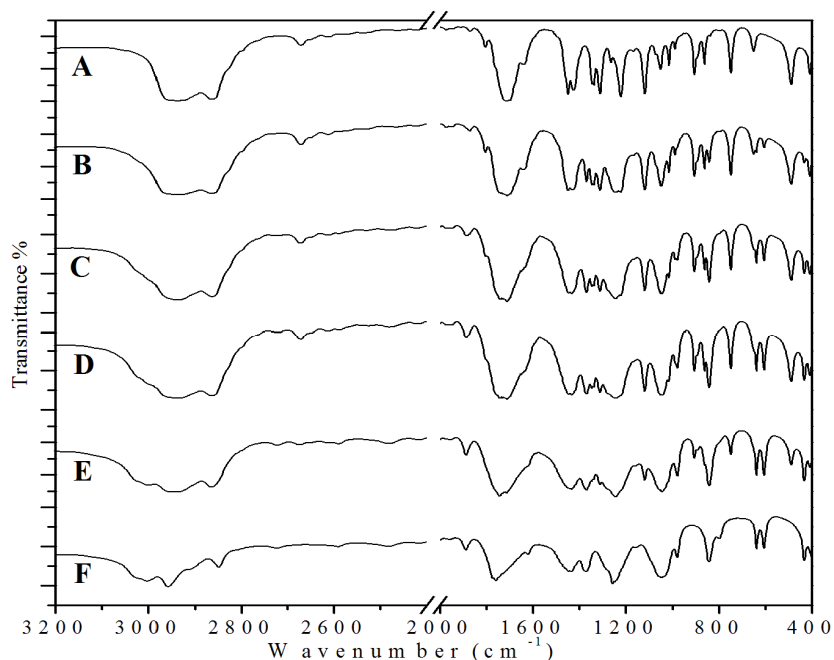


Fig. 8.10. FTIR spectra of the various binary mixtures of CHN (1) + MA (2): A, pure CHN ($x_2 = 0.00$); B, $x_2 = 0.20$; C, $x_2 = 0.40$; D, $x_2 = 0.60$; E, $x_2 = 0.80$; F, pure MA ($x_2 = 1.00$).

Chapter VIII

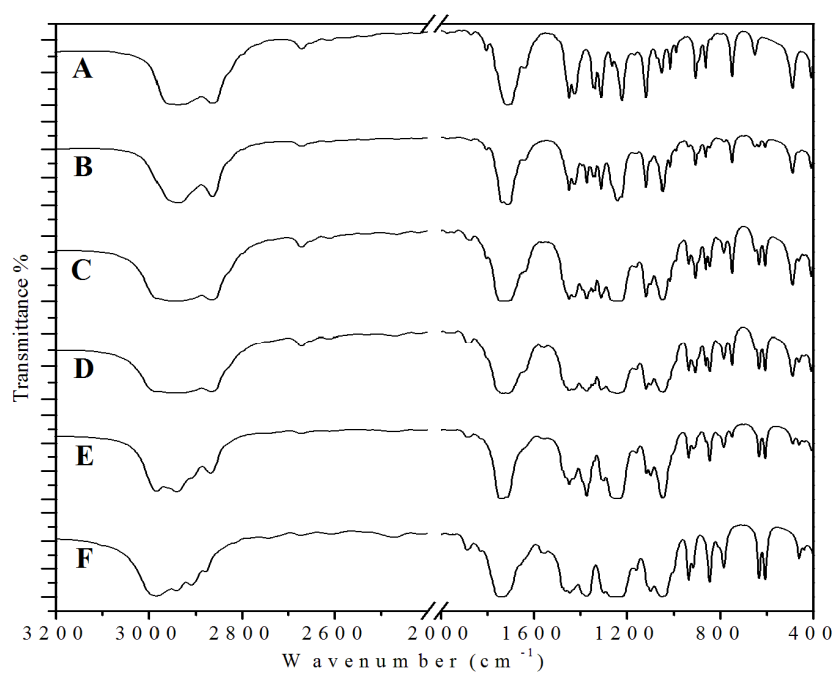


Fig. 8.11. FTIR spectra of the various binary mixtures of CHN (1) + EA (2): A, pure CHN ($x_2 = 0.00$); B, $x_2 = 0.20$; C, $x_2 = 0.40$; D, $x_2 = 0.60$; E, $x_2 = 0.80$; F, pure EA ($x_2 = 1.00$).

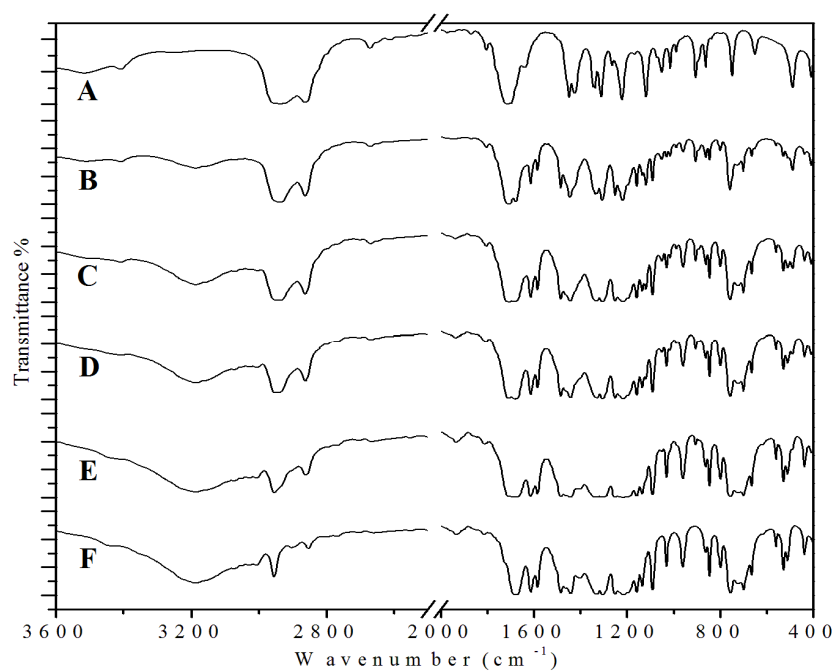


Fig. 8.12. FTIR spectra of the various binary mixtures of CHN (1) + MS (2): A, pure CHN ($x_2 = 0.00$); B, $x_2 = 0.20$; C, $x_2 = 0.40$; D, $x_2 = 0.60$; E, $x_2 = 0.80$; F, pure MS ($x_2 = 1.00$).

Chapter VIII

Again the band near 2960 cm^{-1} due to C-H stretching vibrations of CHN losses intensity on dilution with the esters (MA and EA) and thus behaves like the hydrogen bonded carbonyl band $\nu_{\text{C=O}(\dots\text{H})}$ and shows a blue shifted $\nu_{\text{C-H}(\dots\text{O})}$ mode.³⁹ MS shows characteristic bands around 3180 cm^{-1} and 1676 cm^{-1} due to hydrogen bonded –OH and –C=O groups, respectively. The –C=O stretching band becomes broader as the mole fraction (x_1) of CHN increases in this mixture and splits into a doublet at $x_1 = 0.80$.⁴⁰ Again the broad band at 3180 cm^{-1} losses intensity on dilution with CHN; in consequence the bands appearing in the range $3000\text{-}2800\text{ cm}^{-1}$ due to C-H stretching vibrations appear more intense. These facts corroborate with the presence of strong intermolecular hydrogen bond interactions in the mixture (CHN + MS). However, the weak bands appearing in the region $3600\text{-}3400\text{ cm}^{-1}$ for MA, EA and CHN probably originates from some overtone or other combination bands and as such they were kept out of present analysis.

8.4. Conclusion

In summary, the various derived properties reveal the following order of molecular interactions: (CHN + MS) > (CHN + EA) > (CHN + MA) for the mixtures studied. Such an order of molecular interactions originates from a combined effect of factors like the molecular size, shape and nature of the components. This order can be attributed to the breaking up of dipolar interactions or the three-dimensional hydrogen bonded network (through inter- or intra-molecular), interstitial accommodation as well as intermolecular hydrogen bond interactions on mutual mixing of the components. A comparison of the excess partial molar volumes ($\bar{V}_{m,1}^{0,E}$ and $\bar{V}_{m,2}^{0,E}$) at infinite dilution to the molar volumes of the pure components in the studied mixtures suggests that the molecular compactness increases in the same ascending order of molecular interactions shown above. FT-IR spectra of the mixtures also correlate well with the observed molecular interactions for the mixtures studied.

References

- [1] C.R. Reid, B.E. Poling, *The properties of Gases and Liquids*, McGraw Hill, New York, 1998, Ch.1.
- [2] J.G. Harris, F.H. Stillinger, *J. Chem. Phys.*, 95 (1991) 5953.
- [3] F. Nabi, M.A. Malik, C.G. Jesudason, S.A.Al-Thabaiti, *Korean. J. Chem. Eng.*, 31 (2014) 1505.

Chapter VIII

- [4] G.A. Krestov, *Thermodynamics of Solvation; Solution and Dissolution, Ions and Solvents, Structure and Energetics*, Ellis Horwood, New York, 1991, pp. 151.
- [5] D. Patterson, G. Delmas, *J. Polym. Sci.*, 30 (1970) 1.
- [6] D. Patterson, *Pure. Appl. Chem.*, 47 (1976) 305.
- [7] V.A. Bloomfield, R.K. Dewan, *J. Phys. Chem.*, 75 (1971) 3113.
- [8] D.Y. Peng, D.B. Robinson, *Ind. Eng. Chem. Fundum.*, 15 (1976) 59.
- [9] M.N. Roy, B.K. Sarkar, B. Sinha, *J. Chem. Eng. Data* 54 (2009) 1076.
- [10] J.A. Riddick, W.B. Bunger, T.K. Sakano, *Organic Solvents: Physical Properties and Methods of Purification*, 4th ed., Wiley: New York, 1986.
- [11] R. Venis, R. Rajkumar, *J. Chem. Pharm. Res.*, 2 (2011) 878.
- [12] T.M. Aminabhavi, H.T.S. Phayde, *J. Chem. Eng. Data* 41(1996) 813.
- [13] W.M. Haynes, D.R. Lide, T.J. Bruno, *CRC Handbook of Chemistry & Physics*, 93rd edn., Taylor & Francis, Boca Roton, London, 2012-2013.
- [14] G.M. Smith, H.C. Van Ness, *Introduction to Chemical Engineering Thermodynamics*, McGraw Hill, New York, 1987.
- [15] O. Redlich, A.T. Kister, *Indus. Eng. Chem.*, 40 (1948) 345.
- [16] P.J. Flory, R.A. Orwell, A. Vrijji, *J. Am. Chem. Soc.*, 86 (1964) 3507.
- [17] P.J. Flory, R.A. Orwell, A. Vrijji, *J. Am. Chem. Soc.*, 86 (1964) 3515.
- [18] P.J. Flory, *J. Am. Chem. Soc.*, 87 (1965) 1833.
- [19] A. Abe, P.J. Flory, *J. Am. Chem. Soc.*, 87 (1965) 1838.
- [20] S.I Sandler, *Chemical, Biochemical, and Engineering Thermodynamics*, 4th edn., John Wiley & Sons (Asia), New Delhi, 2006, pp. 242, 258.
- [21] S. Glasstone, K.J. Laidler, H. Eyring, *The theory of Rate Preocess*, McGraw-Hill Book Comnpany, New York, 1941.
- [22] T.M. Reid, T.E. Taylor, *J. Phys. Chem.*, 63 (1949) 58.
- [23] A.K. Mehrotra, W.D. Monnery, W. Svrcek, *Fluid Phase Equilib.*, 117 (1996) 344.
- [24] R.D. McCarty, *Fluid Phase Equilib.*, 256 (2007) 42.
- [25] L. Grunberg, A.H. Nissan, *Nature*, 164 (1949) 799.
- [26] P.K. Katti, M.M. Chaudhri, *J. Chem. Eng. Data* 9 (1964) 442.
- [27] M.A. Hernandez-Galvan, F. Garcia-Sanchez, R. Macias-Salinas, *Fluid Phase Equilib.*, 262 (2007) 51.
- [28] M.H. Cohen, D. Turnbull, *J. Chem. Phys.*, 31 (1959) 1164.
- [29] G.C. Benson, O.K. Kiyohara, *J. Chem. Thermodyn.*, 11 (1979) 1061.
- [30] W.E. Acree, *J. Chem. Eng. Data* 28 (1983) 215.
- [31] C.B. Salguero, J.G. Fadrique, *J. Chem. Eng. Data* 56 (2011) 3823.

Chapter VIII

- [32] J.M. Resa, J.M. Goenaga, A.I. Sa´nchez-Ruiz, J. Chem. Eng. Data 51 (2006) 1294.
- [33] D.L. Cunha, J.A.P. Coutinho, J.L. Daridon, R.A. Reis, M.L.L. Paredes, J. Chem. Eng. Data 58 (2013) 925.
- [34] S. Nallani, S. Boodida, S.J. Tangeda, J. Chem. Eng. Data 52 (2007) 405.
- [35] M.S. Dhillon, H.S. Chugh, J. Chem. Eng. Data 22 (1977) 262.
- [36] M.I. Aralaguppi, C.V. Jadar, T.M. Aminabhavi, J. Chem. Eng. Data 44 (1999) 441.
- [37] A. Ali, A.K. Nain, D. Chand, R. Ahmad, J. Chinese. Chem. Soc., 53 (2006) 531.
- [38] J.R. Partington, *An Advanced Treatise on Physical Chemistry*, Longmans & Green, London, 1953, Vol.4, Sec X.
- [39] P.D. Vaz, P.J.A.R.-. Claro, J. Raman. Spectros., 34 (2003) 863.
- [40] H. Yamada, Bull. Chem. Soc. Jpn., 32 (1959) 1051.

CHAPTER IX

Thermophysical properties of the ternary mixtures of cyclohexane and cyclohexanone with some esters at $T = (298.15-318.15)$ K

9.1. Introduction

Reliable thermodynamic and transport properties of multi-component liquid systems are of great importance to both the chemists and the chemical engineers. These properties are valuable tools for designing the industrial equipments with better precision and testing the predictive ability of various theoretical models. These properties depend on the binding forces amongst the liquids in liquid mixtures and are found to be very sensitive to the liquid structure and composition.¹ Hence these properties help to understand the molecular interactions operating between the component molecules in liquid-liquid mixtures. Such knowledge of molecular interactions are of major significance in relation to their industrial applications.²⁻⁴ Experimental measurements of these properties through the measurements of the physical properties like density, viscosity, ultrasonic speed of sound and refractive indices for the different binary systems have been carried out widely and the data obtained are summarized in various data banks. But for the ternary systems such experimental data are often scarce and could not be adequate. In the absence of experimental data, reliable correlating models and predictive methods or models are necessary, particularly which are simple and requires only the information of the constituent binary mixtures. Therefore in this chapter thermophysical properties of the ternary mixtures consisting of cyclohexane (CH) and cyclohexanone (CHN) with methyl acetate (MA), ethyl acetate (EA) and methyl salicylate (MS) at 298.15, 308.15 and 318.15 K under ambient pressure were studied.

9.2. Experimental section

9.2.1. Materials

All the chemicals involved in this work were purchased from Sigma-Aldrich, Germany (Reagent Plus, purity > 99%) and were used as received from the vendor. The purity of all the chemicals used was ascertained by comparing their densities and viscosities at the experimental temperatures with the literature data as presented in previous chapters (VII and VIII).

Chapter IX

9.2.2. Apparatus and procedure

The binary and ternary mixtures were prepared afresh by mass in specially designed air-tight bottles with stopper inside a dry box at 298.15 K. The measurement of densities (ρ), viscosities (η), ultrasonic speeds of sound (u) and refractive indices (n_D) under the experimental temperatures were carried out as described in the previous chapters. An average of the triplicate measurements for all the properties were taken into consideration and adequate precautions were taken to minimize evaporation losses during all the measurements.

9.3. Results and discussion

The experimental densities and viscosities of three binary mixtures, *i.e.*, (MA + EA), (MA + MS) and (EA + MS) and the ternary mixtures of CH and CHN with MA, EA and MS studied at 298.15, 308.15 and 318.15 K were used to determine the excess molar volumes (V_m^E) and viscosity deviations ($\Delta\eta$). Also the experimental ultrasonic speeds (u) of sound, the refractive indices (n_D) and the other derived properties for the above binary and the ternary mixtures were determined. All these properties for the other binary mixtures, *viz.*, (CH + MA), (CH + EA), (CH + MS), (CHN + MA), (CHN + EA) and (CHN + MS) have already been presented in previous chapters (VII and VIII).

9.3.1. Excess molar volumes and excess partial molar volumes

Excess molar volumes (V_m^E) were calculated for the binary and ternary mixtures using the following expression:

$$V_m^E = \sum_{i=1}^n x_i M_i \left(\frac{1}{\rho} - \frac{1}{\rho_i} \right) \quad (1)$$

where ρ is the density of the mixture and n , x_i , M_i and ρ_i are the number of components in the mixture, the mole fraction, the molar mass and the density of the i^{th} component in the mixture, respectively. The estimated uncertainty for excess molar volumes (V_m^E) was evaluated to be $\pm 0.005 \text{ cm}^3 \cdot \text{mol}^{-1}$. The molecular interactions for the binary mixtures (CH + MA), (CH + EA), (CH + MS), (CHN + MA), (CHN + EA) and (CHN + MS) in terms of various excess or deviation properties have already been discussed in previous chapters (VII and VIII), the molecular interactions for the remaining binary mixtures (MA + EA), (MA + MS) and (EA + MS) are discussed

Chapter IX

herein this chapter. The experimental densities and viscosities of three binary mixtures, *viz.*, (MA + EA), (MA + MS) and (EA + MS) studied at 298.15, 308.15 and 318.15 K are presented in Table 9.1. It shows that while the excess molar volumes (V_m^E) are positive for the mixture (MA + EA) throughout the entire composition range, such values are negative for the mixtures (MA + MS) and (EA + MS) over the entire composition range at all the experimental temperatures. These results are quite obvious from the nature of the interacting components in these mixtures. Due to similar nature of the alkyl acetates, their mixture, *i.e.*, (MA + EA) is characterized by dominance of dispersion forces and weak dipole-dipole interactions. It is because these two alkyl acetates have nearly similar dipole moments ($\mu_{D,MA} = 1.72$ D and $\mu_{D,EA} = 1.78$ D)⁵ and small difference in their molar volumes ($V_{m,EA} - V_{m,MA} = 18.56$ cm³·mol⁻¹ at 298.15 K). On the contrary, the negative V_m^E values for the mixtures (MA + MS) and (EA + MS) suggest the dominance of chemical or specific interactions along with the geometrical fitting of one component into another's structure due to appreciable difference in their molar volumes. The ester molecules being dipolar associates and hydrogen bond acceptors are capable of forming intermolecular hydrogen bond involving the -OH group of MS molecules and the >C=O of MA and EA molecules in their mixtures.⁶ Again due to the difference in their molar volumes ($V_{m,MS} - V_{m,MA} = 49.09$ cm³·mol⁻¹ and $V_{m,MS} - V_{m,EA} = 30.52$ cm³·mol⁻¹), the MA and EA molecules are interstitially accommodated in the voids of planar MS molecules.⁷ These geometrical fitting enhance the molecular compactness leading to volume contraction. Also a comparison of the V_m^E values suggests that the geometrical fitting of MA molecules in voids of MS molecules is more favorable than that of EA molecules. The variations in V_m^E values for all the nine binary mixtures as a function of their composition (x_1) at 298.15 K are depicted in Figure. 9.1, which suggests the following order of molecular interactions: (MA + MS) > (EA + MS) > (CH + MS) \approx (CHN + MS) > (CHN+EA) > (CHN + MA) > (CH + EA) > (CH + MA) > (MA + EA) based on the V_m^E values. Furthermore, for all the mixtures V_m^E values increase as the experimental temperature increase. Hence the degree of molecular interactions between the unlike molecule becomes weaker at higher temperatures.

Chapter IX

Table 9.1. Densities (ρ), viscosities (η), excess molar volumes (V_m^E) and viscosity deviations ($\Delta\eta$) for the three binary mixtures studied at $T = (298.15 \text{ to } 318.15) \text{ K}$.

x_1	$\rho \cdot 10^{-3}$ ($\text{kg} \cdot \text{m}^{-3}$)	η ($\text{mPa} \cdot \text{s}$)	$V_m^E \cdot 10^6$ ($\text{m}^3 \cdot \text{mol}^{-1}$)	$\Delta\eta$ ($\text{mPa} \cdot \text{s}$)
MA (1) + EA (2)				
$T = 298.15 \text{ K}$				
0	0.89455	0.4262	0	0
0.1167	0.89413	0.3782	0.382	-0.042
0.2292	0.89254	0.3400	0.874	-0.075
0.3376	0.89188	0.3143	1.252	-0.096
0.4422	0.89116	0.2934	1.623	-0.112
0.5432	0.89328	0.2873	1.694	-0.114
0.6408	0.89532	0.2822	1.771	-0.114
0.7351	0.89853	0.2933	1.734	-0.099
0.8263	0.90403	0.3130	1.485	-0.075
0.9146	0.91193	0.3464	1.033	-0.038
1	0.92681	0.3809	0	0
$T = 308.15 \text{ K}$				
0	0.88267	0.3874	0	0
0.1167	0.88165	0.3223	0.462	-0.060
0.2292	0.88031	0.2709	0.942	-0.107
0.3376	0.87973	0.2428	1.324	-0.131
0.4422	0.87846	0.2260	1.765	-0.144
0.5432	0.88141	0.2166	1.753	-0.150
0.6408	0.88325	0.2213	1.855	-0.141
0.7351	0.88686	0.2349	1.779	-0.124
0.8263	0.89213	0.2706	1.549	-0.085
0.9146	0.89951	0.3066	1.135	-0.046
1	0.91524	0.3491	0	0
$T = 318.15 \text{ K}$				
0	0.86994	0.3564	0	0
0.1167	0.86792	0.2823	0.587	-0.069
0.2292	0.86698	0.2323	1.032	-0.114
0.3376	0.86637	0.2008	1.424	-0.140
0.4422	0.8665	0.1871	1.722	-0.150
0.5432	0.86754	0.1785	1.912	-0.154
0.6408	0.86975	0.1800	1.974	-0.148
0.7351	0.87263	0.1954	1.966	-0.129
0.8263	0.87871	0.2295	1.642	-0.091
0.9146	0.88599	0.2629	1.222	-0.054
1	0.90225	0.3132	0	0
MA (1) + MS (2)				
$T = 298.15 \text{ K}$				
0	1.17931	1.5358	0	0
0.1858	1.15343	1.2172	-0.561	0.032
0.3393	1.12836	1.0039	-0.995	0.047
0.4682	1.10471	0.8585	-1.393	0.059
0.5779	1.08116	0.7551	-1.651	0.069
0.6726	1.05689	0.6723	-1.724	0.071
0.7550	1.03404	0.6050	-1.817	0.069

Chapter IX

0.8274	1.00970	0.5455	-1.689	0.061
0.8915	0.98461	0.4901	-1.415	0.047
0.9487	0.95780	0.4411	-0.923	0.032
1	0.92681	0.3809	0	0
<hr/>				
<i>T</i> = 308.15 K				
0	1.16931	1.4024	0	0
0.1858	1.14133	1.0995	-0.382	0.016
0.3393	1.11589	0.9045	-0.823	0.030
0.4682	1.09024	0.7705	-1.064	0.039
0.5779	1.06524	0.6709	-1.221	0.043
0.6726	1.03937	0.5932	-1.176	0.043
0.7550	1.01360	0.5299	-1.033	0.039
0.8274	0.98813	0.4752	-0.822	0.031
0.8915	0.96322	0.4307	-0.574	0.025
0.9487	0.93852	0.3865	-0.263	0.012
1	0.91524	0.3491	0	0
<hr/>				
<i>T</i> = 318.15 K				
0	1.15942	1.3027	0	0
0.1858	1.13057	1.0121	-0.354	0.013
0.3393	1.10337	0.8293	-0.674	0.026
0.4682	1.07696	0.7027	-0.893	0.034
0.5779	1.05048	0.6091	-0.951	0.038
0.6726	1.02486	0.5343	-0.966	0.035
0.7550	0.99892	0.4747	-0.833	0.031
0.8274	0.97293	0.4216	-0.594	0.021
0.8915	0.9483	0.3793	-0.385	0.014
0.9487	0.92502	0.3429	-0.212	0.006
1	0.90225	0.3132	0	0
<hr/>				
EA (1) + MS (2)				
<hr/>				
<i>T</i> = 298.15 K				
0	1.17931	1.5358	0	0
0.1610	1.14674	1.2724	-0.413	0.023
0.3015	1.11657	1.0814	-0.841	0.038
0.4253	1.08748	0.9383	-1.171	0.048
0.5352	1.05943	0.8354	-1.419	0.062
0.6333	1.03177	0.7440	-1.531	0.062
0.7215	1.00565	0.6691	-1.646	0.060
0.8012	0.97856	0.5989	-1.513	0.049
0.8735	0.95159	0.5372	-1.252	0.036
0.9396	0.92392	0.4816	-0.788	0.021
1	0.89455	0.4262	0	0
<hr/>				
<i>T</i> = 308.15 K				
0	1.16931	1.4024	0	0
0.1610	1.13555	1.1514	-0.333	0.011
0.3015	1.10438	0.9767	-0.698	0.025
0.4253	1.07512	0.8470	-1.048	0.036
0.5352	1.0467	0.7419	-1.288	0.038
0.6333	1.01905	0.6553	-1.425	0.034
0.7215	0.99176	0.5816	-1.435	0.027
0.8012	0.96454	0.5198	-1.297	0.020
0.8735	0.93647	0.4665	-0.917	0.011
0.9396	0.90962	0.4212	-0.535	0.003
1	0.88267	0.3874	0	0

Chapter IX

$T = 318.15 \text{ K}$				
0	1.15942	1.3027	0	0
0.1610	1.12406	1.0656	-0.223	0.008
0.3015	1.09176	0.9021	-0.524	0.021
0.4253	1.06068	0.7792	-0.726	0.029
0.5352	1.03031	0.6822	-0.794	0.031
0.6333	1.00019	0.6016	-0.692	0.028
0.7215	0.97116	0.5338	-0.532	0.023
0.8012	0.94346	0.4758	-0.352	0.015
0.8735	0.91735	0.4273	-0.192	0.007
0.9396	0.89257	0.3892	-0.043	0.004
1	0.86994	0.3564	0	0

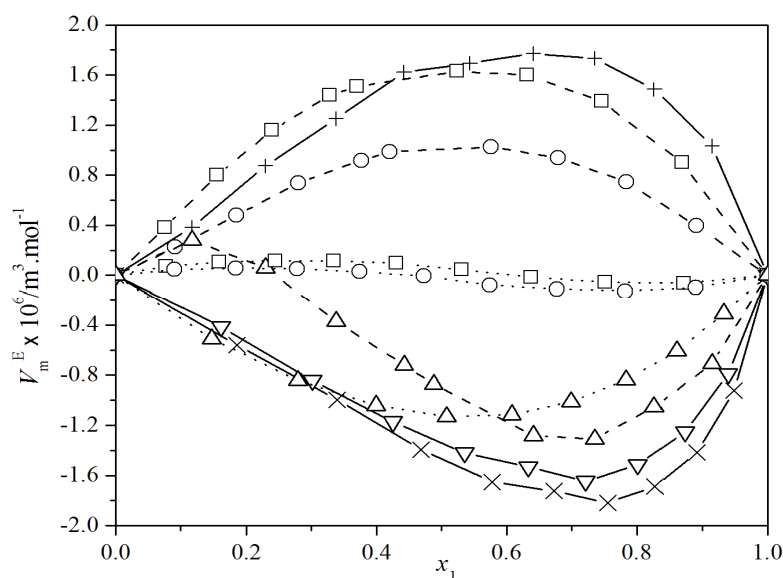


Fig. 9.1. Excess molar volume (V_m^E) versus the mole fractions (x_1) of the first component in all the binary mixtures studied at $T = 298.15 \text{ K}$. The graphical points represent the V_m^E values for the mixtures containing: \square , MA; \circ , EA; Δ , MS. While dashed lines represent the mixtures with CH as the first component and dotted lines represent the mixtures with CHN as the first component. Solid lines represent the binary mixtures of two esters only. Symbols: +, (MA + EA); \times , (MA + MS); ∇ , (EA + MS).

The partial molar volumes ($\bar{V}_{m,i}$) of the i^{th} component in the binary mixtures were obtained at 298.15 K from the relation:⁸

$$\bar{V}_{m,i} = V_{m,i}^E + V_{m,i}^* + (1 - x_i)(dV_{m,i}^E/dx_i)_{T,P} \quad (2)$$

where $V_{m,i}^*$ is the molar volume of the i^{th} component in the binary mixtures. The derivatives $(\partial V_{m,i}^E/\partial x_i)_{T,P}$ were obtained by following a procedure (as detailed in

Chapter IX

chapter II) using the Redlich-Kister coefficients (a_i)⁹ calculated for the excess molar volumes (V_m^E) for each binary mixture at 298.15 K. The coefficients are: $a_0 = 6.7158$, $a_1 = 2.8518$, $a_2 = 0.7375$, $a_3 = 4.3874$, $a_4 = 2.1587$ for the mixture (MA + EA); $a_0 = -5.9147$, $a_1 = -4.8813$, $a_2 = -1.0535$, $a_3 = -3.1460$, $a_4 = -7.8724$ for the mixture (MA + MS) and $a_0 = -5.3419$, $a_1 = -4.0579$, $a_2 = -3.1205$, $a_3 = -3.1935$ for the mixture (EA + MS) with standard deviations (σ) 0.027, 0.021, 0.019 for the corresponding mixtures, respectively. The optimum number of the Redlich-Kister coefficients (a_i)⁹ were determined by using Marquardt algorithm.¹⁰ Partial molar volumes ($\bar{V}_{m,1}^0$ and $\bar{V}_{m,2}^0$) at infinite dilution, excess partial molar volumes ($\bar{V}_{m,i}^E$) and excess partial molar volumes ($\bar{V}_{m,i}^{0,E}$) at infinite dilution were determined at 298.15 K by using the standard relations described in chapter II. Molar volumes ($V_{m,1}^*$ and $V_{m,2}^*$), partial molar volumes ($\bar{V}_{m,1}^0$ and $\bar{V}_{m,2}^0$) and excess partial molar volumes ($\bar{V}_{m,i}^{0,E}$) at infinite dilution for each component in the mixtures at 298.15 K are listed in Table 9.2. Excess partial molar volumes ($\bar{V}_{m,1}^E$ and $\bar{V}_{m,2}^E$) of each component in the binary mixtures are depicted in Figure 9.2 against the mole fraction (x_1) of the first component in the binary mixtures. This figure shows that $\bar{V}_{m,1}^E$ and $\bar{V}_{m,2}^E$ values behave in opposite fashion to each other with increasing mole fraction (x_1) of the first component in these binary mixtures. Partial molar volumes ($\bar{V}_{m,1}^0$ and $\bar{V}_{m,2}^0$) at infinite dilution for both the components in the mixture (MA + EA) were found to be greater than their respective molar volumes, *i.e.*, in this mixture both the components expand in volume on mutual mixing. However, the partial molar volumes ($\bar{V}_{m,1}^0$ and $\bar{V}_{m,2}^0$) at infinite dilution for both the components in the mixtures (MA + MS) and (EA + MS) were found to be lower than their respective molar volumes leading to negative excess partial molar volumes ($\bar{V}_{m,1}^{0,E}$ and $\bar{V}_{m,2}^{0,E}$) at infinite dilution. These results corroborate with the interstitial accommodation of these ester molecules in the voids of MS molecules resulting into compact structures for these mixtures. The mixture (MA + MS), with more negative $\bar{V}_{m,1}^{0,E}$ and $\bar{V}_{m,2}^{0,E}$ values than those of the mixture (EA + MS), is much more compact in structure. These results, therefore, suggest the following order of packing efficiency

Chapter IX

Table 9.2. Molar volumes ($V_{m,1}^*$ and $V_{m,2}^*$), partial molar volumes at infinite dilution ($\bar{V}_{m,1}^0$ and $\bar{V}_{m,2}^0$) and excess partial molar volumes at infinite dilution ($\bar{V}_{m,1}^{0,E}$ and $\bar{V}_{m,2}^{0,E}$) for each component in the studied binary mixtures at 298.15 K.

Volume Parameters	MA (1) + EA (2)	MA (1) + MS (2)	EA (1) + MS (2)
$V_{m,1}^*$	79.93	79.93	98.49
$\bar{V}_{m,1}^0$	82.30	73.12	97.29
$V_{m,2}^*$	98.49	129.02	129.02
$\bar{V}_{m,2}^0$	115.35	106.15	113.30
$\bar{V}_{m,1}^{0,E}$	2.37	-6.81	-1.20
$\bar{V}_{m,2}^{0,E}$	16.86	-22.87	-15.72

Volume parameters are given in $\text{cm}^3 \cdot \text{mol}^{-1}$.

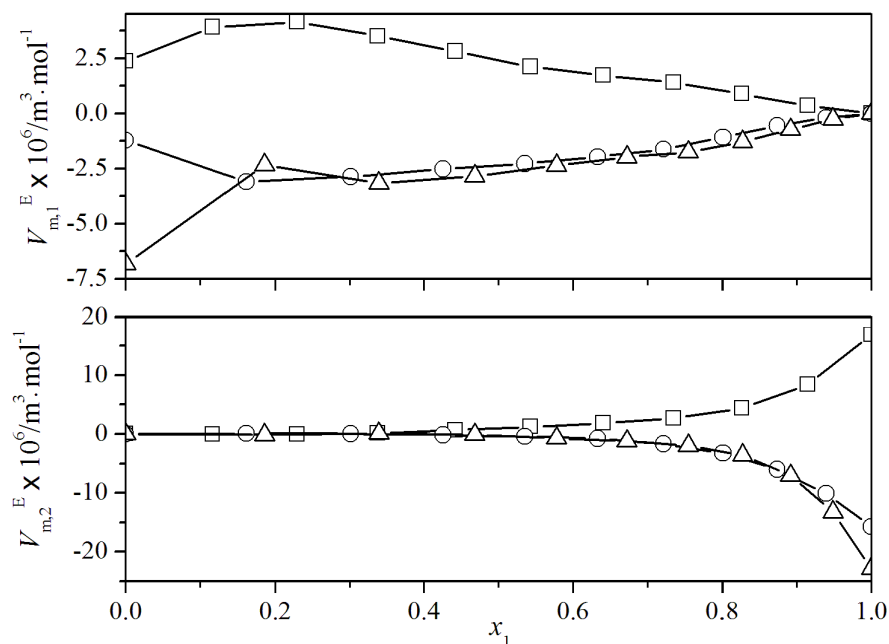


Fig. 9.2. Excess partial molar volume ($\bar{V}_{m,i}^E$) for the i^{th} component against mole fraction (x_1) of the first component in the studied binary mixtures at $T = 298.15$ K. The graphical points represent the $\bar{V}_{m,i}^E$ values for the binary mixtures: \square , (MA + EA); Δ , (MA + MS); \circ , (EA + MS).

Chapter IX

or structure compactness in these mixtures: (MA + EA) < (EA + MS) < (MA + MS) and an overall order of packing efficiency or structure compactness in the related nine binary mixtures is: (MA + MS) > (EA + MS) > (CHN + MS) > (CH + MS) > (CHN + EA) > (CHN + MA) > (CH + EA) > (CH + MA) > (MA + EA) based on the $\bar{V}_{m,1}^{0,E}$ and $\bar{V}_{m,2}^{0,E}$ values. The $\bar{V}_{m,1}^{0,E}$ and $\bar{V}_{m,2}^{0,E}$ values for the binary mixtures of CH and CHN with these esters have already been discussed in previous chapters (VII and VIII). The experimental densities, viscosities, excess molar volumes and viscosity deviations of the seven ternary mixtures of CH and CHN with MA, EA and MS studied at 298.15, 308.15 and 318.15 K were presented in Table 9.3. The $V_{m,123}^E$ values for the ternary mixtures (CH + MA + EA) and (CHN + MA + EA) are found to be positive over the entire composition range studied at all the experimental temperatures. For the mixtures (CH + MA + MS) and (CH + EA + MS), $V_{m,123}^E$ values are found to be negative at lower mole fractions (x_1) of CH but are positive at higher mole fractions (x_1) of CH. However, for the mixtures (CHN + MA + MS) and (CHN + EA + MS), $V_{m,123}^E$ values are negative throughout the entire composition range studied at all the experimental temperatures. For the ternary mixture (MA + EA + MS), $V_{m,123}^E$ values are negative when the mole fractions of MS are higher than those of the alkyl acetates at all the experimental temperatures. These results are quite obvious from the nature of the mixing components of the respective ternary mixtures and the molecular interactions in the associated binary mixtures mentioned earlier. The $V_{m,123}^E$ values for all the ternary mixtures studied were fitted to Cibulka equation:¹¹

$$X_{123}^E = X_{\text{Bin}}^E + x_1 x_2 x_3 (c_1 + c_2 x_1 + c_3 x_2) \quad (3)$$

$$X_{\text{Bin}}^E = X_{m,12}^E + X_{m,13}^E + X_{m,23}^E \quad (4)$$

where $X_{123}^E = V_{m,123}^E$, $X_{\text{Bin}}^E = \sum X_{m,ij}^E$ and $X_{ij}^E = V_{m,ij}^E$. $V_{m,ij}^E$ values were obtained by substituting the Redlich-Kister coefficients (a_i) of respective binary mixtures and the mole fractions of their components in the ternary mixtures in the Redlich-Kister polynomial.⁹ The coefficients (c_i) were calculated by multi-linear regression and are listed in Table 9.4. Although the second term in the right hand side of Eq. (3) is asymmetric, the correlations provided for the ternary mixtures do not depend on the particular subscript.¹²

Chapter IX

Table 9.3. Densities (ρ), viscosities (η), excess molar volumes ($V_{m,123}^E$) and viscosity deviations ($\Delta\eta_{123}$) for the ternary mixtures studied at $T = (298.15 \text{ to } 318.15) \text{ K}$.

x_1	x_2	$\rho \cdot 10^{-3}$ ($\text{kg} \cdot \text{m}^{-3}$)	η ($\text{mPa} \cdot \text{s}$)	$V_{m,123}^E \cdot 10^6$ ($\text{m}^3 \cdot \text{mol}^{-1}$)	$\Delta\eta_{123}$ ($\text{mPa} \cdot \text{s}$)
CH (1) + MA (2) + EA (3)					
$T = 298.15 \text{ K}$					
0.0413	0.0704	0.88872	0.4234	0.234	-0.013
0.0819	0.1163	0.88246	0.4270	0.453	-0.020
0.1217	0.1613	0.87627	0.4312	0.669	-0.027
0.1408	0.2057	0.87315	0.4313	0.846	-0.031
0.1596	0.2494	0.87014	0.4320	1.010	-0.034
0.1977	0.2921	0.86439	0.4380	1.186	-0.039
0.2352	0.3341	0.85877	0.4439	1.353	-0.045
0.2720	0.3753	0.85327	0.4501	1.512	-0.050
0.3081	0.4159	0.84786	0.4564	1.666	-0.054
0.3436	0.4557	0.84257	0.4631	1.811	-0.059
0.3786	0.4948	0.83741	0.4703	1.947	-0.063
0.4129	0.5333	0.83246	0.4783	2.063	-0.066
0.4535	0.4833	0.82654	0.4941	2.052	-0.070
0.4947	0.4325	0.82081	0.5119	2.028	-0.073
0.5365	0.3811	0.81527	0.5316	1.990	-0.076
0.5788	0.3290	0.80992	0.5537	1.938	-0.076
0.6218	0.2761	0.80476	0.5783	1.869	-0.076
0.6654	0.2224	0.79979	0.6058	1.784	-0.074
0.7096	0.1680	0.79505	0.6365	1.675	-0.070
0.7544	0.1128	0.79060	0.6711	1.533	-0.064
$T = 308.15 \text{ K}$					
0.0413	0.0704	0.87585	0.3766	0.367	-0.019
0.0819	0.1163	0.86982	0.3801	0.580	-0.025
0.1217	0.1613	0.86393	0.3843	0.783	-0.030
0.1408	0.2057	0.86094	0.3793	0.956	-0.039
0.1596	0.2494	0.85746	0.3856	1.185	-0.036
0.1977	0.2921	0.85273	0.3850	1.263	-0.046
0.2352	0.3341	0.84714	0.3848	1.445	-0.056
0.2720	0.3753	0.84172	0.3823	1.612	-0.068
0.3081	0.4159	0.83630	0.3859	1.784	-0.073
0.3436	0.4557	0.83076	0.3889	1.975	-0.080
0.3786	0.4948	0.82590	0.3922	2.092	-0.086
0.4129	0.5333	0.82133	0.3953	2.180	-0.093
0.4535	0.4833	0.81555	0.4055	2.163	-0.099
0.4947	0.4325	0.81013	0.4208	2.111	-0.101
0.5365	0.3811	0.80473	0.4324	2.066	-0.108
0.5788	0.329	0.79946	0.4460	2.012	-0.113
0.6218	0.2761	0.79426	0.4610	1.957	-0.118
0.6654	0.2224	0.78888	0.4852	1.934	-0.115
0.7096	0.1680	0.78458	0.5054	1.775	-0.117
0.7544	0.1128	0.78019	0.5276	1.632	-0.118

Chapter IX

$T = 318.15 \text{ K}$					
0.0413	0.0704	0.86200	0.3395	0.525	-0.023
0.0819	0.1163	0.85613	0.3437	0.743	-0.026
0.1217	0.1613	0.85012	0.3416	0.982	-0.035
0.1408	0.2057	0.84700	0.3344	1.183	-0.044
0.1596	0.2494	0.84439	0.3357	1.324	-0.045
0.1977	0.2921	0.83842	0.3333	1.567	-0.055
0.2352	0.3341	0.83357	0.3345	1.682	-0.060
0.2720	0.3753	0.82843	0.3297	1.837	-0.072
0.3081	0.4159	0.82347	0.3196	1.975	-0.089
0.3436	0.4557	0.81874	0.3275	2.090	-0.088
0.3786	0.4948	0.81375	0.3301	2.241	-0.093
0.4129	0.5333	0.80921	0.3317	2.342	-0.098
0.4535	0.4833	0.80344	0.3389	2.342	-0.105
0.4947	0.4325	0.79848	0.3491	2.251	-0.109
0.5365	0.3811	0.79307	0.3585	2.223	-0.114
0.5788	0.3290	0.78789	0.3695	2.175	-0.119
0.6218	0.2761	0.78265	0.3831	2.143	-0.122
0.6654	0.2224	0.77793	0.4032	2.049	-0.120
0.7096	0.1680	0.77327	0.4162	1.953	-0.125
0.7544	0.1128	0.76923	0.4341	1.776	-0.126
CH (1) + MA (2) + MS (3)					
$T = 298.15 \text{ K}$					
0.0660	0.1125	1.13703	1.2716	-0.014	0.005
0.1236	0.1756	1.10404	1.1326	-0.109	0.008
0.1743	0.2311	1.07297	1.0220	-0.198	0.010
0.1942	0.2838	1.05325	0.9415	-0.268	0.011
0.2124	0.3320	1.03377	0.8721	-0.283	0.011
0.2518	0.3720	1.00485	0.8031	-0.181	0.006
0.2872	0.4081	0.97701	0.7428	-0.037	-0.001
0.3194	0.4408	0.95027	0.6896	0.137	-0.009
0.3486	0.4705	0.92461	0.6419	0.332	-0.018
0.3753	0.4977	0.90001	0.5985	0.542	-0.027
0.3999	0.5227	0.87641	0.5588	0.763	-0.038
0.4225	0.5457	0.85379	0.5219	0.993	-0.049
0.4659	0.4965	0.84901	0.5448	1.036	-0.052
0.5104	0.4462	0.84466	0.5706	1.034	-0.054
0.5558	0.3948	0.84072	0.6001	0.989	-0.055
0.6022	0.3422	0.83717	0.6336	0.901	-0.054
0.6497	0.2885	0.83397	0.6714	0.771	-0.051
0.6983	0.2335	0.83109	0.7144	0.602	-0.045
0.7481	0.1771	0.82852	0.7632	0.391	-0.036
0.7991	0.1195	0.82619	0.8183	0.146	-0.024
$T = 308.15 \text{ K}$					
0.0660	0.1125	1.12692	1.1462	-0.028	-0.007
0.1236	0.1756	1.09323	1.0086	-0.062	-0.012
0.1743	0.2311	1.06187	0.9118	-0.133	-0.005
0.1942	0.2838	1.04172	0.8376	-0.167	-0.005
0.2124	0.3320	1.02207	0.7849	-0.171	0.006
0.2518	0.3720	0.99370	0.7183	-0.129	-0.002
0.2872	0.4081	0.96909	0.6649	-0.331	-0.006
0.3194	0.4408	0.93906	0.6088	0.201	-0.020

Chapter IX

0.3486	0.4705	0.91197	0.5536	0.560	-0.039
0.3753	0.4977	0.88787	0.5097	0.724	-0.052
0.3999	0.5227	0.86413	0.4656	0.973	-0.069
0.4225	0.5457	0.84216	0.4305	1.142	-0.081
0.4659	0.4965	0.83761	0.4453	1.172	-0.088
0.5104	0.4462	0.83414	0.4646	1.078	-0.092
0.5558	0.3948	0.82962	0.4913	1.113	-0.091
0.6022	0.3422	0.82709	0.5158	0.909	-0.094
0.6497	0.2885	0.82318	0.5600	0.875	-0.079
0.6983	0.2335	0.82005	0.5965	0.746	-0.073
0.7481	0.1771	0.81848	0.6312	0.412	-0.072
0.7991	0.1195	0.81513	0.6706	0.307	-0.069
<hr/>					
<i>T</i> = 318.15 K					
0.0660	0.1125	1.11663	1.0497	-0.027	0.315
0.1236	0.1756	1.08250	0.9165	-0.038	0.222
0.1743	0.2311	1.05077	0.8239	-0.090	0.142
0.1942	0.2838	1.03017	0.7501	-0.092	0.111
0.2124	0.3320	1.01011	0.6989	-0.066	0.063
0.2518	0.3720	0.98192	0.6412	-0.053	0.051
0.2872	0.4081	0.95416	0.5902	0.080	0.034
0.3194	0.4408	0.92676	0.5354	0.331	-0.014
0.3486	0.4705	0.90023	0.4745	0.634	-0.023
0.3753	0.4977	0.87550	0.4361	0.875	-0.045
0.3999	0.5227	0.85253	0.3955	1.043	-0.057
0.4225	0.5457	0.83016	0.3651	1.267	-0.069
0.4659	0.4965	0.82596	0.3739	1.275	-0.068
0.5104	0.4462	0.82211	0.3758	1.244	-0.075
0.5558	0.3948	0.81846	0.4121	1.192	-0.070
0.6022	0.3422	0.81578	0.4326	1.021	-0.076
0.6497	0.2885	0.81175	0.4725	1.022	-0.084
0.6983	0.2335	0.80910	0.5024	0.847	-0.080
0.7481	0.1771	0.80730	0.5326	0.554	-0.077
0.7991	0.1195	0.80457	0.5602	0.383	-0.079
<hr/>					
CH (1) + EA (2) + MS (3)					
<hr/>					
<i>T</i> = 298.15 K					
0.0672	0.0963	1.13424	1.3119	-0.039	0.003
0.1271	0.1519	1.09876	1.1903	-0.050	0.010
0.1809	0.2017	1.06629	1.0881	-0.156	0.013
0.2034	0.2499	1.04517	1.0137	-0.240	0.015
0.2243	0.2947	1.02463	0.9477	-0.291	0.016
0.2676	0.3325	0.99546	0.8758	-0.274	0.009
0.3072	0.3670	0.96754	0.8154	-0.217	0.003
0.3435	0.3986	0.94083	0.760	-0.129	-0.005
0.3768	0.4277	0.91529	0.7089	-0.016	-0.015
0.4076	0.4545	0.89088	0.6641	0.116	-0.023
0.4362	0.4794	0.86757	0.6226	0.257	-0.033
0.4627	0.5024	0.84531	0.5838	0.406	-0.044
0.5059	0.4533	0.84209	0.6074	0.429	-0.045
0.5494	0.4039	0.83922	0.6334	0.411	-0.046
0.5930	0.3542	0.83668	0.6619	0.353	-0.045
0.6369	0.3043	0.83444	0.693	0.258	-0.043
0.6810	0.2542	0.83245	0.7271	0.133	-0.039
0.7253	0.2039	0.83062	0.7644	-0.013	-0.034

Chapter IX

0.7698	0.1533	0.8289	0.8049	-0.173	-0.026
0.8145	0.1024	0.82715	0.8494	-0.329	-0.016
<hr/>					
<i>T</i> = 308.15 K					
0.0672	0.0963	1.12333	1.1594	0.030	-0.031
0.1271	0.1519	1.08777	1.0566	0.011	-0.013
0.1809	0.2017	1.05501	0.9545	-0.077	-0.017
0.2034	0.2499	1.03362	0.8692	-0.142	-0.032
0.2243	0.2947	1.01316	0.8037	-0.212	-0.037
0.2676	0.3325	0.98291	0.7549	-0.074	-0.025
0.3072	0.3670	0.95561	0.7017	-0.089	-0.027
0.3435	0.3986	0.92719	0.6582	0.208	-0.027
0.3768	0.4277	0.90155	0.5947	0.343	-0.052
0.4076	0.4545	0.87712	0.5405	0.488	-0.073
0.4362	0.4794	0.85293	0.5042	0.754	-0.08
0.4627	0.5024	0.83154	0.4726	0.809	-0.086
0.5059	0.4533	0.82781	0.4799	0.916	-0.100
0.5494	0.4039	0.82500	0.4915	0.907	-0.111
0.5930	0.3542	0.82238	0.5181	0.876	-0.107
0.6369	0.3043	0.82010	0.5316	0.801	-0.118
0.6810	0.2542	0.81753	0.5559	0.767	-0.119
0.7253	0.2039	0.81622	0.5795	0.564	-0.122
0.7698	0.1533	0.81376	0.6168	0.517	-0.112
0.8145	0.1024	0.81191	0.6432	0.388	-0.115
<hr/>					
<i>T</i> = 318.15 K					
0.0672	0.0963	1.11272	1.0434	0.068	-0.055
0.1271	0.1519	1.07629	0.9293	0.123	-0.052
0.1809	0.2017	1.04256	0.8509	0.127	-0.037
0.2034	0.2499	1.02223	0.7879	-0.080	-0.033
0.2243	0.2947	1.00074	0.7158	-0.044	-0.048
0.2676	0.3325	0.96828	0.6621	0.354	-0.044
0.3072	0.3670	0.94016	0.6108	0.437	-0.047
0.3435	0.3986	0.91368	0.5545	0.506	-0.061
0.3768	0.4277	0.88692	0.5066	0.787	-0.073
0.4076	0.4545	0.86295	0.4625	0.885	-0.086
0.4362	0.4794	0.84041	0.4274	0.953	-0.094
0.4627	0.5024	0.81964	0.3955	0.934	-0.101
0.5059	0.4533	0.81655	0.4095	0.978	-0.105
0.5494	0.4039	0.82048	0.4276	0.090	-0.105
0.5930	0.3542	0.81111	0.4371	0.975	-0.114
0.6369	0.3043	0.80897	0.4474	0.898	-0.123
0.6810	0.2542	0.80704	0.4664	0.794	-0.125
0.7253	0.2039	0.80565	0.4839	0.615	-0.128
0.7698	0.1533	0.80352	0.5001	0.539	-0.134
0.8145	0.1024	0.80160	0.5325	0.435	-0.125
<hr/>					
CHN (1) + MA (2) + EA (3)					
<hr/>					
<i>T</i> = 298.15 K					
0.0356	0.0708	0.89718	0.4377	0.113	-0.009
0.0711	0.1177	0.89920	0.4425	0.225	-0.027
0.1062	0.1642	0.90099	0.4500	0.362	-0.044
0.1232	0.2099	0.90271	0.4561	0.408	-0.048
0.1401	0.2552	0.90440	0.4574	0.458	-0.057
0.1745	0.3006	0.90702	0.4719	0.508	-0.068
0.2087	0.3457	0.90960	0.4909	0.563	-0.076

Chapter IX

0.2427	0.3904	0.91212	0.5097	0.625	-0.085
0.2764	0.4349	0.91494	0.5356	0.658	-0.088
0.3099	0.4791	0.91783	0.5624	0.686	-0.091
0.3432	0.5230	0.92112	0.5937	0.675	-0.091
0.3763	0.5666	0.92450	0.6279	0.658	-0.090
0.4159	0.5166	0.92488	0.6849	0.654	-0.083
0.4565	0.4653	0.92592	0.7445	0.583	-0.078
0.4982	0.4126	0.92674	0.8137	0.533	-0.069
0.5411	0.3585	0.92782	0.8865	0.455	-0.063
0.5851	0.3028	0.92912	0.9715	0.352	-0.052
0.6304	0.2457	0.93055	1.0639	0.233	-0.042
0.6770	0.1869	0.93239	1.1707	0.067	-0.026
0.7249	0.1264	0.93420	1.2866	-0.099	-0.011
<hr/>					
<i>T</i> = 308.15 K					
0.0356	0.0708	0.88510	0.3857	0.146	-0.019
0.0711	0.1177	0.88723	0.3857	0.256	-0.039
0.1062	0.1642	0.88913	0.3924	0.392	-0.052
0.1232	0.2099	0.89084	0.3923	0.445	-0.061
0.1401	0.2552	0.89259	0.3922	0.493	-0.070
0.1745	0.3006	0.89521	0.4056	0.551	-0.078
0.2087	0.3457	0.89799	0.4229	0.594	-0.083
0.2427	0.3904	0.90048	0.4372	0.668	-0.092
0.2764	0.4349	0.90334	0.4565	0.705	-0.097
0.3099	0.4791	0.90640	0.4332	0.723	-0.145
0.3432	0.5230	0.90964	0.5037	0.725	-0.100
0.3763	0.5666	0.91290	0.5336	0.727	-0.097
0.4159	0.5166	0.91344	0.5813	0.711	-0.091
0.4565	0.4653	0.91437	0.6308	0.655	-0.086
0.4982	0.4126	0.91544	0.6890	0.583	-0.076
0.5411	0.3585	0.91666	0.7496	0.493	-0.070
0.5851	0.3028	0.91784	0.8192	0.405	-0.059
0.6304	0.2457	0.91933	0.8957	0.282	-0.048
0.6770	0.1869	0.92071	0.9840	0.168	-0.032
0.7249	0.1264	0.92266	1.0780	-0.012	-0.018
<hr/>					
<i>T</i> = 318.15 K					
0.0356	0.0708	0.87224	0.3421	0.184	-0.028
0.0711	0.1177	0.87459	0.3408	0.291	-0.046
0.1062	0.1642	0.87654	0.3395	0.443	-0.063
0.1232	0.2099	0.87840	0.3409	0.489	-0.069
0.1401	0.2552	0.88025	0.3405	0.537	-0.076
0.1745	0.3006	0.88307	0.3498	0.594	-0.084
0.2087	0.3457	0.88596	0.3592	0.645	-0.093
0.2427	0.3904	0.88875	0.3697	0.708	-0.101
0.2764	0.4349	0.89188	0.3846	0.736	-0.105
0.3099	0.4791	0.89503	0.4032	0.765	-0.107
0.3432	0.5230	0.89847	0.4270	0.765	-0.103
0.3763	0.5666	0.90184	0.4504	0.775	-0.101
0.4159	0.5166	0.90266	0.4912	0.751	-0.094
0.4565	0.4653	0.90367	0.5329	0.707	-0.090
0.4982	0.4126	0.90493	0.5771	0.635	-0.086
0.5411	0.3585	0.90653	0.6305	0.524	-0.078
0.5851	0.3028	0.90790	0.6904	0.437	-0.067
0.6304	0.2457	0.90932	0.7548	0.342	-0.056

Chapter IX

0.6770	0.1869	0.91101	0.8325	0.214	-0.038
0.7249	0.1264	0.91312	0.9132	0.037	-0.023
<hr/>					
CHN (1) + MA (2) + MS (3)					
<hr/>					
<i>T</i> = 298.15 K					
0.0571	0.1136	1.15252	1.3572	-0.380	0.026
0.1079	0.1787	1.13242	1.2662	-0.677	0.034
0.1533	0.2369	1.11219	1.1912	-0.859	0.041
0.1713	0.2919	1.09705	1.1171	-0.956	0.046
0.1879	0.3423	1.08192	1.0543	-1.007	0.052
0.2240	0.3858	1.06184	1.0125	-0.996	0.060
0.2569	0.4255	1.04217	0.9726	-0.955	0.063
0.2870	0.4617	1.02301	0.9345	-0.897	0.062
0.3147	0.4951	1.00439	0.8982	-0.830	0.059
0.3402	0.5258	0.98634	0.8660	-0.758	0.057
0.3637	0.5542	0.96885	0.8277	-0.685	0.045
0.3856	0.5805	0.95192	0.7974	-0.612	0.038
0.4281	0.5317	0.95399	0.8582	-0.561	0.036
0.4721	0.4811	0.95628	0.9259	-0.528	0.033
0.5177	0.4287	0.95874	1.0002	-0.510	0.027
0.5650	0.3743	0.96135	1.0851	-0.505	0.022
0.6141	0.3178	0.96408	1.1848	-0.510	0.018
0.6651	0.2592	0.96690	1.2957	-0.524	0.012
0.7181	0.1982	0.96976	1.4288	-0.540	0.010
0.7733	0.1348	0.97262	1.5772	-0.555	0.004
<hr/>					
<i>T</i> = 308.15 K					
0.0571	0.1136	1.13950	1.2377	-0.086	0.016
0.1079	0.1787	1.11864	1.1523	-0.330	0.020
0.1533	0.2369	1.09752	1.0841	-0.442	0.027
0.1713	0.2919	1.08167	1.0199	-0.486	0.033
0.1879	0.3423	1.06627	0.9631	-0.526	0.037
0.2240	0.3858	1.04617	0.9224	-0.526	0.042
0.2569	0.4255	1.02680	0.8874	-0.524	0.047
0.2870	0.4617	1.00815	0.8547	-0.524	0.049
0.3147	0.4951	0.98984	0.8172	-0.492	0.043
0.3402	0.5258	0.97171	0.7836	-0.417	0.036
0.3637	0.5542	0.95472	0.7555	-0.394	0.033
0.3856	0.5805	0.93820	0.7303	-0.363	0.029
0.4281	0.5317	0.94069	0.7780	-0.342	0.026
0.4721	0.4811	0.94341	0.8312	-0.343	0.022
0.5177	0.4287	0.94577	0.8931	-0.305	0.020
0.5650	0.3743	0.94830	0.9621	-0.283	0.017
0.6141	0.3178	0.95099	1.0398	-0.274	0.014
0.6651	0.2592	0.95327	1.1262	-0.221	0.009
0.7181	0.1982	0.95609	1.2280	-0.222	0.008
0.7733	0.1348	0.95841	1.3392	-0.167	0.001
<hr/>					
<i>T</i> = 318.15 K					
0.0571	0.1136	1.12892	1.1233	-0.037	0.012
0.1079	0.1787	1.10738	1.0314	-0.223	0.015
0.1533	0.2369	1.08624	0.9582	-0.346	0.021
0.1713	0.2919	1.07043	0.8932	-0.409	0.025
0.1879	0.3423	1.05487	0.8401	-0.445	0.032
0.2240	0.3858	1.03472	0.7992	-0.445	0.038
0.2569	0.4255	1.01507	0.7614	-0.419	0.040

Chapter IX

0.2870	0.4617	0.99596	0.7293	-0.376	0.043
0.3147	0.4951	0.97746	0.6938	-0.327	0.039
0.3402	0.5258	0.95968	0.6593	-0.286	0.031
0.3637	0.5542	0.94289	0.6305	-0.283	0.027
0.3856	0.5805	0.92670	0.6064	-0.283	0.024
0.4281	0.5317	0.92945	0.6509	-0.263	0.025
0.4721	0.4811	0.93222	0.6925	-0.243	0.018
0.5177	0.4287	0.93505	0.7438	-0.227	0.015
0.5650	0.3743	0.93766	0.8014	-0.185	0.012
0.6141	0.3178	0.94057	0.8703	-0.171	0.012
0.6651	0.2592	0.94341	0.9425	-0.148	0.007
0.7181	0.1982	0.94616	1.0279	-0.113	0.004
0.7733	0.1348	0.94908	1.12510	-0.092	0.001
<hr/>					
CHN (1) + EA (2) + MS (3)					
<hr/>					
<i>T</i> = 298.15 K					
<hr/>					
0.0582	0.0972	1.14929	1.3956	-0.372	0.018
0.1111	0.1546	1.12664	1.3244	-0.609	0.026
0.1593	0.2070	1.10428	1.2616	-0.763	0.031
0.1797	0.2574	1.08719	1.1967	-0.844	0.037
0.1988	0.3044	1.0704	1.1361	-0.896	0.038
0.2387	0.3456	1.04913	1.0957	-0.910	0.043
0.2756	0.3837	1.02841	1.0613	-0.893	0.048
0.3098	0.4190	1.00829	1.0312	-0.855	0.054
0.3416	0.4519	0.98878	0.9959	-0.803	0.051
0.3712	0.4825	0.96991	0.9685	-0.743	0.052
0.3989	0.5110	0.95165	0.9392	-0.677	0.049
0.4248	0.5378	0.93399	0.9122	-0.607	0.046
0.4676	0.4884	0.93798	0.9785	-0.576	0.045
0.5112	0.4381	0.94213	1.0517	-0.558	0.044
0.5556	0.3868	0.94644	1.1277	-0.553	0.038
0.6008	0.3346	0.95089	1.2120	-0.559	0.033
0.6468	0.2815	0.95545	1.3073	-0.573	0.029
0.6937	0.2273	0.96006	1.4123	-0.587	0.024
0.7415	0.1721	0.96472	1.5282	-0.603	0.018
0.7903	0.1158	0.96930	1.6591	-0.605	0.015
<hr/>					
<i>T</i> = 308.15 K					
<hr/>					
0.0582	0.0972	1.13581	1.2599	-0.026	0.010
0.1111	0.1546	1.11174	1.1847	-0.133	0.014
0.1593	0.2070	1.08958	1.1219	-0.330	0.018
0.1797	0.2574	1.07235	1.0591	-0.411	0.021
0.1988	0.3044	1.05516	1.0030	-0.433	0.023
0.2387	0.3456	1.03419	0.9579	-0.491	0.022
0.2756	0.3837	1.01363	0.9229	-0.499	0.027
0.3098	0.4190	0.99389	0.8938	-0.509	0.033
0.3416	0.4519	0.97451	0.8656	-0.475	0.035
0.3712	0.4825	0.95583	0.8416	-0.438	0.040
0.3989	0.5110	0.93802	0.8150	-0.423	0.038
0.4248	0.5378	0.92088	0.7878	-0.410	0.034
0.4676	0.4884	0.92487	0.8396	-0.370	0.031
0.5112	0.4381	0.92941	0.9005	-0.386	0.031
0.5556	0.3868	0.93358	0.9637	-0.357	0.028
0.6008	0.3346	0.93772	1.0326	-0.320	0.025
0.6468	0.2815	0.94220	1.1119	-0.316	0.024

Chapter IX

0.6937	0.2273	0.94629	1.1923	-0.263	0.017
0.7415	0.1721	0.95107	1.2866	-0.283	0.015
0.7903	0.1158	0.95549	1.3878	-0.257	0.010
<i>T</i> = 318.15 K					
0.0582	0.0972	1.12564	1.1538	-0.021	0.001
0.1111	0.1546	1.10200	1.0811	-0.189	0.008
0.1593	0.2070	1.07865	1.0162	-0.266	0.011
0.1797	0.2574	1.06092	0.9594	-0.307	0.016
0.1988	0.3044	1.04397	0.9056	-0.368	0.017
0.2387	0.3456	1.02268	0.8631	-0.395	0.019
0.2756	0.3837	1.00197	0.8293	-0.390	0.024
0.3098	0.4190	0.98190	0.7977	-0.364	0.027
0.3416	0.4519	0.96264	0.7685	-0.343	0.029
0.3712	0.4825	0.94416	0.7385	-0.328	0.026
0.3989	0.5110	0.92640	0.7147	-0.316	0.027
0.4248	0.5378	0.90947	0.6912	-0.325	0.026
0.4676	0.4884	0.91397	0.7353	-0.316	0.024
0.5112	0.4381	0.91840	0.7832	-0.294	0.023
0.5556	0.3868	0.92296	0.8345	-0.282	0.019
0.6008	0.3346	0.92736	0.8917	-0.246	0.017
0.6468	0.2815	0.93168	0.9530	-0.195	0.014
0.6937	0.2273	0.93651	1.0189	-0.197	0.009
0.7415	0.1721	0.94149	1.0949	-0.210	0.007
0.7903	0.1158	0.94612	1.1774	-0.178	0.004
MA (1) + EA (2) + MS (3)					
<i>T</i> = 298.15 K					
0.0757	0.0954	1.14687	1.2350	-0.203	0.012
0.1420	0.1493	1.12377	1.0587	-0.469	0.018
0.2007	0.1968	1.10040	0.9254	-0.583	0.023
0.2249	0.2432	1.08289	0.8467	-0.646	0.025
0.2474	0.2860	1.06420	0.7791	-0.530	0.025
0.2935	0.3208	1.04165	0.6996	-0.470	0.023
0.3351	0.3522	1.01848	0.6259	-0.261	0.013
0.3729	0.3807	0.99786	0.5618	-0.224	0.001
0.4074	0.4067	0.97622	0.5087	-0.009	-0.008
0.4389	0.4305	0.95610	0.4600	0.129	-0.020
0.4679	0.4524	0.93554	0.4185	0.379	-0.029
0.4946	0.4726	0.91723	0.3825	0.472	-0.038
0.5379	0.4240	0.92079	0.3796	0.474	-0.042
0.5808	0.3757	0.92499	0.3799	0.417	-0.042
0.6235	0.3277	0.93001	0.3826	0.285	-0.040
0.6660	0.2800	0.93427	0.3858	0.231	-0.038
0.7082	0.2326	0.93969	0.3892	0.073	-0.036
0.7501	0.1855	0.94480	0.3961	-0.050	-0.029
0.7917	0.1387	0.95097	0.4055	-0.262	-0.021
0.8331	0.0922	0.95558	0.4151	-0.328	-0.012
<i>T</i> = 308.15 K					
0.0757	0.0954	1.13571	1.1228	-0.120	0.006
0.1420	0.1493	1.11197	0.9634	-0.350	0.013
0.2007	0.1968	1.08869	0.8402	-0.500	0.017
0.2249	0.2432	1.07048	0.7691	-0.508	0.019
0.2474	0.2860	1.05234	0.7068	-0.461	0.019
0.2935	0.3208	1.02985	0.6287	-0.421	0.012

Chapter IX

0.3351	0.3522	1.00741	0.5637	-0.295	0.004
0.3729	0.3807	0.98558	0.5056	-0.145	-0.006
0.4074	0.4067	0.96498	0.4571	-0.040	-0.015
0.4389	0.4305	0.94356	0.4086	0.226	-0.029
0.4679	0.4524	0.92066	0.3693	0.716	-0.040
0.4946	0.4726	0.90100	0.3349	0.945	-0.049
0.5379	0.4240	0.90420	0.3295	0.981	-0.055
0.5808	0.3757	0.90830	0.3284	0.928	-0.057
0.6235	0.3277	0.91261	0.3294	0.858	-0.057
0.6660	0.2800	0.91715	0.3329	0.770	-0.055
0.7082	0.2326	0.92265	0.3381	0.595	-0.050
0.7501	0.1855	0.92814	0.3443	0.428	-0.045
0.7917	0.1387	0.93417	0.3548	0.218	-0.035
0.8331	0.0922	0.94088	0.3658	-0.046	-0.025
<hr/>					
$T = 318.15 \text{ K}$					
0.0757	0.0954	1.12468	1.0358	-0.058	0.002
0.1420	0.1493	1.10029	0.8840	-0.265	0.007
0.2007	0.1968	1.07668	0.7699	-0.421	0.012
0.2249	0.2432	1.05808	0.7038	-0.413	0.014
0.2474	0.2860	1.03968	0.6428	-0.360	0.011
0.2935	0.3208	1.01707	0.5712	-0.334	0.005
0.3351	0.3522	0.99459	0.5079	-0.224	-0.004
0.3729	0.3807	0.97253	0.4554	-0.066	-0.012
0.4074	0.4067	0.95113	0.4085	0.108	-0.022
0.4389	0.4305	0.92996	0.3629	0.340	-0.036
0.4679	0.4524	0.90706	0.3280	0.832	-0.044
0.4946	0.4726	0.88739	0.2949	1.060	-0.054
0.5379	0.4240	0.89059	0.2898	1.095	-0.060
0.5808	0.3757	0.89449	0.2881	1.060	-0.062
0.6235	0.3277	0.89907	0.2891	0.960	-0.061
0.6660	0.2800	0.90390	0.2917	0.840	-0.059
0.7082	0.2326	0.90878	0.2972	0.720	-0.054
0.7501	0.1855	0.91441	0.3041	0.533	-0.048
0.7917	0.1387	0.92010	0.3115	0.349	-0.041
0.8331	0.0922	0.92651	0.3246	0.104	-0.028

Chapter IX

Table 9.4. Coefficients (c_i) of the Cibulka equation for different excess or deviation properties of the ternary mixtures at 298.15 K.

Mixture property	c_1	c_2	c_3	σ
CH (1) + MA (2) + EA (3)				
$V_{m,123}^E \cdot 10^6 \text{ (m}^3 \cdot \text{mol}^{-1}\text{)}$	-33.160	-70.292	-101.141	0.727
$\Delta\eta_{123} \text{ (mPa} \cdot \text{s)}$	3.089	6.269	5.013	0.057
$\kappa_{S,123}^E \text{ (TPa}^{-1}\text{)}$	69.327	-96.356	119.839	0.501
$R_{m,123}^E \cdot 10^6 \text{ (m}^3 \cdot \text{mol}^{-1}\text{)}$	-61.838	-33.661	22.744	0.573
CH (1) + MA (2) + MS (3)				
$V_{m,123}^E \cdot 10^6 \text{ (m}^3 \cdot \text{mol}^{-1}\text{)}$	-139.638	255.342	284.283	0.995
$\Delta\eta_{123} \text{ (mPa} \cdot \text{s)}$	4.197	-7.789	-10.455	0.038
$\kappa_{S,123}^E \text{ (TPa}^{-1}\text{)}$	-180.031	262.334	446.651	1.237
$R_{m,123}^E \cdot 10^6 \text{ (m}^3 \cdot \text{mol}^{-1}\text{)}$	-117.976	232.117	378.906	1.409
CH (1) + EA (2) + MS (3)				
$V_{m,123}^E \cdot 10^6 \text{ (m}^3 \cdot \text{mol}^{-1}\text{)}$	-114.234	218.228	251.157	0.836
$\Delta\eta_{123} \text{ (mPa} \cdot \text{s)}$	3.543	-6.443	-9.283	0.034
$\kappa_{S,123}^E \text{ (TPa}^{-1}\text{)}$	-184.307	221.504	456.626	0.968
$R_{m,123}^E \cdot 10^6 \text{ (m}^3 \cdot \text{mol}^{-1}\text{)}$	-118.068	218.682	358.956	1.213
CHN (1) + MA (2) + EA (3)				
$V_{m,123}^E \cdot 10^6 \text{ (m}^3 \cdot \text{mol}^{-1}\text{)}$	-23.577	6.380	-68.538	0.366
$\Delta\eta_{123} \text{ (mPa} \cdot \text{s)}$	10.234	-0.831	-2.293	0.079
$\kappa_{S,123}^E \text{ (TPa}^{-1}\text{)}$	-76.506	19.862	143.757	0.221
$R_{m,123}^E \cdot 10^6 \text{ (m}^3 \cdot \text{mol}^{-1}\text{)}$	-173.781	-83.553	46.788	1.461
CHN (1) + MA (2) + MS (3)				
$V_{m,123}^E \cdot 10^6 \text{ (m}^3 \cdot \text{mol}^{-1}\text{)}$	-79.219	187.614	259.229	0.987
$\Delta\eta_{123} \text{ (mPa} \cdot \text{s)}$	3.941	-5.066	5.224	0.035
$\kappa_{S,123}^E \text{ (TPa}^{-1}\text{)}$	-177.799	77.390	222.36	0.424
$R_{m,123}^E \cdot 10^6 \text{ (m}^3 \cdot \text{mol}^{-1}\text{)}$	-96.775	157.157	97.069	0.327
CHN (1) + EA (2) + MS (3)				
$V_{m,123}^E \cdot 10^6 \text{ (m}^3 \cdot \text{mol}^{-1}\text{)}$	-71.820	170.773	238.72	0.854
$\Delta\eta_{123} \text{ (mPa} \cdot \text{s)}$	3.031	-5.963	-0.124	0.008
$\kappa_{S,123}^E \text{ (TPa}^{-1}\text{)}$	-143.309	21.471	247.433	0.337
$R_{m,123}^E \cdot 10^6 \text{ (m}^3 \cdot \text{mol}^{-1}\text{)}$	-103.201	156.926	227.432	0.692
MA (1) + EA (2) + MS (3)				
$V_{m,123}^E \cdot 10^6 \text{ (m}^3 \cdot \text{mol}^{-1}\text{)}$	-89.779	130.158	288.616	0.920
$\Delta\eta_{123} \text{ (mPa} \cdot \text{s)}$	4.591	-4.168	-6.071	0.007
$\kappa_{S,123}^E \text{ (TPa}^{-1}\text{)}$	-218.421	100.827	569.888	0.878
$R_{m,123}^E \cdot 10^6 \text{ (m}^3 \cdot \text{mol}^{-1}\text{)}$	-120.962	133.731	337.254	0.865

Chapter IX

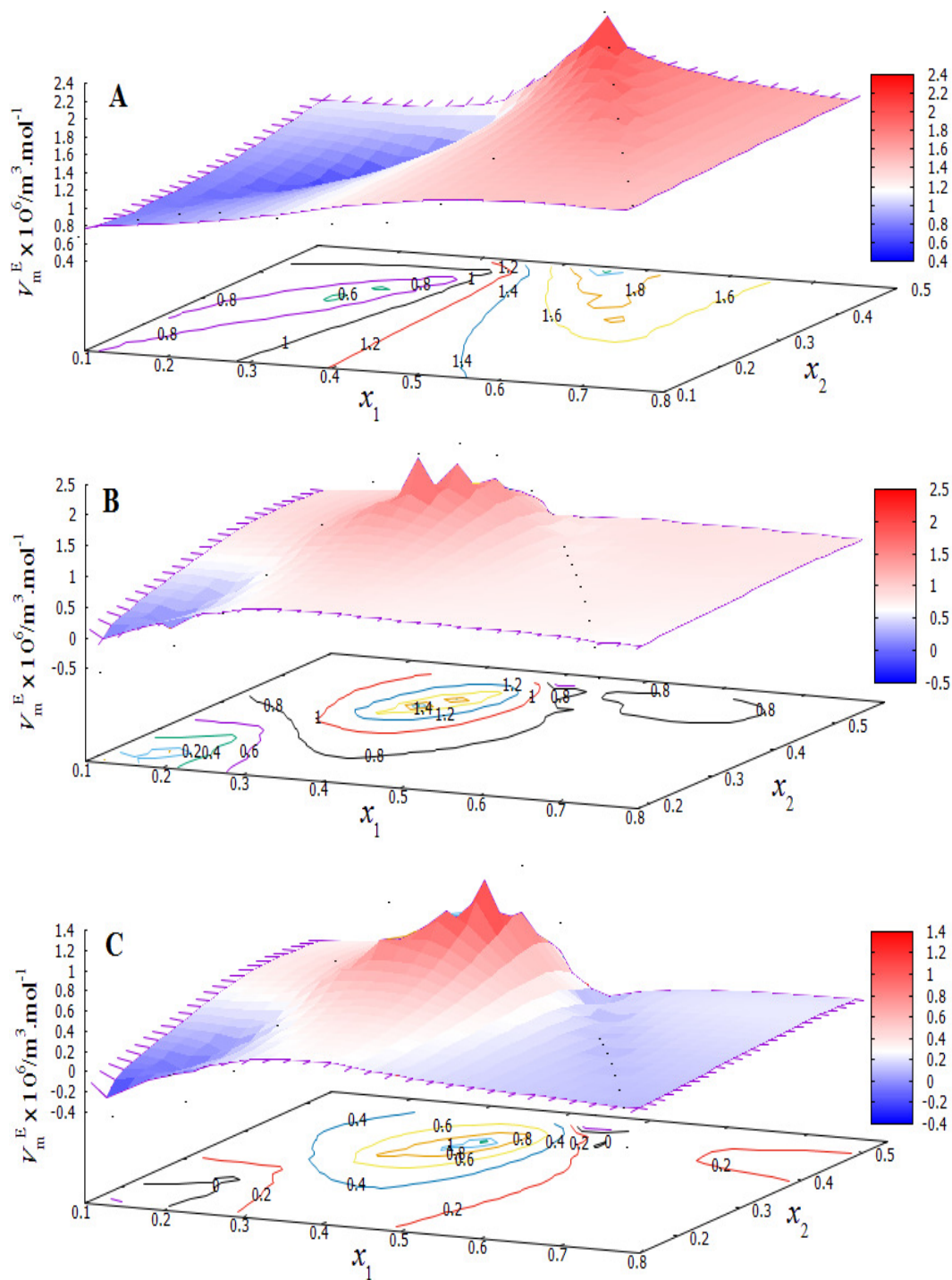


Fig. 9.3. Three-dimensional mesh plots of excess molar volumes ($V_{m,123}^E$) for the ternary mixtures: A, CH (1) + MA (2) + EA (3); B, CH (1) + MA (2) + MS (3) and C, CH (1) + EA (2) + MS (3) and the corresponding pseudo-two dimensional contour plot of constant $V_{m,123}^E$ values for these mixtures at 298.15 K.

Chapter IX

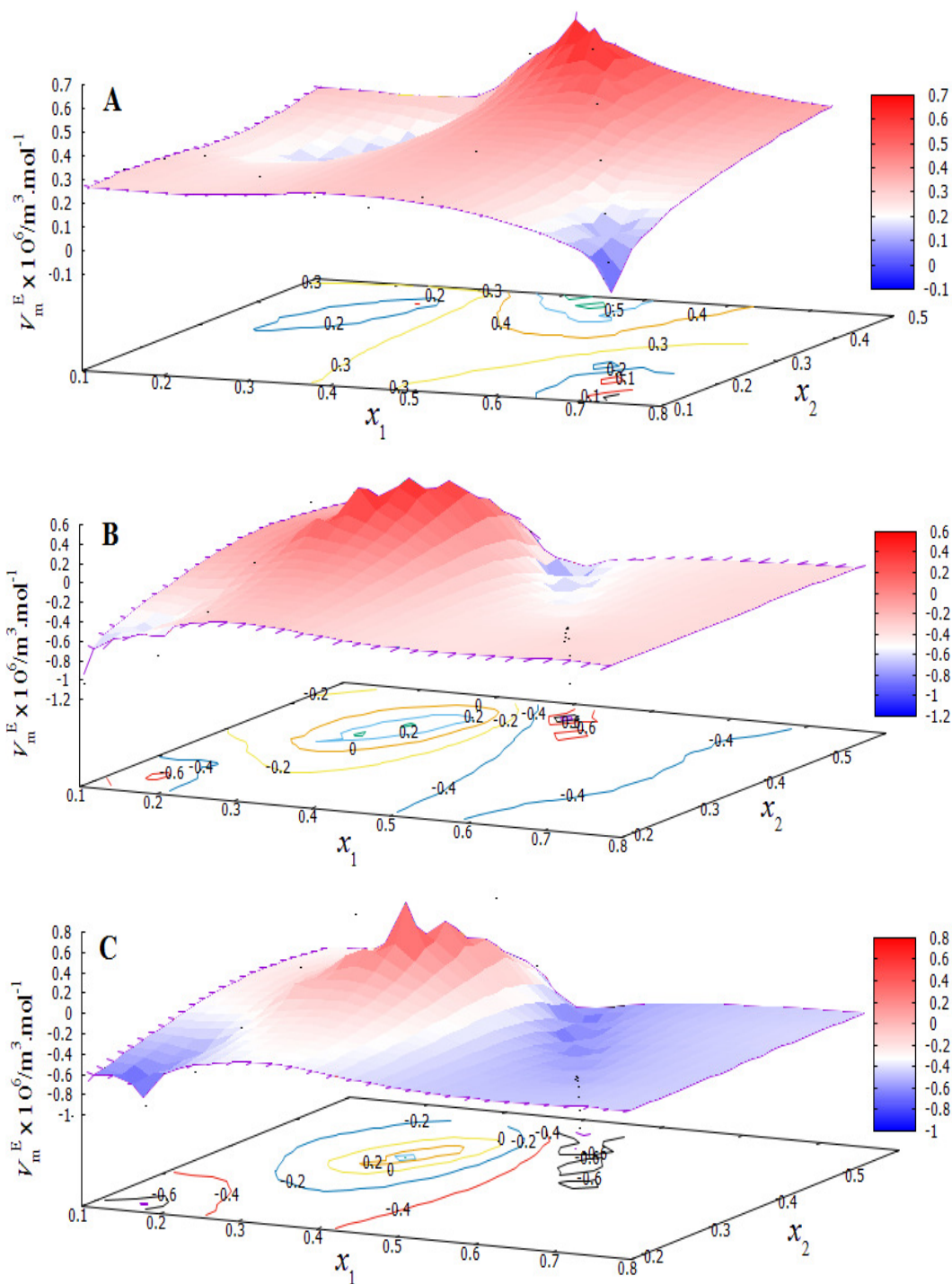


Fig. 9.4. Three-dimensional mesh plots of excess molar volumes ($V_{m,123}^E$) for the ternary mixtures: A, CHN (1) + MA (2) + EA (3); B, CHN (1) + MA (2) + MS (3) and C, CHN (1) + EA (2) + MS (3) and the corresponding pseudo-two dimensional contour plot of constant $V_{m,123}^E$ values for these mixtures at 298.15 K.

Chapter IX

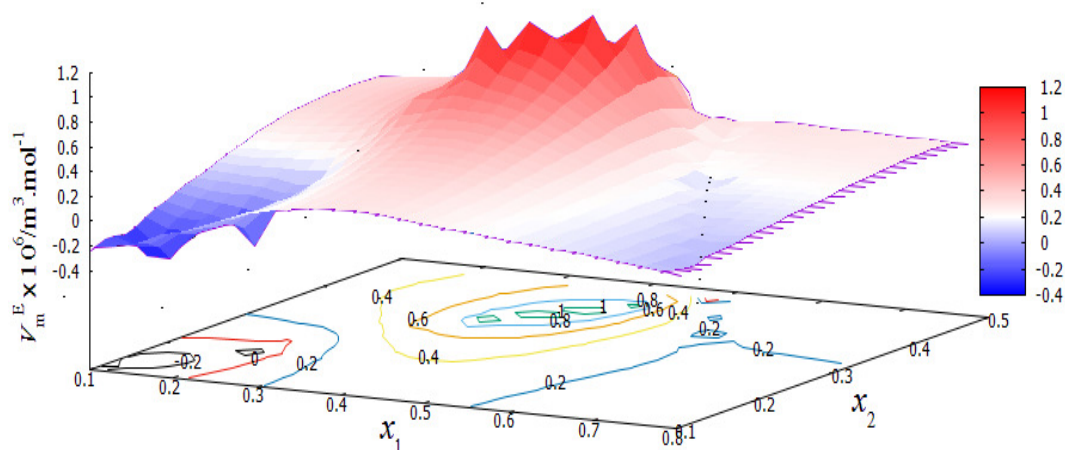


Fig. 9.5. Three-dimensional mesh plots of excess molar volumes ($V_{m,123}^E$) for the ternary mixture MA (1) + EA (2) + MS (3) and the corresponding pseudo-two dimensional contour plot of constant $V_{m,123}^E$ values at 298.15 K.

Table 9.5. Maxima and minima of the ternary contributions to different excess or deviation properties of the ternary mixtures at 298.15 K.

Ternary contributions	x_1 x_2 x_1 x_2							
	CH (1) + MA (2) + EA (3)							
$(V_{m,123}^E - V_{Bin}^E)^a$	max	-0.1115	0.0413	0.0704	min	-3.4263	0.3081	0.4159
$(\Delta\eta_{123} - \Delta\eta_{Bin})^b$	max	0.2513	0.0413	0.0704	min	0.0096	0.3081	0.4159
$(\kappa_{S,123}^E - \kappa_{S,Bin}^E)^c$	max	3.1717	0.2720	0.3753	min	0.1147	0.7544	0.1128
$(R_{m,123}^E - R_{m,Bin}^E)^d$	max	-0.1592	0.0413	0.0704	min	-2.2488	0.2720	0.3753
CH (1) + MA (2) + MS (3)								
$(V_{m,123}^E - V_{Bin}^E)^a$	max	2.4665	0.3486	0.4705	min	-0.8846	0.1236	0.1756
$(\Delta\eta_{123} - \Delta\eta_{Bin})^b$	max	0.0213	0.1236	0.1756	min	-0.1020	0.3486	0.4705
$(\kappa_{S,123}^E - \kappa_{S,Bin}^E)^c$	max	3.6070	0.3486	0.4705	min	-1.0522	0.1236	0.1756
$(R_{m,123}^E - R_{m,Bin}^E)^d$	max	4.1899	0.3486	0.4705	min	-0.3662	0.0660	0.1125
CH (1) + EA (2) + MS (3)								
$(V_{m,123}^E - V_{Bin}^E)^a$	max	2.3760	0.3768	0.4277	min	-0.6730	0.1271	0.1519
$(\Delta\eta_{123} - \Delta\eta_{Bin})^b$	max	0.0183	0.1271	0.1519	min	-0.0900	0.3768	0.4277
$(\kappa_{S,123}^E - \kappa_{S,Bin}^E)^c$	max	2.9759	0.3768	0.4277	min	-1.2082	0.1271	0.1519
$(R_{m,123}^E - R_{m,Bin}^E)^d$	max	3.7132	0.3768	0.4277	min	-0.4976	0.1271	0.1519
CHN (1) + MA (2) + EA (3)								
$(V_{m,123}^E - V_{Bin}^E)^a$	max	-0.0635	0.0356	0.0708	min	-1.7914	0.2764	0.4349
$(\Delta\eta_{123} - \Delta\eta_{Bin})^b$	max	0.3176	0.2764	0.4349	min	0.0226	0.0356	0.0708

Chapter IX

$(\kappa_{S,123}^E - \kappa_{S,Bin}^E)^c$	max	0.1512	0.3763	0.5666	min	-0.8212	0.1745	0.3006
$(R_{m,123}^E - R_{m,Bin}^E)^d$	max	-0.3906	0.0356	0.0708	min	-6.1261	0.2764	0.4349
CHN (1) + MA (2) + MS (3)								
$(V_{m,123}^E - V_{Bin}^E)^a$	max	3.2055	0.3147	0.4951	min	-0.2101	0.0571	0.1136
$(\Delta\eta_{123} - \Delta\eta_{Bin})^b$	max	0.1688	0.2569	0.4255	min	0.0070	0.7733	0.1348
$(\kappa_{S,123}^E - \kappa_{S,Bin}^E)^c$	max	-0.1432	0.3856	0.5805	min	-2.6743	0.1713	0.2919
$(R_{m,123}^E - R_{m,Bin}^E)^d$	max	0.4295	0.6651	0.2592	min	-1.1144	0.1713	0.2919
CHN (1) + EA (2) + MS (3)								
$(V_{m,123}^E - V_{Bin}^E)^a$	max	3.0090	0.3416	0.4519	min	-0.2011	0.1111	0.1546
$(\Delta\eta_{123} - \Delta\eta_{Bin})^b$	max	0.0543	0.1988	0.3044	min	-0.0156	0.7415	0.1721
$(\kappa_{S,123}^E - \kappa_{S,Bin}^E)^c$	max	-0.0096	0.4248	0.5378	min	-1.9726	0.1797	0.2574
$(R_{m,123}^E - R_{m,Bin}^E)^d$	max	1.6976	0.3712	0.4825	min	-0.6504	0.1593	0.2070
MA (1) + EA (2) + MS (3)								
$(V_{m,123}^E - V_{Bin}^E)^a$	max	2.4855	0.4074	0.4067	min	-0.4238	0.1420	0.1493
$(\Delta\eta_{123} - \Delta\eta_{Bin})^b$	max	0.0633	0.2249	0.2432	min	-0.0026	0.4946	0.4726
$(\kappa_{S,123}^E - \kappa_{S,Bin}^E)^c$	max	1.7562	0.4389	0.4305	min	-2.0473	0.2007	0.1968
$(R_{m,123}^E - R_{m,Bin}^E)^d$	max	2.1771	0.4074	0.4067	min	-0.7756	0.1420	0.1493

Units: $a, 10^6 (\text{m}^3 \cdot \text{mol}^{-1})$; $b, \text{mPa}\cdot\text{s}$; c, TPa^{-1} ; $d, 10^6 (\text{m}^3 \cdot \text{mol}^{-1})$

Figures 9.3, 9.4 and 9.5 illustrate three dimensional mesh and contour plots of $V_{m,123}^E$ values of the ternary mixtures calculated from Eqs (3) and (4) against the mole fractions of their components in the ternary mixtures at 298.15 K; the contour plots are for the constant $V_{m,123}^E$ values as defined by the mole fractions of the components. The so-called ternary contributions, defined as $(V_{m,123}^E - V_{Bin}^E)$, represent the difference between the experimental excess molar volumes ($V_{m,123}^E$) of the ternary property and the value (V_{Bin}^E) predicted by the corresponding data of the binary mixtures; the maximum and minimum values of such contributions are given in Table 9.5. The positive contributions arise from the breakup interactions¹³ of similar molecular species; the maximum and minimum ternary contributions¹³ support non-homogeneous behavior of the ternary mixtures.

Chapter IX

9.3.2. Viscosity Deviations

The viscosity deviations ($\Delta\eta$) of the binary and ternary mixtures were obtained from the differences between the measured viscosity (η) and the ideal viscosity (η_{id}) as follows:

$$\Delta\eta = \eta - \eta_{id} \quad (5)$$

and the ideal viscosity (η_{id}) is given by:¹⁴

$$\eta_{id} = \exp\left(\sum_{i=1}^n x_i \ln \eta_{id}\right) \quad (6)$$

where n is the number of components in a mixture and other symbols have their usual meanings as expressed in previous chapters. The uncertainty in viscosity deviation ($\Delta\eta$) was evaluated to be ± 0.004 mPa.s. Table 9.1 shows that $\Delta\eta$ values are negative for the mixture (MA + EA) but for the mixtures (MA + MS) and (EA + MS) such values are positive. It was observed if V_m^E values are positive, $\Delta\eta$ values become negative for many binary mixtures and *vice-versa*. Such a coincidence was found for these binary mixtures. However, for each mixture $\Delta\eta$ values decrease as the experiment temperature increases indicating that the interactions between the dissimilar molecules become weaker at higher temperatures (Table 9.1). The variations in $\Delta\eta$ values for all the nine binary mixtures as a function of composition (x_1) at 298.15 K are depicted in Figure 9.6, which suggests more or less the same order of molecular interactions as obtained from the V_m^E values discussed earlier. The $\Delta\eta_{123}$ values for the mixtures (CH + MA + EA) and (CHN + MA + EA) are found to be negative over the entire composition range studied at all the experimental temperatures. For the mixtures (CH + MA + MS) and (CH + EA + MS), $\Delta\eta_{123}$ values are found to be positive at lower mole fractions (x_1) of CH but are negative at higher mole fractions (x_1) of CH. For the mixtures (CHN + MA + MS) and (CHN + EA + MS), $\Delta\eta_{123}$ values are negative throughout the entire composition range studied at all the experimental temperatures. For the mixture (MA + EA + MS), $\Delta\eta_{123}$ values are positive when the mole fractions of MS are higher than those of the alkyl acetates at all the experimental temperatures. So the correlation that the $V_{m,123}^E$ values are positive

Chapter IX

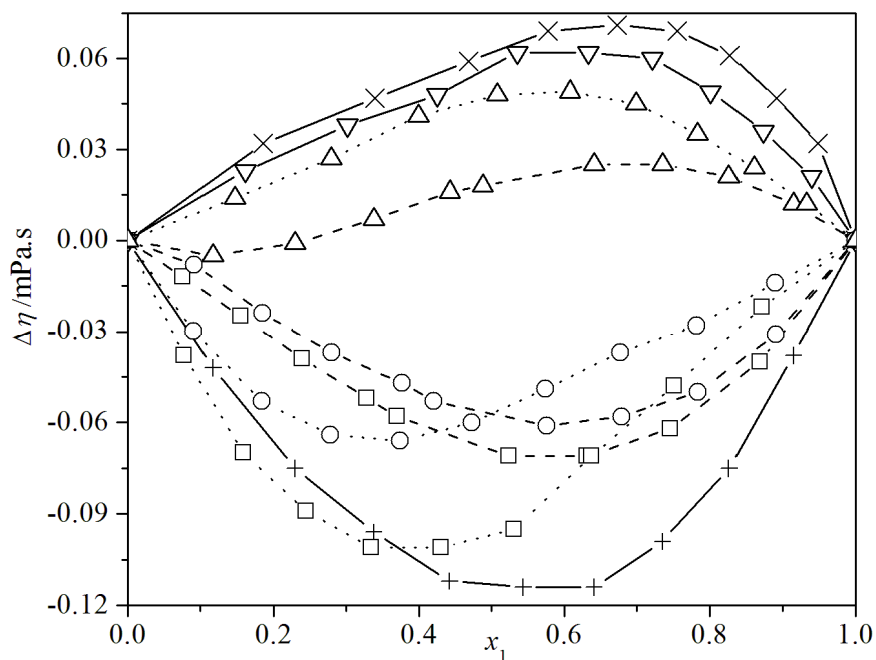


Fig. 9.6. Viscosity deviations ($\Delta\eta$) versus the mole fractions (x_1) of the first component in all the binary mixtures at $T = 298.15$ K. The graphical points represent the $\Delta\eta$ values for the mixtures containing: \square , MA; \circ , EA; Δ , MS. While dashed lines represent the mixtures with CH as the first component and dotted lines represent the mixtures with CHN as the first component. Solid lines represent binary mixtures of two esters only. Symbols: +, (MA + EA); \times , (MA + MS); ∇ , (EA + MS).

for negative $\Delta\eta_{123}$ values and *vice-versa* also holds good for the all these ternary mixtures and the nature of molecular interactions in these mixtures can well be explained from the nature of the mixing components and the molecular interactions in the associated binary mixtures. Similar to V_m^E values, $\Delta\eta$ values of the binary mixtures were fitted to the Redlich-Kister polynomial and the corresponding coefficients (a_i)⁹ are: $a_0 = -0.4649$, $a_1 = -0.118$, $a_2 = 0.0068$, $a_3 = 0.1044$ for the mixture (MA + EA); $a_0 = 0.2469$, $a_1 = 0.0904$, $a_2 = 0.1706$, $a_3 = 0.2201$ for the mixture (MA + MS) and $a_0 = 0.2261$, $a_1 = 0.132$, $a_2 = 0.0479$, $a_3 = -0.0281$ for the mixture (EA + MS) with standard deviations (σ) 0.0024, 0.0038, 0.0023 for the mixtures, respectively.

Chapter IX

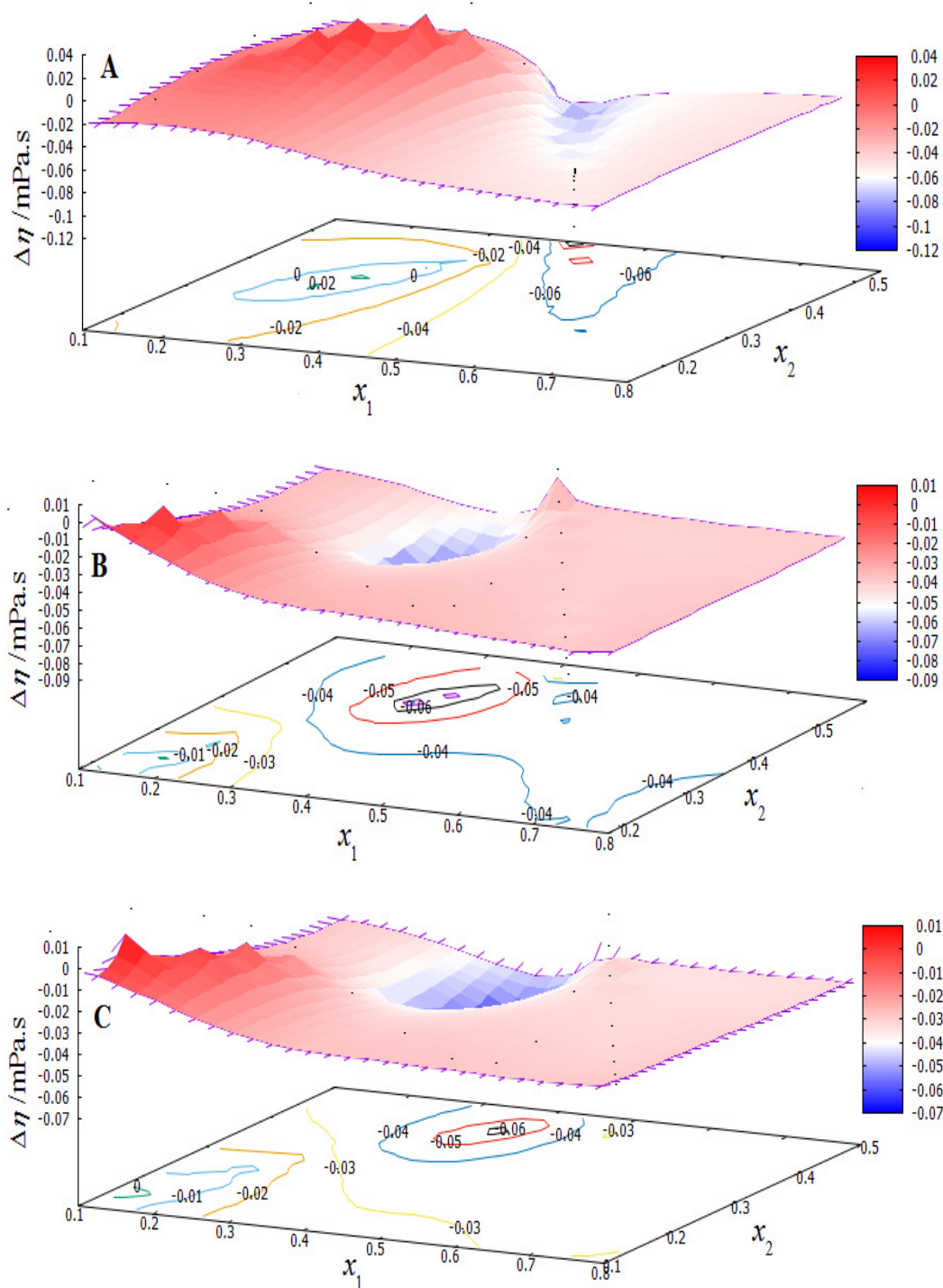


Fig. 9.7. Three-dimensional mesh plots of viscosity deviations ($\Delta\eta_{123}$) for the ternary mixtures: A, CH (1) + MA (2) + EA (3); B, CH (1) + MA (2) + MS (3) and C, CH (1) + EA (2) + MS (3) and the corresponding pseudo-two dimensional contour plot of constant $\Delta\eta_{123}$ values for these mixtures at 298.15 K.

Chapter IX

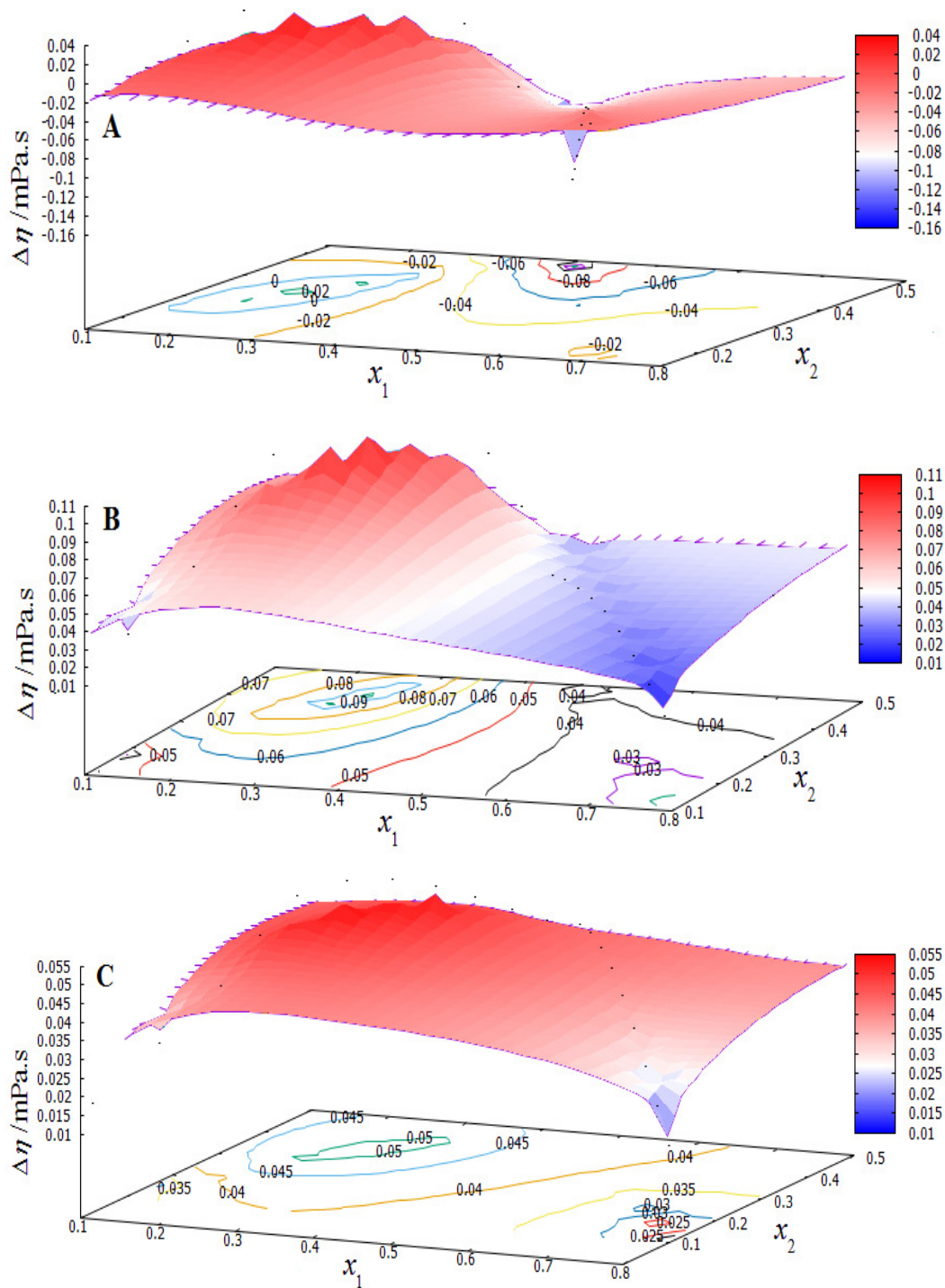


Fig. 9.8. Three-dimensional mesh plots of viscosity deviations ($\Delta\eta_{123}$) for the ternary mixtures: A, CHN (1) + MA (2) + EA (3); B, CHN (1) + MA (2) + MS (3) and C, CHN (1) + EA (2) + MS (3) and the corresponding pseudo-two dimensional contour plot of constant $\Delta\eta_{123}$ values for these mixtures at 298.15 K.

Chapter IX

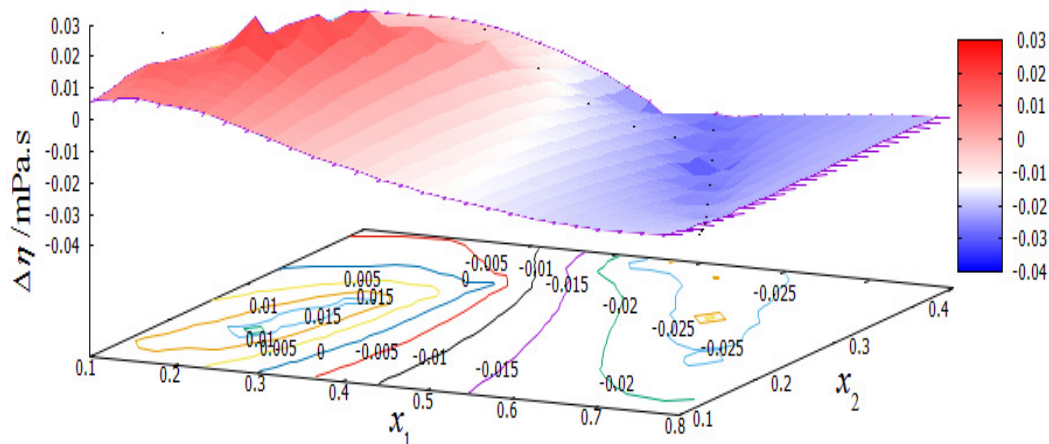


Fig. 9.9. Three-dimensional mesh plots of viscosity deviations ($\Delta\eta_{123}$) for the ternary mixture MA (1) + EA (2) + MS (3) and the corresponding pseudo-two dimensional contour plot of constant $\Delta\eta_{123}$ values at 298.15 K.

$\Delta\eta_{123}$ values of the ternary mixtures at 298.15 K were also fitted to the Cibulka equation (Eq. 3) in a similar fashion to $V_{m,123}^E$ values and the coefficients (c_i) are listed in Table 9.4. Figures 9.7, 9.8 and 9.9 illustrate three-dimensional mesh and contour plots of the calculated $\Delta\eta_{123}$ values of the ternary mixtures against the mole fractions of their components. The so-called ternary contributions, defined as $(\Delta\eta_{123} - \Delta\eta_{Bin})$, were calculated; the maximum and minimum values of such contributions are given in Table 9.5.

9.3.3. Excess Isentropic Compressibility

The experimental speeds of sound (u) and the densities (ρ) of the binary and ternary mixtures at 298.15 K were used to determine the isentropic compressibilities (κ_s) and the excess isentropic compressibilities (κ_s^E) of the mixtures. The excess isentropic compressibilities (κ_s^E) were obtained from the relation:

$$\kappa_s^E = \kappa_s - \kappa_s^{id} \quad (7)$$

where κ_s is the isentropic compressibility and was calculated using the Laplace relation, $\kappa_s = 1/\rho u^2$ and κ_s^{id} is the isentropic compressibility for an ideal mixture. According to Benson and Kiyohara¹⁵ and Acree,¹⁶ κ_s^{id} for a n-component mixture is given by the relation:

Chapter IX

$$\kappa_S^{\text{id}} = \sum_{i=1}^n \tau_i \left[\kappa_{S,i} + \frac{TV_{m,i}^* \alpha_i^2}{c_{P,i}} \right] - \left\{ \frac{T \sum_{i=1}^n (x_i V_{m,i}^*) \sum_{i=1}^n (\tau_i \alpha_i)^2}{\sum_{i=1}^n (x_i c_{P,i})} \right\} \quad (8)$$

where τ_i is the volume fraction of the i^{th} component in the mixture, $\kappa_{S,i}$, $V_{m,i}^*$, α_i and $c_{P,i}$ are the isentropic compressibility, molar volume, isobaric expansion coefficient and molar isobaric heat capacity of the pure components, respectively. Isobaric expansion coefficients (α_i) were obtained from experimental densities and $c_{P,i}$ values were adapted from the literature.⁵ The parameters u , κ_s and κ_s^E at 298.15 K are listed in Table 9.6. The experimental speeds of sound of each pure liquid were in good agreement with the literature values¹⁷⁻²¹ at 298.15 K. Figure 9.10 represents the variation of excess isentropic compressibilities (κ_s^E) against the mole fractions (x_1) of the first component in the binary mixtures at 298.15 K. While excess isentropic compressibilities (κ_s^E) for the mixture (MA + EA) were positive, those for the mixtures (MA + MS) and (EA + MS) were negative. Positive κ_s^E values for the mixture (MA + EA) suggest perturbation of the associated structures of the alkyl acetates (through dipolar association) or molecular order in the pure liquids on mutual mixing leading to volume expansion. Negative κ_s^E values for the mixtures (MA + MS) and (EA + MS) are associated with structure making or more compact packing of the dissimilar molecules due to combined effects of hydrogen bond interactions, dipole-dipole interactions and interstitial accommodation leading to volume contraction for these two binaries. Thus the study of the isentropic compressibilities (κ_s) and the excess isentropic compressibilities (κ_s^E) of different mixtures also stand in support of the order of molecular interactions discussed earlier on the basis of excess molar volumes and viscosity deviations. κ_s^E values of the binary mixtures were also fitted to the Redlich-Kister polynomial and the corresponding coefficients (a_i)⁹ are: $a_0 = 2.3276$, $a_1 = -0.9972$, $a_2 = 0.8128$, $a_3 = 1.2091$ for the mixture (MA + EA); $a_0 = -2.218$, $a_1 = -2.3509$, $a_2 = -0.8534$, $a_3 = 1.1304$ for the mixture (MA + MS) and $a_0 = -1.797$, $a_1 = -1.4454$, $a_2 = 0.0392$, $a_3 = 1.1186$ for the mixture (EA + MS) with standard deviations (σ) 0.0112, 0.0072, 0.0127 for the mixtures, respectively.

Chapter IX

Table 9.6. Ultrasonic speeds (u), isentropic compressibility (κ_s), excess isentropic compressibility (κ_s^E), refractive indices (n_D), molar refractions (R_m) and excess molar refractions (R_m^E) for the binary mixtures at 298.15 K.

x_1	u ($\text{m} \cdot \text{s}^{-1}$)	n_D	κ_s (TPa^{-1})	κ_s^E (TPa^{-1})	$R_m \cdot 10^6$ ($\text{m}^3 \cdot \text{mol}^{-1}$)	$R_m^E \cdot 10^6$ ($\text{m}^3 \cdot \text{mol}^{-1}$)
MA (1) + EA (2)						
0	1144.3	1.3712	853.7	0	22.343	0
0.1167	1126.2	1.3843	881.8	31.4	22.627	0.831
0.2292	1116.9	1.3925	898.1	51.2	22.675	1.406
0.3376	1114.7	1.4003	902.4	58.8	22.677	1.916
0.4422	1115.7	1.4060	9.015	61.5	22.576	2.305
0.5432	1119.3	1.4072	893.6	57.1	22.190	2.392
0.6408	1125.1	1.4048	882.3	49.5	21.650	2.309
0.7351	1130.5	1.3973	870.8	41.6	20.864	1.965
0.8263	1135.1	1.3869	858.5	33.0	19.922	1.450
0.9146	1140.1	1.3756	843.6	21.8	18.924	0.865
1	1148.5	1.3604	818.0	0	17.658	0
MA (1) + MS (2)						
0	1410.9	1.5352	426.0	0	40.179	0
0.1858	1373.4	1.5001	459.6	-20.4	35.105	-0.890
0.3393	1340.0	1.4725	493.6	-36.5	31.213	-1.325
0.4682	1312.2	1.4480	525.7	-50.5	28.013	-1.622
0.5779	1290.2	1.4250	555.6	-63.3	25.314	-1.850
0.6726	1265.8	1.4052	590.5	-68.1	23.117	-1.914
0.7550	1238.9	1.3887	630.1	-65.2	21.304	-1.872
0.8274	1211.1	1.3758	675.2	-54.2	19.888	-1.657
0.8915	1185.8	1.3666	722.3	-38.8	18.808	-1.294
0.9487	1164.4	1.3608	770.1	-20.5	18.028	-0.785
1	1148.5	1.3604	818.0	0	17.658	0
EA (1) + MS (2)						
0	1410.9	1.5352	426.0	0	40.179	0
0.1610	1358.3	1.5035	472.7	-15.4	36.595	-0.713
0.3015	1316.1	1.4779	517.1	-27.5	33.671	-1.130
0.4253	1284.9	1.4546	557.0	-39.2	31.141	-1.452
0.5352	1256.3	1.4324	598.1	-45.3	28.882	-1.751
0.6333	1234.4	1.4153	636.1	-50.3	27.102	-1.782
0.7215	1211.4	1.4017	677.6	-48.2	25.635	-1.675
0.8012	1188.9	1.3905	723.0	-39.0	24.456	-1.433
0.8735	1168.2	1.3805	770.0	-25.1	23.447	-1.152
0.9396	1154.2	1.3762	812.5	-13.2	22.854	-0.566
1	1144.3	1.3712	853.7	0	22.343	0

Chapter IX

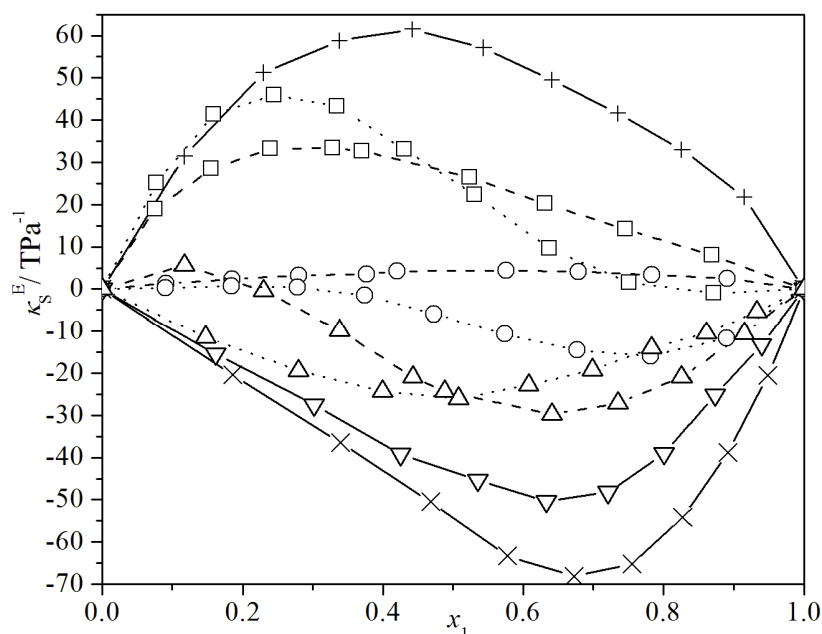


Fig. 9.10. Excess isentropic compressibility (κ_s^E) versus the mole fractions (x_1) of the first component in all the binary mixtures studied at $T = 298.15$ K. The graphical points represent the κ_s^E values for the mixtures containing: \square , MA; \circ , EA; Δ , MS. While dashed lines represent the mixtures with CH as the first component and dotted lines represent the mixtures with CHN as the first component. Solid lines represent binary mixtures of two esters only. Symbols: +, (MA + EA); \times , (MA + MS); ∇ , (EA + MS).

For the ternary mixtures $\kappa_{S,123}^E$ values were observed to follow similar trends as those of $V_{m,123}^E$ values against the composition of the ternary mixtures and $\kappa_{S,123}^E$ values at 298.15 K were also fitted to the Cibulka equation; the coefficients (c_i) are listed in Table 9.4. Figures 9.11, 9.12 and 9.13 illustrate three-dimensional mesh and contour plots of the calculated $\kappa_{S,123}^E$ values of the ternary mixtures against the mole fractions of their components and the maximum and minimum values of the so-called ternary contributions ($\kappa_{S,123}^E - \kappa_{S,Bin}^E$) were given in Table 9.5.

Chapter IX

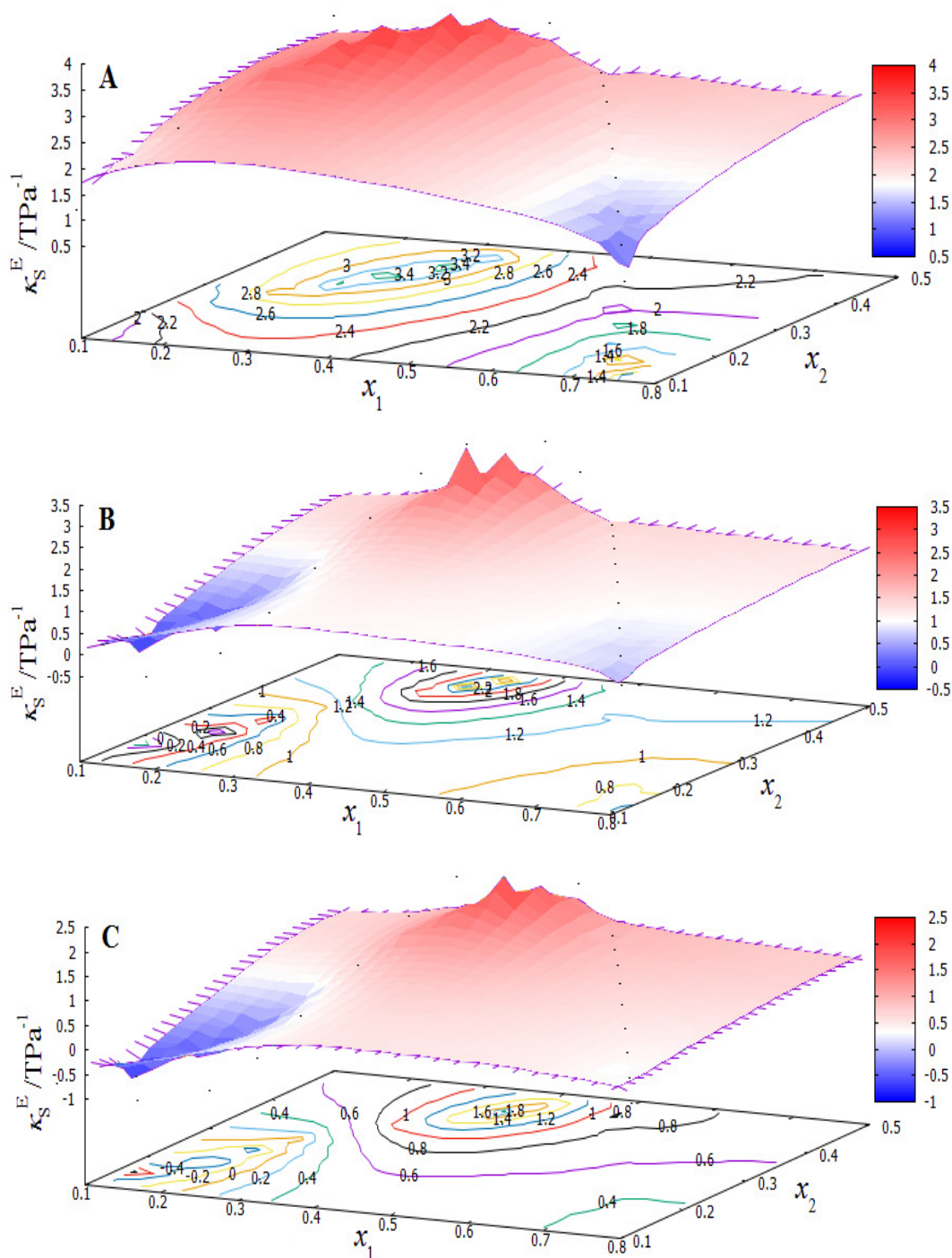


Fig. 9.11. Three-dimensional mesh plots of excess isentropic compressibility ($\kappa_{S,123}^E$) for the ternary mixtures: A, CH (1) + MA (2) + EA (3); B, CH (1) + MA (2) + MS (3) and C, CH (1) + EA (2) + MS (3) and the corresponding pseudo-two dimensional contour plot of constant $\kappa_{S,123}^E$ values for these mixtures at 298.15 K.

Chapter IX

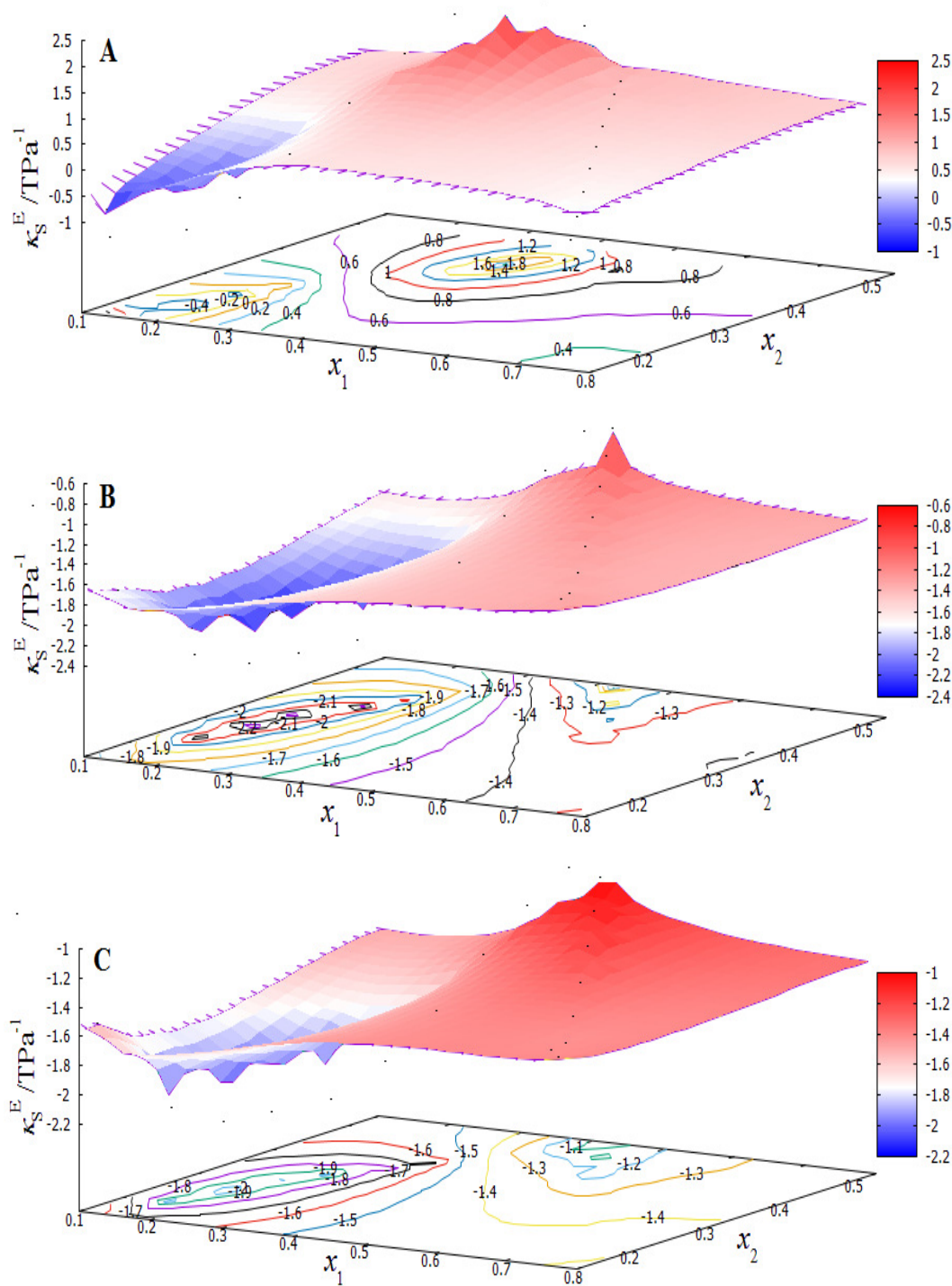


Fig. 9.12. Three-dimensional mesh plots of excess isentropic compressibility ($\kappa_{S,123}^E$) for the ternary mixtures: A, CHN (1) + MA (2) + EA (3); B, CHN (1) + MA (2) + MS (3) and C, CHN (1) + EA (2) + MS (3) and the corresponding pseudo-two dimensional contour plot of constant $\kappa_{S,123}^E$ values for these mixtures at 298.15 K.

Chapter IX

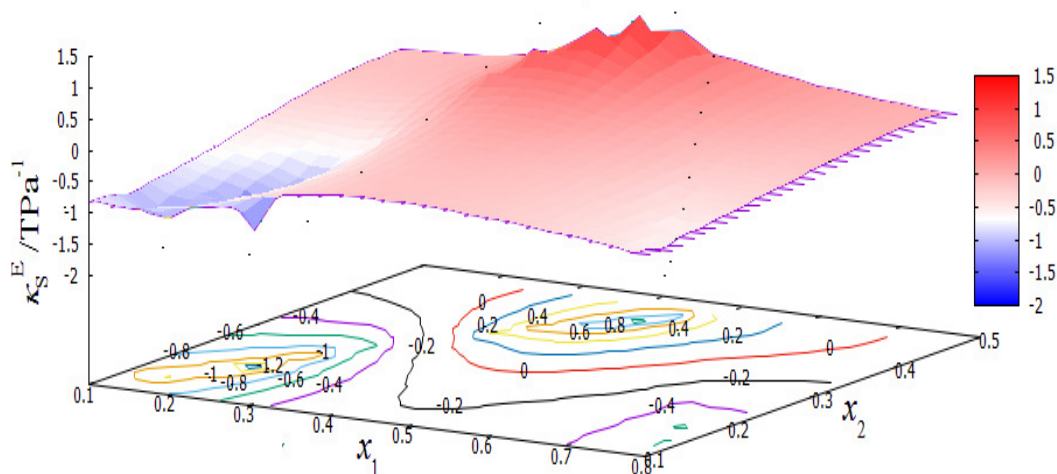


Fig. 9.13. Three-dimensional mesh plots of excess isentropic compressibility ($\kappa_{S,123}^E$) for the ternary mixture MA (1) + EA (2) + MS (3) and the corresponding pseudo-two dimensional contour plot of constant $\kappa_{S,123}^E$ values at 298.15 K.

9.3.4. Excess Molar Refraction

The study of refractive indices (n_D), molar refractions (R_m) and the excess molar refractions (R_m^E) plays an important role in explaining the molecular interactions in the multi-component liquid mixtures. The excess molar refractions (R_m^E) for the n-component mixtures can be had from relation:²²

$$R_m^E = R_m - \sum_{i=1}^n (x_i R_{m,i}) \quad (9)$$

where $R_{m,i}$ is the molar refraction of the i^{th} component in the mixture and the molar refractions (R_m) for a mixture can be had from the relation:²²

$$R_m = \frac{n_D^2 - 1}{n_D^2 + 2} \frac{\sum_{i=1}^n x_i M_i}{\rho} \quad (10)$$

where n_D is the refractive index of the mixture and other symbols have their usual meanings as detailed in Chapter II. Molar refractions (R_m), excess molar refractions (R_m^E) and the experimental refractive indices (n_D) for the three binaries and the ternary mixtures studied are listed in Tables 9.6 and 9.7, respectively.

Chapter IX

Table 9.7. Ultrasonic speeds (u), isentropic compressibility (κ_s), excess isentropic compressibility (κ_s^E), refractive indices (n_D), molar refractions (R_m) and excess molar refractions (R_m^E) for the ternary mixtures at 298.15 K.

x_1	x_2	u ($\text{m} \cdot \text{s}^{-1}$)	n_D	κ_s (TPa^{-1})	κ_s^E (TPa^{-1})	$R_m \cdot 10^6$ ($\text{m}^3 \cdot \text{mol}^{-1}$)	$R_m^E \cdot 10^6$ ($\text{m}^3 \cdot \text{mol}^{-1}$)
CH (1) + MA (2) + EA (3)							
0.0413	0.0704	1150.0	1.3749	850.82	0.592	22.393	0.158
0.0819	0.1163	1155.5	1.3786	848.72	1.263	22.540	0.302
0.1217	0.1613	1161.1	1.3833	846.49	1.779	22.741	0.499
0.1408	0.2057	1164.3	1.3862	844.85	2.190	22.788	0.651
0.1596	0.2494	1167.5	1.3899	843.13	2.514	22.874	0.841
0.1977	0.2921	1172.9	1.3931	840.95	3.016	22.987	0.948
0.2352	0.3341	1178.5	1.3970	838.42	3.160	23.135	1.091
0.2720	0.3753	1184.1	1.3997	835.87	3.242	23.219	1.170
0.3081	0.4159	1189.8	1.4024	833.16	3.151	23.303	1.248
0.3436	0.4557	1195.5	1.4050	830.41	2.997	23.380	1.321
0.3786	0.4948	1201.1	1.4068	827.76	2.909	23.415	1.351
0.4129	0.5333	1206.6	1.4077	825.11	2.801	23.400	1.331
0.4535	0.4833	1210.8	1.4105	825.26	2.446	23.873	1.351
0.4947	0.4325	1214.8	1.4110	825.56	2.24	24.232	1.251
0.5365	0.3811	1218.7	1.4104	825.86	2.044	24.535	1.088
0.5788	0.3290	1222.6	1.4104	826.02	1.716	24.871	0.951
0.6218	0.2761	1226.4	1.4103	826.17	1.388	25.202	0.802
0.6654	0.2224	1230.0	1.4084	826.44	1.189	25.435	0.549
0.7096	0.1680	1233.6	1.4084	826.53	0.804	25.770	0.391
0.7544	0.1128	1236.8	1.4092	826.88	0.701	26.147	0.268
CH (1) + MA (2) + MS (3)							
0.0660	0.1125	1356.3	1.5233	478.10	-0.038	37.332	-0.150
0.1236	0.1756	1323.2	1.5047	517.33	-0.538	34.921	-0.328
0.1743	0.2311	1296.4	1.4873	554.54	-0.752	32.791	-0.490
0.1942	0.2838	1278.5	1.4764	580.85	-0.527	31.300	-0.488
0.2124	0.3320	1263.2	1.4665	606.22	-0.269	29.979	-0.443
0.2518	0.3720	1247.6	1.4537	639.36	0.220	28.550	-0.418
0.2872	0.4081	1235.5	1.4447	670.53	0.450	27.435	-0.221
0.3194	0.4408	1225.9	1.4391	700.23	0.819	26.588	0.119
0.3486	0.4705	1218.7	1.4335	728.20	0.915	25.810	0.422
0.3753	0.4977	1213.1	1.4281	755.02	1.239	25.100	0.701
0.3999	0.5227	1209.0	1.4213	780.62	1.590	24.371	0.879
0.4225	0.5457	1206.3	1.4137	804.89	1.799	23.646	0.990
0.4659	0.4965	1211.5	1.4172	802.49	1.972	24.219	0.991
0.5104	0.4462	1216.8	1.4206	799.61	1.626	24.789	0.978
0.5558	0.3948	1221.7	1.4211	796.93	1.448	25.211	0.802
0.6022	0.3422	1226.5	1.4232	794.06	1.062	25.717	0.698
0.6497	0.2885	1230.9	1.4245	791.41	0.881	26.182	0.538
0.6983	0.2335	1235.0	1.4253	788.89	0.792	26.621	0.338
0.7481	0.1771	1239.1	1.4267	786.11	0.418	27.095	0.158
0.7991	0.1195	1242.9	1.4305	783.52	0.202	27.707	0.102

Chapter IX

CH (1) + EA (2) + MS (3)							
0.0672	0.0963	1353.5	1.5215	481.26	-0.497	37.996	-0.299
0.1271	0.1519	1319.5	1.5012	522.73	-0.802	35.885	-0.580
0.1809	0.2017	1292.3	1.4846	561.56	-1.210	34.095	-0.728
0.2034	0.2499	1273.7	1.4746	589.76	-0.843	32.928	-0.699
0.2243	0.2947	1258.1	1.4645	616.60	-0.724	31.817	-0.698
0.2676	0.3325	1242.3	1.4534	650.91	-0.341	30.616	-0.621
0.3072	0.3670	1230.0	1.4447	683.16	-0.156	29.629	-0.441
0.3435	0.3986	1220.3	1.4389	713.77	0.115	28.870	-0.131
0.3768	0.4277	1212.6	1.4332	743.03	0.629	28.166	0.150
0.4076	0.4545	1206.9	1.4279	770.62	0.935	27.528	0.420
0.4362	0.4794	1202.8	1.4206	796.73	1.109	26.814	0.548
0.4627	0.5024	1200.0	1.4139	821.53	1.242	26.167	0.681
0.5059	0.4533	1205.4	1.4193	817.30	1.316	26.630	0.801
0.5494	0.4039	1210.7	1.4227	812.93	1.215	26.975	0.801
0.5930	0.3542	1215.9	1.4225	808.43	0.963	27.110	0.590
0.6369	0.3043	1220.9	1.4250	803.98	0.717	27.389	0.520
0.6810	0.2542	1225.6	1.4253	799.73	0.655	27.537	0.318
0.7253	0.2039	1230.3	1.4265	795.38	0.452	27.732	0.162
0.7698	0.1533	1235.2	1.4261	790.72	-0.087	27.834	-0.090
0.8145	0.1024	1239.9	1.4292	786.40	-0.321	28.137	-0.141
CHN (1) + MA (2) + EA (3)							
0.0356	0.0708	1152.2	1.3748	839.59	0.066	22.307	0.098
0.0711	0.1177	1160.3	1.3789	826.04	0.134	22.397	0.209
0.1062	0.1642	1168.8	1.3839	812.46	0.245	22.537	0.371
0.1232	0.2099	1173.1	1.3869	804.97	0.382	22.528	0.481
0.1401	0.2552	1177.5	1.3897	797.48	0.541	22.508	0.580
0.1745	0.3006	1186.1	1.3956	783.68	0.659	22.667	0.759
0.2087	0.3457	1195.1	1.3998	769.73	0.722	22.738	0.850
0.2427	0.3904	1204.5	1.4042	755.67	0.770	22.819	0.951
0.2764	0.4349	1214.0	1.4082	741.60	0.904	22.870	1.022
0.3099	0.4791	1223.9	1.4118	727.35	0.965	22.898	1.070
0.3432	0.5230	1234.0	1.4157	712.94	0.955	22.930	1.121
0.3763	0.5666	1244.5	1.4186	698.40	0.922	22.909	1.120
0.4159	0.5166	1254.1	1.4214	687.46	0.813	23.336	1.092
0.4565	0.4653	1263.4	1.4237	676.62	0.793	23.731	1.020
0.4982	0.4126	1273.3	1.4249	665.55	0.559	24.089	0.898
0.5411	0.3585	1283.2	1.4257	654.56	0.407	24.429	0.745
0.5851	0.3028	1293.2	1.4247	643.57	0.265	24.680	0.490
0.6304	0.2457	1303.5	1.4226	632.47	0.014	24.879	0.169
0.6770	0.1869	1313.8	1.4215	621.36	-0.236	25.126	-0.121
0.7249	0.1264	1324.3	1.4200	610.36	-0.370	25.359	-0.438
CHN (1) + MA (2) + MS (3)							
0.0571	0.1136	1374.4	1.5175	459.33	-1.162	36.832	-0.742
0.1079	0.1787	1353.0	1.4975	482.39	-1.722	34.235	-1.148
0.1533	0.2369	1334.4	1.4781	504.95	-1.846	31.915	-1.508
0.1713	0.2919	1318.2	1.4654	524.58	-1.968	30.290	-1.613
0.1879	0.3423	1303.8	1.4537	543.73	-1.997	28.837	-1.669
0.2240	0.3858	1291.9	1.4401	564.27	-1.926	27.291	-1.723
0.2569	0.4255	1281.7	1.4291	584.10	-1.802	25.994	-1.659
0.2870	0.4617	1272.9	1.4198	603.30	-1.606	24.876	-1.532
0.3147	0.4951	1265.4	1.4125	621.79	-1.442	23.935	-1.331

Chapter IX

0.3402	0.5258	1259.0	1.4063	639.62	-1.299	23.109	-1.102
0.3637	0.5542	1253.5	1.4011	656.89	-1.105	22.385	-0.851
0.3856	0.5805	1248.9	1.3940	673.51	-1.000	21.613	-0.720
0.4281	0.5317	1261.6	1.4014	658.59	-0.998	22.311	-0.598
0.4721	0.4811	1274.6	1.4090	643.68	-0.904	23.035	-0.470
0.5177	0.4287	1288.1	1.4141	628.64	-0.851	23.653	-0.471
0.5650	0.3743	1302.2	1.4193	613.43	-0.887	24.293	-0.472
0.6141	0.3178	1317.0	1.4229	598.02	-1.028	24.870	-0.561
0.6651	0.2592	1332.4	1.4264	582.57	-1.126	25.461	-0.662
0.7181	0.1982	1348.6	1.4301	566.98	-1.274	26.083	-0.759
0.7733	0.1348	1365.6	1.4321	551.33	-1.399	26.638	-0.953
CHN (1) + EA (2) + MS (3)							
0.0582	0.0972	1370.5	1.5205	463.25	-0.948	37.799	-0.597
0.1111	0.1546	1348.0	1.5019	488.47	-1.576	35.683	-0.943
0.1593	0.2070	1328.5	1.4830	513.09	-1.697	33.696	-1.314
0.1797	0.2574	1311.6	1.4711	534.68	-1.835	32.391	-1.411
0.1988	0.3044	1296.5	1.4603	555.79	-1.745	31.214	-1.458
0.2387	0.3456	1284.3	1.4469	577.88	-1.769	29.823	-1.552
0.2756	0.3837	1273.8	1.4363	599.28	-1.609	28.669	-1.508
0.3098	0.4190	1265.0	1.4276	619.77	-1.531	27.684	-1.381
0.3416	0.4519	1257.5	1.4205	639.56	-1.386	26.841	-1.191
0.3712	0.4825	1251.2	1.4139	658.59	-1.268	26.069	-1.000
0.3989	0.5110	1245.8	1.4079	677.06	-1.021	25.368	-0.802
0.4248	0.5378	1241.6	1.3998	694.54	-1.105	24.586	-0.741
0.4676	0.4884	1254.1	1.4060	677.86	-1.074	25.040	-0.641
0.5112	0.4381	1267.2	1.4122	661.00	-1.082	25.495	-0.547
0.5556	0.3868	1280.8	1.4169	644.09	-0.979	25.868	-0.541
0.6008	0.3346	1295.2	1.4214	626.90	-0.997	26.231	-0.552
0.6468	0.2815	1310.5	1.4242	609.42	-1.139	26.503	-0.661
0.6937	0.2273	1326.6	1.4278	591.86	-1.201	26.822	-0.730
0.7415	0.1721	1343.8	1.4305	574.02	-1.378	27.095	-0.852
0.7903	0.1158	1362.2	1.4320	555.98	-1.591	27.309	-1.041
MA (1) + EA (2) + MS (3)							
0.0757	0.0954	1351.2	1.5165	477.58	-0.613	36.935	-0.501
0.1420	0.1493	1313.3	1.4952	515.93	-1.431	34.137	-0.748
0.2007	0.1968	1282.0	1.4744	552.93	-1.889	31.661	-0.970
0.2249	0.2432	1261.2	1.4611	580.56	-1.818	30.165	-1.038
0.2474	0.2860	1243.8	1.4495	607.40	-1.640	28.893	-0.988
0.2935	0.3208	1223.5	1.4350	641.31	-1.302	27.229	-0.928
0.3351	0.3522	1207.1	1.4226	673.85	-0.979	25.839	-0.761
0.3729	0.3807	1192.1	1.4148	705.19	-0.558	24.748	-0.440
0.4074	0.4067	1180.2	1.4053	735.43	-0.034	23.691	-0.208
0.4389	0.4305	1169.8	1.3996	764.32	0.278	22.879	0.159
0.4679	0.4524	1161.7	1.3914	792.04	0.512	22.025	0.389
0.4946	0.4726	1154.0	1.3820	818.67	0.654	21.128	0.491
0.5379	0.4240	1155.3	1.3819	813.67	0.585	20.975	0.440
0.5808	0.3757	1156.1	1.3817	808.86	0.730	20.804	0.371
0.6235	0.3277	1156.7	1.3820	803.66	0.537	20.641	0.310
0.6660	0.2800	1157.9	1.3799	798.34	0.259	20.382	0.152
0.7082	0.2326	1158.6	1.3761	792.77	-0.220	20.020	-0.109
0.7501	0.1855	1159.5	1.3727	787.26	-0.609	19.690	-0.340
0.7917	0.1387	1159.8	1.3697	781.75	-0.951	19.361	-0.570
0.8331	0.0922	1161.2	1.3657	776.10	-1.390	19.021	-0.811

Chapter IX

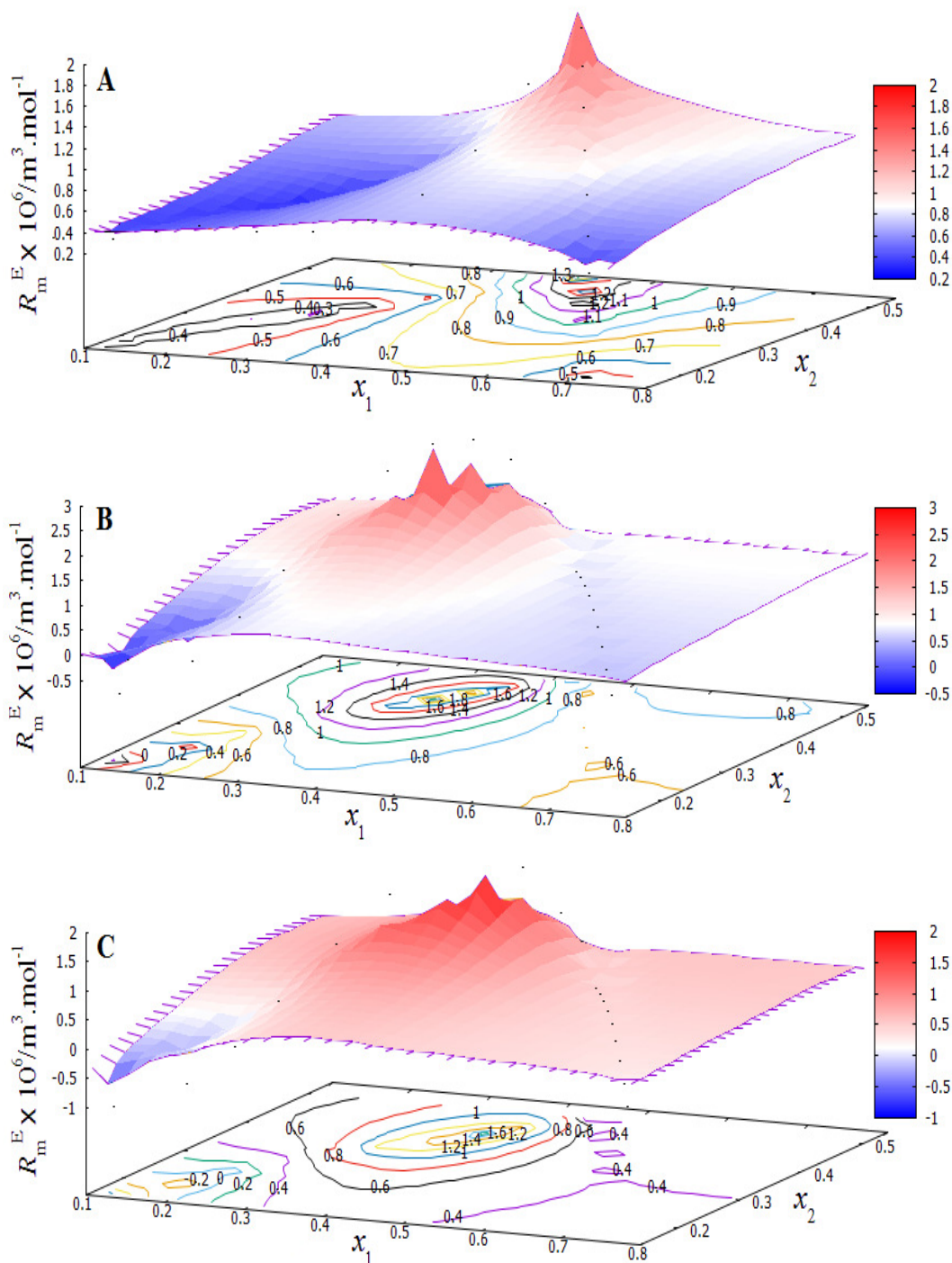


Fig. 9.14. Three-dimensional mesh plots of excess molar refractions ($R_{m,123}^E$) for the ternary mixtures: A, CH (1) + MA (2) + EA (3); B, CH (1) + MA (2) + MS (3) and C, CH (1) + EA (2) + MS (3) and the corresponding pseudo-two dimensional contour plot of constant $R_{m,123}^E$ values for these mixtures at 298.15 K.

Chapter IX

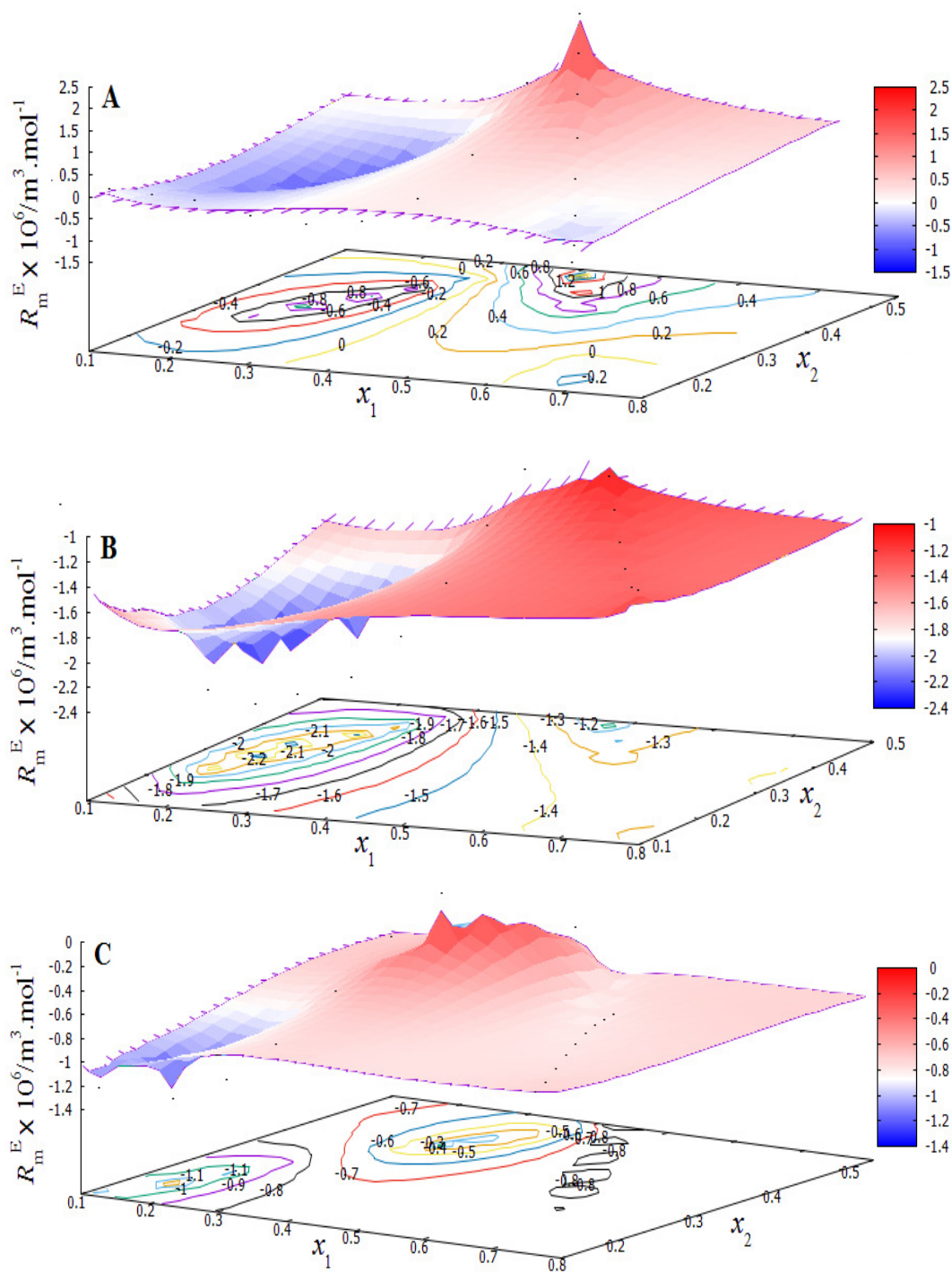


Fig. 9.15. Three-dimensional mesh plots of excess molar refractions ($R_{m,123}^E$) for the ternary mixtures: A, CHN (1) + MA (2) + EA (3); B, CHN (1) + MA (2) + MS (3) and C, CHN (1) + EA (2) + MS (3) and the corresponding pseudo-two dimensional contour plot of constant $R_{m,123}^E$ values for these mixtures at 298.15 K.

Chapter IX

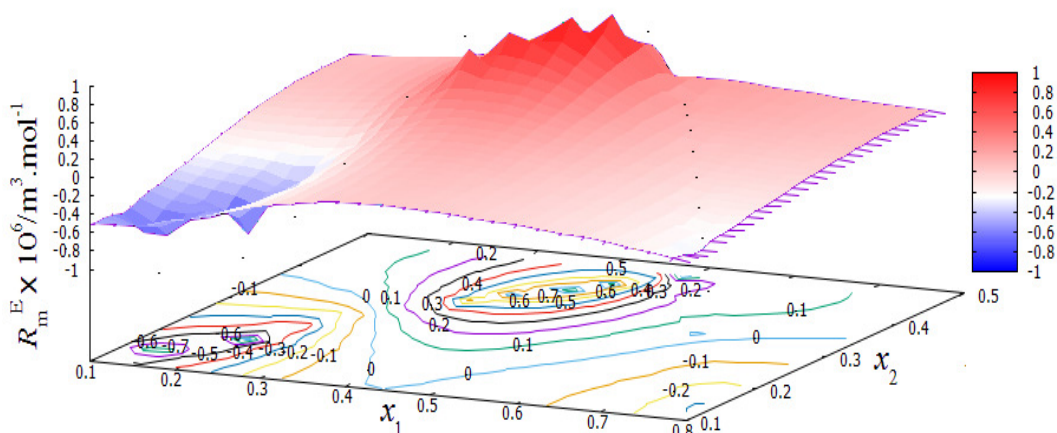


Fig. 9.16. Three-dimensional mesh plots of excess molar refractions ($R_{m,123}^E$) for the ternary mixture MA (1) + EA (2) + MS (3) and the corresponding pseudo-two dimensional contour plot of constant $R_{m,123}^E$ values at 298.15 K.

The experimental refractive indices (n_D) of the pure liquids were in good agreement with literature values^{21,23-25} at 298.15 K and the trends in excess molar refractions (R_m^E) for the binary mixtures as well as for the ternary mixtures with respect to compositions were found to be in line with the molecular interactions discussed above. R_m^E values of the binary mixtures were also fitted to the Redlich-Kister polynomial and the corresponding coefficients (a_i)⁹ are: $a_0 = 9.3329$, $a_1 = 1.9361$, $a_2 = -0.0747$, $a_3 = -0.1481$ for the mixture (MA + EA); $a_0 = -6.7548$, $a_1 = -3.1881$, $a_2 = -4.7298$, $a_3 = -3.3078$ for the mixture (MA + MS) and $a_0 = -6.5478$, $a_1 = -4.0145$, $a_2 = -1.8834$, $a_3 = 1.8893$ for the mixture (EA + MS) with standard deviations (σ) 0.0553, 0.0404, 0.0461 for the mixtures, respectively. $R_{m,123}^E$ values of the ternary mixtures at 298.15 K were fitted to the Cibulka equation and the coefficients (c_i) are listed in Table 9.4 Figures 9.14, 9.15 and 9.16 illustrate three-dimensional mesh and contour plots of the calculated $R_{m,123}^E$ values of the ternary mixtures against the mole fractions of their components at 298.15 K and the so-called ternary contributions ($R_{m,123}^E - R_{Bin}^E$) were determined; the maximum and minimum values of such contributions are given in Table 9.5.

Chapter IX

9.3.5. Empirical and correlative models

During the last few decades, several different symmetrical as well as asymmetrical models have been suggested to predict and compare the thermodynamic and transport properties of the binary and ternary mixtures. Although some of them were originally proposed to predict specific properties like excess molar enthalpy, Gibbs free energy, *etc.*, they can also be applied to any other excess or deviation properties^{26,27} Most of them are still popular and suitable for the prediction of the excess or deviation properties. Herein this chapter symmetrical models proposed by Rastogi,²⁸ Köhler,²⁹ Jacob-Fitzner,³⁰ Colinet³¹ and the asymmetrical models of Tsao-Smith,³² Toop,³³ Scatchard,³⁴ and Mathieson-Thyne³⁵ were used to predict different excess or deviation properties of the ternary solutions by utilizing the available data of the constituent binary mixtures. A brief detail of these models has already been given in Chapter II.

Table 9.8. Standard deviations between the experimental and calculated excess or deviation properties for the ternary mixtures derived from different semi-empirical equations at 298.15 K.

Various models	Standard deviations (σ)			
	$(V_{m,123}^E)^a$	$(\Delta\eta_{123})^b$	$(\kappa_{S,123}^E)^c$	$(R_{m,123}^E)^d$
CH (1) + MA (2) + EA (3)				
Rastogi	0.4693	0.0092	0.2530	0.3303
Köhler	0.0958	0.0328	0.3707	0.2677
Jacob-Fitzner	0.1390	0.0230	0.3324	0.3771
Colinet	0.1633	0.0365	0.3947	0.2242
Tsao-Smith	0.3626	0.0488	0.4896	0.3681
Toop	0.2277	0.0315	0.3828	0.2865
Scatchard	0.3160	0.0098	0.2386	0.6089
Mathieson-Thyne	10.8554	0.4066	2.3926	1.2218
CH (1) + MA (2) + MS (3)				
Rastogi	0.5049	0.0257	0.0683	0.2101
Köhler	0.0918	0.0092	0.0673	0.0847
Jacob-Fitzner	0.1632	0.0056	0.1024	0.0847
Colinet	0.1048	0.0096	0.0603	0.1127

Chapter IX

Tsao-Smith	0.2003	0.0169	0.0963	0.3611
Toop	0.1060	0.0059	0.0579	0.0758
Scatchard	0.4123	0.0129	0.1144	0.4478
Mathieson-Thyne	3.5110	0.1546	0.8400	1.5583
CH (1) + EA (2) + MS (3)				
Rastogi	0.2741	0.0217	0.1288	0.2424
Köhler	0.0548	0.0062	0.1520	0.2464
Jacob-Fitzner	0.1908	0.0021	0.1085	0.1438
Colinet	0.0619	0.0073	0.1590	0.2841
Tsao-Smith	0.1603	0.0123	0.1852	0.4950
Toop	0.1592	0.0039	0.1182	0.2294
Scatchard	0.3198	0.0126	0.0689	0.2774
Mathieson-Thyne	2.0359	0.1222	0.3039	1.2738
CHN (1) + MA (2) + EA (3)				
Rastogi	0.0802	0.0151	0.3677	0.5363
Köhler	0.1974	0.0476	0.2511	0.1335
Jacob-Fitzner	0.2133	0.0350	0.2845	0.1335
Colinet	0.2012	0.0520	0.2411	0.2092
Tsao-Smith	0.3930	0.0662	0.1938	0.5297
Toop	0.2073	0.0474	0.2396	0.2308
Scatchard	0.3019	0.0268	0.3917	0.5389
Mathieson-Thyne	1.5233	0.8582	2.5221	11.7386
CHN (1) + MA (2) + MS (3)				
Rastogi	0.2162	0.0492	0.0606	0.6195
Köhler	0.0956	0.068	0.1033	0.1518
Jacob-Fitzner	0.2047	0.0772	0.1408	0.1518
Colinet	0.1122	0.0674	0.0909	0.178
Tsao-Smith	0.2229	0.0633	0.111	0.2913
Toop	0.0956	0.0746	0.0918	0.1018
Scatchard	0.4148	0.0886	0.1594	0.5504
Mathieson-Thyne	1.6864	0.1469	0.9196	3.6363
CHN (1) + EA (2) + MS (3)				
Rastogi	0.2268	0.0375	0.9818	0.3649
Köhler	0.1029	0.0474	0.2326	0.141
Jacob-Fitzner	0.1677	0.0559	0.9315	0.141

Chapter IX

Colinet	0.1161	0.0465	0.2415	0.1685
Tsao-Smith	0.1904	0.0439	0.9464	0.2718
Toop	0.1037	0.0535	0.9353	0.1064
Scatchard	0.3116	0.0627	0.9798	0.3982
Mathieson-Thyne	1.4480	0.0613	0.2893	1.7002
MA (1) + EA (2) + MS (3)				
Rastogi	0.2270	0.0134	0.2270	0.626
Köhler	0.2577	0.0220	0.2577	0.1152
Jacob-Fitzner	0.5733	0.0332	0.5733	0.2926
Colinet	0.2892	0.0212	0.2824	0.0832
Tsao-Smith	0.4242	0.0230	0.4242	0.2142
Toop	0.5491	0.0312	0.5491	0.2553
Scatchard	0.5877	0.0354	0.5887	0.3573
Mathieson-Thyne	6.1063	0.2098	0.2893	6.1074
Units: $a, 10^6 (\text{m}^3 \cdot \text{mol}^{-1})$; $b, \text{mPa}\cdot\text{s}$; c, TPa^{-1} ; $d, 10^6 (\text{m}^3 \cdot \text{mol}^{-1})$				

With these models lower standard deviations (σ) as given in Table 9.9 are usually obtained for those ternary properties for which the ternary contributions are of little or no importance; therefore the lower standard deviations (σ) stand in support of the view that the ternary mixtures studied are characterized by non-homogeneity and moderate to weak interactions. Again the least σ values for the symmetric model given by Köhler suggest it to be most suitable for the prediction of $V_{m,123}^E$ for all the studied ternaries compared to other models. However, it is observed that almost all the models are suitable for the prediction of $\Delta\eta_{123}$ values.

9.4. Conclusion

Based on various excess or deviation properties like $V_m^E, \Delta\eta$, etc., for the three binary mixtures (MA + EA), (MA + MS) and (EA + MS), it can be concluded that the degree of molecular interactions in these binary mixtures follows the order: (MA + MS) > (EA + MS) > (MA + EA). The excess partial molar volumes ($\bar{V}_{m,1}^{0,E}$ and $\bar{V}_{m,2}^{0,E}$) at infinite dilution of these binary mixtures also support the above order of molecular interactions. Various excess or deviation properties of the studied ternary mixtures (CH + MA + EA), (CH + MA + MS), (CH + EA + MS), (CHN + MA + EA), (CHN +

Chapter IX

MA + MS), (CHN + EA + MS) and (MA + EA + MS) suggest that these mixtures are characterized by the nature of their mixing components as well as by the nature of molecular interactions in the associated binary mixtures. These excess or deviation properties of the ternary mixtures were fitted to Cibulka equation and the so called ternary contributions ($X_{m,123}^E - X_{Bin}^E$) were derived; although these contributions are rather small but their maximum and minimum values suggest non-homogeneity in these ternary mixtures and the binary contributions (X_{Bin}^E) play a significant role in characterizing the ternary mixtures studied.

References

- [1] C.R. Reid, B.E. Poling, *The properties of Gases and Liquids*, McGraw Hill, New York, 1998, Ch. 1.
- [2] J. George, N.V. Sastry, *J. Chem. Eng. Data* 49 (2004) 1116.
- [3] A.R. Mahajan, S.R. Mirgane, *Chem. Eng. Comm.*, 200 (2013) 1666.
- [4] L. Venkatramana, R.L. Gardas, K.S. Kumar, K.D. Reddy, *Fluid. Phase. Equilib.*, 367 (2014) 7.
- [5] W.M. Haynes, D.R. Lide, T.J. Bruno, *CRC Handbook of Chemistry & Physics*, 93rd edn., Taylor & Francis, Boca Roton, London, 2012-2013.
- [6] R. Pradhan, B. Sinha, *J. Serb. Chem. Soc.*, 82 (2017) 189.
- [7] S. Aparicio, R. Alcalde, *Eur. J. Chem.*, 1 (2010) 162.
- [8] G.M. Smith, H.C. Van Ness, *Introduction to Chemical Engineering Thermodynamics*, McGraw Hill, New York, 1987.
- [9] O. Redlich, A.T. Kister, *Indus. Eng. Chem.*, 40 (1948) 345.
- [10] D.W. Marquardt, *J. Soc. Ind. Appl. Math.*, 11, (1963) 431.
- [11] I. Cibulka, *Collect. Czech. Chem. Commun.*, 47 (1982) 1414.
- [12] M.N. Roy, B.K. Sarkar, B. Sinha, *J. Chem. Eng. Data* 54 (2009) 1076.
- [13] B. Garcia, R. Alcalde, S. Aparicio, J.M. Leal, J. S. Matos, *Phys. Chem. Phys. Chem.*, 3 (2001) 2866.
- [14] S. Glasstone, K.J. Laidler, H. Eyring, *The theory of Rate Preocess*. McGraw-Hill Book Comnpany, New York, 1941.
- [15] G.C. Benson, O. K. Kiyohara, *J. Chem. Thermodyn.*, 11 (1979) 1061.
- [16] W.E. Acree, *J. Chem. Eng. Data* 28 (1983) 215.

Chapter IX

- [17] D.L. Cunha, J.A.P. Coutinho, J.L. Daridon, R.A. Reis, M.L.L. Paredes, *J. Chem. Eng. Data* 58 (2013) 2925.
- [18] S. Nallani, S. Boodida, S.J. Tangeda, *J. Chem. Eng. Data* 52 (2007) 405.
- [19] V. Vyas, T. Nautiyal, *Pramana-J. Phys.*, 59 (2002) 663.
- [20] J.M. Resa, J.M. Goenaga, A.I. Sanchez-Ruiz, *J. Chem. Eng. Data* 51 (2006) 1294.
- [21] C.B. Salguero, J.G. Fadrique, *J. Chem. Eng. Data* 56 (2011) 3823.
- [22] M.S. Dhillon, H.S. Chugh, *J. Chem. Eng. Data* 22 (1977) 262.
- [23] M.I. Aralaguppi, C.V. Jadar, T.M. Aminabhavi, *J. Chem. Eng. Data* 44 (1999) 441.
- [24] T.M. Aminabhavi, H.T.S. Phayde, *J. Chem. Eng. Data* 41(1996) 813.
- [25] H. Eyring, J. F. Kincaid, *J. Chem. Phys.*, 6 (1938) 620.
- [26] J.W. McCargar, W.E. Acree, *Thermochimica. Acta*, 149 (1989) 363.
- [27] M. Hillert, *Ber. Bunsenges. Phys. Chem.*, 87 (1983) 762.
- [28] R.P. Rastogi, J. Nath, S.S. Das, *J. Chem. Eng. Data* 22 (1977) 249.
- [29] F. Kohler, *Monatsh. Chem.*, 91 (1960) 738.
- [30] K.T. Jacob, K. Fitzner, *Thermochim. Acta*, 18 (1977) 197.
- [31] C. Colinet, Ph. D Thesis, University of Grenoble, France, 1967.
- [32] C.C. Tsao, J.M. Smith, *Chem. Eng. Prog. Symp. Series*, 49 (1953) 107.
- [33] G.W. Toop, *TMS-AIME*, 233 (1965) 850.
- [34] G. Scatchard, L.B. Ticknor, J.R. Goates, E.R. McCartney, *J. Am. Chem. Soc.*, 74 (1952) 3721.
- [35] A.R. Mathieson, J.C.J. Thynne, *J. Chem. Soc.*, (1956) 3713.

CHAPTER X

Thermophysical properties of the quaternary mixtures of cyclohexane and cyclohexanone with some esters at $T = (298.15-318.15)$ K

10.1. Introduction

Multi-component liquid mixtures due to their unusual behavior have drawn much attention recently. It is because they often exhibit properties that cannot be found in pure liquids. Again the liquid mixtures (binary/ternary/quaternary) have often been preferred in a number of engineering and scientific applications as in chemical industries, process design and in subsequent operations like heat transfer, mass transfer, fluid flow, *etc.* There is always a quest for better solvents or solvent mixtures from both theoretical and practical applications as in paints, varnishes, printing ink, *etc.* Thus the research works on pure liquids and liquid mixtures are never ending. Reliable thermodynamic, transport and acoustic properties of multi-component liquid mixtures are important to both the chemists and the chemical engineers; because such properties are of primary interest for designing and process optimization in chemical and other industries¹⁻³ as well as these properties reflect the binding forces amongst the liquids and found to be very much sensitive to the liquid state structure and composition.⁴ Thus the importance of these properties are not only for the fundamental understanding of mixing processes, but also for understanding the molecular interactions operating between the component liquids. Experimental determinations of these properties for various binary and ternary mixtures are frequently available in the literature and various data banks. But such determinations for the quaternary systems are scarce and sufficient in the literature. Hence in this chapter thermophysical properties of two quaternary mixtures consisting of cyclohexane (CH) and cyclohexanone (CHN) with methyl acetate (MA), ethyl acetate (EA) and methyl salicylate (MS) at 298.15, 308.15 and 318.15 K under ambient pressure were studied.

10.2. Experimental section

10.2.1. Materials

All the chemicals involved in this work were purchased from Sigma-Aldrich, Germany (Reagent Plus, purity > 99%) and were used as received from the vendor.

Chapter X

The purity of all the chemicals used was ascertained by comparing their densities and viscosities at the experimental temperatures with the available literature data, already presented in our previous chapters (VII and VIII).

10.2.2. Apparatus and procedure

The quaternary mixtures were prepared afresh before use by mass in specially designed air-tight bottles with stopper inside a dry box at 298.15 K so as to cover the entire composition range for most of the components as much as possible. The measurement of densities (ρ), viscosities (η), ultrasonic speeds of sound (u) and refractive indices (n_D) under the experimental temperatures were carried out as described in the previous chapters. An average of the triplicate measurements for all the properties were taken into consideration and adequate precautions were taken to minimize evaporation losses during all the measurements.

10.3. Results and discussion

The experimental densities and viscosities of two quaternary mixtures, *i.e.*, (CH + MA + EA + MS) and (CHN + MA + EA + MS) studied at 298.15, 308.15 and 318.15 K were used to determine the excess molar volumes (V_m^E) and viscosity deviations ($\Delta\eta$). Also the experimental ultrasonic speeds (u) of sound, the refractive indices (n_D) and the other derived properties for the above quaternary mixtures were determined. All these properties for the associated binary and ternary mixtures have already been presented in previous chapters (VII, VIII and IX).

10.3.1. Excess molar volumes

Excess molar volumes (V_m^E) were calculated for the quaternary mixtures using the following expression:

$$V_m^E = \sum_{i=1}^n x_i M_i \left(\frac{1}{\rho} - \frac{1}{\rho_i} \right) \quad (1)$$

where ρ is the density of the mixture and n , x_i , M_i and ρ_i are the number of components in the mixture, the mole fraction, the molar mass and the density of the i^{th} component in the mixture, respectively. The estimated uncertainty for excess molar volumes (V_m^E) was evaluated to be $\pm 0.005 \text{ cm}^3 \cdot \text{mol}^{-1}$.

Chapter X

Table 10.1. Densities (ρ), viscosities (η), excess molar volumes (V_m^E) and viscosity deviations ($\Delta\eta$) for the quaternary mixtures studied at $T = (298.15 \text{ to } 318.15) \text{ K}$.

x_1	x_2	x_3	$\rho \cdot 10^{-3}$ ($\text{kg} \cdot \text{m}^{-3}$)	η ($\text{mPa} \cdot \text{s}$)	$V_m^E \cdot 10^6$ ($\text{m}^3 \cdot \text{mol}^{-1}$)	$\Delta\eta$ ($\text{mPa} \cdot \text{s}$)
CH (1) + MA (2) + EA (3) + MS (4)						
$T = 298.15 \text{ K}$						
0.0599	0.6802	0.1716	0.94547	0.3993	-0.347	-0.063
0.0988	0.1622	0.6296	0.93076	0.4391	-0.512	-0.079
0.1595	0.2720	0.1271	1.03265	0.7152	-0.164	-0.104
0.1446	0.6246	0.1935	0.90237	0.3847	0.425	-0.079
0.1979	0.1000	0.5988	0.91052	0.4641	-0.185	-0.093
0.2820	0.0763	0.2182	1.00043	0.7601	0.099	-0.136
0.2441	0.5201	0.1458	0.90373	0.4379	0.642	-0.103
0.2743	0.3118	0.2621	0.91749	0.4946	0.523	-0.118
0.2865	0.1809	0.4563	0.88469	0.4549	0.563	-0.114
0.3664	0.2360	0.0934	0.95612	0.6646	0.389	-0.139
0.3579	0.2466	0.2695	0.89296	0.5076	0.814	-0.127
0.3667	0.3474	0.2239	0.86734	0.4529	1.172	-0.129
0.4481	0.1306	0.2306	0.90273	0.5971	0.652	-0.150
0.4480	0.1576	0.3058	0.86420	0.5094	1.039	-0.144
0.4706	0.1902	0.2698	0.85352	0.4949	1.222	-0.151
0.5393	0.1532	0.1396	0.88354	0.6108	0.737	-0.163
0.5048	0.3488	0.1135	0.83525	0.4691	1.558	-0.152
0.5442	0.3093	0.0963	0.83794	0.4976	1.372	-0.159
0.6484	0.0776	0.0978	0.87477	0.6771	0.364	-0.178
0.6682	0.1139	0.0639	0.86497	0.6643	0.430	-0.176
$T = 308.15 \text{ K}$						
0.0599	0.6802	0.1716	0.93358	0.3391	-0.315	-0.082
0.0988	0.1622	0.6296	0.91860	0.3704	-0.471	-0.099
0.1595	0.2720	0.1271	1.02141	0.6097	-0.121	-0.133
0.1446	0.6246	0.1935	0.89075	0.3195	0.467	-0.102
0.1979	0.1000	0.5988	0.89898	0.3899	-0.176	-0.112
0.2820	0.0763	0.2182	0.98946	0.6507	0.130	-0.155
0.2441	0.5201	0.1458	0.89031	0.3661	0.917	-0.122
0.2743	0.3118	0.2621	0.90552	0.4056	0.644	-0.146
0.2865	0.1809	0.4563	0.87216	0.3673	0.739	-0.144
0.3664	0.2360	0.0934	0.94535	0.5651	0.418	-0.156
0.3579	0.2466	0.2695	0.88164	0.4138	0.889	-0.155
0.3667	0.3474	0.2239	0.85319	0.3754	1.592	-0.146
0.4481	0.1306	0.2306	0.89204	0.5046	0.674	-0.162
0.4480	0.1576	0.3058	0.85180	0.4273	1.273	-0.155
0.4706	0.1902	0.2698	0.84240	0.4033	1.312	-0.172
0.5393	0.1532	0.1396	0.87212	0.5051	0.879	-0.183
0.5048	0.3488	0.1135	0.82170	0.3861	1.977	-0.167
0.5442	0.3093	0.0963	0.82694	0.4162	1.483	-0.167
0.6484	0.0776	0.0978	0.86420	0.5544	0.419	-0.201
0.6682	0.1139	0.0639	0.85465	0.5441	0.463	-0.198
$T = 318.15 \text{ K}$						
0.0599	0.6802	0.1716	0.91919	0.3148	-0.126	-0.065
0.0988	0.1622	0.6296	0.90437	0.3455	-0.236	-0.082

Chapter X

0.1595	0.2720	0.1271	1.00979	0.5821	-0.072	-0.091
0.1446	0.6246	0.1935	0.87858	0.2914	0.481	-0.086
0.1979	0.1000	0.5988	0.88706	0.3507	-0.156	-0.104
0.2820	0.0763	0.2182	0.97803	0.5926	0.199	-0.135
0.2441	0.5201	0.1458	0.87846	0.3256	0.958	-0.110
0.2743	0.3118	0.2621	0.89187	0.3669	0.915	-0.127
0.2865	0.1809	0.4563	0.86074	0.3340	0.750	-0.125
0.3664	0.2360	0.0934	0.93234	0.4923	0.676	-0.151
0.3579	0.2466	0.2695	0.87049	0.3623	0.902	-0.145
0.3667	0.3474	0.2239	0.84164	0.3154	1.665	-0.148
0.4481	0.1306	0.2306	0.88104	0.4232	0.707	-0.169
0.4480	0.1576	0.3058	0.84039	0.3519	1.359	-0.165
0.4706	0.1902	0.2698	0.83050	0.3382	1.466	-0.171
0.5393	0.1532	0.1396	0.86152	0.4205	0.894	-0.186
0.5048	0.3488	0.1135	0.81103	0.3110	1.999	-0.175
0.5442	0.3093	0.0963	0.81617	0.3269	1.521	-0.185
0.6484	0.0776	0.0978	0.85230	0.4584	0.632	-0.204
0.6682	0.1139	0.0639	0.84418	0.4425	0.492	-0.206
<hr/>						
CHN (1) + MA (2) + EA (3) + MS (4)						
<hr/>						
T = 298.15 K						
<hr/>						
0.0518	0.6861	0.1731	0.95052	0.4332	0.344	-0.046
0.0860	0.1646	0.6386	0.94892	0.4788	-0.504	-0.073
0.1400	0.2783	0.1300	1.06722	0.8370	-0.595	-0.080
0.1267	0.6377	0.1975	0.92797	0.4350	0.763	-0.072
0.1747	0.1028	0.6161	0.95130	0.5514	-0.726	-0.082
0.2520	0.0795	0.2273	1.05927	0.9947	-0.741	-0.106
0.2169	0.5388	0.1510	0.95565	0.5372	0.235	-0.096
0.2449	0.3244	0.2728	0.97466	0.6283	-0.067	-0.108
0.2562	0.1886	0.4757	0.94350	0.5790	-0.184	-0.109
0.3316	0.2490	0.0985	1.03410	0.9161	-0.651	-0.132
0.3235	0.2598	0.2839	0.96786	0.6938	-0.169	-0.118
0.3319	0.3665	0.2362	0.94429	0.6239	0.237	-0.122
0.4105	0.1395	0.2463	0.99470	0.8879	-0.607	-0.144
0.4105	0.1683	0.3266	0.95665	0.7617	-0.339	-0.133
0.4326	0.2038	0.2892	0.95068	0.7534	-0.210	-0.145
0.5011	0.1660	0.1512	0.99287	0.9980	-0.646	-0.154
0.4666	0.3757	0.1223	0.94173	0.7376	0.069	-0.146
0.5060	0.3352	0.1044	0.95179	0.8084	-0.206	-0.159
0.6127	0.0854	0.1078	0.99993	1.2460	-0.846	-0.159
0.6333	0.1259	0.0706	0.99477	1.2393	-0.838	-0.161
<hr/>						
T = 308.15 K						
<hr/>						
0.0518	0.6861	0.1731	0.93855	0.3443	0.394	-0.092
0.0860	0.1646	0.6386	0.93654	0.3846	-0.454	-0.113
0.1400	0.2783	0.1300	1.05562	0.7095	-0.535	-0.115
0.1267	0.6377	0.1975	0.91605	0.3429	0.823	-0.115
0.1747	0.1028	0.6161	0.93891	0.4364	-0.666	-0.130
0.2520	0.0795	0.2273	1.04751	0.8256	-0.661	-0.152
0.2169	0.5388	0.1510	0.94361	0.4189	0.315	-0.147
0.2449	0.3244	0.2728	0.96284	0.4991	-0.013	-0.156
0.2562	0.1886	0.4757	0.93121	0.4635	-0.103	-0.147
0.3316	0.2490	0.0985	1.02217	0.7696	-0.551	-0.154
0.3235	0.2598	0.2839	0.95565	0.5772	-0.069	-0.139
0.3319	0.3665	0.2362	0.93214	0.5151	0.337	-0.142

Chapter X

0.4105	0.1395	0.2463	0.98262	0.7192	-0.507	-0.182
0.4105	0.1683	0.3266	0.94404	0.6204	-0.194	-0.160
0.4326	0.2038	0.2892	0.93813	0.6137	-0.065	-0.169
0.5011	0.1660	0.1512	0.98051	0.8212	-0.501	-0.175
0.4666	0.3757	0.1223	0.92934	0.6081	0.214	-0.160
0.5060	0.3352	0.1044	0.94021	0.6567	-0.144	-0.180
0.6127	0.0854	0.1078	0.98690	1.0173	-0.611	-0.183
0.6333	0.1259	0.0706	0.98348	1.0115	-0.788	-0.183
<hr/>						
<i>T</i> = 318.15 K						
0.0518	0.6861	0.1731	0.92569	0.2796	0.456	-0.113
0.0860	0.1646	0.6386	0.92367	0.3213	-0.362	-0.131
0.1400	0.2783	0.1300	1.04381	0.6087	-0.443	-0.138
0.1267	0.6377	0.1975	0.90394	0.2775	0.855	-0.132
0.1747	0.1028	0.6161	0.92698	0.3452	-0.634	-0.166
0.2520	0.0795	0.2273	1.03678	0.6958	-0.629	-0.183
0.2169	0.5388	0.1510	0.93132	0.3360	0.415	-0.167
0.2449	0.3244	0.2728	0.95132	0.4018	0.035	-0.183
0.2562	0.1886	0.4757	0.91927	0.3702	-0.020	-0.175
0.3316	0.2490	0.0985	1.01070	0.6471	-0.429	-0.173
0.3235	0.2598	0.2839	0.94448	0.4776	-0.023	-0.157
0.3319	0.3665	0.2362	0.91912	0.4137	0.579	-0.166
0.4105	0.1395	0.2463	0.97064	0.5767	-0.316	-0.218
0.4105	0.1683	0.3266	0.93188	0.5001	-0.002	-0.187
0.4326	0.2038	0.2892	0.92730	0.4963	-0.009	-0.191
0.5011	0.1660	0.1512	0.96984	0.6695	-0.409	-0.201
0.4666	0.3757	0.1223	0.91831	0.4915	0.306	-0.177
0.5060	0.3352	0.1044	0.92969	0.5194	-0.089	-0.207
0.6127	0.0854	0.1078	0.97497	0.8316	-0.319	-0.208
0.6333	0.1259	0.0706	0.97337	0.8180	-0.696	-0.213

The molecular interactions for the various associated binary and ternary mixtures in terms of various excess or deviation properties have already been discussed in previous chapters (VII, VIII and IX). The experimental densities, viscosities, excess molar volumes and viscosity deviations of the quaternary mixtures (CH + MA + EA + MS) and (CHN + MA + EA + MS) studied at 298.15, 308.15 and 318.15 K under ambient pressure were presented in Table 10.1. A perusal of Table 10.1 shows that the V_m^E values for the mixture (CH + MA + EA + MS) are mostly positive over the composition range studied particularly with higher mole fractions (x_1) of CH at all the experimental temperatures. For the mixture (CHN + MA + EA + MS), V_m^E values are mostly negative over the composition range studied at all the experimental temperatures with some positive V_m^E values when the mole fractions (x_4) of MS are very low in this mixture. Positive V_m^E values generally suggest the dominance of dispersion forces and weak dipole-dipole interactions in the mixtures but the negative

Chapter X

V_m^E values suggest the dominance of chemical or specific interactions along with the geometrical fitting of one component into another's structure due to appreciable difference in their molar volumes.⁵ Therefore the results based on V_m^E values suggest the dominance of dispersion forces and weak dipole-dipole interactions in the mixture (CH + MA + EA + MS) but the dominance of chemical or specific interactions as well as geometrical fitting on mixing in the mixture (CHN + MA + EA + MS). Again the V_m^E values for both the quaternary mixtures increase in magnitude as the experimental temperature increases; this fact suggests decrease in the degree of molecular interactions in these mixtures at higher temperatures. Previously as discussed in chapter IX that the ternary mixture (MA + EA + MS) is characterized by negative $V_{m,123}^E$ values when the mole fractions of MS are higher than those of the alkyl acetates at all the experimental temperatures. This fact is quite obvious from the nature of the mixing components for this ternary mixture and the molecular interactions in the associated binary mixtures. Addition of CH or CHN to this ternary mixture results into the formation of the two quaternary mixtures studied herein this chapter. So the trends in V_m^E values for the quaternary mixtures can simply be attributed to the nature of CH and CHN.

The V_m^E values for the quaternary mixtures at 298.15 K were fitted to Cibulka equation⁶ extended for quaternary mixtures as follows:

$$X_{1234}^E = X_{\text{Bin}}^E + x_1 x_2 x_3 x_4 (c_1 + c_2 x_1 + c_3 x_2 + c_4 x_3) \quad (2)$$

$$X_{\text{Bin}}^E = X_{m,12}^E + X_{m,13}^E + X_{m,23}^E + X_{m,24}^E + X_{m,34}^E \quad (3)$$

where $X_{1234}^E = V_m^E$, $X_{\text{Bin}}^E = \sum X_{m,ij}^E$ and $X_{ij}^E = V_{m,ij}^E$. $V_{m,ij}^E$ values were obtained by substituting the Redlich-Kister coefficients (a_i) of the constituent binary mixtures (these coefficients have already been presented in chapters VII, VIII and IX) and the mole fractions of their components in the quaternary mixtures in the Redlich-Kister polynomial.⁷ The coefficients (c_i) were calculated by multi-linear regression and are listed in Table 10.2.

Chapter X

Table 10.2. Coefficients (c_i) of the Cibulka equation for different excess or deviation properties of the quaternary mixtures at 298.15 K.

Mixture property	c_1	c_2	c_3	c_4	σ
	CH (1) + MA (2) + EA (3) + MS (4)				
$V_m^E \cdot 10^6 (\text{m}^3 \cdot \text{mol}^{-1})$	-1264.025	925.049	338.704	1668.307	0.408
$\Delta\eta (\text{mPa} \cdot \text{s})$	-9.498	-38.638	22.839	-56.401	0.036
$\kappa_s^E (\text{TPa}^{-1})$	-1228.126	1700.621	1883.897	1111.411	0.331
$R_m^E \cdot 10^6 (\text{m}^3 \cdot \text{mol}^{-1})$	6458.734	-3435.095	-7436.126	-4770.848	1.933
Mixture property	CHN (1) + MA (2) + EA (3) + MS (4)				σ
	c_1	c_2	c_3	c_4	
$V_m^E \cdot 10^6 (\text{m}^3 \cdot \text{mol}^{-1})$	-1401.404	-470.698	3572.244	4625.905	0.855
$\Delta\eta (\text{mPa} \cdot \text{s})$	26.857	-117.397	60.608	-43.650	0.029
$\kappa_s^E (\text{TPa}^{-1})$	-514.139	362.650	1006.065	403.163	0.258
$R_m^E \cdot 10^6 (\text{m}^3 \cdot \text{mol}^{-1})$	6975.414	-7553.246	-9412.688	-5432.255	1.401

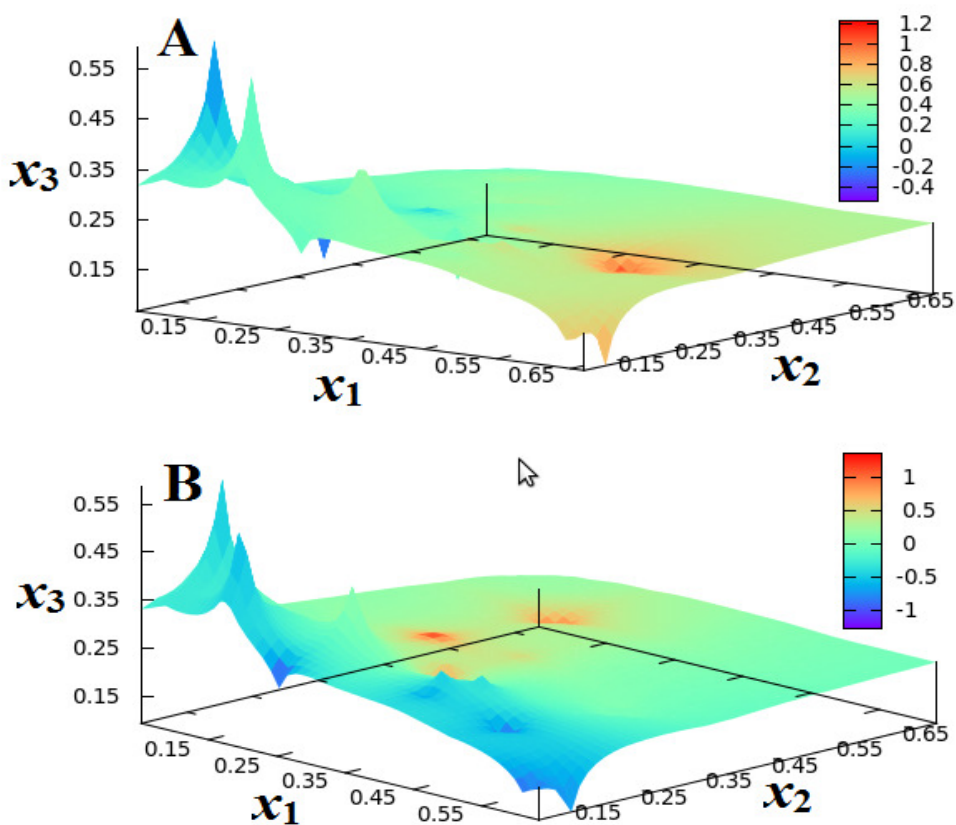


Fig 10.1. Three-dimensional mesh plots of excess molar volumes (V_m^E) for the quaternary mixtures: A, CH (1) + MA (2) + EA (3) + MS (4); B, CHN (1) + MA (2) + EA (3) + MS (4) at 298.15 K. Adjacent colour map represents the V_m^E values for these quaternary mixtures.

Chapter X

Figure 10.1 illustrate the three-dimensional mesh plots of V_m^E values of the quaternary mixtures calculated from Eqs (2) and (3) against the mole fractions of their components in the quaternary mixtures at 298.15 K.

10.3.2. Viscosity Deviations

The viscosity deviations ($\Delta\eta$) of the quaternary mixtures were obtained from the differences between the measured viscosity (η) and the ideal viscosity (η_{id}) as follows:

$$\Delta\eta = \eta - \eta_{id} \quad (4)$$

and the ideal viscosity (η_{id}) is given by:⁸

$$\eta_{id} = \exp\left(\sum_{i=1}^n x_i \ln \eta_{id}\right) \quad (5)$$

where n is the number of components in a mixture and other symbols have their usual meanings as expressed in previous chapters. The uncertainty in viscosity deviation ($\Delta\eta$) was evaluated to be ± 0.004 mPa.s. The $\Delta\eta$ values were found to be negative for both the mixtures (CH + MA + EA + MS) and (CHN + MA + EA + MS) over the composition range studied at all the experimental temperatures (Table 10.1). The correlation, that the V_m^E values are positive when $\Delta\eta$ values are negative and *vice-versa* for many multi-component liquid mixtures,⁹ was observed for the mixture (CH + MA + EA + MS). But for the mixture (CHN + MA + EA + MS), V_m^E values are more negative than the $\Delta\eta$ values. So the $\Delta\eta$ values again suggest the dominance of dispersion forces and weak dipole-dipole interactions in the mixture (CH + MA + EA + MS) but the dominance of chemical or specific interactions as well as geometrical fitting on mixing in the mixture (CHN + MA + EA + MS). Again for both the quaternary mixtures, $\Delta\eta$ values decrease as the experiment temperature increases indicating weaker interactions between the dissimilar molecules of the respective mixtures at higher temperatures (Table 10.1). $\Delta\eta$ values of the quaternary mixtures at 298.15 K were also fitted to the Cibulka equation (Eq. 2) in a fashion similar to V_m^E values and the coefficients (c_i) are listed in Table 10.2. Figure 10.2 illustrates three-dimensional mesh plots of the calculated $\Delta\eta$ values of the quaternary mixtures against the mole fractions of their components at 298.15 K.

Chapter X

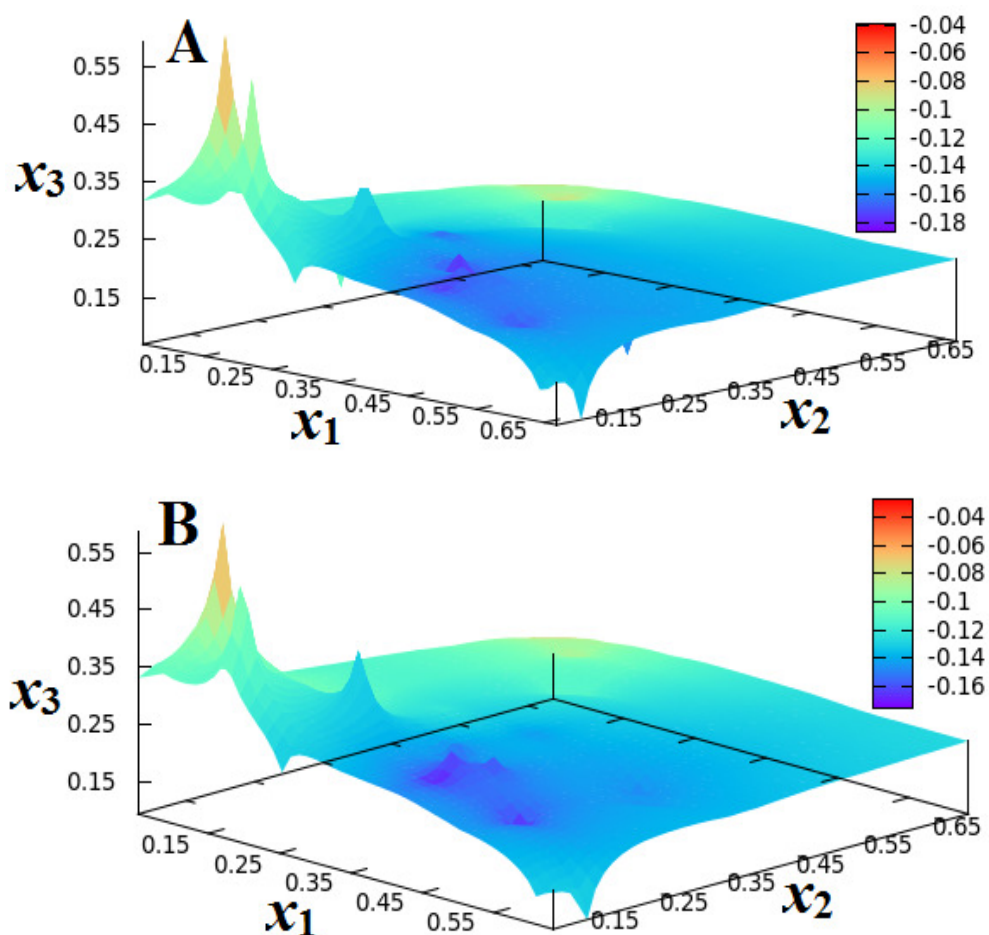


Fig 10.2. Three-dimensional mesh plots of viscosity deviations ($\Delta\eta$) for the quaternary mixtures: A, CH (1) + MA (2) + EA (3) + MS (4); B, CHN (1) + MA (2) + EA (3) + MS (4) at 298.15 K. Adjacent colour map represents the $\Delta\eta$ values for these quaternary mixtures.

10.3.3. Excess Isentropic Compressibility

The experimental speeds of sound (u) and the densities (ρ) of the quaternary mixtures at 298.15 K were used to determine the isentropic compressibilities (κ_s) and the excess isentropic compressibilities (κ_s^E) of the mixtures. The excess isentropic compressibilities (κ_s^E) were obtained from the relation:

$$\kappa_s^E = \kappa_s - \kappa_s^{\text{id}} \quad (6)$$

where κ_s is the isentropic compressibility and was calculated using the Laplace relation, $\kappa_s = 1/\rho u^2$ and κ_s^{id} is the isentropic compressibility for an ideal mixture.

Chapter X

Table 10.3. Ultrasonic speeds (u), isentropic compressibility (κ_s) and excess isentropic compressibility (κ_s^E) for the quaternary mixtures at 298.15 K.

x_1	x_2	x_3	u ($\text{m} \cdot \text{s}^{-1}$)	κ_s (TPa^{-1})	κ_s^E (TPa^{-1})
CH (1) + MA (2) + EA (3) + MS (4)					
0.0599	0.6802	0.1716	1141.4	811.8	36.8
0.0988	0.1622	0.6296	1177.2	775.3	-10.0
0.1595	0.2720	0.1271	1279.2	591.8	-25.4
0.1446	0.6246	0.1935	1163.8	818.2	12.9
0.1979	0.1000	0.5988	1163.6	811.1	22.8
0.2820	0.0763	0.2182	1268.6	621.1	-15.2
0.2441	0.5201	0.1458	1177.8	797.7	21.3
0.2743	0.3118	0.2621	1194.6	763.7	11.8
0.2865	0.1809	0.4563	1168.6	827.7	30.7
0.3664	0.2360	0.0934	1256.8	662.1	-17.1
0.3579	0.2466	0.2695	1198.6	779.5	13.2
0.3667	0.3474	0.2239	1172.4	838.8	42.9
0.4481	0.1306	0.2306	1209.2	757.6	20.4
0.4480	0.1576	0.3058	1187.6	820.4	33.3
0.4706	0.1902	0.2698	1184.4	835.2	39.9
0.5393	0.1532	0.1396	1205.2	779.2	33.9
0.5048	0.3488	0.1135	1169.6	875.2	67.4
0.5442	0.3093	0.0963	1178.4	859.4	60.6
0.6484	0.0776	0.0978	1226.8	759.5	17.1
0.6682	0.1139	0.0639	1230.8	763.2	12.1
CHN (1) + MA (2) + EA (3) + MS (4)					
0.0518	0.6861	0.1731	1164.9	775.3	18.3
0.0860	0.1646	0.6386	1186.4	748.7	-10.0
0.1400	0.2783	0.1300	1310.7	545.4	-26.9
0.1267	0.6377	0.1975	1182.6	770.5	8.5
0.1747	0.1028	0.6161	1203.5	725.8	-9.4
0.2520	0.0795	0.2273	1321.1	540.9	-18.6
0.2169	0.5388	0.1510	1204.7	721.0	17.1
0.2449	0.3244	0.2728	1241.7	665.4	-8.4
0.2562	0.1886	0.4757	1222.8	708.8	-9.2
0.3316	0.2490	0.0985	1323.2	552.3	-22.9
0.3235	0.2598	0.2839	1254.2	656.8	-8.2
0.3319	0.3665	0.2362	1232.8	696.8	6.8
0.4105	0.1395	0.2463	1293.8	600.6	-11.5
0.4105	0.1683	0.3266	1264.5	653.7	-8.2
0.4326	0.2038	0.2892	1266.5	655.8	-6.7
0.5011	0.1660	0.1512	1311.2	585.8	-6.8
0.4666	0.3757	0.1223	1264.0	664.6	4.9
0.5060	0.3352	0.1044	1289.0	632.3	-7.4
0.6127	0.0854	0.1078	1347.9	550.4	-9.4
0.6333	0.1259	0.0706	1348.7	552.6	-8.3

Chapter X

According to Benson and Kiyohara¹⁰ and Acree,¹¹ κ_s^{id} for a n-component mixture is given by the relation:

$$\kappa_s^{\text{id}} = \sum_{i=1}^n \tau_i \left[\kappa_{s,i} + \frac{TV_{m,i}^* \alpha_i^2}{c_{p,i}} \right] - \left\{ \frac{T \sum_{i=1}^n (x_i V_{m,i}^*) \sum_{i=1}^n (\tau_i \alpha_i)^2}{\sum_{i=1}^n (x_i c_{p,i})} \right\} \quad (7)$$

where τ_i is the volume fraction of the i^{th} component in the mixture, $\kappa_{s,i}$, $V_{m,i}^*$, α_i and $c_{p,i}$ are the isentropic compressibility, molar volume, isobaric expansion coefficient and molar isobaric heat capacity of the pure components, respectively. Isobaric expansion coefficients (α_i) were obtained from experimental densities and $c_{p,i}$ values were adapted from the literature.¹² The parameters u , κ_s and κ_s^E at 298.15 K are listed in Table 10.3. The experimental speeds of sound of each pure liquid were in good agreement with the literature values¹³⁻¹⁷ at 298.15 K. For the quaternary mixtures κ_s^E values were observed to follow similar trends as those of V_m^E values against the composition of the mixtures at 298.15 K and these κ_s^E values were also fitted to the Cibulka equation; the coefficients (c_i) are listed in Table 10.2. Figure 10.3 illustrates three-dimensional mesh plots of the calculated κ_s^E values of the quaternary mixtures against the mole fractions of their components at 298.15 K.

10.3.4. Excess Molar Refraction

The excess molar refractions (R_m^E) for a n-component mixture can be had from relation:¹⁸

$$R_m^E = R_m - \sum_{i=1}^n (x_i R_{m,i}) \quad (8)$$

where $R_{m,i}$ is the molar refraction of the i^{th} component in the mixture and the molar refractions (R_m) for a mixture can be had from the relation:¹⁸

$$R_m = \frac{n_D^2 - 1}{n_D^2 + 2} \frac{\sum_{i=1}^n x_i M_i}{\rho} \quad (9)$$

where n_D is the refractive index of the mixture and other symbols have their usual meanings as detailed in Chapter II. Molar refractions (R_m), excess molar refractions (R_m^E) and the experimental refractive indices (n_D) for the quaternary mixtures studied

Chapter X

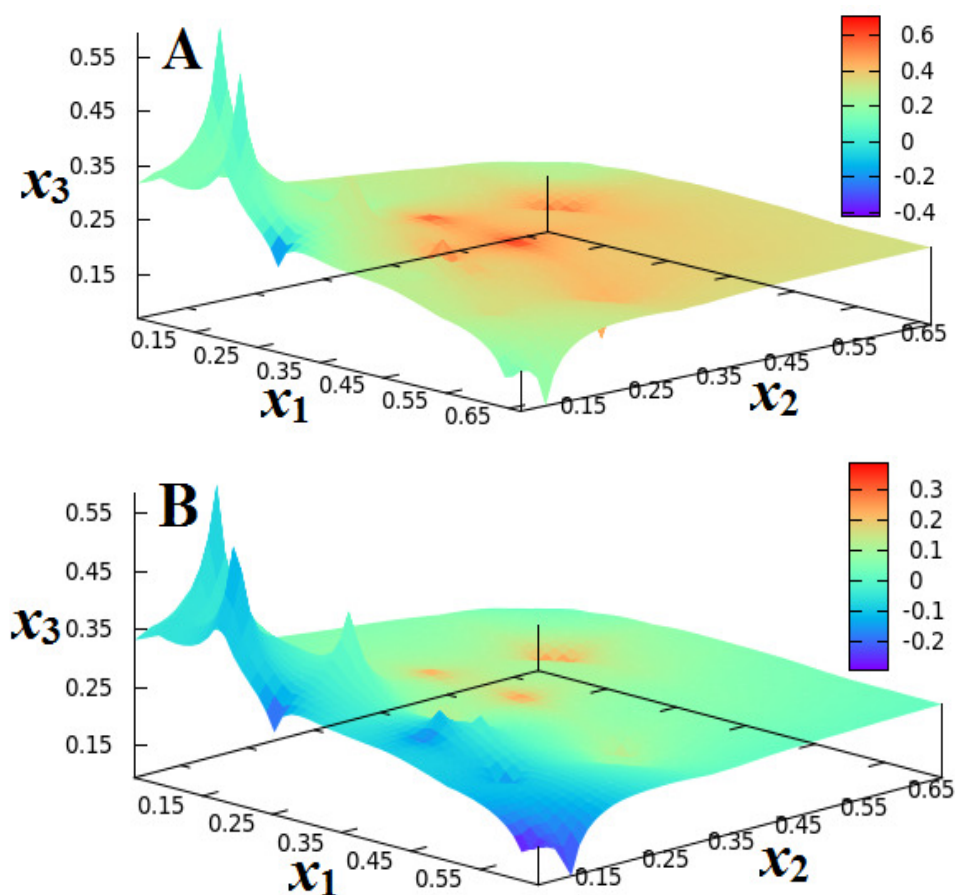


Fig 10.3. Three-dimensional mesh plots of excess isentropic compressibility (κ_S^E) for the quaternary mixtures: A, CH (1) + MA (2) + EA (3) + MS (4); B, CHN (1) + MA (2) + EA (3) + MS (4). Adjacent colour map represents κ_S^E values for these quaternary mixtures.

at 298.15 K are listed in Table 10.4. These R_m^E values of the quaternary mixtures were fitted to the Cibulka equation and the coefficients (c_i) are listed in Table 10.2 Figure 10.4 illustrates three-dimensional mesh plots of the calculated R_m^E values of the quaternary mixtures against the mole fractions of their components at 298.15 K.

10.3.5. Empirical and correlative models

During the last few decades, several different symmetrical as well as asymmetrical models have been suggested to predict and compare the thermodynamic and transport properties of multi-component mixtures. Although some of them were originally proposed to predict specific properties like excess molar enthalpy,

Chapter X

Table 10.4. Refractive indices (n_D), molar refractions (R_m) and excess molar refractions (R_m^E) for the quaternary mixtures at 298.15 K.

x_1	x_2	x_3	n_D	$R_m \times 10^6$ ($\text{m}^3 \cdot \text{mol}^{-1}$)	$R_m^E \times 10^6$ ($\text{m}^3 \cdot \text{mol}^{-1}$)
CH (1) + MA (2) + EA (3) + MS (4)					
0.0599	0.6802	0.1716	1.3864	1.386	-0.240
0.0988	0.1622	0.6296	1.4366	1.437	1.849
0.1595	0.2720	0.1271	1.6419	1.642	8.992
0.1446	0.6246	0.1935	1.4036	1.404	1.089
0.1979	0.1000	0.5988	1.4583	1.458	2.885
0.2820	0.0763	0.2182	1.5883	1.588	6.651
0.2441	0.5201	0.1458	1.4532	1.453	2.719
0.2743	0.3118	0.2621	1.4752	1.475	3.171
0.2865	0.1809	0.4563	1.4342	1.434	1.847
0.3664	0.2360	0.0934	1.6097	1.610	8.399
0.3579	0.2466	0.2695	1.4673	1.467	2.928
0.3667	0.3474	0.2239	1.4179	1.418	1.069
0.4481	0.1306	0.2306	1.4779	1.478	2.629
0.4480	0.1576	0.3058	1.4614	1.461	2.872
0.4706	0.1902	0.2698	1.4480	1.448	2.335
0.5393	0.1532	0.1396	1.4956	1.496	3.598
0.5048	0.3488	0.1135	1.4217	1.422	1.301
0.5442	0.3093	0.0963	1.4376	1.438	1.802
0.6484	0.0776	0.0978	1.5147	1.515	4.242
0.6682	0.1139	0.0639	1.5011	1.501	3.663
CHN (1) + MA (2) + EA (3) + MS (4)					
0.0518	0.6861	0.1731	1.3701	20.162	-0.906
0.0860	0.1646	0.6386	1.4275	25.396	1.294
0.1400	0.2783	0.1300	1.6229	37.840	7.629
0.1267	0.6377	0.1975	1.3915	21.243	0.495
0.1747	0.1028	0.6161	1.4483	26.815	2.030
0.2520	0.0795	0.2273	1.5757	36.780	5.229
0.2169	0.5388	0.1510	1.4380	24.365	1.640
0.2449	0.3244	0.2728	1.4751	27.774	2.688
0.2562	0.1886	0.4757	1.4236	25.167	0.844
0.3316	0.2490	0.0985	1.6181	36.764	7.820
0.3235	0.2598	0.2839	1.4621	27.335	1.991
0.3319	0.3665	0.2362	1.4200	24.251	0.617
0.4105	0.1395	0.2463	1.4621	28.561	0.863
0.4105	0.1683	0.3266	1.4369	26.264	0.737
0.4326	0.2038	0.2892	1.4414	26.231	1.125
0.5011	0.1660	0.1512	1.4922	29.948	2.295
0.4666	0.3757	0.1223	1.4207	24.164	0.408
0.5060	0.3352	0.1044	1.4382	25.376	0.864
0.6127	0.0854	0.1078	1.5074	31.418	2.557
0.6333	0.1259	0.0706	1.5088	31.087	2.749

Chapter X

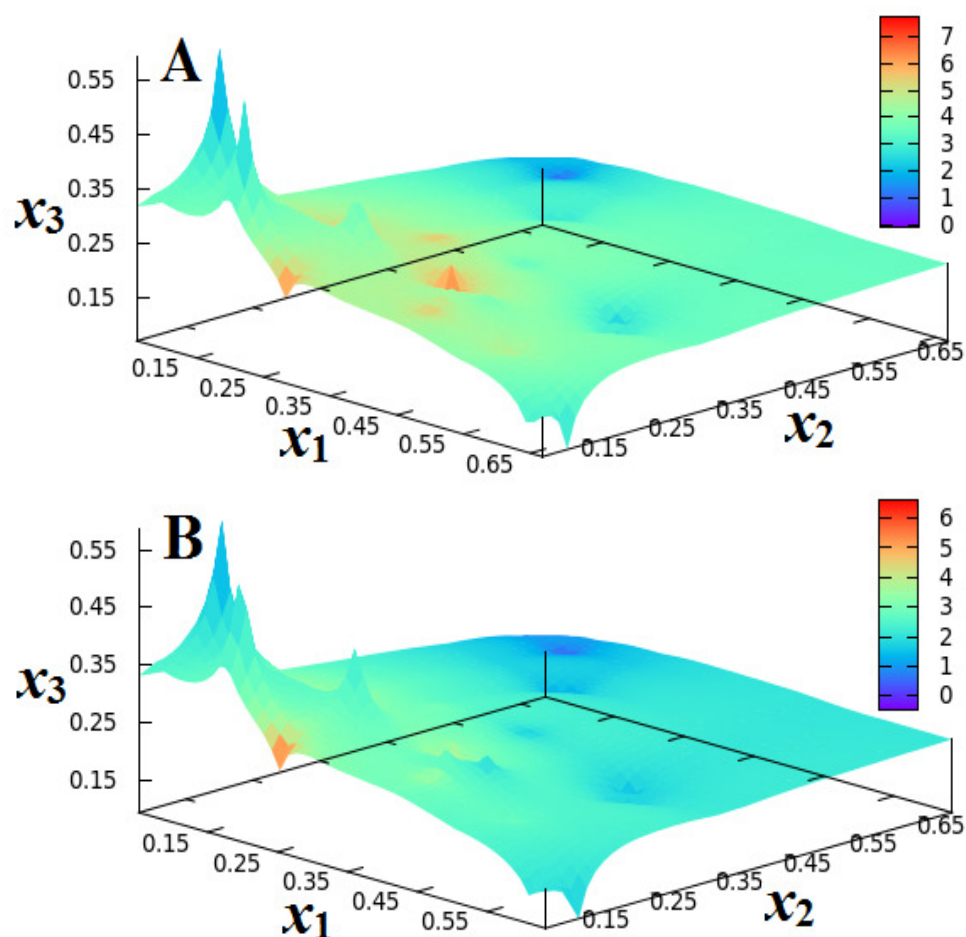


Fig 10.4. Three-dimensional mesh plots of excess molar refractions (R_m^E) for the quaternary mixtures: A, CH (1) + MA (2) + EA (3) + MS (4); B, CHN (1) + MA (2) + EA (3) + MS (4). Adjacent colour map represents the R_m^E values for these quaternary mixtures.

Gibbs free energy, *etc.*, they can also be applied to any other excess or deviation properties^{19,20} Most of them are still popular and suitable for the prediction of the excess or deviation properties. Herein this chapter models proposed by Köhler²¹ and Jacob-Fitzner²² were used in their extended form (as detailed in chapter II) to predict different excess or deviation properties of the quaternary mixtures by utilizing the available data of the constituent binary mixtures only. The predictive capability of these models was judged by calculating the standard deviation (σ) between the experimental and the calculated values at 298.15 K. These standard deviations (σ) are shown in Table 10.5.

Chapter X

Table 10.5. Standard deviations (σ) between the experimental and calculated excess or deviation properties for the quaternary mixtures derived from Köhler and Jacob-Fitzner model at 298.15 K.

Various models	Standard deviations (σ)			
	$(V_m^E)^a$	$(\Delta\eta)^b$	$(\kappa_S^E)^c$	$(R_m^E)^d$
CH (1) + MA (2) + EA (3) + MS (4)				
Köhler	0.1625	0.1022	0.2499	0.1285
Jacob-Fitzner	0.1473	0.0933	0.2319	0.1032
CHN (1) + MA (2) + EA (3) + MS (4)				
Köhler	0.1022	0.0797	0.1756	0.2292
Jacob-Fitzner	0.1020	0.0689	0.1581	0.2132

Units: $a, 10^6(\text{m}^3 \cdot \text{mol}^{-1})$; $b, \text{mPa}\cdot\text{s}$; c, TPa^{-1} ; $d, 10^6(\text{m}^3 \cdot \text{mol}^{-1})$

The small standard deviations (σ) reveal that both the symmetric models suggested by Köhler and Jacob-Fitzner work well for the quaternary mixtures studied in this chapter.

10.4. Conclusion

Based on various excess or deviation properties like V_m^E , $\Delta\eta$, etc., for the two quaternary mixtures (CH + MA + EA + MS) and (CHN + MA + EA + MS), it can be concluded that the degree of molecular interactions in these mixtures follows the order: (CHN + MA + EA + MS) > (CH + MA + EA + MS). Also the composition dependence of these derived properties reveal that these mixtures are characterized by the nature of the components as well as by the nature and degree of molecular interactions in the associated mixtures.

References

- [1] C.R. Reid, B.E. Poling, *The properties of Gases and Liquids*, McGraw Hill, New York, 1998, Ch. 1.
- [2] J. George, N.V. Sastry, *J. Chem. Eng. Data* 49 (2004) 1116.
- [3] A.R. Mahajan, S.R. Mirgane, *Chem. Eng. Comm.*, 200 (2013) 1666.
- [4] G. Nath, *Chem. Sci. Trans.*, 1 (2012) 516.
- [5] R. Pradhan, B. Sinha, *J. Serb. Chem. Soc.*, 82 (2017) 189.
- [6] I. Cibulka, *Collect. Czech. Chem. Commun.* 47 (1982) 1414.
- [7] O.J. Redlich, A.T. Kister, *Ind. Eng. Chem.* 1948, 40, 345.

Chapter X

- [8] S. Glasstone, K.J. Laidler, H. Eyring, *The theory of Rate Process*. McGraw-Hill Book Company, Inc., New York, 1941.
- [9] R. Pradhan, A. Kamath, D. Brahman, B. Sinha, *Fluid Phase Equilib.* 404 (2015) 131.
- [10] G.C. Benson, O.K. Kiyohara, *J. Chem. Thermodyn.* 11 (1979) 1061.
- [11] W.E. Acree, *J. Chem. Eng. Data*, 28 (1983) 215.
- [12] W.M. Haynes, D.R. Lide, T.J. Bruno, *CRC Handbook of Chemistry & Physics*, 93rd edn., Taylor & Francis, Boca Roton, London, 2012-2013.
- [13] D.L. Cunha, J.A.P. Coutinho, J.L. Daridon, *J. Chem. Eng. Data* 58 (2013) 925.
- [14] S. Nallani, S. Boodida, S.J. Tangeda, *J. Chem. Eng. Data* 52 (2007) 405.
- [15] V. Vyas, T. Nautiyal, *Pramana-J. Phys.*, 59 (2002) 663.
- [16] J.M. Resa, J.M. Goenaga, A.I. Sanchez-Ruiz, *J. Chem. Eng. Data* 51 (2006) 1294.
- [17] C.B. Salguero, J.G. Fadrique, *J. Chem. Eng. Data* 56 (2011) 3823.
- [18] M.S. Dhillon, H.S. Chugh, *J. Chem. Eng. Data* 22 (1977) 262.
- [19] J.W. McCargar, W.E. Acree, *Thermochimica. Acta.*, 149 (1989) 363.
- [20] M. Hillert, *Ber. Bunsenges. Phys. Chem.*, 87 (1983) 762.
- [21] F. Köhler, *Monatsh. Chem.* 91 (1960) 738.
- [22] K.T. Jacob, K. Fitzner, *Thermochim. Acta* 18 (1977) 197.

CHAPTER XI

Concluding Remarks

The present thesis involves the experimental measurements of the densities, viscosities, ultrasonic velocities and refractive indices of binary, ternary and quaternary liquid mixtures. These experimental data helps in the investigation of the nature and molecular interactions amongst the unlike components of the various multi-component liquid mixtures in terms of various derived excess or deviation properties.

In chapter IV thermophysical properties of the binary mixtures of N, N-dimethylformamide (DMF) with tetrahydrofuran (THF), 1,3-dioxolane (1,3-DO) and 1,4-dioxane (1,4-DO) at several temperatures were studied. The nature and magnitude of various excess or deviation properties (V_m^E , $\Delta\eta$ and κ_S^E) suggests the following order of molecular interactions: (DMF + THF) > (DMF + 1,3-DO) > (DMF + 1,4-DO) and the molecular interactions also increase with the increase of temperature. The excess partial molar volumes ($\bar{V}_{m,1}^E$ and $\bar{V}_{m,2}^E$) were found to be negative for all the binary systems except the binary mixture containing 1,4-DO. Also the excess partial molar volumes at infinite dilution ($\bar{V}_{m,1}^{0,E}$ and $\bar{V}_{m,2}^{0,E}$) were found to be negative for both the components in all the binary mixtures except (DMF + 1,4-DO) mixture. Therefore, while the (DMF + 1,4-DO) mixture is characterised by volume expansion the other two mixtures were characterised by volume contraction. The excess molar volumes of the mixtures were predicted using Prigogine-Flory-Patterson (PFP) and ultrasonic speeds of sound for the studied binary mixtures were also predicted using various empirical and semi-empirical models.

In chapter V the thermophysical properties of the binary mixtures of 2-ethylhexan-1-ol with some 1,2-disubstituted ethanes were studied in terms of various excess or deviation properties. These properties show both positive and negative deviations from ideal ones. An inspection of excess molar volumes, viscosity deviations, isentropic compressibilities, *etc.*, suggests the following order of molecular interactions: (2-EH + MEA) > (2-EH + EDA) > (2-EH + DCE). However, the degree of molecular interactions for each binary systems studied becomes weaker at higher temperatures, probably due to enhanced thermal agitation and kinetic energy

of the component molecules at higher temperatures. The excess partial molar volumes ($\bar{V}_{m,1}^{0,E}$ and $\bar{V}_{m,2}^{0,E}$) for both the components in the mixtures (2-EH + EDA) and (2-EH + MEA) were negative. However, more negative values of these properties for (2-EH + MEA) mixture than (2-EH + EDA) mixture suggest the following order of packing efficiency or structure compactness in the mixtures: (2-EH + MEA) > (2-EH + EDA) > (2-EH + DCE). The excess molar volumes were correlated using Prigogine-Flory-Patterson (PFP) theory and Peng-Robinson Equation of State (PREOS) based model. The viscosities were correlated using PREOS and Bloomfield-Dewan models. The ultrasonic speeds of sound were also predicted using various empirical and semi-empirical models like Collision factor theory (CFT), Nomoto relation (NOM), Impedance dependence relation (IDR), Ideal mixture relation (IMR) and Junjie (JUN). FTIR spectra of the mixtures also supported the nature of molecular interactions observed for the studied binary systems.

In chapter VI physico-chemical properties of the binary mixtures of 1,4-dioxane (1,4-DO) with ethylenediamine (EDA), 1,2-dichloroethane (DCE) and monoethanolamine (MEA) were studied at several temperatures. Various excess or deviation properties were determined for the experimentally measured densities, viscosities, ultrasonic speeds of sound and refractive indices. These properties were interpreted in terms of dipole-dipole interactions and H-bond interactions amongst the mixing components and the following order of molecular interactions: (1,4-DO + MEA) > (1,4-DO + EDA) > (1,4-DO + DCE) has been found. The degree of molecular interactions however decreases at higher temperatures owing to thermal disruption of developing dispersion forces, non-specific interactions and specific interactions (H-bonding) amongst the liquid components of the mixture. A comparison of the partial molar volume ($\bar{V}_{m,1}^0$ and $\bar{V}_{m,2}^0$) at infinite dilution to molar volume of the respective pure liquids reveal that except the mixture (1,4-DO + MEA), the other two mixtures are characterised by volume expansion. For the studied binary systems Prigogine-Flory-Patterson (PFP) and Peng-Robinson Equation of State (PREOS) were found to predict the excess molar volumes satisfactorily. FTIR spectra of these mixtures showed characteristic band shifts in position and intensities in accordance with the nature of the molecular interaction of the mixtures.

Chapter VII describes the thermophysical properties of the binary mixtures of cyclohexane (CH) with methyl acetate (MA), ethyl acetate (EA) and methyl salicylate (MS) at several temperatures. Experimental densities, viscosities ultrasonic speeds of sound and refractive indices were utilised to derive various excess or deviation properties like excess molar volumes, viscosity deviations, excess isentropic compressibilities, excess molar refractions, *etc.* An analysis of these properties revealed the following order of molecular interactions: (CH + MS) > (CH + EA) > (CH + MA). Such an order of molecular interactions originates from a combined effect of several factors like the molecular size, shape and nature of the components; herein the order is attributed to the breaking up of dipolar interactions or the three dimensional hydrogen bonded network as well as interstitial accommodation on mutual mixing of the components. A comparison of the excess partial molar volumes ($\bar{V}_{m,1}^{0,E}$ and $\bar{V}_{m,2}^{0,E}$) at infinite dilution to the molar volumes of the pure components of the mixtures suggests that while the mixtures with MA and EA are characterized by volume expansion, the mixture with MS is characterized by volume contraction on mixing with CH. FTIR spectra of the mixtures also correlate well with the observed molecular interactions for the mixtures studied.

Chapter VIII describes the thermophysical properties of the binary mixtures of cyclohexanone (CHN) with methyl acetate (MA), ethyl acetate (EA) and methyl salicylate (MS) at several temperatures. Various excess or deviation properties determined from the experimental physico-chemical properties like density, viscosity, ultrasonic speed of sound, *etc.*, were interpreted in terms of breaking up of dipolar interactions or three-dimensional hydrogen bonded network as well as interstitial accommodation, *etc.* The study revealed the following order of molecular interactions: (CHN + MS) > (CHN + EA) > (CHN + MA). A comparison of the excess partial molar volumes ($\bar{V}_{m,1}^{0,E}$ and $\bar{V}_{m,2}^{0,E}$) at infinite dilution to the molar volumes of the pure components of these mixtures suggests that the molecular compactness increases in the same order of molecular interactions as shown above. The Applicability of PFP theory, PR-EOS and Bloomfield-Dewan models were tested for the prediction of V_m^E and η values of the mixtures. FT-IR spectra of the mixtures also correlate well with the observed molecular interactions for the mixtures studied.

Chapter IX describes the thermophysical properties of the ternary mixtures of cyclohexane (CH) and cyclohexanone (CHN) with methyl acetate (MA), ethyl acetate (EA) and methyl salicylate (MS) at several temperatures. In this chapter molecular interactions of the binary mixtures between the ester molecules were also studied through the determination of the densities, viscosities, *etc.* Based on the excess or deviation properties like V_m^E , $\Delta\eta$, *etc.*, for the three binary mixtures (MA + EA), (MA + MS) and (EA + MS), the following order of molecular interactions were observed: (MA + MS) > (EA + MS) > (MA + EA). The excess partial molar volumes ($\bar{V}_{m,1}^{0,E}$ and $\bar{V}_{m,2}^{0,E}$) at infinite dilution of these binary mixtures also support the above order of molecular interactions. Various excess or deviation properties of the studied ternary mixtures (CH + MA + EA), (CH + MA + MS), (CH + EA + MS), (CHN + MA + EA), (CHN + MA + MS), (CHN + EA + MS) and (MA + EA + MS) suggest that these mixtures are characterized by the nature of their mixing components as well as by the nature of molecular interactions in the associated binary mixtures. These excess or deviation properties of the ternary mixtures were fitted to Cibulka equation and the so-called ternary contributions ($X_{m,123}^E - X_{Bin}^E$) were derived; although these contributions are rather small but their maximum and minimum values suggest non-homogeneity in these ternary mixtures and the binary contributions (X_{Bin}^E) play a significant role in characterizing the ternary mixtures studied. Further the empirical models like Köhler, Jacob–Fitzner, Colinet, Tsao–Smith, Toop, *etc.*, were tested to estimate theoretically the excess molar volumes, viscosity deviations, *etc.*, and these models were found to be suitable for the studied ternaries.

Chapter X describes the thermophysical properties for the quaternary mixtures of cyclohexane (CH) and cyclohexanone (CHN) with methyl acetate (MA), ethyl acetate (EA) and methyl salicylate (MS) at several temperatures. The various excess or deviation properties like excess molar volumes, viscosity deviations, *etc.*, derived for these quaternary mixtures revealed the following order of molecular interactions: (CHN + MA + EA + MS) > (CH + MA + EA + MS). This order of molecular interactions suggests that these mixtures are characterised by the nature of the component liquids as well as by the molecular interactions prevailing in the associated binary and ternary mixtures. Various excess or deviation properties of these mixtures

were also correlated with two symmetric models given by Köhler and Jacob–Fitzner. Both these models were found to correlate the excess or deviation properties satisfactorily.

In summary the physico-chemical study of multi-component liquid mixtures provide valuable information about the extent and nature of molecular interactions (amongst the component liquids) that ultimately predicts the overall structure of such mixtures in the liquid state. Information on the molecular interactions often helps to develop new theoretical models, which aid to have valuable academic information on various physico-chemical properties of the related mixtures; because it is often difficult to understand, explore and interpret molecular interactions in multi-component liquid mixtures. Information on the physico-chemical properties and the liquid structure of multi-component liquid mixtures are actually very much important for their industrial applications. Therefore, studies on physico-chemical properties of such mixtures can prove handy for their selections in process industries. Therefore, physico-chemical studies on multi-component liquid mixtures are never ending as well as worthy of extensive studies.

APPENDIX I

List of Publications

- [1] Thermophysical properties of binary mixtures of N, N-dimethylformamide with three cyclic ethers, J. Serb. Chem. Soc., 78 (9) (2013) 1443-1460.
- [2] Hydrogen bond interactions in the blends of 1,4-dioxane with some 1,2-disubstituted ethanes at $T = (298.15, 308.15 \text{ and } 318.15) \text{ K}$, Fluid Phase Equilibria, 404 (2015) 131-140.
- [3] Thermophysical properties of the binary blends of cyclohexane with some esters, J. Serb. Chem. Soc., 82 (2017) 189-202.
- [4] Solution thermodynamics of iron(III)-N,N'-ethylene-bis(salicylideneiminato)-chloride in binary mixtures of N,N-dimethylformamide and acetonitrile at $T = (298.15, 303.15, 308.15 \text{ and } 313.15) \text{ K}$, J. Chem. Thermodyn. 75 (2014) 96-105.
- [5] A partial derivatives approach for estimation of the viscosity Arrhenius temperature in N, N-dimethylformamide + 1,4-dioxane binary fluid mixtures at temperatures from 298.15 K to 318.15 K, Phys. Chem. of Liquids, 54 (2016) 615-631.

APPENDIX II

PARTICIPATION IN SEMINAR, SYMPOSIUM & CONVENTIONS

- **National Seminar on Frontiers in Chemistry 2013**, sponsored by University Grants Commission, New Delhi, India, Organized by Department of Chemistry, University of North Bengal, Darjeeling, India on February 28, 2013 as Delegate.
- Workshop on “**Intellectual Property and Innovation Management in Knowledge Era**” sponsored by National Research Development Corporation, New Delhi and organized by University of North Bengal, held at University of North Bengal on February 12, 2013 as Delegate.
- **16th.National Symposium in Chemistry** organized by Chemical Research Society of India, held at Indian Institute of Technology Bombay, on February 7-9, 2014 and presented a Poster.
- **53rd Annual Convention of Chemist (National Conference)** Organized by Indian Chemical Society, held at the GITAM University, Visakapatnam, Andhra Pradesh, India, on December 27-29, 2016 and presented a Poster (PP-16).
- **National Seminar on Frontiers in Chemical and Material Sciences: Theory and Practice 2018**, sponsored by University Grants Commission, New Delhi, India, organized by Department of Chemistry, University of North Bengal, Darjeeling, India on February 8-10, 2018 as Delegate.

BIBLIOGRAPHY

- [1] A. Abe, P.J. Flory, J. Am. Chem. Soc., 87 (1965) 1838.
- [2] A. Ali, A. K. Nain, D. Chand, R. Ahmad, J. Chinese. Chem. Soc., 53 (2006) 531.
- [3] A. Ali, A.K Nain, J. Pure. Appl. Ultrason., 22 (2000) 121.
- [4] A. Ali, A.K. Nain, N. Kumar, M. Ibrahim, J. Pure Appl. Ultrason., 24 (2002) 27.
- [5] A. Ali, A.K. Nain, S. Hyder, J. Pure Appl. Ultrason., 23 (2001) 73.
- [6] A. Ali, H. soghra, Ind. J. phys., 76 (2002) 23.
- [7] A. Ali, K. Tewari, A.K. Nain, V. Chakravorthy, Phys. Chem. Liq., 38 (2000) 459.
- [8] A. Ali, M. Tariq, F. Nabi, Ind. J. Pure App. Phys., 46 (2008) 545.
- [9] A. Blanco, A. García-Abuín, D. Gómez-Díaz, J.M. Navaza, J. Chem. Eng. Data 57 (2012) 3136.
- [10] A. Chatterjee, B. Das, J. Chem. Eng. Data 51 (2006) 1352.
- [11] A. Henni, J.H. Jonathan. T. Paitoon, C. Amit, J. Chem. Eng. Data 48 (2003) 1062.
- [12] A. Inglese, J.E. Groller, E. Willhelm, J. Chem. Eng. Data 28 (1983) 124.
- [13] A. Lorentz, Weid. Ann., 9 (1880) 641.
- [14] A. Pal and A. Kumar, J. Chem. Eng. Data 43 (1998) 143.
- [15] A. Pal and H. Kumar, J. Mol. Liq., 89 (2000) 189.
- [16] A. Pal, G. Dass, Ind. J. Chem., 38 (1999) 237.
- [17] A. Pal, H. Kumar, Ind. J. Phys., 78 (2004) 1319.
- [18] A. Pal, H. Kumar, J. Mol. Liq., 89 (2000) 189.
- [19] A. Pal, Y.P. Singh, J. Chem. Thermodyn., 28 (1996) 143.
- [20] A. Pineiro, P. Brocos, A. Amigo, M. Pintos, R. Bravo, J. Chem. Thermodyn., 31 (1999) 931.
- [21] A. Pineiro, P. Brocos, A. Amigo, M. Pintos, R. Bravo, Phys. Chem. Liq., 38 (2000) 251.
- [22] A. Sinha, M.N. Roy, J. Mol. Liq., 140 (2008) 39.
- [23] A. Valen, I. Gascon, C. Lafuente, J.S. Urieta, F.M. Royo, M. Postigo, Int. J. Thermophys., 23 (2002) 1587.
- [24] A. Villares, S. Martin, M. Haro, B. Giner, H. Artigas, J. Chem. Thermodyn., 36 (2004) 1027.
- [25] A.A. Mistry, V.D. Bhandakkar, O.P. Chimankar, J. Chem. Pharm. Res., 4 (2012) 170.
- [26] A.B. Bhatia, *Ultrasonic Absorption*, Clarendon Press, Oxford, (1967).
- [27] A.B. Pereiro, A. Rodriguez, J. Chem. Eng. Data 52 (2007) 600.
- [28] A.B. Sawant, M. Hasan, V. J. Naukudkar, Chem. Sci. Trans., 2 (2013) 263.
- [29] A.F. Fucaloro, J. Chem. Educ., 79 (2002) 865.
- [30] A.F. Ribeiro, E. Langa, A.M. Mainar, J.J. Pardo, J.S. Urieta, J. Chem. Eng. Data 52 (2006) 1.
- [31] A.G. Peshwe, B.R. Arbad, S.P. Pachaling, Int. J. Chem. Sci., 7 (2009) 1505.
- [32] A.H. Al-Dujali, A.A. Yassen, A.M. Awwad, J. Chem. Eng. Data 45 (2000) 647.
- [33] A.J. Matheson, *Molecular Acoustics*, Wiley Interscience, London, (1971).
- [34] A.J. Queimade, I.M. Marrucho, J.A.P. Coutinho, E.H. Stenby, Int. J. Thermophys, 26 (2005) 47.
- [35] A.J. Treszczanowicz, O. Kiyohora, G.C. Benson, J. Chem. Thermodyn., 13 (1981) 253.
- [36] A.J. Treszczanowicz, T. Treszczanowicz, T.S. Pawlowski, T. Kasprzycka-Guttman, J. Solution Chem., 33 (2004) 1049.
- [37] A.K. Doolittle, J. Appl. Phys., 23 (1952) 236.
- [38] A.K. Mehrotra, W.D. Monnery, W. Svrcek, Fluid Phase Equilib., 117 (1996) 344.
- [39] A.K. Nain, Fluid Phase Equilib., 265 (2008) 56.
- [40] A.K. Nain, J. Solution Chem., 35 (2006) 1417.

Bibliography

- [41] A.K. Nain, P. Chandra, J.D. Pandey, S. Gopal, J. Chem. Eng. Data 53 (2008) 2654.
- [42] A.M. Awaad, R.A. Pethrick, J. Chem. Soc. Faraday Trans., 78 (1982) 3203.
- [43] A.M. Farhan, E.T. Kareem, A.N. Abd, Bag. Sci. J., 8 (2011) 348.
- [44] A.M. Farhan, E.T. Kareem, A.N. Abd, J. Kerb. Univ., 8 (2010) 184.
- [45] A.N. Kannappan, S. Thirumaran, R. Palani, J. Phys. Sci., 20 (2009) 97.
- [46] A.P. Kilimov, M.A. Svechnikova, V.I. Shevchenko, V.V. Smirnov, S.B. Zotov, F.V. Kvasnyuk-Mudryi, Khimiya Geterotsiklicheskikh Soedinenii, 5 (1969) 208.
- [47] A. Pal, Y.P. Singh, Ind. J. Pure Appl. Phys., 35 (1997) 310.
- [48] A.R. Mahajan, S.R. Mirgane, Chem. Eng. Comm., 200 (2013) 1666.
- [49] A.R. Mathieson, J.C.J. Thynne, J. Chem. Soc., (1956) 3713.
- [50] A.R. Ravishankara. Science, 276 (1997) 1058.
- [51] A.R. Venis, R. Rajkumar, Orient. J. Chem., 27 (2011) 105.
- [52] A.T.J. Hayward, Brit. J. Appl. Phys., 18 (1967) 965.
- [53] A.T.J. Hayward, J. Phys. D: Appl. Phys., 4 (1971) 938.
- [54] A.T.J. Hayward, Nature, 221 (1996) 1047.
- [55] B. Celda, R. Gavara, J. E. Figueruelo, J. Chem. Eng. Data 32 (1987) 31.
- [56] B. Garcia, R. Alcalde, J.M. Leal, J.S. Mantos, J. Chem. Soc., Faraday Trans., 93 (1997) 1115.
- [57] B. Garcia, R. Alcalde, S. Aparicio, J.M. Leal, J. S. Matos, Phys. Chem. Phys. Chem., 3 (2001) 2866.
- [58] B. Garcia, R. Alcalde, S. Aparicio, J.M. Leal, Phys. Chem. Chem. Phys., 4 (2002) 5833.
- [59] B. Giner, C. Lafuente, A. Villares, M. Haro, M.C. Lopez, J. Chem. Thermodyn., 3 (2007) 148.
- [60] B. Giner, S. Martin, H. Artigas, M.C. Lopez, C.J. Lafuente, J. Phys. Chem. B., 110 (2006) 17683.
- [61] B. Gracia, R. Alcalde, J. M. Leal, J. Chem. Soc., Faraday Trans., 93 (1997) 1115.
- [62] B. Jacobson, Acta Chem. Scand., 5 (1951) 1214.
- [63] B. Jacobson, Acta Chem. Scand., 6 (1952) 1485.
- [64] B. Jacobson, J. Chem. Phys., 20 (1952) 927.
- [65] B. Jasinski, S. Malanowski, Chem. Eng. Sci., 25 (1970) 913.
- [66] B. Sinha, Phys. Chem. Liq., 48 (2010) 183.
- [67] B. Sinha, R. Pradhan, S. Saha, D. Brahman, A. Sarkar, J. Serb. Chem. Soc., 78 (2013) 1443.
- [68] B. Sinha, R. Pradhan, S. Saha, D. Brahman, J. Serb. Chem. Soc., 78 (2013) 1443.
- [69] B.E. Eichinger, P.J. Flory, Trans Faraday Soc., 64 (1968) 2006.
- [70] B.E. Eichinger, P.J. Flory, Trans Faraday Soc., 64 (1968) 2035.
- [71] B.E. Eichinger, P.J. Flory, Trans Faraday Soc., 64 (1968) 2061.
- [72] B.J.I. Shwara, N.S. Varaprasad, Ind. J. Pure Appl. Phys., 41 (2003) 275.
- [73] B.K. Sarkar, A. Choudhury, B. Sinha, J. Solution Chem., 41 (2012) 53.
- [74] C. Colinet, Ph. D thesis, University of Grenoble, France,(1967).
- [75] C. Lafuente, J. Pardo, J. Santafe, F.M. Royo, J. Chem. Thermodyn., 27 (1995) 541.
- [76] C. Li, J. Zhang, T. Zhang, X. Wei, E. Zhang, N. Yang, N. Zhao, M. Su, H. Zhou, J. Chem. Eng. Data 55 (2010) 4104.
- [77] C. Reichardt, *Solvents and Solvent Effects in Organic Chemistry*, 3rd edn., Wiley-VCH, 2003.
- [78] C.B. Salguero, J.G. Fadrique, J. Chem. Eng. Data 56 (2011) 3823.
- [79] C.C. Tsao, J.M. Smith, Chem. Eng. Prog. Symp. Series, 49 (1953) 107.
- [80] C.C. Wang, H.W. Chen, C.H. Tu, J. Chem. Eng. Data 50 (2005) 1687.
- [81] C.de. Visser, G. Perron, J.E. Desnoyers, J. Chem. Eng. Data 22 (1977) 74.

Bibliography

- [82] C.G. Janz, R.P.T. Tomkins, *Non-Aqueous Electrolytes Handbook*, Academic, New York, 2, 1973.
- [83] C.R Reid, B.E. Poling, *The properties of Gases and Liquids*, McGraw Hill, New York, 1998, Ch.1
- [84] C.V. Surayanarayana, T. Kuppasamy, J. Acou. Soc. Ind., 4 (1976) 75.
- [85] D. Brahman, B. Sinha, J. Chem. Thermodyn., 75 (2014) 136.
- [86] D. Brahman, R. Pradhan, B. Sinha, J. Chem. Thermodyn., 75 (2014) 96.
- [87] D. Kiyohora, G.C. Benson, J. Chem. Thermodyn., 11 (1979) 861.
- [88] D. Patterson, A.K. Rastogi, J. Phys. Chem., 74 (1970) 1067.
- [89] D. Patterson, G. Delmas, Discuss Faraday Soc., 49 (1970) 98.
- [90] D. Patterson, G. Delmas, J. Polym. Sci., 30 (1970) 1.
- [91] D. Patterson, Pure. Appl. Chem., 47 (1976) 305.
- [92] D.W. Marquardt, J. Soc. Ind. Appl. Math., 11, (1963) 431.
- [93] D.B. Karuna Kumar, K.R. Reddy, G.S. Rao, P.B. Sandhyasri, Z. Begum, C. Rambabu, J. Mol. Liq., 183 (2013) 31.
- [94] D.D. Perin, W.L.F. Armarego, *Purification of Laboratory Chemicals*, 3rd edn., Oxford, New York, 1988, pp. 164.
- [95] D.F.J. Arago, J.B. Biot, Mem. Acad. Fr., 17 (1806) 7.
- [96] D.K. Sravana, D.K. Rao D. Ind. J. Pure Appl. Phys., 45 (2007) 210.
- [97] D.L. Cunha, J.A.P. Coutinho, J.L. Daridon, J. Chem. Eng. Data 58 (2013) 925.
- [98] D.L. Cunha, J.A.P. Coutinho, J.L. Daridon, R.A. Reis, M.L.L. Paredes, J. Chem. Eng. Data 58 (2013) 2925.
- [99] D.N. Bajpai, *Advanced Physical Chemistry*, S. Chand and Company Ltd., 2nd edn., New Delhi, 1998.
- [100] D.S. Gill, K.N. Arora, J. Tiwari, J. Chem. Soc. Faraday Trans., 1, 84 (1988) 1729.
- [101] D.S. Gill, T. Kaur, H. Kaur, I.M. Joshi, J. Chem. Soc. Faraday Trans., 89 (1993) 1737.
- [102] D.S. Wankaede, N.N. Wankhede, M.K. Lande, B. R. Arbad, Ind. J. Pure Appl. Phys., 44 (2006) 909.
- [103] D.S. Wankhede, Int. J. Chem. Res., 2 (2011) 23.
- [104] D.W. Marquardt, J. Soc. Ind. Appl. Math., 11, (1963) 431.
- [105] D.W.A. Sharp, *Miall's Dictionary of Chemistry*, Essex, 5th edn., UK, Longman, 1981, pp. 121.
- [106] D.Y. Peng, D.B. Robinson, Ind. Eng. Chem. Fundum., 15 (1976) 59.
- [107] E. Aicart, G. Tardajos, M. Dlaz Peia, J. Chem. Eng. Data 26 (1981) 22.
- [108] E. Rajgopal, S.V. Subrahmanyam, Bull. Chem. Soc. Jpn., 54 (1981) 282.
- [109] E. Vercher, F.J. Llopis, M.V. Gonza'lez-Alfaro, A. Mart'inez-Andreu, J. Chem. Eng. Data 55 (2010) 1377.
- [110] E. Zorebski, M. Dzida, E. Wysocka, J. Chem. Eng. Data 56 (2011) 2680.
- [111] E. Zorebski, M.G. Rybczynska, B. Maciej, J. Chem. Eng. Data 55 (2010) 1025.
- [112] E.D. Dikio1, S.M. Nelana, D.A. Isabirye, E.E. Ebenso, Int. J. Electrochem. Sci., 7 (2012) 11101.
- [113] E.L. Heric, J. G. Brewer, J. Chem. Eng. Data 12 (1967) 574.
- [114] E.R. Dobbs, L. Finegold, Ibid, 32 (1960) 1215.
- [115] E.T. Kareem, Nat. J. Chem., 39 (2010) 515.
- [116] F. Corradini, L. Marcheselli, A. Marchetti, M. Tagliazucchi, L. Tassi, G. Tosi, Bull. Chem. Soc. Jpn., 65 (1992) 503.
- [117] F. Gladstone, D. Dale, Philos. Trans. R. Soc. London, 148 (1858) 887.
- [118] F. Köhler, Monatsh. Chem. 91 (1960) 738.
- [119] F. Nabi, M.A. Malik, C.G. Jesudason, S.A. Al-Thabaiti, Korean. J. Chem. Eng. Data 31 (2014) 1505.

Bibliography

- [120] F.J. Millero, Chem. Rev., 71 (1971) 147.
- [121] F.R. Jensen, D.S. Noyce, C. H. Sederholm, A. J. Berlin, J. Am. Chem. Soc., 84 (1962) 386.
- [122] Farid I. El-Dossoki, J. Chin. Chem. Soc., 54 (2007) 1129.
- [123] G. C. Benson, O. K. Kiyohara, J. Chem. Thermodyn. 11 (1979) 1061.
- [124] G. Copetti, R. Lapasin, E. R. Morris, *Proceedings of the 4th European Rheology Conference*, Seville, Spain, 1994, pp. 215.
- [125] G. Douheret, M.I. Davis, Chem. Soc. Rev., 22 (1993) 43.
- [126] G. Nath, Chem. Sci. Trans., 1 (2012) 516.
- [127] G. Scatchard, L.B. Ticknor, J.R. Goates, E.R. McCartney, J. Am. Chem. Soc., 74 (1952) 3721.
- [128] G. Schmidt, H. Wenzel, Chem. Eng. Sci., 35 (1980) 1503.
- [129] G. Soave, Chem. Eng. Sci., 27 (1972) 1197.
- [130] G.A. Krestov, *Thermodynamics of Solvation; Solution and Dissolution, Ions and Solvents, Structure and Energetics*, Ellis Horwood, New York, 1991, pp. 151.
- [131] G.A. Shabir, T.K. Bradshaw, Turk J. Pharm. Sci., 8 (2011) 117.
- [132] G.C. Benson, C.J. Halpin, Canad. J. Chem., 65 (1987) 322.
- [133] G.C. Benson, J. Singh, J. Phys. Chem., 72 (1968) 1345.
- [134] G.C. Benson, O.K. Kiyohara, J. Chem. Thermodyn., 11 (1979) 1061.
- [135] G.J. Moody, J.D.R. Thomas, *Dipole Moments in Inorganic Chemistry*; Edward Arnold: London, 1971.
- [136] G.L. Bertrand, W.E. Acree (Jr), J. Solution Chem., 12 (1983) 755.
- [137] G.L. Bertrand, W.E. Acree (Jr), T.E. Burhfield, J. Solution Chem., 12 (1983) 327.
- [138] G.M. Smith, H.C. Van Ness, *Introduction to Chemical Engineering Thermodynamics*, McGraw Hill, New York, 1987.
- [139] G.P. Dubey, K. Kumar, J. Chem. Eng. Data 56 (2011) 2995.
- [140] G.R. Bedare1, V. D. Bhandakkar, B.M. Suryavanshi, Euro. J. Appl. Eng. Sci. Res., 1 (2012) 1.
- [141] G.V.R. Rao, A.V. Sarma, J.S.R. Krishna, C. Rambabu, Ind. J. Pure Appl. Phys., 43 (2005) 345.
- [142] G.V.R. Rao, A.V. Sharma, D. Ramachandran, C. Rambabu, Ind. J. pure Appl. Phys., 43 (2005) 602.
- [143] G.W. Toop, Trans. TMS-AIME, 233 (1965) 850.
- [144] H. Eyring, J.F. Kincaid, J. Chem. Phys., 6 (1938) 520.
- [145] H. Eyring J. Chem. Phys., 4 (1936) 283.
- [146] H. Eyring, F. Comuschi, J. Chem. Phys., 7 (1939) 547.
- [147] H. Eyring, J. F. Kincaid, J. Chem. Phys., 6 (1938) 620.
- [148] H. Eyring, J. Hirschfelder, J. Phys. Chem., 41 (1937) 249.
- [149] H. Eyring, M.S. John, *Significant Liquid Structures*, John Willey and Sons, New York, 1969.
- [150] H. Houkhani, J.B. Parsa, S. Azizian, J. Chem. Eng. Data 44 (1999) 152.
- [151] H. Iloukhani, H.A. Zarei, Phys. Chem. Liq., 46 (2008) 154.
- [152] H. Kumar, D. Kumar, Int. J. Thermodyn., 16 (2013) 123.
- [153] H. Kumar, D. Kumar, S. Yadav, J. Pure Appl. Ind. Phys., 2 (2012) 248.
- [154] H. Renon, Fluid Phase Equilib., 13 (1983) 15.
- [155] H. Vogel, A. Weiss, Phys. Chem. Chem. Phys., 86 (1982) 193.
- [156] H. Yamada, Bull. Chem. Soc. Jpn, 32 (1959) 1051.
- [157] H.A. Zarei, J. Mol. Liq., 130 (2007) 74.
- [158] I. Cibulka, Collect. Czech. Chem. Commun., 47 (1982) 1414.
- [159] I. Gascon, A.M. Mainar, F.M. Royo, J.S. Urieta, J. Chem. Eng. Data 45 (2000) 751.

Bibliography

- [160] I. Johnson, M. Kalidoss, R. Srinivasamoorthy, *J. Chem. Eng. Data* 47 (2002) 1388.
- [161] I. Prigogine, A. Bellemans, *J. Chem. Phys.*, 21 (1953) 561.
- [162] I. Prigogine, G. Garikian, *Physica*, 16 (1950) 239.
- [163] I. Prigogine, R. Defay, *Chemical Thermodynamics*, 5th ed., Longman, London, 1994, pp. 8.
- [164] I. Prigogine, V. Mathot, *J. Chem. Phys.*, 20 (1952) 49.
- [165] I. Prigogine, *Molecular Theories of Solutions*, North-Holland publishing Co., Amsterdam, 1957.
- [166] I.A. McLure, J.E. Benette, A.E. Watson, *J. Phys. Chem.*, 69 (1965) 2759.
- [167] I.R. Radovic, M. Lj. Kijevcanin, A.Ž. Tasic, B.D. Djordjevic, S.P. Šerbanovic, *J. Serb. Chem. Soc.*, 75 (2010) 283.
- [168] I.R. Radovic, M.L. Kijevcanin, A.Z. Tasic, B.D. Djordjevic, S.P. Serbanovic, *J. Serb. Chem. Soc.*, 74 (2009) 1303.
- [169] *Intermolecular force*, Rory Adams Free High School Science Text Project Heather Williams, Version 1.2, July 7, 2001.
- [170] J. Asghar1, F.L.A. Khan, K. Subramani, *Rasay. J. Chem.*, 3 (2010), 697.
- [171] J. Burgess, *Metal Ions in Solutions*, Ellis Horwood, New York, 1978.
- [172] J. Canosa, A. Rodriguez, J. Tojo, *J. Chem. Eng. Data* 43 (1998) 961.
- [173] J. George, N.V. Sastry, *J. Chem. Eng. Data* 49 (2004) 1116.
- [174] J. Israelachvili, *Intermolecular and surface Force*, Academic Press, London, 1992.
- [175] J. Krautkramer, H. Krautkramer, *Ultrasonic Testing of Materials*, Springer Verlag, New York, 1969.
- [176] J. Nath, A.P. Dixit, *J. Chem. Eng. Data* 29 (1984) 320.
- [177] J. Nath, G. Singh, *J. Chem. Eng. Data* 33 (1988) 58.
- [178] J. Nath, *J. Chem. Thermodyn.*, 34 (2002) 1857.
- [179] J. Nath, M. Tewari, *J. Chem. Soc. Faraday Trans.*, 88 (1992) 2197.
- [180] J. Nath, S.N. Dubey, *J. Phys. Chem.*, 84 (1980) 2166.
- [181] J. Pellicer, *Sinergia Viscosa*, Valencia, Spain, October, 1997.
- [182] J. Singh, H.D. Pflug, G.C. Benson, *J. Phys. Chem.*, 72 (1968) 1939.
- [183] J.A. Acosta, E. Rodil, A. Soto, *J. Chem. Eng. Data* 46 (2001) 1176.
- [184] J.A. Al-Kandary, A.S. Al-Jimaz, A. Haq, A. Latif, *J. Chem. Eng. Data* 51 (2006) 2074.
- [185] J.A. Al-Kandary, A.S. Al-Jimaz, A.M. Abdul-Latif, *Phys. Chem. Liq.*, 47 (2009) 210.
- [186] J.A. Dean, *Lange's Handbook of Chemistry*, 11th ed., McGraw Hill, New York, 1973.
- [187] J.A. Pal, S. Sharma, G. Dass, *J. Chem. Thermodyn.*, 31 (1999) 273.
- [188] J.A. Riddick, W.B. Bunger, T.K. Sakano, *Organic solvents. Techniques of Chemistry*, Vol. 2, 4th edn., Wiley Interscience, New York, 1986.
- [189] J.A. Riddick, W.B. Bunger, T.K. Sakano, *Organic Solvents, Physical Properties and Methods of Purification, Techniques of Chemistry*, vol. 2, 4th edn., Wiley-Interscience, New York, 1986.
- [190] J.B. Irving, *The Effectiveness of Mixture Equations*, NEL Report No31, National Eng. Lab., East Kilbride, Glasgow, 1977.
- [191] J.B. Irving, *Viscosity of Binary Liquid Mixtures, A Survey of Mixture Equations*, NEL Report No. 630, National Eng. Lab., East Kilbride, Glasgow, 1977.
- [192] J.D. Panday, A.D.M. David, *Chemica Scr.*, 19 (1982) 39.
- [193] J.D. Panday, *Electrochimica Acta*, 27 (1982) 1097.
- [194] J.D. Panday, N. Pant, *J. Am. Chem. Soc.*, 104 (1982) 3299.
- [195] J.D. Panday, R.K. Upadhyay, U. Gupta, *Acoustics Letters*, 5 (1982) 120.
- [196] J.D. Panday, R.P. Panday, *Phys. Chem. Letters* 14 (1985) 253.
- [197] J.D. Panday, U. Gupta, *Electrochimica Acta*, 28 (1983) 1047.
- [198] J.D. Panday, U. Gupta, *J. Phys. Chem.*, 86 (1982) 5234.

Bibliography

- [199] J.D. Panday, V. Sanguri, M.K. Yadav, A. Singh, *Ind. J. chem.*, 47 (2008) 1020.
- [200] J.D. Panday, V.N.P. Srivastava, V. Vyas, N. Pant, *Ind. J. Pure and Appl. Phys.*, 25 (1987) 467.
- [201] J.D. Pandey, *J. Chem. Soc., Faraday Trans I*, 75 (1979) 2160.
- [202] J.D. Pandey, N. Pant, N. Agarwal, Shikha. *Acustica*, 68 (1969) 225.
- [203] J.D. Pandey, V. Vyas, G.P. Dubey, N. Tripathi, R. Dey, *J. Mol. Liq.*, 81 (1999) 123.
- [204] J.D. Van der Waals, *Essay on the continuity of the gaseous and liquid States*, London, 1873.
- [205] J.D. van der Waals, *On the Continuity of the Gaseous and Liquid States*. Ph. D. Dissertation, University Leiden, Leiden, Netherland, 1873.
- [206] J.E. Gordon, *The Organic Chemistry of Electrolyte Solutions*, Wiley-Interscience, 1975.
- [207] J.F. Coetzee, T.-H. Chang, *Pure. Appl. Chem.*, 57 (1985) 633.
- [208] J.F. Eykman, A.F. Holleman, *Research Refractometers*, De Erven Loosjes, 1919.
- [209] J.G. Harris, F.H. Stillinger, *J. Chem. Phys.*, 95 (1991) 5953.
- [210] J.H. Dymond, *Chem. Soc. Rev.*, 14 (1985) 417.
- [211] J.J. McKetta, W.A. Cunningham, *Encyclopedia of Chemical Processing and Design*, Vol-36, Marcel Dekker, New York, 1991, pp. 99.
- [212] J.K. Gladden, *J. Chem. Eng. Data* 17 (1972) 468.
- [213] J.M. Resa, J.M. Goenaga, A.I. Sanchez-Ruiz, *J. Chem. Eng. Data* 51 (2006) 1294.
- [214] J.O. Hirschfelder, C.F. Curtis, R.B. Bird, *Molecular Theory of Gases and Liquids*, Wiley, New York, corrected printing, 1964, Chap. 5, 11.
- [215] J.P. O'Connell, J.M. Haile, *Thermodynamics: Fundamentals for Applications*, Cambridge University Press, New York, 2005.
- [216] J.R. Partington, *An Advanced Treatise on Physical Chemistry*, Longmans & Green, London, 1953, Vol.4, Sec X.
- [217] J.S. Rowlinson, F.L. Swinton, *Liquid and Liquid Mixtures*, Butterworths, London, 3rd edn., 1982, pp. 16,17.
- [218] J.V. Herraез, R. Belda, *J. Solution Chem.*, 33 (2004) 217.
- [219] J.W. Leland, P.S. Chappellear, *Ind. Eng. Chem.*, 60 (1968) 15.
- [220] J.W. McCargar, W.E. Acree, *Thermochemica. Acta.*, 149 (1989) 363.
- [221] K. Ibuki, M. Nakahara *J. Phys. Chem.*, 94 (1990) 8370.
- [222] K. Rajathi, S.J.A. Ali, A. Rajendra, *J. Chem. Pharma. Res.*, 3 (2011) 348.
- [223] K. Rettinger, C. Burschka, P. Scheeben, H. Fuchs, A. Mosandl, *Tetrahedron Asymmetry*, 2 (1991) 965.
- [224] K. Saravanakumar, R. Basharan, T.R. Kubendra, *E-J. Chem.*, 9 (2012) 1711.
- [225] K. Saravanakumar, T.G. Lavanya, T.R. Kubendran, *Chem. Sci. Trans.*, 1 (2012) 269.
- [226] K. Sreekanth, D.S. Kumar, M. Kondaiah, D.K. Rao, *J. Phys. B.*, 406 (2011) 854.
- [227] K. Tamura, S. Murakami, S. Doi, S. Takagi, *J. Chem. Thermodyn.*, 18 (1986) 489.
- [228] K. Vasudha, D. Vijaya Kumari, G. Yuvaraja, A. Krishnaiah, *J. Chem. Pharm. Res.*, 3 (2011) 108.
- [229] K.B. Wiberg, T.A. Keith, M.J. Frisch, M. Murcko, *J. Phys. Chem.*, 99 (1995) 9072.
- [230] K.C. Kalra, K.C. Singh, D.C. Spah, *J. Chem. Thermodyn.*, 21 (1989) 1243.
- [231] K.F. Hertzfeld, T.A. Litovitz, *Absorption and Dispersion of Ultrasonic Waves*, Academic Press, New York, 1959.
- [232] K.M. Kadish, J.E. Anderson, *Pure. Appl. Chem.*, 59 (1987) 703.
- [233] K.M. Marstokk, H. Mollendal, *J. Mol. Struc.*, 49 (1978) 221.
- [234] K.N. Marsh, *Recommended Reference Materials for the Realisation of Physicochemical Properties*, Blackwell Scientific Publications, Oxford, U. K., 1987.
- [235] K.N. Marsh, *TRC Data Bases for Chemistry and Engineering-TRC Thermodynamic Tables*, Texas A & M University System, College Station, TX, 1994.

Bibliography

- [236] K.P. Rao, K.S. Reddy, *J. Chem. Eng. Data* 33 (1988) 130.
- [237] K.R. Harris, P.J. Dunlop, *J. Chem. Thermodyn.*, 2 (1970) 813.
- [238] K.S. Pitzer, J.C. Peiper, R.H. Busey, *J. Phys. Chem. Ref. Data*, 13 (1984) 1.
- [239] K.T. Jacob, K. Fitzner, *Thermochim. Acta* 18 (1977) 197.
- [240] L. Asselineau, G. Bogdanic, J. Vidal, *Chem. Eng. Sci.*, 33 (1978) 1269.
- [241] L. Grunberg, A.H. Nissan, *Nature*, 164 (1949) 799.
- [242] L. Lorenz, *Weid. Ann.*, 11 (1880) 70.
- [243] L. Sarkar, M.N. Roy, *J. Chem. Eng. Data* 54 (2009) 3307.
- [244] L. Venkatramana, R.L. Gardas, K.S. Kumar, *Fluid. Phase. Equilib.*, 367 (2014) 7.
- [245] L.M. Harwood, C.J. Moody, *Experimental organic chemistry: Principles and Practice*, (Illustrated edn.), Wiley-Blackwell, 1989, pp. 292.
- [246] M. Aravinthraj, C. Venkatesan, D. Meera, *J. Chem. Pharm. Res.*, 3 (2009) 623.
- [247] M. Aravinthraj, S. Venkatesan, M. Kamaraj, *Int. J. Chem. Enviro. Pharm. Res.*, 2 (2011) 5.
- [248] M. Born, E. Wolf, *Principles of Optics: Electromagnetic Theory of Propagation, Interference and Diffraction of Light*, 7th edn., Cambridge University Press, London, 1999.
- [249] M. Das, M.N. Roy, *J. Chem. Eng. Data* 51 (2006) 2225.
- [250] M. Deetlefs, K. Seddon, M. Shara, *Phys. Chem. Chem. Phys.*, 8 (2006) 642.
- [251] M. Fermeglia, G. Torriano, *J. Chem. Eng. Data* 44 (1999) 965.
- [252] M. Gowrisankar, P. Venkateswarlu, K. Sivakumar, S. Sivarambabu, *J. Sol. Chem.*, 42 (2013) 916.
- [253] M. Gupta and I. Vibhu, J.P. Shukla, *J. Phys. Chem. Liq.*, 41 (2003) 575.
- [254] M. H. Cohen, D. Turnbull, *J. Chem. Phys.*, 31 (1959) 1164.
- [255] M. Hillert, *Ber. Bunsenges. Phys. Chem.*, 87 (1983) 762.
- [256] M. Indhumathi, G. Meenakshi, *Mid. East. J. Sci. Res.*, 20 (2014) 546.
- [257] M. Kalidoss, R. Srinivasamoorthy, *J. Pure. Appl. Ultrason.*, 19 (1997) 9.
- [258] M. Karvo, *J. Chem. Thermodyn.*, 15 (1986) 809.
- [259] M. Kondaiah, D. K. Rao, *Int. J. Res. Pure. Appl. Phys.*, 3 (2013) 43.
- [260] M. Mayer, R. Mayer, *J. Chem. Phys.*, 63 (1971) 143.
- [261] M. Meyappan, Sethupathy, *J. Pure Appl. Ultrason.*, 25 (2003) 1.
- [262] M. Palaiologou, G.K. Arianas, N.G. Tsierkezo, *J. Sol. Chem.*, 35 (2006) 1551.
- [263] M. Rastogi, A. Awasthi, M. Gupta, J.P. Shukla, *Ind. J. Pure Appl. Phys.*, 40 (2002) 256.
- [264] M. Shafiq, S. Asif, M. Farooqui, *Asian J. Biochem. Pharm. Res.*, 1 (2011) 419.
- [265] M. Shafique, S. Hussain, S. Asif, V. Pradhan, M. Farooqui, *Res. J. Chem. Sci.*, 3 (2013) 98.
- [266] M. Tamura, M. Kurata, *Bull. Chem. Soc. Jpn.*, 25 (1952) 32.
- [267] M. Tjahjono, L. Guo, M. Garland, *Chem. Eng. Sci.*, 60 (2005) 3239.
- [268] M. Tjahjono, M. Garland, *J. Solution Chem.*, 36 (2007) 221.
- [269] M. Yasmin, M. Gupta, *J. Solution Chem.*, 40 (2011) 1458.
- [270] M.A. Hernandez-Galvan, F. Garcia-Sanchez, R. Macias-Salinas, *Fluid. Phase. Equilib.* 262 (2007) 51.
- [271] M.A. Iglesias-Otero, J. Troncoso, E. Carballo, L. Romani, *J. Chem. Thermodyn.*, 40 (2008) 949.
- [272] M.A. Saleh, M.S. Ahmed, M.S. Islam, *Phys. Chem. Liq.*, 40 (2002) 477.
- [273] M.A. Saleh, S. Akhtar, M. S. Ahmed, *Phys. Chem. Liq.*, 44 (2006) 551.
- [274] M.A. Tejjraj, H.T.S. Phayde, R.S. Khinnavar, G.K. Bindu, *J. Chem. Eng. Data* 39 (1994) 251.
- [275] M.H. Cohen, D. Turnbull, *J. Chem. Phys.*, 31 (1959) 1164.
- [276] M.I. Aralaguppi, C.V. Jadar, T.M. Aminabhavi, *J. Chem. Eng. Data* 44 (1999) 441.

Bibliography

- [277] M.I. Aralaguppi, C.V. Jadar, T.M. Aminabhavi, J. Chem. Eng. Data 44 (1999) 446.
- [278] M.I. Aralaguppi, T. M. Aminabhavi, R. H. Balundgi, S. S. Joshi, J. Phys. Chem., 95 (1991) 299.
- [279] M.I. Aralaguppi, T.M. Aminabhavi, S.B. Harogoppad, R.H. Balundgi, J. Chem. Eng. Data 37 (1992) 298.
- [280] M.I. Aralaguppi, C.V. Jadar, T. M. Aminabhavi, J.D. Ortego, S.C. Mehrotra, J. Chem. Eng. Data 42 (1977) 301.
- [281] M.I. Davis, Chem. Soc. Rev., 22 (1993) 127.
- [282] M.J. Blandamer, Chem. Soc. Rev., 27 (1998) 73.
- [283] M.J. Blandamer, *Introduction to Chemical Ultrasonics*, Academic Press, London, 1973.
- [284] M.J. Huron, D.N. Dufour, J. Vidal, Fluid Phase Equilib., 1 (1978) 247.
- [285] M.L. Haber, R.A. Perkins, Fluid Phase Equilib., 227 (2005) 44.
- [286] M.L. Williams, R.F. Landel, J.D. Ferry, J. Am. Chem. Soc., 77 (1955) 3701.
- [287] M.M. Cox, *Molecular Biology*, Palgrave Macmillan, 18 November, 2011, pp. 73.
- [288] M.M. Hossain Bhuiyan and Kaxuhiro Tamura, J. Chem. Thermodyn., 36 (2004) 549.
- [289] M.N. Roy, B.K. Sarkar, B. Sinha, J. Chem. Eng. Data 54 (2009) 1076.
- [290] M.N. Roy, R. Dey, A. Jha, J. Chem. Eng. Data 46 (2001) 1327.
- [291] M.R.V. Krishnan, G.S. Laddha, Ind. Eng. Chem. Fundam., 7 (1968) 324.
- [292] M.S. Dhillon, H.S. Chugh, J. Chem. Eng. Data 22 (1977) 262.
- [293] M.S. Graboski, T.E. Daubert, Ind. Eng. Chem. Process. Des. Dev., 17 (1978) 443.
- [294] M.T. Musser "Cyclohexanol and Cyclohexanone" in *Ullmann's Encyclopedia of Industrial Chemistry*, Wiley-VCH, Weinheim, 2005.
- [295] M.V. Garcia, M.I. Redondo, J. Chem. Edu., 62 (1985) 887.
- [296] M.V. Rathnam, Proc. Indian. Natn. Sci. Acad., 53A (1987) 588.
- [297] M.V. Rathnam, S. Mohite, M.S. Kumar, J. Serb. Chem. Soc., 76 (2011) 1.
- [298] M.V. Rathnam, S. Mohite, M.S. Kumar, J. Serb. Chem. Soc., 77 (2012) 507.
- [299] N. Auerbach, Experientia, 4 (1948) 473.
- [300] N. Mohanty, R. Paikaray, Res. J. Chem. Sci., 3 (2013) 71.
- [301] N.I. Malek, S.P. Ijardar, S.B. Oswal, Thermochemica Acta, 539 (2012) 71.
- [302] N.N. Wankhede, M.K. Lande, B.R. Arbad. J. Chem. Eng. Data 50 (2005) 969.
- [303] N.V. Sastry, M.C. Patel, J. Chem. Eng. Data 48 (2003) 1019.
- [304] N.V. Sastry, N.M. Vaghela, P.M. Mac, J. Mol. Liq., 180 (2013) 12.
- [305] O. Ciocirlan, O. Iulian, J. Serb. Chem. Soc., 74 (2009) 317.
- [306] O. Nomoto, J. Phys. Soc. Jpn., 13 (1958) 1528.
- [307] O. Popvyich, R.P.T. Tomkins, *Nonaqueous Solution Chemistry*, Wiley-Interscience, New York, (198), Ch 4.
- [308] O. Redlich, A.T. Kister, Indus. Eng. Chem., 40 (1948) 345.
- [309] O. Redlich, J.N.S. Kwong, Chem. Rev., 44 (1949) 233.
- [310] O. Weiner, Berichte (Leipzig), 62 (1910). 256.
- [311] O.K. Patrick, P.J.D. Arcy, G.C. Benson, Canad. J. Chem., 57 (1978) 1006.
- [312] Oscillating U-tube. Electronic document, [http://en.m.wikipedia.org/wiki/Oscillating U-tube](http://en.m.wikipedia.org/wiki/Oscillating_U-tube), accessed on Oct 12, 2013.
- [313] P. Atkins, J. de Paula, *Elements of Physical Chemistry*, Fifth Edition, W. H. Freeman and Company, New York, 2009, pp. 351.
- [314] P. Brocos, A. Pineiro, R. Bravo, A. Amigo, Phys. Chem. Chem. Phys., 5 (2003) 550.
- [315] P. Brocos, E. Calvo, A. Pineiro, R. Bravo, A. Amigo, J. Chem. Eng. Data 44 (1999) 1341.
- [316] P. Brocos, E. Calvo, R. Bravo, M. Pintos, A. Amigo, J. Chem. Eng. Data 44 (1999) 67.
- [317] P. Griffiths, J.A. de Haseth, *Fourier Transform Infrared Spectrometry*, 2nd edn., Wiley-Blackwell, 18 May, 2007.

Bibliography

- [318] P. Muller, *Pure Appl. Chem.*, 66 (1994) 1077.
- [319] P. Pacak, *J. Solution Chem.*, 16 (1987) 71.
- [320] P. Tancrede, P. Bothorel, P. St. Romain, D. Patterson. *J. Chem. Soc. Faraday Trans., II* 73 (1977) 15.
- [321] P. Vigoureux, *Ultrasonics. Chapman and Hall Ltd.*, London, 1952.
- [322] P.D. Vaz, P.J.A.R.-. Claro, *J. Raman. Spectros.*, 34 (2003) 863.
- [323] P.J. Flory *J. Am. Chem. Soc.*, 87(1965) 1833.
- [324] P.J. Flory, A. Abe, *J. Am. Chem. Soc.*, 87 (1965) 1838.
- [325] P.J. Flory, A. Vrij, R.A. Orwall, *J. Am Chem. Soc.*, 86 (1964) 3507.
- [326] P.J. Flory, *Discuss Faraday Soc.*, 49 (1970) 7.
- [327] P.J. Flory, R.A. Orwall, A. Vrij, *J. Am. Chem. Soc.*, 86 (1964) 3515.
- [328] P.K. Katti, M. M. Choudhri, *J. Chem. Eng. Data* 9 (1964) 442.
- [329] P.N. Tshibangu, S.N. Ndwandwe, E.D. Dikio, *Int. J. Electrochem. Sci.*, 6 (2011) 2201.
- [330] P.P. Singh, R.K. Nigam, K.C. Singh, V.K. Sharma, *Thermochim. Acta*, 46 (1981) 175.
- [331] P.S Naidu, K.R. Prasad, *J. Pure Appl. Ultrason.*, 24 (2002) 1824.
- [332] P.S. Nikam, S.J. Kharat, *J. Chem. Eng. Data* 50 (2005) 455.
- [333] P.W. Atkins, *Physical Chemistry*, 6th edn., Oxford University Press, Oxford, Ch. 22, 1998.
- [334] P.W. Atkins, *Physical Chemistry*, 6th edn., Oxford University Press, Oxford, 1993, pp. 763.
- [335] Q. Li, F. Sha, G. Zhao, M. Yang, L. Zhao, Q. Zhang, J. Zhang, *J. Chem. Eng. Data* 61 (2016) 1718.
- [336] R. Azevedo, J. Szydowski, *J. Chem. Thermodyn.*, 36 (2004) 211.
- [337] R. Battino, *Chem. Reviews*, 71 (1971) 5.
- [338] R. Abraham, M. Abdulkhadar, C.V. Asokan, *J. Chem. Thermodyn.*, 32 (2000) 1.
- [339] R. Chanda, A. Banerjee, M.N. Roy, *J. Serb. Chem. Soc.*, 75 (2010) 1721.
- [340] R. Dean, J. Moulins, A. MacInnis, R.M. Palepu, *Phys. Chem. Liq.*, 47 (2009) 302.
- [341] R. Dey, A. Harshavardhan, *J. Ener. Chem. Eng.*, 2 (2014) 1.
- [342] R. Dey, A. Harshavardhan, S. Verma, *J. Mol. Liq.*, 211 (2015) 686.
- [343] R. Gopal, S. Agarwal, D.K. Agarwal, *J. Chem. Thermodyn.*, 8 (1976) 1205.
- [344] R. Hammker, R. Clegg, P. Paderson, P. Ridder, S. Rock, *J. Phys. Chem.*, 72 (1968) 1837.
- [345] R. Macias-Salinas, F. Garcia-Sanchez, G. Eliosa-Jimencz. *Fluid Phase Equilib.*, 210 (2003) 319.
- [346] R. Mehra, A. Gupta, R. Israni, *Ind. J. Chem.*, 40 (2001) 505.
- [347] R. Mehra, R. Israni, *Ind. J. Pure Appl. Phys.*, 38 (2000) 81.
- [348] R. Meyer, M. Meyer, J. Metzger, A. Peneloux, *J. Chim. Phys.*, 62 (1971) 405.
- [349] R. Palepu, B. Hawrylak, K. Gracia, *Canad. J. Chem.*, 76 (1998) 464.
- [350] R. Pradhan, A. Kamath, D. Brahman, B. Sinha, *Fluid Phase Equilib.*, 404 (2015) 131.
- [351] R. Pradhan, B. Sinha, *J. Serb. Chem. Soc.*, 82 (2017) 189.
- [352] R. Thiagarajan, L. Palaniappan. *Ind. J. Pure. Appl. Phys.*, 46 (2008) 852.
- [353] R. Truell, C. Elbaum, B.B. Chick, *Ultrasonic Methods in Solid State Physics*, Academic Press, New York, 1969.
- [354] R. Venis, R. Rajkumar, *J. Chem. Pharm. Res.*, 3 (2011) 878.
- [355] R.A. McAllister, *AIChE J.*, 6 (1960) 427.
- [356] R.A. Orwall, P.J. Flory, *J. Am. Chem. Soc.*, 86 (1964) 3515.
- [357] R.A. Orwall, P.J. Flory, *J. Am. Chem. Soc.*, 89 (1967) 6814.
- [358] R.A. Patil, P.B. Dabrase, B.M. Suryavanshi, *J. Chem. Pharm. Res.*, 5 (2013) 745.
- [359] R.C.L. Bosworth, *Trans Faraday Soc.*, 43 (1947) 308.

Bibliography

- [360] R.D. McCarty, *Fluid Phase Equilib.*, 256 (2007) 42.
- [361] R.D. Singh, M. Gupta, *Int. J. Inno. Res. Adv. Stud.*, 3 (2016) 407.
- [362] R.G. Pearson, *Hard and Soft Acids and Bases*, Dowden, Hutchinson and Ross, Stroudsburg, 1973.
- [363] R.J. Fort, W.R. Moore, *Trans Faraday Soc.*, 61 (1965) 2102.
- [364] R.J. Hunter, *Fundation of colloidal science*, 2nd edn., Oxford University Press, Oxford, 2004, pp. 533.
- [365] R.K. Nigam, P.P. Singh, *Trans. Faraday Soc.*, 65 (1969) 950.
- [366] R.K. Biswas, R.A. Banu, M.N. Islam, *Hydrometallurgy*, 69 (2003) 157.
- [367] R.K. Dewan, C.M. Gupta, S.K. Mehta, *Acustics*, 66 (1988) 245.
- [368] R.K. Hind, E. McLaughlin, A.R. Ubbelohde, *Trans. Faraday. Soc.*, 56 (1960) 328.
- [369] R.K. Sreeruttun, R. Ramasami, *Phys. Chem. Liq.*, 44 (2006) 315.
- [370] R.M. Pires, H.F. Costa, A.G.M. Ferreira, I.M.A. Fonseca, *J. Chem. Eng. Data* 52 (2007) 1240.
- [371] R.M. Pires, H.F. Costa, A.G.M. Ferreira, *J. Chem. Eng. Data* 52 (2007) 1240.
- [372] R.P. Rastogi, J. Nath, S.S. Das, *J. Eng. Chem. Data* 22 (1977) 249.
- [373] R.P. Rastogi, R.R. Misra, *An Introduction to Chemical Thermodynamics*, Vikash Publishing House, New Delhi, 1978.
- [374] R.T. Beyer, S.V. Letcher, *Physical Ultrasonics*, Academic Press, New York, 1969.
- [375] R.W. Kershaw, G.N. Makcolm, *Trans. Faraday Soc.*, 64 (1968) 323.
- [376] R.W. Missen, *Ind. Eng. Chem. Fundam.*, 8 (1969) 81.
- [377] S. Akhtar, A.N.Q. Faruk, M.A. Saleh, *Phys. Chem. Liq.*, 39 (2001) 383.
- [378] S. Aparicio, R. Alcalde, *Eur. J. Chem.*, 1 (2010) 162.
- [379] S. Azhagiri, S. Jayakumar, R. Padmanaban, S. Gunasekaran, S. Srinivasan, *J. Sol. Chem.*, 38 (2009) 441.
- [380] S. Balakrisnan, R. Palani, *J. Pure App. Indust. Phys.*, 5 (2015) 25.
- [381] S. Bhatiya, J. Sagnwan, R. Bhatiya, *J. Mol. Liq.*, 161 (2011) 96.
- [382] S. Glasstone, K.J. Laidler, H. Eyring, *The theory of Rate Preocess*, McGraw-Hill Book Company, Inc., New York, 1941.
- [383] S. Glasstone, *Textbook of Physical Chemistry*, 2nd ed.; D. Van Nostrand Co., London, 1949.
- [384] S. Glasstone, *Thermodynamic for Chemist*, D. Van Nostrand Co., Inc., New York, 62 1947.
- [385] S. Ismadji, *J. Chem. Eng. Data* 53 (2008) 2207.
- [386] S. Kumar, A. Maken, S. Agarwal and S. Maken, *J. Mol. Liq.*, 155 (2010) 115.
- [387] S. Kumar, W. Lim, Y. Lee, J.S. Yadav, D. Sharma, V.K. Sharma, Il Moon, *J. Mol. Liq.*, 155 (2010) 8.
- [388] S. Nallani, S. Boodida, S.J. Tangeda, *J. Chem. Eng. Data* 52 (2007) 405.
- [389] S. Ranjbar, K. Fakhri, B. Jahan, J. Ghasemi, *J. Chem. Eng. Data* 54 (2009) 3284.
- [390] S. Sharma, J. Bhalodia, J. Ramani, R. Patel, *Int. J. Phys. Sci.*, 7 (2012) 1205.
- [391] S. Singh, S. Parveen, D. Shukla, M. Gupta and J.P. Shukla, *Acta Physi. Polo. A*, 111 (2007) 847.
- [392] S. Yamagishi, Y. Takahshi, K. Shiba, *J. Phys. E: Sci. Instrum.*, 17 (1984) 359.
- [393] S.C. Bhatia, J. Sangwan, R. Rani, V. Kiran, *Int. J. Thermophys.*, 34 (2013) 2076.
- [394] S.C. Bhatia, R. Bhatia ·G.P. Dubey, *Int. J. Thermophys.*, 31(2010) 2119.
- [395] S.C. Bhatia, R. Bhatia, G.P. Dubey, *J. Mol. Liq.*, 144 (2009) 163.
- [396] S.E. Burke, B. Hawryla, R. Palepu, *Thermochim. Acta* 345 (2002) 101.
- [397] S.H. Canzonieri, M.A. Postigo, J.A. Salas, M. Katz, *J. Argen. Chem. Soc.*, 1 (2002) 31.
- [398] S.I Sandler, *Chemical, Biochemical, and Engineering Thermodynamics*, 4th edn., John Wiley India (P) Ltd., 2007, New Delhi, pp. 242, 258, 371, 423.

Bibliography

- [399] S.I. Oswal, N.B. Patel, J. Chem. Eng. Data 40 (1995) 845.
- [400] S.K. Jangra, N. Saini, J.S. Yadav, R.K. Siwach, D. Sharma and V.K. Sharma, J. Mol. Liq., 158 (2011) 192.
- [401] S.K. Mehta, A.K. Sharma, K.K. Bhasin, Fluid Phase Equilib., 201 (2002) 203.
- [402] S.L. Oswal, A.V. Rao, Ind. J. Chem. Sec. A, 24 (1985) 545.
- [403] S.L. Oswal, H.S. Desai, Fluid Phase Equilib., 186 (2001) 81.
- [404] S.M. Bardavid, G.C. Pedrosa, M. Katz, M.A. Postigo, P. Garcia, J. Solution Chem., 25 (1996) 1125.
- [405] S.M. Contreras, J. Chem. Eng. Data 46 (2001) 1149.
- [406] S.S. Kurtz, A.L. Ward, J. Franklin Inst., 222 (1936) 563.
- [407] S.S. Nandre, U.G. Deshpande, S.R. Patil, J. Chem. Pharm. Res., 7 (2015) 328.
- [408] S.S. Patil, S.R. Mirgane, B.R. Arbad, Adv. Appl. Sci. Res., 3 (2012) 2378.
- [409] T. M. Reed, T. E. Taylor, J. Phys. Chem., 63 (1959) 58.
- [410] T.B. Hoover, J. Phys. Chem., 73 (2002) 57.
- [411] T.H. Van, D. Patterson, J. Solution Chem., 11 (1982) 793.
- [412] T.J. Aminabhavi, V.B. Patil, J. Chem. Eng. Data 43 (1998) 497.
- [413] T.M. Aminabhavi, H.T.S. Phayde, J. Chem. Eng. Data 41(1996) 813.
- [414] T.M. Aminabhavi, H.T.S. Phayde, R.S. Khinnavar, B. Gopalakrishna, K.C. Hansen, J. Chem. Eng. Data 39 (1994) 251.
- [415] T.M. Aminabhavi, K. Banerjee and R.H. Balundgi, Ind. J. Chem., 38 (1999) 768.
- [416] T.M. Aminabhavi, V.B. Patil, M.I. Aralaguppi, H.T.S. Phayde, J. Chem. Eng. Data 41 (1996) 521.
- [417] T.M. Reid, T.E. Taylor, J. Phys. Chem., 63 (1949) 58.
- [418] T.S. Banipal, A.P. Toor, V.K. Rattan, Ind. J. Chem., 39 (2000) 809.
- [419] T.W. Richards, Chem. Rev., 2 (1925) 315.
- [420] U. Mayer, V. Gutmann, Adv. Inorg. Chem. Radiochem, 17 (1975) 189.
- [421] U.B. Tumberphale, R.S. Kawale, N.P. Pawar, V.G. Kalamse, Int. J. Phys. Math. Sci., 5 (2015) 25.
- [422] U.R. Kapadi, D.G. Hundiwale, N.B. Patil, M.K. Lande, Fluid Phase Equilib., 201 (2002) 335.
- [423] V. Chakravorty, B.K. Rout, Ind. J. Chem., 33 (1994) 303.
- [424] V. Gutmann, Electrochim. Acta, 21 (1967) 661.
- [425] V. Kannapan, R.J. Santhi, Ind. J. Pure and Appl. Phys., 43 (2005) 750.
- [426] V. Rajendran, Ind. J. Pure Appl. Phys., 34 (1996) 152.
- [427] V. Vanathi, S. Mullainathan, S. Nithiyantham, Rus. J. Phys. Chem. A, 86 (2012) 1204.
- [428] V. Vyas, T. Nautiyal, Pramana-J. Phys., 59 (2002) 663.
- [429] V.A. Bloomfield and R.K. Dewan, J. Phys. Chem., 75 (1971) 3113.
- [430] V.A. Tavhane, B.A. Pataki, Ind. J. Pure Appl. Phys., 22 (1984) 447.
- [431] V.D. Bhandakkar, S. Rode, S. Jajodia, Arch. Appl. Sci. Res., 5 (2013) 12.
- [432] V.D. Spassjevic, B.D. Bjordjevic, S.P. Serbanovic, I.R. Radovic, M.Lj. Kijevcanin, J. Chem. Eng. Data 59 (2014) 1817.
- [433] V.F. Nozdrev, *The Use of Ultrasonics in Molecular Physics*, Pergamon, London, 1965.
- [434] V.K. Dakua, B. Sinha, M.N. Roy, Ind. J. Chem., 45 (2006) 1381.
- [435] V.K. Sharma, R. Dua, D. Sharma, J. Chem. Thermodyn., 78 (2014) 241.
- [436] V.M. Lobe, M.Sc. Thesis University of Rochester, New York, 1973.
- [437] W. Kauzman, H. Eyring, J. Am. Chem. Soc., 62 (1940) 3113.
- [438] W. Haijum, Z. Guokang, C. Mingzhi, J. Chem Thermodyn., 25 (1993) 949.
- [439] W. Heller, Phys. Rev., 68 (1945) 5.
- [440] W. Schaaffs, Acoustica, 33 (1975) 272.

Bibliography

- [441] W. Schaaffs, *Molekularakustic*, Springer Verlag, Berlin, (1963) Chap. 11,12.
- [442] W. Van Dael, E. Vangael, in abst. paper: *Proc. 1st International Conference on Calorimetry and thermodynamics*, Warsaw Poland, 1969, pp. 555.
- [443] W.A. Duncan, J.P. Sheridan and F.L. Swinton, *Trans. Faraday Soc.*, 62 (1966) 1090.
- [444] W.E. Streeti, L.A.K. Stavely, *J. Chem. Phys.*, 47 (1967) 2449.
- [445] W.E. Acree, *J. Chem. Eng. Data* 28 (1983) 215.
- [446] W.J. Moore, *Physical Chemistry*, 2nd edn., Prentice-Hall, New Jersey, 1972.
- [447] W.M. Haynes, D.R. Lide, T.J. Bruno, *CRC Handbook of Chemistry & Physics*, 93rd edn., Taylor & Fransis, Boca Roton, London, 2012-2013.
- [448] W.T. Keeton, J.L. Gould, *Biological Science*, 5th edn., W. W. Norton & Co, New York, 1993.
- [449] X. Esteve, K.R. Patil, J. Fernandez, A. Coronas, *J. Chem. Thermodyn.*, 27 (1995) 281.
- [450] Y. Mahan, C.N. Liew, A.E. Mather, *J. Solution Chem.*, 31 (2002) 743.
- [451] Y. Marcus, *Solvent Mixtures: Properties and Selective Solvation*, Marcel Dekker, Inc., New York, Basel, 2002.
- [452] Y. Zhao, J. Wang, X. Xuan, J. Lu, *J. Chem. Eng. Data* 45 (2000) 440.
- [453] Y.L. Hunter, H.D. Dardy, *J. Acoust. Soc. Amer.*, 36 (1964) 1914.
- [454] Z. Junjie, *J. China Univ. Sci. Tech.*, 14 (1984) 298.

===

INDEX

	Page No.
A	
Abbe refractometer	88,89
Absolute viscosity	86
Acentric factor	53,54
Acoustic impedance	47,69
Anton Paar densitometer	84,98
Available volume	69,70
B	
Binary interaction parameter	60,142,175,209,238
Binary mixture	83,95
Bloomfield-Dewan viscosity model	60,143,176,209,238
C	
Cannon type Ubbelohde viscometer	86,87,99,124,161,191,222
Characteristic pressure	56,58,108,168,200,231
Characteristic temperature	56,108,168,231
Characteristic Volume	56,,108,110,168,231
Cibulka polynomial equation	65,259,301
Colinet model	66
Compressibility factor	54,137,170,202,232
Correlative model	52,62,64
Corresponding state	52,57
Critical pressure	54,136,170,202
Critical temperature	70,136,170,202
Cubic equation of state	59,135,141,174
Cyclohexane	82,83,158,189
Cyclohexanone	82,83,221,222

D	
Density	84
1,2-dichloroethane	82,83,123,159
Differential solvation	4
Dimethylformamide	82,83,97
1,4-dioxane	82,83,58,159
1,3-dioxolane	82,83,97
Dipole-dipole interaction	30
Dipole induced dipole interaction	31
Dipole moment	30,31
E	
Effective molecular weight	48
Empirical model	52,59,64,68
2-ethyl-1-hexanol	82,83
Ethylacetate	82,83
Ethylenediamine	82,83
Excess acoustic impedance	47
Excess free volume	48
Excess function	29
Excess Gibb's free energy of activation of viscous flow	42
Excess internal pressure	16
Excess isentropic compressibility	46
Excess molar refraction	51
Excess molar volume	52, 94
Excess partial molar volume	40,
Excess partial molar volume at infinite dilution	40
Eykman relation	72
Eyring John relation	71

	Page No.
Eyring's theory	59
F	
Flory's theory	52,57
Fourier transform infrared spectroscopy	93
Free volume	48
Free volume contribution	46,58
Free volume theory	61
Fugacity coefficient	60
G	
Gibb's free energy	36,
Gladstone-Dale relation	71
Grunberg-Nissan model	62
H	
Heller relation	72
Heric Brewer model	63
Hind model	63,207
Hydrogen bonding	30,137,165,196,228
I	
Ideal behaviour	6,30,35,62,
Impedance dependence relation	69
Induced dipole interaction	,31
Instantaneous dipole induced dipole interaction	31
Intermolecular force	30
Intermolecular free length	46,47,69
Intermolecular hydrogen bonding	20,33
Intermolecular interaction	41,44,47,49
Internal pressure	48,49
Intramolecular hydrogen bonding	33,34

	Page No.
Isentropic compressibility	45
J	
Jacob-Fitzner model	66,291
Jacobson's free length theory	69
Junjie's equation	70,
K	
Katti-Chaudhri model	64
Kohler Model	65,291
Krishnan-Laddha model	64
L	
Lobe model	,64
London force	32
Lorentz-Lorentz relation	71
M	
McAllister model	63,207
Methyl salicylate	82,83,189,221,251,
Methylacetate	82,83,190,251
Molar enthalpy	43,65
Molar entropy	43,
Molar refraction	51
Molar speed of sound	51
Monoethanolamine	82,83,123,159
N	
Newton relation	72
Newton-Laplace equation	45
Nomoto relation	68
Non-ideal solution	38

	Page No.
P	
Partial molar quantities	37,38
Partial molar refraction	72
Partial molar volume	37,39
Partial molar volume at infinite dilution	72
Peng Robinson Equation of state	53,135,141,169,174,200,232,238
Percent root mean square deviation	73
Percent standard deviation	73
Predictive models	51,64
Preferential solvation	6,7
Prigogine-Flory-Patterson theory	52,57,108,133,168,198,230
Q	
Quaternary mixture	83,296
R	
Redlich-Kister polynomial equation	39,64
Reduced excess volume per segment	57
Reduced Pressure	55
Reduced temperature	55
Reduced volume	55
Refractive index	49,70
Residual free energy of mixing	143,239
Response surface model	72
S	
Scatchard model	67,291
Schaaff's collision factor theory	68
Selective solvation	6
Solvation	4,5
Solvation Shell	5,6

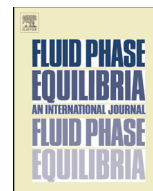
	Page No.
Specific acoustic impedance	47,69
Standard deviation	73
Symmetrical model	65,291
T	
Tamura-Kurata model	62
Tsao-Smith model	69,291
Ternary mixture	83,94,251,294
Tetrahydrofuran	82,83,98
Thermodynamic property	37,128,
Toop model	67,291
Transport property	40
U	
Ultrasonic interferometer	90,91,92
Ultrasonic speed of sound	44
V	
van der Waals	49,52,53,55,57,69
Vandael Vangeal ideal mixture relation	69
Viscosity	20,40,86
Viscosity deviation	40
Viscous antagonism	41
Viscous synergy	41
Viscosity models	59,62
W	
Weiner Model	71



ELSEVIER

Contents lists available at ScienceDirect

Fluid Phase Equilibria

journal homepage: www.elsevier.com/locate/fluid

Hydrogen bond interactions in the blends of 1,4-dioxane with some 1, 2- disubstituted ethanes at $T=(298.15, 308.15$ and $318.15)$ K

Rajendra Pradhan^a, Amarjit Kamath^b, Dhiraj Brahman^a, Biswajit Sinha^{b,*}^aDepartment of Chemistry, St. Joseph's College, Darjeeling, India^bDepartment of Chemistry, University of North Bengal, Darjeeling, India

ARTICLE INFO

Article history:

Received 24 February 2015

Received in revised form 22 June 2015

Accepted 25 June 2015

Available online 2 July 2015

Keywords:

Excess properties

1,4-Dioxane

1, 2-Disubstituted ethanes

Prigogine–Flory–Patterson theory

Peng–Robinson equation of state

ABSTRACT

Densities (ρ), viscosities (η), ultrasonic speeds (u) and refractive indices (n_D) of the binary blends of 1,4-dioxane (DO) with ethylenediamine (EDA), 1,2-dichloroethane (DCE) and monoethanolamine (MEA) were measured at $T=(298.15\text{--}318.15)$ K under atmospheric pressure over the entire composition range. Various experimental data were utilized to estimate the excess molar volumes (V_m^E), excess viscosities (η^E), excess molar refractions (R_m^E), excess isentropic compressibility (κ_s^E), excess intermolecular free length (L_f^E), etc., and analyzed in terms of molecular interactions and structural effects. Partial molar volumes ($\bar{V}_{m,1}^0$ and $\bar{V}_{m,2}^0$) and excess partial molar volumes ($\bar{V}_{m,1}^{0,E}$ and $\bar{V}_{m,2}^{0,E}$) at infinite dilution of the components were derived and discussed in terms of volume changes. Prigogine–Flory–Patterson theory and Peng–Robinson equation of state were used to predict V_m^E and η values of the blends. IR spectra of the blends were correlated to the molecular interactions therein the blends.

© 2015 Elsevier B.V. All rights reserved.

1. Introduction

Molecular interactions, operating between different liquids in liquid–liquid systems, control their physico-chemical properties and knowledge of such molecular interactions is of major significance in relation to their industrial applications [1–3] as well as in the elucidation of the structural properties of the molecules [4] in the liquid state. Mixed solvents have been used for studying complex reactions and developing theoretical understanding of chemical separations, fluid flow and heat transfers, etc. The basis for any design process in chemical industries is a reliable set of chemical and physical pure component along with mixture properties. Thus the determination of density, viscosity and speed of sound, etc are valuable tools for exploring the liquid state [5], because of the close relation between the liquid structure and macroscopic properties. Experimental values of these properties are many-a-time not at hand and the measurements are often expensive or even difficult and thus estimation methods are of great interest. These properties are functionally dependent on temperature and the composition of the liquid–liquid systems. For example, density and ultrasonic speed of sound depend on the binding forces between the liquids and are very much sensitive to the liquid structure and composition [6]. Hence studies on the

physico-chemical properties of liquid–liquid systems stand as an efficient guide for the selection of such systems regarding their practical utilization in industrial and consumer applications.

Therefore in continuation of our systematic study [7–10] on the physico-chemical properties of non-aqueous liquid blends, the present study attempts to unravel the nature of molecular interactions in the binary blends of 1,4-dioxane (DO) with ethylenediamine (EDA), 1,2-dichloroethane (DCE) and monoethanolamine (MEA) at 298.15, 308.15 and 318.15 K under ambient pressure. 1, 2-disubstituted ethanes are excellent prototype for conformational studies and it is reported that relative stability of the *gauche* and *trans* conformation of 1, 2-disubstituted ethanes depend on the substituents as well as on the dielectric constant of the medium [11]. Sreeruttun and Ramasami [12] studied the conformational behavior of 1,2-dichloroethanes in several solvents by ¹H NMR, IR, refractive index and theoretical studies. It was found that *gauche* conformers become preferentially stabilized in media with higher dielectric constants. Nath and Singh [13] studied the binary blends of 1,2-dichloroethane with benzene, toluene, *p*-xylene, quinoline and cyclohexane. Anyway, to the best of our knowledge reports on the physico-chemical properties of the binary blends under investigation are rare in the literature. Among the selected liquids DO is a non-polar, aprotic, non-hydrogen bonded cyclic diether and finds numerous applications in industrial processes as a solvent for saturated and unsaturated hydrocarbons [14]. The other three solvents also have industrial

* Corresponding author.

importance and consumer applications, e.g., EDA is an important raw material for the production of polymers, pharmaceuticals, pesticides, herbicides and dye fixing agent, etc; DCE is a σ -acceptor and is used as a solvent, degreaser, etc [13]; MEA is used in the purification of petroleum, as a solvent in dry cleaning, as a CO₂ adsorbent and as an ingredient in paints and pharmaceuticals [15]. Thus the pure liquid components for the present study were chosen based on their varied applications.

The well-established thermodynamic approach to study liquid blends is based on the interpretation of various excess properties. Hence the experimental data (ρ, η, u and n_D) were utilized to estimate the excess molar volumes (V_m^E), excess viscosities (η^E), acoustic parameters like isentropic compressibility (κ_S), intermolecular free length (L_f), specific acoustic impedance (z_{im}), excess isentropic compressibility (κ_S^E), excess intermolecular free length (L_f^E), excess specific acoustic impedance (z_{im}^E) and excess molar refractions (R_m^E) for the binary blends. Partial molar volumes ($\bar{V}_{m,1}^0$ and $\bar{V}_{m,2}^0$) and excess partial molar volumes ($\bar{V}_{m,1}^{0,E}$ and $\bar{V}_{m,2}^{0,E}$) at infinite dilution of each component were derived from the excess molar volumes (V_m^E) of the binary blends. All these functions were discussed in terms of molecular interactions, structural effects and the nature of liquid blends. Furthermore, a quantitative estimation of different contributions (i.e., interaction contribution, free volume contribution and internal pressure contribution) to the excess molar volumes (V_m^E) of the binary blends at ambient temperature and pressure was determined from PFP theory [16,17]. A comparison was made between the experimental and calculated V_m^E and η values (based on PFP [16,17] or Bloomfield–Dewan viscosity model [18] and PREOS [19]) to assess the predictive capability of these theories. Moreover, ultrasonic speeds of sound and refractive indices for all the binary blends were theoretically predicted on the basis of several empirical and semi-empirical relations. In addition, IR spectra of the blends were correlated to the molecular interactions therein the blends studied.

2. Experimental

2.1. Chemicals

All the chemicals used in this work were of Reagent/Reagent Plus grade (Sigma–Aldrich, Germany, purity >99%) were used as received from the vendor. Table 1 contains provenance and purity of the chemicals used in this work. Purity of the solvents was ascertained by GLC and also by comparing their densities and viscosities at the experimental temperatures with the literature data [20–31], whenever available, as shown in Table S1 of the Supporting information.

2.2. Measurements

The binary blends were prepared by mass in air-tight bottles with stopper inside a dry box at 298.15 K and each solution thus prepared was distributed into three recipients to perform all the measurements in triplicate with the aim of the determining possible dispersion of the results obtained. The mass measurements were made on a digital electronic analytical balance (Mettler, AG 285, Switzerland) with an uncertainty of $\pm 1 \cdot 10^{-4}$ g. All solutions were prepared afresh before use. The uncertainty in mole fraction was evaluated to be ± 0.0002 . The densities were measured with a vibrating-tube density meter (Anton Paar, DMA 4500 M). The densitometer was calibrated at the experimental temperatures with doubly distilled and degassed water and dry air at atmospheric pressure. The temperature was automatically kept constant with an accuracy of $\pm 1 \cdot 10^{-2}$ K by using the built-in Peltier technique. The stated repeatability and accuracy of the densities were $\pm 1 \cdot 10^{-5}$ gcm⁻³ and $\pm 5 \cdot 10^{-5}$ gcm⁻³, respectively. However, the estimated uncertainty of the density measurements for most of the pure liquids and solutions was found to be within the range 0.01–0.1%.

The viscosity was measured by means of a suspended Canon-type Ubbelohde viscometer thoroughly cleaned, dried and calibrated at the experimental temperatures with triply distilled, degassed water and purified methanol. It was filled with experimental liquid and placed vertically in a glass sided thermostat maintained constant to ± 0.01 K. After attainment of thermal equilibrium, the efflux times of flow of liquids were recorded with a digital stopwatch correct to ± 0.01 s. In all determinations, an average of triplicate measurements was taken into account and adequate precautions were taken to minimize evaporation losses during the actual measurements. The estimated uncertainty in viscosity measurements was 1.5%.

Ultrasonic speeds of sound (u) were measured with an accuracy of 0.3% by using a single crystal variable-path ultrasonic interferometer (Mittal Enterprise, New Delhi, F-05) working at 2 MHz. It was calibrated with doubly distilled water and purified methanol maintained at $T = (298.15 \pm 0.01)$ K by circulating thermostated water around the jacketed cell (of 2 MHz) containing the experimental liquids with a circulating pump. The uncertainty of ultrasonic speeds measurements was around ± 0.2 ms⁻¹. Refractive indices were measured with an Abbe's refractometer. It was calibrated by measuring the refractive indices of doubly distilled water and purified methanol maintained at $T = (298.15 \pm 0.01)$ K similarly as done with the ultrasonic interferometer cell. The estimated uncertainty in the refractive indices was 0.02%. The details of the methods and measurement techniques have been described elsewhere [32,33].

Table 1
Provenance and purity of the chemicals used.

Chemicals	Source	Purification method	Mass fraction purity ^e	CAS No
DO ^a	Sigma–Aldrich, Germany	Non	>0.998	123-91-1
EDA ^b	Sigma–Aldrich, Germany	Non	>0.990	107-15-3
DCE ^c	Sigma–Aldrich, Germany	Non	>0.998	106-06-2
MEA ^d	Sigma–Aldrich, Germany	Non	>0.990	141-43-5

^a DO = 1, 4-dioxane.

^b EDA = 1, 2-ethylenediamine.

^c DCE = 1, 2-dichloroethane.

^d MEA = Monoethanolamine.

^e Purity as prescribed by the vendor.

3. Results and discussion

The experimental densities (ρ), viscosities (η), excess molar volumes (V_m^E) and excess viscosities (η^E) of the binary blends at the experimental temperatures are listed in Table S2 of the supporting information. In order to understand the nature of the molecular interactions between the components of the liquid blends, excess parameters are of immense help. Non-ideal liquid mixtures show deviations from a rectilinear dependence of their properties such as molar volume, viscosity, etc on the component mole fractions. Such deviations can be ascribed to arise from the strong or weak interactions between the liquid components. The extent of such deviation depends upon the nature of the constituents and composition of the blends.

3.1. Excess molar volumes

The excess molar volumes, V_m^E , of the solutions were calculated using the equation:

$$V_m^E = \sum_{i=1}^2 x_i M_i (1/\rho - 1/\rho_i) \quad (1)$$

where ρ is the density of the mixture and x_i , M_i and ρ_i are the mole fraction, molar mass and density of i th component in the blend, respectively. The estimated uncertainty for excess molar volumes (V_m^E) was evaluated to be $\pm 0.005 \text{ cm}^3 \text{ mol}^{-1}$. Fig. 1 (V_m^E versus x_1 at 298.15 K) illustrate that the V_m^E values are positive for DO + EDA and DO + DCE blends but are negative for DO + MEA blend over the entire range of compositions at all the experimental temperatures. The excess molar volume depends upon two factors: (i) variation of intermolecular forces between two components in contact; the physical effects involve dispersion forces and non-specific interactions in the mixture and thus contribute positively to V_m^E . The chemical or specific interactions result in volume decrease and involve hydrogen bond formation or rupture, charge transfer type forces and other complex forming interactions between dissimilar species and thus contribute negatively to V_m^E ; (ii) variation in molecular packing due to interstitial accommodation of one component into other owing to difference in free volume and molar volume of the components.

If the interactions between dissimilar molecules are weaker than those between similar molecules excess molar volume (V_m^E)

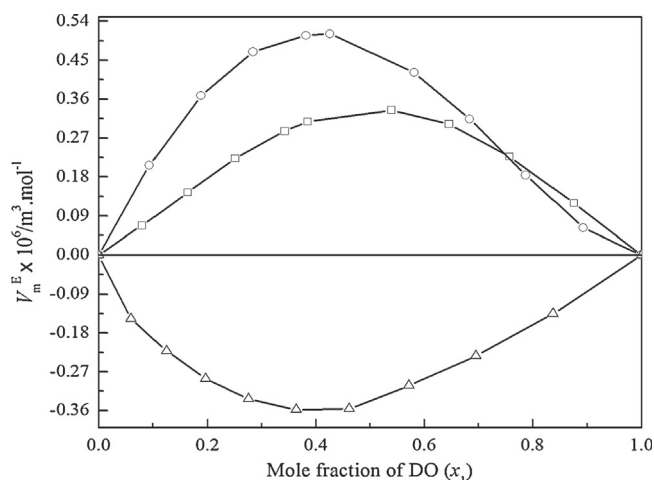


Fig. 1. Excess molar volume (V_m^E) versus mole fraction of DO (x_1) for the binary blends of DO + 1,2-disubstituted ethanes at $T = 298.15 \text{ K}$. Symbols: \square , EDA; \circ , DCE; \triangle , MEA.

will be positive. 1, 2-disubstituted ethanes used in this work prefer *gauche* conformation and possess intra-molecular hydrogen bonding except DCE [34]. However, the *gauche* conformer of DCE is polar and stabilized by electrostatic interaction between their dipole moments [34]. A comparison of the relative permittivity [35] of the liquid components $\{\epsilon_{r,DO} (2.21) < \epsilon_{r,DCE} (10.42) < \epsilon_{r,EDA} (13.82) < \epsilon_{r,MEA} (31.94)\}$ suggests that the approximate order of molecular interaction between similar molecules in the subject liquids is: MEA-MEA > EDA-EDA > DCE-DCE > DO-DO. The positive V_m^E values for DO + EDA and DO + DCE blends indicate breaking of liquid order on mixing and dispersion interaction between dissimilar components. Dispersion interaction may arise from the breaking of cohesive forces or intra-molecular hydrogen bonds present between similar molecules on addition of DO to the ethanes. So mixing of DO probably breaks the weak dipole-dipole cohesive forces present amongst the DCE molecules [34] and intra-molecular hydrogen bonds present in EDA molecules [34]. DO can also form hydrogen bond through its two ethereal O-atoms with NH_2 groups of EDA molecule and hampers intra-molecular hydrogen bonds in EDA molecules. That is why V_m^E values of DO + EDA blend are lower than those of DO + DCE blend. Similarly if the interactions between dissimilar molecules are higher than those between similar molecules the excess molar volume (V_m^E) will be negative. In the case of DO + MEA blend, the negative V_m^E values suggest the presence of specific interactions like intermolecular hydrogen bonds between the dissimilar components (through the involvement of the ethereal O-atoms of DO and the highly polar $-\text{OH}$ and $-\text{NH}_2$ group present in MEA molecule) and geometrical fitting of the molecules ($V_{m,DO} - V_{m,MEA} = 25.36 \text{ cm}^3 \text{ mol}^{-1}$ at 298.15 K) on mixing. Thus the magnitude of V_m^E values show the order: DO + DCE > DO + EDA > DO + MEA; this indicates that the molecular interaction is least for DO + DCE blend and highest for DO + MEA blend. Furthermore, Table S2 shows that in each case V_m^E values increase as the temperature increases over the whole composition range from 298.15 to 318.15 K. Such a trend in temperature dependence of V_m^E values indicates that temperature enhancement causes a decrease in the interaction between the component molecules due to thermal agitation that probably breaks or disturbs the developing dispersion forces and non-specific interactions as well as specific interactions between the liquid components in the blends.

The partial molar volumes ($\bar{V}_{m,i}$) of the i th component in the binaries over the entire composition range at 298.15 K were obtained from the relation [36]:

$$\bar{V}_{m,i} = V_{m,i}^E + V_{m,i}^* + (1 - x_i)(dV_{m,i}^E/dx_i)_{T,P} \quad (2)$$

where $V_{m,i}^*$ is the molar volume of the i th component in the binaries. The derivatives, $(dV_{m,i}^E/dx_i)_{T,P}$ used in Eq. (2) were obtained by following a procedure described elsewhere [37] by using the Redlich-Kister coefficients (a_i) [38] for the excess molar volumes (V_m^E): $a_0 = 1.3439, a_1 = 0.0760, a_2 = -0.5266, a_3 = -0.0272$ for DO + EDA; $a_0 = 1.9370, a_1 = -1.0974, a_2 = -0.6155, a_3 = 0.0604$ for DO + DCE and $a_0 = -1.3210, a_1 = 0.4367, a_2 = -0.4153, a_3 = 0.8004$ for DO + MEA with standard deviations (σ) 0.0008, 0.0051, 0.0147 for the three blends, respectively. Partial molar volumes ($\bar{V}_{m,1}^0$ and $\bar{V}_{m,2}^0$) at infinite dilution, excess partial molar volumes ($\bar{V}_{m,i}^E$) and excess partial molar volumes ($\bar{V}_{m,i}^{0,E}$) at infinite dilution were determined from the standard relations described elsewhere [36]. Partial molar volumes ($\bar{V}_{m,1}^0$ and $\bar{V}_{m,2}^0$) and excess partial molar volumes ($\bar{V}_{m,i}^{0,E}$) at infinite

Table 2

Molar volumes ($V_{m,1}^*$ and $V_{m,2}^*$), partial molar volumes at infinite dilution ($\bar{V}_{m,1}^0$ and $\bar{V}_{m,2}^0$) and excess partial molar volumes at infinite dilution ($\bar{V}_{m,1}^{0,E}$ and $\bar{V}_{m,2}^{0,E}$) for each component in the binary mixtures at 298.15 K

Volume parameters	DO (1) +		
	EDA (2)	DCE (2)	MEA (2)
$V_{m,1}^* \times 10^6 (\text{m}^3 \text{mol}^{-1})$	85.73	85.73	85.73
$\bar{V}_{m,1}^0 \times 10^6 (\text{m}^3 \text{mol}^{-1})$	86.50	88.09	82.75
$V_{m,2}^* \times 10^6 (\text{m}^3 \text{mol}^{-1})$	67.15	79.41	60.37
$\bar{V}_{m,2}^0 \times 10^6 (\text{m}^3 \text{mol}^{-1})$	68.02	79.69	59.87
$\bar{V}_{m,1}^{0,E} \times 10^6 (\text{m}^3 \text{mol}^{-1})$	0.769	2.358	-2.973
$\bar{V}_{m,2}^{0,E} \times 10^6 (\text{m}^3 \text{mol}^{-1})$	0.866	0.285	-0.499

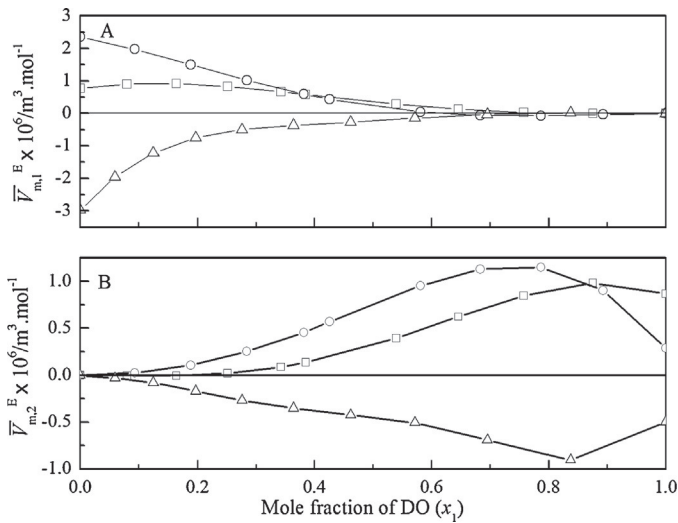


Fig. 2. Excess partial molar volume ($\bar{V}_{m,i}^E$) against mole fraction of DO (x_1) for the binary blends of DO + 1, 2-disubstituted ethanes at $T=298.15\text{ K}$: A, for DO; B, for 1, 2-disubstituted ethanes. Symbols: \square , EDA; \circ , DCE; Δ , MEA.

dilution for each component in the binary blends are listed in Table 2. Excess partial molar volumes ($\bar{V}_{m,1}^E$ and $\bar{V}_{m,2}^E$) of each component in the studied blends were depicted in Fig. 2 as a function of x_1 . Partial molar volume ($\bar{V}_{m,1}^0$ and $\bar{V}_{m,2}^0$) at infinite dilution of each liquid were found to be greater than the molar volume of the respective pure liquid for the studied blends except the DO + MEA blend. Also, the excess partial molar volumes ($\bar{V}_{m,1}^{0,E}$ and $\bar{V}_{m,2}^{0,E}$) at infinite dilution were positive for both components in the blends DO + EDA and DO + DCE except the blend DO + MEA. This suggests that while the systems with EDA and DCE are characterized by volume expansion on mixing with DO, the blend with MEA is characterized by volume contraction on mixing with DO, i.e., for DO + MEA blend is characterized by a better packing efficiency and intermolecular hydrogen bonds between the dissimilar molecules were not broken at dilute regions.

3.1.1. Predictions of excess molar volumes

i) Prigogine–Flory–Paterson theory (PFPP):

In recent years, Flory's statistical theory [39–42] and its modified version known as the Prigogine–Flory–Paterson (PFPP) theory [16,17] has been employed to estimate and analyze excess thermodynamic functions theoretically. The Flory's parameters such as reduced volume (\bar{v}), reduced temperature (\bar{T}),

characteristic volume (V^*), characteristic pressure (P^*) and characteristic temperature (T^*) for each liquid component are given in Table S3 of the supporting information. The PFPP theory considers excess molar volumes (V_m^E) of binary blends to be the sum of three contributions: (i) the interaction contribution (V_{int}^E) is proportional to the interaction parameter, $\chi_{1,2}$; (ii) the free volume contribution (V_{fv}^E) arises from the dependence of the reduced volume upon the reduced temperature as a result of the difference between the degree of expansion of the two components; and (iii) the internal pressure contribution (V_{p}^E) which depends both on the differences of the characteristic pressures and on the differences of reduced volumes of the components. The following equation was used to estimate V_m^E values:

$$\begin{aligned} x_1 V_1^* + x_2 V_2^* = & \frac{(\bar{v}^{1/3} - 1)\bar{v}^{2/3}\psi_1\theta_2}{[(4/3)\bar{v}^{-1/3} - 1]P_1^*} \chi_{1,2} (\chi_{1,2} \text{contribution}) \\ & - \frac{(\bar{v}_1 - \bar{v}_2)^2 [14/9]\bar{v}^{-1/3} - 1}{[(4/3)\bar{v}^{-1/3} - 1]\bar{v}} \psi_1 \psi_2 (\bar{v} \text{contribution}) \\ & + \frac{(\bar{v}_1 - \bar{v}_2)(P_1^* - P_2^*)\psi_1 \psi_2}{(P^* \text{contribution})} \end{aligned} \quad (3)$$

where ψ_1 and ψ_2 stand for the molecular contact energy fractions of liquid 1 and liquid 2 in a mixture; θ_2 is the molecular site fraction of liquid 2 in a mixture and other symbols have their usual significance [16,17]. The interaction contributions to V_m^E were obtained from Eq. (3) by using a computer program as detailed elsewhere [10]. The optimized $\chi_{1,2}$ values, calculated and experimental V_m^E values, their deviation and different contributions to V_m^E values for near equimolar ($x_1 \approx 0.5$) composition at 298.15 K are given in Table S4 of the Supporting information. It reveals that the calculated excess molar volumes ($V_{m,\text{PFPP}}^E$) reasonably agree well with the experimental excess molar volumes (V_m^E) for all the blends studied.

ii) Peng–Robinson Equation of State (PREOS):

Cubic equations of state are extensively used in process simulations for the prediction of thermodynamic properties and phase equilibria of hydrocarbon systems due to their simplicity, robustness and computational efficiency. Here in this work we have used the classical cubic Peng–Robinson equation of state (PREOS) for predicting the excess molar volumes ($V_{m,\text{PREOS}}^E$) of the blends studied at 298.15 K. PREOS is given by [19]:

$$P = \frac{RT}{V-b} - \frac{a}{V(V+b) + b(V-b)} \quad (4)$$

For a pure component the energy a and co-volume b parameters can be obtained from the relations:

$$a = a(T) = a(T_c) \left[1 + \xi \left(1 - \sqrt{\frac{T}{T_c}} \right) \right]^2 \quad (5)$$

$$b = b(T) = b(T_c) \quad (6)$$

$$a(T_c) = 0.45724 \frac{R^2 T_c^2}{P_c} \quad (7)$$

$$b(T_c) = 0.07780 \frac{RT_c}{P_c} \quad (8)$$

where T_c and P_c are critical temperature and pressure of a pure component. The parameter ξ in terms of acentric factor (ω) [43] is defined by:

$$\xi = 0.37464 + 1.54226\omega - 0.26992\omega^2 \quad (9)$$

T_c , P_c and ω values of the pure liquids used in the present study were taken from the literature [25,44]. For a binary blend the energy a and co-volume b parameter can be given by [43]:

$$a(T) = \sum_{i=1}^2 \sum_{j=1}^2 x_i x_j \sqrt{a_i a_j} (1 - k_{ij}) \quad (10)$$

$$b(T) = \sum_{i=1}^2 x_i b_i \quad (11)$$

where k_{ij} is the interaction coefficient for a binary blend of components i and j . Rearranging Eq. (4) in terms of the compressibility factor (Z), we have:

$$Z^3 - (1 - B)Z^2 + (A - 3B^2 - 2B)Z - (AB - B^2 - B^3) = 0 \quad (12)$$

where $Z = PV/RT$, $B = Pb/RT$ and $A = aP/(RT)^2$. Thus from a knowledge of the compressibility factors for the components and their blends, the corresponding excess molar volumes (V_m^E) of the blends were calculated. The values of the interaction coefficient (k_{ij}) were found to be 0.0582, 0.0679 and 0.0206 with standard deviations (σ) 0.019, 0.086 and 0.056, respectively for the blends DO+EDA, DO+DCE and DO+MEA. A comparison between the experimental excess molar volumes (V_m^E) and the calculated excess molar volumes ($V_{m,PPF}^E$ and $V_{m,PREOS}^E$) from PFP theory and PREOS for the studied blends at 298.15 K was depicted in Fig. 3.

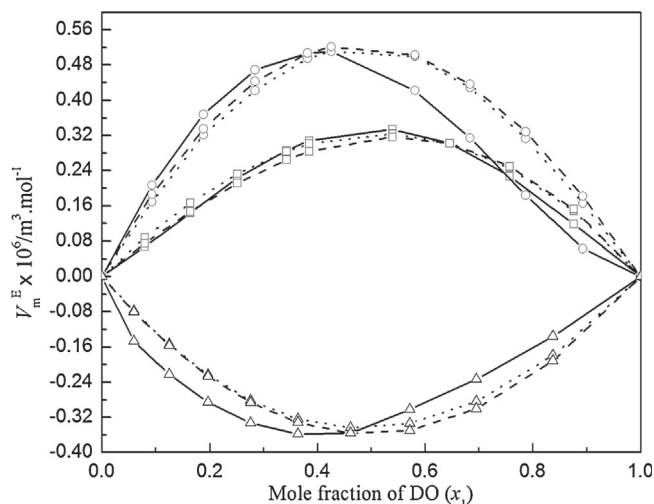


Fig. 3. A comparison between the excess molar volumes (V_m^E) against mole fraction of DO (x_1) for the binary blends of DO+1, 2-disubstituted ethanes at $T=298.15$ K. Symbols: \square , EDA; \circ , DCE; Δ , MEA. Solid lines, dashed lines and dotted lines represent excess molar volumes (V_m^E) obtained from experimental density values, PREOS and PFP theory, respectively.

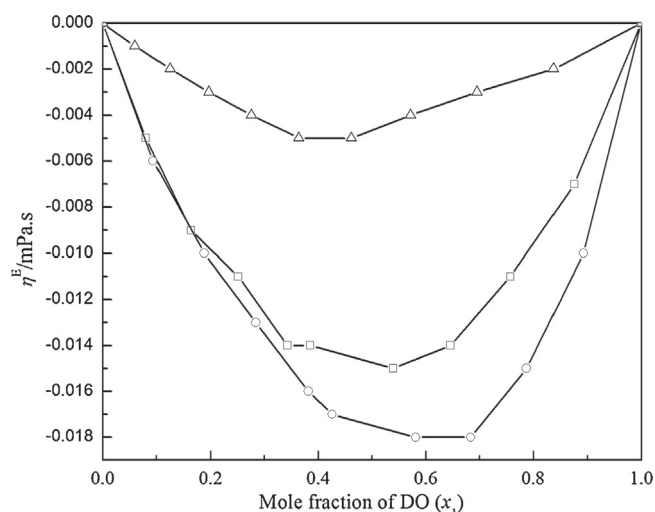


Fig. 4. Excess viscosities (η^E) versus mole fraction of DO (x_1) for the binary blends of DO+1, 2-disubstituted ethanes at $T=298.15$ K. Symbols: \square , EDA; \circ , DCE; Δ , MEA.

3.3. Excess viscosities

The excess viscosity (η^E) can be obtained from the difference between the measured viscosity (η) and the ideal viscosity (η_{id}) of a solution as follows [9,10]:

$$\eta^E = \eta - \eta_{id} \quad (13)$$

and the ideal viscosity (η_{id}) is given by [45]:

$$\eta_{id} = \exp\left(\sum_{i=1}^2 x_i \ln \eta_{id}\right) \quad (14)$$

The estimated uncertainty for excess viscosities (η^E) was evaluated to be ± 0.0002 mPa.s. Fig. 4 (η^E versus x_1 at 298.15 K) shows that the η^E values are negative over the whole composition range for the blends at the experimental temperatures. It was observed if V_m^E values are positive, η^E values become negative for many binary blends and vice-versa. Such a coincidence was found for DO+EDA and DO+DCE blends but for DO+MEA blend both V_m^E and η^E values are negative. However, for each blend η^E values decrease as the experiment temperature increases indicating that the interaction between the dissimilar molecules becomes weaker at higher temperatures (Table S2).

According to Eyring's viscosity relation [45], the free energy of viscous flow (ΔG^*) is given by the relation:

$$\eta = \left(\frac{hN}{V}\right) \exp\left(\frac{\Delta G^*}{RT}\right) \quad (15)$$

where h is Planck's constant, N is Avogadro's number and other symbols have their usual meanings. Rearranging Eq. (15) and putting $\Delta G^* = \Delta H^* - T\Delta S^*$ we get the relation:

$$R \ln\left(\frac{\eta V}{hN}\right) = \frac{\Delta H^*}{T} - \Delta S^* \quad (16)$$

Thus, linear regressions of $R \ln(\eta V/hN)$ against $(1/T)$ give the enthalpy (ΔH^*) and entropy (ΔS^*) of activation of viscous flow from the corresponding slope and negative intercept, respectively. ΔG^* , ΔH^* , ΔS^* and the regression coefficients (R^2) are given in Table S5 of the supporting information. It shows that while ΔH^* values are positive, ΔS^* values are negative for all the binary blends except the blend DO+MEA. According to Corradini et al. [46] the

enthalpy of activation of viscous flow is regarded as a measure of the degree of cooperation between the species taking part in viscous flow. In a highly structured liquid there will be considerable degree of order; hence for cooperative movement of the entities a large heat of activation is required for the flow process. Thus the ΔH^* values indicate that the ease of formation of activated species necessary for viscous flow follows the order: DO + DCE \approx DO + EDA > DO + MEA. This order is also supported by negative values of ΔS^* for the blends DO + DCE and DO + EDA and positive values of ΔS^* for the blend DO + MEA.

3.3.1. Viscosity prediction

Several empirical models can simulate the viscosity of liquids or liquid mixtures and practical implications of such viscosity models were reviewed by Mehrotra et al. [47] Empirical methods have also been developed using the corresponding state principle based on van der Waals' hypothesis [48] that the properties of substances in terms of reduced thermodynamic properties show similar behavior. For the blends studied viscosities were predicted using Peng–Robinson cubic equation of state [19] and Bloomfield–Dewan model [18].

i) Peng–Robinson Equation of State:

The excess activation free energy of viscous flow (ΔG^{*E}) for the binary blends can be obtained from the relation:

$$\Delta G^{*E} = \Delta G^* - \sum_{i=1}^2 (x_i \Delta G_i^*) \quad (17)$$

A simple rearrangement of Eq. (17) gives the viscosity for a mixture [49]:

$$\eta = \frac{(\eta V)^{\text{id}}}{V_m} \exp\left(\frac{\Delta G^{*E}}{RT}\right) \quad (18)$$

where V_m and $(\eta V)^{\text{id}}$ are the molar volume and kinematic viscosity of an ideal mixture, respectively. $(\eta V)^{\text{id}}$ is defined as follows:

$$(\eta V)^{\text{id}} = \exp\left[\sum_{i=1}^2 x_i \ln(\eta_i V_i)\right] \quad (19)$$

In order to incorporate the binary interaction parameter g_{12} ($g_{ii} = 0$ and $g_{ij} = g_{ji}$), ΔG^{*E} for a binary blend is given as:

$$\frac{\Delta G^{*E}}{RT} = \frac{G^{*E}}{RT} + \frac{1}{2} \sum_{i=1}^2 \sum_{j=1}^2 x_i x_j g_{ij} = \frac{G^{*E}}{RT} + x_1 x_2 g_{12} \quad (20)$$

The interaction parameter g_{12} can be evaluated from a comparison of the experimental viscosities to those obtained from Eq. (18). The value of G^{*E} can also be obtained from the relation:

$$\frac{G^{*E}}{RT} = \sum_{i=1}^2 x_i (\ln \varphi_i - \ln \varphi_i^0) \quad (21)$$

where φ_i^0 and φ_i stand for the fugacity coefficients of i th component in pure state and in the mixture, respectively. As per PREOS, fugacity coefficient for a pure component is given by:

$$\ln \varphi = (Z - 1) - \ln(Z - B) - \frac{A}{2\sqrt{2}B} \ln\left(\frac{Z + (1 + \sqrt{2})B}{Z + (1 - \sqrt{2})B}\right) \quad (22)$$

and fugacity coefficient for the i th component in a binary blend is given by:

$$\ln \varphi_i = \frac{b_i}{b} (Z - 1) - \ln(Z - B) - \frac{A}{2\sqrt{2}B} \left(\frac{2}{a} \sum_{j=1}^2 x_j (a_i a_j) \frac{1}{2} (1 - k_{ij}) - \frac{b_i}{b} \right) \ln\left(\frac{Z + (1 + \sqrt{2})B}{Z + (1 - \sqrt{2})B}\right) \quad (23)$$

Combining Eqs. (18)–(23) we get,

$$\eta = \frac{(\eta V)^{\text{id}}}{V_m} \exp\left[\sum_{i=1}^2 x_i (\ln \varphi_i - \ln \varphi_i^0) + \frac{1}{2} \sum_{i=1}^2 \sum_{j=1}^2 x_i x_j g_{ij}\right] \quad (24)$$

In order to obtain the binary interaction parameter (g_{12}), a non-linear regression analysis was performed iteratively by using a C-program to have minimum standard deviation (σ) for a binary blend. The binary interaction parameters (g_{12}) were found to be -0.294 ($\sigma = 0.001$), -0.053 ($\sigma = 0.002$) and -0.116 ($\sigma = 0.001$) for the blends DO + EDA, DO + DCE and DO + MEA, respectively.

ii) Bloomfield–Dewan viscosity model:

It combines two major semi-empirical theories of liquid viscosities in order to assess excess viscosity of liquid blends. The first one is the absolute reaction rate theory [45] that relates the viscosity to the free energy required by a molecule to overcome the attractive force field of its neighbors in order to jump to a new equilibrium position, *i.e.*, to flow. The second one is the free volume theory [50] that relates the viscosity to the probability of occurrence of an empty neighboring site into which a molecule can jump and the probability depends exponentially on the free volume of the liquid. Thus the probability of viscous flow has been considered as a product of the probabilities of acquiring sufficient activation energy and the occurrence of an empty site. All the thermodynamic quantities involved in Bloomfield–Dewan model can be had from Flory's statistical thermodynamic theory for liquid mixtures [39–42]. Bloomfield and Dewan [18] developed the following expression:

$$\Delta \ln \eta = f(\tilde{v}) - \frac{\Delta G^R}{RT} \quad (25)$$

where

$$\Delta \ln \eta = \ln \eta - \sum_{i=1}^2 (x_i \eta_i) \quad (26)$$

and

$$f(\tilde{v}) = \frac{1}{\tilde{v} - 1} - \sum_{i=1}^2 \frac{x_i}{\tilde{v}_i - 1} \quad (27)$$

ΔG^R is the residual free energy of mixing and can be had from the relation:

$$\Delta G^R = \Delta G^E + RT \sum_{i=1}^2 x_i \ln(x_i / \phi_i) \quad (28)$$

where ϕ_i is the segment fraction of the i th component in a binary blend and is defined in the literature [39–42]. The excess energy ΔG^E can be obtained from the Flory's statistical theory of liquid blends by using the relation:

$$\Delta G^E = \sum_{i=1}^2 x_i P_i^* V_i^* \left[(1/\tilde{v}_i - 1/\tilde{v}) + 3\tilde{T}_i \ln\{(1/\tilde{v}_i^{1/3} - 1)/(\tilde{v}^{1/3} - 1)\} \right] + (x_1 \theta_2 V_1^* \chi_{12}) / \tilde{v} \quad (29)$$

The standard deviations (σ) between the experimental viscosities and those calculated from Bloomfield and Dewan model were 0.03, 0.39 and 4.99 for the blends with EDA, DCE and MEA, respectively. A comparison between the experimental viscosities and the

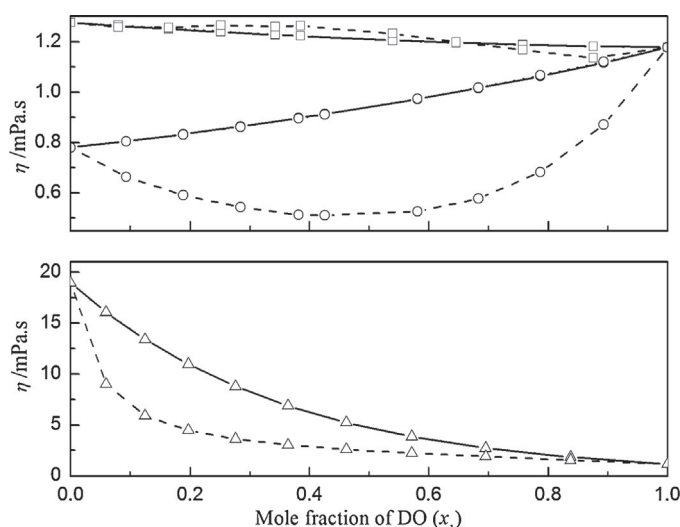


Fig. 5. A comparison between the excess viscosities (η^E) against mole fraction of DO (x_1) for the binary blends of DO + 1, 2-disubstituted ethanes at $T=298.15$ K. Symbols: \square , EDA; \circ , DCE; Δ , MEA. Solid lines, dashed lines and dotted lines represent excess molar volumes (η^E) obtained from experimental viscosity values, Bloom Field–Dewan theory and PREOS, respectively.

calculated viscosities from these two viscosity prediction models are depicted in Fig. 5. It is evident that PREOS predicted the viscosities for the blends very well.

3.4. Ultrasonic speed of sound and derived functions

The speeds of sound (u) and the densities (ρ) of the binary blends at 298.15 K were used to determine their isentropic compressibilities (κ_S), excess isentropic compressibilities (κ_S^E) and the other acoustic parameters. The experimental speeds of sound of each pure liquid were in good agreement with the literature values [10,30,51,52] at 298.15 K. The excess isentropic compressibilities (κ_S^E) were calculated by using the relation:

$$\kappa_S^E = \kappa_S - \kappa_S^{\text{id}} \quad (30)$$

where $\kappa_S = 1/\rho u^2$ and κ_S^{id} , the isentropic compressibility for an ideal mixture, is given by the relation [53]:

$$\kappa_S^{\text{id}} = \sum_{i=1}^2 \tau_i \left[\kappa_{S,i} + \frac{TV_{m,i}^* \alpha_i^2}{C_{p,i}} \right] - \left\{ \frac{T \sum_{i=1}^2 (x_i V_{m,i}^*) (\sum_{i=1}^2 \tau_i \alpha_i)^2}{\sum_{i=1}^2 (x_i C_{p,i})} \right\} \quad (31)$$

where τ_i is the volume fraction of the component 'i' in the mixture, $\kappa_{S,i}$, $V_{m,i}^*$, α_i and $C_{p,i}$ are the isentropic compressibility, the molar volume, the expansion coefficient and the molar isobaric heat capacity of the pure components, respectively. The expansion coefficients (α_i) were obtained from experimental density values and the values of $C_{p,i}$ were taken from the literature [35]. The other acoustic parameters like intermolecular free length (L_f), specific acoustic impedance (z_{im}) and their excess/deviation functions were calculated by using the standard relations available elsewhere [9,54].

The parameters u , κ_S and κ_S^E at 298.15 K are listed in Table S6 of the Supporting information. Fig. 6 illustrates the variation of excess isentropic compressibilities (κ_S^E) of the blends against mole fraction of DO (x_1) at 298.15 K. It is evident that while the excess isentropic compressibilities (κ_S^E) for the blends DO + EDA and DO + DCE are positive, those for the blend DO + MEA are negative over the entire composition range at 298.15 K. The positive κ_S^E values for the blends DO + EDA and DO + DCE are indicative of dispersion interaction between mixing component like breaking up of the weak dipole–dipole cohesive forces present among the DCE molecules and intermolecular hydrogen bonding present in EDA molecules upon mixing. For the blend DO + MEA, the negative κ_S^E values suggest the presence of specific interaction like intermolecular hydrogen bond between the components as well as mutual geometrical fitting of the dissimilar molecules on mixing. The magnitude of κ_S^E values follows the order: DO + DCE > DO + EDA > DO + MEA, indicating that the molecular interaction is least for the blend DO + DCE and highest for DO + MEA blend. Thus the results stand in parallel to those obtained earlier from excess molar volumes and excess viscosities.

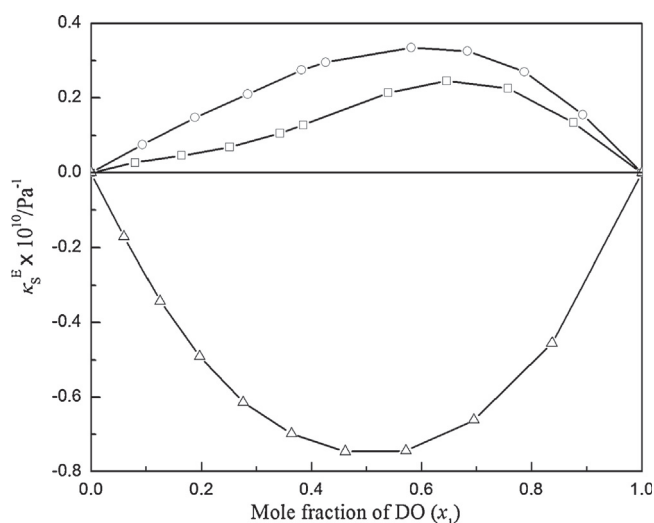


Fig. 6. Excess isentropic compressibility (κ_S^E) versus mole fraction of DO (x_1) for the binary blends of DO + 1, 2-disubstituted ethanes at $T=298.15$ K. Symbols: \square , EDA; \circ , DCE; Δ , MEA.

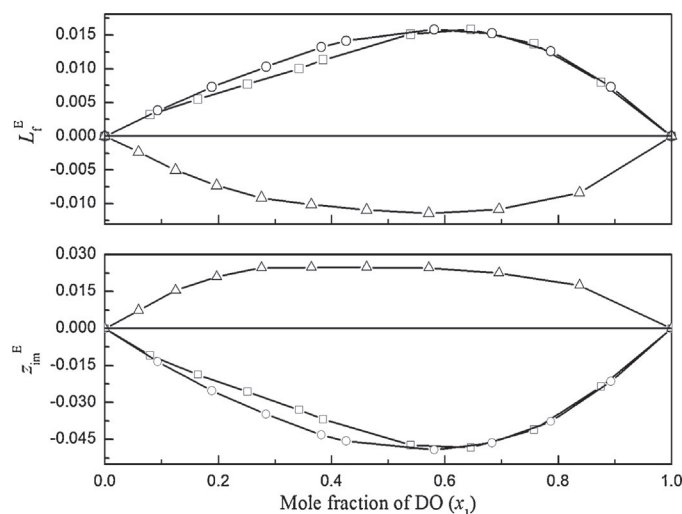


Fig. 7. Excess intermolecular free length (L_f^E) and excess acoustic impedances (z_{im}^E) versus mole fraction of DO (x_1) for the binary blends of DO + 1, 2-disubstituted ethanes at $T=298.15$ K. Symbols: \square , EDA; \circ , DCE; Δ , MEA.

Intermolecular free length (L_f) and specific acoustic impedance (z_{im}) for the studied binaries at 298.15 K are listed in Table S7 of the supporting information. According to King-Kincaid [55], a regular rise in intermolecular free length causes a fall in speeds of sound for the mixtures and *vice-versa*. This is also in accordance with the expected increase in the isentropic compressibility and decrease in specific acoustic impedance. Table S7 shows that while the specific acoustic impedances (z_{im}) decrease, the intermolecular free lengths (L_f) increase as the mole fraction (x_1) of DO in the mixtures increase. The magnitude of the intermolecular free lengths (L_f) has the order: DO+DCE > DO+EDA > DO+MEA; this indicates that the molecular interaction between dissimilar molecules is also increasing in the same order. The excess intermolecular free lengths (L_f^E) and excess acoustic impedances (z_{im}^E) are plotted in Fig 7 against the mole fraction of DO in the mixtures. The negative excess intermolecular free lengths (L_f^E) and positive excess acoustic impedances (z_{im}^E) for DO+MEA blend reflect the stronger interaction between the two components in contrast to the blends DO+EDA and DO+DCE for which z_{im}^E values are negative and L_f^E values are positive. The negative L_f^E and positive z_{im}^E values for the blend DO+MEA are due to stronger hetero-association between MEA and DO molecules and such hetero-association may be attributed to both hydrogen bonding and interstitial accommodation of MEA molecules within the voids of DO structure.

3.5. Molar refractions

The molar refractions (R_m) for the binary blends were calculated from the relation:

$$R_m = \frac{n_{D,1}^2 - 1}{n_{D,2}^2 + 2} \frac{\sum_{i=1}^2 x_i M_i}{\rho} \quad (32)$$

where ρ is the density of the mixture and x_i , M_i are the mole fraction and molar mass of i th component in the blend, respectively; $n_{D,1}$ and $n_{D,2}$ are the refractive indices of the 1st and 2nd component in a blend. The excess molar refractions (R_m^E) were obtained from relation,

$$R_m^E = R_m - \sum_{i=1}^2 x_i R_{m,i} \quad (33)$$

where $R_{m,i}$ is the molar refraction of i th component in the blend. Excess molar refractions (R_m^E) along with the experimental the refractive indices (n_D) for the three binaries are listed in Table S8 of the supporting information. The experimental the refractive indices (n_D) were in good agreement with literature values [26,56–58] at 298.15 K. The variation of excess refractive indices (R_m^E) with the mole fraction of DO (x_1) at 298.15 K also reveals that the same order of molecular interactions for the studied blends as discussed above.

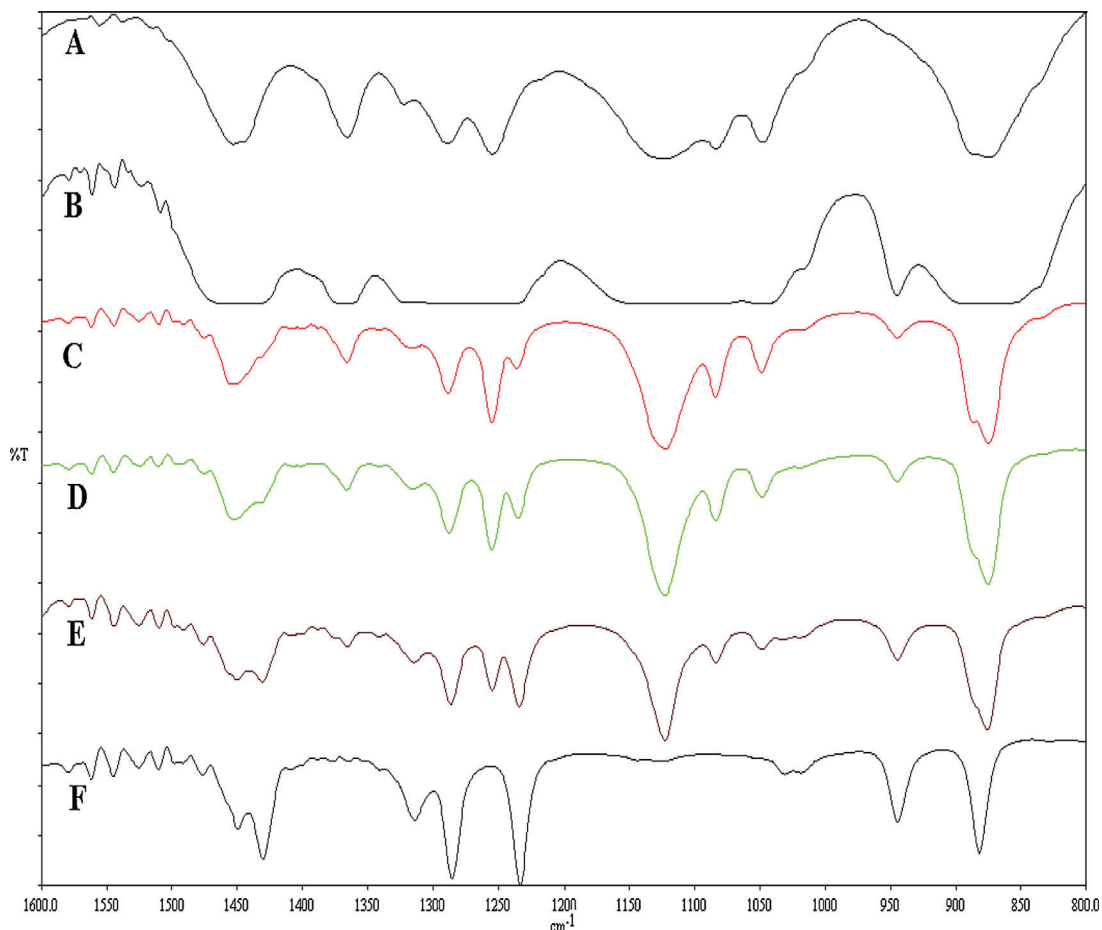


Fig. 8. FTIR spectra of the various binary blends of DO+DCE. A, pure DO ($x_{DCE} = 0.0000$); B, $x_{DCE} = 0.1820$; C, $x_{DCE} = 0.3725$; D, $x_{DCE} = 0.5718$; E, $x_{DCE} = 0.7807$; F, Pure DCE ($x_{DCE} = 1.0000$).

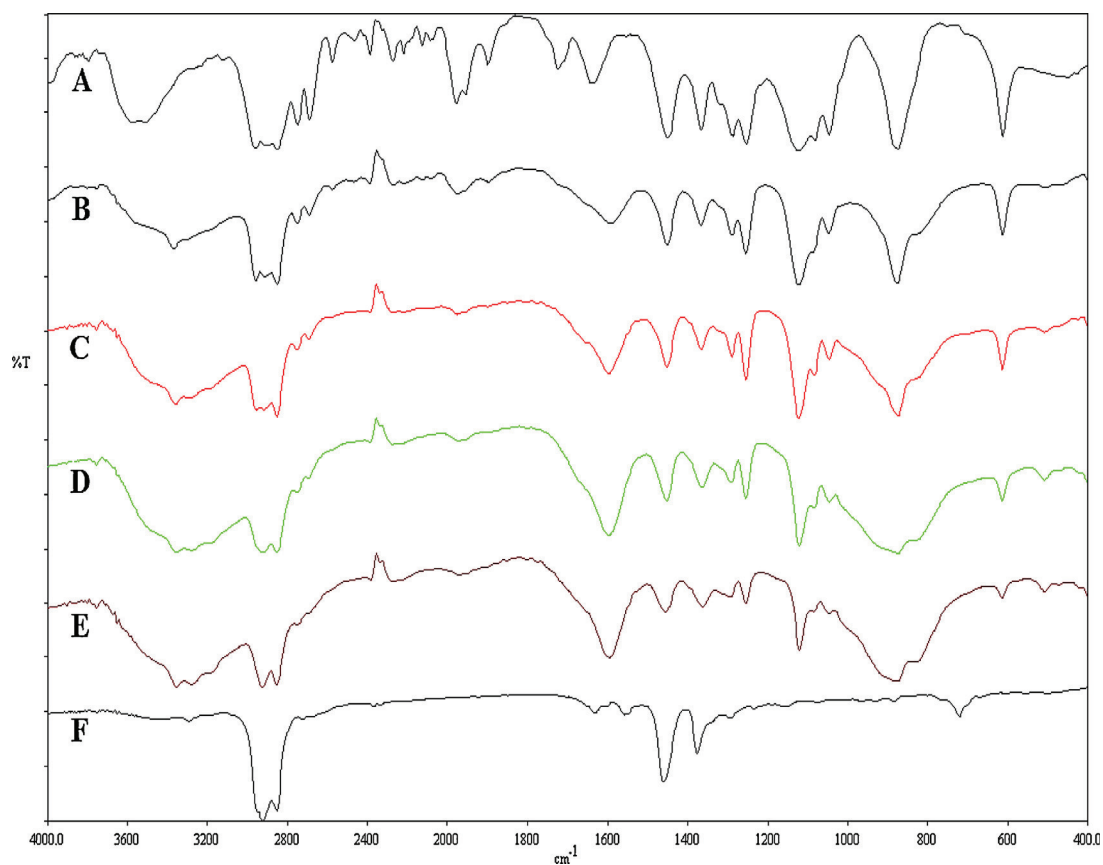


Fig. 9. FTIR spectra of the various binary blends of DO + EDA. A, pure DO ($x_{\text{EDA}} = 0.0000$); B, $x_{\text{EDA}} = 0.2682$; C, $x_{\text{EDA}} = 0.4943$; D, $x_{\text{EDA}} = 0.6874$; E, $x_{\text{EDA}} = 0.8543$; F, Pure EDA ($x_{\text{EDA}} = 1.0000$).

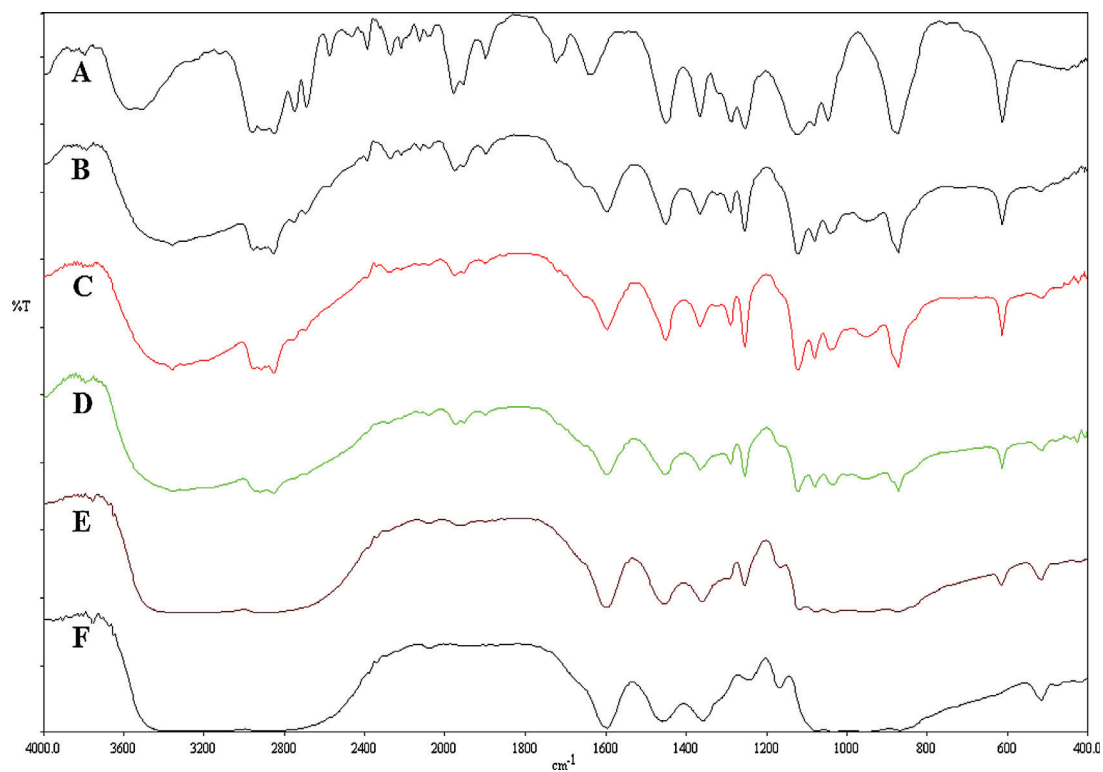


Fig. 10. FTIR spectra of the various binary blends of DO + MEA. A, pure DO ($x_{\text{MEA}} = 0.0000$); B, $x_{\text{MEA}} = 0.2651$; C, $x_{\text{MEA}} = 0.4902$; D, $x_{\text{MEA}} = 0.6839$; E, $x_{\text{MEA}} = 0.8523$; F, Pure MEA ($x_{\text{MEA}} = 1.0000$).

3.6. IR spectroscopic study

The results obtained so far are also well reflected in FT-IR spectra of the binary blends (Figs. 8–10). The spectra were recorded in a demountable KBr cell for liquid samples with spacer of path length of 0.5 mm at ambient temperature with a PerkinElmer Spectrum FT-IR spectrometer (RX-1). Pure DO shows characteristic bands at the range 1600–800 cm^{-1} due to vibrations of the ring (1122 cm^{-1}), the wagging vibrations (800–1050 cm^{-1}) and fan-like vibrations (1250–1300 cm^{-1}) for CH_2 groups and scissor vibrations (1453 cm^{-1}) [59]. DCE has characteristic peaks around 1232 cm^{-1} for *trans* conformer and two peaks around 1313 and 1285 cm^{-1} for *gauche* conformer [12]. These bands shift slightly in peak position and intensity for the blend DO + DCE as the mole fraction (x_1) of DO increases in the blends and thus stand for weak interactions between the components.

Of note for the blend DO+EDA is that the N–H and N– CH_2 stretching bands (around 3296 and 2855 cm^{-1} , respectively) of EDA become less intense and broad as the mole fraction of DO (x_1) in the blend increases. This indicates formation of inter-molecular hydrogen bonds between dissimilar molecules in the blend DO+EDA. Similarly for the blend DO+MEA the bands due to –OH and NH_2 groups (falling within the range 3335–2850 cm^{-1}) become broader and their intensity decreases significantly as the mole fraction (x_1) of DO decreases in the blend suggesting that the blends are characterized by intra-molecular and inter-molecular hydrogen bonds.

4. Conclusion

The physico-chemical study revealed that degree of molecular interactions in the binary blends follows the order: DO + MEA > DO + EDA > DO + DCE. This order of molecular interactions originates from the disruption of weak dipole–dipole interaction/cohesion forces or intra-molecular hydrogen bonds amongst the similar molecules on mixing with DO, because mixing of DO results in the formation of hetero-associates due to inter-molecular hydrogen bond formation and mutual interstitial fitting. Interestingly, a comparison of the partial molar volume ($\bar{V}_{m,1}^0$ and $\bar{V}_{m,2}^0$) at infinite dilution to the molar volume of the respective pure liquid for the studied blends revealed that except the DO + MEA blend other two blends are characterized by volume increase. Anyway, FTIR spectra of the blends showed characterized band shifts in position and intensity as per the above order of molecular interactions.

Acknowledgements

The authors are grateful to the Departmental Special Assistance Scheme under the University Grants Commission, New Delhi (SAP-DRS-III, No. 540/12/DRS/2013) for financial support.

Appendix A. Supplementary data

Supplementary data associated with this article can be found, in the online version, at <http://dx.doi.org/10.1016/j.fluid.2015.06.041>.

References

- [1] C.R. Reid, B.E. Poling, *The Properties of Gases and Liquids*, McGraw Hill, New York, 1998 Ch. 1.

- [2] J. George, N.V. Sastry, *J. Chem. Eng. Data* 49 (2004) 1116–1126.
- [3] A.R. Mahajan, S.R. Mirgane, *Chem. Eng. Comm.* 200 (2013) 1666–1682.
- [4] L. Venkatramana, R.L. Gardas, K.S. Kumar, K.D. Reddy, *Fluid Phase Equilib.* 367 (2014) 7–21.
- [5] Y. Mahan, C.N. Liew, A.E. Mather, *J. Solution Chem.* 31 (2002) 743–756.
- [6] G. Nath, *Chem. Sci. Trans.* 1 (2012) 516–521.
- [7] M.N. Roy, B.K. Sarkar, B. Sinha, *J. Chem. Eng. Data* 54 (2009) 1076–1083.
- [8] B. Sinha, *Phys. Chem. Liq.* 48 (2010) 183–198.
- [9] B.K. Sarkar, A. Choudhury, B. Sinha, *J. Solution Chem.* 41 (2012) 53–74.
- [10] B. Sinha, R. Pradhan, S. Saha, D. Brahman, A. Sarkar, *J. Serb. Chem. Soc.* 78 (2013) 1443–1460.
- [11] K.B. Wiberg, T.A. Keith, M.J. Frisch, M. Murcko, *J. Phys. Chem.* 99 (1995) 9072–9079.
- [12] R.K. Sreeruttan, R. Ramasami, *Phys. Chem. Liq.* 44 (2006) 315–328.
- [13] J. Nath, G. Singh, *J. Chem. Eng. Data* 33 (1988) 58–60.
- [14] P. Brocos, E. Calvo, A. Pineiro, R. Bravo, A. Amigo, *J. Chem. Eng. Data* 44 (1999) 1341–1347.
- [15] V.D. Spasjjevic, B.D. Bjordjevic, S.P. Serbanovic, I.R. Radovic, *J. Chem. Eng. Data* 59 (2014) 1817–1829.
- [16] D. Patterson, G. Delmas, *J. Polym. Sci.* 30 (1970) 1.
- [17] D. Patterson, *Pure. Appl. Chem.* 47 (1976) 305–314.
- [18] V.A. Bloomfield, R.K. Dewan, *J. Phys. Chem.* 75 (1971) 3113–3119.
- [19] D.-Y. Peng, D.B. Robinson, *Ind. Eng. Chem. Fundum.* 15 (1976) 59–64.
- [20] A. Villares, S. Martin, M. Haro, B. Giner, H. Artigas, *J. Chem. Thermodyn.* 36 (2004) 1027–1036.
- [21] M. Das, M.N. Roy, *J. Chem. Eng. Data* 51 (2006) 2225–2232.
- [22] S. Akhtar, A.N. Qamar Faruk, M.A. Saleh, *Phys. Chem. Liq.* 39 (2001) 383–399.
- [23] L. Sarkar, M.N. Roy, *J. Chem. Eng. Data* 54 (2009) 3307–3312.
- [24] K.P. Rao, K.S. Reddy, *J. Chem. Eng. Data* 33 (1988) 130–133.
- [25] C. Li, J. Zhang, T. Zhang, X. Wei, E. Zhang, N. Yang, N. Zhao, M. Su, H. Zhou, *J. Chem. Eng. Data* 55 (2010) 4104–4107.
- [26] J.K. Gladden, *J. Chem. Eng. Data* 17 (1972) 468–471.
- [27] M.A. Saleh, M.S. Ahmed, M.S. Islam, *Phys. Chem. Liq.* 40 (2002) 477–490.
- [28] S. Ranjbar, K. Fakhri, B. Jahan, J. Ghasemi, 2009, *J. Chem. Eng. Data* 54 (2009) 3284–3290.
- [29] R.K. Biswas, R.A. Banu, M.N. Islam, 2003, *Hydrometallurgy* 69 (2003) 157–168.
- [30] S.E. Burke, B. Hawryla, R. Palepu, *Thermochim. Acta* 345 (2002) 101–107.
- [31] U.R. Kapadi, D.G. Hundiwale, N.B. Patil, M.K. Lande, *Fluid Phase Equilib.* 201 (2002) 335–341.
- [32] D. Brahman, R. Pradhan, B. Sinha, *J. Chem. Thermodyn.* 75 (2014) 96–105.
- [33] D. Brahman, B. Sinha, *J. Chem. Thermodyn.* 75 (2014) 136–144.
- [34] K.M. Marstokk, H. Mollendal, *J. Mol. Struct.* 49 (1978) 221–237.
- [35] W.M. Haynes, D.R. Lide, T.J. Bruno, *CRC Handbook of Chemistry & Physics*, 93rd ed., Taylor & Francis, Boca Roton, London, 2012–2013.
- [36] G.M. Smith, H.C. Van Ness, *Introduction to Chemical Engineering Thermodynamics*, McGraw Hill, New York, 1987.
- [37] A.K. Nain, *J. Solution Chem.* 35 (2006) 1417–1439.
- [38] O. Redlich, A.T. Kister, *Indus. Eng. Chem.* 40 (1948) 345–348.
- [39] P.J. Flory, R.A. Orwell, A. Vrijji, *J. Am. Chem. Soc.* 86 (1964) 3507–3514.
- [40] P.J. Flory, R.A. Orwell, A. Vrijji, *J. Am. Chem. Soc.* 86 (1964) 3515–3520.
- [41] P.J. Flory, *J. Am. Chem. Soc.* 87 (1965) 1833–1838.
- [42] A. Abe, P.J. Flory, *J. Am. Chem. Soc.* 87 (1965) 1838–1846.
- [43] S.I. Sandler, *Chemical, Biochemical, and Engineering Thermodynamics*, 4th ed., John Wiley & Sons (Asia, New Delhi, 2006) 242–258.
- [44] J.J. McKetta, W.A. Cunningham, *Encyclopedia of Chemical Processing and Design*, Vol-36, Marcel Dekker, New York, 1991 99–108.
- [45] S. Glasstone, K.J. Laidler, H. Eyring, *The Theory of Rate Process*, McGraw-Hill Book Company, New York, 1941.
- [46] F. Corradini, L. Marcheselli, A. Marchetti, M. Tagliuzucchi, L. Tassi, G. Tosi, *Bull. Chem. Soc. Jpn.* 65 (1992) 503–511.
- [47] A.K. Mehrotra, W.D. Monnery, W. Svrcek, *Fluid Phase Equilib.* 117 (1996) 344–355.
- [48] R.D. McCarty, *Fluid Phase Equilib.* 256 (2007) 42–46.
- [49] M.A. Hernandez-Galvan, F. Garcia-Sanchez, R. Macias-Salinas, *Fluid Phase Equilib.* 262 (2007) 51–60.
- [50] M.H. Cohen, D. Turnbull, *J. Chem. Phys.* 31 (1959) 1164–1169.
- [51] G.P. Dubey, K. Kumar, *J. Chem. Eng. Data* 56 (2011) 2995–3003.
- [52] S.C. Bhatia, R. Bhatia, G.P. Dubey, *Int. J. Thermophys.* 31 (2010) 2119–2146.
- [53] W.E. Acree, *J. Chem. Eng. Data* 28 (1983) 215–216.
- [54] M.N. Roy, B. Sinha, V.K. Dakua, *J. Mol. Liq.* 136 (2007) 128–137.
- [55] H. Eyring, J.F. Kincaid, *J. Chem. Phys.* 6 (1938) 620–629.
- [56] T.J. Aminabhavi, V.B. Patil, *J. Chem. Eng. Data* 43 (1998) 497–503.
- [57] K.M. Kadish, J.E. Anderson, *Pure Appl. Chem.* 59 (1987) 703–714.
- [58] M. Yasmin, M. Gupta, *J. Solution Chem.* 40 (2011) 1458–1472.
- [59] A.P. Kilimov, M.A. Svechnikova, V.I. Shevchenko, V.V. Smirnov, S.B. Zotov, F.V. Kvasnyuk-Mudryi, *Khimiya Geterotsiklicheskikh Soedinenii* 5 (1969) 208–211.